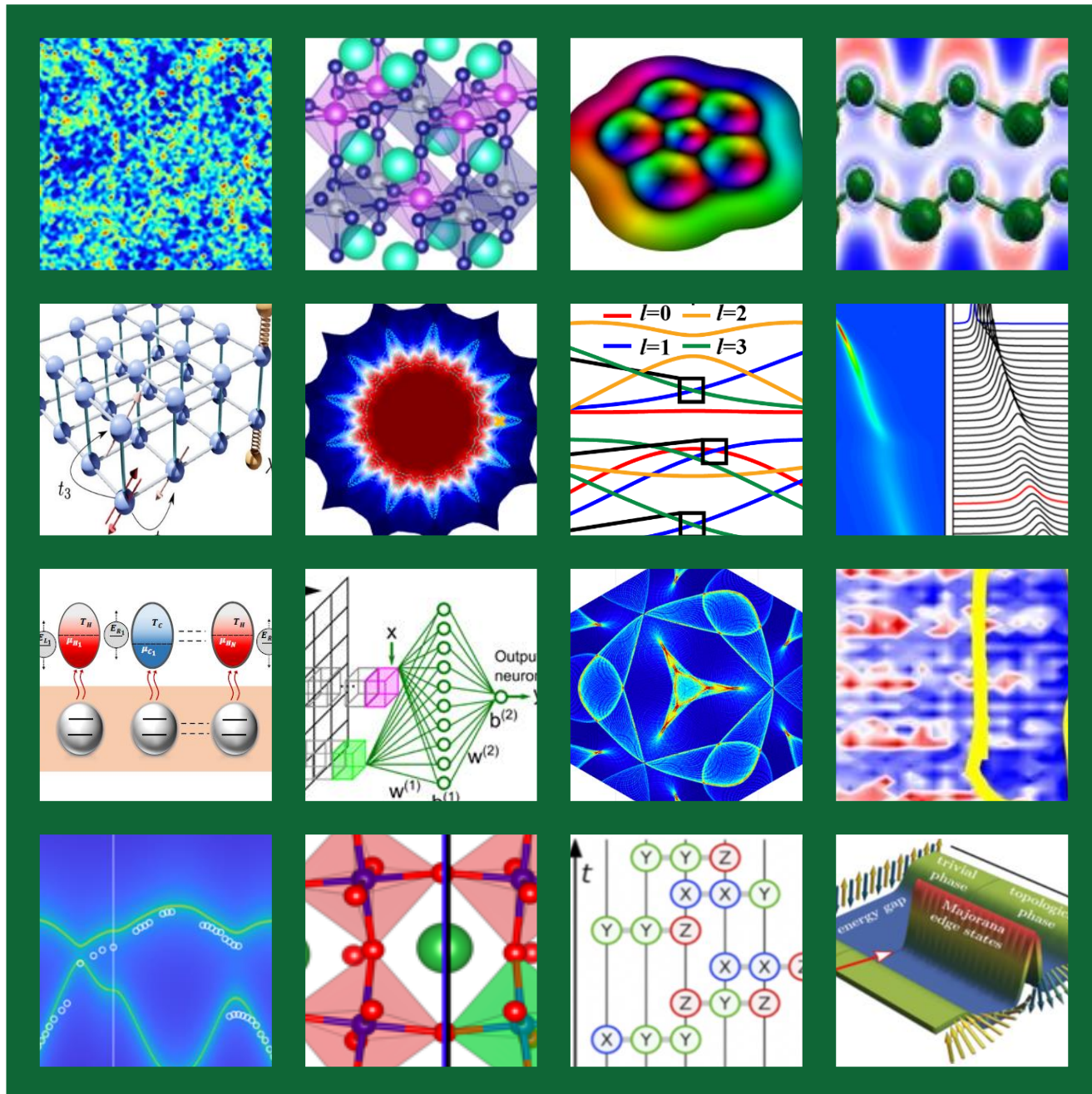


Theoretical Condensed Matter Physics Principal Investigators' Meeting

Virtual Meeting, October 26-28, 2021

Program and Abstracts

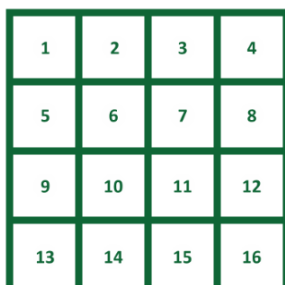


U.S. DEPARTMENT OF
ENERGY

Office of
Science

Office of Basic Energy Sciences
Materials Sciences and Engineering Division

On the Cover



1. Gia-Wei Chern, Machine Learning Aided Modeling of Resistive Switching Phenomena in Correlated Electron, shown is a snapshots of spin-spin correlations during phase separation.
2. Feliciano Giustino, Toward exascale computing of electron-phonon couplings for finite-temperature materials design, shown is the atomic structure of lead-free double perovskite $\text{Cs}_2\text{AgBiBr}_6$ for photovoltaics.
3. Jiadong Zang, Topological spin textures in chiral magnets: from 2D to 3D, shown is the spin configuration of a skyrmion bundle.
4. Lilia M. Woods, Dispersive Interactions in Quantum Materials: Interplay between Anisotropy, Doping, and Non-linearity, shown is the side view of the AA bilayer.
5. Richard Scalettar, Quantum Simulations of the Interplay of Charge Density Wave, Magnetic, and Pairing Correlations, shown is a sketch of a Holstein Hamiltonian with intralayer and interlayer hopping.
6. Sahar Sharifzadeh, First-Principles Understanding of Optical Excitations within Low-Dimensional Materials, shown is the real part of the in-plane dielectric function for 1T-TaS₂.
7. Lucas Lindsay, Elucidating the Nature of Chiral and Topological Phonons in Materials for Energy Technologies, shown is the DFT-derived electronic band structure for α -TeO₂ along the chiral c-axis.
8. Steven G. Louie, Theory of Materials Program, shown are *Ab initio* ARPES spectrum and momentum distribution curves (MDC) of La_{2-x}Sr_xCuO₄ calculated with the GWPT method.
9. Andrew N. Jordan, Solid State Quantum Refrigeration Superconducting, Absorption and Measurement Based, shown is a series of electronic nanocavities connected to external reservoirs and coupled to each other via quantum dots with prescribed resonant energies. The cavities are exchanging energy in the form of heat with ancillary quantum systems.
10. Eun-Ah Kim, Machine Learning Quantum Emergence, shown is part of the quantum loop topography.
11. Allan H. MacDonald, Magnetism in Moiré Materials, shown is the momentum-dependence of low-energy particle-hole phase space in MATBG.
12. Badri Narayanan, Controlling reversible phase transitions in rare-earth nickelates for novel memory devices, shown is the spatial distribution of oxygen near the end of 0.2 ns CMD simulations under applied electric fields in WO_{3- δ} memristors.
13. Liqin Ke, Quantum Control and Tuning of Magnetic 2D van der Waals Heterostructures, shown is the spinwave spectrum in CrI₃ calculated with QSGW+U.
14. Fernando Reboledo, Advanced theoretical and computational methods for quantum materials, shown is the laterally modulated unit cell of epitaxial LaCoO₃.
15. Vedika Khemani, The Non-Equilibrium Quantum Frontier, shown is the measurement-only circuit dynamics with measurements drawn from ensembles of three-site Pauli strings.
16. Elbio Dagotto, Theoretical Studies of Complex Collective Phenomena, shown is a sketch of Majorana's DMRG results in helical spin backgrounds, in a multiorbital Hubbard chain geometry.

This document was produced under contract number DE-SC0014664 between the U.S. Department of Energy and Oak Ridge Associated Universities.

The research grants and contracts described in this document are supported by the U.S. DOE Office of Science, Office of Basic Energy Sciences, Materials Sciences and Engineering Division.

Foreword

This book contains abstracts for presentations made at the 2021 Theoretical Condensed Matter Physics (TCMP) Principal Investigators' Meeting sponsored by the Materials Sciences and Engineering Division of the US Department of Energy, Office of Basic Energy Sciences (DOE-BES). The meeting convenes scientists supported within the TCMP program by the DOE-BES to present the most exciting, new research accomplishments and proposed future research directions in their BES supported awards. The meeting affords Principal Investigators (PIs) in the program an opportunity to see the full range of research currently being supported. We hope the meeting fostered a collegial environment to (1) stimulate the discussion of new ideas, (2) provide unique opportunities to develop or strengthen collaborations among PIs, and (3) identify and pursue new scientific directions and energy frontiers. In addition, the meeting provides valuable feedback to DOE-BES management in its assessment of the state of the program and in identifying program needs and future programmatic research directions. The meeting was attended by approximately 130 TCMP-supported scientists.

The mission of the BES program is to support fundamental research to understand, predict, and ultimately control matter and energy at the electronic, atomic, and molecular levels. Condensed matter theory contributes to the knowledge base for the discovery and design of new materials with novel structures, functions, and properties. This knowledge serves as a basis for the development of new materials for the efficient generation, storage, and use of energy and for mitigation of the environmental impacts of energy use.

More specifically, the core research areas of the TCMP program support research in quantum physics with an emphasis on quantum materials, materials discovery and design, out-of-equilibrium quantum dynamics, and fundamental research in materials related to energy technologies. Specific themes include strong electron correlations; quantum phases of matter, including topological states, magnetism, and superconductivity; multiferroic materials; and excited states phenomena and photon science. Research spans from purely analytical to computational with an emphasis on methods and technique development, as well as prediction and interpretation of novel quantum phenomena. This includes data-driven materials science, as well as high throughput computations.

The TCMP program also supports research relevant to the Materials Genome Initiative (MGI) and exascale computing through small and large team projects in Computational Materials Sciences (CMS). These integrated team-science projects develop widely applicable open-source software utilizing DOE's current leadership class and future exascale computing facilities. Researchers are expected to make use of current generation petaflop supercomputers and prepare for next-generation exaflop machines scheduled for deployment in the coming years. The goal of these CMS projects is to provide the software platforms and data for the design of new functional materials with a broad range of applications, including alternative and renewable energy, electronics, data storage and materials for quantum information science (QIS).

Complementing this computational materials ecosystem, next-generation high-performance computing science projects are supported in the Scientific Discovery Through Advanced Computing (SciDAC) partnership with the Office of Advanced Scientific Computing Research (ASCR). The SciDAC projects support interdisciplinary teams. These bring together experts in

key areas of science and energy research, applied mathematics, and computer science to address computing challenges and take maximum advantage of DOE's supercomputers, allowing them to quicken the pace of scientific discovery. Their focus is on computational methods, algorithms, and software to further materials research, specifically for simulating quantum phenomena of many-particle systems driven far from equilibrium by going beyond the use of existing quantum-based methods in their traditional regimes.

More recently, the TCMP program expanded into QIS to include research focused on the discovery and modeling of fundamental physical properties of next-generation quantum systems and the development of quantum computing algorithms and applications relevant to the core research areas of TCMP.

The meeting was held in a virtual format organized into six oral and six poster sessions covering the range of activities supported by the program. This structure attempted to capture in a virtual setting fewer oral and more poster sessions with the intent to provide enhanced virtual PI interactions in poster rooms using a video chat platform. Co-chairs for the scientific program were Dr. Lucas Lindsay (ORNL) and Dr. Brian Moritz (SLAC). To these two we express our sincere appreciation for their invaluable help in organizing the meeting. We also want to gratefully acknowledge the excellent support provided by Ms. Tia Moua and Mr. Andrew Fowler of the Oak Ridge Institute for Science and Education and by Ms. Teresa Crockett of BES, for their efforts in organizing the meeting.

Drs. Matthias Graf and Claudia Mewes
Program Managers, Theoretical Condensed Matter Physics
Division of Materials Sciences and Engineering
Basic Energy Sciences, Office of Science, U.S. Department of Energy

Table of Contents

Agenda	xiii
Poster Listing	xix
 <u>Abstracts</u>	
Superconductivity in Quantum Materials <i>Daniel Agterberg</i>	1
Theory of Fluctuating and Critical Quantum Matter <i>Leon Balents</i>	6
Quantum Phenomena in Few-Layer Group IV Monochalcogenides: Interplay Among Structural, Thermal, Optical, Spin, and Valley Properties in 2D <i>Salvador Barraza-Lopez</i>	11
Topological Magnetic Quantum Chemistry and Twisted Engineered Materials <i>B. Andrei Bernevig</i>	16
Spin-Orbit Interactions in Transdimensional Heterostructures <i>Igor Bondarev</i>	20
Coupled Electron-Phonon Transport from First Principles <i>David Broido</i>	25
QMC-HAMM: High Accuracy Multiscale Models from Quantum Monte Carlo <i>David Ceperley, Elif Ertekin, Harley Johnson, Matthew Turk, Lucas Wagner and Andriy Nevidomskyy</i>	30
Designing Topological Quantum Matter <i>Claudio Chamon</i>	33
Ab Initio Complete Cell Quantum Embedding and Diagrammatic Coupled Cluster for Correlated Materials Phase Diagrams <i>Garnet Kin-Lic Chan</i>	37
Traversing the “Death Valley” Separating Short and Long Times in Non-equilibrium Quantum Dynamical Simulations of Real Materials <i>Garnet Kin-Lic Chan, Marco Bernardi, Emanuel Gull, Andrew Millis, Eran Rabani, David Reichman, Carol Woodward, and Chao Yang</i>	39

Theoretical Studies of Polar Systems near Ferroelectric Quantum Critical Points <i>Premala Chandra</i>	41
Computational Mesoscale Science and Open Software for Quantum Materials <i>L. Q. Chen, V. Gopalan, I. Dabo, J. Xu, and R. Engel-Herbert</i>	44
Machine Learning Aided Modeling of Resistive Switching Phenomena in Correlated Electron Systems <i>Gia-Wei Chern</i>	49
Quantum Anisotropic-Exchange Magnets <i>Alexander Chernyshev</i>	54
Machine-Assisted Quantum Magnetism <i>S. Chowdhury, A. Bansil, J. Turner, M. Amoo, A. Feiguin, C. Jia, A. Lindenberg, Y. Nashed, J. Thayer, and C. Yoon</i>	58
Competing Orders in Multi-Orbital Systems <i>Andrey V. Chubukov</i>	60
Topology Driven Quantum and Thermal Dynamics of Low-Dimensional Magnetic and Superconducting Systems <i>Eugene M. Chudnovsky</i>	65
Spin and Orbital Physics in Novel Quantum Materials <i>Piers Coleman</i>	69
Simulation, Design, and Discovery of Complex Materials <i>Valentino R. Cooper, T. Berlijn, R. S. Fishman, L. R. Lindsay, and D. S. Parker</i>	72
Theoretical Studies of Complex Collective Phenomena <i>Elbio Dagotto, Thomas Maier, Adriana Moreo, and Satoshi Okamoto</i>	77
Theory Institute for Materials and Energy Spectroscopies (TIMES) <i>T. P. Devereaux, B. Moritz, C. Jia, C. D. Pemmaraju, H. Jiang, J. Rehr, J. Kas, F. Vila, and J.E. Moore</i>	82
MemComputing the Spectrum of Correlated Quantum Systems <i>Massimiliano Di Ventra</i>	88
Time-Dependent Phenomena in Correlated Materials <i>Adrian Feiguin</i>	91
Intertwined and Vestigial Electronic Orders in Correlated Systems <i>Rafael M. Fernandes</i>	93

Theory for Pump/Probe Experiments in Charge-Density-Wave Materials <i>James K. Freericks</i>	98
Simulating Long-Time Evolution of Driven Many-Body Systems with Next Generation Quantum Computers <i>James K. Freericks and Alexander Kemper</i>	103
Midwest Integrated Center for Computational Materials (MICCoM): A Brief Overview <i>G. Galli, Maria Chan, Juan de Pablo, Marco Govoni, Joseph Heremans, Andrew Ferguson, Dmitri Talapin, François Gygi, and Jonathan Whitmer</i>	108
Theory of Fluctuations in Strongly Correlated Materials <i>Victor Galitski</i>	111
Toward Exascale Computing of Electron-Phonon Couplings for Finite-Temperature Materials Design <i>Feliciano Giustino and Emmanouil Kioupakis</i>	114
Non-equilibrium Effects in Conventional and Topological Superconducting Nanostructures <i>Leonid Glazman</i>	119
Optical Control of Spin-polarization in Quantum Materials <i>Marco Govoni</i>	124
Mapping the Genome of Coherent Quantum Defects for Quantum Information Science <i>Geoffroy Hautier, Alp Sipahigil, Sinéad Griffin, Archana Raja, and Alexander Weber-Bargioni</i>	126
Symmetry in Correlated Quantum Matter <i>Michael Hermele</i>	128
Theory of Novel Superconductors <i>P. J. Hirschfeld</i>	133
Data Science Enabled Discovery of Superconductors <i>P. J. Hirschfeld, J. A. Hamlin, G. R. Stewart, and R. G. Hennig</i>	137
Nontrivial Consequences of Non-centrosymmetry in Topological and Trivial Metals <i>Pavan Hosur</i>	142
Van der Waals Reprogrammable Quantum Simulator <i>Benjamin M. Hunt, Jeremy Levy, Patrick Irvin, Chang-Beom Eom, Roman Engel-Herbert, Erica Carlson, Prineha Narang, and Di Xiao</i>	146

Quantitative Studies of the Fractional Quantum Hall Effect <i>Jainendra Jain</i>	149
Mapping and Manipulating Materials Phase Transformation Pathway <i>Duane D. Johnson, William A. Shelton, Prashant Singh and Andrey V. Smirnov</i>	154
Artificial Intelligence and Data Science Enabled Predictive Modeling of Collective Phenomena in Strongly Correlated Quantum Materials <i>Steven Johnston, Cristian Batista, Adrian Del Maestro, Jian Liu, Richard Scalettar, Ehsan Khatami, Mark Dean, Thomas Maier, Alan Tennant, Kipton Barros, and Ying Wai Li</i>	158
Solid State Quantum Refrigeration Superconducting, Absorption and Measurement Based <i>Andrew N. Jordan</i>	163
Quantum Control and Tuning of Magnetic 2D van der Waals Heterostructures <i>Liqin Ke</i>	167
Center for Predictive Simulation of Functional Materials <i>P. R. C. Kent, A. Benali, A. Bhattacharya, O. Heinonen, Y. Luo, H. Shin, R. Clay, L. Shulenburger, J. Townsend, P. Ganesh, J. Krogel, H. N. Lee, L. Mitas, and B. Rubenstein</i>	172
The Non-Equilibrium Quantum Frontier <i>Vedika Khemani</i>	177
Machine Learning Quantum Emergence <i>Eun-Ah Kim</i>	182
Quantum Probes of the Materials Origins of Decoherence <i>S. Kolkowitz, V. Brar, J. Choy, J. Dubois, M. Eriksson, L. Faoro, M. Friesen, A. Levchenko, V. Lordi, R. McDermott, K. Ray, and Y. Rosen</i>	186
Comscope: Center for Computational Design of Functional Strongly Correlated Materials and Theoretical Spectroscopy <i>Gabriel Kotliar, Robert Konik, Sangkook Choi, Mark Dean, Andrey Kutepov, Corey Melnick, Cedomir Petrovic, Yongxin Yao, Kipton Barros, Martha Greenblatt, Kristjan Haule, Manish Parashar, and Gia-Wei Chern</i>	191
Spin Currents in Magnetic Systems and Heterostructures <i>Alexey Kovalev</i>	196
Correlated Electronic Structure and Phase Stability in Real Materials <i>Walter R. L. Lambrecht</i>	201

Strongly Correlated Electronic Systems: Local Moments and Conduction Electrons <i>Patrick A. Lee</i>	206
Elucidating the Nature of Chiral and Topological Phonons in Materials for Energy Technologies <i>Lucas Lindsay</i>	211
Theory of Materials Program <i>Steven G. Louie, Marvin L. Cohen, Dung-Hai Lee, Jeffrey B. Neaton, and Lin-Wang Wang</i>	216
Center for Computational Study of Excited-State Phenomena in Energy Materials <i>Steven G. Louie, Jeffrey B. Neaton, James R. Chelikowsky, Jack R. Deslippe, Naomi S. Ginsberg, Felipe H. da Jornada, Daniel Neuhauser, Diana Y. Qiu, Eran Rabani, Feng Wang, and Chao Yang</i>	221
Non-Abelian Quasiparticles and Topological Superconductivity for Quantum Information Science <i>Yuli Lyanda-Geller</i>	226
Materials for Ultra-Coherent, Mobile, Electron-Spin Qubits <i>S. A. Lyon, M. I. Dykman, M. D. Henry, and E. A. Shaner</i>	231
Magnetism in Moiré Materials <i>Allan H. MacDonald</i>	235
A New Approach to the Interacting Phonon Problem <i>Chris A. Marianetti</i>	238
Less Common Topological Phenomena in Bulk Materials <i>Igor I. Mazin</i>	243
Structure and Electronic Properties of Dirac Materials <i>E. J. Mele</i>	247
Metals and Quantum Materials with Spin-Orbit Interactions by Quantum Monte Carlo Methods <i>Lubos Mitas</i>	251
Nonequilibrium Phenomena in Topological Insulators <i>Aditi Mitra</i>	255
Localization in Energy Materials <i>Juana Moreno</i>	257
Non-equilibrium Physics at the Nanoscale <i>Dirk K. Morr</i>	262

Duality and Strongly Interacting Systems <i>Michael Mulligan</i>	267
Fractons and Beyond <i>Rahul Nandkishore</i>	272
Controlling Reversible Phase Transitions in Rare-Earth Nickelates for Novel Memory Devices <i>Badri Narayanan, Dillon Fong, and Subramanian Sankaranarayanan</i>	276
Correlations and Dynamics in Quantum Materials <i>Michael Norman, Olle Heinonen, Peter Littlewood, Ivar Martin, Kostya Matveev, and Hyowon Park</i>	281
Center for Nonperturbative Studies of Functional Materials Under Nonequilibrium Conditions <i>Tadashi Ogitsu, Xavier Andrade, Alfredo Correa, Liang Z. Tan, David Prendergast, C. D. Pemmaraju, and Aaron M. Lindenberg</i>	286
Identification of Fractionalized Excitations in Quantum Spin Liquids and Related Materials <i>Natalia Perkins</i>	291
Materials Project <i>Kristin Persson</i>	295
Complex (Anti)Ferroic Oxides: Statics and Dynamics at Finite Temperatures <i>Inna Ponomareva</i>	300
First Principles Approach to Exciton Transport in Energy Materials <i>Diana Qiu</i>	304
Emergent Properties of Highly Correlated Electron Materials <i>Srinivas Raghu</i>	307
Theoretical and Computational Studies of Excitations in Functional Nanomaterials <i>Talat S. Rahman</i>	312
Ab initio Prediction of Novel Optoelectronic Properties for Topological Materials <i>Andrew M. Rappe</i>	317
Advanced Theoretical and Computational Methods for Quantum Materials <i>F. A. Reboredo, M.-H. Du, M. Eisenbach, J. Krogel, and M. Yoon</i>	322
New Developments in the Theory of Excited States and X-ray Spectra <i>J. J. Rehr and J. J. Kas</i>	327

Applications of Nickelate Perovskites for Neuromorphic Computing from Electronic Structure and Machine Learning <i>Aldo H. Romero</i>	331
Optoelectronic Properties of Bent Two-Dimensional Materials from First-Principles Methods Combined with Machine Learning <i>Adrienn Ruzsinszky</i>	334
Quantum Simulation of Correlated Quantum Matter <i>Subir Sachdev</i>	338
Quantum Simulations of the Interplay of Charge Density Wave, Magnetic, and Pairing Correlations <i>Richard T. Scalettar</i>	341
Holographic Quantum Simulation of Strongly Correlated Electron Systems <i>Shyam Shankar and Andrew Potter</i>	346
First-Principles Understanding of Optical Excitations within Low-Dimensional Materials <i>Sahar Sharifzadeh</i>	350
Theoretical Studies in Very Strongly Correlated Matter <i>B. Sriram Shastry</i>	355
Fractional Topological States in Disorder Quantum Hall and Graphene Based Superlattice Systems <i>Dong-Ning Sheng</i>	360
Electron Correlations, Bad-Metal Behavior and Unconventional Superconductivity <i>Qimiao Si</i>	365
Frontiers in Magnetic Materials <i>David J. Singh</i>	370
Late Stages in the Ordering of Magnetic Skyrmion Lattices <i>Uwe C. Täuber and Michel Pleimling</i>	375
Unconventional Metals in Strongly Correlated Systems <i>Senthil Todadri</i>	380
Orbital-Free Quantum Simulation Methods for Applications to Warm Dense Matter <i>Samuel B. Trickey and J. W. Dufty</i>	383
Interaction and Transport Effects in Driven Magnetic and Topological Materials <i>Wang-Kong Tse</i>	388

Nonequilibrium Thermodynamics in Magnetic Nanostructures <i>Yaroslav Tserkovnyak</i>	393
Condensed Matter Theory <i>Alexei Tsvetlik, Robert Konik, Weiguo Yin, Andreas Weichselbaum, and Laura Classen</i>	398
Time-Dependent Density-Functional Approaches for Spin-Dependent Nonequilibrium Phenomena <i>Carsten A. Ullrich</i>	403
<i>Ab Initio</i> Theory of Unconventional Superconductivity <i>Mark van Schilfgaarde, Stephan Lany, and Dimitar Pashov</i>	407
Quantum Criticality and Topology in Non-equilibrium Systems <i>Romain Vasseur</i>	410
Real-Time Dynamics of Driven Correlated Electrons in Quantum Materials <i>Vojtech Vlcek, Khaled Ibrahim, Gabriel Kotliar, Lin Lin, Daniel Neuhauser, K. Birgitta Whaley, Chao Yang, and Dominika Zgid</i>	415
Exploratory Development of Theoretical Methods <i>Cai-Zhuang Wang, Vladimir Antropov, Yongxin Yao, Kai-Ming Ho, and Feng Zhang</i>	418
Disorder and Interaction in Correlated Electron Materials <i>Ziqiang Wang</i>	422
Exploiting Locality in Electronic Structure: Tensor Networks, Gausslets, Blue Electrons, and Machine-Learning <i>Steven R. White and Kieron Burke</i>	427
First Principles Thermodynamics of Intrinsically Disordered Matter <i>Michael Widom</i>	432
DECODE: Data-driven Exascale Control of Optically Driven Excitations in Chemical and Material Systems <i>Bryan M. Wong, Christian Shelton, Zizhong Chen, Ibrahim Khaled, and Mauro Del Ben</i>	437
Dispersive Interactions in Quantum Materials: Interplay between Anisotropy, Doping, and Non-linearity <i>Lilia M. Woods</i>	441
First Principles Investigations for Magnetic Properties of Innovative Materials <i>Ruqian Wu</i>	446

Synthesis of Motif and Symmetry for Accelerated Learning, Discovery, and Design of Electronic Structures for Energy Conversion Applications <i>Qimin Yan</i>	450
Quantum Computing Enhanced Gutzwiller Variational Embedding Method for Correlated Multi-Orbital Materials <i>Yongxin Yao, Cai-Zhuang Wang, Kai-Ming Ho, and Peter P. Orth</i>	452
Topological Spin Textures in Chiral Magnets: From 2D to 3D <i>Jiadong Zang</i>	457
Fundamental and Defect Properties of Electronic Materials <i>Shengbai Zhang and Damien West</i>	462
Data-driven Discovery of Inorganic Electrides for Energy Applications <i>Qiang Zhu</i>	467
Reconsidering Electronic Phases: The Role of Other Microscopic Degrees of Freedom <i>Alex Zunger</i>	471
Spin-Orbit Coupled Systems: From Triplet Superconductivity to Topological Kink States <i>Igor Zutic</i>	474
Author Index	481
Participant List	487

**Theoretical Condensed Matter Physics
Virtual Principal Investigators' Meeting Agenda
October 26 – 28, 2021**

Co-Chairs: Lucas Lindsay (ORNL) and Brian Moritz (SLAC)
(Times listed in Eastern Time Zone)

Tuesday, October 26, 2021

Opening Session

11:00–11:15 **Matthias Graf**, Department of Energy
Welcome and Introductory Remarks

11:15–11:30 **Andrew Schwartz**, Acting MSE Division Director, Department of Energy
Remarks from BES

**Oral Session 1
(QIS / noneq)**

Chair: **Matthias Graf**

11:30–11:45 **Alexander Kemper**, North Carolina State University
*Many body thermodynamics on quantum computers via partition function zeros
(Poster: Simulating long-time evolution of driven many-body systems with next
generation quantum computers)*

11:45–12:00 **Yongxin Yao**, Ames Laboratory
*Adaptive variational quantum computing algorithm for nonequilibrium dynamics
simulations
(Poster: Quantum computing enhanced Gutzwiller variational embedding approach
for correlated materials)*

12:00–12:15 **Shimon Kolkowitz**, University of Wisconsin, Madison
*Correlated errors in superconducting qubits
(Poster: Quantum probes of the materials origins of decoherence)*

12:15–12:30 **Vedika Khemani**, Stanford University
*Out-of-equilibrium phases in non-unitary dynamics
(Poster: Non-unitary dynamics via spacetime duality)*

12:30–12:50 **20 Minute Break**

12:50–1:00 **Poster Session 1 – Introductions**

1:00–2:15 **Poster Session 1 (GatherTown)**

2:15–2:30 **15 Minute Break**

Oral Session 2 (Low D / multi-/ ferro / data)	Chair: Claudia Mewes
2:30–2:45	Kristin Persson , Lawrence Berkeley National Lab and University of California, Berkeley <i>The Materials Project for Data-driven Energy Materials Discovery</i> (Poster: <i>The Materials Project</i>)
2:45–3:00	Salvador Barraza-Lopez , University of Arkansas <i>Engineering static topological vortices on 2D ferroelectrics</i> (Poster: <i>Quantum phenomena in few-layer group IV monochalcogenides: interplay among structural, thermal, optical, spin, and valley properties in 2D</i>)
3:00–3:15	Lilia Woods , University of South Florida <i>Probing the universal Casimir force with novel materials</i> (Poster: <i>Materials with nontrivial topology and fluctuation induced interactions</i>)
3:15–3:30	Lucas Wagner , University of Illinois, Urbana Champaign <i>Accurate excited states computed via quantum Monte Carlo</i> (Poster: <i>QMC-HAMM P1: Quantum Monte Carlo database for machine learning accurate interatomic potentials of dense hydrogen</i>)
3:30–3:45	Adrienn Ruzsinszky , Temple University <i>Tunable band gaps and optical absorption properties of bent MoS₂ nanoribbons</i> (Poster: <i>same</i>)
3:45–4:00	Liqin Ke , Ames Laboratory <i>Critical role of electron correlations on exchange interactions and spin excitations</i> (Poster: <i>Electron correlation effects on magnetic interactions and spin excitations in 2D van der Waals materials</i>)
4:00–4:20	20 Minute Break
4:20–4:35	Let's talk diversity – Talat Rahman , University of Central Florida <i>Bridge to PhD – Diversity matters</i>
4:35–4:45	Poster Session 2 – Introductions
4:45–6:00	Poster Session 2 (GatherTown)

Wednesday, October 27, 2021

11:00–11:05 **Welcome to Day Two**

Oral Session 3
(Noneq / transp / data) Chair: **Matthias Graf**

11:05–11:20 **Alexei Tselik**, Brookhaven National Laboratory
Dynamically induced topological phase transitions in ZrTe₅
(Poster: *Understanding and manipulating phases of matter in correlated and topological systems*)

11:20–11:35 **David Broido**, Boston College
Coupled electron-phonon transport from first principles
(Poster: *same*)

11:35–11:50 **Feliciano Giustino**, University of Texas, Austin
Origin of low carrier mobility in lead-free halide perovskites
(Poster: *Phonon-limited mobility and electron-phonon coupling in lead-free halide double perovskites*)

11:50–12:05 **Long-Qing Chen**, Pennsylvania State University
Coupled electronic and structural transitions and oscillation
(Poster: *Phase-field models of coupled structural and electronic processes*)

12:05–12:20 **Qimin Yan**, Temple University
Motif centric learning framework for crystalline materials
(Poster: *Physical principle enhanced machine learning frameworks for solid-state materials and molecules*)

12:20–12:40 **20 Minute Break**

12:40–12:50 **Poster Session 3 – Introductions**

12:50–2:05 **Poster Session 3 (GatherTown)**

2:05–2:20 **15 Minute Break**

Oral Session 4
(Comp spectroscopy /
CMS / photo / data) Chair: **Lucas Lindsay**

2:20–2:35 **John Rehr**, University of Washington
Advanced calculations of X-ray spectroscopies with FEFY10 and Corvus
(Poster: *New developments in the theory of excited states and X-ray spectra*)

2:35–2:50 **Adrian Feiguin**, Northeastern University
A time-dependent numerical approach to non-equilibrium ARPES
(Poster: *Beyond perturbation theory: a time dependent numerical approach to non-equilibrium spectroscopies*)

- 2:50–3:05 **Tadashi Ogitsu**, Lawrence Livermore National Laboratory
Effect of surface defects on carrier dynamics in lead halide perovskites (LHP)
(Poster: *INQ: A state of the art implementation of density functional theory for GPU-based supercomputers*)
- 3:05–3:20 **Giulia Galli**, Argonne National Laboratory and University of Chicago
Midwest Integrated Center for Computational Materials (MICCoM)
(Poster: *same*)
- 3:20–3:25 **5 Minute Break**
- 3:25–3:40 **Andrew Rappe**, University of Pennsylvania
Ab initio prediction of novel optoelectronic properties for topological materials
(Poster: *same*)
- 3:40–3:55 **Steven Louie**, Lawrence Berkeley National Lab and University of California, Berkeley
Exciton-enhanced photophysics: Giant shift currents and excitons in time-resolved ARPES
(Poster: *Center for Computational Study of Excited-State Phenomena in Energy Materials*)
- 3:55–4:10 **Gia-Wei Chern**, University of Virginia
Anomalous phase separation dynamics in strongly correlated electron systems
(Poster: *Anomalous phase separation dynamics in strongly correlated electron systems — Machine-learning enabled large-scale simulations*)
- 4:10–4:30 **20 Minute Break**
- 4:30–4:40 **Poster Session 4 – Introductions**
- 4:40–6:00 **Poster Session 4 (GatherTown)**

Thursday, October 28, 2021

- 11:00–11:05 **Welcome to Day Three**
- Oral Session 5**
(SC / dynamics / data) Chair: **Matthias Graf**
- 11:05–11:20 **Richard Hennig**, University of Florida
Data-driven superconductor discovery: Metastable superconductivity in WB2 at high pressure
(Poster: *Metastable superconducting materials*)
- 11:20–11:35 **Qimiao Si**, Rice University
Multiorbital spin-singlet pairing and d+d superconductivity
(Poster: *Matrix spin-singlet pairing and d+d superconductivity*)

- 11:35–11:50 **Patrick Lee**, Massachusetts Institute of Technology
Superconducting-like response in systems near the Mott transition under external drive
(Poster: same)
- 11:50–12:05 **Thomas Devereaux**, SLAC National Acceleratory Laboratory and Stanford University
Tuning nickelate superconductivity via rare-earth
(Poster: Theory of monovalent nickelates)
- 12:05–12:20 **Gabriel Kotliar**, Brookhaven National Laboratory and Rutgers University
Theoretical spectroscopy of the infinite layer nickelates
(Poster: COMSCOPE: Center for Computational Material Spectroscopy and Design)
- 12:20–12:40 **20 Minute Break**
- 12:40–12:50 **Poster Session 5 – Introductions**
- 12:50–2:05 **Poster Session 5 (GatherTown)**
- 2:05–2:20 **15 Minute Break**

Oral Session 6
(Topo spin / mag / QSL
/ data)

Chair: **Brian Moritz**

- 2:20–2:35 **Andrei Bernevig**, Princeton University
Magnetic stoichiometric and Moiré topological materials
(Poster: same)
- 2:35–2:50 **Elbio Dagotto**, University of Tennessee and Oak Ridge National Laboratory
Interaction-induced Majorana edge states
(Poster: Unveiling new states of matter by computer simulation)
- 2:50–3:05 **Aditi Mitra**, New York University
Long lived π edge-modes of clean, interacting spin-chains
(Poster: Strong modes and almost strong modes of Floquet spin chains)
- 3:05–3:20 **Yuli Lyanda-Geller**, Purdue University
Transport in helical Luttinger liquids in the fractional quantum Hall regime
(Poster: same)
- 3:20–3:35 **Dong-ning Sheng**, California State University Northridge
Electrical detection of spin physics in double Moiré layers: Spin liquids and supersolids
(Poster: Fractional topological states in disorder quantum Hall and graphene based superlattice systems—Chiral spin liquid/supersolids)

3:35–3:50	Subir Sachdev , Harvard University <i>Probing topological spin liquids in Rydberg atom arrays</i> (Poster: <i>Probing topological spin liquids on a programmable quantum simulator</i>)
3:50–4:10	20 Minute Break
4:10–4:20	Poster Session 6 – Introductions
4:20–5:35	Poster Session 6 (GatherTown)
5:35–5:40	5 Minute Break
Closing Session	
5:40–5:59	Matthias Graf , Department of Energy <i>Concluding Remarks</i>
6:00	Meeting Adjourns

Theoretical Condensed Matter Physics Principal Investigators' Meeting

POSTER SESSION 1 Tuesday, October 26, 2021 12:50–2:15PM

1. *Odd Parity Superconductivity in CeRh₂As₂*
Daniel Agterberg, University of Wisconsin, Milwaukee
2. *Electronic nematicity in twisted Moiré systems*
Rafael Fernandes, University of Minnesota
3. *Propagation, localization, and interaction of collective excitations in Josephson junction arrays*
Leonid Glazman, Yale University
4. *Optical control of spin-polarization in quantum materials*
Marco Govoni, Argonne National Laboratory
5. *Mapping the genome of coherent quantum defects for Quantum Information Science*
Geoffroy Hautier, Dartmouth College
6. *Theory of STM on Sr₂RuO₄*
Peter Hirschfeld, University of Florida
7. *Van der Waals reprogrammable quantum simulator*
Benjamin Hunt, Carnegie Mellon University
8. *Simulating long-time evolution of driven many-body systems with next generation quantum computers*
Alexander Kemper, North Carolina State University
9. *Non-unitary dynamics via spacetime duality*
Vedika Khemani, Stanford University
10. *Quantum probes of the materials origins of decoherence*
Shimon Kolkowitz, University of Wisconsin, Madison
11. *Ultra-coherent, mobile, electron-spin qubits*
Stephen Lyon, Princeton University
12. *Scar states in a system of interacting chiral fermions*
Michael Norman, Argonne National Laboratory
13. *Advanced theoretical and computational approaches for quantum materials*
Fernando Reboredo, Oak Ridge National Laboratory
14. *Holographic quantum simulation of strongly correlated electron systems*
Shyam Shankar, University of Texas, Austin
15. *Quantum computing enhanced Gutzwiller variational embedding approach for Correlated Materials*
Yongxin Yao, Ames Laboratory

POSTER SESSION 2
Tuesday, October 26, 2021
4:35–6:00PM

1. *Quantum phenomena in few-layer group IV monochalcogenides: interplay among structural, thermal, optical, spin, and valley properties in 2D*
Salvador Barraza-Lopez, University of Arkansas
2. *Transdimensional quantum heterostructure: Electromagnetic response peculiarities and collective many-particle effects*
Igor Bondarev, North Carolina Central University
3. *QMC-HAMM P1: Quantum Monte Carlo database for machine learning accurate interatomic potentials of dense hydrogen*
David Ceperley, University of Illinois, Urbana-Champaign
4. *Quantum states of a skyrmion in a two-dimensional antiferromagnet*
Eugene Chudnovsky, The City University of New York
5. *Electron correlation effects on magnetic interactions and spin excitations in 2D van der Waals materials*
Liqin Ke, Ames Laboratory
6. *Magnon Landau levels and spin resonances in antiferromagnets*
Alexey Kovalev, University of Nebraska, Lincoln
7. *Topological transitions in monolayer Sb*
Walter Lambrecht, Case Western Reserve University
8. *Phase interference of twisted quasiparticles*
Lucas Lindsay, Oak Ridge National Laboratory
9. *Pseudospin paramagnon theory of MATBG superconductivity*
Allan MacDonald, University of Texas, Austin
10. *Real space quantum cluster formulation for the typical medium t Theory (TMT) of Anderson localization*
Juana Moreno, Louisiana State University
11. *Topological superconductivity in skyrmion lattices*
Dirk Morr, University of Illinois, Chicago
12. *The Materials Project*
Kristin Persson, Lawrence Berkeley National Laboratory
13. *Tunable band gaps and optical absorption properties of bent MoS₂ nanoribbons*
Adrienn Ruzsinszky, Temple University
14. *Single layer cuprates experimental resistivity versus theory*
Sriram Shastry, University of California, Santa Cruz
15. *Materials with nontrivial topology and fluctuation induced interactions*
Lilia Woods, University of South Florida

POSTER SESSION 3
Wednesday, October 27, 2021
12:40–2:05PM

1. *Coupled electron-phonon transport from first principles*
David Broido, Boston College
2. *Phase-field models of coupled structural and electronic processes*
Long-Qing Chen, The Pennsylvania State University
3. *Phonon-limited mobility and electron-phonon coupling in lead-free halide double perovskites*
Feliciano Giustino, University of Texas, Austin
4. *Thermal control of a chain of nanocavities*
Andrew Jordan, University of Rochester
5. *Machine learning for simulation of strongly correlated systems*
Eun-Ah Kim, Cornell University
6. *A new approach to the interacting phonon problem*
Chris Marianetti, Columbia University
7. *Achieving reliable cohesive energies, band gaps and band edges using real-space quantum Monte Carlo*
Lubos Mitas, North Carolina State University
8. *Exciton-phonon interactions in monolayer germanium selenide from first principles*
Sahar Sharifzadeh, Boston University
9. *Artifactual character of hydrogen liquid-liquid phase transition from a machine learning potential*
Samuel Trickey, University of Florida
10. *Understanding and manipulating phases of matter in correlated and topological systems*
Alexei Tsvelik, Brookhaven National Laboratory
11. *SciDAC: Real-time dynamics of driven correlated electrons in quantum materials*
Vojtech Vitek, University of California, Santa Barbara
12. *Information-based approaches to thermodynamic entropy*
Michael Widom, Carnegie Mellon University
13. *DECODE: Data-driven exascale control of optically driven excitations in chemical and material systems*
Bryan Wong, University of California, Riverside
14. *Physical principle enhanced machine learning frameworks for solid-state materials and molecules*
Qimin Yan, Temple University
15. *Data-driven discovery of inorganic electrides for energy applications*
Qiang, Zhu, University of Nevada, Las Vegas

POSTER SESSION 4
Wednesday, October 27, 2021
4:30–6:00PM

1. *Anomalous phase separation dynamics in strongly correlated electron systems — machine-learning enabled large-scale simulations*
Gai-Wei Chern, University of Virginia
2. *Twisted bilayer graphene—an itinerant perspective*
Andrey Chubukov, University of Minnesota
3. *MemComputing the spectrum of correlated quantum systems*
Massimiliano Di Ventra, University of California, San Diego
4. *Beyond perturbation theory: a time dependent numerical approach to non-equilibrium spectroscopies*
Adrian Feiguin, Northeastern University
5. *Theory for pump/probe experiments in charge-density-wave materials*
James Freericks, Georgetown University
6. *Midwest Integrated Center for Computational Materials (MICCoM) s*
Giulia Galli, Argonne National Laboratory
7. *Advances in quantum Monte Carlo for the predictive simulation of functional materials*
Paul Kent, Oak Ridge National Laboratory
8. *Center for Computational Study of Excited-State Phenomena in Energy Materials*
Steven Louie, Lawrence Berkeley National Laboratory
9. *Theory of Materials Program*
Jeff Neaton, Lawrence Berkeley National Laboratory
10. *INQ: a state-of-the-art implementation of density functional theory for GPU-based supercomputers*
Tadashi Ogitsu, Lawrence Livermore National Laboratory
11. *First principles approach to exciton transport in energy materials*
Diana Qiu, Yale University
12. *Theoretical and computational studies of excitations in functional nanomaterials*
Talat Rahman, University of Central Florida
13. *Ab initio prediction of novel optoelectronic properties for topological materials*
Andrew Rappe, University of Pennsylvania
14. *New developments in the theory of excited states and X-ray spectra*
John Rehr, University of Washington
15. *Accurate and fast self-consistent ab initio calculations for correlated-electron materials*
Cai-Zhuang Wang, Ames Laboratory

POSTER SESSION 5
Thursday, October 28, 2021
12:40–2:05PM

1. *SciDAC: Traversing the “death valley” separating short and long times in non-equilibrium quantum dynamical simulations of real materials*
Garnet Chan, Caltech
2. *Machine-assisted quantum magnetism*
Sugata Chowdhury, Howard University
3. *Designing disorder in functional materials*
Valentino Cooper, Oak Ridge National Laboratory
4. *Theory of monovalent nickelates*
Thomas Devereaux, SLAC
5. *Metastable superconducting materials*
Richard Hennig, University of Florida
6. *Artificial intelligence and data science enabled predictive modeling of collective phenomena in strongly correlated quantum materials*
Steven Johnston, University of Tennessee
7. *COMSCOPE: Center for Computational Material Spectroscopy and Design*
Gabi Kotliar, Brookhaven National Laboratory
8. *Superconducting-like response in systems near the Mott transition under external drive*
Patrick Lee, Massachusetts Institute of Technology
9. *Controlling reversible phase transitions in rare-earth nickelates for novel memory devices*
Badri Narayanan, University of Louisville
10. *Quantum critical points and the sign problem*
Richard Scalettar, University of California, Davis
11. *Matrix spin-singlet pairing and d+d superconductivity*
Qimiao Si, Rice University
12. *Robust dx²-y² wave pairing in infinite layer nickelates*
Raghu Srinivas, SLAC
13. *Indirect exchange interaction in floquet driven systems*
Wang-Kong Tse, University of Alabama
14. *Fundamental properties of electronic materials: Bulk quadrupole, polarization and surface workfunction*
Shengbai Zhang, Rensselaer Polytechnic Institute
15. *The peculiarities of para phases of oxide perovskites explained as consequences of symmetry breaking*
Alex Zunger, University of Colorado, Boulder

POSTER SESSION 6
Thursday, October 28, 2021
4:10–5:35PM

1. *Magnetic stoichiometric and Moire topological materials*
Andrei Bernevig, Princeton University
2. *Systematic electronic structure in the cuprate parent state from quantum many-body simulations*
Garnet Chan, Caltech
3. *Unveiling new states of matter by computer simulation*
Elbio Dagotto, Oak Ridge National Laboratory
4. *Subdimensional criticality: continuous quantum phase transitions out of fracton phases*
Michael Hermele, University of Colorado, Boulder
5. *Nontrivial consequences of non-centrosymmetry in topological and trivial metals: preliminary results*
Pavan Hosur, University of Houston
6. *Exactly solvable model for strongly interacting electrons in a magnetic field*
Jainendra Jain, Pennsylvania State University
7. *Transport in helical Luttinger liquids in the fractional quantum Hall regime*
Yuli Lyanda-Geller, Purdue University
8. *Strong modes and almost strong modes of Floquet spin chains*
Aditi Mitra, New York University
9. *Partial equilibration of anti-Pfaffian edge modes at $\nu = 5/2$*
Michael Mulligan, University of California, Riverside
10. *Spectroscopic fingerprints of spin liquids, conventional and fractonic*
Rahul Nandkishore, University of Colorado, Boulder
11. *Footprints of the Kitaev spin liquid in the Fano lineshapes of the Raman active optical phonons*
Natalia Perkins, University of Minnesota
12. *Probing topological spin liquids on a programmable quantum simulator*
Subir Sachdev, Harvard University
13. *Fractional topological states in disorder quantum Hall and graphene based superlattice systems—Chiral spin liquid/supersolids*
Dong-ning Sheng, Cal State University Northridge
14. *Frontiers in magnetic materials*
David Singh, University of Missouri
15. *Energy storage in magnetic textures driven by vorticity flow*
Yaroslav Tserkovnyak, University of California, Los Angeles
16. *Spin waves in doped graphene*
Carsten Ullrich, University of Missouri

17. *Ab initio theory of unconventional superconductivity*
Mark van Schilfgaarde, National Renewable Energy Laboratory
18. *Superdiffusive spin transport in isotropic spin chains*
Romain Vasseur, University of Massachusetts, Amherst
19. *First principles investigations for magnetic properties of innovative materials*
Ruqian Wu, University of California, Irvine
20. *Topological spin textures in chiral magnets: from 2D to 3D*
Jiadong Zang, University of New Hampshire

Superconductivity in quantum materials

Daniel Agterberg, University of Wisconsin-Milwaukee

Program Scope

This project addresses unconventional superconductivity of quantum materials. It does so by solving effective theories of correlated fermions guided by experimental results and by collaboration with density functional theory experts. A key emphasis is to move beyond the commonly used single-band picture to include the spin, orbital, valley, sublattice, and non-symmorphic degenerate electronic degrees of freedom needed to properly describe quantum materials. This project focuses on the role of these electronic degrees of freedom on the physics of unconventional superconducting states. Current research emphasizes three topics: i) the role of non-symmorphic symmetries and Dirac-line fermions in stabilizing odd-parity superconductivity in CeRh_2As_2 ; ii) the physics of topologically protected Bogoliubov Fermi surfaces, a newly found nodal superconducting state; and iii) the topological properties and the interplay of superconductivity and magnetism in the odd-parity superconductor UTe_2 .

Keywords: Correlated superconductors, Bogoliubov Fermi surfaces, Weyl superconductivity

Recent Progress

Field induced odd-parity superconductivity in CeRh_2As_2 : As discussed in detail in Ref. [1], we have carried out a collaborative effort between experiment and theory to show that a magnetic field along the c-axis drives an even to odd-parity (possibly topological) superconducting transition in tetragonal

CeRh_2As_2 . Underlying this transition is an electronic spin-orbit coupling enabled by the lack of inversion symmetry at the two Ce atomic sites in the unit cell. Inversion symmetry then implies on-site singlet Cooper pairs give rise to global even-parity and odd-parity superconducting states. A “c-axis hopping”

between the two Ce sites ensures that the even-parity superconducting state has the higher

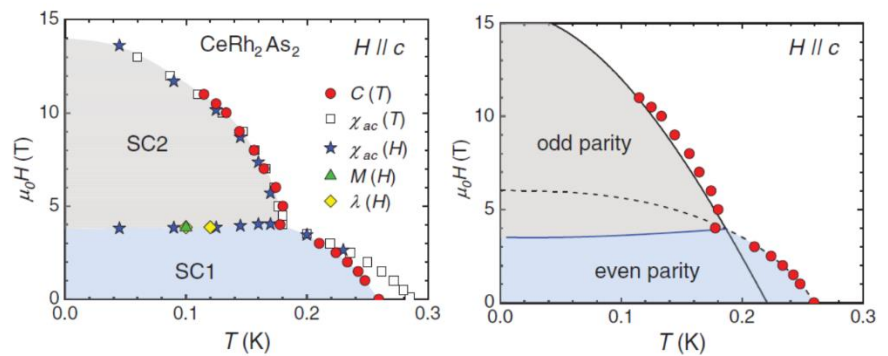


Fig.1 Superconducting magnetic-field (H) temperature (T) phase diagram of tetragonal CeRh_2As_2 for field along the c-axis. Left is the experimental phase diagram revealing a field induced transition. Right is the theory phase diagram based on a field-driven even to odd parity transition.

transition temperature (T_c). The electronic spin-orbit coupling ensures that the odd-parity state is robust against a c-axis while the even-parity state is not, allowing a field induced to transition to occur [1,2].

Key to the existence of the above observed transition is that the spin-orbit energy scale is larger than the c-axis hopping – a property that is unexpected in a 3D material such as CeRh_2As_2 . In Ref. [3], we show that this is a natural consequence of the non-symmorphic $P4/nmm$ space group of CeRh_2As_2 . In particular, we have carried out renormalized band structure calculations that yields the

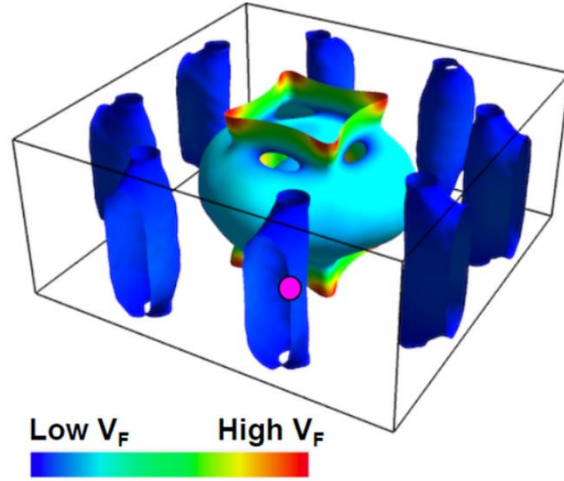


Fig.2 Fermi surface of CeRh_2As_2 calculated using a renormalized band structure approach. The Fermi surfaces at the zone edges contain 80% the density of states.

Fermi surface shown in Fig. 2. This Fermi surface reveals that the largest contribution from the density of states collaborators comes from electron pockets on the Brillouin zone faces. Importantly, the non-symmorphic structure makes it possible to prove that on the zone faces, the spin-orbit coupling dominates over the c-axis hopping.

Interplay of magnetism and superconductivity in UTe_2 : In Ref. [4], we have carried out an experiment and theory collaboration to understand the development of broken time-reversal symmetry in the superconducting state of UTe_2 . This work follows up on an earlier collaboration on the superconducting state, Ref. [5], in which the observation of a zero applied field polar Kerr effect and the observation of two specific heat anomalies were used to deduce that superconducting Weyl nodes are likely in UTe_2 . In Ref. [4], the evolution of the polar Kerr signal in an applied magnetic field has been measured. The results reveal that there are two contributions to the polar Kerr signal: a field independent contribution associated with the broken time-reversal superconducting state; and a field dependent contribution that is interpreted as originating from the development of ferromagnetism in vortex cores. This sheds new insight into interplay of odd-parity superconductivity and magnetism in this important superconductor.

Using disorder to identify Bogoliubov Fermi surfaces: In Ref. [6] it was previously shown that even parity superconductors that break time-reversal symmetry must either be nodeless or exhibit topologically protected Bogoliubov Fermi surfaces in the low energy limit. A key question is how to observe Bogoliubov Fermi surfaces in the superconducting state. In Ref. [7], in collaboration with Hanbit Oh and Eun-Gook Moon, we have shown that response of Bogoliubov Fermi surfaces to impurity scattering is qualitatively different that line nodal, point nodal, or fully gapped superconducting states. As shown in Fig. 3, the density of states of a Bogoliubov Fermi surfaces generically increases linearly with respect to the impurity scattering rate, a feature

that is not true for other nodal superconductors. These calculations were carried using a Born approximation for the impurity scattering and a total angular momentum $j=3/2$ basis for the band representations at the Brillouin zone center.

Future Plans

Odd parity superconductivity in $CeRh_2As_2$: The theory and experiment collaboration begun in Ref. [1] will be continued, initially by comparing theory and experiment for the superconducting phase diagram for a variety of field orientations. In addition, our theory will be extended to other superconducting materials, including those that belong to the same $P4/nmm$ space group. One promising material in this context is FeSe, for which an unexplained magnetic field induced phase transition has also been seen in the superconducting state [8].

Weyl Superconductivity in UTe_2 : The discovery of broken time-reversal symmetry and likely Weyl superconductivity in UTe_2 [5] motivates a deeper understanding of Weyl nodes in odd-parity superconductors. This is currently being carried out, a key finding is that previous studies of Weyl nodes have neglected novel symmetry allowed terms in the Hamiltonian.

Superconducting symmetries and classification of 2D superconductors: In 3D, time-reversal (T) and inversion (I) symmetries are key to a superconducting instability, since these ensure all electronic states at momenta \mathbf{k} and $-\mathbf{k}$, needed to make Cooper pairs, are degenerate. In 2D, there are additional superconducting symmetries that ensure this, for example a two-fold rotation about the axis normal to the system. Recently, in Ref. [9], the PI and collaborators have carried out a topological classification of 2D superconductors when neither T nor I are present. Analysis of the properties of the resultant superconducting states and an extension to include all 2D superconducting symmetries that require degenerate states at momenta \mathbf{k} and $-\mathbf{k}$ is being carried out. This is timely since the field of 2D superconductivity has recently been rapidly advancing.

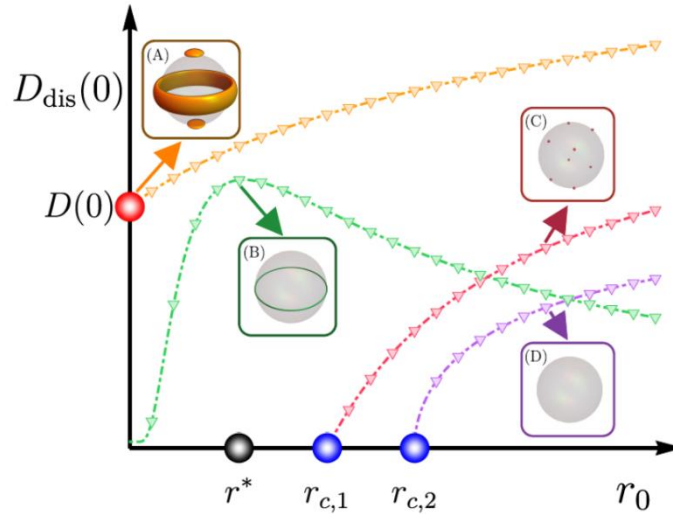


Fig.3 Density of states as a function of impurity scattering rate for different nodal superconductors. Here (A) gives the impurity response of a Bogoliubov Fermi surface, (B) the response of a line-nodal superconductor, (C) the response of a point nodal superconductor, and (D) the response of a fully gapped superconductor.

References

- 1- S. Khim, J. F. Landaeta, J. Banda, N. Bannor, M. Brando, P. M. R. Brydon, D. Hafner, R. Küchler, R. Cardoso-Gil, U. Stockert, A. P. Mackenzie, D. F. Agterberg, C. Geibel, and E. Hassinger, *Field-induced transition within the superconducting state of CeRh₂As₂*, Science **373**, 1012 (2021).
- 2- T. Yoshida, M. Sigrist, and Y. Yanase, *Pair-density wave states through spin-orbit coupling in multilayer superconductors*, Phys. Rev. B **86**, 134514 (2012).
- 3- D.C. Cavanagh, T. Shishidou, M. Weinert, P. M. R. Brydon, and D.F. Agterberg, *Non-symmorphic symmetry and field-driven odd-parity pairing in CeRh₂As₂*, arXiv:2106.02698 (2021).
- 4- D. S. Wei, D. Saykin, O. Y. Miller, S. Ran, S. R. Saha, D. F. Agterberg, J. Schmalian, N. P. Butch, J. Paglione, and A. Kapitulnik, *Interplay between magnetism and superconductivity in UTe₂*, arXiv:2108.09838 (2021).
- 5- I. M. Hayes, D. S. Wei, T. Metz, J. Zhang, Y. S. Eo, S. Ran, S. R. Saha, J. Collini, N. P. Butch, D. F. Agterberg, A. Kapitulnik, and J. Paglione, *Multicomponent superconducting order parameter in UTe₂*, Science **373**, 797 (2021).
- 6- D. F. Agterberg, P. M. R. Brydon, and C. Timm, *Bogoliubov Fermi surfaces in superconductors with broken time-reversal symmetry*, Phys. Rev. Lett. **118**, 127001 (2017).
- 7- H. Oh, D. F. Agterberg, and E. -G. Moon, *Using disorder to identify Bogoliubov Fermi-surface states*, arXiv:2105.09317 (2021).
- 8- T. Shibauchi, T. Hanaguri, and Y. Matsuda, *Exotic superconducting states in FeSe-based materials*, J. Phys. Soc. Jap. **89**, 102002 (2020).
- 9- M. H. Fischer, M. Sigrist, and D. F. Agterberg, *Superconductivity without inversion and time-reversal symmetries*, Phys. Rev. Lett. **121**, 157003 (2018).

Publications

- 1- S. Khim, J. F. Landaeta, J. Banda, N. Bannor, M. Brando, P. M. R. Brydon, D. Hafner, R. Küchler, R. Cardoso-Gil, U. Stockert, A. P. Mackenzie, D. F. Agterberg, C. Geibel, and E. Hassinger, *Field-induced transition within the superconducting state of CeRh₂As₂*, Science **373**, 1012 (2021).
- 2- D.C. Cavanagh, T. Shishidou, M. Weinert, P. M. R. Brydon, and D.F. Agterberg, *Non-symmorphic symmetry and field-driven odd-parity pairing in CeRh₂As₂*, arXiv:2106.02698 (2021).

3- H. Oh, D. F. Agterberg, and E. -G. Moon, *Using disorder to identify Bogoliubov Fermi-surface states*, arXiv:2105.09317 (2021).

4- D. S. Wei, D. Saykin, O. Y. Miller, S. Ran, S. R. Saha, D. F. Agterberg, J. Schmalian, N. P. Butch, J. Paglione, and A. Kapitulnik, *Interplay between magnetism and superconductivity in UTe_2* , arXiv:2108.09838 (2021).

Theory of Fluctuating and Critical Quantum Matter

Leon Balents, University of California, Santa Barbara

Program Scope

This is a program of theoretical research into many body quantum phenomena involving unconventional states and correlations of electrons in solids. The current research divides largely into two thrusts: frustrated quantum magnets, and moiré materials. In the former area, the aims are to identify and model magnetic materials supporting novel excitations and phases of matter, developing both fundamental theory and connections to experiments. In the latter, the research strives to describe and predict how correlated states can be manipulated by imposing moiré patterns upon known two dimensional materials.

In the thrust on quantum magnets, the research has been comprised (1) studies of quantum spin liquids, the description of different spin liquid phases, and of candidate materials in which they are being sought; and (2) formation of unusual spin complexes beyond simple magnons, including bound states and spontaneously formed dimers.

The research in the thrust on moiré materials includes (1) the theoretical derivation of continuum models for electronic and magnetic two dimensional incommensurate stacked materials, (2) prediction of non-collinear magnetic phases in moiré magnets, and (3) study of the quantum anomalous Hall effect in twisted bilayer graphene.

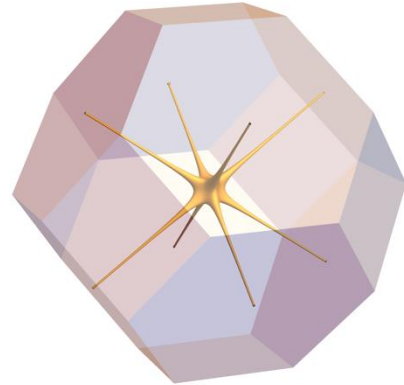
Keywords:

Quantum spin liquids, moiré materials,

Recent Progress

Spin liquids: In **paper 7** of the Publications list below, we collaborated with the Wilson group in the UCSB materials department to study a promising spin liquid candidate material, NaYbO₂. This consists of layers of triangular lattices of Yb ions, importantly arranged in a staggered fashion, which adds additional frustration in the third dimension. In this paper, we made detailed comparisons of theoretical structure factors to inelastic neutron scattering spectra, at a sequence of different applied magnetic fields, which tune the system from the spin liquid state at low field, through an ordered three-sublattice state at intermediate fields, to a third phase at the highest measured fields. Our theoretical calculations explain the observed spectra, and suggest that the high field state is a canted “V” state, with non-collinear spin order.

Paper 9 is an exhaustive theoretical study of different quantum spin liquids states which may occur in three-dimensional pyrochlore lattice antiferromagnets. This complements prior studies pyrochlore spin liquids based on the strong anisotropy quantum spin-ice limit. It also greatly extends early pioneering work which assumed $SU(2)$ spin rotation symmetry (this is a very bad assumption for nearly all pyrochlore magnets). We obtained a full list of different spin liquid states based on a fermionic parton construction, under a variety of assumed symmetries present and broken. From the theory, wavefunctions suitable for variational Monte Carlo can be directly constructed. Interestingly, we find that several $U(1)$ spin liquid classes possess an unusual gapless multi-nodal-line structure (“nodal star”) in the spinon bands, which is protected by the projective actions of the threefold rotation and screw symmetries of the pyrochlore space group; we studied the gauge theory which describes the low energy physics of this state.



Nodal star – a low energy surface of spinons in momentum space in certain spin liquids.

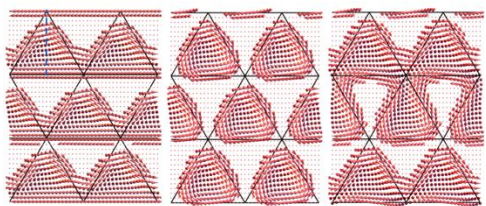
Spin complexes: It is well-known theoretically since the 1980s that generalizing the $SU(2)$ symmetry group of spins to $SU(N)$ with $N > 2$ can favor non-magnetic “quantum disordered” ground states. These are becoming accessible in ultra-cold atoms and in certain moiré lattice Mott insulators. For intermediate N , however, the precise nature of such ground states remains unclear. In **paper 2**, we studied the formation of dimerized or valence bond solid states in an $SU(4)$ antiferromagnet on the triangular lattice. Here the spins are bound into dimer units as emergent degrees of freedom. We developed a new type of quantum dimer model expansion, and compared it to density matrix renormalization group and exact diagonalization studies, finding evidence for a 12-site valence bond solid ground state, which can be driven through a quantum phase transition to a magnetically ordered state by a particular $SU(4)$ symmetry breaking perturbation.

Paper 3 studied the formation of magnon bound states in a one-dimensional chain system with large spin $S=2$. This is another collaboration with the Wilson group, who experimentally synthesized the material NaMnO_2 , and studied it via neutron scattering. They observed several unexpected non-spin-wave modes spectroscopically, prompting us to calculate the dynamical structure factor using matrix product operator methods. Our theory showed that, surprisingly, such a “large” spin system, which might be expected to be semiclassical, actually has a series of quantum bound states of magnons, of which at least 2 and 3 magnon states were directly observed.

Continuum models for moiré materials: Much of the theoretical work on twisted graphene structures is based on the continuum model first derived by Bistritzer and Macdonald[1]. In **paper 1**, we presented an alternative derivation of their continuum model, which is much simpler

and more direct than the original one, and which is more general. It is based on concepts of effective field theory, and among other things directly describes not only twisting but strain and inhomogeneity. Insight gained from this work led our group to develop continuum models for intrinsically magnetic van der Waals materials with incommensurate layered structures (**papers 5,10**).

Moiré magnets: Chemists and experimental physicists have recently extended the catalog of exfoliatable two dimensional van der Waals materials to include a growing number of intrinsically magnetic substances, both ferromagnets and antiferromagnets, with different spin sizes, types of magnetic anisotropies, etc. By stacking these together, one may produce a variety of moiré patterns, which can modify strongly the magnetism. In **paper 5**, we introduced a continuum formalism which greatly simplifies the study of such structures. Using it, we found that twisted bilayer of antiferromagnets, as well as certain ferromagnets, are profoundly effected by their moiré structure. In particular, we predict that twisting generates inter-layer frustration which, for small twist angles, results in conversion of formerly collinear antiferromagnets and ferromagnets to non-collinear twisted spin patterns with controllable size. Varying twist angle and/or applied magnetic fields can induce phase transitions between different ordered states. Our predictions were recently confirmed by experiments on CrI₃[2].



Three non-collinear states of inversion breaking moiré ferromagnets. The middle image is a skyrmion lattice.

In **paper 10**, we extended this treatment to inversion-breaking moiré ferromagnets, which are known in bulk and thin films to display skyrmion lattices. In the moiré framework, the skyrmion structure is further enriched, as there is a delicate interplay between the skyrmion scale (set by Dzyaloshinskii-Moriya interactions) and the moiré length (set by incommensurability, twist, etc.). We showed that this gives rise to a complex phase diagram of skyrmion and other textured states, which may be of interest to spintronics.

Quantum anomalous Hall effect: **Paper 6** reports the striking experimental discovery of spontaneous ferromagnetism of twisted bilayer graphene in zero magnetic field and concurrent quantized anomalous Hall effect. Our theoretical input to this paper was the interpretation as valley polarization combined with a known phenomena of valley Chern number formation in moiré graphene, and most importantly in addition to explain the observation of current-induced reorientation of magnetization and consequently sign change of the Hall conductivity. We described how this occurs at low temperature via the current-induced repopulation of low energy electronic states at the sample and domain wall edges. These repopulations modify the energy difference of the two ferromagnetic domains and thereby allow one to be favored over another.

Future Plans

Future work will address both spin liquid and moiré aspects of the project.

In the spin liquid thrust, we intend to apply the classification results for the pyrochlore variationally to realistic model Hamiltonians for rare earth materials. We would also like to deepen the connections between our fermionic parton wavefunctions and the bosonic ones discussed earlier for quantum spin ice, and intend to work to see how the two can be related. Finally, we plan to seek new spin liquid candidate materials with triangular lattices in the same structural family as NaYbO_2 , but involving transition metal ions rather than rare earths. This has the advantage that the exchange energy is much larger in transition metal magnets and hence spin liquid behavior, if found, should persist to much higher temperature. The challenge is that many materials in this family may be much less strongly insulating, requiring consideration of proximity to a metal-insulator transition.

In the moiré materials thrust, we plan to seek more strongly fluctuating magnetic states in this setting. The strict low dimensionality of 2d materials makes it ideal to observe both quantum and thermal fluctuations. We will consider how such phenomena can be modeled and measured, and moreover extend the continuum models for moiré magnets to include non-ordered states such as quantum spin liquids, and in materials such as transition metal dichalcogenides.

References

1. Bistrizter, Rafi, and Allan H. MacDonald. *Moiré bands in twisted double-layer graphene*. Proceedings of the National Academy of Sciences **108**, 12233-12237 (2011).
2. Y. Xu et al, *Emergence of a noncollinear magnetic state in twisted bilayer CrI_3* , arXiv: 2103.09850 (2021).

Publications

1. L. Balents. *General continuum model for twisted bilayer graphene and arbitrary smooth deformations*. SciPost Phys., **7**:48, 2019.
2. A. Keselman, L. Savary, and L. Balents. *Dimer description of the $SU(4)$ antiferromagnet on the triangular lattice*. SciPost Phys., **8**:76, 2020.
3. R. L. Dally, A. J. R. Heng, A. Keselman, M. M. Bordelon, M. B. Stone, L. Balents, and S. D. Wilson. *Three-magnon bound state in the quasi-one-dimensional antiferromagnet $\alpha\text{-NaMnO}_2$* . Phys. Rev. Lett., **124**:197203, 2020.
4. L. Balents, C. R. Dean, D. K. Efetov, and A. F. Young. *Superconductivity and strong correlations in moiré flat bands*. Nature Physics, **16**:725–733, 2020.
5. K. Hejazi, Z.-X. Luo, and L. Balents. *Noncollinear phases in moiré magnets*. Proceedings of the National Academy of Sciences, **117**(20):10721–10726, 2020.

6. M. Serlin, C. L. Tschirhart, H. Polshyn, Y. Zhang, J. Zhu, K. Watanabe, T. Taniguchi, L. Balents, and A. F. Young. *Intrinsic quantized anomalous hall effect in a moiré heterostructure*. *Science*, **367**(6480):900–903, 2020.
7. M. M. Bordelon, C. Liu, L. Posthuma, P. M. Sarte, N. P. Butch, D. M. Pajerowski, A. Banerjee, L. Balents, and S. D. Wilson. *Spin excitations in the frustrated triangular lattice antiferromagnet NaYbO_2* . *Phys. Rev. B*, **101**:224427, 2020.
8. M. M. Bordelon, C. Liu, L. Posthuma, E. Kenney, M. J. Graf, N. P. Butch, A. Banerjee, S. Calder, L. Balents, and S. D. Wilson. *Frustrated heisenberg $J_1 - J_2$ model within the stretched diamond lattice of LiYbO_2* . *Phys. Rev. B*, **103**:014420, 2021.
9. C. Liu, G. B. Halász, and L. Balents. *Symmetric $U(1)$ and Z_2 spin liquids on the pyrochlore lattice*. *Phys. Rev. B*, **104**:054401, 2021.
10. K. Hejazi, Z.-X. Luo, and L. Balents. *Heterobilayer moiré magnets: Moiré skyrmions and commensurate-incommensurate transitions*. *Phys. Rev. B*, **104**:L100406, 2021.

Quantum phenomena in few-layer group IV monochalcogenides: interplay among structural, thermal, optical, spin, and valley properties in 2D

Salvador Barraza-Lopez, Department of Physics, University of Arkansas

Program Scope

The PI investigates the physical properties of a new and experimentally-available [1,2] family of two-dimensional ferroelectrics. Research includes a comparison among models developed to describe the ferroelectric-to-paraelectric phase transition [3], a verification of the electronic structure within a theory-experiment collaboration [4], a study of thermoelectricity on materials undergoing phase transformations [5], the creation of static vortices on paraelectric-ferroelectric in-plane heterojunctions [6-8], and a study of the elastic properties of 2D ferroelectrics at finite temperature [9-10].

Keywords: Two-dimensional ferroelectrics, thermally-driven structural transformations, thermoelectricity, elasticity.

Recent Progress

Figure 1(a) shows the atomistic structure of a bulk, orthorhombic group-IV monochalcogenide. These materials have an inversion center, and hence lack an intrinsic electric dipole moment.

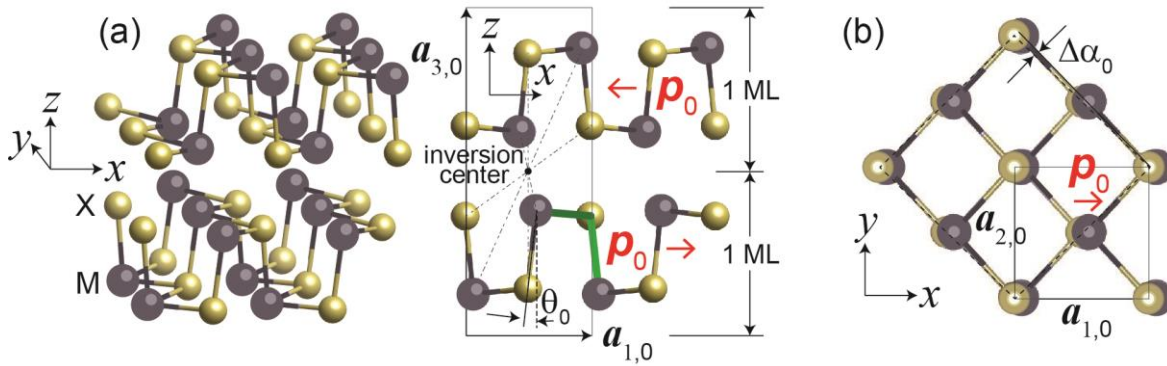


Figure 1. (a) Structure of bulk orthorhombic group-IV monochalcogenides, indicating geometrical variables θ_0 , tilt \mathbf{p}_0 , and lattice constants. The group-IV atom is labeled M, and the group-IV atom X. (b) A group-IV monochalcogenide monolayer, highlighting \mathbf{p}_0 , and $\Delta\alpha_0$.

Nevertheless, single layers of these materials [1,2] do possess a net in-plane intrinsic dipole, which is related to geometrical variables θ and $\Delta\alpha$, shown in Figure 1(a) and 1(b). The 0-subindex in the figure refers to values at zero temperature. As it turns out, there were two models set to describe the structural transition in these materials. In our approach, lattice parameters evolve through the transition, but there was another model in which a transition was discussed whereby θ changed without a modification of lattice constants.

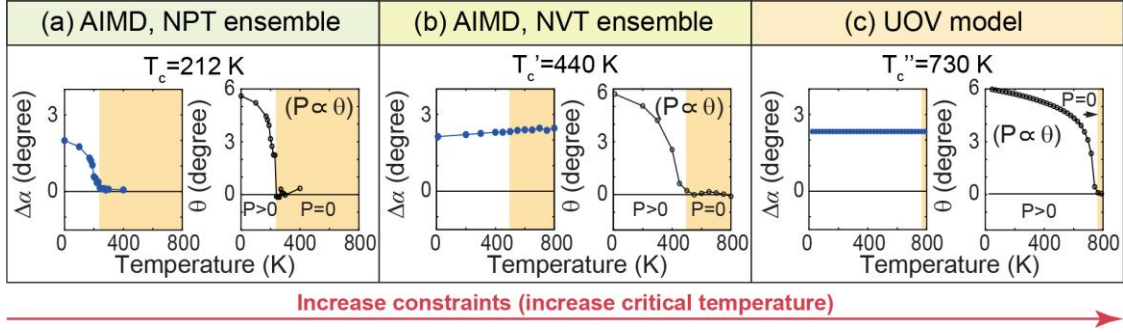


Figure 2. Thermal evolution of geometrical parameters $\Delta\alpha$ and θ within (a) *ab initio* molecular dynamics (AIMD) using the NPT ensemble, (b) AIMD within the NVT ensemble, and (c) competitors' model [2,3].

A comparison of the predictions from the two models is shown in Figure 2 [3]. Experimentally, $\Delta\alpha$ becomes zero at the critical temperature; this result can only be reproduced by our theory, in which lattice constants are allowed to evolve (Figure 2(a)). The more constrained the model is (for example, by fixing lattice constants to zero-temperature magnitudes Figure 2(b), or by fixing all the structure and allowing just a single optical phonon mode to vibrate, as in the competing theory), the larger the critical temperature at which θ becomes zero.

A second contribution concerns determining the electronic dispersion of a SnTe monolayer, by means of standing waves on parallel ferroelectric domains [4]. Figure 3(a) depicts 90-degree in-plane ferroelectric domains on the SnTe monolayer. Scanning tunneling spectroscopy images (Fig. 3(b)) for the valence valley display a standing wave pattern, that the PI determined to be due to the lack of transmission in between valleys, because there is only a two-fold symmetry in a rectangular lattice, and hence only two available valleys, that turn mismatched upon a 90 degree rotation across valleys (Fig. 3(c)). Figure 3(d) shows standing waves on a larger domain, and the dashed curve in Fig. 3(e) is the distance among the edges of a valley, when the energy is measured away from the valence band edge: The distance among the two ends of the valley is the momentum transferred q , which explains the standing wave phenomena in subplots (b) and (d). The colored pattern in Fig. 3(e) is the Fourier transform of the standing wave pattern in Fig. 3(c).

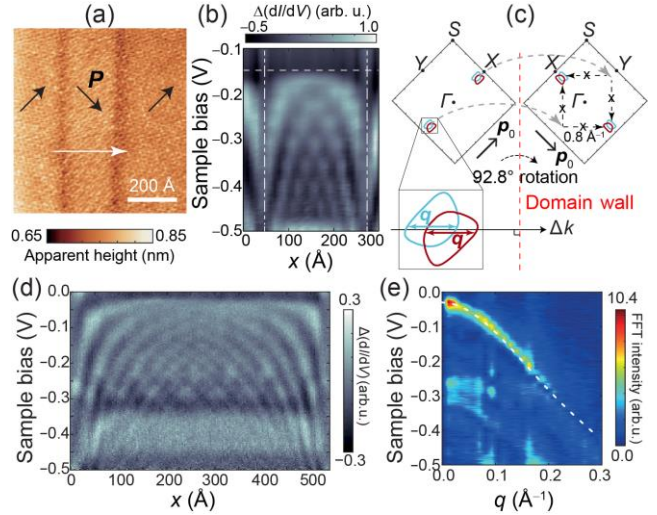


Figure 3. (a) Parallel 90-degree domains on a SnTe monolayer. (b) Standing wave pattern on the valence band valley. (c) Mismatched valleys lead to the creation of standing waves. (d) A second standing wave pattern, and (e) its Fourier transform. The dashed curve is theory prediction.

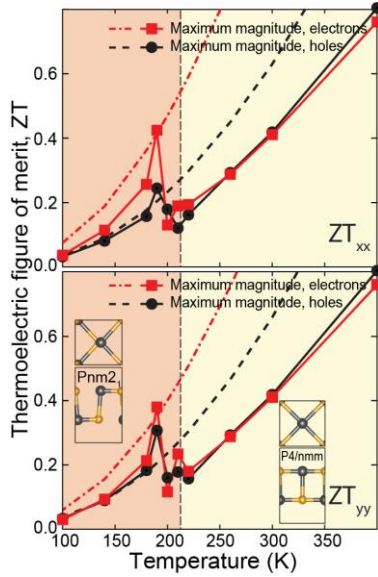


Figure 4. ZT for SnSe monolayer.

Another recent contribution [5] is the creation of a model for thermoelectricity that takes structural transformations of group-IV monochalcogenide monolayers into account. Its basic ingredient is finite-temperature data. For example, the electronic structure is always computed with relation to the finite-temperature average unit cell, and the vibrational properties are derived from vibrational spectra directly obtained from the copious *ab initio* molecular dynamics data that gave rise to Fig. 1. A highlight is exemplified on a SnSe monolayer in Fig. 4. Previous results (shown in dashed lines) exaggerate the thermoelectric figure of merit (ZT). A model that accounts for the structural transition shows a spike slightly below T_c , and subsequent smaller values of ZT, due to the softening of vibrational modes at the transition.

Figure 5 contains a second highlight of the experiment-theory collaboration among the PI and experimental groups in China

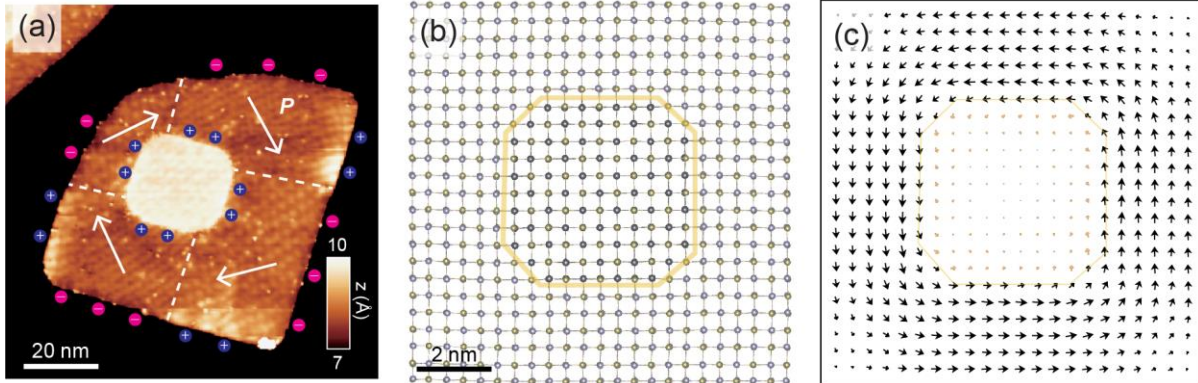


Figure 5. (a) Experimental creation and characterization of a PbTe/SnTe monolayer lateral heterojunction, with the (paraelectric) PbTe monolayer at the center, and the ferroelectric SnTe monolayer around. A static vortex is created as a result. (b) Simulated ground state structure of a similar heterojunction and (c) intrinsic moment.

and Germany [6] leading to structurally stable vortex-like structures in PbTe/SnTe monolayer lateral heterojunctions. Figure 5(a) is experimental, and Figures 5(b) and 5(c) depict simulated lowest-energy heterojunctions. Additional experiment/theory collaborative results can be found in References [7] and [8].

More recent and ongoing work concerns an analysis of mechanical properties of group-IV monochalcogenide monolayers at finite temperature: the usual approach is to perform DFT calculations at zero temperature, fit to a quadratic (harmonic) energy profile, and be done. Here, we are making use of the elastic energy landscape to ascertain the elastic properties at finite

temperature. The methodology has been developed in References [9] and [10], and preliminary results can be seen in Figure 6.

Future Plans

Recent funding through Award DE-SC0022120 became available in July, 2021, and the PI is starting to study non-linear optical properties of these materials.

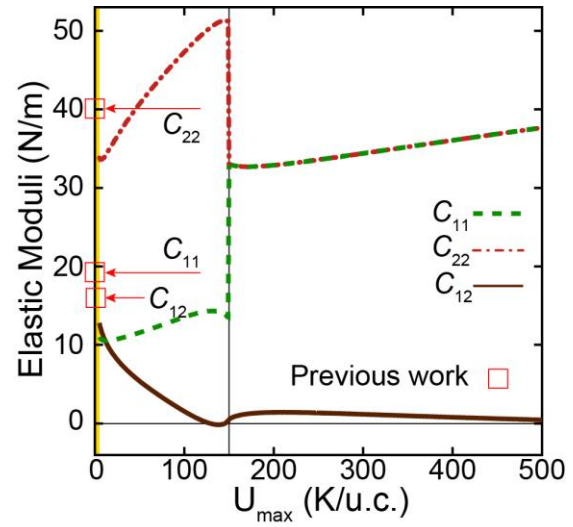


Figure 6. Elastic behavior of 2D ferroelectrics at finite temperature (in progress).

References and publications resulting from supported work

1. Microscopic manipulation of ferroelectric domains in SnSe monolayers at room temperature. K Chang, F Küster, BJ Miller, JR Ji, JL Zhang, P Sessi, S Barraza-Lopez, SSP Parkin. *Nano Lett.* **20**, 6590 (2020)
2. Colloquium: Physical properties of group-IV monochalcogenide monolayers. S Barraza-Lopez, BM Fregoso, JW Villanova, SSP Parkin, K Chang. *Rev. Mod. Phys.* **93**, 011001 (2021)
3. Theory of finite-temperature two-dimensional structural transformations in group-IV monochalcogenide monolayers. JW Villanova, P Kumar, S Barraza-Lopez. *Phys. Rev. B* **101**, 184101 (2020)
4. Standing waves induced by valley-mismatched domains in ferroelectric SnTe monolayers. K Chang, BJ Miller, H Yang, H Lin, SSP Parkin, S Barraza-Lopez, QK Xue, X Chen, S-H Ji. *Phys. Rev. Lett.* **122**, 206402 (2019)
5. Anomalous thermoelectricity at the two-dimensional structural transition of SnSe monolayers. JW Villanova, S Barraza-Lopez. *Phys. Rev. B* **103**, 035421 (2021)
6. Vortex-oriented ferroelectric domains in SnTe/PbTe monolayer lateral heterostructures. K Chang, JW Villanova, JR Ji, S Das, F Küster, S Barraza-Lopez, P Sessi, SSP Parkin. *Adv. Mater.* **33**, 2102267 (2021)
7. From an atomic layer to the bulk: low-temperature atomistic structure, ferroelectric and electronic properties of SnTe films. T Kaloni, K Chang, BJ Miller, QK Xue, X Chen, SH Ji, SSP Parkin, S Barraza-Lopez. *Phys. Rev. B* **99**, 134108 (2019)
8. Enhanced spontaneous polarization in ultrathin SnTe films with layered antipolar structure. K Chang, T Kaloni, H Lin, A Bedoya-Pinto, AK Pandeya, I Kostanovskiy, K Zhao, Y Zhong, X Hu, QK Xue, X Chen, S-H Ji, S Barraza-Lopez, SSP Parkin. *Adv. Mater.* **31**, 1804428 (2019)
9. Evolution of elastic moduli through a two-dimensional structural transformation. A Pacheco-Sanjuan, TB Bishop, EE Farmer, P Kumar, S Barraza-Lopez. *Phys. Rev. B* **99**, 104108 (2019)
10. Quantum paraelastic two-dimensional materials. TB Bishop, EE Farmer, A Sharmin, A Pacheco-Sanjuan, P Darancet, S Barraza-Lopez. *Phys. Rev. Lett.* **122**, 015703 (2019)

Topological Magnetic Quantum Chemistry and Twisted Engineered Materials

DOE Grant No. DE-SC0016239

B. Andrei Bernevig
Princeton University

Program Scope

We are developing a full theory of magnetic symmetry groups and magnetic structures, which encompasses classifications based on topological invariants, and are applying it to both stoichiometric as well as moire materials. Our program is a synergistic, wide-ranging theoretical effort to combine the most exciting areas of topological materials, quantum interactions, and material engineering. The goal is the discovery of new phases of matter, of new quantum phenomena with technological applications and the control of topological excitations in both stoichiometric crystals and in engineered artificial materials. We are focusing on the prediction, classification, and discovery of all magnetic topological phases detectable by symmetry in all 1651 magnetic space groups; material prediction, with possible use in magnetic low power devices. We are then trying to use the information in magnetic space groups to characterize new phenomena in the physics of the flat bands of different types of moiré lattices.

Keywords: magnetism, topology, moire, magnetic topological quantum chemistry

Recent Progress

We have made considerable progress on a series of fronts. First, we developed the full theory of magnetic symmetry groups and magnetic topology. Second, we developed databases showing the results. The first database of all symmetry operations/representations of magnetic groups was developed, capping about 100 years of incomplete results in the field. The first theory and data of topological invariants and topological states in magnetic groups. We further applied theory to ab-initio calculations of topological materials. We then provided the first database of magnetic topological materials (with interactions).

The discoveries of intrinsically magnetic topological materials, including semimetals with a large anomalous Hall effect and axion insulators, have directed fundamental research in solid-state materials. Our recent theory, topological quantum chemistry has enabled the understanding of and the efficient search for paramagnetic topological materials. For over 100 years, the group-theoretic characterization of crystalline solids has provided the foundational language for diverse problems in physics and chemistry. However, the group theory of crystals with commensurate magnetic order has remained incomplete for the past 70 years, due to the complicated symmetries of magnetic crystals. In our Magnetic Topological Quantum Chemistry work, we

complete the 100-year-old problem of crystalline group theory by deriving the small corepresentations, momentum stars, compatibility relations, and magnetic elementary band corepresentations of the 1,421 magnetic space groups (MSGs) (the 230 non-magnetic groups had already been solved by the Topological Quantum Chemistry). We have made our work freely accessible through tools on the Bilbao Crystallographic Server. We extended Topological Quantum Chemistry to the MSGs to form a complete, real-space theory of band topology in magnetic and nonmagnetic crystalline solids - Magnetic Topological Quantum Chemistry (MTQC). Using MTQC, we derived the complete set of symmetry-based indicators of electronic band topology, for which we identified symmetry-respecting bulk and anomalous surface and hinge states [6,7].

- Improved U.I..
- More than 38k unique materials (71k unique ICSDs).
- With and without SOC.
- Dynamical plots.
- Fragile phases.
- Wiki and more.

Topological Materials Database
 Total Materials: 38423
 Topological Insulators: 6171
 Semi-Metals: 14111

NAVIGATION
 Search
 Predict
 About
 Wiki

SETTINGS
 UI Mode

Compound Contains: Only these elements Exclude
 e.g. Bi1 Se2 Ge
 e.g. O1 N
 ICSD Number: e.g. 123456
 Search

Show Advanced Search

When using the data and information on this website in a publication, please cite the following three papers and two websites:
 • Topological Quantum Chemistry
 Nature 547, 298–305 (2017)
 • A Complete Catalogue of High-Quality Topological Materials
 Nature 566, 480–485 (2019)

<https://www.topologicalquantumchemistry.fr/magnetic/>
<https://www.topologicalquantumchemistry.com>

Figure 1: Database of topological magnetic and non-magnetic materials

Using magnetic topological indices obtained from magnetic topological quantum chemistry (MTQC), we further performed [1,5] a high-throughput search for magnetic topological materials based on first-principles calculations. We used as our starting point the Magnetic Materials Database on the Bilbao Crystallographic Server, which contains more than 549 magnetic compounds with magnetic structures deduced from neutron-scattering experiments, and identify 130 enforced semimetals (for which the band crossings are implied by symmetry eigenvalues), and topological insulators. For each compound, we performed complete electronic structure calculations, which include complete topological phase diagrams using different values of the Hubbard potential. We wrote a custom code to find the magnetic corepresentations of all bands in all magnetic space groups, we generate data to be fed into the algorithm of MTQC to determine the topology of each magnetic material. Several of these

materials display previously unknown topological phases, including symmetry-indicated magnetic semimetals, three-dimensional anomalous Hall insulators and higher-order magnetic semimetals. We analyze topological trends in the materials under varying interactions: 60 per cent of the 130 topological materials have topologies sensitive to interactions, and the others have stable topologies under varying interactions. We provided (<https://www.topologicalquantumchemistry.fr/magnetic/>, Fig[1]) a materials database for future experimental studies and open-source code for diagnosing topologies of magnetic materials.

Future Plans

Our plan is to develop more material calculations, including interactions for the magnetic topological insulators, semimetals, moire systems. We will, using magnetic topological quantum Chemistry, develop many-body twisted bilayer graphene calculations that map the problem into a heavy fermion problem. Using the heavy fermion machinery, we will then solve for the superconductivity.

Magic-angle ($\theta = 1.05^\circ$) twisted bilayer graphene (MATBG) has shown two seemingly contradictory characters: the localization and quantum-dot-like behavior in STM experiments[2,4], and delocalization in transport experiments. We will construct a model, which naturally captures the two aspects, from the well-known twisted bilayer Bistritzer-MacDonald (BM) model in a first principles spirit. A set of local flat-band orbitals (f) centered at the AA-stacking regions will be responsible to the localization. A set of extended topological conduction bands (c), which are at small energetic separation from the local orbitals, are responsible to the delocalization and transport. The topological flat bands of the BM model appear as a result of the hybridization of f - and c -electrons. This model then provides a new perspective for the strong correlation physics, which is now described as strongly correlated f -electrons coupled to nearly free c -electrons — we hence name our model as the topological heavy fermion model. Using this model, we obtain a manifold of $U(4)$ and $U(4) \times U(4)$ symmetries in TBG as well as the correlated insulator phase and their energies. Simple rules for the ground states and their Chern numbers are derived. Moreover, features such as the large dispersion of the charge ± 1 excitations, and the minima of the charge gap at the Γ point can now, for the first time, be understood both qualitatively and quantitatively in a simple physical picture. Our mapping will open the prospect of using heavy-fermion physics machinery to the superconducting physics of TBG, which is one of our future plans.

References and Publications

1. High-throughput calculations of magnetic topological materials

Yuanfeng Xu, Luis Elcoro, Zhi-Da Song, Benjamin J. Wieder, M. G. Vergniory, Nicolas Regnault, Yulin Chen, Claudia Felser, B. Andrei Bernevig

Nature, 586, pages702–707(2020)

2. Cascade of electronic transitions in magic-angle twisted bilayer graphene
Dillon Wong, Kevin P. Nuckolls, Myungchul Oh, Biao Lian, Yonglong Xie, Sangjun Jeon, Kenji Watanabe, Takashi Taniguchi, B. Andrei Bernevig, Ali Yazdani
Nature 582, 198-202 (2020)
3. Axionic charge-density wave in the Weyl semimetal (TaSe4)2I
J. Gooth, B. Bradlyn, S. Honnali, C. Schindler, N. Kumar, J. Noky, Y. Qi, C. Shekhar, Y. Sun, Z. Wang, B. A. Bernevig, C. Felser
Nature volume 575, pages315–319(2019)
4. Spectroscopic signatures of many-body correlations in magic-angle twisted bilayer graphene
Y. Xie, B. Lian, B. Jäck, X. Liu, CL. Chiu, K. Watanabe, T. Taniguchi, B. A. Bernevig, A. Yazdani
Nature, 572, pages101–105 (2019)
5. A complete catalogue of high-quality topological materials
M. G. Vergniory, L. Elcoro, C. Felser, N. Regnault, B. A. Bernevig, Z. Wang
Nature 566, 480-485 (2019)
6. Twisted bulk-boundary correspondence of fragile topology
Zhi-Da Song, Luis Elcoro, B. Andrei Bernevig.
Science, 2020; 367 (6479): 794 DOI: [10.1126/science.aaz7650](https://doi.org/10.1126/science.aaz7650)
7. Experimental characterization of fragile topology in an acoustic metamaterial
Valerio Peri, Zhi-Da Song, Marc Serra-Garcia, Pascal Engeler, Raquel Queiroz, Xueqin Huang, Weiyin Deng, Zhengyou Liu, B. Andrei Bernevig, Sebastian D. Huber.
Science, 2020; 367 (6479): 797 DOI: [10.1126/science.aaz7654](https://doi.org/10.1126/science.aaz7654)

Spin-Orbit Interactions in Transdimensional Heterostructures

Principle Investigator: Igor Bondarev, Professor of Physics, PhD, DSc (Habilitation)
Department of Mathematics & Physics, North Carolina Central University, Durham, NC 27707
ibondarev@ncsu.edu

Project Scope

This project focuses on the development of the theoretical understanding for intrinsic electronic processes and interactions in transdimensional heterostructures. The transdimensional (TD) regime lies in between three (3D) and two (2D) dimensions. Current research has been largely focused on purely 2D or conventional 3D materials, being guided by the traditional view that only the dimensionality and the chemical composition are important to control the physical properties of quantum materials. The transitional, TD regime has been greatly overlooked. This project is intended to fill in this gap by developing the relativistic theory of the spin-orbit interactions, the associated electromagnetic (EM) response, and collective many-particle effects for ultrathin films of metals and semiconductors in the TD regime. As an example, in ultrathin metallic films of controlled thickness (TD plasmonic films) the stronger spin-orbit interactions can lead to sizable pseudomagnetic effects, making their spatially dispersive EM response nonreciprocal and the film optically active, or gyrotropic. This can result in novel parity-time symmetry-breaking effects controlled by the film thickness.

Keywords: Transdimensional, Epsilon-Near-Zero Modes, Charged Interlayer Excitons, Quaternions

Recent Progress

- Transdimensional Epsilon-Near-Zero Modes in Planar Plasmonic Nanostructures— We use Quantum Electrodynamics (QED) and the confinement-induced nonlocal EM response model based on the Keldysh-Rytova (KR) pairwise electron interaction potential [1] to study epsilon-near-zero (ENZ) modes and their coupling to a point-like dipole emitter (DE) close to an ultrathin plasmonic film in the TD regime. Contrary to conventional thin film models that rely either on 2D material properties or on 3D materials with boundary conditions on their top and bottom interfaces, our model takes into account the electron vertical confinement explicitly. Our results generalize the seminal work by Drexhage [2] and recent work [3] by showing how the light-matter coupling in TD films evolves as their thickness decreases from bulk material properties to those of 2D plasmonic materials. We report new remarkable effects. They are: (i) the lifting of the surface plasmon mode degeneracy and (ii) the DE coupling to the split ENZ modes with biexponential DE-surface distance dependence of the spontaneous emission at rates 2 to 3 orders of magnitude greater than in free space. These effects can be controlled due to the thickness-dependent plasma frequency of the TD film – a unique microscopic property that cannot be obtained from macroscopic boundary conditions on the bulk metal film interfaces. The electron vertical confinement turns the Coulomb potential into the much stronger thickness-dependent KR potential, leading to thickness-dependent plasma oscillations and thus providing the way to control the light-matter coupling, the EM response, and the near-field properties of the ultrathin plasmonic films in the TD regime. Knowledge of these features is advantageous both for the fundamental understanding of EM properties and for the development of the new design principles for efficient photonic nanodevices built on the ultrathin plasmonic TD films. [Figure 1; I.V.Bondarev, H.Mousavi, and V.M.Shalaev, Physical Review Research 2, 013070 (2020)]

- Crystal Phases of Charged Interlayer Excitons in van der Waals Heterostructures— The topic of strongly correlated coherent states of excitons has recently boomed due to new emerging quantum materials such as van der Waals (vdW) bound monolayers of transition metal dichalcogenides (TMDs). The analytical equal electron-hole (e-h) mass theory we developed for the complexes of indirect (aka interlayer, or dipolar) excitons such as trion (aka X^\pm charged interlayer exciton, CIE) and biexciton in bilayer semiconductor heterostructures [4], has recently been confirmed experimentally [5]. The CIE binding energies ~ 10 meV are reported, just as our theory predicts. Additionally, experiments exhibited the fact of the X^- trion binding energy being greater (by a factor of ~ 1.5) than that of the X^+ trion. To explain this theoretically we extend our model to include the most general case of unequal e-h masses. New CIE binding energy equations we have obtained exhibit an interesting crossover behavior whereby

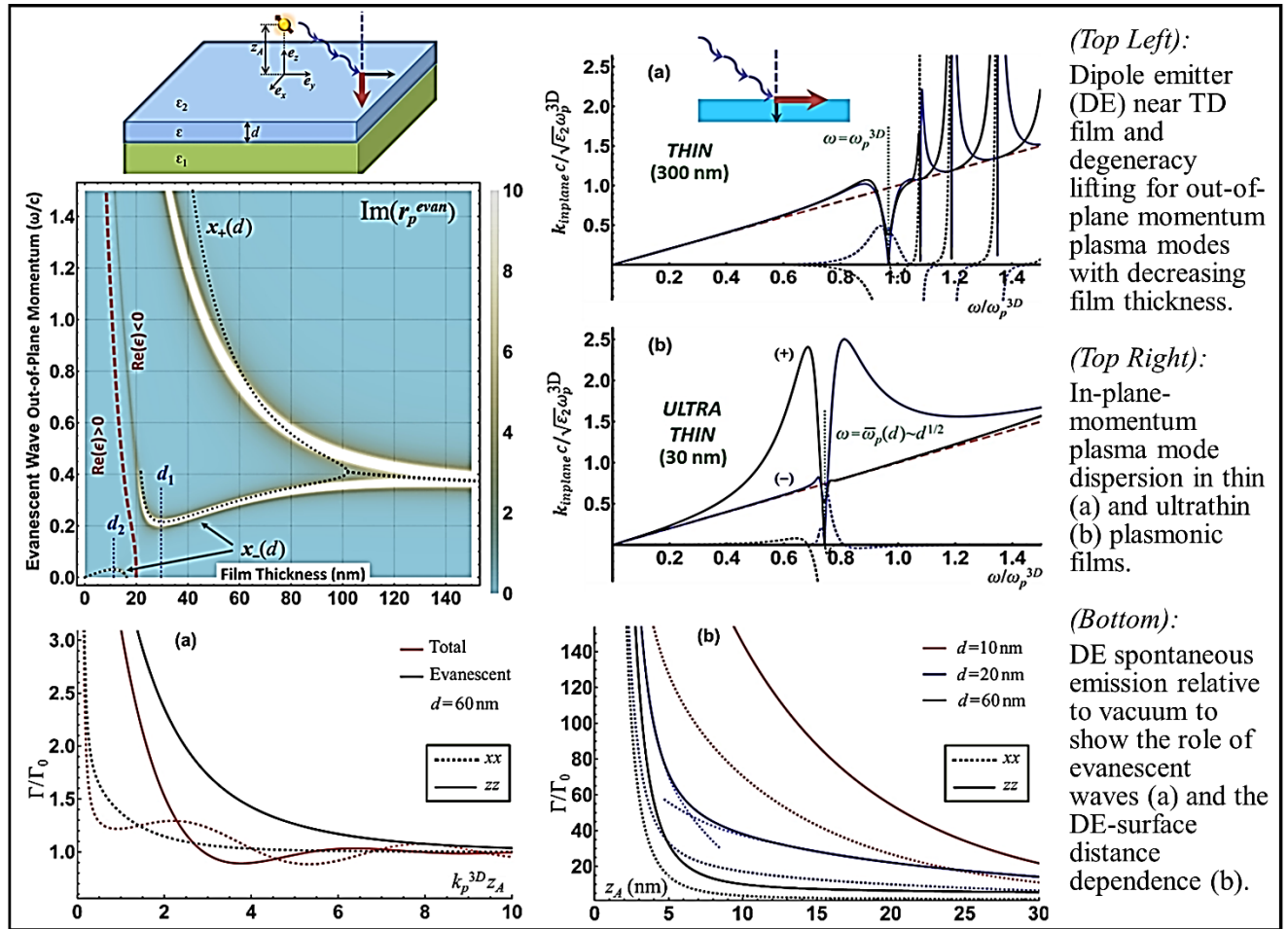


Fig. 1: Summary of research results on the TD epsilon-near-zero modes in ultrathin planar plasmonic nanostructures.

the difference in the negative and positive CIE binding energy changes its sign as the interlayer distance increases. This explains the experimental evidence reported. Our analysis of X^\pm pairwise interactions exhibits two scenarios for crystallization phase transitions in the collective multiparticle CIE system. They are: (i) the unlike-charge CIE crystallization and (ii) the like-charge CIE Wigner crystallization. We predict the existence of the new strongly correlated collective CIE states in highly excited vdW heterostructures such as TMD bilayers and double bilayer graphene. We evaluate the critical densities and temperatures for such state formation. We show that they can be selectively realized with TMD bilayers of properly chosen e-h mass ratio by varying the interlayer separation distance. Our results can be used for a variety of spinoptronics applications with vdW heterostructures. [Figure 2; I.V.Bondarev, O.L.Berman, R.Ya.Kezerashvili, and Yu.E.Loikov, Communications Physics 4, 134 (2021)]

• Quaternion Complexes in Bilayer Semiconductors near Metallic Surfaces— In 1996, V.I.Yudson proposed the existence of stable doubly charged four-carrier complexes in bilayer semiconductor nanostructures, which may be called “quaternions” [6]. The geometry he considered is shown in Fig. 3 (a). Two semiconductor layers are placed side by side to make a bilayer structure. The structure is placed parallel to a metal surface. Under optical pumping, an interlayer exciton can be created which then picks up two free electrons (or two holes). The metal surface produces image charges to cancel much of the repulsive interaction in the quaternion. Such four-particle complexes are charged bosons as they consist of an even number of fermions. Similar quaternion complexes have been recently observed in the photoluminescence (PL) spectroscopy experiments on the p -doped bilayer WSe_2 -hBN- WSe_2 TMD heterostructures placed near the niobium metal surface at a distance controlled by extra

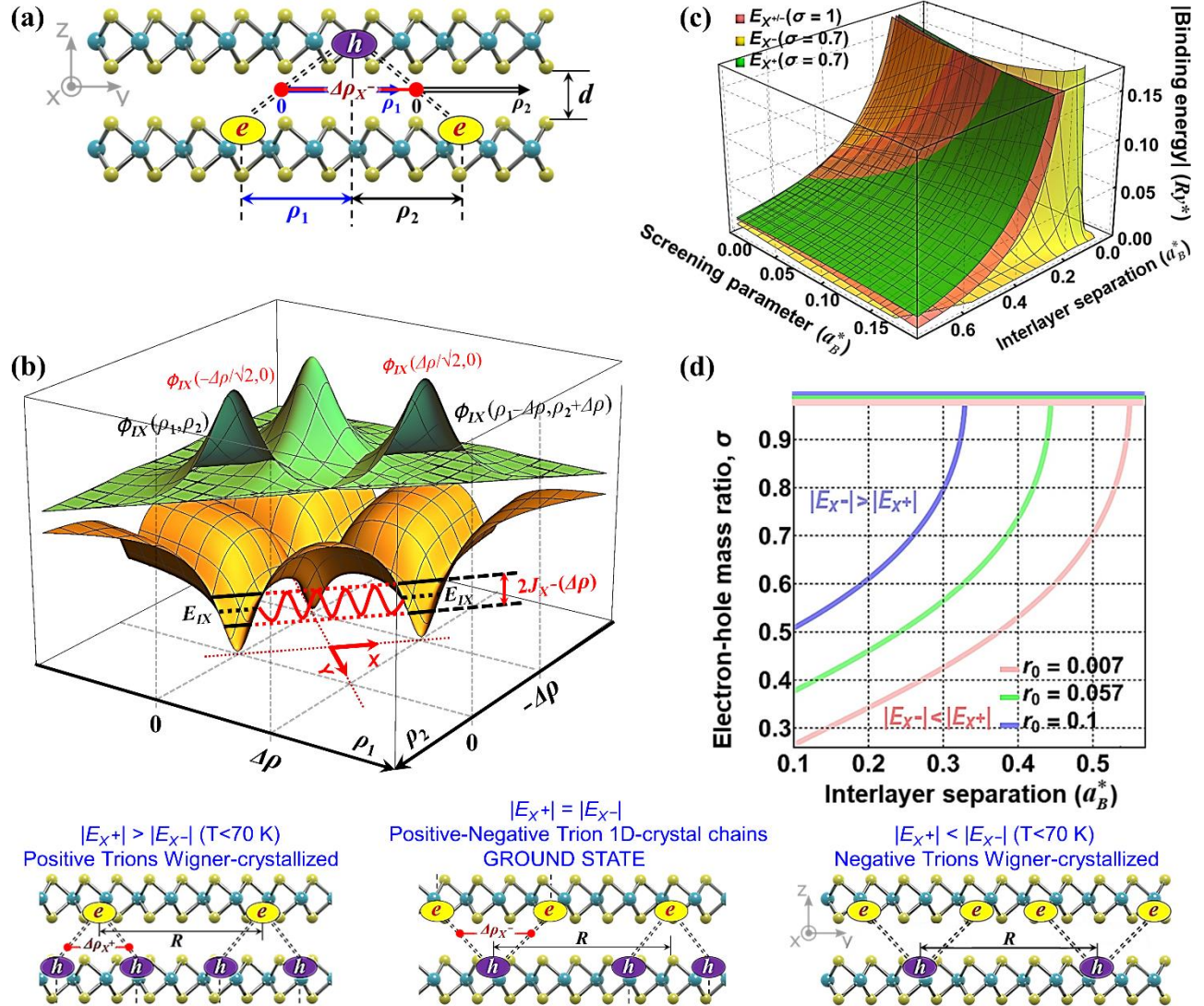


Fig. 2: (a) Sketch of a negative CIE complex (X^- trion) in a TMD bilayer. (b) Crosscut of the e - h potential/wavefunctions (yellow/green) in the configuration space (ρ_1, ρ_2) to show the tunneling between the equivalent IE configurations, ρ_1 and ρ_2 , to form the CIE in (a). (c) X^\pm trion binding energies calculated within the tunnel-exchange model sketched in (b) for varied problem parameters. (d) Equal-binding-energy solutions calculated for the X^+ and X^- trions with e - h potential screening length r_0 fixed. **Bottom:** X^\pm trion crystal phases as it follows from (d) per the total-energy minimum principle.

hBN separation layers [7]. The spectra exhibit an extra PL line that shows up in between the trion and exciton PL lines at temperatures up to ~ 100 K, only in the presence of the metal layer. To explain the experiments, we develop the theory for a variant of the Yudson geometry, which is structurally a trion in one layer bound to a carrier in a parallel layer as shown in Fig. 3 (b). To evaluate the trion and quaternion recombination energies, we employ the configuration space approach developed by the PI (Bondarev) previously, with metal surface included by the method of electrical images [7]. In this approach, a singly charged exciton complex (X^+ or X^- trion) is regarded as a bound system of the two equivalent excitons sharing the same hole (or electron). The trion bound state forms due to the tunneling between the equivalent configurations of the e - h system (see Refs.[4,8,9] and Fig.2). The binding and recombination energies are controlled by the tunneling rate. Our calculations shown in Fig. 3 (c) are fully consistent with the experiments to indicate that: (i) our variant of the quaternion complex does exist, (ii) is more stable than the Yudson geometry, and (iii) manifests itself as the PL line that pops up in between the trion and exciton PL lines in the presence of a metallic surface. A Bose-Einstein

condensate (BEC) of such quaternions would be a Schafroth superconductor [10] – a collective multi-particle superfluid state of doubly charged bosons – a state that does not require Cooper pairing and so paves the way to a new kind of unconventional high-temperature superconductivity. [Figure 3; Z.Sun, J.Beaumariage, Q.Wan, H.Alnatah, N.Houglan, J.Chisholm, Q.Cao, K.Watanabe, T.Taniguchi, B.M.Hunt, I.V.Bondarev, and D.W.Snoke, Nano Letters (2021), DOI: 10.1021/acs.nanolett.1c02422]

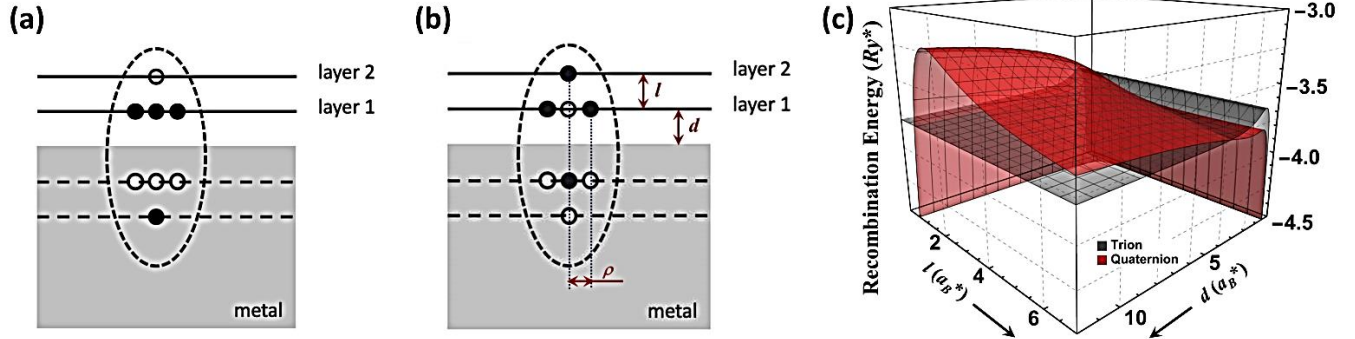


Fig. 3: (a) Yudson quaternion of three holes and one electron. (b) Quaternion geometry to explain the experimental PL data theoretically [7]. (c) Trion and quaternion recombination energies (counted down from exciton recombination energy) calculated in atomic units using the configuration space approach of Refs.[4,8] supplemented with the image charge method as sketched in (b).

Future Plans

Quaternions in TMD bilayers close to a Metal Layer: Stability Control and BEC— Currently in progress is the effort to obtain the relativistic spin-orbit contribution to the magneto-optical response of ultrathin plasmonic films of heavy metals with outer s- and d-orbitals hybridized. We already see the plasmon propagation nonreciprocity effect due to the d-wave-correction to the plasma frequency. The effect comes from the thickness-dependent pseudomagnetic field associated with the spin-orbit coupling, which makes the TD plasmonic film optically active (gyrotropic). The effect goes away as the film thickness increases. Once this work is finished and submitted for publication, the focus will be shifted towards the theory development for the quaternion stability control, Wigner crystallization, and BEC. We will work to gain a better understanding of how, under which conditions, these doubly charged interacting bosons can form strongly correlated long-range states, and how stable they can possibly be if one uses ultrathin metal films of controlled finite thickness (TD films) in place of the semi-infinite metal interface. Utilizing TD films allows for more adjustment parameters to increase the quaternion stability and hence the temperature at which they can exist. The first observation of quaternions by our experimental collaborator (Prof. David Snoke group, University of Pittsburgh) at temperature ~ 100 K is in excellent agreement with our theory [7]. The natural next step is to guide the experiments towards the quaternion high-temperature superconductivity observation under an in-plane electric field applied. This is a very timely crucial effort to go on with in the near future.

References

- [1] L.V.Keldysh, JETP Lett. 29, 658 (1979); N.S.Rytova, Proc. MSU Phys. Astron. 3, 30 (1967).
- [2] K.H.Drexhage, J. Lumin. 1-2, 693 (1970).
- [3] S.Campione, I.Brener, and F.Marquier, Phys. Rev. B 91, 121408 (2015).
- [4] I.V.Bondarev and M.R.Vladimirova, Phys. Rev. B 97, 165419 (2018).
- [5] L.A.Jauregui, *et al.*, Science 366, 870 (2019).
- [6] V.I.Yudson, Phys. Rev. Lett. 77, 1564 (1996).
- [7] Z.Sun, *et al.*, Nano Letters 2021, DOI: 10.1021/acs.nanolett.1c02422.
- [8] I.V.Bondarev, *et al.*, Communications Physics 4, 134 (2021).
- [9] I.V.Bondarev, Mod. Phys. Lett. B 30, 1630006 (2016).
- [10] M.R.Schafroth, Phys. Rev. 100, 463 (1955).

Publications

(2020-21)

I.V.Bondarev, H.Mousavi, and V.M.Shalaev, Transdimensional Epsilon-near-Zero Modes in Planar Plasmonic Nanostructures, Physical Review Research 2, 013070 (2020)

I.V.Bondarev, O.L.Berman, R.Ya.Kezerashvili, and Y.E.Loikov, Crystal Phases of Charged Interlayer excitons in van der Waals Heterostructures, Communications Physics 4, 134 (2021)

Z.Sun, J.Beaumariage, Q.Wan, H.Alnatah, N.Houglund, J.Chisholm, Q.Cao, K.Watanabe, T.Taniguchi, B.M.Hunt, I.V.Bondarev, and D.W.Snoke, Charged Bosons Made of Fermions in Bilayer Structures with Strong Metallic Screening, Nano Letters 2021, DOI: 10.1021/acs.nanolett.1c02422

Coupled Electron-Phonon Transport from First Principles

Principal Investigator: David Broido

Department of Physics, Boston College, Chestnut Hill, MA 02467

Email: broido@bc.edu

Program Scope

The major goals of this project are (i) to develop and implement a predictive *ab initio* approach, free of adjustable parameters, to explore the regime in which the mutual interaction between electrons and phonons dominates thermoelectric transport behavior resulting in strong drag effects; (ii) To validate the predictive capability of the approach through demonstrating agreement between calculated and measured thermoelectric transport coefficients for a range of materials; (iii) To computationally identify new materials in which strong phonon drag behavior occurs.

Our approach is based on an efficient computational scheme to fully solve the coupled electron/phonon Boltzmann transport equations (eBTE/pBTE). It accurately describes the momentum-conserving (normal) and momentum-relaxing (Umklapp) intrinsic electron-phonon and phonon-phonon scattering processes. In addition, it goes beyond the commonly-used Bloch assumption in which phonons (electrons) are taken to remain in equilibrium when describing electron (phonon) transport. Thus, it can capture the strong phonon drag enhancement of thermopower and mobility in doped semiconductors. A key feature of the computational approach is that it satisfies the Kelvin-Onsager relation, a fundamental requirement of thermodynamics, by construction, even in the strong drag regime.

Keywords: Electron-phonon coupling; thermoelectric transport; phonon drag.

Recent Progress

Phonon drag enhancement of thermopower and mobility in Silicon

Working with our collaborators at the Catalan Institute for Nanoscience [1], we have applied our *ab initio* approach and computational code (known as elphbolt; now publicly available [1]) to calculate the thermoelectric transport coefficients (electrical conductivity/mobility, thermal conductivity, thermopower and Peltier coefficients) of silicon as a function of temperature. In Fig. 1 (left panel), our calculated thermopower magnitudes are compared to measured values [2]. Excellent agreement is found across a wide temperature range. The Seebeck thermopower (black curve), obtained by solving the eBTE/pBTE under an imposed temperature gradient, includes a large phonon drag contribution. This can be seen by solving the eBTE/pBTE in the Peltier picture, where an applied electric field generates a heat current whose electronic (blue dashed) and phonon (green dashed) thermopower contributions sum to match the Seebeck thermopower. The Peltier

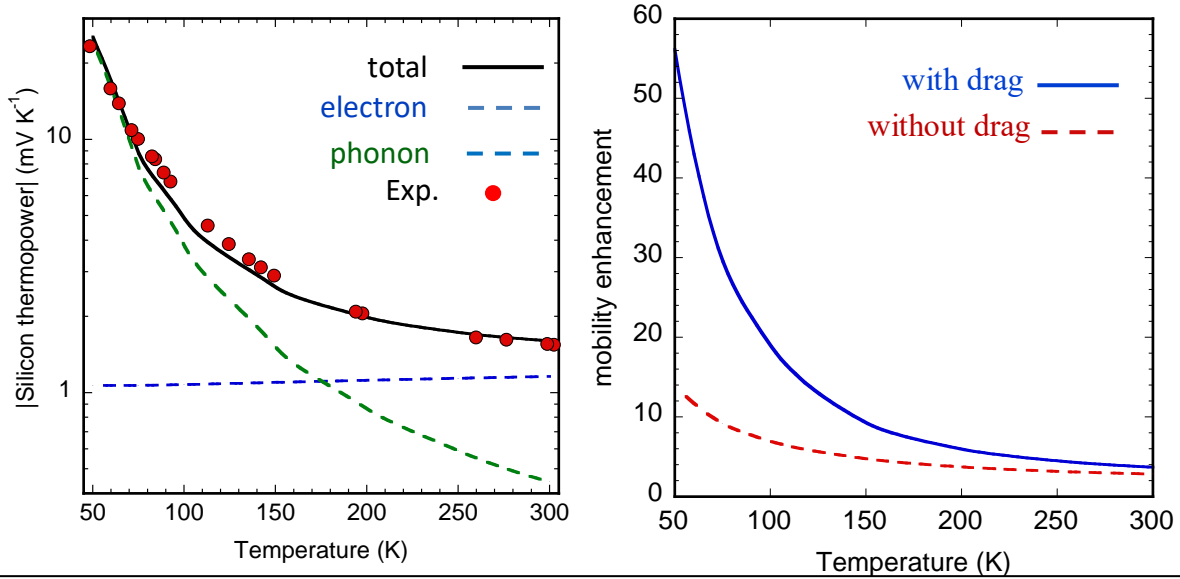


Figure 1. Left panel: *Ab initio* calculations of total thermopower magnitude of silicon (black curve) as a function of temperature for electron density of $2.75 \times 10^{14} \text{ cm}^{-3}$, compared to measurement [2]. Strong phonon drag contributions (green curve) below around 200K reflect failure of Bloch assumption. Right panel: Calculation of enhancement of silicon mobility for electron density of $2 \times 10^{19} \text{ cm}^{-3}$, when removing electron scattering from charged donors. Significantly larger mobility enhancements are found at low T when including phonon drag (solid blue curve) than when requiring phonons in equilibrium (Red dashed curve).

picture also allows a clean separation of the electronic and the phonon contributions. The electronic thermopower corresponds to the Bloch assumption in which phonons remain in equilibrium. A 40% phonon drag contribution to the Seebeck thermopower is found even at room temperature, which increases to an astounding factor of 25 at 50K.

The right panel in Fig. 1 compares the enhancement in the Si mobility from removing the electron scattering from charged dopant atoms. The dashed red curve gives the enhancement within the Bloch assumption, while the solid blue curve gives the corresponding enhancement upon including drag effects. At room temperature, factors of two enhancements are found in both cases indicating negligible phonon drag boost. In contrast, at 50K, the mobility enhancement including phonon drag is four times larger than that predicted from ignoring it. These results highlight simultaneously the dominance of the phonon drag contributions to thermopower and mobility at low T and the catastrophic failure of the commonly used Bloch assumption in this regime.

***Ab initio* thermoelectric transport in metals: Breakdown of Wiedemann-Franz law**

An important task of this project is to verify that the theoretical approach has predictive capability. Since the theory has no adjustable parameters, demonstrating good agreement with measured data for a number of materials gives strong support to the accuracy of the calculations. The thermopower results illustrated above for Si contribute to this goal for semiconductors. We have also calculated electrical and thermal conductivities as functions of temperature for several common metals including copper (Cu), silver (Ag), gold (Au) and tungsten (W). These metals are

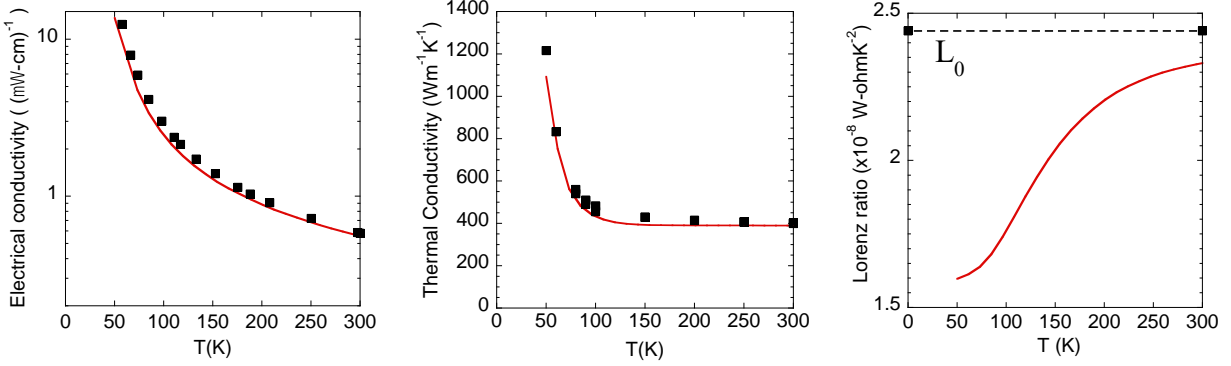


Figure 2. Comparison of calculated (red curves) and measured (black squares; [3, 4]) electrical (left panel) and thermal conductivities (center panel) for copper (Cu) as a function of temperature, T. Right panel: Lorenz ratio and breakdown of Wiedemann-Franz ($L_0=2.44 \times 10^{-8} \text{ W-ohmK}^{-2}$) for Cu at low temperatures.

chosen in part because of the relatively high sample quality for which measured data is available. Also, prior theoretical studies of these metals are either not fully first principles or do not extend well below room temperature. We note that the calculated results include both the electron and phonon contributions to the thermal conductivity; the electronic contribution is found to dominate across the full range of T considered.

We find good agreement between our calculated electrical and thermal conductivities for Cu, Ag, Au and W compared with experiment, extending from room temperature down to 50K. Results for Cu are presented in Fig. 2. These results along with similarly good agreement found previously for aluminum build support for the developed theoretical approach to interrogate thermoelectric transport in normal metals. We have also found an increasing breakdown of the Wiedemann-Franz law for all of these metals well below room temperature, which is illustrated for Cu in the right panel of Fig. 2. This breakdown, which occurs due to the increasingly inelastic nature of electron-phonon scattering and the different way that this affects the electrical and heat currents, is accurately captured by our *ab initio* approach.

Thermal expansion in the classical Invar alloy

In a side project, we have been working to understand the anomalously low thermal expansion observed in the "classical Invar" alloy, Fe_{0.65}Ni_{0.35}, which is referred to as the Invar effect. Over 100 years since its discovery, the nature of magnetism in Invar is still not understood, and no satisfactory theoretical explanation of the Invar effect has been given. Working with collaborator, Dr. Olle Hellman, we have developed a general first principles approach to calculate temperature-dependent phonons and thermal expansion in magnetic materials in the absence of any microscopic model for the magnetism. The model fully includes thermal disorder in both lattice and spin subsystems as well as the temperature dependent spin-lattice coupling between the two subsystems, and it is guided by the measured changes in magnetization with temperature and pressure. The calculated phonon dispersions are in excellent agreement with the measured data.

Exploiting the theoretical/computational expertise and understanding gained from this work, we are collaborating with an experimental group at CalTech [7], to investigate the Invar thermal expansion coefficient through studies of pressure-dependent changes in its entropy.

Future Plans

- 1) *Continued code development and testing*: We will continue to develop code efficiencies that will allow us to interrogate behavior in the regime of strong phonon drag, where electron-phonon coupling dominates. A particular focus will be to solve the coupled electron-phonon BTEs at lower temperatures where extremely fine electron/phonon wavevector grids are needed.
- 2) *Ab initio phonon drag studies*: We have identified several candidate materials, including semiconducting, semimetallic and metallic ones, that may show strong phonon drag behavior, possibly even occurring at relatively high temperatures. We will use our developed *ab initio* computational approach to investigate thermoelectric transport and phonon drag in these candidate materials.
- 3) *Joint Theory/Experiment study of thermal expansion in Invar*: Calculations of the magnetization, and the vibrational and magnetic entropy as a function of pressure and temperatures are ongoing to compare with the measurements. It is anticipated that this project will be completed in the fall/winter of 2021.

References

- [1] Nakib H. Protik, Chunhua Li, Miguel Pruneda, David Broido, Pablo Ordejón, elphbolt: *An ab initio solver for the coupled electron-phonon Boltzmann transport equations*, under review (2021); <https://arxiv.org/abs/2109.08547>.
- [2] T. Geballe, G. Hull, *Seebeck effect in silicon*, Physical Review 98, 940 (1955).
- [3] K.-H. Hellwege, J. L. Olsen, Ed., *Metals: Electronic Transport Phenomena: Electrical Resistivity, Kondo and Spin Fluctuation Systems, Spin Glasses and Thermopower*, Landolt-Börnstein, New Series III/15a (1982).
- [4] O. Madelung, G. K. White, Ed., *Metals: Electronic Transport Phenomena · Thermal Conductivity of Pure Metals and Alloys*, Landolt-Börnstein, New Series III/15c (1991).
- [5] E. D. Hallman and B. N. Brockhouse, *Crystal dynamics of nickel–iron and copper–zinc alloys*, Canadian Journal of Physics, 47, 1117–1131 (1969).
- [6] E. Maliszewski and S. Bednarski; *Lattice dynamics of Fe_{0.65}Ni_{0.35} classical invar*, Physica Status Solidi (b), 211, 621–629, (1999).
- [7] S. Lohaus, M. Heine, P. Guzman, C. Bernal, G. Shen, E. E. Alp, O. Hellman, D. Broido, and B. Fultz, to be submitted (2021).

Publications

- [1] Nakib H. Protik, Chunhua Li, Miguel Pruneda, David Broido, Pablo Ordejón, elphbolt: *An ab initio solver for the coupled electron-phonon Boltzmann transport equations*, under review (2021); <https://arxiv.org/abs/2109.08547>.

QMC-HAMM: High accuracy multiscale models from quantum Monte Carlo

PI: David Ceperley, University of Illinois Champaign-Urbana

Co-PIs: Elif Ertekin, Harley Johnson, Matthew Turk, Lucas Wagner (Univ. of Illinois at Urbana-Champaign); Andriy Nevidomskyy (Rice Univ.)

Program Scope

The state of the art in creating mesoscopic models starting from the microscopic behavior is based on density functional theory (DFT) calculations. In recent years, modern machine learning techniques have been able to reproduce potential energy surfaces from standard DFT functionals to a very high accuracy; the accuracy of the potential energy surfaces is often limited by the underlying DFT data. In quantum materials such as twisted bilayer graphene, effective electron interactions and weak van der Waals interactions can be critical to their behavior, which DFT does not treat accurately. Similarly, the phase diagram of hydrogen at high pressures and temperatures depends sensitively on the energy difference between very different phases, which are hard to treat with simple off-the-shelf electronic structure



To improve the quality of data on which mesoscopic models are based, it is necessary to move beyond density functional theory and to base mesoscopic models on more accurate microscopic calculations. The QMC-HAMM project uses quantum Monte Carlo (QMC) techniques to compute the properties of materials very accurately. Multiscale models are then derived based on these accurate calculations, using software and data to glue highly accurate QMC calculations to lattice-scale and continuum models of materials.

Keywords: Quantum Monte Carlo, Machine Learning, Dense Hydrogen, Graphene

Recent Progress

Machine-learned interatomic potentials trained on Ab initio data have been applied in large-scale molecular dynamics simulations to approach the accuracy of the *ab initio* methods. Historically, these potentials have relied on density functional theory to generate the training data. We have developed the first large-scale publicly accessible database of quantum Monte Carlo (QMC) force calculations for dense hydrogen enabling more accurate machine-learned potentials. As a first study with this data, we determine the melting temperature of molecular hydrogen as a function of pressure in the range 50-200 GPa. While at lower pressure our result agrees with previous theory and experiment, we find a substantially higher melting temperature for higher pressures.

Layering van der Waals (vdW) materials has shown the capability to create new functional materials, such as small-twist-angle bilayer graphene with strongly correlated phases. These phases as determined by the electronic properties are sensitive to geometry relaxations, the determination of which requires an accurate description of the vdW interaction between bilayers. However, there does not exist enough accurate data to fully parameterize the dependence on registry between the bilayers.

We used diffusion Monte Carlo (DMC) to parameterize the interaction between layers of graphene. The DMC method is able to compute the vdW energy accurately [1], and is efficient enough that we can use the Summit supercomputer to compute the binding curve for multiple different stacking types. We present the DMC data set and compare it to other approximations for the binding curve of graphene. We anticipate this data will be used to develop accurate classical potentials and total energy tight binding models, which then can be used to study the long-wavelength relaxations in bilayer graphene.

An exciting new task in condensed matter physics is understanding the microscopic mechanisms behind flat band superconductivity in twisted bilayer graphene (TBLG). A major hurdle to understanding superconductivity in TBLG are the roles of lattice relaxation and electronic structure on isolated band flattening near magic twist angles. State of the art tight binding calculations indicate that lattice relaxation is required to achieve isolated flat bands with fragile topology in TBLG, however the phenomenological origin of commonly used tight binding models obfuscates whether the lattice relaxation or model inaccuracy leads to this conclusion. We have developed an accurate local environment tight binding model (LETB) and fit it using training data from first principles density functional theory calculations. By computing the band structures using the LETB, we observe the emergence of flat bands near the magic twist angle accompanied by Wannier obstruction, associated with a fragile topology, without needing lattice relaxation. Geometry relaxation is shown only to quantitatively enhance band flattening and band gaps. Our work demonstrates that an accurate electronic structure model for TBLG can generate topological flat bands without geometric relaxation, in contrast to conclusions made using phenomenological models for TBLG.

Future Plans

We plan to add functionality to the database to the database for dense hydrogen forces, for example to allow users to compare results with different DFT functionals and potentials and to save developed potentials. Using the machine-learned potentials we plan to study molecular and metallic phase of hydrogen to develop a much more accurate phase diagram of dense hydrogen. We are also studying the impact of long-range coulombic forces on the machined-learned force fields. We have developed machined-learned potentials for use with lanthanum

hydrides and using QMC forces have computed phonon dispersions in those materials at various high pressures and plan to study superconductivity and its phase diagram.

On the graphene side, we are pursuing two main avenues. The first is using quantum Monte Carlo to derive large length scale models that include interactions for the electrons using the density matrix downfolding technique invented in our collaboration. The second avenue is to marry the structural models to electronic models, which will allow us to investigate the effects of electron-phonon coupling on twisted bilayer graphene. Such a model is currently of high interest in light of new observations of superconductivity in untwisted trilayer graphene, which may be due to electron-phonon interactions.

References

[1] Mostaani, Drummond, Falko. Phys. Rev. Letts. **115**, 115501 (2015).

Publications

1. Shivesh Pathak, Brian Busemeyer, João N. B. Rodrigues, and Lucas K. Wagner. “Excited States in Variational Monte Carlo Using a Penalty Method.” J. Chem. Phys. **154** (2021): 034101. <https://doi.org/10.1063/5.0030949>.

Designing Topological Quantum Matter

Claudio Chamon, Boston University

Program Scope

Systems whose properties rely on intrinsically quantum mechanical effects such as interference or entanglement hold the promise to serve as the building blocks for novel technologies for computing and energy applications. Topological quantum matter, in particular, may provide ways to realize fault tolerant platforms for quantum computation and quantum information processing.

Keywords: Topological matter, quantum spin liquids, topological qubits

Recent Progress

We put forward in publication [P9] a theoretical framework to construct topological quantum spin liquids with exact gauge symmetries in systems with realistic two-body interactions. That one can generate effective multi-spin interactions in some low energy limit of a two-spin Hamiltonian is not unexpected; what is novel in our work is that the gauge symmetries we discuss are *exact*.

We introduced the notion of combinatorial gauge symmetry — a local transformation that includes single spin rotations plus permutations of spins (or swaps of their quantum states) — that preserve the commutation and anticommutation relations among the spins. We showed that Hamiltonians with simple two-body interactions contain this symmetry if the coupling matrix is a Hadamard matrix, with the combinatorial gauge symmetry being associated with the automorphism of these matrices with respect to monomial transformations. Armed with this symmetry, we addressed the physical problem of how to build \mathbb{Z}_2 quantum spin liquids with physically accessible interactions. In addition to its intrinsic physical significance, the problem is also tied to that of how to build topological qubits.

We showed that combinatorial gauge symmetry can be extended to other Abelian groups, and presented a realization of a \mathbb{Z}_3 quantum double in an array of superconducting wires coupled via Josephson junctions in publication [P13]. With a suitably chosen magnetic flux threading the system, the inter-wire Josephson couplings take the form of a complex Hadamard matrix, which possesses combinatorial gauge symmetry — a local \mathbb{Z}_3 symmetry involving permutations and shifts by $\pm 2\pi/3$ of the superconducting phases. The sign of the star potential resulting from the Josephson energy is inverted in this physical realization, leading to a massive degeneracy in the non-zero flux sectors. A dimerization pattern encoded in the capacitances of the array lifts up

these degeneracies, resulting in a \mathbb{Z}_3 topologically ordered state. Moreover, this dimerization pattern leads to a larger effective vison gap as compared to the canonical case with the usual (uninverted) star term. Our work highlights that combinatorial gauge symmetry can serve as a design principle to build quantum double models using systems with realistic interactions.

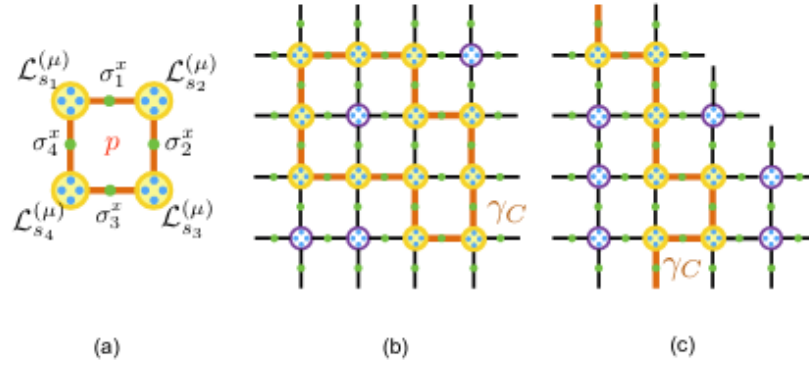


Figure 1: (a) Operator generating the local \mathbb{Z}_2 gauge transformation on an elementary plaquette, G_p (b) A closed loop operator along a path γ_C . (c) An open string operator along a path in a system with boundaries.

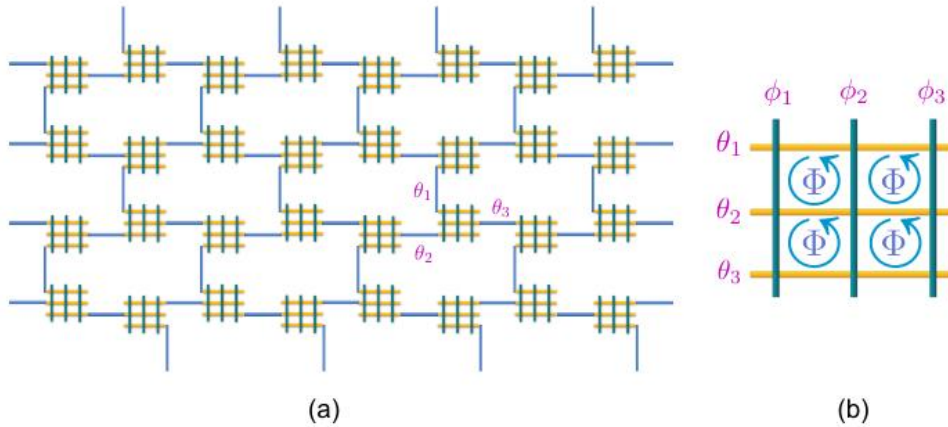


Figure 2: An array of superconducting wires forming a two-dimensional honeycomb lattice. An elementary building block is depicted in (b), which contains three horizontal (yellow) gauge wires with superconducting phases θ_i coupled to three vertical (green) matter wires with phases ϕ_a via Josephson junctions, forming a “waffle” like geometry. An external magnetic flux of $\Phi = (n+1/3) \Phi_0$ threads each elementary plaquette of the waffle, leading to a complex coupling matrix W with combinatorial gauge symmetry. On the full lattice, the gauge wires are shared between two neighboring sites via the blue wires, whereas the matter wires are localized on each lattice site.

Future Plans

A front opened by this work is that one can now program spin liquid systems with two-body interactions in available quantum hardware. For instance, we implemented our ideas on a D-Wave annealer, for the case of the \mathbb{Z}_2 spin liquid. However, the parameter regime that is accessible in these devices is such that the spinon gap is larger than the operating temperature, while the vison gap is smaller. In effect, this regime is a realization of a classical, but not a quantum, spin liquid. Nonetheless, it may be possible to probe the effects of the mutual statistics between vison and spinons (a quantum effect) in this intermediate temperature regime by studying the localization of the spinons propagating on a random flux background due to the visons. We plan to undertake these studies in the near future, in collaboration with Claudio Castelnovo's group at the University of Cambridge.

On a broader scope, the successful theoretical construction of the \mathbb{Z}_2 and \mathbb{Z}_3 spin liquids on top of combinatorial gauge symmetry points to the promise that other quantum doubles – Abelian and, more interestingly, non-Abelian – could be constructed for realistic models with at most two-body interactions. We plan to now extend the construction to non-Abelian states as a challenging theoretical undertaking.

Publications

- [P1] S. Kourtis, C. Chamon, E. R. Mucciolo, and A. E. Ruckenstein, “Fast counting with tensor networks”, *SciPost Phys.* 7, 60 (2019), DOI:10.21468/SciPostPhys.7.5.060.
- [P2] Z.-C. Yang, T. Iadecola, C. Chamon, and C. Mudry, “Hierarchical Majoranas in a programmable nanowire network”, *Phys. Rev. B* 99, 155138 (2019), DOI:10.1103/PhysRevB.99.155138.
- [P3] J.-H. Chen, C. Mudry, C. Chamon, and A. M. Tsvelik, “Model of spin liquids with and without time-reversal symmetry”, *Phys. Rev. B* 99, 184445 (2019), DOI:10.1103/PhysRevB.99.184445.
- [P4] O. Hart, G. Goldstein, C. Chamon, and C. Castelnovo, “Steady-state superconductivity in electronic materials with repulsive interactions”, *Phys. Rev. B* 100, 060508 (2019), DOI:10.1103/PhysRevB.100.060508.
- [P5] D. V. Efremov, A. Shtyk, A. W. Rost, C. Chamon, A. P. Mackenzie, and J. J. Betouras, “Multicritical Fermi surface topological transitions”, *Phys. Rev. Lett.* 123, 207202 (2019), DOI:10.1103/PhysRevLett.123.207202.

- [P6] L. Zhang, S. Kourtis, C. Chamon, E. R. Mucciolo, and A. E. Ruckenstein, “Ultraslow dynamics in a translationally invariant spin model for multiplication and factorization”, *Phys. Rev. Research* 1, 033001 (2019), DOI:10.1103/PhysRevResearch.1.033001.
- [P7] S. Ok, K. Choo, C. Mudry, C. Castelnovo, C. Chamon, and T. Neupert, “Topological many-body scar states in dimensions one, two, and three”, *Phys. Rev. Research* 1, 033144 (2019), DOI:10.1103/PhysRevResearch.1.033144.
- [P8] J. Noh, T. Schuster, T. Iadecola, S. Huang, M. Wang, K. P. Chen, C. Chamon, and M. C. Rechtsman, “Braiding photonic topological zero modes”, *Nature Physics* 16, 989(2020), DOI:10.1038/s41567-020-1007-5.
- [P9] C. Chamon, D. Green, and Z.-C. Yang, “Constructing quantum spin liquids using combinatorial gauge symmetry”, *Phys. Rev. Lett.* 125, 067203 (2020), DOI:10.1103/PhysRevLett.125.067203.
- [P10] C. Aron and C. Chamon, “Landau Theory for Non-Equilibrium Steady States”, *SciPost Phys.* 8, 74 (2020), DOI:10.21468/SciPostPhys.8.5.074.
- [P11] A. Chandrasekaran, A. Shtyk, J. J. Betouras, and C. Chamon, “Catastrophe theory classification of Fermi surface topological transitions in two dimensions”, *Phys. Rev. Research* 2, 013355 (2020), DOI:10.1103/PhysRevResearch.2.013355.
- [P12] W. B. Fontana, P. R. S. Gomes, and C. Chamon, “Lattice Clifford fractons and their Chern-Simons-like theory”, *SciPost Phys. Core* 4, 12 (2021), DOI:10.21468/SciPostPhysCore.4.2.012.18
- [P13] Z.-C. Yang, D. Green, H. Yu, and C. Chamon, “ Z_3 quantum double in a superconducting wire array”, *PRX Quantum* 2, 030327 (2021), DOI:10.1103/PRXQuantum.2.030327.
- [P14] W. B. Fontana, P. R. S. Gomes, and C. Chamon, “Field theories for type-II fractons”, *ArXiv e-prints* 2103.02713 (2021).
- [P15] A. Khudorozhkov, A. Tiwari, C. Chamon, and T. Neupert, “Hilbert space fragmentation in a 2d quantum spin system with subsystem symmetries”, *ArXiv e-prints* 2107.09690 (2021).

Ab initio complete cell quantum embedding and diagrammatic coupled cluster for correlated materials phase diagrams

Garnet Kin-Lic Chan (PI, Caltech)

Program Scope

The aim of our work is (i) to develop and apply ab initio complete cell quantum embedding methods. The quantum embedding methods considered include both density matrix embedding theory and dynamical mean-field theory. The complete cell methodology avoids downfolding by embedding all the atoms and their corresponding atomic orbitals (including virtual states) in a cell (or multiple cells) of the crystal. The corresponding quantum many-body problem is solved using a variety of quantum chemistry methods which target the wide range of energy scales in the resulting impurity. (ii) Out of the various quantum chemistry methods, one particular focus is on coupled cluster methods for condensed phase problems. Coupled cluster methods provide a systematic hierarchy of diagrammatic theories. Our efforts aim to extend the methods to anomalous orders such as superconducting orders, as well as finite-temperature and non-equilibrium systems, in order to study bulk phases in- and out-of-equilibrium.

Keywords: Non-equilibrium, quantum dynamics, many-body physics

Recent Progress: The funding period for this grant started this summer. Since the start we have completed a number of works including (i) a comprehensive formulation of coupled cluster dynamics at finite temperatures, maintaining conservation laws [1]. Although conserving conditions have been known for Green's function theories since Kadanoff and Baym, conserving coupled cluster approximations cannot be constructed in the same way. We describe how conservation laws arise in coupled cluster dynamics and demonstrated the numerical utility of the method in the simulation of non-equilibrium Kondo transport. (ii) Uncovering the origin of lack of convergence of the DMET algorithm. In collaboration with the group of Lin Lin, we found that the reason for the non-convergence of DMET self-consistency is from density matrices that are not pure-state v -representable. We formulated a numerical algorithm that therefore converges DMET without assuming pure-state v -representability, allowing DMET to be converged for previously difficult problems [2]. (iii) The first fully ab initio quantum many-body simulation of the cuprates in their parent state. Through our extensions of DMET into the ab initio setting it is now possible to simulate a 2×2 supercell of typical cuprates in a fully ab initio calculation. Since no downfolding is performed, the only approximations in the calculation are the finite size of the cell, the basis, and the solver error, each of which can be estimated. We applied this methodology first to understand systematics of the cuprate parent state across the mercury barium layer compounds. We found that we could indeed reproduce the systematic layer trend in the strength of the exchange couplings across the compounds (which increase with the number of copper oxygen layers). Further, by turning on and off excitation pathways within the ab initio calculation itself, it was possible to see the mechanism of the layer effect. In particular,

excitations to the empty Hg-O buffer layer orbitals compete with the copper-oxygen superexchange pathways in the plane, effectively leading to the suppression of the exchange and the observed layer effect on the magnetic couplings [3].

Publications:

[1] Conservation laws in coupled cluster dynamics at finite temperature, Ruoqing Peng, Alec F. White, Huanchen Zhai, Garnet Kin-Lic Chan, *J. Chem. Phys.*, 155, 044103 (2021)

[2] On the pure-state v -representability of density matrix embedding theory, Fabian Faulstich, Raehyun Kim, Zhi-Hao Cui, Zaiwen Wen, Garnet Kin-Lic Chan, Lin Lin, in preparation

[3] Systematic electronic structure in the cuprate parent state from quantum many-body simulations, Zhi-Hao Cui, Huanchen Zhai, Xing Zhang, Garnet Kin-Lic Chan, under review

SciDAC: Traversing the “death valley” separating short and long times in non-equilibrium quantum dynamical simulations of real materials

Marco Bernardi (Caltech), Garnet Kin-Lic Chan (Lead, Caltech), Emanuel Gull (Michigan), Andrew Millis (Columbia), Eran Rabani (Berkeley), David Reichman (Columbia), Carol Woodward (LLNL, FASTMath), Chao Yang (LBL, FASTMath)

Program Scope

We aim to tackle the fundamental bottlenecks that inhibit the faithful simulation of non-equilibrium quantum materials: the need to incorporate realistic interactions and the need to cross the “death valley” separating the very short times accessible to brute force simulation and the long times where hydrodynamics takes over. We will achieve this via (i) new simulation algorithms - built on the recent contributions of the PIs in the first principles treatment of interactions out of equilibrium, diagrammatic quantum Monte Carlo in the time domain, and insights into the structure of entanglement in dynamics, (ii) new applied mathematical advances into compressed representations in the time domain, improved time-propagation methods, and higher-dimensional tensor algebra, and (iii) new computational implementations, leveraging scalable parallelism and heterogeneous compute platforms, building on the established open-source libraries developed within this collaboration. We will also validate our methods via target applications, including simulating state-of-the-art ultrafast spectroscopies and coherently driven phonons; thereby modeling systems ranging from semiconductors driven out of equilibrium, to dynamical phases in complex correlated materials.

Current activities are centered around the following areas:

Algorithms and Computational formulations: The methods to be advanced include (i) first principles diagrammatic methods for the low-order treatment of interactions out of equilibrium, (ii) exact diagrammatic quantum Monte Carlo methods in the time domain, extended to multi-orbital and cluster impurity models; (iii) tensor networks for numerically controlled long time dynamics. By simultaneously advancing the full suite of techniques from first principles to low energy models, we aim to extend to the study of materials far from equilibrium the kind of multi-pronged attack that has proven fruitful in the equilibrium context.

Target phenomena: A plethora of target systems of intense current experimental interest are known, and theories to date have been formulated on the qualitative model-system level, often based on a time dependent mean-field analysis or extrapolating conclusions based on very short times. Crucial questions of flow of energy and coherence remain unaddressed. We are currently coordinating activities of the collaboration in four critical non-equilibrium areas: linear and non-linear response in materials with strong electron-phonon and electron-electron couplings; ultrafast optical control of electronic and lattice properties and competing orders; photo-induced superconductivity; and the dynamics of exciton formation.

Software development and leadership computational implementations: An important output will be the software, which includes tensor network methods (QUIMB); diagrammatic MC methods (ALPS); time-dependent coupled cluster methods (PYSCF); methods for the real-time Boltzmann equation and the related lowest-order interactions (PERTURBO). We are currently working on scaling up a wide variety of algorithms on leadership CPU and GPU architectures. In addition, contributions from the FASTMath members in the areas of time-integration, solvers and low-dimensional representations are being abstracted out as reusable math components.

Keywords: Non-equilibrium, quantum dynamics, many-body physics

Recent Progress

The collaboration started its activities one month ago and has completed its initial kickoff and coordination meeting.

Theoretical Studies of Polar Systems near Ferroelectric Quantum Critical Points

Premala Chandra, Center for Materials Theory, Department of Physics and Astronomy, Rutgers University

Program Scope

The emergence of complex states of quantum matter in the vicinity of zero-temperature phase transitions suggests that such quantum phenomena should be explored in a variety of settings. Quantum phase transitions are typically studied in magnetic systems with links to novel metallic behavior, whereas the interest in insulating polar materials is often motivated by room-temperature functionalities. There is much to be gained at the confluence of these two areas. Paraelectric materials near polar quantum critical points can be viewed as “economy” quantum critical systems whose propagating dynamics and few degrees of freedom allow for detailed interplay between analytic approaches, first-principles calculations and laboratory measurements. Additional degrees of freedom like spin and charge can be added and characterized systematically. Quantum critical metals are known to host strongly correlated phases where their behaviors depend crucially on the nature of the quantum critical points involved; it is thus natural to explore this phenomenon in quantum critical polar metals. Anomalous superconductivity in dilute quantum critical polar metals remains enigmatic. Therefore quantum critical polar metals, like their magnetic counterparts, do host exotic strongly correlated phases and provide accessible settings for careful study both theoretically and experimentally.

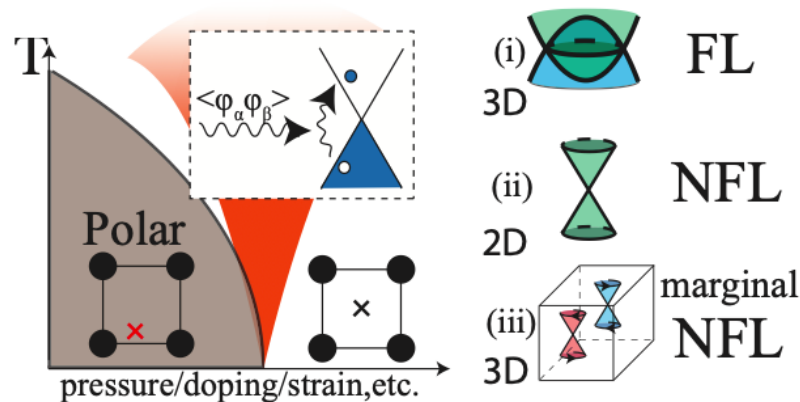


Fig. 1 (a) Schematic Phase Diagram of a polar metal with a critical region around the QCP. Inset illustrates that the critical region couple to an interband excitation. (b) Summary of the QCP behavior near typical band crossing: (i) a 3D nodal line, (ii) a 2D nodal point, and (iii) 3D Weyl point. (N)FL is (non-)Fermi liquid and in all case the polar mode is strongly renormalized. Coulomb interaction introduce anisotropy for (i) and (ii), and gap the longitudinal mode for (iii).

Keywords: polar criticality, quantum critical polar metals, strongly correlated phases

Recent Progress

Experimentally most insulating polar materials display first-order classical phase transitions due to strong electromechanical coupling, and yet in many cases low-temperature experiments suggest pressure-induced quantum criticality associated with zero-temperature continuous transitions. We have developed a theoretical framework for this phenomenon with specific predictions for the behavior of observable properties with decreasing temperature.

We have also explored the emergence of strong correlations in polar metals driven by critical polar fluctuations. Overcoming previously discussed challenges we demonstrate a robust mechanism for coupling between electrons and the critical transverse mode in multiband metals. We identify and characterize several novel interacting phases (see Figure 1), including non-Fermi liquids, when band crossings are close to the Fermi level with predictions for experiment in each case.

Superconductivity in dilute quantum critical polar metals challenges the conventional electron-phonon theory due to the absence of retardation required to overcome Coulomb repulsion. In quantum critical polar metals the Coulomb repulsion is heavily screened, and the critical transverse optical phonons decouple from the electric charge. In the resulting vacuum, long-range attractive interactions emerge from the energy fluctuations of the critical phonons leading to superconducting pairing. We provide predictions for the enhancement of superconductivity near polar criticality in two- and three-dimensional materials that can be used to test our theory.

Many anomalous properties of polar metals, particularly in the superconducting state, have been predicted by invoking spin-orbit mediated coupling between polar fluctuations (arising from soft polar phonons) and electrons. However, to date there is no consensus on the magnitude of this coupling, and we propose a mechanism to probe it experimentally. More specifically we demonstrate the presence of a spin-phonon resonance in the presence of applied magnetic field; the hybridization of the soft transverse optical mode and the electronic spin-flip mode leads to an energy splitting that is a function of coupling strength. Analyzing the static limit, we find that the polar order parameter can be oriented in magnetic field, providing possibilities for new switching protocols in polar metallic materials. We demonstrate that the effects we predict can be observed with current experimental techniques, suggesting promising material candidates.

Future Plans

We plan to work with our colleagues who perform first-principles calculations to identify promising polar materials to host the strongly correlated phases we have predicted. We will also explore dynamical quantum phase transitions in polar insulators, particularly since most non-equilibrium studies are performed in cold atom systems restricting the types of measurements possible. In parallel we will continue to study critical spin systems, quantum critical magnetic metals and disordered topological systems with the aim of learning new concepts that may prove useful in our overall study of quantum critical polar materials.

Publications

1. Spin-Phonon Resonances in Nearly Polar Metals with Spin-Orbit Coupling, A. Kumar, P. Chandra and P.A. Volkov, arXiv:2110.02051 (2021).
2. Superconductivity from Energy Fluctuations in Dilute Quantum Critical Polar Metals, P.A. Volkov, P. Chandra and P.Coleman, arXiv:2106.11295 (2021).
3. Emergent Potts Order in a Coupled Hexatic-Nematic XY model, V. Drouin-Touchette, P. P. Orth, P. Coleman, P. Chandra, T. C. Lubensky, arXiv:2103.01878 (2021).
4. Quantum Annealed Criticality: A Scaling Description, P. Chandra, P. Coleman, M.A. Continentino and G.G. Lonzarich, Physical Review Research 2, 043440 (2020).
5. Multiband Quantum Criticality of Polar Metals, P.A. Volkov and P. Chandra, Phys. Rev. Lett. 124, 237601 (2020).

Computational Mesoscale Science and Open Software for Quantum Materials

(PI) L. Q. Chen; Co-PIs: V. Gopalan, I. Dabo, J. Xu, R. Engel-Herbert
The Pennsylvania State University, University Park, PA 16802

Program Scope

The central goal of this Computational Mesoscale Materials Science (COMMS) center is to advance the mesoscale science of quantum and functional materials. The main objectives of the proposed program are to: (1) understand the thermodynamic stability of mesoscale topological structures and predict their responses to external thermal, mechanical, electrical, and magnetic stimuli; (2) develop computational models and innovative numerical algorithms toward exascale computations and implement them into an open-source software (Q-POP) for the discovery and manipulation of emerging mesoscale phenomena; and (3) experimentally validate and refine the computational tools using atom-resolution materials synthesis in tandem with cutting-edge characterization methods. The research is expected to advance the fundamental understanding of the mesoscale pattern formation in metal-insulator transitions, topological mesoscale textures, co-evolution of coupled spin, lattice, electron, and polarization order parameters, as well as the coupling between mesoscale materials textures and superconducting order parameters.

Keywords: Phase-field Method, Mesoscale Structures, Quantum Materials

Recent Progress

We made major progress in developing phase-field models of coupled lattice and electronic processes and applying them to materials undergoing structural and electronic phase transitions and mesoscale structure evolution. We also developed a dynamical version of phase-field method by coupling polarization dynamics and elastodynamics and are currently extending it to include mobile carrier dynamics. We successfully predicted the formation of transient metallic monoclinic phase formation and the phase oscillation during voltage-driven insulator-metal transition in VO₂ and the formation and dynamics of vortices in ferroelectric heterostructures with experimental validation in collaboration with ANL, SLAC, LBL, and BNL. We are developing multigrid-based finite-element solver modules and the I/O tools for the phase-field software package Q-POP (Quantum Phase-field OPen source).

Phase-field Model of Coupled Electronic Insulator-metal and Structural Transitions [1-4]

We completed the development of a phase-field model for coupled electronic and structural transitions as well as electronic carrier dynamics incorporating stress/strain and electrostatic contributions. Using VO₂ as a prototypical correlated system undergoing both electronic and structural phase transitions, we predicted that an insulator-metal transition driven by ultrafast photoexcitation may experience an intermediate charge density wave state with a temperature-dependent characteristic wavelength through a spinodal mechanism. In collaboration with Lindenberg group at SLAC, we discovered the formation of transient metallic monoclinic phase during the voltage-driven insulator-metal transition in VO₂ thin films. Upon applying a voltage, the metallic rutile phase nucleates at regions with lower transition temperature and grows into the surrounding insulating monoclinic phase, turning it into a metallic monoclinic phase (Figure 1b). We computationally demonstrated the oscillation of alternating insulator and metal phases in VO₂ actuated by a direct bias voltage (Figure 1a), leading to oscillating voltage outputs with

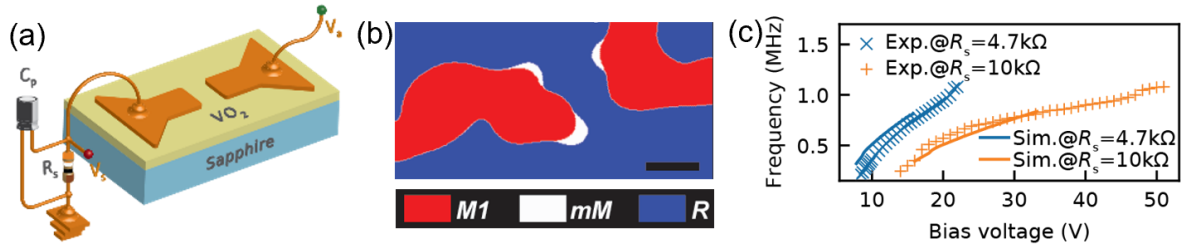


Figure 1 (a) A schematic of a VO_2 device; (b) A temporal snapshot of the calculated phase distribution during the voltage-driven insulator-metal transition in VO_2 , showing the metallic monoclinic (mM) phase stabilized between the equilibrium insulating monoclinic (M1) and metallic rutile (R) phases on a microsecond time scale; (c) Phase-field predicted (lines) and experimentally measured (markers) frequency scaling with the direct bias voltage of the voltage oscillation in VO_2 .

characteristic frequencies (Figure 1c), and the results are validated by experiments from Purdue and Draper Lab. We showed that the nonequilibrium carrier dynamics is critical to the emergence of the voltage oscillation and imposes a fundamental limit to the maximal frequency, which is crucial to both the fundamental science and the device engineering of Mott-insulator-based oscillators. We are currently in collaboration with several experimental groups at LBL, BNL, ANL, and SLAC to further explore the mesoscale evolution dynamics of this fascinating system.

Dynamical Phase-field Model of Collective Dynamics of Topological Structures

We developed a dynamical phase-field model of polarization dynamics and elastodynamics [5-6] and are extending it to allow interaction between polarization/elastodynamics and electronic carriers generated by ultrafast stimuli. We predicted two sub-THz collective phonon modes unique to polar vortices in $\text{PbTiO}_3/\text{SrTiO}_3$ superlattices (see Figure 2a for a schematic of the vortex structure) using dynamical phase-field simulations. The phase-field predictions of structural response are validated by ultrafast X-ray diffraction measurement as shown in Figure 2b by Wen and Freeland groups at ANL. In particular, the slower mode represents a vertical motion of the vortex cores as indicated by phase-field and atomistic simulations (see Figure 2c). We further developed an analytical model of the energetics of the phonon modes and calculated their frequencies, which are consistent with the experimental measurements and phase-field simulations (Figure 2d). We showed that elastic modulation of the energy function and spring constants lead to a condensation of a collective mode upon a second-order structural transition from symmetric to asymmetric vortices at a critical strain, analogous to the ferroelectric soft phonon mode at a ferroelectric transition. The work offers a theoretical framework for predicting and manipulating the ultrafast collective dynamics of polar nanostructures.

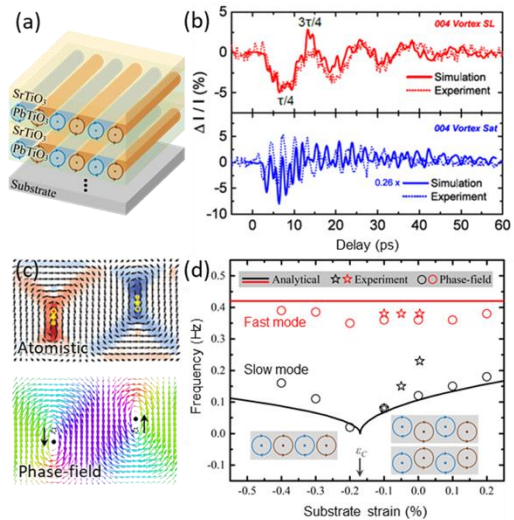


Figure 2 (a) Schematic of polar vortices in $\text{PbTiO}_3/\text{SrTiO}_3$ superlattice (b) Time evolution of SL and Sat XRD peak intensities upon electric-field excitation, from phase-field and experiment (c) Collective motion of vortices from atomistic and phase-field simulations; (d) Slow and fast mode frequencies vs strain from analytical model, phase-field, and experiment.

Phase-field Model of Coupled Light-Excited Carrier and Ferroelectric Domain Dynamics

Upon excitation by external stimuli like light or current pulses, electronic carrier concentrations in solids can be transiently raised by orders of magnitude from their ground state, thus, giving rise to properties and phenomena vastly different from those at equilibria. We developed a phase-field model for modeling the simultaneous evolution dynamics of carriers and ferroelectric domains upon external excitation [7]. As an illustrative example, we simulate the transient response of the most common 90° twin domains in a PbTiO_3 crystal excited by an ultrafast above-bandgap light pulse (see Figure 3a). We discover a two-stage relaxational carrier concentration evolution across picosecond to nanosecond timescales around charged domain walls (Figure 3b). Meanwhile, a transient structural response is induced with two fast oscillation components and a slower relaxational component which signifies dynamics of domains, domain walls, and charges, respectively (see Figure 3c for the strain evolution). The work offers a theoretical framework for predicting and manipulating carrier-related ultrafast dynamics of ferroelectric domains and is expected to stimulate future ultrafast experiments on the rich coupled evolution dynamics of domains, domain walls, and charge carriers. In collaboration with ANL and LBL, we are currently applying this model to understand the influence of the light-excited electronic carriers on mesoscale supercrystal formation and evolution dynamics in ferroelectric heterostructures.

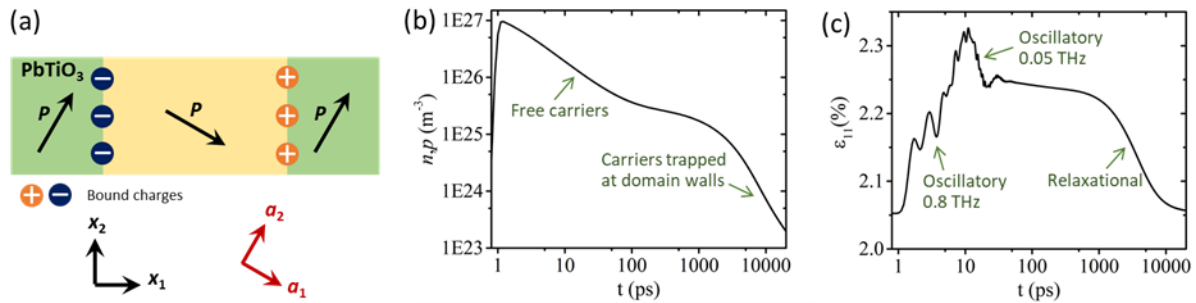


Figure 3 (a) Schematic of charged 90° domain walls in PbTiO_3 (b-c) Simulated evolution of (b) average carrier concentration and (c) average strain after applying a light pulse at $t = 1\text{ps}$.

Open-Source Software Package Development

We established an open-source framework for a computer software package termed Q-POP, an important first step towards building flexible and easily maintainable phase-field library modules. We are developing solver modules for the general set of static and dynamic phase-field equations using the multigrid finite element method as well as special numerical schemes to handle complex boundary conditions [8] and processes at very different timescales [9]. We are building common utilities, including a standard I/O interface, a high-throughput first-principles calculation software to provide thermodynamic and kinetic input data for phase-field simulations, and a tool for calculating the equilibrium temperature-strain phase diagrams which can be used drastically reduce the number of phase-field simulations [10]. We are automating the construction of energy functions for inputs to phase-field simulations. We developed post-processing routines to identify the types and locations of topological features in mesoscale structures from phase-field simulations [11]. We are developing routines to compute the x-ray diffraction patterns to allow direct comparisons between phase-field simulations and diffraction experiments.

Future Plans

- To develop the phase-field models and codes for electron and lattice dynamics involving spin ordering for predicting the coupled spatiotemporal evolution of electron, spin, and lattice and experimentally validate them using the strongly correlated $\text{Ca}_3\text{Ru}_2\text{O}_7$ system as a test example and for coupled structural and superconducting phase transitions with elasticity and experimentally validate them using FeSe films on SrTiO_3 substrates as examples.
- Continue to develop scalable multigrid finite-element solvers for phase-field equations of metal-insulator transitions, electron carrier dynamics, polarization dynamics, spin dynamics, superconducting phase transitions, and implement them into the software package Q-POP.
- Explore the oscillation of VO_2 filaments under fundamental frequencies and search for potential chaotic voltage oscillations in VO_2 systems.
- Study the formation and dynamics of topological structures in ferroelectric heterostructures under the influence of electronic carrier generation from ultrafast stimuli.

References

1. Y. Shi and L.Q. Chen, Spinodal Electronic Phase Separation During Insulator-Metal Transitions. *Physical Review B*, 2020. 102(19): 195101.
2. A. Sood, X.Z. Shen, Y. Shi, S. Kumar, S.J. Park, M. Zajac, Y.F. Sun, L.Q. Chen, S. Ramanathan, X.J. Wang, W.C. Chueh, and A.M. Lindenberg, Universal Phase Dynamics in VO_2 Switches Revealed by Ultrafast Operando Diffraction. *Science*, 2021. 373(6552): 352-+
3. Y. Shi, A.E. Duwel, D.M. Callahan, Y.F. Sun, F.A. Hong, H. Padmanabhan, V. Gopalan, R. Engel-Herbert, S. Ramanathan, and L.Q. Chen, Dynamics of Voltage-Driven Oscillating Insulator-Metal Transitions. *Physical Review B*, 2021. 104(6): 064308.
4. Y. Shi and L. Q. Chen, "Intrinsic Insulator-Metal Phase Oscillations", Submitted to *Physical Review Letters*, 2021.
5. Q. Li, V.A. Stoica, M. Pasciak, Y. Zhu, Y.K. Yuan, T.N. Yang, M.R. McCarter, S. Das, A.K. Yadav, S. Park, C. Dai, H.J. Lee, Y. Ahn, S.D. Marks, S.K. Yu, C. Kadlec, T. Sato, M.C. Hoffmann, M. Chollet, M.E. Kozina, S. Nelson, D.L. Zhu, D.A. Walko, A.M. Lindenberg, P.G. Evans, L.Q. Chen, R. Ramesh, L.W. Martin, V. Gopalan, J.W. Freeland, J. Hlinka, and H.D. Wen, Subterahertz Collective Dynamics of Polar Vortices. *Nature*, 2021. 592(7854): 376-+
6. T. N. Yang, C. Dai, Q. Li, H. D. Wen, and L. Q. Chen, Condensation of Collective Polar Vortex Modes. *Physical Review B*, 2021. 103(22): L220303.
7. T. N. Yang and L. Q. Chen, "Phase-field Model of Coupled Light-Excited Carrier and Ferroelectric Domain Dynamics", submitted to *Nature Computational Science*, 2021.
8. X. Xu, L. Zhang, Y. Shi, L.-Q. Chen, and J. Xu, "Integral Boundary Conditions in Phase-field Models", 2021. <https://arxiv.org/abs/2108.06769>
9. Jacob A. Zorn, L. M. Ma, J. C. Xu, and L. Q. Chen, "An Adaptive Time-Stepping Scheme for Phase-Field Calculations", submitted to *Computers and Mathematics with Applications*, 2021.
10. J. A. Zorn, B. Wang, L. Q. Chen, "Q-POP-Thermo: A General-Purpose Thermodynamics Solver for Ferroelectric Materials", submitted to *Computer Physics Communications* 2021.
11. J. A. Zorn, T. N. Yang, L. Q. Chen, "Vector Decomposition of Novel Polar States: An Analysis of Polar Vortex Identification Methods", submitted to *Computational Materials Science* 2021.

Publications

1. Y. Shi and L.Q. Chen, Spinodal Electronic Phase Separation During Insulator-Metal Transitions. *Physical Review B*, 2020. 102(19): 195101.
2. K.N. Zhang, J.J. Wang, Y.H. Huang, L.Q. Chen, P. Ganesh, and Y. Cao, High-Throughput Phase-Field Simulations and Machine Learning of Resistive Switching in Resistive Random-Access Memory. *npj Computational Materials*, 2020. 6(1): 198.
3. W. Peng, J.A. Zorn, J. Mun, M. Sheeraz, C.J. Roh, J. Pan, B. Wang, K. Guo, C.W. Ahn, Y.P. Zhang, K. Yao, J.S. Lee, J.S. Chung, T.H. Kim, L.Q. Chen, M. Kim, L.F. Wang, and T.W. Noh, Constructing Polymorphic Nanodomains in BaTiO₃ Films Via Epitaxial Symmetry Engineering. *Advanced Functional Materials*, 2020. 30(16): 1910569.
4. S.B. Cheng, M.H. Lee, R. Tran, Y. Shi, X. Li, H. Navarro, C. Adda, Q.P. Meng, L.Q. Chen, R.C. Dynes, S.P. Ong, I.K. Schuller, and Y.M. Zhu, Inherent Stochasticity During Insulator-Metal Transition in VO₂. *Proceedings of the National Academy of Sciences of the United States of America*, 2021. 118(37): e2105895118.
5. S. Das, Z. Hong, V.A. Stoica, M.A.P. Goncalves, Y.T. Shao, E. Parsonnet, E.J. Marks, S. Saremi, M.R. McCarter, A. Reynoso, C.J. Long, A.M. Hagerstrom, D. Meyers, V. Ravi, B. Prasad, H. Zhou, Z. Zhang, H. Wen, F. Gomez-Ortiz, P. Garcia-Fernandez, J. Bokor, J. Iniguez, J.W. Freeland, N.D. Orloff, J. Junquera, L.Q. Chen, S. Salahuddin, D.A. Muller, L.W. Martin, and R. Ramesh, Local Negative Permittivity and Topological Phase Transition in Polar Skyrmions. *Nature Materials*, 2021. 20(2): 194-+
6. Q. Li, V.A. Stoica, M. Pasciak, Y. Zhu, Y.K. Yuan, T.N. Yang, M.R. McCarter, S. Das, A.K. Yadav, S. Park, C. Dai, H.J. Lee, Y. Ahn, S.D. Marks, S.K. Yu, C. Kadlec, T. Sato, M.C. Hoffmann, M. Chollet, M.E. Kozina, S. Nelson, D.L. Zhu, D.A. Walko, A.M. Lindenberg, P.G. Evans, L.Q. Chen, R. Ramesh, L.W. Martin, V. Gopalan, J.W. Freeland, J. Hlinka, and H.D. Wen, Subterahertz Collective Dynamics of Polar Vortices. *Nature*, 2021. 592(7854): 376-+
7. A.S. McLeod, A. Wieteska, G. Chiriaco, B. Foutty, Y. Wang, Y. Yuan, F. Xue, V. Gopalan, L.Q. Chen, Z.Q. Mao, A.J. Millis, A.N. Pasupathy, and D.N. Basov, Nano-Imaging of Strain-Tuned Stripe Textures in a Mott Crystal. *npj Quantum Materials*, 2021. 6(1): 46.
8. Y. Shi, A.E. Duwel, D.M. Callahan, Y.F. Sun, F.A. Hong, H. Padmanabhan, V. Gopalan, R. Engel-Herbert, S. Ramanathan, and L.Q. Chen, Dynamics of Voltage-Driven Oscillating Insulator-Metal Transitions. *Physical Review B*, 2021. 104(6): 064308.
9. A. Sood, X.Z. Shen, Y. Shi, S. Kumar, S.J. Park, M. Zajac, Y.F. Sun, L.Q. Chen, S. Ramanathan, X.J. Wang, W.C. Chueh, and A.M. Lindenberg, Universal Phase Dynamics in VO₂ Switches Revealed by Ultrafast Operando Diffraction. *Science*, 2021. 373(6552): 352-+
10. A. J. Sternbach, F. L. Ruta, Y. Shi, Tetiana V. Slusar, Jacob S. Schalch, G. Duan, Alexander S. McLeod, X. D. Zhang, M. Liu, A. Millis, H.-T. Kim, L-Q. Chen, R. D. Averitt, D. N. Basov "Anchored heterogeneous nucleation in the light-induced insulator-to-metal transformation of Vanadium Dioxide, Submitted to *Nano Letters* 2021.
11. F. Xue, T.N. Yang, and L.Q. Chen, Theory and Phase-Field Simulations of Electrical Control of Spin Cycloids in a Multiferroic. *Physical Review B*, 2021. 103(6): 064202.
12. T.N. Yang, C. Dai, Q. Li, H.D. Wen, and L.Q. Chen, Condensation of Collective Polar Vortex Modes. *Physical Review B*, 2021. 103(22): L220303.
13. S. Chen, Q. Hong, J. Xu, and K. Yang, "Robust block preconditioners for poroelasticity", *Computer Methods in Applied Mechanics and Engineering*. 2020; 369:113229.

Machine Learning Aided Modeling of Resistive Switching Phenomena in Correlated Electron Systems

Gia-Wei Chern, University of Virginia

Program Scope

The overarching goal of this project is to develop theoretical modeling of nonequilibrium dynamical phenomena, and particularly the resistive switching phenomena, in strongly correlated electron systems through machine-learning enabled large-scale dynamical simulations. Novel functionalities of correlated electron materials often originate not only from the microscopic electron dynamics and correlation effects, but also from the intriguing spatial-temporal textures at the mesoscopic scale. Comprehensive modeling of such phenomena, however, requires accurate quantum calculation at the microscale as well as large-size dynamical simulations in order to take into account the crucial role of spatial fluctuations and inhomogeneity. Such an integration is especially difficult for correlated electron systems since the many-body techniques required to properly describe the quantum state of correlated electrons is very time-consuming. We propose in this project to employ modern machine learning (ML) methods to overcome the computational difficulties of incorporating sophisticated quantum calculation into large-scale dynamical simulations in strongly correlated electron systems.

A three-stage research program is proposed to achieve the objective of multi-scale modeling. In the first step, the nonequilibrium Green's function method will be integrated with real-space dynamics simulation, such as Landau-Lifshitz-Gilbert and Langevin dynamics, on relatively small-scale systems. The results from these studies will shed light on the microscopic mechanisms of resistive switching as well as the mesoscopic building blocks (domain walls, filaments) of the associated inhomogeneous states. The second stage is to build machine-learning models using datasets generated from the small-scale simulations. Major activities include implementation of the appropriate descriptor, training the artificial neural network, benchmark and validations. And finally, with the trained neural nets, we will conduct large-scale dynamics simulation of the switching phenomena and investigate the structural and statistical properties, as well as the dynamical characteristics of the resistance transition.

Keywords: Machine learning potentials, Nonequilibrium dynamics, Strongly correlated electron materials.

Recent Progress

Our first goal in this project is to develop the ML-potential for adiabatic dynamical simulations of well-known correlated electron models in condensed matter physics. To this end, we have demonstrated the first-ever machine-learning enabled large-scale quantum Landau-

Lifshitz-Gilbert (LLG) dynamics simulation of the double-exchange (DE) model [1], which plays a crucial role in the colossal magnetoresistance effect. In particular, we have developed a novel magnetic descriptor that preserves both the spin-rotation and lattice symmetries for describing the local spin configurations. A multi-layer neural network (NN) combined with the magnetic descriptor is trained using dataset from exact diagonalization on small lattices; see Figure 1. Not only that our trained NN potential can successfully reproduce the spin-dynamics on small lattices, we have also carried out large-scale ML-LLG simulations to uncover truly new physics of the nonequilibrium phase-separation phenomena in this canonical correlated electron system.

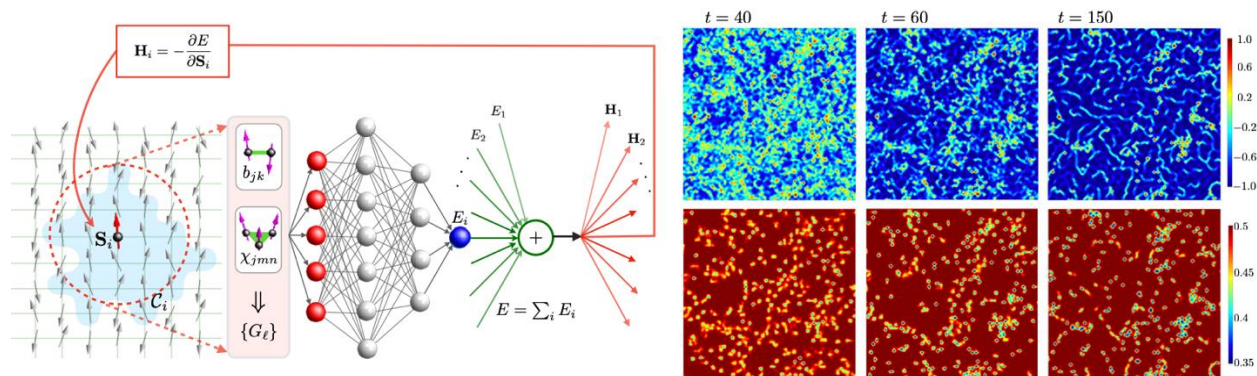


Figure 1. (Left) Machine learning potential for force prediction of the DE model. (Right) Snapshots of spin-spin correlation (top panels) and local electron density (bottom panels) during phase separation.

We uncover an intriguing correlation-induced freezing behavior as doped holes are segregated from half-filled insulating background during equilibration. While the aggregation of holes is stabilized by the formation of ferromagnetic clusters through Hund's coupling between charge carriers and local magnetic moments, this stabilization also creates confining potentials for holes when antiferromagnetic spin-spin correlation is well developed in the background. The dramatically reduced mobility of the self-trapped holes prematurely disrupts further growth of the ferromagnetic clusters, leading to an arrested phase separation, as shown in Figure 1.

The ML techniques have also been applied to enable the first-ever large-scale quantum kinetic Monte Carlo (kMC) simulations in the Falicov-Kimball model [2], which is another representative correlated electron systems. We discover an unusual phase-separation scenario where domain coarsening occurs simultaneously at two different scales: the growth of checkerboard clusters at smaller length scales and the expansion of super-clusters, which are aggregates of the checkerboard patterns of the same sign, at a larger scale. We show that the emergence of super-clusters is due to a hidden dynamical breaking of the sublattice symmetry. A self-trapping mechanism related to the super-clusters gives rise to the arrested growth of the checkerboard patterns and of the super-clusters themselves. Glassy behaviors similar to the one reported in this work could be generic for other correlated electron systems.

In tandem with the effort of ML-potential for force predictions from quasi-equilibrium electron subsystem, we have also developed numerical methods for dynamical simulations of driven correlated electron systems far from equilibrium. Specifically, we have combined the nonequilibrium Green's function (NEGF) method with the LLG dynamics for driven double-exchange (DE) systems, as well as NEGF integrated with effective dynamics for Gutzwiller slave bosons for driven Hubbard models. In particular, we show that the insulator-to-metal transition induced by an applied voltage in the DE is initiated by the nucleation of a thin ferromagnetic conducting layer at the anode. The metal-insulator interface separating the two phases is then driven toward the opposite electrode by the voltage stress, giving rise to a growing metallic region. We further show that the initial transformation kinetics is well described by the Kolmogorov-Avrami-Ishibashi model with an effective spatial-dimension that depends on the applied voltage.

While ML-potential for adiabatic quasi-equilibrium electronic forces have been widely used in *ab initio* molecular dynamics research, and generalized to correlated electron system by our group, the method cannot be directly applied to *nonequilibrium* electronic forces. This is because almost all ML-potential relies on the so-called Behler–Parrinello (BP) scheme [3], which implicitly assumes a conservative force, namely the force is given by the derivative of an effective energy, which is computed from the ML-model; see Figure 1 for details. However, since the nonequilibrium force is in general nonconservative, hence is beyond the conventional BP approach. One of the most important results of this project is our development of a novel NN potential that is capable of representing the non-equilibrium electronic forces for quantum spin dynamics; see Figure 2 (left). Taking advantage of the fact that spin-dynamics needs to conserve the length of the magnetic moment, we obtain a general expression for the forces which can be expressed as derivatives of two potentials. This then allows us to develop a generalized BP-type NN that can predict the local energies for these two potentials. LLG simulations based on our new ML-potential agrees very well with those using the exact NEGF method; see Figure 2.

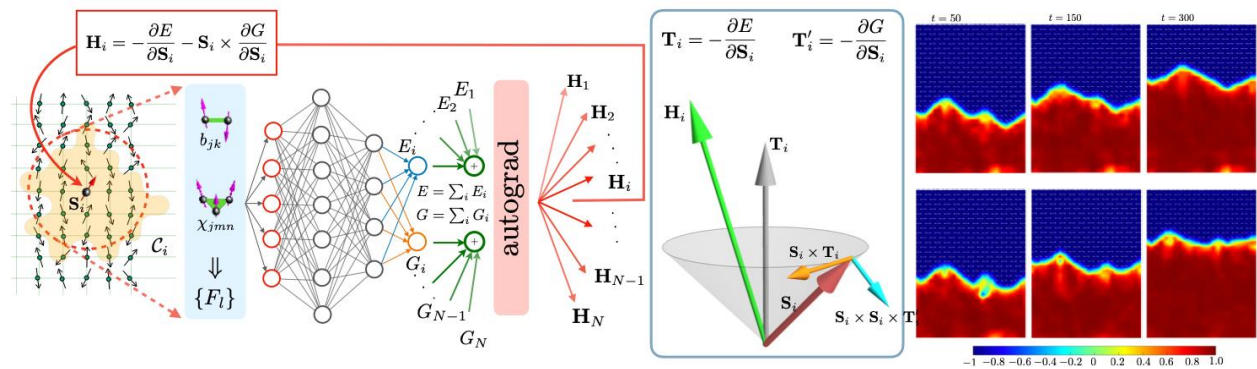


Figure 2. (Left) Machine learning potential for *nonequilibrium* force prediction of the DE model. (Middle) Generalized potentials for nonequilibrium forces. (Right) Comparison of the ML-LLG (top) with exact NEGF-LLG simulations of domain-wall propagation in a driven DE system.

Future Plans

One unexpected outcome of our generalized NN for nonequilibrium forces is the efficient prediction of the spin-transfer torques (STT). These are forces generated by itinerant electrons in metallic ferromagnets widely used in spintronics research. To further explore this application, we have implemented NEGF-LLG simulations for the Rashba s-d metal, and successfully reproduce the first-ever full-microscopic nonequilibrium simulation of the Skyrmion Hall effect. Using datasets generated from these exact simulations, we have seen very promising training. One of our future plans is to demonstrate large-scale simulations of current-driven Skyrmion dynamics based on the our generalized NN model shown in Figure 2.

Kinetic Monte Carlo is one of the most widely used tools in the study of resistive-switching in conventional materials (for example, those based on ion-migration dynamics). Encouraged by our previous works on ML-enabled kMC simulations for temperature-quench dynamics on Falicov-Kimball (FK) model, we plan to generalize the kMC simulations and the ML-models for the non-equilibrium dynamics of voltage-driven FK model. One crucial step is to generalize the Metropolis/Glauber dynamics to the out-of-equilibrium setup.

We will also integrate both the Hartree-Fock and Gutzwiller methods with the NEGF calculation for quantum molecular dynamics (QMD) simulations of Hubbard-type model with on-site Holstein or Peierls electron-lattice coupling. The additional self-consistent iteration significantly increases the computational overhead for simulating such full interacting systems. Further code optimization with massive parallelization is underway.

While we have successfully developed NN-potential for nonequilibrium force prediction in quantum spin dynamics, such as the NEGF-LLG simulations, it remains unclear how to develop a similar ML scheme for the nonequilibrium forces in QMD simulations. We have succeeded in developing generalized potentials (similar to the spin case) for two-dimensional MD simulations. We are currently exploring different formulations for the most general three-dimensional case. Successful development of this formulation is crucial to the ML-application for large-scale QMD simulation of out-of-equilibrium systems. This tool not only is important for our proposed multi-scale modeling of correlated electron systems, but also has tremendous implications for the DFT-based MD widely used in the quantum chemistry and materials science communities.

References

- [1] E. Dagotto, *Nanoscale phase separation and colossal magnetoresistance* (Springer 2002).
- [2] L. M. Falicov and J. C. Kimball, *Phys. Rev. Lett.* **22**, 997 (1969).
- [3] J. Behler and M. Parrinello, *Phys. Rev. Lett.* **98**, 146401 (2007).

Publications

1. Puhang Zhang and G.-W. Chern, Arrested Phase Separation in Double-Exchange Models: Large-Scale Simulation Enabled by Machine Learning, *Physical Review Letters* **127**, 146401 (2021).
2. Sheng Zhang, Puhang Zhang, and G.-W. Chern, Anomalous phase separation and hidden coarsening of super-clusters in the Falicov-Kimball model, arXiv:2105.13304.
3. G.-W. Chern, Spatio-temporal dynamics of voltage-induced resistance transition in the double-exchange model, arXiv:2105.11076.
4. Lingnan Shen and G.-W. Chern, Cell dynamics simulation of coupled charge and magnetic phase transformation in correlated oxides, *Physical Review E* **103**, 032134 (2021).
5. Puhang Zhang, Preetha Saha, and G.-W. Chern, Machine learning dynamics of phase separation in correlated electron magnets, arXiv:2006.04205.

Quantum Anisotropic-Exchange Magnets

Principal Investigator: Alexander Chernyshev

Institution: Department of Physics and Astronomy, University of California, Irvine

Keywords: strongly-anisotropic exchange, dynamics in quantum magnets, spin-orbit interaction

Project Scope

The central objective of this program is to advance understanding of the extensive family of quantum materials with spin-orbit-generated interactions, which offer an unusually rich spectrum of opportunities for realizing unconventional ordered and exotic quantum-disordered phases. Our research is focused on their enigmatic ground states, their unusual excitations, unconventional disorder-induced phenomena in them, and their anomalous magneto-thermal transport properties. Our effort can be expected to significantly deepen the fundamental knowledge of the physical properties of a diverse group of quantum materials, provide an immediate impact in the experimental research, yield predictions of new phenomena, and offer crucial insights into the potentially transformative properties of anisotropic-exchange magnets and into the nature of their excitations.

Recent Progress

Fingerprinting Triangular Antiferromagnet by Excitation Gaps.-- CeCd_3As_3 is a notable representative of a rapidly growing class of the rare-earth-based triangular-lattice materials, in which the paradigmatic geometric frustration due to a triangular motif of their lattice structure is inherently combined with the celebrated Kitaev-like bond-dependent interactions, originating from the strong spin-orbit coupling in the rare-earth ions. However, recent avalanche of new materials has uncovered the lack of a clear roadmap to their comprehensive understanding. In our recent work [1], we presented a joint experimental-theoretical study that offers CeCd_3As_3 as if not a Rosetta stone for this field, but at least as an essential keystone for such a comprehensive understanding. In our work with LANL colleagues [1], the low-T heat capacity measurements of CeCd_3As_3 enabled us to study the field-evolution of its spin-excitation gaps. Our theoretical insights into the phase diagram and excitation spectrum, based on a recent progress by our group in understanding of a generic anisotropic-exchange model on a triangular

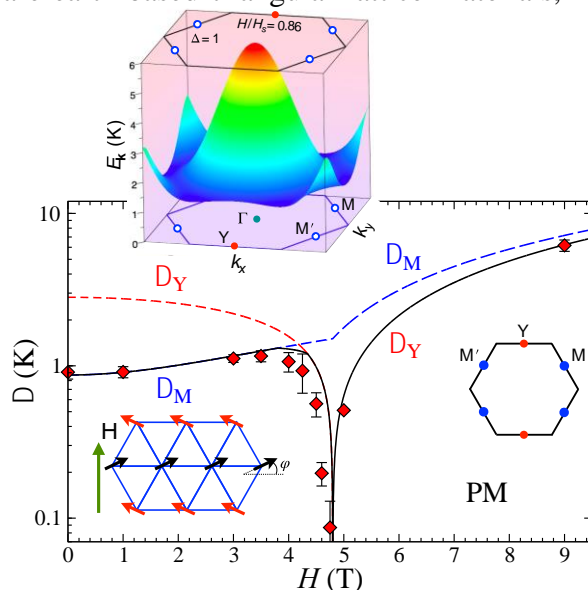


Figure 1. From [1]. Field-dependence of spin-excitation gaps in CeCd_3As_3 , experiment and theory. Insets: Stripe phase in a field. Excitation spectrum at $H/H_s=0.86$ throughout Brillouin zone.

lattice, allowed us to unequivocally identify the ground state of CeCd_3As_3 as belonging to a stripe phase and yielded a close agreement with a non-trivial field-dependence of the gaps. The phenomenological constraints on the parameters of the microscopic model resulted in an unprecedented level of certainty regarding the ground state and parameter region of the general phase diagram where CeCd_3As_3 is likely to belong. This is unique among the rare-earth-based triangular-lattice systems and is expected to enable a better understanding of this important class of materials. Our study provides a much-needed framework to this area of research, creates a foundation for future studies of a large group of materials with anisotropic exchanges, connects and extends different approaches used in this broad field of study, clears the path to a consistent interpretation of the current and future experiments, and gives important new insights into fundamental properties of quantum magnets with spin-orbit-generated low-energy spin systems.

Spin texture induced by a non-magnetic doping and spin dynamics in 2D triangular lattice antiferromagnet.-- Novel effects induced by nonmagnetic impurities in frustrated quantum magnets and spin liquids is a highly nontrivial and interesting problem. A theoretical proposal of extended modulated spin structures induced by doping of such magnets and are distinct from the well-known skyrmions has attracted significant interest. Recent experimental neutron-scattering study was initiated by a theoretical proposal originating in an earlier work by our group [2]. We have suggested that a seemingly benign dilution-like impurities in the frustrated magnets must necessarily result in spin textures, which, in turn, should induce a very unusual features in the magnet's excitation spectra. This prediction was validated in the recent neutron-scattering experiments that has measured the full dynamical structure factor in Al-doped h-YMnO_3 , a triangular antiferromagnet with noncollinear magnetic order, and confirmed the presence of magnon damping with a clear momentum dependence, in agreement with our original proposal. The theoretical calculations presented in our work can reproduce the key features of the INS data, supporting the formation of the proposed spin textures and our group has contributed to the analysis of the data and a positive interpretation of the effect [2]. Our study has provided the first experimental confirmation of the impurity-induced spin textures and offered new insights and understanding of the impurity effects in a broad class of noncollinear magnetic systems and to the broader area of unconventional disorder-induced phenomena.

Phase Diagram of YbZnGaO_4 in Applied Magnetic Field.-- Among the rare-earth-based anisotropic-exchange materials, a system that sparked an explosion of experimental and theoretical interest is the triangular-lattice antiferromagnet YbMgGaO_4 , which has led to a broad research effort that currently involves a number of related compounds. In our recent joint work with the neutron-scattering group at Duke University, we have proposed that the experimental and theoretical investigations of the field-induced phases offer a powerful instrument to significantly narrow the allowed parameter space to a region that is consistent with the material's phenomenology [3]. This enriched map of the phase space serves as a basis to restrict the values of parameters describing the magnetic Hamiltonian with broad application to recently discovered related materials. More specifically, we have found that the external field tends to stabilize the

three-sublattice structures in a region of parameters that far exceeds the nominal three-sublattice footprint of the zero-field phase diagram, see Fig. 2. This finding is in a close accord with the sensitive magnetic torque and inelastic neutron scattering experiments, which suggested a migration of the scattering intensity to the three-sublattice ordering vector vs field. We have demonstrated the power of these experimental and theoretical insights in identifying relevant parameter spaces of YbMgGaO_4 and YbZnGaO_4 . We have shown that despite their disorder-induced pseudo-SL ground states we can significantly narrow the allowed regions of their phase diagram that are compatible with their phenomenologies. More experimental and theoretical investigations were suggested for exploring the phase diagram of this group of compounds and shedding further light on their rich physics. Our work will serve as a guide in the search of quantum spin liquids and other intriguing phenomena in frustrated triangular-lattice compounds.

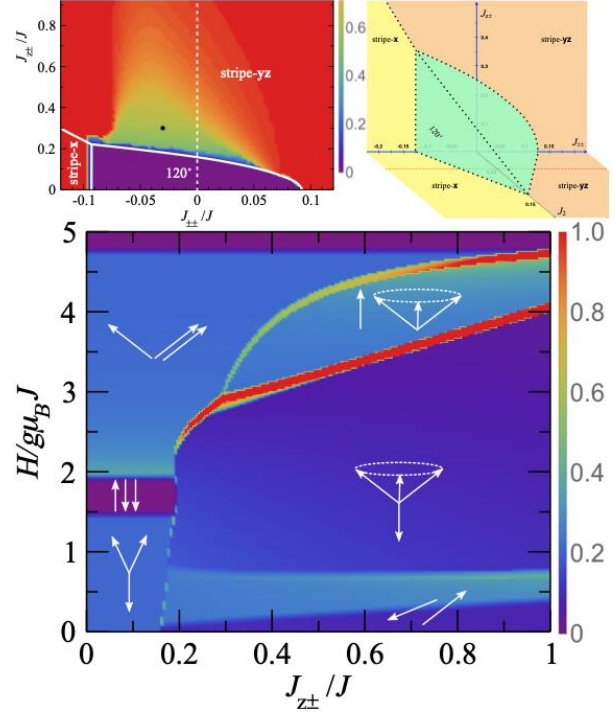


Figure 2. From Ref. 3. Magnetic susceptibility, in the $J_{z\pm}$ - H plane for $\Delta=1.1$, $J_2=0.05J$, and $J_{\pm\pm}=0$. Singularities correspond to phase transitions. Upper panels: Region of transitions from the four- to three-sublattice state in $J_{z\pm}$ - $J_{\pm\pm}$ axes, dot: parameters for YbZnGaO_4 ; Zero-field $J_{z\pm}$ - $J_{\pm\pm}$ - J_2 phase diagram.

Generalized J - K - Γ - Γ' - J_3 model on the honeycomb lattice, α - RuCl_3 , and strong anharmonic couplings of magnons.—In two recent studies [4,5], we have investigated the phase diagram and a variety of dynamical properties of the extended J - K - Γ - Γ' - J_3 model on the honeycomb lattice, a model that is of great current interest as it is related to α - RuCl_3 and several other new materials. These works continue to advocate a scenario originally proposed in our group, that the broad features in the spectrum of α - RuCl_3 are due to strong anharmonic coupling of the single-magnon excitations at higher energies to the two-magnon continua of the lower-energy magnons. In these recent works [4,5], this scenario was demonstrated to be applicable to a vastly wider regions of the parameter space of the anisotropic-exchange model,—roughly speaking, to the entire phase diagram except where the off-diagonal exchange terms are artificially suppressed,—without the need of an artificial fine-tuning of the parameters in the “proximate-Kitaev” spin-liquid scenario. Using explicit calculations of the dynamical structure factor for representative parameters, we strongly substantiated our proposal by showing a coexistence of the broad continua with the well-defined low-energy modes in the inelastic neutron scattering spectrum in a close agreement with experiments. In Ref. [4], we have demonstrated that empirical constraints lead to significant restrictions and rather drastic revisions of the physically reasonable parameter space for the effective microscopic spin model of α - RuCl_3 . Specifically, the ESR and THz data in the

field-induced paramagnetic regime, combined with the analysis of the in-plane critical fields, out-of-plane tilt angle, bandwidth of the magnetic signal, and the zigzag nature of the ground state, produce convincing bounds on the parameters of this model. It is concluded that the relevant physics of α - RuCl_3 is not related to a model with a dominating Kitaev term, affiliated with a proximate spin-liquid state. The only proximity in the phase diagram that is present in this case is that to an incommensurate phase, which is continuously connected to a ferromagnetic one. For the much-discussed spectral properties of α - RuCl_3 , the conclusion of this work also unambiguously points toward the physics of the strongly interacting and mutually decaying magnons, not to that of the fractionalized excitations.

Future Plans

For the next years, we plan to continue our studies of quantum effects in anisotropic-exchange magnets with a focus on their dynamical and transport properties and on the role of disorder in them. Specifically, we have several ongoing projects:

- A study into the ground state and spectral properties of the anisotropic-exchange honeycomb-lattice Kitaev-Heisenberg magnets in the proximity of the zigzag-to-ferromagnet phase boundary is ongoing.
- We have a close understanding of a rather astonishing behavior of the magnetoresistance in the magnetically-intercalated graphite EuC_6 .
- In a light of recent progress in new honeycomb-lattice materials, we plan to focus on the easy-plane version of their model.
- A study of the transverse-field Ising material and its intricate dynamical properties is planned.
- A study of the longitudinal component of the dynamical response in the anisotropic-exchange magnets is expected.

Publications (August 2019 – August 2021)

1. K. E. Avers, P. A. Maksimov, P. F. S. Rosa, S. M. Thomas, J. D. Thompson, W. P. Halperin, R. Movshovich, and A. L. Chernyshev, “*Fingerprinting Triangular-Lattice Antiferromagnet by Excitation Gaps,*” *Phys. Rev. B* **103**, L180406 (2021). (Editors' Suggestion).
2. P. Park, K. Park, J. Oh, K. H. Lee, J. C. Leiner, H. Sim, T. Kim, J. Jeong, K. C. Rule, K. Kamazawa, K. Iida, T. G. Perring, H. Woo, S.-W. Cheong, M. E. Zhitomirsky, A. L. Chernyshev, and J.-G. Park, “*Spin texture induced by non-magnetic doping and spin dynamics in 2D triangular lattice antiferromagnet $h\text{-Y}(\text{Mn,Al})\text{O}_3$,*” *Nat. Commun.* **12**, 2306 (2021).
3. W. Steinhardt, P. A. Maksimov, S. Dissanayake, Z. Shi, N. P. Butch, D. Graf, A. Podlesnyak, Y. Liu, Y. Zhao, G. Xu, J. W. Lynn, C. Marjerrison, A. L. Chernyshev, and S. Haravifard, “*Phase Diagram of YbZnGaO_4 in Applied Magnetic Field,*” *npj Quantum Materials* **6**, 78 (2021).
4. P. A. Maksimov and A. L. Chernyshev, “*Rethinking α - RuCl_3 ,*” *Phys. Rev. Research* **2**, 033011 (2020).
5. R. L. Smit, S. Keupert, O. Tsyplatyev, P. A. Maksimov, A. L. Chernyshev, and P. Kopietz, “*Magnon damping in the zigzag phase of the Kitaev-Heisenberg-Gamma model on a honeycomb lattice,*” *Phys. Rev. B* **101**, 054424 (2020).

Machine-Assisted Quantum Magnetism

S. Chowdhury, Howard University (Principal Investigator/Project Director)
A. Bansil, Northeastern University (Co-Investigator, Lead Northeastern)
J. Turner, Stanford University/SLAC (Co-Investigator, Lead SLAC/Stanford)
M. Amoo, Howard University (Co-Investigator)
A. Feiguin, Northeastern University (Co-Investigator)
C. Jia, Stanford University/SLAC National Accelerator Laboratory (Co-Investigator)
A. Lindenberg, Stanford University (Co-Investigator)
Y. Nashed, SLAC National Accelerator Laboratory (Co-Investigator)
J. Thayer, SLAC National Accelerator Laboratory (Co-Investigator)
C. Yoon, SLAC National Accelerator Laboratory (Co-Investigator)
sugata.chowdhury@howard.edu

Some of the most exciting and exotic physics occurs in the field of quantum magnetism, where strong electron correlations and entanglement lead to topological magnets and emergent magnetic excitations.¹ This can lead to new states of matter, such as the long-sought but elusive spin liquid. One key issue limiting progress in this field is the lack of experimental capabilities to study low-energy excitations in materials at equilibrium as well as that of comprehensive theoretical modeling schemes. By taking advantage of the innovative capabilities of the DOE's Linac Coherent Light Source (LCLS) to provide novel experimental data on low-energy modes of magnetic materials that are not accessible anywhere else with x-rays,^{2,3} together with a theoretical framework that includes three of the most powerful, modern computational approaches (exact diagonalization (ED), advanced density-functional theory (DFT), and the density-matrix renormalization group (DMRG)), we will make fundamental advances in the understanding of quantum magnetism. This project will combine the scientific domains of quantum materials (experiment, theory, and computation) with that of high-performance computing and multimodal experimental workflows to achieve real-time, machine-assisted control and analysis of x-ray scattering studies at LCLS to significantly reduce time to discovery. Specific research activities include investigations of: (1) skyrmions⁴⁻⁶ in systems such as Fe/Gd multilayers⁵ and CrI₃⁶; (2) the pyroxene family of 1D Mott insulators and 1D-cuprate CuGeO₃; and (3) new materials, such as the α -RuCl₃/graphene heterostructure⁷. Experimental techniques are X-ray photon fluctuation spectroscopy, ultrafast x-ray and electron diffraction, and THz spectroscopy. The proposed work will give insight into areas of spontaneous fluctuations, quantum criticality, and the discovery of exotic phases.

Keywords: Machine learning, quantum magnetism, quantum spin liquid, DFT, DMRG, ED, skyrmions, Mott insulators, THz spectroscopy.

Reference:

1. A. Banerjee et al. *Science* **356**, 1055 (2017)
2. M. Seaberg et al., *Phys. Rev. Lett.* **119**, 067403 (2017)
3. L. Shen, et al., *MRS Advances* (accepted for publication).
4. V. Esposito, et al., *Appl. Phys. Lett.* **116**, 181901 (2020)
5. M. H. Seaberg, et. Al. *Phys. Rev. Research.* 3, 033249 (2021)
6. A. Behera, et. al. *Appl. Phys. Lett.* **114**, 232402 (2019).
7. S. Biswas et. al. *Phys. Rev. Lett.* 123, 237201, (2019).

Competing Orders in Multi-Orbital Systems

Andrey V Chubukov, University of Minnesota

Program Scope

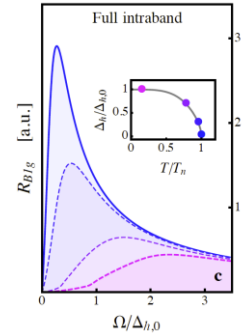
This main scope of this program is to understand the interplay between superconductivity and competing orders, such as magnetism, nematicity, and valley and orbital order, in two set of systems -- twisted bilayer graphene (TBG) and related systems, e.g., rhombohedral trilayer graphene, and multi-orbital Fe-based superconductors (FeSCs), most notably pure and doped FeSe. The overarching theme of these two classes of materials is the presence of an additional symmetry - valley symmetry in TBG and orbital symmetry in FeSCs. Breaking of valley or orbital symmetry leads to particular electronic orders and affects the pairing. Both TBG and FeSCs currently attract high level of interest in the physics community [R1-R3]. The key goal of my research is to unravel new physics in these systems by departing from a model of interacting electrons and analyzing mutually affecting instabilities in particle-particle and particle-hole channels. For TBG and related systems, my primary goal is to derive the low-energy itinerant fermion model, analyze the manifold of ordered states that break spin and valley symmetry, either separately or together, at various fillings, including the ones near van Hove singularities, find the number of associated Goldstone modes and the splitting of the fermionic levels, analyze the interplay between spin/valley orders and superconductivity, and compare with strong coupling approaches [R4,R5]. For FeSe and related systems, my key goal is to analyze how normal state behavior and superconductivity are affected by orbital transmutation -- the change of orbital composition of low-energy excitations in the presence of a nematic order. This non-linear feedback from breaking the orbital symmetry affects the physics beyond widely discussed mixing of s-wave and d-wave pairing channels in the nematic phase. The effect is particularly strong in FeSe, where it makes all Fermi pockets nearly mono-orbital deep in the nematic phase.

Another scope of my program is to analyze the experimentally detectable fermionic spectral function and bosonic response in a superconductor with pairing mediated by soft nematic fluctuations [R6]. This is relevant both doped FeSeS and nematic superconductivity in TBG. In this part of my research, I explore the fact that near a nematic transition the couplings in different pairing channels are nearly identical and investigate how this near degeneracy affects the nematic resonance in a superconductor and the spectral function of fermions. To do this analysis, I include the dressing of particle-hole contributions and terms that couple particle-hole and particle-particle responses.

Keywords: Superconductivity and competing orders in twisted bilayer graphene, orbital transmutation in multi-orbital superconductors, fermionic and bosonic spectral functions near a nematic transition.

Recent Progress

1. With my student D. Chichinadze, my colleagues from Minnesota and Rome, I analyzed several effects associated with orbital physics in FeSCs. In Ref. [1], we analyzed the magnitude of the jump of a specific heat at superconducting T_c in a situation when the mass of a fermion on the d_{xy} orbital is substantially larger than those on d_{xz} and d_{yz} orbitals. In this situation, we argued that the jump of the specific heat is substantially smaller than in BCS theory because heavy d_{xy} fermions give the largest contribution to specific heat in the normal state, but contribute little to its jump at T_c . Below T_c specific heat first tends to a finite value at T decreases, and drops only $T \ll T_c$, when d_{xy} fermions pair. We favorably compared the results with the experiments on hole doped KFe_2As_2 and similar materials. In Ref. [2] we provided theoretical explanation of Raman experiments in FeSCs, which show that in the nematic phase, Raman intensity in B_{1g} (nematic) channel nearly vanishes at small frequencies, but at higher frequencies recovers to the same value as in the tetragonal (non-nematic) phase. Such a vanishing would be expected in a superconductor, but not in the normal state. We argued that deep in the nematic phase Fermi pockets become almost mono-orbital, and B_{1g} Raman susceptibility nearly coincides with density susceptibility, which vanishes by charge conservation. At larger frequencies, Fermi pockets recover their multi-orbital character, and B_{1g} Raman intensity recovers the value it had without nematic order. In Ref. [3] we applied similar reasoning to explain ARPES data in non-superconducting nematic state of FeSe. I also collaborated with the experimental group from IFW Dresden on the co-existence of nematic and superconducting orders in LiFeAs (Ref. [4]) and with my Minnesota colleagues on how one can experimentally detect an antiferromagnetic critical point under a superconducting dome (Ref. [5]). We argued that the temperature dependence of the specific heat deep inside the fully gapped superconductor becomes singular at the onset of antiferromagnetism, and a conventional exponential behavior is replaced by a T^2 power-law behavior.



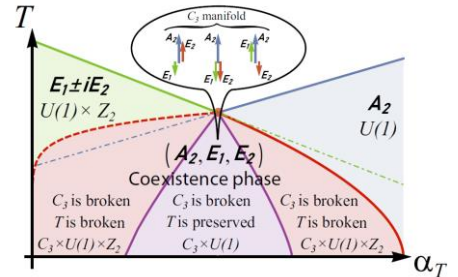
B_{1g} Raman intensity above the nematic transition (blue) and in the nematic phase.

2. With a postdoc A. Klein and my colleagues D. Maslov and L.P. Pitaevskii, we analyzed zero-sound type collective excitations in a 2D Fermi liquid near and away a nematic instability. (Refs. [6-9]). The "conventional" view of the zero-sound mode is that for repulsive interaction it resides outside the particle-hole continuum and gives rise to a sharp peak in the corresponding susceptibility, while for attractive interaction it is a damped mode inside the particle-hole continuum. We showed that there exist two additional types of zero sound: hidden and mirage modes. A hidden mode resides outside the particle-hole continuum already for attractive interaction. It does not appear as a sharp peak in the susceptibility, but determines the long-time transient response of a Fermi liquid and can be identified in pump-probe experiments. A mirage mode emerges for strong enough repulsion. Unlike the conventional zero sound, it is not a true propagating mode, yet it gives rise to a peak in the particle-hole susceptibility and can be

identified by measuring the width of the peak, which for a mirage mode is larger than the single-particle scattering rate.

3. Inspired by renewed experimental interest to superconductivity in SrTiO₃ and other systems with low density of carriers [R7], I analyzed, together with colleagues from Amherst [10], the interplay between electron-phonon and electron-electron interaction in an s-wave superconductor, with predominantly repulsive interaction, particularly the threshold for the pairing and the sign change of the gap $\Delta(\omega)$ between small and large frequencies. I also wrote a review article with colleagues from Stanford and Texas on superconductivity in a system with electron-phonon interaction brought about to a CDW instability (Ref. [11]).

4. With L. Classen from BNL, we analyzed in Ref. [12] the interplay between superconductivity and competing orders near a higher-order van Hove point with power-law singularity in the density of states, suggested for magic angle TBG. We used an effective low-energy model for electrons near higher-order Van Hove points and analyze the competition between different ordering tendencies using an unbiased renormalization group approach. For purely repulsive interactions, we find that the two key competitors are ferromagnetism and chiral superconductivity. With Chichinadze and Classen, I did two works on TBG. In the first work, we analyzed electron-mediated superconductivity near the van-Hove filling within the flat band [13] and found that in some circumstances superconducting order necessary breaks lattice rotational symmetry (see Fig. on the right for the summary plot). In the second work [14], we analyzed spin and valley orders near the van Hove filling in the ladder approximation and found that the system develops either a magnetic or valley order. A magnetic order is ferromagnetic within a valley, but the angle between magnetic moments in the two valleys is arbitrary.



Superconducting phases for TBG near van Hove filling. The co-existence phase with C3 symmetry broken is a nematic superconductor

Future Plans

One future plan is to advance the itinerant approach to TBG and to trilayer graphene. With Chichinadze, Classen, and Y. Wang from UF, we derived [15] the Landau functionals for the particle-hole order parameters at van Hove fillings and for a smaller filling, when the Fermi surface consists of disconnected pockets near K and K' points, and found that the order parameter manifold in the cases has an approximate SU(4) symmetry, but differ in the sign of the quartic terms. We determined the structure of the degenerate ground state and analyzed its excitations. For small fillings, we find a strong 1st-order transition to an SU(3) * U(1) manifold of orders that break spin-valley symmetry and induce a 3-1 splitting of fermionic excitations. Importantly, the ordered states from the manifold are necessary the combinations of spin and valley orders. For Van Hove filling, we find a weak 1st-order transition from an ordinary metal to an SO(4)*U(1) manifold of orders that preserves the two-fold band degeneracy and gives rise

to 2-2 splitting. My next plan is to move continuously from charge neutrality to maximal doping and analyze how the system evolves if the order, that develops near a particular doping, remains finite at larger doping. Along these lines, I also plan to study superconductivity in the presence of a spin/valley order.

Another plan is to study in more detail novel physics in Fe-based superconductors. I plan to analyze how orbital transmutation affects the thermodynamics in the nematic state and the angular variation of pairing gap (both have been extensively analyzed experimentally). I also plan to analyze Te-doped FeSe, for which ARPES experiments detected parity change along k_z for a band that does not cross the Fermi level. My goal is to verify whether may give rise to specific, ARPES detectable k_z variation of the superconducting gap, and, more generally, affect the pairing mechanism.

Finally, I plan to study the structure of collective excitations (e.g., a neutron resonance peak) for a superconductor in which pairing is mediated by charge nematic fluctuations. This topic is directly related to FeSe doped by S, which at 20% S doping undergoes a $T=0$ transition between a nematic and a tetragonal phase under the dome of superconductivity, and it is likely relevant to TBG and related systems as there a superconducting order co-exists with nematicity in some region under superconducting dome, at least at hole doping, where superconducting T_c is the largest.

References

- R1. Y. Cao, V. Fatemi, S. Fang, K. Watanabe, T. Taniguchi, E. Kaxiras, and P. Jarillo-Herrero, *Nature* 556, 43 (2018).
- R2. E. Y. Andrei and A. H. MacDonald, *Nature materials* 19, 1265 (2020).
- R3. A. I. Coldea and M. D. Watson, *Annual Review of Condensed Matter Physics* 9, 125 (2018).
- R4. N. Bultinck, E. Khalaf, S. Liu, S. Chatterjee, A. Vishwanath, and M. P. Zaletel, *Phys. Rev. X* 10, 031034 (2020).
- R5. D. Wong, K. P. Nuckolls, M. Oh, B. Lian, Y. Xie, S. Jeon, K. Watanabe, T. Taniguchi, B. A. Bernevig, and A. Yazdani, *Nature* 582, 198 (2020).
- R6. S. Lederer, Y. Schattner, E. Berg, and S. A. Kivelson, *Phys. Rev. Lett.* 114, 097001 (2015).
- R7. C. Collignon, X. Lin, C. W. Rischau, B. Fauqué, and K. Behnia, *Annual Review of Condensed Matter Physics* 10, 25 (2019).

Publications

- [1] D. V. Chichinadze and A. V. Chubukov, *Phys. Rev. B* 99, 024509 (2019).
- [2] M. Udina, M. Grilli, L. Benfatto, and A. V. Chubukov, *Phys. Rev. Lett.* 124, 197602 (2020).
- [3] M. H. Christensen, R. M. Fernandes, and A. V. Chubukov, *Phys. Rev. Research* 2, 013015 (2020).
- [4] Y. S. Kushnirenko, D. V. Evtushinsky, T. K. Kim, I. Morozov, L. Harnagea, S. Wurmehl, S. Aswartham, B. Büchner, A. V. Chubukov, and S. V. Borisenko, *Phys. Rev. B* 102, 184502 (2020).
- [5] V. S. de Carvalho, A. V. Chubukov, and R. M. Fernandes, *Phys. Rev. B* 102, 045125 (2020).
- [6] A. Klein, D. L. Maslov, L. P. Pitaevskii, and A. V. Chubukov, *Phys. Rev. Research* 1, 033134 (2019).
- [7] A. Klein, D. L. Maslov, and A. V. Chubukov, *npj Quantum Materials* 5, 1 (2020).
- [8] A. Klein, Y.-M. Wu, and A. V. Chubukov, *npj Quantum Materials* 4, 1(2019).
- [9] X. Y. Xu, A. Klein, K. Sun, A. V. Chubukov, and Z. Y. Meng, *npj Quantum Materials* 5, 1 (2020).
- [10] A. Chubukov, N. V. Prokof'ev, and B. V. Svistunov, *Phys. Rev. B* 100, 064513 (2019).
- [11] A. V. Chubukov, A. Abanov, I. Esterlis, and S. A. Kivelson, *Annals of Physics* 417, 168190 (2020).
- [12] L. Classen, A. V. Chubukov, C. Honerkamp, and M. M. Scherer, *Phys. Rev. B* 102, 125141 (2020).
- [13] D. V. Chichinadze, L. Classen, and A. V. Chubukov, Nematic superconductivity in twisted bilayer graphene, *Phys. Rev. B* 101, 224513 (2020).
- [14] D. V. Chichinadze, L. Classen, and A. V. Chubukov, *Phys. Rev. B* 102, 125120 (2020).
- [15] D. V. Chichinadze, L. Classen, Y. Wang and A. V. Chubukov, arXiv: 2108.05334.
- [16] D. Mozyrsky and A. V. Chubukov, *Phys. Rev. B* 99, 174510 (2019).
- [17] D. Pimenov, A. Kamenev, and A. V. Chubukov, *Phys. Rev. B* 103, 214519 (2021).

TOPOLOGY DRIVEN QUANTUM AND THERMAL DYNAMICS OF LOW-DIMENSIONAL MAGNETIC AND SUPERCONDUCTING SYSTEMS
DOE/BES Grant No. DE-FG02-93ER45487

Principal Investigator: Dr. Eugene M. Chudnovsky, Distinguished Professor
Department of Physics and Astronomy
Herbert H. Lehman College & CUNY Graduate School
The City University of New York
250 Bedford Park Boulevard West, Bronx, NY 10468-1589
Email: Eugene.Chudnovsky@Lehman.CUNY.edu

Project Scope

The work on the DOE/BES grant at CUNY Lehman College and Graduate School, and research planned in the nearest future, are focused on analytical and large-scale numerical studies of topology-driven phenomena in low-dimensional magnetic and superconducting systems. Recent publications acknowledging DOE support report studies of breathing dynamics of individual skyrmions (PRB-2020), interaction between skyrmions (JPhys-2020), formation of biskyrmion lattices (PRR-2019), skyrmions in the oblique field with an eye on developing binary and quaternary skyrmion-based memory (JMMM-2021), behavior of skyrmions near defects (JPhys-2021), and the origin of skyrmion mass (PRB-2021). This abstract reports our most recent work on quantization of nanoscale skyrmions in two-dimensional magnetic systems (PRB-2021). Quantum states of a skyrmion in a 2D antiferromagnetic lattice have been obtained by quantizing the scaling parameter of Belavin-Polyakov model. Skyrmion classical collapse due to violation of the translational invariance of the continuous spin-field model by the lattice is replaced in quantum mechanics by transitions between discrete energy levels of the skyrmion. Rates of transitions due to the emission of magnons have been computed and ways of detecting quantization of skyrmion states have been discussed. Future research will address quantization of and emission of magnons by ferromagnetic skyrmions, as well as quantum phenomena in skyrmion lattices. The effect of the underlying atomic lattice on the symmetry of the skyrmion lattice will be studied with an eye on structural phase transitions induced by the magnetic field.

Keywords: topology, skyrmions, quantum dynamics

Recent Progress

Even the smallest nanoscale skyrmions experimented with are still comprised of hundreds of spins. Such skyrmions have been imaged by the Lorentz transmission electron microscopy and are generally perceived as classical objects. As the skyrmion becomes smaller, however, one must expect that at some point quantum mechanics comes into play. This work is motivated by the observation that classical collapse of an unstable skyrmion into a point contradicts the uncertainty principle the same way as the classical collapse of an electron onto a proton does. Huge number of spin degrees of freedom possessed by the skyrmion resembles the problem of the many-electron atom for which analytical computation of quantum states is impossible. In Ref. 1 we took a different approach. A Belavin-Polyakov skyrmion is characterized by a scaling parameter λ that can be roughly interpreted as its size. In a continuous spin-field model the

energy of the skyrmion is independent of λ . However, as we have shown in Ref. 2, in a discrete model with a finite lattice spacing a the energy acquires a small term proportional to $-(a/\lambda)^2$. In the absence of stabilizing interactions, such as, e.g., Dzyaloshinskii-Moriya interaction (DMI), it leads to the collapse of a classical skyrmion. In quantum mechanics the lattice term can be interpreted as a potential well $U(\lambda)$ inside which the skyrmion must have quantized energy levels. In antiferromagnets, inertia associated with the dynamics of the Neel vector allows one to introduce the conjugate momentum associated with the generalized coordinate λ , making quantization of the problem conceptually similar to the quantization of a string loop collapsing under tension. We consider a 2D exchange model of antiferromagnetic spins in a square lattice that is relevant to parental compounds of high-temperature superconductors where copper spins belonging to weakly interacting CuO layers are arranged in a square lattice and coupled antiferromagnetically with negligible magnetic anisotropy and no DMI.

Wave functions and energy levels of the quantized skyrmion states are shown in Figs. 1a and 1b respectively. Here $x = \lambda/a$, parameter l is the lateral size of the system in units of a , and S is the spin of the lattice site.

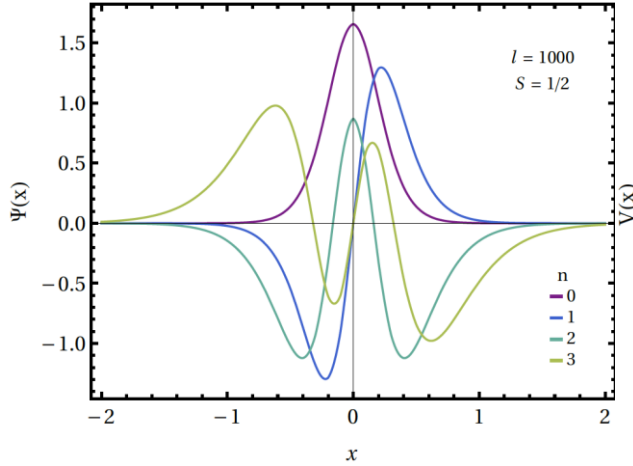


Fig. 1a: Wave functions of quantum skyrmion states.

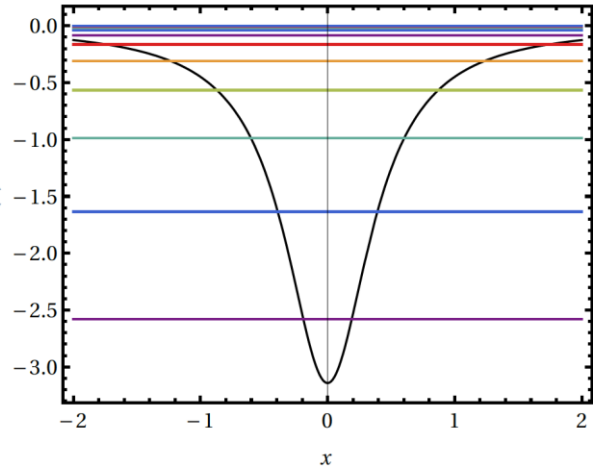


Fig. 1b: Skyrmion energy levels.

We also developed quantum theory of the skyrmion interaction with magnons and computed the rates of transitions between skyrmion states accompanied by the radiation of magnons. They are shown in Table 1 in units of J/\hbar , where J is the exchange constant. Due to quantum transitions, the collapse of a classically unstable skyrmion occurs in quantum mechanics as well, but the existence of quasi-stationary quantum states slows it down substantially.

nm	0	1	2	3	4	5	6	7	8
0	0	0.970×10^{-3}	0	1.36×10^{-3}	0	0.659×10^{-3}	0	2.00×10^{-4}	0
1	0	0	0.284×10^{-3}	0	0.389×10^{-4}	0	1.60×10^{-4}	0	0.439×10^{-4}
2	0	0	0	0.471×10^{-4}	0	0.603×10^{-4}	0	2.25×10^{-5}	0
3	0	0	0	0	0.512×10^{-5}	0	0.604×10^{-5}	0	2.01×10^{-6}
4	0	0	0	0	0	0.389×10^{-6}	0	0.417×10^{-6}	0
5	0	0	0	0	0	0	2.17×10^{-8}	0	2.11×10^{-8}
6	0	0	0	0	0	0	0	0.941×10^{-9}	0
7	0	0	0	0	0	0	0	0	0.328×10^{-10}

Table 1: Transition rates in units of J/\hbar from the state m to the state n of a skyrmion for $S = 1/2$ and $l = 1000$.

When many small skyrmions are thermally nucleated at elevated temperatures, we predict that quantization of their energies must lead to the observable peaks in the absorption and noise spectra corresponding to the transitions between skyrmion energy levels.

Future Plans

We are currently working on implementing a similar quantization procedure for a ferromagnetic skyrmion. This problem is more challenging than the antiferromagnetic problem because the conventional ferromagnetic dynamics corresponds to precession and it does not possess inertia.

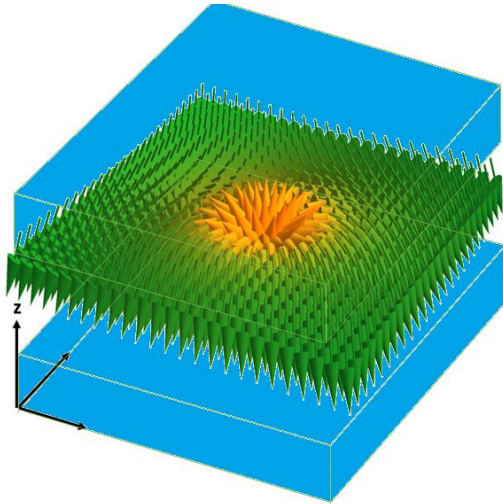


Fig. 2: Skyrmion in a magnetic film confined between nonmagnetic layers.

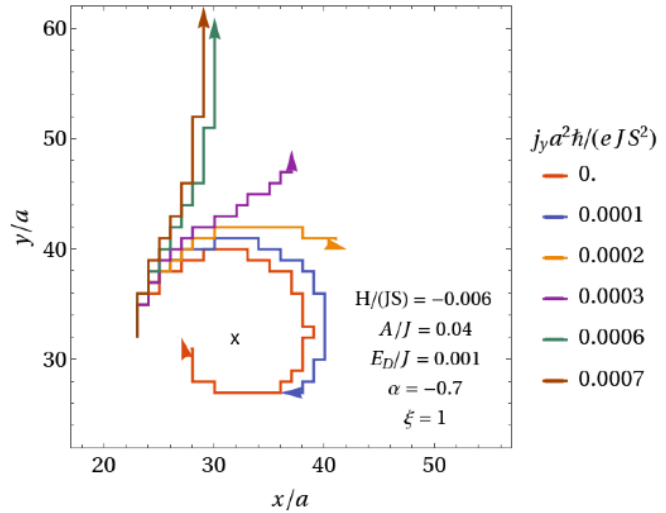


Fig. 3: Trajectories of a skyrmion driven by spin-polarized current in the vicinity of a defect.

Within the Heisenberg model the inertial mass of a ferromagnetic skyrmion is formally zero unless it is localized inside a potential well. In Ref. 3 we addressed the problem of generation of the skyrmion mass by a spin-phonon interaction in the absence of a confining potential. We studied a 2D magnetic film sandwiched between nonmagnetic layers as is shown in Fig. 2.

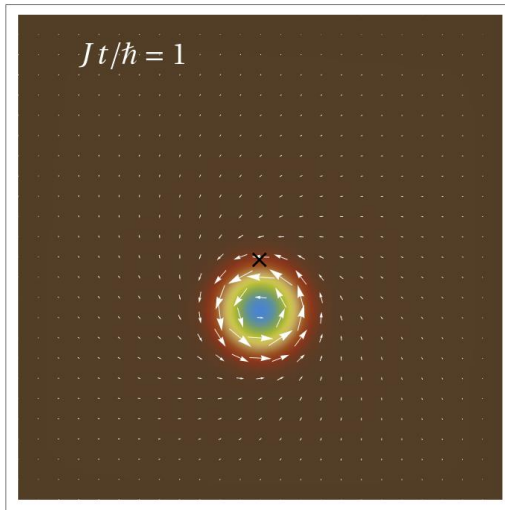


Fig. 4a: Skyrmion placed near defect.

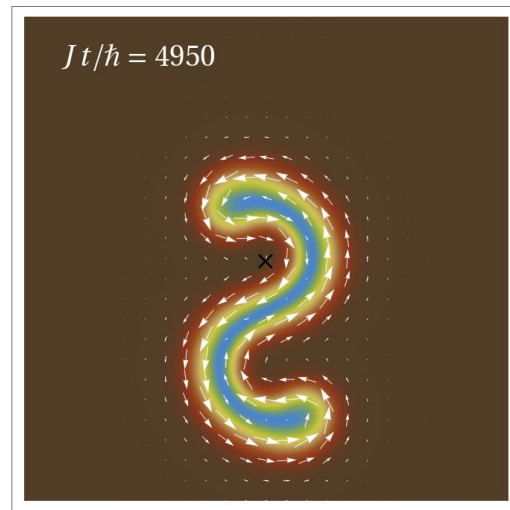


Fig. 4b: Time evolution of a skyrmion near defect.

The time-dependent spin field of a moving skyrmion induces, through magnetoelastic coupling, the motion of atoms whose inertia contributes to the mass of the skyrmion. This effect can be large in materials with high magnetostriction where it can contribute to quantum dynamics.

In Ref. 4 we also studied pinning of a skyrmion by a crystal defect and the classical motion of the skyrmion induced by a spin polarized current j , for various strengths of the exchange J , the DMI constant A , the dipole-dipole interaction E_D , the magnetic field H , as well as the strength of the exchange modification by the defect α and its spatial extent ξ , see Fig. 3. Within a certain parameter range the skyrmion deforms into a snake-like structure on approaching the defect, see Figs. 4a and 4b. Quantum states of a skyrmion coupled to a defect is the next problem on our list.

Most of the skyrmion lattices observed in experiments are triangular. This should be expected when the spacing between skyrmions is large compared to the atomic spacing. On reducing the distance between skyrmions by increasing magnetic field, one should expect the symmetry of the underlying atomic lattice to come into play. Such structural phase transitions will be investigated numerically. We also plan to study quantum spin excitations in dense skyrmion lattices.

References

1. A. Derras-Chouk, E. M. Chudnovsky, and D. A. Garanin, Quantum states of a skyrmion in a two-dimensional antiferromagnet, *Physical Review B* **103**, 224423-(8) (2021).
2. L. Cai, E. M. Chudnovsky, and D. A. Garanin, Collapse of skyrmions in two-dimensional ferromagnets and antiferromagnets, *Physical Review B* **86**, 024429-(4) (2012).
3. D. Capic, E. M. Chudnovsky, and D. A. Garanin, Skyrmion mass from spin-phonon interaction, *Physical Review B* **102**, 060404(R) (2020).
4. A. Derras-Chouk and E. M. Chudnovsky, Skyrmions near defects, *Journal of Physics: Condensed Matter* **33**, 195802 (2021).

Publications (October 2019 – October 2021, DOE/BES support acknowledged)

1. D. Capic, D. A. Garanin, and E. M. Chudnovsky, Biskyrmion lattices in centrosymmetric magnetic films, *Physical Review Research* **1**, 033011-(8) (2019).
2. D. A. Garanin, R. Jaafar, and E. M. Chudnovsky, Breathing mode of a skyrmion on a lattice, *Physical Review B* **101**, 014418-(11) (2020).
3. D. Capic, D. A. Garanin, and E. M. Chudnovsky, Skyrmion-skyrmion interaction in a magnetic film, *Journal of Physics: Condensed Matter* **32**, 415803 (2020).
4. D. Capic, E. M. Chudnovsky, and D. A. Garanin, Skyrmion mass from spin-phonon interaction, *Physical Review B* **102**, 060404(R) (2020).
5. D. A. Garanin and E. M. Chudnovsky, Conservation of angular momentum in the elastic medium with spins, *Physical Review B* **103**, L100412-(4) (2021).
6. A. Derras-Chouk and E. M. Chudnovsky, Skyrmions near defects, *Journal of Physics: Condensed Matter* **33**, 195802 (2021).
7. A. Derras-Chouk, E. M. Chudnovsky, and D. A. Garanin, Quantum states of a skyrmion in a two-dimensional antiferromagnet, *Physical Review B* **103**, 224423-(8) (2021).
8. D. Capic, D.A. Garanin, and E. M. Chudnovsky, Skyrmions in an oblique field, *Journal of Magnetism and Magnetic Materials* **537**, 168215 (2021).

Spin and Orbital Physics in Novel Quantum Materials

Piers Coleman, Center for Materials Theory, Department of Physics and Astronomy, Rutgers University.

Program Scope

The current program of research is interested in novel forms of superconductivity and spin order, including order that involves additional orbital degrees of freedom. The work to be presented will focus on triplet pairing driven by Hund's and by anisotropic ferromagnetic interactions. This is a topic motivated by a wide range of correlated quantum materials, including the iron-based superconductors[1], transition metal chalcogenides and the recently discovered heavy fermion materials UTe_2 [2] and $CeRh_2As_2$ [3].

One of our key areas of research has been to extend the idea of resonating valence bond theory to triplet pairing. Here, the key idea is that a spin-triplet RVB (tRVB) state, driven by spatially, or orbitally anisotropic ferromagnetic interactions can provide the parent state for triplet superconductivity. This idea is particularly interesting for Hund's coupled systems where the center of symmetry lies away from the atomic sites, for in these systems the entangled triplet pairs inside an atom can coherently admix with triplet Cooper pairs on the Fermi surface[4], providing the triplet condensate has an odd mirror symmetry about the center of inversion.

We have applied apply this idea to the iron-based superconductors [5] arguing that strong onsite Hund's interactions develop intra-atomic tRVBs between the t_{2g} orbitals. On doping, the presence of two iron atoms per unit cell allows these inter-orbital triplets to coherently delocalize onto the Fermi surface, forming a fully gapped triplet superconductor. This mechanism gives rise to a unique staggered structure of onsite pair correlations, detectable as an alternating π phase shift in a scanning tunnelling Josephson microscope.

Recently, we have extended the idea of tRVB to triangular lattices with anisotropic ferromagnetic couplings[6], with a perceived application to transition metal chalcogenide compounds.

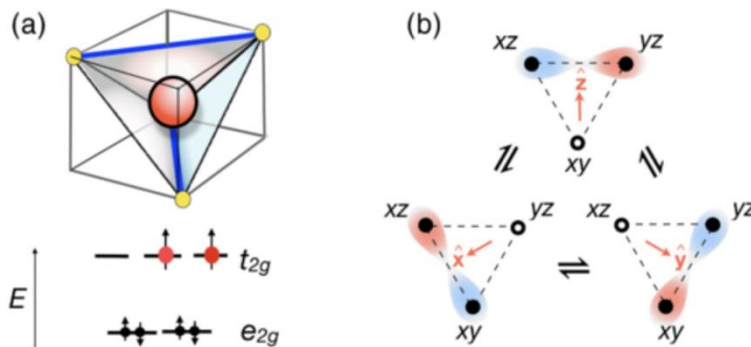


Figure 1. (a) Isolated tetrahedron in iron-based superconductors, showing the two electrons forming a $S=1$ triplet in the t_{2g} orbitals. b) Triplet resonating valence bond (tRVB) as the ground state of a Hund's metal atom. The blue and red colors reflect the odd parity of the triplet pairs, while the red arrows denote the quantization axis (d vector) of the $m=0$ triplet pair.

Keywords: Triplet superconductivity, Hund's metals, Resonating Valence Bonds.

Recent Progress

Working with Alexei Tsvelik (BNL) we have recently discovered a set of almost-integrable Kondo lattice models involving the Kondo coupling of a Majorana spin liquid (described by the Yao-Lee variant of the Kitaev spin liquid) to a conduction band[7]. Unlike conventional treatments of Kondo lattice systems, these take advantage of the pre-existing fractionalization of spins into Majorana fermions in the Yao-Lee model[8]. In work nearing completion, We are able to show that these models exhibit the phenomenon of “order fractionalization” whereby the developing order is described by a charge e , spin $\frac{1}{2}$ spinor, and a decoupled neutral Fermi surface. This work is available for a talk presentation, and a preprint will shortly be available.

Future Plans

Under development is an approach to tRVB that can take into account the strong energy dependence of interactions, we have developed a Schwinger boson scheme that describes Hund's coupled orbitals in t_{2g} orbitals. We are currently seeking to extend this Schwinger boson description to incorporate tRVB triplet pairing. We are also seeking to extend this work to describe UTe₂. UTe₂ is a likely triplet superconductor, yet its intersite spin correlations are known to be antiferromagnetic, making ferromagnetic Hund's coupling a compelling driver for the pairing.

References

- [1] T.-H. Lee, A. Chubukov, H. Miao, and G. Kotliar, *Phys. Rev. Lett.* **121**, 187003 (2018).
- [2] S. Ran, C. Eckberg, Q.-P. Ding, Y. Furukawa, T. Metz, S. R. Saha, I.-L. Liu, M. Zic, H. Kim, J. Paglione, N. P. Butch, Nearly ferromagnetic spin-triplet superconductivity. *Science* **365**, 684–687 (2019).
- [3] S. Khim, J. F. Landaeta, J. Banda, N. Bannor, M. Brando, P. M. R. Brydon, D. Hafner, R. Küchler, R. Cardoso-Gil, U. Stockert, A. P. Mackenzie, D. F. Agterberg, C. Geibel, E. Hassinger. Field-induced transition within the superconducting state of CeRh₂As₂. *Science*, 2021; 373 (6558)
- [4] P. W. Anderson, Further consequences of symmetry in heavy-electron superconductors, *Phys. Rev. B* 32, 499 (1985).
- [5] Piers Coleman, Yashar Komijani, Elio J. König, The Triplet Resonating Valence Bond State and Superconductivity in Hund's Metals, *Phys. Rev. Lett.* 125, 077001 (2020).

[6] Elio J. König, Yashar Komijani, Piers Coleman, Triplet resonating valence bond theory and transition metal chalcogenides , arXiv:2109.03851, (2021).

[7] P. Coleman and A. M. Tsvelik, Order Fractionalization in a Kitaev Kondo model, in preparation (2021)

[8] H. Yao and D.-H. Lee, Fermionic magnons, non-abelian spinons, and the spin quantum Hall effect from an exactly solvable spin-1/2 Kitaev model with SU(2) symmetry, Phys. Rev. Lett. 107, 087205 (2011).

Publications

1. Triplet resonating valence bond theory and transition metal chalcogenides , Elio J. König, Yashar Komijani, Piers Coleman, arXiv:2109.03851, (2021).
2. Emergent Potts Order in a Coupled Hexatic-Nematic XY model , Victor Drouin-Touchette, Peter P. Orth, Piers Coleman, Premala Chandra, Tom C. Lubensky, arXiv:2103.01878, (2021).
3. Emergent moments in a Hund's impurity, Victor Drouin-Touchette, Elio J. König, Yashar Komijani, Piers Coleman, arXiv:2101.10332 Phys. Rev. B 103, 205147 (2021).
4. Frustrated Kondo impurity triangle: A simple model of deconfinement. Elio J. König, Piers Coleman, Yashar Komijani, arXiv:2002.12338, Phys. Rev. B 104, 115103 (2021).
5. Spin magnetometry as a probe of stripe superconductivity in twisted bilayer graphene , Elio, J. König, Piers Coleman and A. M. Tsvelik, arXiv:2006.10684, Phys. Rev. B 102, 104514 (2020).
6. Tunneling spectroscopy of quantum spin liquids, Elio J. König, Mallika T. Randeria and Berthold Jack, arXiv:1912.06142, Phys. Rev. Lett. 125, 2672-6 (2020).
7. Soluble limit and criticality of fermions in Z₂ gauge theories, Elio J. König, Piers Coleman, Alexei M. Tsvelik, arXiv:1912.11106, Phys. Rev. B 102, 155143 (2020).
8. The Triplet Resonating Valence Bond State and Superconductivity in Hund's Metals, Piers Coleman, Yashar Komijani, Elio J. König, arXiv:1910.03168, Phys. Rev. Lett. 125, 077001 (2020).
9. Strongly interacting spin-orbit coupled Bose-Einstein condensates in one dimension, Siddhartha Saha, E. J. König, Junhyun Lee, J. H. Pixley, arXiv:1912.06142 Phys. Rev. Research 2, 013252 (2020).
10. Magic-Angle Semimetals with Chiral Symmetry, Yang-Zhi Chou, Yixing Fu, Justin H. Wilson, E. J. König, J. H. Pixley, arXiv:1908.09837, Phys. Rev. B 101, 235121 (2020).

Simulation, Design, and Discovery of Complex Materials

V. R. Cooper, T. Berlijn, R. S. Fishman, L. R. Lindsay, D. S. Parker (Oak Ridge National Laboratory)

Program Scope

The competition between energetically comparable phases determines whether a material can be synthesized and whether it will exhibit favorable properties under relevant operating conditions. While electronic structure theory and simulation offer exciting possibilities for accelerating the design of new materials, they often neglect phase transitions and competing secondary phases. The overarching goal of this project is to understand how defects and disorder, affect functionality and stability across a material's phase diagram. Addressing this challenge, we examine two key specific aims: (1) connecting phase stability to emergent material functionality in multicomponent, disordered compounds and (2) building insights into defect- and disorder-driven vibrational behaviors. We focus on bulk, multicomponent ceramics and metals. Central to this effort, has been the development and application of first-principles-derived methods to create realistic, materials-specific, predictive models that link phase-stability and material imperfections to functionality. This combined effort provides crucial insights into materials behavior, with direct relevance to experimental synthesis and characterization efforts with the aim of developing physical and chemical rules to accelerate materials design and discovery.

Keywords: Entropy stabilized materials, disorder, spin waves

Recent Progress

Novel approach to predicting the formability and ultimate synthesizability of bulk oxides: In 2015, the discovery of the entropy stabilized oxides added a new family to the class of high entropy materials. By mixing MgO, CoO, NiO, CuO and ZnO it was found that $\text{Mg}_{0.2}\text{Co}_{0.2}\text{Ni}_{0.2}\text{Cu}_{0.2}\text{Zn}_{0.2}\text{O}$ (hereafter MgO-HEO) could be stabilized in a rock-salt structure in which the cations are fully disordered [1]. The entropy stabilized oxides are not only interesting from a fundamental scientific point of view but may engender a wide variety of promising chemical, thermal, and electrical properties. Our research effort seeks to identify the relevant competing phases and structures that emerge to understand how materials responses to extrinsic factors such as magnetic/electric fields and temperature can be tuned through the control of disorder.

Using first-principles calculations, we demonstrated the ability to predict which 5-member oxides form stable, single-component high entropy compounds [2]. Using descriptors based on the average and standard deviations of binary oxide formation energies, we show that the original MgO-HEO was unique in its ability to form a single component oxide. The energies obtained from first-principles calculations were subsequently used to build a nearest-neighbor bond potential. Employing this potential with Monte Carlo simulations, we were able to reproduce the experimentally observed transition from a two-component phase mixture to a high-temperature

single phase material [1]. Surprisingly, our results allowed us to identify a previously hidden phase, obscured in X-ray diffraction data due to potentially overlapping Bragg reflection peaks. This study builds a foundation for further exploration of the temperature- and composition-dependent phase diagrams of disordered solid solutions. Our recent application to pyrochlores illustrates the strength of our approach for understanding the origin of the short range-order observed in neutron scattering [3].

Similarly, using first-principles thermodynamic calculations we demonstrated the origins of the formation of a ferromagnetic spinel upon Li doping into BiFeO_3 . The Li-doped perovskite was previously thought to be the ground state compound that would drive the material into a ferrimagnetic configuration. Our calculations showed that for most of the phase diagram, the LiFe_5O_8 spinel is substantially more stable (Fig. 1), thus making the Li-doped perovskite phase inaccessible [4]. These results represent a new direction towards understanding *how to place atoms* in the race towards accelerating the materials discovery process.

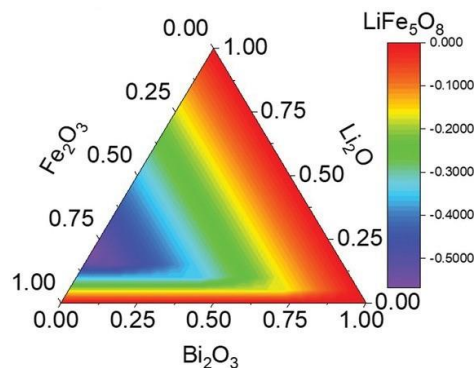


Figure 1 Computational phase diagram for the synthesis from Bi_2O_3 , Fe_2O_3 and Li_2O showing the strong thermodynamic preferences for the formation of LiFe_5O_8 rather than Li-doped BiFeO_3 [4].

Spin-waves keep on propagating despite extreme disorder: Recent neutron diffraction studies reported that bulk MgO-HEO displays antiferromagnetic (AFM) order with a Néel temperature on the order of 120K [5, 6]. Interestingly, inelastic neutron scattering measurements also demonstrated that spin-wave excitations persist up to room temperature. The discovery of magnetic long-range order and spin-wave excitations in MgO-HEO raises several questions. How can the experimentally observed AFM long range order be stabilized in the presence of randomly distributed moments of Co, Ni and Cu and 40% spin vacancies created by non-magnetic Mg and Zn ions? and What is the nature of spin-wave excitations in extremely disordered magnetic environments?

In our recent work [7], we theoretically investigated the magnetic ground state and spin-wave excitations in the high entropy oxide MgO-HEO. To treat the full effects of disorder we analyzed the magnetic properties via linear spin-wave theory in combination with the supercell approximation. We found that to stabilize the experimentally observed antiferromagnetic ground state, large next-nearest neighbor exchange couplings and large rhombohedral distortions are required. The spin-wave excitation spectrum of our

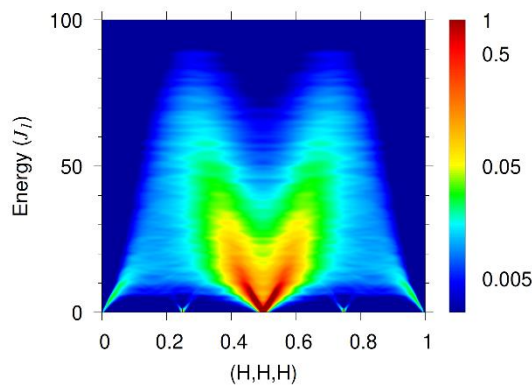


Figure 2 Spin-wave spectrum MgO-HEO obtained from averaging over 100 disordered supercells with 250 lattice sites on average.

J_1 - J_2 FCC spin-model for MgO-HEO (Fig. 2) is found to consist of a well-defined low-energy coherent spectrum in the background of an incoherent continuum at higher energies. From a general perspective, our study not only gives insight into the magnetic excitation spectrum of entropy-stabilized oxides, but also reveals the nature of spin-waves in extremely disordered magnets.

Success and Breakdown of the T-matrix Approximation for Phonon-Disorder Scattering: The ability to predict the thermal conductivity of materials with defects and disorder has grown increasingly crucial considering recent technological and environmental trends, from the miniaturization of electronics to the global energy crisis [8, 9]. First-principles T-matrix and perturbative approximations are commonly used to evaluate phonon-defect interactions in disordered materials. However, their success in predicting the thermal conductivity of strongly disordered alloys reported in Refs. [10-12] is surprising, given that these methods are only appropriate in the dilute limit. Additionally, the T-matrix approximation has not been critically evaluated for phonon-disorder scattering of flexure modes in two-dimensional and van der Waals layered materials, which typically carry a large proportion of the heat.

In our recent work [13], we examined the validity of the T-matrix approximation for treating phonon-defect scattering by implementing a linear scaling unfolding algorithm capable of *simulating tens of millions of atoms* and generalizing its applicability to mass disorder. We demonstrate that the T-matrix approximation fails to describe flexure phonon lifetimes in monolayers with vacancy concentrations greater than a few percent, which is typical for some prominent materials such as MoS₂. In particular, we show that the T-matrix approximation strongly underestimates the scattering rates of the low-energy flexure phonons (green-shaded region in Fig. 3) that are critically important for understanding thermal conductivity in two-dimensional monolayers and van der Waals layered materials with defects. Furthermore, we connect the phonon unfolding method to the popular Boltzmann transport formalism despite the breakdown of the phonon quasiparticle picture in alloys, building insights into the apparent success of T-matrix and perturbative approaches in these systems. Our methodology closes an existing modeling gap in the thermal transport of materials with medium and high concentrations of defects, elucidating the role of defect-limited thermal transport beyond the dilute limit.

Future Plans

We will continue to explore magnetism in entropy stabilized oxides. Of particular interest are open

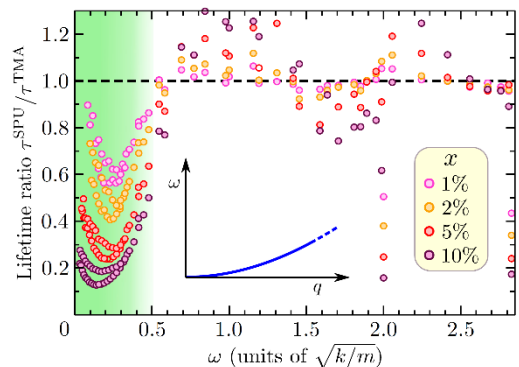


Figure 3 Ratio of phonon lifetimes from supercell phonon unfolding (SPU) and the T-matrix approximation (TMA) in 2D flexure phonon model for varying vacancy concentrations x . Ratios are plotted as a function of the clean mode frequencies. Inset: Sketch of quadratic flexure phonon dispersion.

questions, such as why does the AFM phase transition occur across a broad temperature range, what role does magnetic frustration play and why do spin-waves persist above the Neel temperature.

To further investigate the validity of the perturbative approximations for phonon-disorder scattering, we will perform large scale super cell simulations again, this time for the realistic first-principles model of $\text{Mg}_2(\text{Sn},\text{Si})$, a promising thermoelectric candidate material. In addition, we will simulate phonons-disorder scattering and chemical phase segregation in large supercells to examine correlated disorder as a novel way to control thermal conductivity. We will study stacking fault limited thermal conductivity in van der Waals Kitaev materials such as $\alpha\text{-RuCl}_3$, which has recently been shown to play a critical role in the search for fractionized Majorana fermions.

References

1. C.M. Rost, E. Sachet, T. Borman, A. Moballeggh, E.C. Dickey, D. Hou, J.L. Jones, S. Curtarolo, J.-P. Maria, Entropy-stabilized oxides, *Nat. Commun.* **6**, 8485 (2015).
2. K.C. Pitike, S. Kc, M. Eisenbach, C.A. Bridges, V.R. Cooper, Predicting the phase stability of multicomponent high-entropy compounds, *Chem. Mater.* **32**, 7507 (2020).
3. B. Jiang, C.A. Bridges, R.R. Unocic, K.C. Pitike, V.R. Cooper, Y. Zhang, D.-Y. Lin, K. Page, Probing the local site disorder and distortion in pyrochlore high-entropy oxides, *J. Am. Chem. Soc.* **143**, 4193 (2021).
4. Y. Sharma, R. Agarwal, L. Collins, Q. Zheng, A.V. Ievlev, R.P. Hermann, V.R. Cooper, S. KC, I.N. Ivanov, R.S. Katiyar, et al., Self-Assembled Room Temperature Multiferroic $\text{BiFeO}_3\text{-LiFe}_5\text{O}_8$ Nanocomposites, *Adv. Funct. Mater.* **30**, 1906849 (2020).
5. J. Zhang, J. Yan, S. Calder, Q. Zheng, M.A. McGuire, D.L. Abernathy, Y. Ren, S.H. Lapidus, K. Page, H. Zheng, et al., Long-range antiferromagnetic order in a rocksalt high entropy oxide, *Chem. Mater.* **31**, 3705 (2019).
6. M.P. Jimenez-Segura, T. Takayama, D. Bérardan, A. Hoser, M. Reehuis, H. Takagi, N. Dragoë, Long-range magnetic ordering in rocksalt-type high-entropy oxides, *Appl. Phys. Lett.* **114**, 122401 (2019).
7. T. Berlijn, G. Alvarez, D.S. Parker, R.P. Hermann, R.S. Fishman, Simulating spin waves in entropy stabilized oxides, *Phys. Rev. Res.* **3**, 033273 (2021).
8. G.J. Snyder, E.S. Toberer, Complex thermoelectric materials, *Nat. Materials* **7**, 105 (2008).
9. M. Beekman, D.G. Cahill, Inorganic crystals with glass-like and ultralow thermal conductivities, *Cryst. Res. Technol.* **52**, 1700114 (2017).
10. J. Garg, N. Bonini, B. Kozinsky, N. Marzari, Role of disorder and anharmonicity in the thermal conductivity of silicon-germanium alloys: A first-principles study, *Phys. Rev. Lett.* **106**, 045901 (2011).
11. W. Li, L. Lindsay, D.A. Broido, D.A. Stewart, N. Mingo, Thermal conductivity of bulk and nanowire $\text{Mg}_2\text{Si}_x\text{Sn}_{1-x}$ alloys from first principles, *Phys. Rev. B* **86**, 174307 (2012).
12. J. Ma, W. Li, X. Luo, Intrinsic thermal conductivities and size effect of alloys of wurtzite AlN , GaN , and InN from first-principles, *J. Appl. Phys.* **119**, 125702 (2016).
13. S. Thébaud, C.A. Polanco, L. Lindsay, T. Berlijn, Success and breakdown of the T-matrix approximation for phonon-disorder scattering, *Phys. Rev. B* **102**, 094206 (2020).

Publications (16/35)

1. T. Berlijn, G. Alvarez, D. S. Parker, R. P. Hermann, and R. S. Fishman, Simulating spin waves in entropy stabilized oxides accepted in *Phys. Rev. Research* (2021).
2. R. S. Fishman, Single-Ion Anisotropy is Necessary and Appropriate to Study the Magnetic Behavior of Tb^{3+} Moments with $J_{\text{eff}} = 1/2$ on the Honeycomb Lattice in $Tb_2Ir_3Ga_9$ *PRB* **103**, 214440 (2021)
3. V. R. Cooper, J. T. Krogel and K. J. Donald, From molecules to solids: A vdW-DF-C09 case study of the mercury dihalides *J. Phys. Chem. A* **125**, 3978 (2021)
4. J. T. Krogel, S. F. Yuk, P. R. C. Kent, V. R. Cooper, Perspectives on van der Waals density functionals: The case of TiS_2 *J. Phys. Chem.* **124**, 9867 (2020).
5. S. Thébaud, C. A. Polanco, L. Lindsay, and T. Berlijn, Success and breakdown of the T-matrix approximation for phonon-disorder scattering, *PRB* **102**, 094206 (2020).
6. G. D. Nguyen, K. Pitike, P. Wadley, V. R. Cooper, M. Yoon, T. Berlijn and A.-P. Li, Emerging edge states on the surface of the epitaxial semimetal CuMnAs thin film, *Appl. Phys. Lett.* **116**, 061603 (2020). *Berlijn co-corresponding author
7. C. A. Polanco, T. Pandey, T. Berlijn, and L. Lindsay, Defect-limited thermal conductivity in MoS_2 , *Phys. Rev. Mater.* **4**, 014004 (2020).
8. T. Pandey, L. Lindsay, B. C. Sales, and D. S. Parker, Lattice instabilities and phonon thermal transport in TlBr, *Phys. Rev. Mater.* **4**, 045403 (2020).
9. K. Pitike, S. KC, M. Eisenbach, C. A. Bridges, V. R. Cooper, Predicting the phase stability of multi-component high entropy compounds, *Chem. Mater.* **32**, 7507 (2020).
10. H. Sims, D. N. Leonard, A. Y. Birenbaum, Z. Ge, T. Berlijn, L. Li, V. R. Cooper, M. F. Chisholm, and S. T. Pantelides, Intrinsic interfacial van der Waals monolayers and their effect on the high-temperature superconductor $FeSe/SrTiO_3$, *PRB. B* **100**, 144103 (2019).
11. S. Mu, R. Olsen, B. Dutta, L. Lindsay, G. D. Samolyuk, T. Berlijn, E. D. Specht, K. Jin, H. Bei, T. Hickel, B. C. Larson, and G. M. Stocks, Unfolding the complexity of phonon quasi-particle physics in disordered materials, *npj Comp. Mat.* **6**, 4 (2020).
12. B. Jiang, C. A. Bridges, R. R. Unocic, K. Pitike, V. R. Cooper, Y. Zhang, D.-Y. Lin, K. Page Probing the local site disorder and distortion in pyrochlore high-entropy oxides *JACS* **143**, 4193 (2021).
13. V. V. Klepov, K. A. Page, A. A. Berseneva, J. B. Felder, S. Calder, G. Morrison, Q. Zhang, M. J. Kirkham, D. S. Parker and H. C. Zur Loye. Chloride Reduction of Mn^{3+} in Mild Hydrothermal Synthesis of a Charge Ordered Defect Pyrochlore, $CsMn^{2+}Mn^{3+}F_6$, a Canted Antiferromagnet with a Hard Ferromagnetic Component *JACS* **143**, 11554 (2021).
14. M.-H. Du, J. Yan, V. R. Cooper, M. Eisenbach Tuning Fermi levels in intrinsic antiferromagnetic topological insulators $MnBi_2Te_4$ and $MnBi_4Te_7$ by Defect Engineering and Chemical Doping *Adv. Funct. Mater.* **31**, 2006516 (2021).
15. G. Sala, M. B. Stone, B. K. Rai, A. F. May, P. Laurell, V. O. Garlea, N. P. Butch, M. D. Lumsden, G. Ehlers, G. Pokharel, A. Podlesnyak, D. Mandrus, D. S. Parker, S. Okamoto, G. B. Halász, A. D. Christianson Van Hove singularity in the magnon spectrum of the antiferromagnetic quantum honeycomb lattice *Nat. Commun.* **12**, 171 (2021).
16. Y. Sharma, R. Agarwal, L. Collins, Q. Zheng, A. V. Ievlev, R. P. Hermann, V. R. Cooper, S. KC, I. Ivanov, R. S. Katiyar, S. V. Kalinin, H. N. Lee, S. Hong, and T. Z. Ward, Self-assembled room temperature multiferroic $BiFeO_3$ - $LiFe_5O_8$ nanocomposites, *Adv. Funct. Mater.*, 1906849 (2019).

Theoretical Studies of Complex Collective Phenomena (Oak Ridge National Laboratory)

Elbio Dagotto PI ^(a,b). Co-PIs: Thomas Maier ^(a), Adriana Moreo ^(a,b), Satoshi Okamoto ^(a)

(a) Oak Ridge National Laboratory and (b) University of Tennessee, Knoxville

Program Scope

Our overarching goal is the quantitative understanding of the many-body states generated in electronic models for quantum materials, involving both strong correlation and spin-orbit coupling (SOC), with simultaneously active spin, charge, and orbital degrees of freedom.

Keywords:

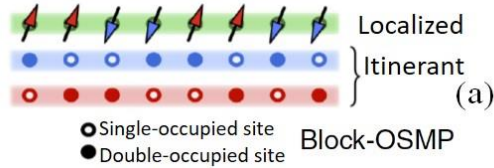
- *Mixing correlation and topology*: How does SOC affect the properties of strongly correlated electrons? Does correlation help or destroy topology?
- *Orbital degree of freedom*: How does the orbital affect superconductivity, exciton formation, and magnetic states? Can topology be affected by the orbital? In general, what new states can emerge by mixing spins, charge, orbital, and SOC?
- *Exotic spin textures and topological superconductivity*: What kind of skyrmionic patterns emerge from the Dzyaloshinskii-Moriya (DM) interaction in stacked layers? Can we create Majoranas in superconducting models by adding Rashba SOC?

Recent Progress

(1) Spin dynamics of the block orbital-selective Mott phase. The competition among electronic, orbital, and spin degrees of freedom leads to emergent states in multiorbital Hubbard models. These states *cannot* be deduced from weak coupling perturbation theory nor from strong coupling spin-only models, but numerical techniques are needed. One example is the orbital-selective Mott phase (OSMP), where orbitals with different bandwidths and crystal fields can become gapped or remain gapless, leading to coexisting insulating and metallic characteristics. While the localized spins prefer an antiferromagnetic (AFM) arrangement, the itinerant electrons develop ferromagnetic (FM) tendencies to optimize the kinetic energy. This induces exotic “block” phases, with FM blocks (of various lengths), AFM coupled among them. The case of block-2 is in Fig.1 (a). The generalization to two-leg ladders has 2×2 blocks, and was experimentally confirmed via powder neutron scattering in BaFe_2Se_3 . In anticipation of the availability of single crystals, we performed DMRG calculations to predict the dynamical spin structure factor $S(q,\omega)$ of the block state, Fig.1 (b). The results have an “acoustic mode” with high intensity at wavevector $q = \pi/2$. These are blocks slightly oscillating in unison without disrupting each block. There is also a flat optical mode, with high intensity between $q = \pi/2$ and π , reflecting intra-block excitations [1].

The analysis of the complete phase diagram of the multi-orbital model generated a surprise: varying Hubbard U , Hund J_H , and density n , a *spiral* state was unveiled. This occurs without any obvious source of frustration and without SOC (i.e. “hidden frustration”). Moreover, the spiral is

not canonical, with the same angle between neighboring spins, but instead is a “block spiral” where the spins in the individual blocks remain collinear but the spiral angle is between blocks, as shown in Fig.1 (c) [2]. Clearly, the complexity of novel states arising from competing tendencies is



“emergent” in the sense that it is unpredictable *a priori*, and only unbiased reliable many-body techniques can unveil the true phase diagrams of multi-orbital interacting models.

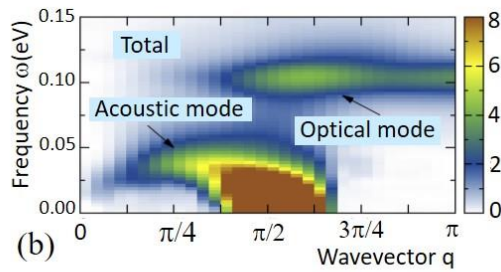
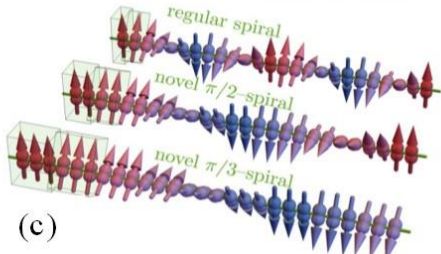


Fig. 1. (a) “Block” spin phase ($\uparrow\uparrow\downarrow\downarrow$) emerging from the three-orbital one-dimensional Hubbard model studied with DMRG. This phase appears within the OSMP, with one localized and two itinerant bands. (b) Dynamical spin structure factor $S(q, \omega)$ using DMRG [1]. The acoustic mode is the block-state spin wave, while the optical mode arises from internal excitations within each block. (c) Varying U , J_H , and electronic density n , the collinear block state evolves into a spin spiral [2]. This spiral is not “regular”, but “novel” because the block spins remain collinear, but the spiral’s angle is between blocks.



(2) Topological Hall Effect and skyrmion crystal at manganite-iridate interfaces. At the interface between $\text{La}_{1-x}\text{Sr}_x\text{MnO}_3$ and SrIrO_3 , the iridate with active $5d$ orbitals induces a finite spin-orbit-driven DM interaction $\mathbf{D}_{ij}(\mathbf{S}_i \times \mathbf{S}_j)$ at the manganite with $3d$ orbitals. Using Monte Carlo (MC) techniques, a two-orbital double exchange model for manganites, supplemented by the DM coupling D was studied [3]. Our model system, with both localized t_{2g} spins and itinerant e_g electrons, is challenging due to the frequent

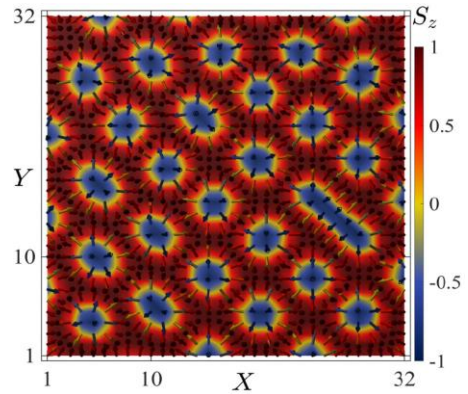


Fig. 2: MC results for the double-exchange model with two orbitals [3], DM coupling $D=0.1$, easy-plane anisotropy $A=0.05$, and magnetic field $h_z=0.1$, all in hopping units. Lattice is 32×32 and temperature $T=0.001$. Skyrmions (circles) spontaneously form a triangular lattice.

diagonalization in the fermionic sector during the MC evolution, as compared with simpler spin-only models. However, this effort allows us to calculate the Hall conductance, because itinerant fermions are degrees of freedom in the model.

Phase diagrams were obtained varying temperature and magnetic fields perpendicular to the interface. In a range of couplings, skyrmions emerge upon cooling, condensing into a triangular lattice, as in Fig. 2. In these regimes, the topological Hall effect appears, driven by the non-zero scalar spin chirality $\chi_{ijk} = \mathbf{S}_i \cdot (\mathbf{S}_j \times \mathbf{S}_k)$ induced by DM interactions.

Related to the previous item, we developed the Landau Lifshitz (LL) formalism studying the $S(\mathbf{q}, \omega)$ of skyrmion crystals [4]. In Fig. 3 using classical spin models, multiple bands were shown to emerge in interfaces of manganites with iridates, via a nonzero DM interaction transmitted from the Ir to the Mn oxide. Together with expertise in RPA and DCA, we can address FM or AFM variations of the kagome or honeycomb lattices with SOC. For topological magnons, edge modes should develop in the open direction of a cluster with cylindrical boundary conditions.

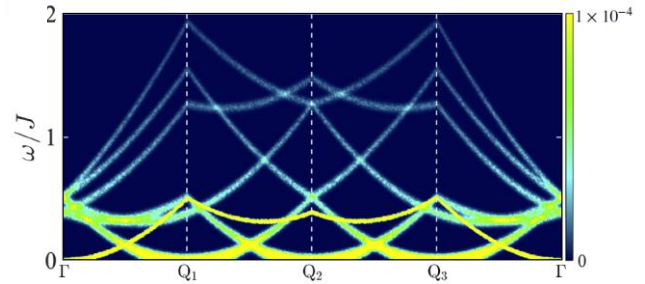


Fig. 3: Skyrmion lattice spin-wave spectrum obtained using a classical spin Heisenberg model with DM interactions and a magnetic field, via the LL equations.

Future Plans

(1) Topological superconductors (TS) in multi-orbital systems. TS have a bulk pairing gap and gapless Majorana fermion states at the surface, edges, defects, or vortex cores. What special properties develop in the Majoranas when many orbitals are active in the system? Recent work by our team [5], illustrated this phenomenon in a one-dimensional model with one itinerant band in interaction with localized spins $\frac{1}{2}$. By proximity effect the itinerant band is coupled to an s -wave pairing field. Previous work (see above) showed that the combined effects of couplings U and J_H spontaneously cause tendencies to form spirals. In this context we recently observed Majorana states at the ends of the chains [5], as shown schematically in Fig. 4: increasing the Hubbard U a transition from collinear to spiral magnetic order is induced, concomitant with a transition from canonical to proximity-induced TS. Because the system is one dimensional, DMRG provides accurate results and its open boundary conditions are ideal to generate Majoranas. Next, we will study Majoranas searching for internal orbital dependency, and via ladders the two dimensional limit will slowly be approached.

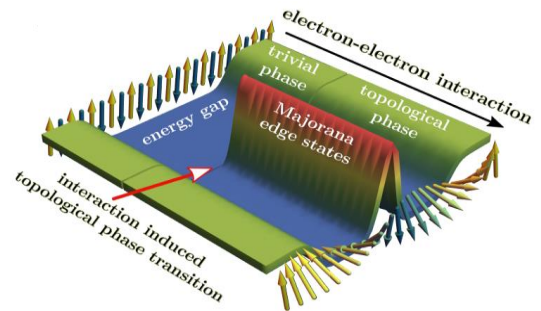


Fig. 4: Sketch of Majorana's DMRG results in helical spin backgrounds, in a multiorbital Hubbard chain geometry. In the actual calculations, the SC gap is $\sim 0.1W$, $U/W=2$, and $\Delta_{SC}/W=0.5$ (see [5]), with W the bandwidth.

(2) Multitude of topological phase transitions in bipartite dice and Lieb Lattices with interacting electrons and Rashba coupling. Using Hartree-Fock, we studied [6] Hubbard U interacting electrons including Rashba spin-orbit coupling λ , in two bipartite lattices: the dice (see Fig. 5) and Lieb lattices, both at half-filling. Both lattices have ferrimagnetic order in the phase diagram. Our main result is the observation of an unexpected multitude of *topological phases* for both lattices, differing among themselves in their set of six Chern numbers (six numbers because the unit cells have three atoms). The Chern numbers observed in our study range from 0 to 3, showing that large Chern numbers can be obtained by the effect of electronic correlation.

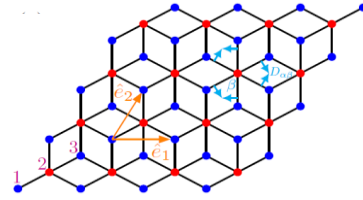
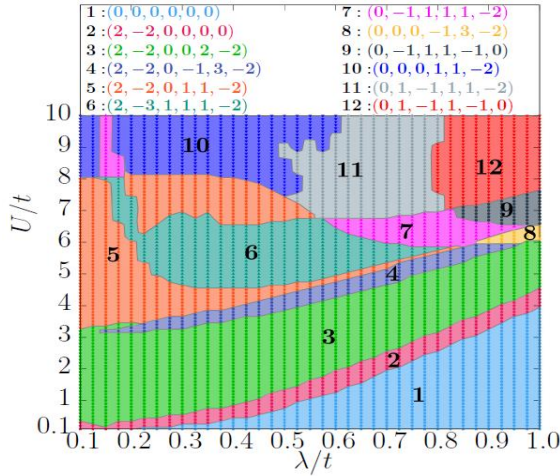


Fig. 5: Left panel is the Hartree Fock phase diagram varying Hubbard and Rashba SOC couplings, in the dice lattice shown above. The multitude of phases only differ in the Chern numbers of their six bands (unit cell has three sites). All the phases are ferrimagnetic [6].

(3) Magnetization dynamics fingerprints of an excitonic condensate $(t_2g)^4$ magnet. The competition between **L.S** spin-orbit coupling λ and electron-electron interaction U leads to novel states of matter, extensively studied in materials, such as ruthenates and iridates. Excitonic magnets (the AFM state of bounded electron-hole pairs) is an example of phenomena driven by those competing energy scales. Interestingly, recent DMRG studies predicted that excitonic magnets exist in the ground-state of $(t_2g)^4$ spin-orbit-coupled Hubbard models. Recently [7], we finished a detailed computational study of the magnetic excitations in that excitonic magnet, employing DMRG and Lanczos. We showed that the low-energy spectrum (Fig. 6) is dominated by a spin-wave mode, with extra features arising from the $\lambda = 0$ state. More importantly, we found a novel magnetic excitation forming a high-energy optical mode with highest intensity at $q \sim 0$. These features do not appear all together in any of the neighboring states in the phase diagram, and thus constitute unique fingerprints of the $(t_2g)^4$ excitonic magnet, of importance in neutron and RIXS experiments.

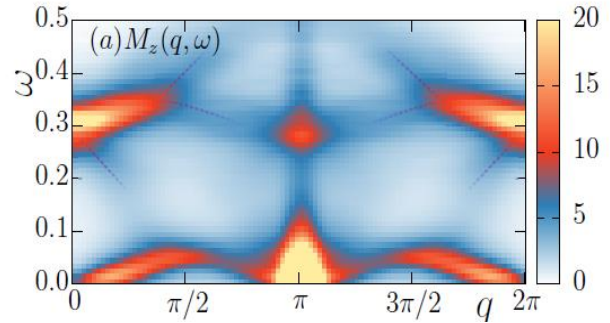


Fig. 6: $S(q, \omega)$ of a one-dimensional multiorbital Hubbard model with SOC, obtained via DMRG. Results were gathered in an excitonic condensate phase [7].

References

[1] J. Herbrych et al., *Nat. Commun.* **9**, 3736 (2018).
 [2] J. Herbrych et al., *Proc. Natl. Acad. Sci. USA* **117**, 16226 (2020).
 [3] N. Mohanta et al., *Phys. Rev. B* **100**, 064429 (2019).
 [4] N. Mohanta et al., *Commun. Phys. (Nature)* **3**, 229 (2020).
 [5] J. Herbrych et al., *Nat. Commun.* **12**, 2955 (2021).
 [6] R. Soni et al., in preparation.
 [7] N. Kaushal et al., in preparation.

Publications: selection from FY2020 and FY 2021 (from a total of 54 publications).

1. N. D. Patel et al., *npj Quantum Mater.* **5**, 27 (2020).
2. N. Kaushal et al., *Phys. Rev. B* **101**, 245147 (2020).
3. J. Herbrych et al., *Proc. Natl. Acad. Sci. USA* **117**, 16226 (2020).
4. R. Soni, N. Kaushal, S. Okamoto, and E. Dagotto, *Phys. Rev. B* **102**, 045105 (2020).
5. B. Pandey et al., *Phys. Rev. B* **102**, 035149 (2020).
6. N. Mohanta, S. Okamoto, and E. Dagotto, *Phys. Rev. B* **102**, 064430 (2020).
7. J. Herbrych, G. Alvarez, A. Moreo, and E. Dagotto, *Phys. Rev. B* **102**, 115134 (2020).
8. L-F. Lin, Y. Zhang, A. Moreo, E. Dagotto, and S. Dong, *Phys. Rev. Mater.* **3**, 111401 (2019).
9. A. Moreo and E. Dagotto, *Phys. Rev. B* **100**, 214502 (2019).
10. T. Miao et al., *Proc. Natl. Acad. Sci. USA* **117**, 7090 (2020).
11. S. Bhattacharyya, P. Hirschfeld, T. Maier, and D. Scalapino, *Phys. Rev. B* **101**, 174509 (2020).
12. Y. Wang et al., *Phys. Rev. X* **10**, 021030 (2020).
13. E. Skoropata et al., *Sci. Adv.* **6**, eaaz3902 (2020).
15. Y. Zhang et al., *Phys. Rev. B* **102**, 195117 (2020) (Editor's choice).
16. N. Mohanta et al., *Commun. Phys. (Nature)* **3**, 229 (2020).
17. J. Herbrych et al., *Nat. Commun.* **12**, 2955 (2021).
18. S. Shen, Z. Li, Z. Tian, W. Luo, S. Okamoto, and P. Yu, *Phys. Rev. X* **11**, 021018 (2021).
19. M.-W. Yoo et al., *Nat. Commun.* **12**, 3283 (2021).
20. X. Huang et al., *Nat. Phys.* **17**, 715 (2021).
21. N. Mohanta, S. Okamoto, and E. Dagotto, *Commun. Phys. (Nature)* **4**, 163 (2021).
22. L-F. Lin, Y. Zhang, G. Alvarez, A. Moreo, and E. Dagotto, *Phys. Rev. Lett.* **127**, 077204 (2021).
23. J. M. Ok et al., *Sci. Adv.* **7**, ebf9631 (2021)

Theory Institute for Materials and Energy Spectroscopies (TIMES, SLAC FWP 100291)
T. P. Devereaux, B. Moritz, C. Jia, C. D. Pemmaraju, H. Jiang (SLAC), J. Rehr, J. Kas, F. Vila (UW), J.E. Moore (LBL)

Program Scope

The primary mission of TIMES is to develop a world class program on the theory of spectroscopy, with the goal of understanding and controlling and non-equilibrium phenomena and the emergent dynamics of coupled charge, spin, lattice, and orbital degrees of freedom at their natural time- and length-scales. Our approach utilizes advanced theoretical techniques and numerical simulations for a broad range of spectroscopies, spanning THz to x-rays, with particular emphasis on science that is enabled by the West Coast light sources: the Linac Coherent Light Source (LCLS) & Stanford Synchrotron Radiation Lightsource (SSRL) at SLAC National Accelerator Laboratory & the Advanced Light Source (ALS) at Lawrence Berkeley National Laboratory (LBL).

Keywords: Spectroscopy, theory & simulations, non-equilibrium.

Recent Progress

Our FWP reports significant progress during this cycle in three main areas. The first is the continued development of theories especially for equilibrium x-ray spectroscopies, including the launch of FEFF10 and the combination of *ab initio* and multiplet calculations into a single framework. Tutorial-like applications have been launched to help new users become familiar with different aspects of x-ray spectroscopies. The second is the development of theoretical tools that address time-resolved x-ray absorption that matches well with the capabilities of LCLS, setting the stage for much of our proposed work into time-domain spectroscopies. The third area represents our basic research science efforts towards the understanding of dynamics in representative systems, including novel superconductors and certain one-dimensional spin systems.

The key software objectives of the current TIMES FWP have largely been met. Our major objectives included the development and release of an updated version of the x-ray spectroscopy codes FEFF10 together with the Corvus Workflow tools [1-3] in a TIMES Software suite, which includes both open-source codes and documentation. The Corvus platform and its software components have been optimized for parallel computational environments and are installed on the TIMES server and other sites.

This platform includes workflows for finite-temperature XAS, XANES analysis, and XAFS and XRD Debye-Waller factors. The latest Corvus version is compatible with updated versions of Python > 3.7. The TIMES software suite facilitates complex workflows that involve multiple codes and can be extended to include many other scientific software packages. A number of new workflows have been implemented, including XES fitting, and inclusion of many-body satellites in XPS and XAS using RT-TDDFT and the cumulant spectral function.

With an eye towards the anticipated ramp up of time-resolved X-ray spectroscopy experiments at LCLS-II, TIMES researchers have been developing explicitly time-domain simulation methods.

As X-ray pulses advance further towards higher coherence and better temporal resolution, paving the way to non-linear X-ray spectroscopy, theoretical tools that can treat valence and core electron dynamics efficiently and on the same footing become necessary. The velocity-gauge formalism of real-time time dependent density functional theory (VG-RT-TDDFT), which provides an efficient treatment of laser-matter interactions in condensed matter, is well suited to addressing simulation challenges in this space. Our prior work demonstrated an implementation of the VG-RT-TDDFT equations for electron dynamics within a linear combination of atomic orbitals (LCAO) basis set framework [4]. This approach allows for the treatment of low-energy valence and high-energy core-excitations on the same footing in condensed-matter systems while retaining the scalability of RT-TDDFT. Within the current funding cycle, we extended this LCAO platform towards improved accuracy enabled by modern non-local exchange-correlation functionals within the Generalized Kohn-Sham (GKS) framework and demonstrated for the first time a velocity gauge GKS-RT-TDDFT approach for simulating both valence and core-excitonic effects [5]. This represents a key development within RT-TDDFT applied to periodic supercell simulations. Our implementation has also been recently deployed by experiment-theory collaborations to successfully study second harmonic response at extended surfaces within the emerging field of nonlinear X-ray spectroscopy [6].

By providing cutting-edge theoretical spectroscopy expertise to experimental efforts connecting SSRL, LCLS and SIMES, TIMES researchers contributed during the current review period to a number of science outcomes spanning a broad range of interesting materials classes.

Meeting global energy challenges requires higher energy density battery materials and anion redox within Li-ion and Na-ion battery cathodes represents a promising route towards this goal. Anionic redox provides additional high voltage capacity beyond that achieved within transition-metal (TM) redox systems but in most TM oxide cathodes it is associated with the formation of stable oxidized oxygen species that adversely affect cyclability leading to capacity loss. We proposed a mechanism that enables reversible anionic redox in the cathode material $\text{Na}_{2-x}\text{Mn}_3\text{O}_7$ through kinetic stabilization of polaronic oxidized oxygen species associated with weak lattice perturbations and without the formation of short O-O dimers that lead to irreversibility under charge-discharge cycling [7]. A key aspect of our study is the interplay between experimental characterization using XAS/RIXS and detailed atomistic modeling of these spectroscopies within TIMES to relate experimentally observed spectroscopic signatures to specific structural motifs in the charged cathode material. In particular by combining *ab initio* computational-spectroscopy at the level of the Bethe-Salpeter-Equation (BSE), with experimental characterization, we provided unambiguous spectral fingerprints for hole polarons on O in charged $\text{Na}_{2-x}\text{Mn}_3\text{O}_7$ at 4.2 V. These spectral signatures are observed at a lower energy in O *K*-edge XAS compared to the signatures associated with dimerized O-O species. The OCEAN BSE code, a part of the TIMES software ecosystem through a NIST collaboration was instrumental to our study. The Coulombically enhanced kinetic stabilization of O hole polarons observed in our study points the way to future time-resolved experimental efforts to elucidate the path dependence within redox induced structural dynamics in cathode materials.

The recent discovery of superconductivity in oxygen-reduced monovalent nickelates such as $R_{1-x}\text{Sr}_x\text{NiO}_2$ ($R = \text{La}, \text{Nd}, \text{and Pr}$) has raised a new platform for the study of unconventional superconductivity [8]. The lowest energy electronic structure in the nickelate is of multi-orbital

nature, consisting of bands associated with the Nd $5d$ states and the Ni $3d_{x^2-y^2}$ bands. X-ray investigations capitalizing on the atomic specificity of XAS and RIXS have already made headway in probing the fundamental orbital constituents thought to play a role in superconductivity [9]. State-of-the-art charge transfer hybridization full atomic multiplet (CTHFAM) calculations developed within TIMES confirmed the orbital character [9].

To lay the groundwork for future x-ray studies in FWP 10017 (Devereaux) and elsewhere in SIMES, a recent study [10] investigated the family of infinite-layer nickelates $R\text{NiO}_2$ with rare-earth R spanning across the lanthanide series, introducing a new and nontrivial "knob" with which to tune nickelate superconductivity. When traversing from La to Lu, the out-of-plane lattice constant decreases dramatically with an accompanying increase of Ni $3d_{x^2-y^2}$ bandwidth; however, surprisingly, the role of oxygen charge transfer diminishes. In contrast, the magnetic exchange grows across the lanthanides, which may be favorable to superconductivity. The theoretical studies on the electronic structure of infinite-layer nickelates feature a weakly interacting three-dimensional $5d$ metallic state at the rare-earth R spacer layer hybridizing with a quasi-two-dimensional, strongly correlated state with primarily Ni $3d_{x^2-y^2}$ orbital character in the NiO_2 layer.

This scenario shows that compensation effects from the itinerant $5d$ electrons present a closer analogy to Kondo lattices, indicating a more complex interplay between charge transfer, bandwidth renormalization, compensation, and magnetic exchange. These predictions are well suited for the application of RIXS to these compounds.

Future Plans

While our prior TIMES effort has focused primarily on equilibrium spectroscopies and numerical methods focusing on equilibrium ground states and dynamics, we will concentrate our efforts on ultrafast materials science and work towards the development of theories for spectroscopies out of equilibrium and into the time-domain, with a focus on tool development in support of planned experiments at LCLS and beyond. Our proposed research is therefore based on three broad topics with the goal of moving towards more of a focus on time-domain and correlation effects: 1) advancing equilibrium spectroscopy theory; 2) extending our theories and associated software to real-time and non-equilibrium simulations; and 3) applying our theoretical tools to novel materials and real-time (ultrafast) spectroscopic probes.

To this end our proposed effort has two tiers of theoretical and computational development: First, we will continue to develop advanced theories of x-ray spectra, focusing on the treatment of correlation effects, and finite temperature electronic, vibrational, and magnetic properties of materials. For equilibrium properties, we will build on *ab initio* approaches, including FEFF10 - finite temperature multiple scattering, SIESTA real-time TDDFT, OCEAN solution of the Bethe-Salpeter equation, as well as model Hamiltonian methods including exact diagonalization (ED) and DMRG for correlated systems as they are ideal approaches to study the properties of quantum systems with strong correlations. FEFF10 has already become an advanced tool for calculating numerous spectroscopies. Further, as also outlined therein, we have developed efficient ED codes for studying the ground state and dynamical properties of proposed systems on small clusters, and efficient DMRG code for both the ground state properties of large 1D and

quasi-1D systems and dynamical properties of 1D systems. We will continue to develop new methods of coupling *ab initio* and model Hamiltonian based approaches for highly correlated systems and focus them on the development of theories for x-ray and related spectroscopies.

Second, and more importantly, we plan to extend our effort with more emphasis on real-time calculations of dynamical and non-equilibrium properties. We plan to continue our progress in theories of real-time and finite temperature effects, such as real-time TDDFT as implemented in SIESTA, and the finite temperature real-space multiple scattering code FEFF10, as these have already been used for simulations of non-equilibrium properties. We propose to continue the development of new efficient codes, especially DMRG, to study the spectroscopic properties of strongly correlated system for pump-probe problems including XAS, RIXS and ARPES. We also plan to apply the algorithms on various strongly correlated systems for cutting-edge emergent phenomenon, such as the Hubbard model on the triangular lattice, and multi-orbital Hubbard model for superconducting nickelates.

Finally, building upon our track record of collaborations with experimental groups, we propose combined experimental and theoretical investigations of a variety of novel materials, including battery materials, 2d spin liquids, and axion insulators, for materials verification and for applying our developments towards solving important questions regarding these novel systems.

References

1. J. J. Kas, F. D. Vila, J. J. Rehr, C. D. Pemmaraju, and T. S. Tan, “Advanced calculations of x-ray spectroscopies with FEFF10 and Corvus”, arXiv:2106.13334, (in press J. Synchrotron Rad.) (2021).31
2. T. S. Tan, J. J. Kas, and J. J. Rehr, “Real-space green’s function approach for x-ray spectra at hightemperature”, Phys. Rev. B104, 035144 (2021).
3. S. M. Story, F. D. Vila, J. J. Kas, K. B. Raniga, C. D. Pemmaraju, and J. J. Rehr, “Corvus: a frame-work for interfacing scientific software for spectroscopic and materials science applications”, Journal of Synchrotron Radiation 26, 1694–1704 (2019).
4. C. Pemmaraju, F. D. Vila, J. J. Kas, S. A. Sato, J. J. Rehr, K. Yabana, and D. Prendergast, “Velocity-gauge real-time TDDFT within a numerical atomic orbital basis set”, Computer Physics Communications 226, 30–38 (2018).
5. C. D. Pemmaraju, “Valence and core excitons in solids from velocity-gauge real-time TDDFT with range-separated hybrid functionals: An LCAO approach”, Computational Condensed Matter 18, e00348 (2019).
6. T. Helk, E. Berger, S. Jamnuch, L. Hoffmann, A. Kabacinski, J. Gautier, F. Tissandier, J. P. Goddet, H. T. Chang, J. Oh, C. Das Pemmaraju, T. A. Pascal, S. Sebban, C. Spielmann, and M. Zuerch, “Table-top extreme ultraviolet second harmonic generation”, Science Advances 7, eabe2265 (2021).
7. I. Abate, C. D. Pemmaraju, S. Y. Kim, K. H. Hsu, S. Sainio, B. Moritz, J. Vinson, M. F. Toney, W. Yang, W. E. Gent, T. P. Devereaux, L. F. Nazar, and W. C. Chueh, “Coulombically-stabilized oxygen hole polarons enable fully reversible oxygen redox”, Energy Environ. Sci., 10.1039/D1EE01037A (2021).
8. D. Li, K. Lee, B. Y. Wang, M. Osada, S. Crossley, H. R. Lee, Y. Cui, Y. Hikita, and H. Y. Hwang, “Superconductivity in an infinite-layer nickelate”, Nature 572, 624–627 (2019).

9. M. Hepting, D. Li, C. Jia, H. Lu, E. Paris, Y. Tseng, X. Feng, M. Osada, E. Been, Y. Hikita, Y.-D. Chuang, Z. Hussain, K. J. Zhou, A. Nag, M. Garcia-Fernandez, M. Rossi, H. Y. Huang, D. J. Huang, Z. X. Shen, T. Schmitt, H. Y. Hwang, B. Moritz, J. Zaanen, T. P. Devereaux, and W. S. Lee, “Electronic structure of the parent compound of superconducting infinite-layer nickelates”, *Nature Materials* **19**, 381–385 (2020)
10. E. Been, W.-S. Lee, H. Y. Hwang, Y. Cui, J. Zaanen, T. Devereaux, B. Moritz, and C. Jia, “Electronic structure trends across the rare-earth series in superconducting infinite-layer nickelates”, *Phys. Rev. X* **11**, 011050 (2021).

Publications

1. **Web-Based Methods for X-ray and Photoelectron Spectroscopies**, T. P. Devereaux, B. Moritz, C. Jia, J. J. Kas, J. J. Rehr, *Comp. Mat. Sci.* **200**, 110814 (2021).
2. **Spatiotemporal crossover between low- and high-temperature dynamical regimes in the quantum Heisenberg magnet**, M. Dupont, N. Sherman, J. E. Moore, *Physical Review Letters* **127**, 107201 (2021).
3. **Coulombically-stabilized oxygen hole polarons enable fully reversible oxygen redox**, Iwnetim I. Abate, C. Das Pemmaraju, Se Young Kim, Kuan H. Hsu, Sami Sainio, Brian Moritz, John Vinson, Michael F. Toney, Wanli Yang, William E. Gent, Thomas P. Devereaux, Linda F. Nazar, William C. Chueh, *Energy Environ. Sci.*, DOI:10.1039/D1EE01037A (2021).
4. **Dynamical signatures of symmetry protected topology following symmetry breaking**, Jacob A. Marks, Michael Schüler, and Thomas P. Devereaux, *Phys. Rev. Res.* **3**, 023137 (2021).
5. **Correlation-Assisted Quantized Charge Pumping**, Jacob Marks, Michael Schüler, Jan C. Budich, Thomas P. Devereaux, *Phys. Rev. B* **103**, 035112 (2021).
6. **Detection of Kardar–Parisi–Zhang hydrodynamics in a quantum Heisenberg spin-1/2 chain**, A. Scheie, N. E. Sherman, M. Dupont, S. E. Nagler, M. B. Stone, G. E. Granroth, J. E. Moore, and D. A. Tennant, *Nat. Phys.* **17**, 726–730 (2021).
7. **Electronic structure trends across the rare-earth series in superconducting infinite layer nickelates**, Emily Been, Wei-Sheng Lee, Harold Y. Hwang, Yi Cui, Jan Zaanen, Thomas Devereaux, Brian Moritz, Chunjing Jia, *Phys. Rev. X* **11**, 011050 (2021).
8. **Gauge invariance of light-matter interactions in first-principle tight-binding models**, Michael Schüler, Jacob A. Marks, Yuta Murakami, Chunjing Jia, Thomas P. Devereaux, *Phys. Rev. B* **103**, 155409 (2021).
9. **Criticality of Two-Dimensional Disordered Dirac Fermions in the Unitary Class and Universality of the Integer Quantum Hall Transition**, Björn Sbierski, Elizabeth J. Dresselhaus, Joel E. Moore, and Ilya A. Gruzberg, *Phys. Rev. Lett.* **126**, 076801 (2021).
10. **Simulation of attosecond transient soft X-ray absorption in solids using generalized Kohn-Sham real-time time-dependent density functional theory**, C D Pemmaraju, *New J. Phys.* **22**, 083063 (2020).
11. **Ab initio molecular dynamics study of SiO₂ lithiation**, Iwnetim Iwnetu Abate, Chunjing Jia, Brian Moritz, Thomas P Devereaux, *Chemical Physics Letters* **739**, 136933 (2020).

12. **How circular dichroism in time- and angle-resolved photoemission can be used to spectroscopically detect transient topological states in graphene**, Michael Schüler, Umberto De Giovannini, Hannes Hübener, Angel Rubio, Michael A. Sentef, Thomas P. Devereaux, and Philipp Werner, *Phys. Rev. X* **10**, 041013 (2020).
13. **Advanced calculations of x-ray spectroscopies with FEF10 and Corvus**, J. J. Kas, F. D. Vila, J. J. Rehr, C. D. Pemmaraju, T. S. Tan, arXiv:2106.13334 (2021), to appear in *J. Synchrotron Rad.*
14. **Combined multiplet and cumulant Green's function treatment of correlation effects in x-ray photoelectron spectroscopy**, J. J. Kas, J. J. Rehr, T. P. Devereaux, arXiv:2107.10409 [cond-mat.mtrl-sci] (2021).
15. **Orbitally Selective Resonant Photodoping to Enhance Superconductivity**, Ta Tang, Yao Wang, Brian Moritz, Thomas P. Devereaux, arXiv:2106.04742.
16. **Bloch Wavefunction Reconstruction using Multidimensional Photoemission Spectroscopy**, Michael Schüler, Tommaso Pincelli, Shuo Dong, Thomas P. Devereaux, Martin Wolf, Laurenz Rettig, Ralph Ernstorfer, Samuel Beaulieu, arXiv:2103.17168.
17. **Witnessing quantum criticality and entanglement in the triangular antiferromagnet KYbSe₂**, A. Scheie, E. A. Ghioldi, J. Xing, J. A. M. Paddison, N. E. Sherman, M. Dupont, D. Abernathy, D. Pajerowski, Shang-Shun Zhang, L. O. Manuel, A. E. Trumper, C. D. Pemmaraju, D. S. Parker, T. P. Devereaux, J.E. Moore, C. D. Batista, D. A. Tennant, arXiv:2109.11527.
18. **Superconductivity in a minimal two-band model for infinite-layer nickelates**, Cheng Peng, Hong-Chen Jiang, Brian Moritz, Thomas P. Devereaux, Chunjing Jia, arXiv:2110.07593.

MemComputing the Spectrum of Correlated Quantum Systems

Massimiliano Di Ventra, Department of Physics, University of California, San Diego

Program Scope

Finding the ground state (GS) and excited states (the spectrum) of correlated quantum systems is one of the most important and challenging problems in Physics. It has far-reaching implications for both fundamental science and for a wide range of technological applications. The problem is extremely difficult because the elementary units of these systems are strongly coupled. This means that perturbation theory (which treats the interaction between the elementary units as a small perturbation) is inadequate to provide satisfactory answers.

Consequently, *non-perturbative* approaches are needed to tackle such a problem. In fact, finding the GS of correlated systems is like finding the optimum in a corrugated (non-convex) landscape, a variant problem that is also of great technological importance in both academic and industrial settings.

In this respect, the PI has introduced a new computing paradigm, he called *MemComputing* [1], to tackle these types of problems. (See the book [2] for an in-depth discussion of this paradigm.) MemComputing stands for computing *in* and *with* memory (time non-locality). Its digital, hence scalable version brings about a set of machines called digital MemComputing machines (DMMs) that can be built in hardware with, e.g., electrical circuits with memory, and are described by non-linear equations of motion whose point attractors express the solutions of the corresponding problem they tackle.

The important point is that DMMs do not necessarily need to be built in hardware to show their potential: being non-quantum (classical) systems their simulations on conventional computers have already been shown to outperform traditional algorithmic approaches on a wide variety of combinatorial optimization problems [3].

The reason behind this efficiency is that these machines operate at a *critical state* (or the “edge of chaos”) where they take advantage of topological excitations known as *instantons* [4]. The latter ones are the classical analogue of quantum tunneling and, as such, they are *non-perturbative* in nature. The topological character of the solution search by DMMs makes them also robust against noise (both physical and numerical) and perturbations.

In order to apply such a computing paradigm to quantum systems the PI employs neural networks (NNs) as variational wavefunctions of quantum states. This is a particularly promising direction since the PI has already shown that simulations of DMMs can considerably accelerate the pre-training of NNs, as well as efficiently train deep networks in an unsupervised setting, compared to state-of-the-art approaches [5].

Keywords: Correlated Quantum Systems; MemComputing; Machine Learning; Artificial Intelligence.

Recent Progress

In order to test the above theoretical approach, the PI has applied MemComputing to the difficult task of reconstructing the quantum states (quantum tomography) of correlated systems. A particular NN known as restricted Boltzmann machine (RBM) has been used as variational wavefunction. The most difficult part of the training of such NNs is finding the mode of the probability distribution [5].

This is not easy to do with Gibbs sampling (the traditional method to train NNs), while the MemComputing approach performs this task efficiently [5].

Fig. 1 shows how many measurements are required to reach some fixed fidelity (F) for a prototypical entangled state known as W state with N qubits.

When the target fidelity is low (e.g., $F=0.9$) there is not an appreciable advantage in using the MemComputing-assisted training vs. the traditional Gibbs sampling.

In contrast, when the fidelity is raised to $F=0.98$, the RBM with mode training requires substantially less measurements to reach that fidelity, with that difference growing with the number N of qubits in the W state. In addition, it is evident that the MemComputing-assisted training shows a much smaller variance. In other words, not only does the mode-assisted training substantially improve over Gibbs sampling, it also stabilizes the training. This is in agreement with previous results on other data sets [5].

Future Plans

The PI plans to test this approach on various correlated quantum systems and for different spatial dimensions. In particular, the PI is attempting to map the NN variational wavefunctions directly into DMMs so that the training of such NN can be done 'in one shot', as a fully dynamical problem. This direction of study has implications far beyond the present project. In fact, a DMM that trains directly NNs can be implemented in hardware, thus accelerating a wide range of tasks in Machine Learning and Artificial Intelligence.

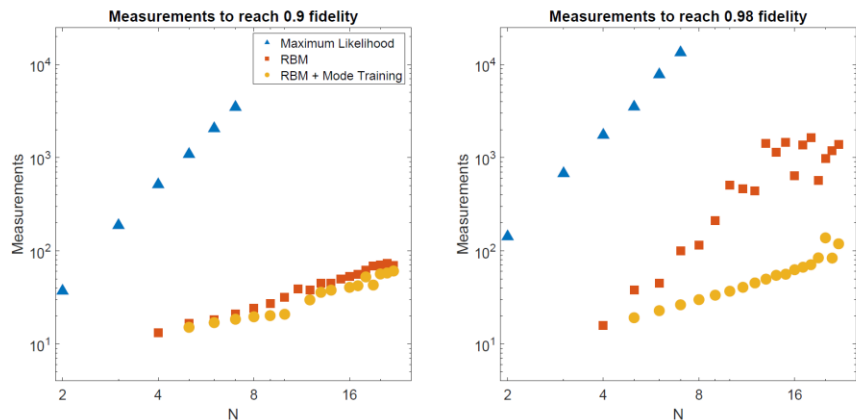


Fig. 1 Number of measurements needed to reach (left panel) $F=0.9$ fidelity, and (right panel) $F=0.98$ fidelity for the W state with three approaches: maximum likelihood, RBM trial wavefunctions trained with Gibbs sampling, and mode-assisted RBM trial wavefunctions. N is the number of qubits.

References

- [1] Di Ventra, M. and Pershin, Y. V. *The parallel approach*, Nature Physics, **9**, 200 (2013).
- [2] Di Ventra, M. *MemComputing: Fundamentals and Applications* (Oxford University Press, 2022).
- [3] Di Ventra, M. and Traversa, F. L. *MemComputing: Leveraging memory and physics to compute efficiently*, J. Appl. Phys., **123**, 180901 (2018).
- [4] Di Ventra, M. and Ovchinnikov, I. V. *Digital MemComputing: from logic to dynamics to topology*, Annals of Physics, **409**, 167935 (2019).
- [5] Manukian, H. and Di Ventra, M. *Mode-assisted joint training of deep Boltzmann machines*, Scientific Reports, **11**, 19000 (2021).

Publications

- 1) M. Di Ventra, Y.V. Pershin, and C.-C. Chen, "Custodial chiral symmetry in SSH memcircuits", arXiv:2109.03428
- 2) A. Norambuena, F. Torres, M. Di Ventra, R. Coto, "Polariton-based quantum memristors", arXiv:2108.09382
- 3) Y.R. Pei and M. Di Ventra, "A Finite-temperature Phase Transition for the Ising Spin-glass in $d \geq 2$ ", arXiv:2105.01188

Time-dependent phenomena in correlated materials

Adrian E. Feiguin, Northeastern University

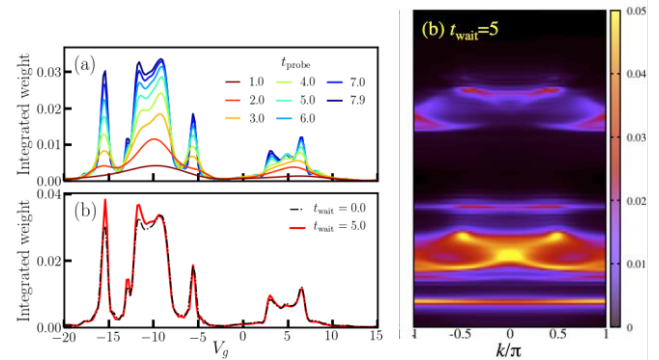
Program Scope

Our project encompasses two main themes: (i) developing and refining computational techniques to study non-equilibrium spectroscopies including non-perturbative effects and (ii) applications to non-equilibrium phenomena. In particular, we are interested in studying the fate of quasi particles when a system is driven away from equilibrium under a pump of electromagnetic radiation and the corresponding signatures in the photoemission or neutron spectra. It is subsequently divided into four (4) thrusts: (i) Inelastic neutron scattering away from equilibrium; (ii) non-perturbative effects in time-resolved ARPES; (iii) validity of the quasi-particle picture away from equilibrium; (iv) resonant inelastic X-Ray scattering.

Keywords: DMRG, ARPES, RIXS

Recent Progress

We have developed a new computational paradigm to simulate time and momentum resolved inelastic scattering spectroscopies in correlated systems. The conventional calculation of scattering cross sections relies on a treatment based on time-dependent perturbation theory, that provides formulation in terms of Green's functions. In equilibrium, it boils down to evaluating a simple spectral function equivalent to Fermi's golden rule, which can be solved efficiently by a variety of numerical methods. However, away from equilibrium, the resulting expressions require a full knowledge of the excitation spectrum and eigenvectors to account for all the possible allowed transitions, a seemingly unsurmountable complication. Similar problems arise when the quantity of interest originates from higher order processes, such as in Auger, Raman, or resonant inelastic X-ray scattering (RIXS) spectroscopies. To circumvent these hurdles, we introduce a time-dependent approach that does not require a full diagonalization of the Hamiltonian: we simulate the full scattering process, including the incident and outgoing particles (neutron, electron, photon) and the interaction terms with the sample, and we solve the time-dependent Schrödinger equation. The spectrum is recovered by measuring the momentum and energy lost by the scattered particles, akin an actual energy-loss experiment. The method can be used to study transient dynamics and spectral signatures of correlation-driven non-equilibrium



Left: time-resolved spectrum of the 1D extended Hubbard model at half-filling after a sudden quench in the interactions from $U_0 = 2, V_0 = 0$ to $U = 20, V = 5$. (a) Integrated spectral weight as a function of V_g for $t_{wait} = 0$ and different probe times (b) Same as (a) but for $t_{wait} = 0$ and 5, at the final $t_{probe} = 7.9$. **Right:** Momentum resolved tunneling spectrum.

processes, as I illustrate with several examples and experimental proposals using the time-dependent density matrix renormalization group method as a solver. Even in equilibrium, we find higher order contributions to the spectra that can potentially be detected by modern instruments.

Future Plans

- 1) We will calculate the non-equilibrium spin dynamic structure factor after pumping the spin ladder and look for signatures of triplon fractionalization into deconfined spinons. We will extend these ideas to dimerized chains.
- 2) Understanding the limits of the sudden approximation in ARPES: We will explicitly introduce the Coulomb interaction between the electron in the continuum and the bulk, and provide exact numerical evidence of the corrections to the sudden approximation and their spectral fingerprints.
- 3) We will study two-photon spectroscopies and “Coincidence ARPES” to extract information about pair binding energies and the spectrum of composite excitations (Cooper pairs).
- 4) We will study the dynamics of the excitations in indirect RIXS using time-resolved tunneling to understand the processes in the d band after the core-hole excitation is created. The results of these studies will help to unveil the physics of the p electron and its role in the screening mechanism.

Publications

- 1) Gannon WJ, Zaliznyak IA, Wu LS, Feiguin AE, Tsvetlik AM, Demmel F, Qiu Y, Copley JRD, Kim MS, Aronson MC. Spinon confinement and a sharp longitudinal mode in Yb₂Pt₂Pb in magnetic fields. Nat Commun. 2019 Mar 8;10(1):1123.
- 2) Feiguin AE, Tsvetlik AM, Yin W, Bozin ES. Quantum Liquid with Strong Orbital Fluctuations: The Case of a Pyroxene Family. Phys Rev Lett. 2019 Dec 6;123(23):237204.
- 3) Zawadzki K, Nocera A, Feiguin AE. A time-dependent scattering approach to core-level spectroscopies. Phys. Rev. X. Forthcoming; Available from: <https://arxiv.org/abs/2002.041424>.
- 4) Zawadzki K, Yang L, Feiguin A. Time-dependent approach to inelastic scattering spectroscopies in and away from equilibrium: Beyond perturbation theory. Phys. Rev. B **102**, 235141. Available from: <https://link.aps.org/doi/10.1103/PhysRevB.102.235141> DOI:10.1103/PhysRevB.102.235141.
- 5) Krissia Zawadzki and Adrian E. Feiguin. Time- and momentum-resolved tunneling spectroscopy of pump-driven nonthermal excitations in Mott insulators. Phys. Rev. B **100**, 195124 (2019).
- 6) Rincon, J and Feiguin AE. Nonequilibrium optical response of a one-dimensional Mott insulator. Phys. Rev. B **104**, 085122 (2021)

Intertwined and Vestigial Electronic Orders in Correlated Systems

Rafael M. Fernandes, University of Minnesota, Minneapolis, MN 55455

Program Scope

The overarching goal of this proposal is to investigate and elucidate the intertwining between various electronic orders realized in correlated materials. To achieve this goal, and to go beyond the competing-order paradigm commonly used to describe the phase diagrams of these systems, particular emphasis is given to the framework of vestigial electronic orders. These fluctuation-driven states, described by composite order parameters, are partially melted versions of phases commonly observed in correlated systems, such as spin and charge density-waves, superconductivity, and ferromagnetism. While this concept has been widely applied to electronic nematic phases, the concept of vestigial order extends well beyond nematicity, encompassing a variety of standard and exotic electronic orders. During this period, the PI demonstrated a route to realize double-Weyl points in iron-based superconductors that either explicitly or spontaneously break the glide plane symmetry of the lattice, e.g. via the onset of a spin-vorticity vestigial order. The PI also shed new light on the issue of intertwined superconducting, magnetic, and Mott insulating phases via state-of-the-art sign-problem-free Quantum Monte Carlo simulations of a multi-band interacting model. Finally, unique properties of the nematic normal state and nematic superconducting state of twisted moiré systems were unveiled, including the possibility of realizing an exotic charge-4e vestigial phase.

Keywords: Correlated-electron systems; intertwined orders; unconventional superconductivity.

Recent Progress

New topological properties of iron-based superconductors. The recent recognition that the band structure of iron-based superconductors (FeSC) can display a band inversion involving an As/Se p-band and Fe d-bands has ignited intense research on the possible realization of exotic topological phenomena in these compounds. In Ref. [1], the PI led an effort that revealed an appealing and experimentally feasible route to realize topological Weyl points involving only the Fe d-bands. The main ingredient is the breaking of the glide plane symmetry, such that the FeAs layers no longer have inversion symmetry. This symmetry-breaking can be explicit or spontaneous. A candidate for the latter is the vestigial spin-vorticity density-wave expected to appear when the magnetic ground state is the spin-vortex crystal. The former scenario is realized in the so-called 1144 compounds, such as $\text{CaKFe}_4\text{As}_4$, due to the existence of alternating Ca and K layers. In either scenario, the degeneracy of the electronic states along the M - A line of the Brillouin zone is lowered from 4 to 2 (see Fig. 1). Application of a magnetic lifts the remaining twofold degeneracy and moves the positions of the bands, which can then cross and form Weyl points. In the case of the 1144 compounds, depending on the ratio between the spin-orbit coupling and the Zeeman-field splitting, the crossing can be of bands with the same or opposite spins, resulting in double-Weyl

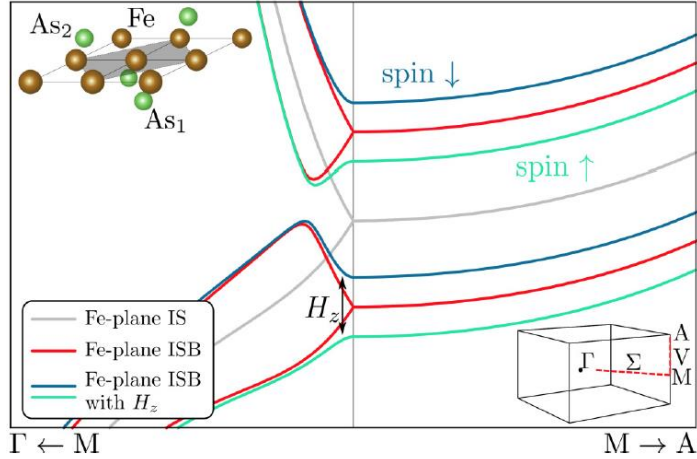


Figure 1: Schematic illustration of the degeneracies of the bands along the Brillouin zone path indicated in the lower inset for a single FeAs layer with P4/nmm space group. The following cases are shown: inversion symmetric (IS, grey); inversion-symmetry breaking (ISB, red); and ISB in the presence of a Zeeman field (blue and green). From Ref. [1].

or single-Weyl points, respectively. Hole-doping and electronic correlations bring these Weyl points close to the Fermi level, which would lead to unique experimental manifestations. The fact that the 1144 compounds display superconductivity below 30K leads to the exciting prospect of investigating the interplay between Weyl points and unconventional superconductivity.

QMC simulations of intertwined orders in an interacting multi-band electronic model. In many correlated-electron materials, interesting phenomena such as unconventional superconductivity emerge in the regime of moderate correlations, where electronic interactions are comparable with the kinetic energy, t . Elucidating this regime is difficult: analytically, well-established perturbative methods become uncontrolled; numerically, Quantum Monte Carlo (QMC) simulations face the hurdles imposed by the fermionic sign problem. In a work led by the PI [2], a multi-band version of the Hubbard model was solved by extensive determinantal QMC simulations. The model, which corresponds essentially to the Hubbard-Kanamori model written in band space, contains two bands and five interaction terms originating from the Coulomb repulsion. The key insight was that, in the limit where the two intra-band interactions vanish and the ratios between the three inter-band interactions is fixed, the model does not suffer from the sign problem, regardless of the magnitude of the remaining interaction U or of the filling. This is to be contrasted with the single-band Hubbard model, for which the sign-problem can only be avoided at half-filling. The resulting phase diagram, shown in Fig. 2, reveals a prominent antiferromagnetic (AFM) dome peaked at $U \sim t$. This dome is intercepted by a metal-to-insulator crossover line, which merges with the left AFM boundary of the dome in a seemingly first-order transition. Interestingly, a superconducting (SC)

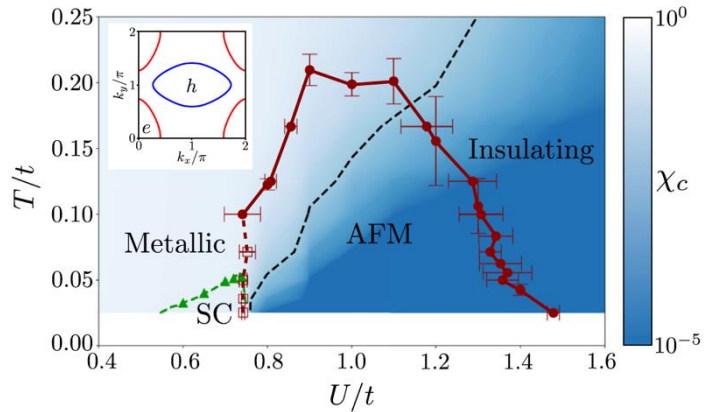


Figure 2: Phase diagram of the two-band version of the Hubbard model (inset) with only inter-band interactions, obtained from sign-problem-free QMC simulations. U/t is the ratio between the inter-band repulsion and the hopping. The red line denotes the antiferromagnetic (AFM) phase; the green line, the superconducting (SC) phase; and the dashed line, the metal-to-insulator transition/crossover. The background color denotes the charge susceptibility. From Ref. [2].

dome is only found near the metallic AFM quantum phase transition, with a maximum transition temperature of about 5% of t , which translates to hundreds of Kelvin for typical values of t . Near the insulating quantum AFM transition, SC is absent. This is attributed to a strong suppression of the quasi-particle spectral weight combined with a change of the magnetic dynamics from overdamped to propagating in the insulating side of the phase diagram – both of which were observed in the QMC simulations. The surprising lack of magnetic order for large U was further explored in Ref. [3] by strong-coupling methods, which revealed that the two-band Hubbard model with only inter-band interactions maps onto the transverse-field Ising J_1 - J_2 model. Depending on the parameters, the ground state may be non-magnetic, antiferromagnetic, or stripe magnetic. This is to be contrasted with the single-band Hubbard model, which reduces to an effective Heisenberg model at half-filling and large U , which has a Néel magnetic ground state for the square lattice.

Electronic nematicity and vestigial charge-4e order in twisted moiré systems. The observation of electronic nematic order in twisted moiré systems raised important new questions about the nature and properties of this correlated state. In contrast to the Ising-nematic order widely observed in correlated systems with rigid tetragonal crystal lattices, the nematic order parameter in moiré systems behaves as that of a 3-state Potts model. In Ref. [4], the PI and collaborator reported other fundamental differences between nematicity in rigid tetragonal crystals and in emergent triangular moiré superlattices. In the former, while uniaxial strain always smears the nematic transition, in the latter it still leaves an in-plane twofold rotational symmetry intact, such that a nematic-related transition can still occur. The coupling to acoustic phonon modes also leads to fundamentally different outcomes. In the rigid lattice case, due to elasticity constraints, this coupling effectively decouples the soft nematic fluctuations from the low-energy electronic states. In contrast, because the moiré lattice is an emergent superlattice subjected to the adhesion potential between the layers, this coupling ensures that low-energy nematic fluctuations are maximally coupled to the electrons.

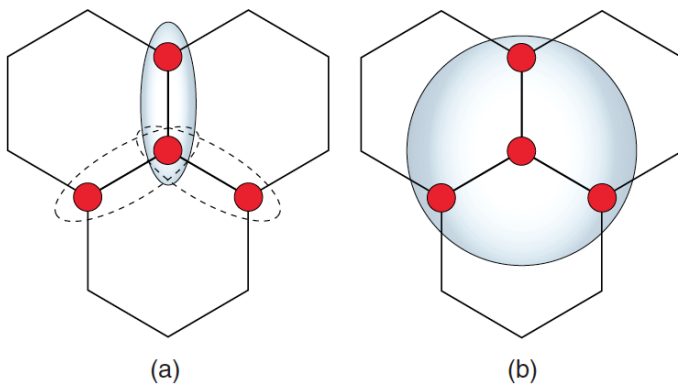


Figure 3: Illustration of the vestigial nematic order (a) and the vestigial charge-4e order (b) that can emerge before the onset of nematic superconductivity in lattices with three- or sixfold rotational symmetry. From Ref. [6].

The PI also developed a phenomenological model of nematicity in Ref. [5], which was a joint theoretical-experimental collaboration exploring the phase diagram of twisted bilayer graphene (TBG). The model provided essential support to the interpretation of the experimental data in terms of a nematic superconducting state and a nematic normal state. In Ref. [6], the PI and collaborator found that a nematic superconducting state in a triangular lattice, such as that revealed by Ref. [5] in TBG, supports two nearly degenerate vestigial phases: a nematic one and a

charge-4e one. The latter is characterized by coherent quartets formed out of pairs of Cooper pairs (see Fig. 3). It was shown that random strain can be used to favor the charge-4e phase over the nematic phase, opening the door for this exotic state being realized in inhomogeneous TBG devices.

Future Plans

One of the topics that will be investigated involves the unusual electronic properties of a newly proposed correlated state of matter, called valley-polarized electronic nematics, which can be realized in twisted moiré systems. The 6-state clock-model symmetry of this order parameter leads to an extended critical phase at finite temperatures, which can have unique manifestations on the electronic spectrum. At zero temperature, there is a wide regime in which the collective nematic mode behaves very similarly to the Goldstone mode of a genuine XY nematic, which is known to cause non-Fermi liquid behavior. Another research direction will involve sign-problem-free QMC simulations of a three-band version of the Hubbard model. Unlike the two-band version studied in Ref. [2], this one allows for a vestigial nematic state supported by the stripe magnetic ground state. The QMC simulations will provide unique unbiased insight onto the role of vestigial phases in correlated systems. The role of random strain on vestigial nematicity will also be investigated numerically. Quite generally, random strain acts as a random nematic field. If the nematic instability is the primary one, then the system can be modeled as the random-field Ising-model. However, if the nematic instability is a vestigial phase of a stripe magnetic state, a richer behavior is likely to emerge, since random strain acts also as a random-bond disorder to the magnetic variables. An appropriate low-energy model that captures some of these unique features is an Ashkin-Teller model with random Baxter field, which is amenable to Monte Carlo simulations.

References

- [1] N. Heinsdorf *et al.*, Phys. Rev. B **104**, 075101 (2021).
- [2] M. H. Christensen, X. Wang, Y. Schattner, E. Berg, and R. M. Fernandes, Phys. Rev. Lett. **125**, 247001 (2020).
- [3] X. Wang, M. H. Christensen, E. Berg, and R. M. Fernandes, in press Annals of Physics, 10.1016/j.aop.2021.168522 (2021).
- [4] R. M. Fernandes and J. W. F. Venderbos, Science Adv. **6**, eaba8834 (2020).
- [5] Y. Cao *et al.*, Science **372**, 264 (2021).
- [6] R. M. Fernandes and L. Fu, Phys. Rev. Lett. **127**, 047001 (2021).

Publications (selected list)

1. *Strong-coupling expansion of multi-band interacting models: mapping onto the transverse-field J_1 - J_2 Ising model*, X. Wang, M. H. Christensen, E. Berg, and R. M. Fernandes, in press *Annals of Physics*, 10.1016/j.aop.2021.168522 (2021).
2. *Degradation of phonons in disordered moiré superlattices*, H. Ochoa and R. M. Fernandes, arXiv:2108.10342 (2021).
3. *Theory of the charge-density wave in AV_3Sb_5 kagome metals*, M. H. Christensen, T. Birol, B. M. Andersen, and R. M. Fernandes, arXiv:2107.04546 (2021).
4. *Prediction of Double-Weyl Points in the Iron-Based Superconductor $CaKFe_4As_4$* , N. Heinsdorf, M. H. Christensen, M. Iraola, S. Zhang, F. Yang, T. Birol, C. D. Batista, R. Valentí, and R. M. Fernandes, *Phys. Rev. B* **104**, 075101 (2021).
5. *Charge-4e superconductivity from multi-component nematic pairing: Application to twisted bilayer graphene*, R. M. Fernandes and L. Fu, *Phys. Rev. Lett.* **127**, 047001 (2021).
6. *Electric-field-tunable electronic nematic order in twisted double-bilayer graphene*, R. Samajdar, M. S. Scheurer, S. Turkel, C. Rubio-Verdú, A. N. Pasupathy, J. W. F. Venderbos, and R. M. Fernandes, *2D Mater.* **8**, 034005 (2021).
7. *Nematicity and Competing Orders in Superconducting Magic-Angle Graphene*, Y. Cao, D. Rodan-Legrain, J. M. Park, F. N. Yuan, K. Watanabe, T. Taniguchi, R. M. Fernandes, L. Fu, and P. Jarillo-Herrero, *Science* **372**, 264 (2021).
8. *Topological and nematic superconductivity mediated by ferro- $SU(4)$ fluctuations in twisted bilayer graphene*, Y. Wang, J. Kang, R. M. Fernandes, *Phys. Rev. B* **103**, 024506 (2021).
9. *Modeling unconventional superconductivity at the crossover between strong and weak electronic interactions*, M. H. Christensen, X. Wang, Y. Schattner, E. Berg, and R. M. Fernandes, *Phys. Rev. Lett.* **125**, 247001 (2020).
10. *Universal moiré nematic phase in twisted graphitic systems*, C. Rubio-Verdú, S. Turkel, L. Song, L. Klebl, R. Samajdar, M. S. Scheurer, J. W. F. Venderbos, K. Watanabe, T. Taniguchi, H. Ochoa, L. Xian, D. Kennes, R. M. Fernandes, A. Rubio, and A. N. Pasupathy, arXiv:2009.11645 (2020).
11. *Nematicity with a twist: rotational symmetry breaking in a moiré superlattice*, R. M. Fernandes and J. W. F. Venderbos, *Science Adv.* **6**, eaba8834 (2020).

Theory for pump/probe experiments in charge-density-wave materials

James Freericks, Department of Physics, Georgetown University

Program Scope

Objectives: This project is focused on theoretically describing pump-probe experiments. One of the most studied classes of materials are charge-density-wave (CDW) ordered quantum materials that illustrate a wide range of complex and interesting behavior. We want to determine the fundamental behavior of electron-driven and phonon driven charge-density-wave materials. We discovered interesting rich behavior in electron driven CDWs. This behavior can be summarized as being an *emergent* quantum critical point—at $T=0$, the system remains in a single phase, but as $T \rightarrow 0$, there is a metal-insulator transition that takes place at a critical value of the interaction strength. This system behaves like a quantum critical point for temperatures above zero, but it has no quantum critical point at $T=0$! We also spent a significant effort to develop new numerical methods for simulating nonequilibrium systems. Our first attempt was based on a real-time solver of the single-impurity Anderson model, but we were not able to stabilize a numerically tractable methodology for completing that work. Instead, we developed an accurate Monte Carlo approach for solving the nonequilibrium problem in CDW systems in two-dimensions—one of the key features is this solver can extend to long times (many 10s of picoseconds). It utilizes special features of the many-body problem in the limit when the phonon frequency goes to zero. If the frequency is exactly zero, then the phonons are static and the system is solved by an annealed average over the phonon distribution. If the frequency is low, then it is well described by a semiclassical approach, similar to the Born-Oppenheimer approximation, where the electrons are treated exactly as quantum particles, but the phonons are treated as classical objects

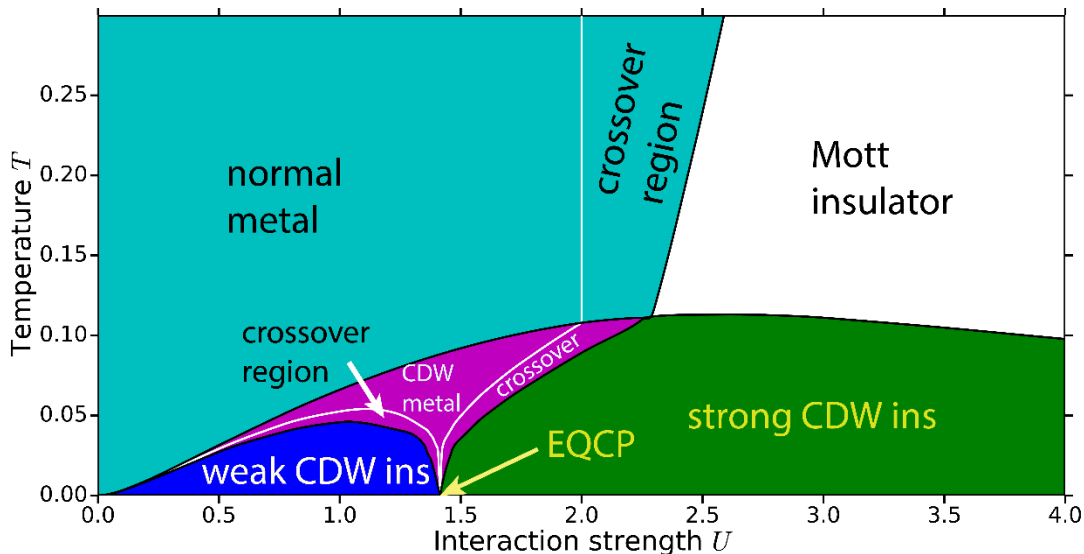


Fig. 1: Emergent quantum critical point for an electron-driven CDW. A nonzero band inside the gap region forms as T is raised. It has the classic V shape of a quantum critical point.

moving according to their Ehrenfest forces. Using this numerical approach, we have discovered a robust mechanism to avoid the heat-death in Floquet-driven electronic systems and we have been able to provide a microscopic description of a number of recent pump/probe experiments in CDW systems.

Recent Progress

We start by discussing the emergent quantum critical point. This arises due to the creation of mid-gap states in a CDW. What we find is that for low U , the midgap states are created near the band gaps. But as U is increased, they are pushed closer and closer to the center of the gap, until they meet at a critical value of U . Then they are pushed beyond the center toward the opposite gap edge, eventually forming the Mott insulator band edge in the normal state. At the critical value of U , the metallic density of states is present for any nonzero temperature (but does not form at $T=0$). Because the weight of the minigap grows exponentially as T is increased, this metallic behavior can be masked into looking like activated insulator transport. But it is not that. It satisfies scaling laws for U values above and below the critical U , and has the same phenomenological V shape for the conductivity as we see in quantum critical points (see Fig. 1) for the emergent quantum critical point phase diagram.

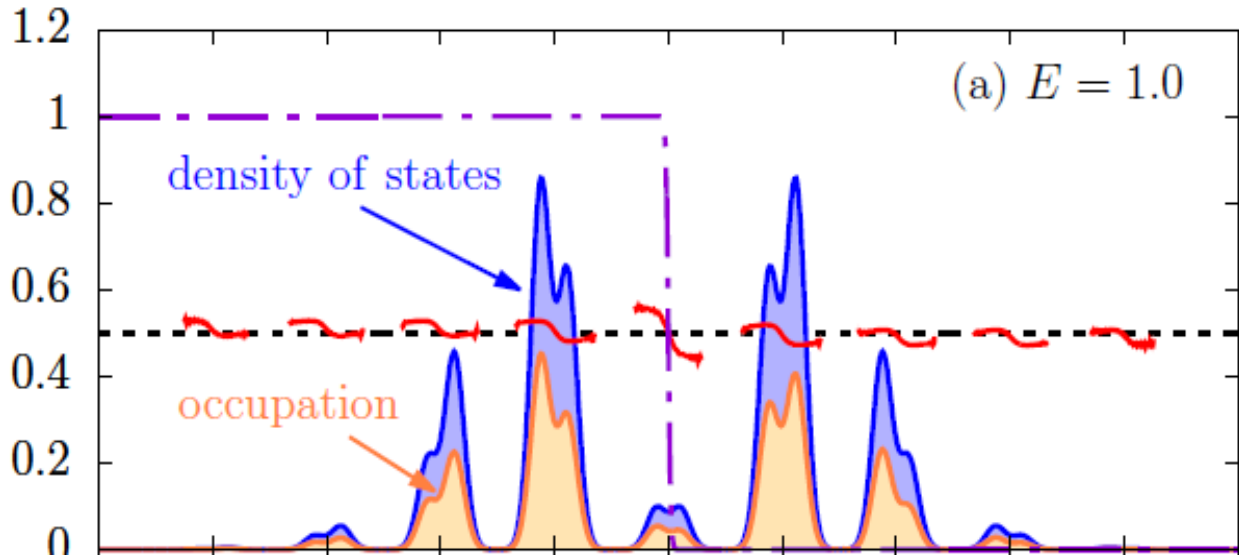


Fig. 2. Nonequilibrium density of states (blue) and occupancy (beige). One can see the individual Wannier-Stark minibands, nearly split by the interactions, with a distribution (red lines) that is given by high-temperature Fermi-Dirac distributions. This behavior is highly nonequilibrium, but is stable, because the runaway heating of typical Floquet systems is shut off due to the dynamical symmetrization of the electron momentum distribution.

The second group of projects we have completed involve nonequilibrium dynamics in electron-phonon coupled systems. We have studied the response of an electron-phonon coupled system to a large DC electric field. The current folklore says this should heat up to infinite temperature. But, instead, we find that the gauge-invariant electronic momentum distribution quickly becomes an even function of momentum. Once this occurs, the current vanishes and the system can no

longer heat, even though an electric field is present (because the Joule heating is given by $E \cdot J$, which vanishes if $J=0$). The steady state that emerges is quite nonequilibrium. The density of states develops broadened Wannier-Stark bands that are occupied by electrons in a Fermi-like distribution for each miniband (rather than an overall Fermi-Dirac distribution for the set of bands). These results are summarized in Fig. 2.

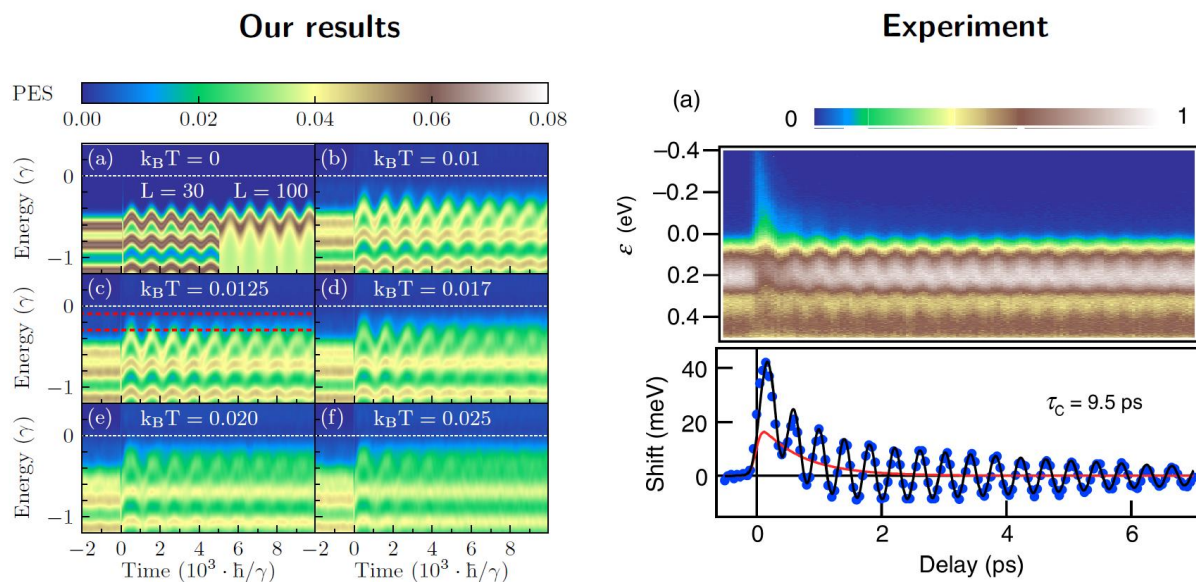


Fig. 3. (Left) Time-resolved photoemission spectroscopy of a CDW system at different initial temperatures and (right) experimental photoemission spectroscopy for a CDW system (from the Perfetti group). As T rises, the excited phonon is more and more damped. The oscillation of the phonon can be seen by the oscillation of the band edge of the photoemission. We see similar damping to experiment at intermediate T s.

We have also have investigated time-resolved photoemission spectroscopy in CDW systems. Our numerical calculations span many picoseconds, so we can faithfully simulate the behavior of these systems on the phonon timescales. We see similar behavior for the oscillation of the band edge of the photoemission spectroscopy with that seen in experiment on a typical CDW system. The results are shown in Fig. 3.

We also have investigated the dynamical transition seen as a function of fluence in CDW systems. When we are in the CDW phase, the phonon potential has a double-well nature to it. As we pump energy in the system, it changes to a single well. Interestingly, if one can tune the fluence to drive the phonon right to the bottom of the single well, then it will just sit there. This leads to a dynamical decoupling of Holstein phonons, since their interaction is proportional to the phonon coordinate. In this case, they would have no interaction on average, and very small interaction in general. The transition is very sharp in the fluence and has been seen by Nuh Gedik's group. We summarize our calculations in Fig. 4.

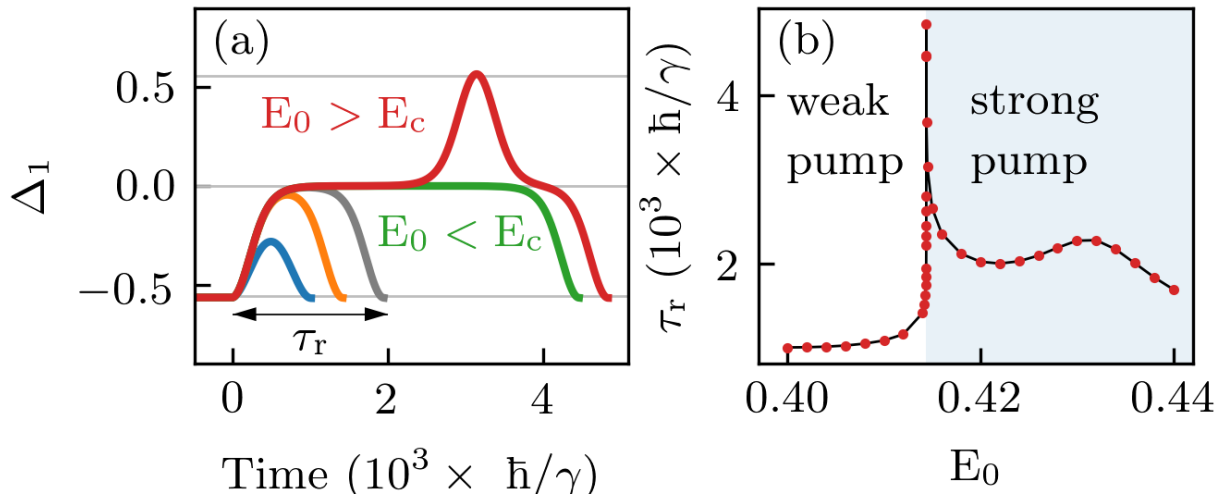


Fig. 4. (Left panel) the phonon coordinate as a function of time for different fluences. For weak fluence, the phonon coordinate oscillates about the CDW-ordered value. At high fluence, it oscillates from one ordered value to the other, as if the double well has become a single well. At the critical fluence, the phonon coordinate is driven to the origin (center of the single well) and stays there. (Right panel) The rise time as a function of fluence measures the time it takes the phonon to reach its maximal variation due to the pump. In the critical region, this rise time sharply increases. Similar results have been seen in Nuh Gedik’s experiments on CDW systems.

Keywords: Nonequilibrium many-body problem, pump/probe spectroscopy, electron-phonon coupled systems

Future Plans

Our work on pump/probe spectroscopy in CDW systems has only just begun. We plan to investigate what happens when the phonon is directly driven by THz radiation, as opposed to indirectly driven by pumping the electrons. We also plan to look into other experimental behavior that has already been measured, but has not yet been explained by a microscopic model, including the difference between diagonal and off-diagonal electron-phonon coupling. The heat-death work and a description of the numerical approach have all been written up and submitted. The pump/probe photoemission work is nearly finished being written up, as is the emergent quantum critical point work.

The plans for next year are to focus on developing new capabilities of our code, in terms of response functions we can measure, and applying it to as many experimental situations as we can. We also plan to investigate systems with off-diagonal electron-phonon coupling (Su-Schrieffer-Heeger model) and to go from one-d systems to two-d systems. We also plan to begin work on time-resolved Raman scattering, which is also planned to be completed during the grant period.

Publications

- [1] Manuel Weber, Francesco Parisen Toldin, and Martin Hohenadler, *Competing orders and unconventional criticality in the Su-Schrieffer-Heeger model*, Phys. Rev. Research **2**, 023013 (2020). Doi: PhysRevResearch.2.023013
- [2] Herbert F. Fotso and James K. Freericks, *Characterizing the Non-equilibrium Dynamics of Field-Driven Correlated Quantum Systems*, Front. Phys. **8**, 324 (2020). Doi: 10.3389/fphy.2020.00324
- [3] Manuel Weber, *Valence bond order in a honeycomb antiferromagnet coupled to quantum phonons*, Phys. Rev. B **103**, L041105 (2021). Doi: 10.1103/PhysRevB.103.L041105
- [4] J. K. Freericks and Alexander F. Kemper, *What do the two times in two-time correlation functions mean for interpreting tr-ARPES?*, J. Elec. Spec. Rel. Phenom. **251**, 147104 (2021). Doi: 10.1016/j.elspec.2021.147104
- [5] Herbert F. Fotso, Eric Dohner, Alexander Kemper and James K. Freericks, *Bridging the Gap Between the Transient and the Steady State of a Nonequilibrium Quantum System*, submitted to Phys. Rev. B. (arxiv: 2101.00795)
- [6] Manuel Weber and James K. Freericks, *Field Tuning Beyond the Heat Death of a Charge-Density-Wave Chain*, submitted to Phys. Rev. Lett. (arXiv: 2107.04096)
- [7] Manuel Weber and James K. Freericks, *Real-time evolution of static electron-phonon models in time-dependent electric fields*, submitted to Phys. Rev. E (arXiv: 2108.05431)

Simulating long-time evolution of driven many-body systems with next generation quantum computers

James Freericks, Department of Physics, Georgetown University and Alexander Kemper, Department of Physics, North Carolina State University

Program Scope

Objectives: This project is focused on performing the best science possible on current generation quantum computers. As such, we have focused on developing techniques that involve robust algorithms that are either insensitive to noise, or are extremely low depth. We also have worked on determining topological properties and employing the robustness of topology to noise to allow for robust quantum computation. The ultimate goal is to be able to do new science on quantum computers that cannot be achieved on classical computers. The main effort of the work we have completed is on time-evolution of quantum systems and robust calculation of properties of systems enabled by being able to perform time evolution.

Recent Progress

The recent work we have completed falls into three main categories: (i) constant depth time evolution circuits (as an alternative to Trotter time evolution); (ii) time evolution for driven-dissipative systems; and (iii) computation of topological invariants of topological quantum systems. We have achieved what we believe to be the world record for time steps in time evolution on a quantum computer, completing 1000 Trotter steps of time evolution for a driven dissipative system. We are able to construct circuits for time evolution that are constant in depth, even for certain classes of time-dependent Hamiltonians; this employs a circuit compression algorithm that is based on group theoretic ideas. We also have demonstrated how to compute a number of different topological properties, including the first ever noise free measurement of the Chern number. Finally, we also showed how one can use a quantum computer to determine Lee-Yang and Fisher zeros and employ them in determining thermodynamics.

The first project we will describe is developing constant depth circuits for time evolution. One of the challenges of time evolution on quantum computers is that the conventional Trotter product formula requires more and more resources for long time evolution. This is because one needs more Trotter steps for a given step size to get to long times, but the situation is even worse, because higher accuracy is also needed, so one must also reduce the step size when going to longer times, which makes the depth of the circuit increase very rapidly.

For Hamiltonians that do not depend on time, one can use the Lie algebraic construction of a Cartan decomposition and the so-called KAK theorem to decompose the time evolution for any time into a product of operators determined by the algebraic results and not relying on Trotter steps. The only challenge with this approach is that the Lie algebra arising from the Hamiltonian must be small enough that the circuit can be constructed as a low-depth circuit. This is possible

for a wide class of oft-studied spin models, and we have completed a project showing how this procedure works. Future work will investigate whether this approach can be generalized to more complex models. But, we have also discovered an even more powerful method for circuit compression. Here, we find that different types of circuit elements from a Trotter decomposition can be recombined and compressed into a much shorter circuit. This then allows us to perform the compression on time-varying Hamiltonians as well. The final result is very efficient, as shown in Fig. 1.

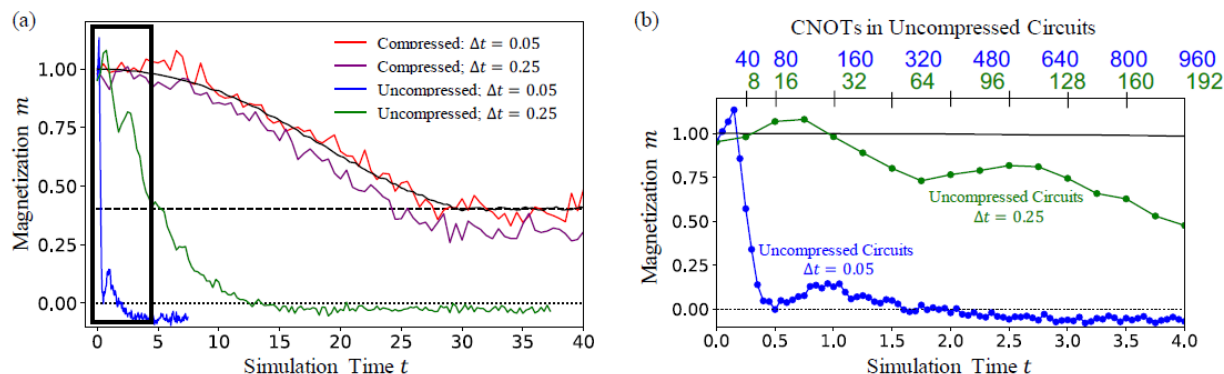


Fig. 1. (Left) Magnetization of a five-site Ising model that has a transverse field slowly turned on starting from $t=0$. The exact magnetization is the solid curve and the red and purple curves are compressed circuits run on the IBM quantum computer. One can see that the conventional circuits (blue and green) fail already at short times.

The second project we examined is simulating driven-dissipative systems. These systems are among the most difficult to simulate on classical computers, because many equilibrium-based algorithms fail for systems that have time dependence. Our goal is to simulate the general Hubbard model. We have not achieved that yet, but we have successfully simulated its two limits: (i) the noninteracting limit and (ii) the atomic limit. In the noninteracting limit, we modeled lattice electrons driven by an electric field and coupled to a fermionic bath at each lattice site. The problem was mapped to a master equation by integrating out the reservoir degrees of freedom and imposing the Markov approximation. The resulting Lindblad equation is then reformulated into a Kraus map, which can be directly implemented on the quantum computer. We were able to run circuits on the IBM quantum computers once mid-circuit resets became available about one year ago. Since these circuits are intrinsically robust, due to their contractive nature, we could run the circuit many times longer than the decoherence time of a qubit. We were able to run for 1000 Trotter steps (which is more than an order of magnitude longer than the recent Google time evolution of the Hubbard model). We believe this is the longest time evolution on any quantum computer. We then used these results to calculate the current of the system as it approaches a steady state. These results appear in Fig. 2.

We also calculated the thermalization of a Hubbard atom in a magnetic field. Here, we have four states, and the doubly occupied one feels an interaction U . Running our circuit shows that even if

the short-time, transient behavior is not too accurate, the system nevertheless does settle in on the correct steady state for long times. These results appear in Fig. 3.

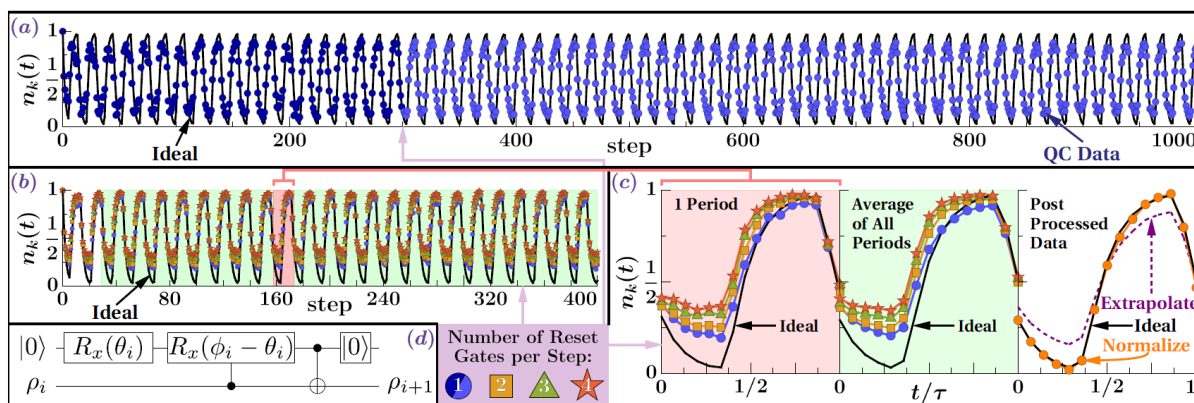


Fig. 2. Momentum distribution as a function of time for a system driven by a DC electric field in the presence of dissipation. (Top panel) raw data from the IBM machine compared to the exact result. (Left) extrapolation method to extrapolate to the zero-reset-time limit and the circuit we ran. (Right) data processing used to extract the error-free result, which nearly lies on top of the exact answer.

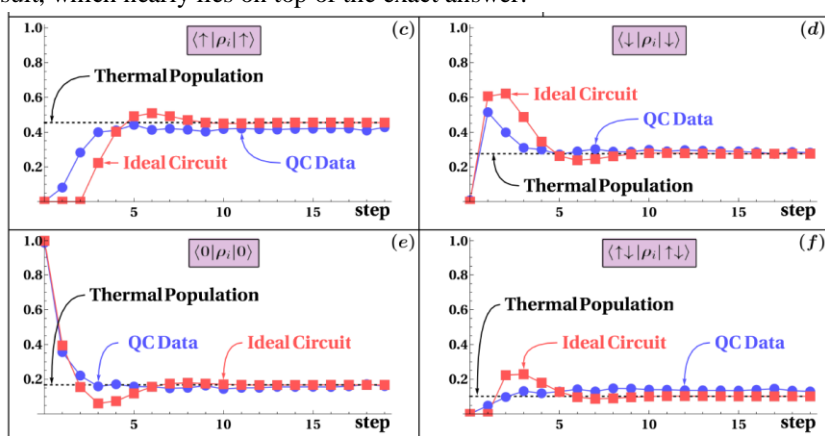


Fig. 3. Time evolution for the thermal-state preparation of the Hubbard atom. The system has a single Hubbard lattice site and is in a magnetic field. The quantum computer data (blue) follows close to the exact result (red), but has larger errors in the transient regime at short times.

We plan to work on determining how to create the Kraus maps that will describe the Hubbard model for intermediate U . This problem is highly nontrivial, but solving it will allow us to use quantum computers to simulate pump/probe spectroscopy experiments. Key to making this happen is a means to determine the Green's function and other response functions on the quantum computer. An algorithm, now called the Hadamard test, was developed at Los Alamos nearly 20 years ago. Unfortunately, that algorithm is very sensitive to decoherence in the ancilla during the time evolution of the system. Indeed, we tried running it on the IBM machines for these systems and it was not successful. We have instead generalized this result to create a robust method for measuring Green's functions on a quantum computer based on the ideas of Ramsey

interferometry. The approach shares many similarities with the Hadamard test, but we entangle the ancilla and then immediately measure it in our protocol, so it is robust against decoherence errors. We have run this algorithm on the Honeywell quantum computer and successfully calculated Green’s functions even for times longer than the decoherence time of the quantum computer. These results are shown in Fig. 4.

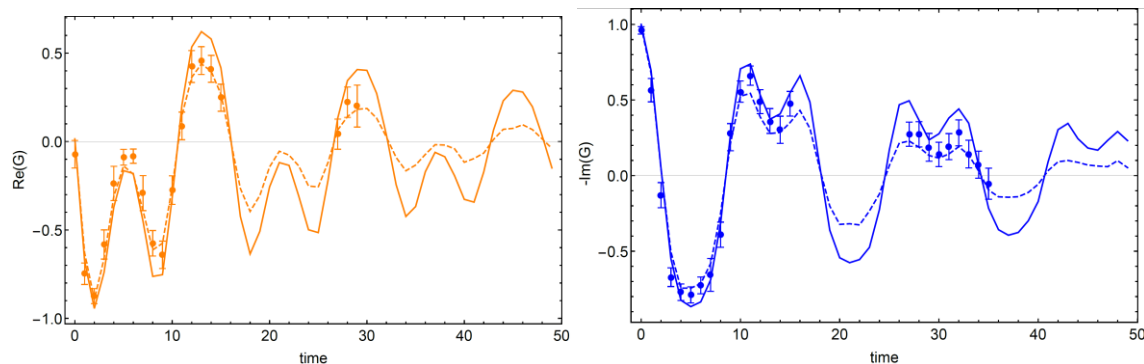


Fig. 4. Retarded Green’s function for a nonequilibrium driven-dissipative system in its steady state. (Left) Real part of G and (right) imaginary part of G . The data points at the longest times lie beyond the coherence time of the Honeywell quantum computer. This is the first step in being able to simulate pump/probe spectroscopies on a quantum computer.

The last set of problems we worked on involved computing topological properties of quantum models with topological invariants. We found that even on a conventional quantum computer, the topology of a quantum model protects the calculation and allows us to determine properties of these systems, sometimes without any errors. We also solved for thermodynamics using Lee-Yang zeros, demonstrating that our developed time evolution techniques can be applied in a wide variety of scenarios.

Keywords: Nonequilibrium many-body problem, quantum computation, time evolution of quantum systems

Future Plans

One of the major pushes of next year’s work will be to see whether pump/probe spectroscopies can be computed on currently available NISQ machines. If successful, this can usher in a new era of theoretical developments for the nonequilibrium many-body problem. We also plan on pushing forward the circuit compression ideas to see if they can be generalized to more complex models as well as generalizing the Lee-Yang zeros work. We plan on examining nonequilibrium topological models, such as the well-known Thouless (quantum) pump. Finally, we will try to see if we can determine how to find approximate Kraus maps that can describe the behavior of the driven dissipative Hubbard model well. For this, we seek a minimal mapping that provides the required dissipation. Since many different reservoirs should produce similar behavior of the system, we believe that finding a minimal model, corresponding to a simplified reservoir, may allow this problem to be solved.

- Publications:** [1] Akhil Francis, J. K. Freericks, and A. F. Kemper, *Quantum computation of magnon spectra*, Phys. Rev. B **101**, 014411 (2020). Doi: 10.1103/PhysRevB.101.014411
- [2] Lorenzo Del Re, Brian Rost, A. F. Kemper, and J. K. Freericks, *Driven-dissipative quantum mechanics on a lattice: Simulating a fermionic reservoir on a quantum computer*, Phys. Rev. B **102**, 125112 (2020). DOI: 10.1103/PhysRevB.102.125112
- [3] M. Reitner, P. Chalupa, L. Del Re, D. Springer, S. Ciuchi, G. Sangiovanni, and A. Toschi, *Attractive Effect of a Strong Electronic Repulsion: The Physics of Vertex Divergences* Phys. Rev. Lett. **125**.196403 (2020). DOI: 10.1103/PhysRevLett.125.196403
- [4] Akhil Francis, D. Zhu, C. Huerta Alderete, Sonika Johri, Xiao Xiao, J. K. Freericks, C. Monroe, N. M. Linke, and A. F. Kemper, *Many Body Thermodynamics on Quantum Computers via Partition Function Zeros*, Science Adv. **7**, eabf2447 (2021). DOI: 10.1126/sciadv.abf2447
- [5] Xiao Xiao, J. K. Freericks, and A. F. Kemper, Determining quantum phase diagrams of topological Kitaev-inspired models on NISQ quantum hardware, Quantum **5**, 553 (2021). DOI: 10.22331/q-2021-09-28-553
- [6] Lorenzo Del Re and Alessandro Toschi, *Dynamical vertex approximation for many-electron systems with spontaneously broken $SU(2)$ symmetry*, Phys. Rev. B **104**, 085120 (2021). DOI: 10.1103/PhysRevB.104.085120
- [7] Xiao Xiao, J. K. Freericks, and A. F. Kemper, Robust measurement of wave function topology on NISQ quantum computers, submitted to Quantum. (arxiv: 2101.07283)
- [8] Bassman L, Urbanek M, Metcalf M, Carter J, Kemper AF, de Jong W, *Simulating Quantum Materials with Digital Quantum Computers*, to appear in Quant. Sci. Tech. (arXiv 2101.0883)
- [9] Metcalf M, Stone E, Klymko K, Kemper AF, Sarovar M, de Jong WA, *Quantum Markov Chain Monte Carlo with Digital Dissipative Dynamics on Quantum Computers* (arXiv 2103.03207)
- [10] Camps D, Kökcü E, Bassman L, de Jong WA, Kemper AF, Van Beeumen R, *An Algebraic Quantum Circuit Compression Algorithm for Hamiltonian Simulation*, submitted to SIAM J. Matrix Anal. Appl. (arxiv 2108.03283)
- [11] Kökcü E, Camps D, Bassman L, Freericks JK, de Jong WA, Van Beeumen R, Kemper AF, *Algebraic Compression of Quantum Circuits for Hamiltonian Evolution*, submitted to Phys Rev A. (arXiv 2108.03282)
- [12] Brian Rost, Barbara Jones, Mariya Vyushkova, Aaila Ali, Charlotte Cullip, Alexander Vyushkov, Jarek Nabrzyski, *Simulation of Thermal Relaxation in Spin Chemistry Systems on a Quantum Computer Using Inherent Qubit Decoherence*, submitted to PRX Quantum (arXiv 2001.00794)

Midwest Integrated Center for Computational Materials (MICCoM): A Brief Overview

PI: G. Galli, Argonne National Laboratory (lead institution), University of Chicago

Co-PIs: Maria Chan, Argonne National Laboratory; Juan de Pablo, Marco Govoni, and Joseph Heremans, Argonne National Laboratory and The University of Chicago; Andrew Ferguson and Dmitri Talapin, The University of Chicago; François Gygi, University of California, Davis; and Jonathan Whitmer, University of Notre Dame

Program Scope:

The Midwest Integrated Center for Computational Materials, MICCoM (<http://miccom-center.org/>) develops and disseminates interoperable computational tools – open-source software, data, simulation methods, and validation procedures – that enable the community to simulate and predict properties of functional materials for energy conversion, and solid-state materials for quantum information science. The center is focused on the prediction of properties of heterogeneous systems composed of atomistic and nanoscale building blocks; the emphasis is placed on understanding and characterizing defects and interfaces, and on predicting finite-temperature spectroscopic and coherence properties.

To predict the properties of heterogeneous systems, the center develops first-principles electronic-structure methods, coupled to appropriate dynamical descriptions of matter and advanced sampling techniques, so as to capture all the relevant length and time scales of importance to materials design [1]. (See Fig.1).

Keywords: quantum simulations, materials for energy, materials for quantum technologies

Recent progress

The ecosystem of coupled codes and frameworks built within MICCoM is summarized in Fig. 2. SSAGES [I] provides a suite of advanced methods for phase space sampling and a framework that can be used as a wrapper for first principles molecular dynamics (FPMD), classical MD and Monte Carlo engines. Qbox [II] is a first principles molecular dynamics code using Density Functional Theory (DFT) and hybrid-DFT to simulate thermodynamic and structural properties of materials and molecules, including simulations under bias; it also performs calculations of vibrational spectra & ionic conductivity. WEST [III-V] performs large-scale many-body perturbation theory calculations (GW, BSE, el-phonon, quantum embedding) to compute electronic and optical properties. In Fig.2 the double arrows indicate codes coupled in client-server

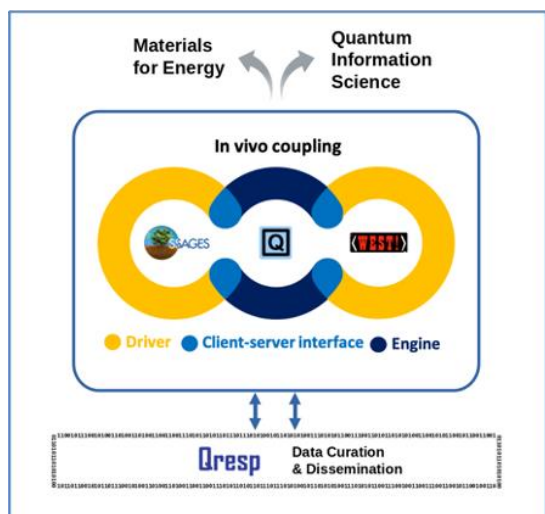


Figure 1. The three main open-source codes developed within MICCoM (the quantum codes Qbox and WEST and the advanced sampling suite of codes SSAGES) are used to compute multiple materials properties for the prediction and design of materials for energy conversion processes and quantum information science [1]. Qresp is a graphical user interface developed to disseminate and enable curation of data on a paper-by-paper basis [2].

mode and the single arrow pointing from the Qbox-WEST coupling to quantum defect embedding theory (QDET) [3-5] indicates the use of the client-server functionality in the implementation of the QDET. We note the presence of all codes developed within MICCoM in our coupling framework, but also of codes developed outside the center (e.g., i-PI, pySCF and Quantum Espresso) to indicate that MICCoM coupling strategy is general and can be easily extended to other codes, as needed.

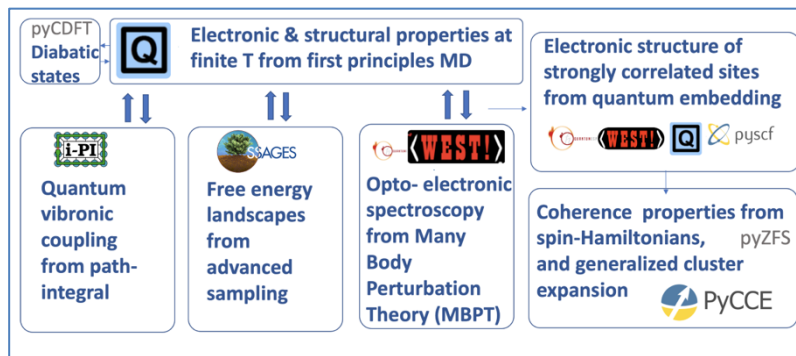


Figure 2. Summary of codes coupled, developed and used within the center.

Recent progress in coupling classical and quantum codes for the description of matter at the atomistic and molecular scales includes the study of chemical reactions at surfaces [6], liquids and aqueous interfaces [7-8], nanostructured materials [9], and solid-state qubits [10-13].

Future Plans

The plans for the center for the current year include the completion of the porting of WEST and pySAGES (two of the main MICCoM codes) onto to GPU architectures, the ongoing optimization of Qbox and WEST, updated documentation on the coupling of the two codes and the development of improved algorithms for first principles molecular dynamics with hybrid functionals and for the calculations of spectroscopic properties of materials using many body perturbation theory.

References

- I) Hythem Sidky, Yamil J. Colón, Julian Helfferich, Benjamin J. Sikora, Cody Bezik, Weiwei Chu, Federico Giberti, Ashley Z. Guo, Xikai Jiang, Joshua Lequieu, Jiyuan Li, Joshua Moller, Michael J. Quevillon, Mohammad Rahimi, Hadi Ramezani-Dakhel, Vikramjit S. Rathee, Daniel R. Reid, Emre Sevgen, Vikram Thapar, Michael A. Webb, Jonathan K. Whitmer, and Juan J. de Pablo, *SSAGES: Software Suite for Advanced General Ensemble Simulations*, J. Chem. Phys. 148, 044104 (2018). DOI: 10.1063/1.5008853
- II) Francois Gygi, *Architecture of Qbox: A scalable first-principles molecular dynamics code*, IBM Journal of Research and Development 52.1.2 (2008): 137-144.
- III) Marco Govoni and Giulia Galli, *Large Scale GW Calculations*, J. Chem. Theory Comput. 11, 2680 (2015). DOI: 10.1021/ct500958p
- IV) Peter Scherpelz, Marco Govoni, Ikutaro Hamada, and Giulia Galli, *Implementation and Validation of Fully Relativistic GW Calculations: Spin-Orbit Coupling in Molecules, Nanocrystals, and Solids*, J. Chem. Theory Comput. 12, 3523 (2016). DOI: 10.1021/acs.jctc.6b00114
- V) Marco Govoni and Giulia Galli, *GW100: Comparison of Methods and Accuracy of Results Obtained with the WEST Code*, J. Chem. Theory Comput. 14, 1895 (2018). DOI: 10.1021/acs.jctc.7b00952

Publications

- [1] Marco Govoni, Jonathan Whitmer, Juan de Pablo, Francois Gygi, and Giulia Galli, *Code interoperability extends the scope of quantum simulations*, npj Comput. Mater. 7, 32, (2021). DOI: 10.1038/s41524-021-00501-z
- [2] Marco Govoni, Milson Munakami, Aditya Tanikanti, Jonathan H. Skone, Hakizumwami B. Runesha, Federico Giberti, Juan de Pablo, and Giulia Galli, *Qresp, a tool for curating, discovering and exploring reproducible scientific papers*, Sci. Data 6, 190002 (2019). DOI: 10.1038/sdata.2019.2
- [3] He Ma, Marco Govoni, Giulia Galli, *Quantum simulations of materials on near-term quantum computers*, npj Comput. Mater. 6, 85 (2020). DOI: 10.1038/s41524-020-00353-z
- [4] He Ma, Nan Sheng, Marco Govoni, Giulia Galli, *First-principles studies of strongly correlated states in defect spin qubits in diamond*, Phys. Chem. Chem. Phys. 22, 25522 (2020). DOI: 10.1039/D0CP04585C
- [5] He Ma, Nan Sheng, Marco Govoni, and Giulia Galli, *Quantum Embedding Theory for Strongly Correlated States in Materials*, J. Chem. Theory Comput. 17, 2116 (2021). DOI: 10.1021/acs.jctc.0c01258
- [6] Elizabeth M. Y. Lee, Thomas Ludwig, Boyuan Yu, Aayush R. Singh, François Gygi, Jens K. Nørskov, and Juan J. de Pablo, *Neural Network Sampling of the Free Energy Landscape for Nitrogen Dissociation on Ruthenium*, J. Phys. Chem. Lett. 12, 2954 (2021). DOI: 10.1021/acs.jpcllett.1c00195
- [7] Katherine J. Harmon, Kendra Letchworth-Weaver, Alex P. Gaiduk, Federico Giberti, Francois Gygi, Maria K. Y. Chan, Paul Fenter, and Giulia Galli, *Validating first-principles molecular dynamics calculations of oxide/water interfaces with x-ray reflectivity data*, Phys. Rev. Materials 4, 113805 (2020). DOI: 10.1103/PhysRevMaterials.4.113805
- [8] Cunzhi Zhang, Federico Giberti, Emre Sevgen, Juan J. de Pablo, Francois Gygi, and Giulia Galli, *Dissociation of salts in water under pressure*, Nat. Commun. 11, 3037 (2020). DOI: 10.1038/s41467-020-16704-9
- [9] Mariami Rusishvili, Stefan Wippermann, Dmitri V. Talapin, and Giulia Galli, *Stoichiometry of the Core Determines the Electronic Structure of Core–Shell III–V/II–VI Nanoparticles*, Chem. Mat. 32, 9798 (2020). DOI: 10.1021/acs.chemmater.0c03939
- [10] Yu Jin, Marco Govoni, Gary Wolfowicz, Sean E. Sullivan, F. Joseph Heremans, David D. Awschalom, and Giulia Galli, *Photoluminescence spectra of point defects in semiconductors: Validation of first-principles calculations*, Phys. Rev. Materials 5, 084603 (2021). DOI: 10.1103/PhysRevMaterials.5.084603
- [11] Krishnendu Ghosh, He Ma, Mykyta Onizhuk, Vikram Gavini, and Giulia Galli, *Spin–spin interactions in defects in solids from mixed all-electron and pseudopotential first-principles calculations*, npj Comput. Mater. 7, 123 (2021). DOI: 10.1038/s41524-021-00590-w
- [12] He Ma, Marco Govoni, and Giulia Galli, *PyZFS: A Python package for first-principles calculations of zero-field splitting tensors*, J. Open Source Softw. 5(47), 2160, (2020). DOI: 10.21105/joss.02160
- [13] Mykyta Onizhuk and Giulia Galli, *PyCCE: A Python Package for Cluster Correlation Expansion Simulations of Spin Qubit Dynamics*, Adv. Theory Simul. 4, 2100254 (2021). DOI: 10.1002/adts.202100254

Title: Theory of Fluctuations in Strongly-Correlated Materials

PI: Victor Galitski (Joint Quantum Institute, University of Maryland)

Program Scope

This research program develops a comprehensive theoretical study of strongly-correlated electronic materials. The foci of the project are electronic hydrodynamics and chaotic dynamics in interacting many-body systems. The physical systems of interest include superconductors, anomalous metals, magnetic materials, and various quantum-critical electronic systems. The proposed investigations involve a coherent combination of fundamental open problems of potentially foundational significance, timely projects of relevance to recent high-impact experiments, and original proposals for new experiments in quantum materials.

The first research direction is develop to an experimental platform and put together a supporting theoretical framework in order to realize hydrodynamic regime of transport in electronic materials. It is proposed to consider strongly-fluctuating materials near phase transitions as a platform for electronic hydrodynamics. The goal is to expand the list of hydrodynamic materials beyond a handful currently available in experiment. In addition, the proximity to criticality will enable to tune the parameters of the macroscopic hydrodynamic equations, which this project will derive.

A second related project is electronic turbulence. An important goal here is to identify key experimental signatures of turbulent electronic dynamics in quantum materials. Of particular interest are the electronic analogue of the Kolmogorov spectrum and turbulent energy cascades. The application also proposes to consider magnetohydrodynamic phenomena in strongly-correlated electron systems. Of particular interest is the dynamo instability – a ubiquitous and well-known effect in magnetohydrodynamics, where hydrodynamic motion of a conducting fluid yields a spontaneous excitation of magnetic field. Superconducting critical points will be explored as promising candidates to observe this phenomenon in solid state.

The third direction is to develop microscopic theory of many-body quantum chaos in order to understand how thermalization, ergodicity, and statistical mechanics emerge in interacting many-body systems. In particular, an ambitious proposed problem is to derive, starting from a microscopic model, the emergence of the chaotic many-body level statistics in a weakly-interacting system. This spectral statistics represents a smoking gun of ergodicity and as such represents a central concept in the theory. It is proposed that spontaneous breaking of unitarity may be a key new ingredient underlying the emergence of ergodicity. This program will explore this ambitious conjecture and make connections between formal theory and experimental observables. In particular, explicit connections between the many-body quantum chaos and energy relaxation/thermalization dynamics in a chaotic system will be studied. Specifically, real-time far-from-equilibrium dynamics of an interacting many body system will be derived from the chaotic many-body level statistics.

All in all, the research program gives new insight into the unconventional properties of several classes of physically interesting materials such as superconductors and unconventional metals. Apart from purely fundamental interest, the research on fluctuating materials has a significant practical component. The proposed research will provide theoretical background for the development of new experimental devices based on the fluctuation transport in the vicinity of critical points in a variety of systems.

Keywords: Quantum chaos, electronic hydrodynamics, strong correlations

Recent Progress

In their recent work, the PI in collaboration with his postdoc Dr. Yunxiang Liao have shown that many-body quantum chaos emerges due to spontaneous breaking of unitarity and via a universal dephasing mechanism similar to Altshuler-Aronov-Khmelnitsky dephasing in the theory of localization.

Future Plans

Extend the theory to justify eigen-state thermalization hypothesis. Apply the theory to interacting quantum circuits. An important question here is whether they are stable against many-body quantum chaos or unitarity-breaking can present a fundamental obstruction for large circuits?

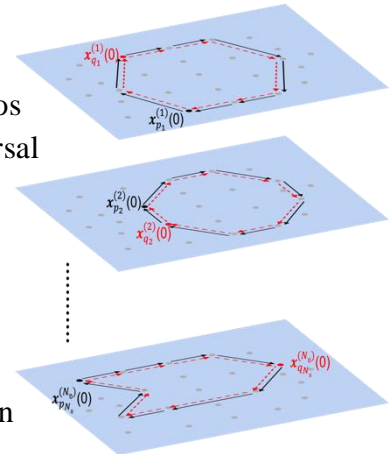
Develop the theory of electronic hydrodynamics and electronic turbulence with an eye on magnetohydrodynamic phenomena in strongly-correlated metals.

References

- [1] Y. Liao & V. Galitski, “Universal Dephasing Mechanism of Many-Body Quantum Chaos,” arXiv:2110.02976 [cond-mat.stat-mech]
- [2] Y. Liao & V. Galitski, “Emergence of many-body quantum chaos via spontaneous breaking of unitarity,” arXiv:2104.05721 [cond-mat.stat-mech]
- [3] Y. Liao, A. Vikram, & V. Galitski, “Many-body level statistics of single-particle quantum chaos,” Phys. Rev. Lett. **125**, 250601 (2020)

Publications

- [1] C. Rylands, A. Parhizkar, & V. Galitski, “Non-Abelian bosonization in a (3+1)-d Kondo semimetal via quantum anomalies,” arXiv:2107.12388 [cond-mat.str-el]



Periodic-orbit theory description of many-body quantum chaos. Without interactions, a massive time-translation symmetry exists, which leads to loss of correlations due to interference of time-translated paths. Interactions lead to dephasing and break it down to a global time-translation.

- [2] S. Balasubramanian, A. Patoary, & V. Galitski, “Solitons in lattice field theories via tight-binding supersymmetry,” *J. High Energ. Phys.* 2021, 55 (2021)
- [3] C. Rylands, A. Parhizkar, A. Burkov, & V. Galitski “Chiral Anomaly in interacting Condensed Matter Systems,” *Phys. Rev. Lett.* **126**, 185303 (2021)
- [4] Y. Liao & V. Galitski, “Universal Dephasing Mechanism of Many-Body Quantum Chaos,” arXiv:2110.02976 [cond-mat.stat-mech]
- [5] Y. Liao & V. Galitski, “Emergence of many-body quantum chaos via spontaneous breaking of unitarity,” arXiv:2104.05721 [cond-mat.stat-mech]
- [6] Y. Liao, A. Vikram, & V. Galitski, “Many-body level statistics of single-particle quantum chaos,” *Phys. Rev. Lett.* **125**, 250601 (2020)
- [7] L. A. Bunimovich, E. B. Rozenbaum, and V. Galitski, “Early-Time Exponential Instabilities in Non-Chaotic Quantum Systems,” *Physical Review Letters* **125**, 014101 (2020)
- [8] C. Rylands, E. B. Rozenbaum, V. Galitski, and R. Konik, “Many-Body Dynamical Localization in a Kicked Lieb-Liniger Gas,” *Physical Review Letters* **124**, 155302 (2020)
- [9] Y. Liao and V. Galitski, “Drag viscosity of metals and its connection to Coulomb drag,” *Physical Review B* **101**, 195106 (2020)
- [10] Z. M. Raines, A. A. Allocca, M. Hafezi, and V. M. Galitski, “Cavity Higgs polaritons,” *Physical Review Research* **2**, 013143 (2020)
- [11]. H. M. Hurst, V. Galitski, and T. T. Heikkila, “Electron-induced massive dynamics of magnetic domain walls,” *Physical Review B* **101**, 054407 (2020)
- [12] S. Balasubramanian, Y. Liao, and V. Galitski, “Many-body localization landscape,” Editors' suggestion in *Physical Review B* 101, 014201 (2020)
- [13] S. Lee et al., “Perfect Andreev reflection due to the Klein paradox in a topological superconducting state,” *Nature* **570** (7761), 3441 (2019)
- [14] J.B. Curtis, Z.M. Raines, A.A. Allocca, M. Hafezi, and V. M. Galitski, “Cavity quantum Eliashberg enhancement of superconductivity,” *Physical Review Letters* **122** (16), 167002 (2019)
- [15] Y. Liao and V. Galitski, “Critical viscosity of a fluctuating superconductor,” *Rapid Communication in Physical Review B* **100**, 060501(R) (2019)
- [16] Z.M. Raines, A.A. Allocca, and V.M. Galitski, “Manifestations of spin-orbit coupling in a cuprate superconductor,” *Physical Review B* **100**, 224512 (2019)
- [17] S.V. Syzranov, A.V. Gorshkov, and V.M. Galitski, “Interaction-induced transition in the quantum chaotic dynamics of a disordered metal,” *Annals of Physics* **405**, 1-137 (2019)

Toward exascale computing of electron-phonon couplings for finite-temperature materials design

Feliciano Giustino, The University of Texas at Austin

Emmanouil Kioupakis, University of Michigan at Ann Arbor

Program Scope

The overarching goal of this project is to enable *ab initio* calculations of the electronic, optical, and transport properties of solids including temperature and quantum nuclear effects. Most materials design approaches based on density-functional theory and beyond rely on the Born-Oppenheimer approximation, whereby electrons are adiabatically decoupled from the atomic motion. Furthermore, the atomic nuclei are most often described as classical particles. These approximations neglect the consequences of temperature, electron-phonon interactions, and phonon-assisted quantum processes in the functional properties of materials. Paradigmatic example of materials properties where electron-phonon interactions play a central role are the electrical conductivity of metals and the carrier mobility of semiconductors.

In this project we are working to systematically incorporate electron-phonon effects in *ab initio* calculations. To this end, we are advancing the theoretical foundations of electron-phonon physics and we are developing *ab initio* computational methods and software for predicting related materials properties. Novel aspects that we are currently investigating within this project include the theory and calculation polaron formation and electron self-trapping and phonon-limited electrical mobility and conductivity. In addition to this foundational work, we are expanding the functionality and improving the efficiency of our flagship code EPW, an open-source software for electron-phonon physics. The goal of the software effort is to refactor EPW in preparation for the exascale transition.

Keywords:

Electron-phonon interactions

Carrier transport in semiconductors

Massively parallel computing

Recent Progress

In the area of carrier transport, we developed new capabilities to predict electron and hole mobilities from first principles. The state-of-the-art approach for computing charge carrier mobilities in semiconductors and electrical conductivities in metals is the *ab initio* Boltzmann Transport Equation (BTE). Our team has been a key player in the development of this methodology, and the community working in this area and using the EPW code is growing rapidly. Our previous implementation of the BTE was restricted to the description of the drift mobility, as it is measured for example in time-of-flight experiments and in terahertz photo-

conductivity experiments. In this type of calculation, we determine the electrical current induced by an applied electric field. However, the most widely employed experimental approach to measure carrier mobilities is the Hall effect. In Hall measurements the mobility is measured in the presence of a driving field in the direction of the current, and a magnetic field applied perpendicular to the current flow. This is a so-called magneto-transport measurement. We recently extended the BTE implementation in EPW to introduce an applied magnetic field to calculate magneto-transport coefficients [1]. As a result of this work, it is now possible to compute Hall effect mobilities from first principles. To validate this methodology and establish its predictive power, we calculated the drift and Hall mobilities of several standard semiconductors, namely diamond, silicon, GaAs, 3C-SiC, AlP, GaP, c-BN, AlAs, AlSb, and SrO. Our most accurate calculations are in good agreement with available experimental data (Fig. 1), but additional work will be required to achieve fully predictive accuracy. For example, we found that even after pushing the accuracy limits of the code (convergence of planewaves and Brillouin zone sampling, dynamical dipole and quadrupole corrections, adaptive smearing, symmetry reduction) the predicted Hall mobility differs from experiments by 50%-100% [1]. This is not a very large error considering that mobilities can vary by several orders of magnitude between materials, but it is symptomatic of some underlying deficiency of density functional theory and density functional perturbation theory. Our current working hypothesis is that the carrier effective masses, band velocities, and electron-phonon matrix elements are not sufficiently accurate in density functional theory, and many-body approaches will be required going forward.

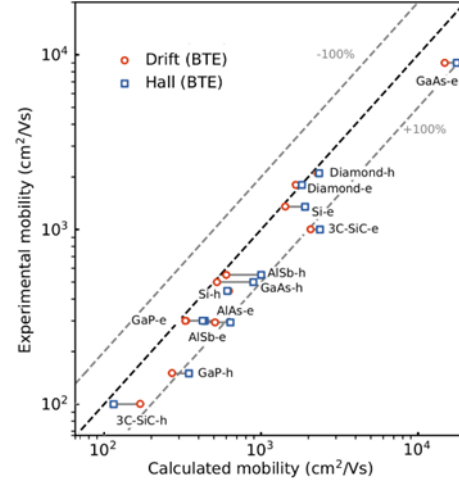


Fig. 1: Comparison between calculated drift and Hall mobility and experiments for ten prototypical semiconductors.

Recently we employed our *ab initio* BTE implementation to explain the transport properties of lead-free halide double perovskites. Halide perovskites have been attracting enormous attention since the discovery of organic-inorganic hybrid lead iodide perovskites at the beginning of the last decade. These materials exhibit extraordinary solar-to-electricity conversion efficiency, and perovskite solar cells are the first solar technology to match the performance of silicon-based photovoltaics. One potential issue with these materials is that Pb is a toxic element hence large-scale deployment may pose a hazard. During the past few years, a new class of halide perovskite has been developed, the lead-free halide double perovskites. The most established lead-free double perovskite is $\text{Cs}_2\text{AgBiBr}_6$. One limitation of these new compounds is that they exhibit relatively poor carrier mobilities, in the range of $10 \text{ cm}^2/\text{Vs}$ at room temperature. The community has been debating whether the much lower mobility of $\text{Cs}_2\text{AgBiBr}_6$ as compared to lead-based perovskites is the result of poor sample quality, or else it is an intrinsic property of materials of this class. To answer this question, we performed the first

ab initio calculations of the carrier mobilities of lead-free halide double perovskites (Fig. 2). Our work indicates that the low mobility can be traced back directly to the heavy carrier effective masses in these materials [2]. For example, the band effective mass in $\text{Cs}_2\text{AgBiBr}_6$ is much heavier than in lead-based perovskites (0.4 vs. 0.1 electron masses).

Based on these findings, we proposed that in order to improve electrical transport in lead-free perovskites it may be possible to control the band structure via cation substitution.

On a related front, we investigated the electrical transport properties of ultra-wide band gap semiconductors to be used in power electronics. The field of power electronics underpins a wide array of applications, for example high-voltage switches for regulating the power grid, and compact antennas for 5G wireless communications and beyond. Power semiconductors need to be able to sustain high voltages while conducting electricity with efficiency comparable to conventional compound semiconductors. High voltage operation requires wide band gaps, however wide gaps imply heavy carrier effective masses and poor transport properties. Therefore the design of new materials in this area requires the balancing of competing trends. In this context, we employed EPW to understand the mobility limits in cubic BN and diamond resulting from phonon- and dopant-induced scattering. We found that the phonon-limited electron and hole mobilities of diamond are similarly high, in agreement with experiments [3]. We also found that the electron mobility of c-BN is similar to diamond, due to the structural and chemical similarity of the two compounds. However, we discovered that the phonon-limited hole mobility in c-BN is much lower than the widely accepted value from experimental measurements. We attributed the discrepancy to the conducting nature of the substrate used in the experiments, which introduces artifacts in the measurements. We further explored the effects of scattering by ionized and non-ionized dopants in both materials (Fig. 3). Our results showed that, owing to the high ionization energies of dopants in these ultra-wide-band-gap semiconductors, the majority of dopants are not ionized, leading to strong carrier scattering by neutral impurities. As a result, the mobility of these compounds is severely suppressed for the high dopant concentrations needed to realize high free-carrier concentrations, which is detrimental to their performance [3]. This work clarified the intrinsic fundamental performance limits of c-BN and diamond in power-electronic devices.

On the front of software engineering, we refactored EPW to harness the capabilities of current and future supercomputing architectures. For example, we redesigned the data structure in order to increase data locality, and we optimized the ratio of MPI to OpenMP tasks. To test these improvements we participated in the Texascale Days initiative during December 2020, and

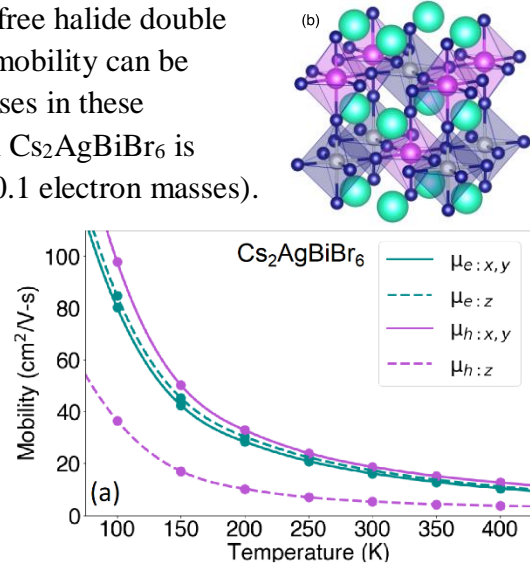


Fig. 2: (a) Calculated mobility of lead-free halide double perovskite $\text{Cs}_2\text{AgBiBr}_6$. (b) Atomic structure of $\text{Cs}_2\text{AgBiBr}_6$.

we were given exclusive access to the entire Frontera supercomputer (448,448 Intel Cascade Lake cores) at the Texas Advanced Computing Center over a period of 24h. During this session we tested EPW to perform the interpolation of the electron-phonon matrix elements for magnesium diboride (MgB_2) onto one million electron and phonon momenta. We successfully executed EPW on up to 7,840 nodes, corresponding to 439,040 compute cores. For the largest test we achieved a speedup of 86%, as given by the ratio of the measured wall-clock time and the execution time of an hypothetical code with perfect scaling. This test constitutes the first demonstration of the execution of the code at 40 petaFLOPs, and indicates that the EPW has reached the pre-exascale regime.

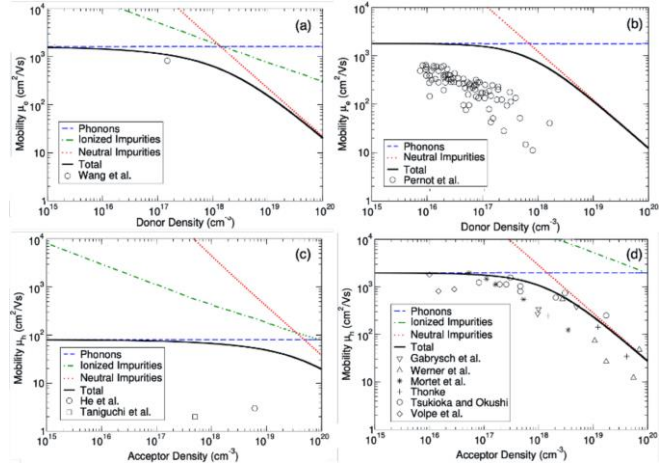


Fig. 3: Calculated room-temperature carrier mobility versus dopant density in (a) n-type c-BN, (b) n-type diamond, (c) p-type cBN, and (d) p-type diamond. The calculations are compared to available experimental data (symbols).

Future Plans

During the second half of the award period we will prioritize the following tasks: 1) To refactor the carrier transport module of EPW by introducing two-level MPI/OpenMP parallelization and re-designing the data structure. 2) To initiate the porting of the interpolation engine of EPW onto GPU architectures. 3) To calculate polarons in several materials classes in order to identify trends and establish the predictive accuracy of our methodology. 4) To finalize the new polaron module of the EPW code for release. 5) To extend the theory of the Fröhlich electron-phonon interaction from bulk three-dimensional materials to two-dimensional materials and van der Waals heterostructures. 6) To develop the theory of phonon-assisted optical absorption and Auger recombination and test our predictions on compound semiconductors.

References

- [1] S. Poncé, [...] and F. Giustino, “First-principles predictions of Hall and drift mobilities in semiconductors”, arXiv:2105.04192; in press, Phys. Rev. Res. (2021).
- [2] J. Leveille, G. Volonakis, and F. Giustino, “Phonon-Limited Mobility and Electron-Phonon Coupling in Lead-Free Halide Double Perovskites”, J. Phys. Chem. Lett. 12, 4474 (2021).
- [3] N. Sanders and E. Kioupakis, “Phonon- and defect-limited electron and hole mobility of diamond and cubic boron nitride: a critical comparison”, Appl. Phys. Lett. 119, 062101 (2021).

Publications (acknowledging this award)

- [1] S. Poncé, [...] and F. Giustino, “First-principles predictions of Hall and drift mobilities in semiconductors”, arXiv:2105.04192; in press, Phys. Rev. Res. (2021).
- [2] V.-A. Ha, G. Volonakis, H. Lee, M. Zacharias, and F. Giustino, “Quasiparticle Band Structure and Phonon-Induced Band Gap Renormalization of the Lead-Free Halide Double Perovskite $\text{Cs}_2\text{InAgCl}_6$ ”, J. Phys. Chem. C 2021 (in press), DOI:10.1021/acs.jpcc.1c06542 .
- [3] J. Leveillee, G. Volonakis, and F. Giustino, “Phonon-Limited Mobility and Electron-Phonon Coupling in Lead-Free Halide Double Perovskites”, J. Phys. Chem. Lett., 12, 4474 (2021).
- [4] T. A. Huang, M. Zacharias, D. K. Lewis, F. Giustino, and S. Sharifzadeh, “Exciton-Phonon Interactions in Monolayer Germanium Selenide from First Principles”, J. Phys. Chem. Lett. 12, 3802 (2021).
- [5] C. Q. Xia, S. Poncé, J. Peng, A. M. Ulatowski, J. B. Patel, A. D. Wright, R. L. Milot, H. Kraus, Q. Lin, L. M. Herz, F. Giustino, and M. B. Johnston, “Ultrafast photo-induced phonon hardening due to Pauli blocking in MAPbI_3 single-crystal and polycrystalline perovskites”, J. Phys. Mater., 4, 044017 (2021).
- [6] C. Q. Xia, J. Peng, S. Poncé, J. Patel, A. D. Wright, T. W. Crothers, M. U. Rothmann, J. Borchert, R. L. Milot, H. Kraus, Q. Lin, F. Giustino, L. M. Herz, and M. B. Johnston, “Limits to Electrical Mobility in Lead-Halide Perovskite Semiconductors”, J. Phys. Chem. Lett., 12, 3607 (2021).
- [7] F. Macheda, S. Poncé, F. Giustino, and N. Bonini, “Theory and computation of the Hall scattering factor in graphene”, Nano Lett. 20, 8861 (2020).
- [8] S. Poncé and F. Giustino, “Structural, electronic, elastic, power, and transport properties of beta- Ga_2O_3 from first principles”, Phys. Rev. Research 2, 033102 (2020).
- [9] M. Zacharias and F. Giustino, “Theory of the special displacement method for electronic structure calculations at finite temperature”, Phys. Rev. Res. 2, 013357 (2020).
- [10] S. Chae, [...], and E. Kioupakis, “Toward the predictive discovery of ambipolarly doped ultra-wide-band-gap semiconductors: The case of rutile GeO_2 ”, Appl. Phys. Lett. 117, 260501 (2021).
- [11] N. Sanders and E. Kioupakis, “Phonon- and defect-limited electron and hole mobility of diamond and cubic boron nitride: a critical comparison”, Appl. Phys. Lett. 119, 062101 (2021).
- [12] K. Bushick, K. A. Mengle, S. Chae, E. Kioupakis, “Electron and hole mobility of rutile GeO_2 from first principles: An ultrawide-bandgap semiconductor for power electronics”, Appl. Phys. Lett. 177, 182104 (2020).
- [13] S. Chae, [...], and E. Kioupakis, “Thermal conductivity of rutile germanium dioxide”, Appl. Phys. Lett. 117, 102106 (2020).

Non-Equilibrium Effects in Conventional and Topological Superconducting Nanostructures

Leonid Glazman, Yale University

Program Scope

Propagation, localization, and interaction of collective excitations in Josephson junction arrays.

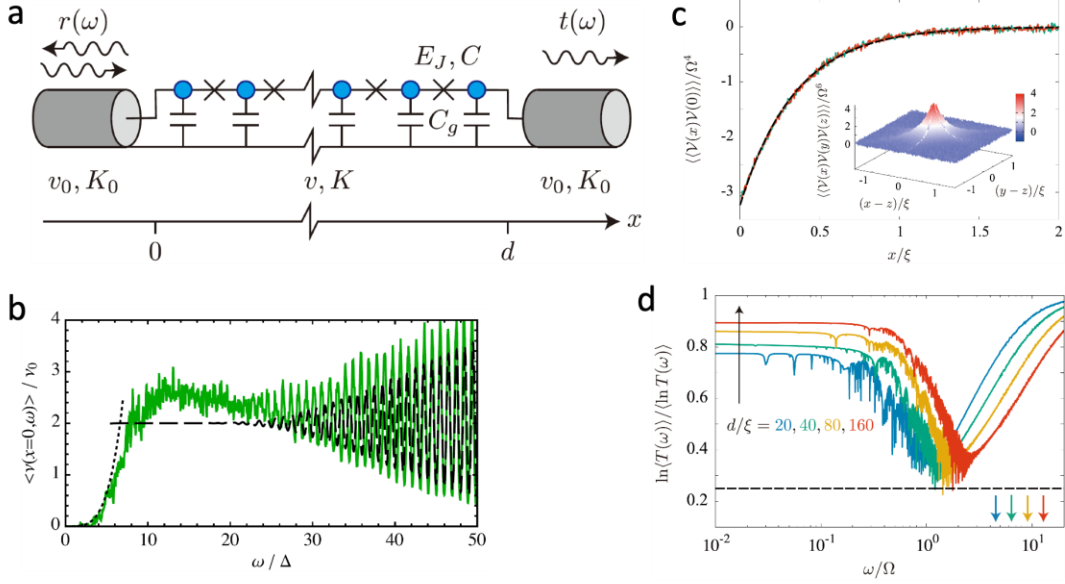
Keywords: quantum phase slips, quantum charge fluctuations, microwave fluorescence.

Recent Progress

Motivated by a number of recent experiments, we addressed the quantum dynamics of one-dimensional arrays of small Josephson junctions, Fig. 1a. The basic properties of an array are controlled by two dimensionless parameters: $\lambda/E_J \sim \exp(-\sqrt{32E_J/E_C})$ and $K = \pi \sqrt{E_J/(2E_g)}$, where the energy λ is the effective bandwidth of a quantum phase slip propagating along an uncompactified phase variable [1] of an isolated junction, and energies E_J , E_C and E_g are defined in Fig. 1a. The first of the two parameters controls the probability amplitude of a quantum phase slip across a single junction, and the other one is responsible for the long-wavelength quantum fluctuations of the superconducting order parameter phase. The possibility of the phase slips makes the array sensitive to the stray charges in the substrate. At $K > 3/2$ that sensitivity is washed out, so a very long array resides in the “superfluid” phase [2]. An array with $K < 3/2$ is in a “bose glass” phase; the long-range phase correlations are destroyed in it, and the distribution of charge among the superconducting islands is weakly pinned. The characteristic pinning length in the classical limit ($K \ll 1$) is known as the “Larkin length”. Its quantum generalization found in Ref. [1], $\xi \propto (E_J/\lambda)^{2/(3-2K)}$, is sensitive to the value of K .

Microwave reflection from and transmission through the array carry information regarding the dynamics of a pinned charge density wave. Our works [1,3] make first steps in extracting it, by focusing on the “classical arrays”, $K \ll 1$. In Ref. [1], we established that the disorder-averaged reflection amplitude $\langle r(\omega) \rangle$ yields the spectral density of the Josephson plasmon excitations capable of reaching an end of the array, $\langle r(\omega) \rangle + 1 = (K/K_0)\langle v(x=0, \omega) \rangle/v_0$; here $v_0 = \pi/v$ is the plasmon spectral density in an ideal, infinitely-long array and v is the plasmon propagation speed. The disorder averaging occurs naturally in the experiments because of the variation of the stray charges configuration on the time scale far exceeding the plasmon propagation time through the array. We identified three frequency ranges for an array with length $N \gg \xi$ (hereinafter, length is identified with the number of junctions). At high, length-specific frequency $\gg (N/\xi)^{1/2}\Omega$, reflection amplitude $\langle r(\omega) \rangle$ preserves a regular Fabry-Perot oscillatory pattern inhomogeneously broadened by the forward-scattering off the quasi-static charge disorder; here $\Omega = v/\xi$ is defined by the Larkin length and plasmon propagation speed. At $(N/\xi)^{1/2}\Omega \gg \omega \gg \Omega$, broadening of the Fabry-Perot resonances exceed the distance between

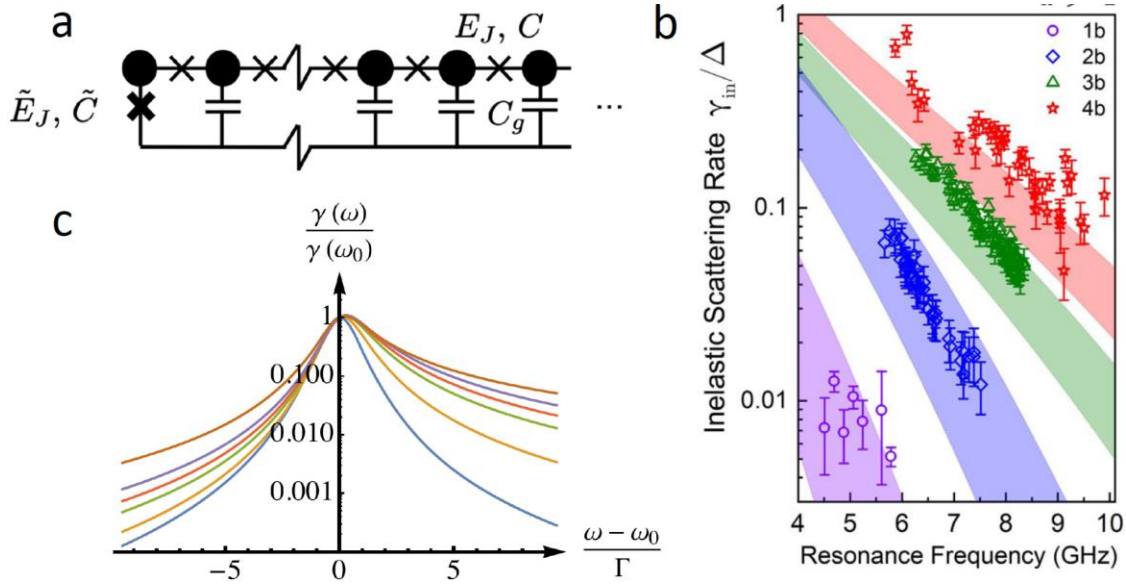
them while a plasmon still is able to explore the entire length of the array; the broadening and consequent suppression of the Fabry-Perot oscillations is associated with the scrambling of plasmons phases. Lastly, at frequencies $\omega \ll \Omega$ reflection amplitude probes the spectral density of plasmons localized by disorder. Using the general arguments of Refs. [4,5] we concluded [1] and checked numerically [3] that $\langle r(\omega) \rangle + 1 \propto \omega^4$ in the limit of low frequencies, see Fig. 1b.



a: One-dimensional array of Josephson junctions with Josephson energy E_J and charging energy $E_c = 4e^2/(2C)$; $E_g = 4e^2/(2C_g)$ is the charging energy of a superconducting island between junctions with respect to the ground. We assume that the ideal array's impedance $Z = \pi\hbar/4e^2K$ is much greater than the impedance $Z_0 = \pi\hbar/4e^2K_0$ of the waveguides attached to the array [1,3]. **b:** Frequency dependence of the disorder-averaged spectral density at the edge, extracted from the reflection amplitude: $\langle r(\omega) \rangle + 1 = (K/K_0)\langle v(x=0, \omega) \rangle / v_0$; green line: numerics, $\Delta = \frac{\pi v}{N}$ is the spacing between Fabry-Perot resonances; dotted line: $\langle v(x=0, \omega) \rangle \propto \omega^4$ [1]. **c:** The smooth part of the second-order correlation function of the effective disorder at $N/\xi = 20$. Green and red lines: two numerical implementations of randomness [3]; dashed line: fit, $-w(x) = -3.24e^{-|x|/0.346}$. Inset: third-order disorder cumulant at non-coinciding points. **d:** Ratio $\ln\langle T(\omega) \rangle / \langle \ln T(\omega) \rangle$ for lengths $N/\xi = 20, 40, 80, 160$ and $K/K_0 = 1.0$. The ratio approaches value $\ln\langle T(\omega) \rangle / \langle \ln T(\omega) \rangle \approx 0.9$ at $\omega \ll \Omega$. Upon increasing the frequency, the ratio decreases while remaining above the value $1/4$ found analytically in the frequency range $(N/\xi)^{1/2}\Omega \gg \omega \gg \Omega$; at larger frequencies, when disorder becomes irrelevant, the ratio increases to the value 1. Arrows show $\omega/\Omega = (N/\xi)^{1/2}$ for each N [3]. Length d in panels (a) and (d) is identified with N in the text.

Weak pinning creates a correlated medium for the wave propagation, with a correlation length R_* . Correlations come from the competition between the white-noise potential of the external stray charges and the compressibility of the charge density along the array; low compressibility results in a large Larkin length ξ . In the high-frequency limit, $\omega \gg \Omega$, we were able to find [3] a comprehensive analytical solution for the disorder-averaged reflection amplitude $\langle r(\omega) \rangle$ and for the average and mesoscopic fluctuations of the transmission coefficient $T(\omega)$. The analytical results were supported and thoroughly checked by extensive numerical simulations, presented in the same work. The key simplification afforded by this high-frequency limit is the weakness of scattering, which makes the statistics of the scattering data dependent only on the two-point correlation function of the disorder. The latter was found numerically, see Fig. 1c, and is

universal, *i.e.*, independent of the type of the pinned elastic medium and relies only on the assumption of weak pinning. At $\omega \gg \Omega$, the universality manifests itself as a fixed ratio of the forward- and back-scattering lengths, $\ell_0(\omega)/\ell_\pi(\omega) \approx 2.277(9)$. The former of the two lengths determines the broadening of the Fabry-Perot resonances at $\omega \gg (d/\xi)^{1/2}\Omega$, while the latter one defines the exponential dependence of transmission coefficient on the array's length at $(d/\xi)^{1/2}\Omega \gg \omega \gg \Omega$. In the latter frequency range, the use of Fokker-Planck formalism for finding the distribution function of $T(\omega)$ is justified and effective. As expected, the analytically-found distribution function shows giant mesoscopic fluctuations of $T(\omega)$, indicated by the ratio $\ln\langle T(\omega) \rangle / \langle \ln T(\omega) \rangle = 1/4$ being different from 1. Results of the numerical simulation of that ratio depicted in Fig. 1d agree with the analytical theory in the proper limit, while indicating strong deviations from 1/4 at $\omega \lesssim \Omega$. Studying the deviations is a part of Future Plans.



a: A transmon qubit (with parameters \tilde{E}_J, \tilde{C}) in a galvanic contact with a Josephson junction array [6].
b: Comparison of experiments (data points) performed on four devices with the theory (stripes) [7].
c: Normalized total inelastic cross-section as a function of incoming microwave frequency; ω_0 is the transmon transition frequency, and Γ is the elastic level width [6].

Quantum slips of the Josephson phase φ lead to a decay of a high-frequency plasmon into plasmons of lower frequency. While such mechanism may seem more exotic than a decay due to the anharmonic Josephson phase-energy relation $E_J(\varphi) = -E_J \cos\varphi$, it turns out to be the most effective one in a decay with a soft-plasmon emission. We realized [6], that quantum phase slips may dominate the total cross-section of inelastic scattering of a Josephson plasmon off a weak junction, representing a “quantum impurity” in a Josephson junction array, see Fig. 2a. Developing a quantitative theory of the effect have led us to introducing an interesting generalization of the boundary sine-Gordon model. Apart from being interesting technically, this generalization is a fair representation of a transmon qubit in a galvanic contact with a Josephson junction array [7]. Our quantitative theory for the total inelastic cross-section explained the detailed in Ref. [7] experiment, see Fig. 2b. Inelastic Josephson plasmon scattering off a transmon is somewhat similar to the resonance fluorescence of an atom. However, there are two major differences: (i) the quantized single plasmon replaces a classical driving field, and (ii) quantum fluctuations of the Josephson junction array dynamically modulate the transmon’s

transition frequency around its nominal value ω_0 . As the result, the total cross-section $\gamma(\omega)$ as a function of frequency ω is not symmetric around $\omega = \omega_0$, see Fig. 2c, and depends of K . We found $\gamma(\omega) \propto \Gamma \tilde{\lambda}_1^2 (\omega_0 - \omega)^{4K-3}$ at $\omega > \omega_0$ and outside the elastic broadening width Γ . Cross-section $\gamma(\omega)$ is not normalizable at $K > 1/2$, indicating the Schmid quantum phase transition [8] affecting the dynamics of the transmon's Josephson phase difference. The phase slips probability amplitude is represented here by parameter $\tilde{\lambda}_1 \propto \exp\left(-\sqrt{32\tilde{E}_J/\tilde{E}_c}\right)$. The current theory, accounting for the phase slips in the excited state of the transmon, is adequate for the needs of experiment [7].

Future Plans

- (1) Develop the theory of microwave elastic transmission through a Josephson junction array at frequencies below the scale defined by the Larkin length.
- (2) Extend the theory to include the plasmon-plasmon interaction and tunneling of localized plasmon modes (finite- K effects). The goal is to account for inelastic plasmon scattering, elucidate the structure of many-body plasmon states in a finite-length array, and find their possible manifestation in microwave experiments.
- (3) Investigate the microwave scattering off a finite-length Josephson junction array containing a charge- and flux-sensitive transmon. We intend to develop a theory for the discrete resonance lines associated with the inelastic photon scattering.
- (4) Extend the theory of Ref. [6] to allow phase slips at any qubit excitation level (including the $n = 0$ state) and investigate the ramifications for the soft inelastic scattering of microwaves.
- (5) Develop theoretical prediction for manifestations of the Schmid transition in microwave experiments with a resistively-shunted charge qubit.

References

- [1] M. Houzet and L. I. Glazman, Phys. Rev. Lett. **122**, 237701 (2019).
- [2] T. Giamarchi and H. J. Schulz, Phys. Rev. B **37**, 325 (1988).
- [3] T. Yamamoto, L. I. Glazman, and M. Houzet, Phys. Rev. B **103**, 224211 (2021).
- [4] I. L. Aleiner and I. M. Ruzin, Phys. Rev. Lett. **72**, 1056 (1994).
- [5] M. M. Fogler, Phys. Rev. Lett. **88**, 186402 (2002).
- [6] M. Houzet and L. I. Glazman, Phys. Rev. Lett. **125**, 267701 (2020).
- [7] R. Kuzmin, N. Grabon, N. Mehta, A. Burshtein, M. Goldstein, M. Houzet, L.I. Glazman, and V.E. Manucharyan, Phys. Rev. Lett. **126**, 197701 (2021).
- [8] A. Schmid, Phys. Rev. Lett. **51**, 1506 (1983).

Publications

- [1] M. Houzet and L. I. Glazman, *Critical fluorescence of a transmon at the Schmid transition*, Phys. Rev. Lett. **125**, 267701 (2020).
- [2] Z. Shi, P. W. Brouwer, K. Flensberg, L. I. Glazman, and F. von Oppen, *Long-distance coherence of Majorana wires*, Phys. Rev. B **101**, 241414(R) (2020).
- [3] C. Murthy, V. D. Kurilovich, P. D. Kurilovich, B. van Heck, L. I. Glazman, and C. Nayak, *Energy spectrum and current-phase relation of a nanowire Josephson junction close to the topological transition*, Phys. Rev. B **101**, 224501 (2020).
- [4] T. Yamamoto, L. I. Glazman, and M. Houzet, *Transmission of waves through a pinned elastic medium*, Phys. Rev. B **103**, 224211 (2021).
- [5] R. Kuzmin, N. Grabon, N. Mehta, A. Burshtein, M. Goldstein, M. Houzet, L.I. Glazman, and V.E. Manucharyan, *Inelastic Scattering of a Photon by a Quantum Phase Slip*, Phys. Rev. Lett. **126**, 197701 (2021).
- [6] L. I. Glazman and G. Catelani, *Bogoliubov quasiparticles in superconducting qubits*, SciPost Phys. Lect. Notes **31** (2021).
- [7] V. D. Kurilovich, C. Murthy, P. D. Kurilovich, B. van Heck, L. I. Glazman, C. Nayak, *Quantum-critical dynamics of a Josephson junction at the topological transition*, Phys. Rev. B **104**, 014509 (2021).

Optical Control of Spin-polarization in Quantum Materials

Marco Govoni, Materials Science Division & Center for Molecular Engineering, Argonne National Laboratory (mgovoni@anl.gov)

Program Scope

The goal of this project is the application of first principles methods to predict the optical properties of spin-defects in wide band-gap semiconductors. We focus on analogues of the NV center in diamond that are relevant for new quantum technologies and nanoscale sensing applications.

A grand challenge in quantum information science (QIS) is the design of materials that can host quantum states that are both robust and easily controllable with light. Point-defects in materials bind electrons to a region on the order of a single lattice constant and can be regarded as molecule-like states trapped inside the crystal. So far, the optical cycle of the spin-polarization of the negatively charged nitrogen-vacancy (NV) center in diamond has represented the most studied prototypical example of an isolated quantum system embedded within a solid-state lattice. The field is currently thriving with several candidate defect host materials under study, which possess a more scalable fabrication process and a longer coherence time for improved quantum functionality. Theoretical insights and broadly applicable computational models offer the opportunity to accelerate the experimental examination of candidate materials.

Key science questions that are guiding this research include: How does the local environment surrounding the defect site influence its spin-polarization? What factors can be controlled in order to generate good quantum functionalities? To address these questions, we use predictive modeling techniques based on first-principles numerical simulations to provide a quantitative description of optically activated processes and better guide and understand experimental activities. In particular, we use hierarchical modeling approaches, from density functional theory to many-body perturbation theory and multi-reference methods. For instance, we model the electronic states of spin defects in proximity to interfaces and near surfaces, and explore new avenues for realizing the optical control of the spin-polarization cycle in quantum materials. The techniques and the results obtained within this program provide the fundamental groundwork to understand and control quantum materials relevant for QIS.

Keywords: defects, quantum information science, polytypes

Recent Progress

Divacancies in silicon carbide (SiC) have electronic states with sharp optical and spin transitions which are compelling analogues of diamond NV centers and have been increasingly recognized as a candidate platform for quantum information and nanoscale sensing [1-2]. Moreover, SiC has hundreds of polytypes, each with unique structural properties and band gap; this presents a materials design parameter that is not available in diamond and has the potential to create and control new solid-state quantum systems. We explored whether we can harness the local environment to tailor quantum functionalities in SiC, focusing on the computation of the spectroscopic features of defects in hetero-polytypic structures. SiC offers the opportunity to localize vacancy-related quantum defects within a polytype layer, providing a distinct local crystallographic environment. We have considered divacancies in SiC located in the 3C, 2H, 4H and 6H polytypes, and we looked at the spin-polarization of such divacancies in close proximity to interfaces between these polytypes. This research identifies the pathways to harness polytypism in SiC for QIS applications where growth processes may be used to embed spin-defects with tailored properties in optoelectronic devices.

Future Plans

Work is in progress to identify the variation of the defect spin and optoelectronic properties as a function of the distance of the divacancy from hetero-polytypic interfaces in SiC. We have initiated simulations of defects at near surface conditions, which we expect will reveal important changes to the spin-defect properties due to variations of the local environment caused by the presence of interfaces or surfaces. Strategically this represents a necessary step towards the simulation of spin-defects in low-dimensional systems.

References

[1] A. L. Falk, B. B. Buckley, G. Calusine, W. F. Koehl, V. V. Dobrovitski, A. Politi, C. A. Zorman, P. X.-L. Feng, D. D. Awschalom. Polytype control of spin qubits in silicon carbide. *Nat. Commun.* 4, 1819 (2013).

[2] D. J. Christle, P. V. Klimov, C. F. de las Casas, K. Szász, V. Ivády, V. Jokubavicius, J. Ul Hassan, M. Syväjärvi, W. F. Koehl, T. Ohshima, N. T. Son, E. Janzén, Á. Gali, D. D. Awschalom, Isolated Spin Qubits in SiC with a High-Fidelity Infrared Spin-to-Photon Interface, *Phys. Rev. X* 7, 021046 (2017).

Mapping the genome of coherent quantum defects for Quantum Information Science

Geoffroy Hautier¹, Alp Sipahigil^{2,3}, Sinéad Griffin³, Archana Raja³, Alexander Weber-Bargioni³

1. Dartmouth College
2. University of California, Berkeley
3. Lawrence Berkeley National Laboratory

Program Scope

Atom-like defects in solids have emerged as potential building blocks for quantum technologies ranging from sensing to communications and computing. The electronic and nuclear spin states of the defects can be isolated from the environmental decoherence mechanisms to realize highly-coherent quantum bits. A few quantum defects (e.g., the NV center in diamond) have shown promising optical and spin properties, and are finding applications in nanoscale quantum sensing and elementary quantum network. The limitations of the NV center has driven interest in investigating new defect and host material combinations. In particular, remote-entanglement generation and quantum networking applications require quantum repeater nodes combining coherent spin and optical transitions, strong light-matter coupling, operation at telecommunication wavelengths and high temperatures, and a mature material platform for scalable fabrication. The discovery of new quantum defects has proceeded so far by chance and on a case-by-case basis.

Our project proposes to change this paradigm and use high-throughput computing to accelerate the search for quantum defects. The general workflow of our project is outlines in **Figure 1**. By evaluating through *ab initio* computations important quantities (e.g., symmetry, formation energies, spin multiplicity, transition wavelengths, and electron-phonon coupling...) for a very large series of potential point defects and complexes in a host material (here silicon and 2D transition metal dichalcogenides (TMDCs)), we will build a large defect database. We will analyze this database to select the most promising defects for quantum networking

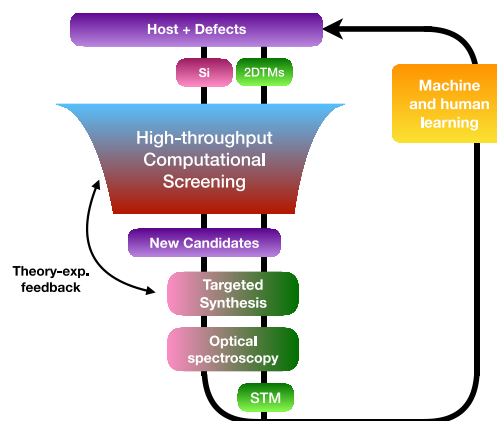


Figure 1: general workflow for high-throughput discovery

applications, and experimentally synthesize them for advanced characterization and theory benchmark. The database will be used not only for selecting promising candidates but also to increase our understanding of defects properties through data analysis and machine learning.

While our project will establish a general framework for high-throughput search for quantum defects, we will focus on two materials platform of great applied and fundamental interest: silicon

and 2D TMDCs such as WS_2 . While most work on quantum defects has targeted wider band gap materials than silicon, recent results have shown that color centers in the infrared are present in silicon. Working with silicon would have tremendous advantages in terms of materials process and integration with current microelectronics. TMDCs on the other hand offer an emerging platform with unprecedented tunability and atomic level control. Following the leads from high-throughput screening, we will perform targeted synthesis of defects in silicon and TMDCs (mono- or bilayers) using ion implantation. Extensive characterization with Zeeman and Stark shift spectroscopy via cryogenic photoluminescence (PL) and photoluminescence excitation (PLE) will elucidate the electronic structure. For selected systems, we will also use scanning tunneling microscopy to provide a direct atomistic comparison between theory and experiment. In addition to the opportunity of improved novel quantum defects in these two important platforms in the near term, the experimental work will provide very valuable feedback on the accuracy of our theoretical framework.

Keywords: first principles computations, quantum defects, high-throughput computing, silicon, transition metal dichalcogenides

Recent Progress

The project has just started and we will report on some early results. First “low-throughput” computations on silicon and WS_2 will be presented and compared to experimental data. Technical benchmarks of supercell size convergence and electrostatic corrections for both systems will be discussed on a two examples: the sulfur vacancy in WS_2 and the T-center in silicon. We will report as well on an approach to incorporate metals such as cobalt in the sulfur vacancy of WS_2 . We will report as well on the first high-throughput computations for simple extrinsic point defects in silicon.

Future Plans

On the silicon-side, the project will focus on producing a first database of DFT-based defects for complexes. Experimental ion implantation runs and characterization will be conducted according to what is suggested by theory. For the 2D TMDCs, the focus will be on finishing our first benchmark tests (including tackling the issue of charge interactions in 2D systems) and start some first high-throughput production of metal substitutions on the sulfur vacancy. Similarly, to silicon, the suggested metal substitutions from theory will drive experimental work. In parallel to these efforts, we will benchmark different approaches to speed up beyond-DFT techniques that will alleviate the band gap problem inherent to DFT.

Publications

No publication yet.

Symmetry in Correlated Quantum Matter

Principal investigator: Michael Hermele

Department of Physics, University of Colorado Boulder, Boulder, CO 80309-0390

Program Scope

The goal of this project is to characterize, classify and elucidate the properties of highly entangled forms of quantum matter, in which symmetry, or the geometry of the crystalline lattice, plays a key role. Current efforts are focused in two main areas, namely (1) fracton phases of matter, and (2) $4f$ and $5d$ materials that combine significant spin-orbit coupling and electron-electron interactions. Some highlights of current work are discussed here:

Fracton phases. Current work on fractonic matter is multi-faceted, reflecting the plethora of open questions pertaining to these states. One area of focus is phase transitions between fracton phases and proximate phases with some more conventional form of order. Our recent work found phase transitions with quasi-2d and quasi-1d character (see below); we are now beginning to investigate whether continuous transitions out of fracton phases *without* such emergent subdimensional character are possible, and to broaden the range of fracton phase transitions that are understood.

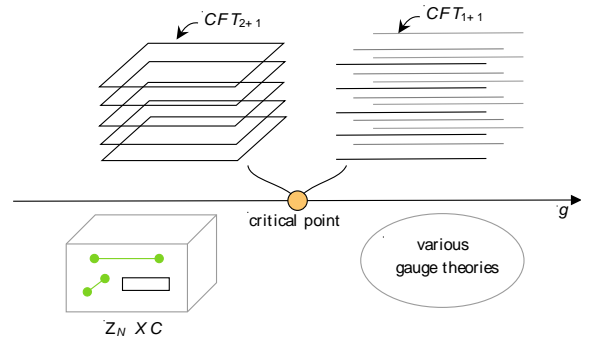
Another line of current work concerns the close relationship between fracton phases and subsystem symmetries; these are symmetries that act *e.g.* by flipping spins on some lower-dimensional subspace, such as a line, plane or even a fractal subspace. We recently discovered a two-dimensional exactly solvable model with the same topological order as Kitaev's toric code, and where linear subsystem symmetries are fractionalized on some of the fractional excitations. Based on an argument of Stephen *et. al.* [1], it was thought that subsystem symmetries cannot be fractionalized on point-like excitations; our model evades this no-go result because the mobility of the model's excitations is restricted under symmetry-preserving dynamics, and indeed the subsystem symmetry fractionalization is intimately tied to restricted mobility. This result is of fundamental interest and also opens the door to fracton-like phenomena in relatively simple two-dimensional topologically ordered systems, which may be realizable in synthetic quantum matter platforms. Current work focuses on obtaining a better understanding of the range of possibilities for subsystem symmetry fractionalization on point-like excitations.

4f and 5d materials. One line of current work consists of providing theoretical support in modeling and understanding thermal transport measurements in $4f$ delafossites in Minhyea Lee's group. Another line of work is based on past experimental work led by Gang Cao on $\text{Ba}_4\text{Ir}_3\text{O}_{10}$ [2]; our collaborators are obtaining effective spin models based on *ab initio* quantum chemistry calculations, and we are analyzing the many-body physics of these models in an effort to understand the frustrated magnetism observed in $\text{Ba}_4\text{Ir}_3\text{O}_{10}$.

Keywords: topological phases of matter, strongly correlated materials, fractons

Recent Progress

Subdimensional critical points between phases with and without fracton order. While theoretical models have now been constructed for a large variety of fracton phases, there is relatively little understanding of critical points between fracton phases and proximate more conventional phases, which might for instance possess symmetry-breaking order or conventional topological order. This is important in part because gapless states – including critical points – typically have a rich set of signatures across a wide range of experimental probes, in contrast to gapped phases (including fracton phases) that can be challenging to probe. With Ethan Lake, we studied various critical points out of the Z_N X-cube phase (a particularly simple paradigmatic example of a fracton phase) [3]; the common feature of these critical points is that they arise upon condensing subdimensional excitations constrained to move either in planes or along lines. In some cases, stable critical points or even stable intermediate gapless phases are found to exist.



Schematic illustration of the phase transitions studied. One starts in the Z_N X-cube phase and enters a phase described by a gauge theory as a control parameter g is increased. The critical point itself is described as a stack or array of coupled $2+1d$ or $1+1d$ conformal field theories, and thus has a low-dimensional character

Odd fracton theories and proximate orders. In systems at fractional filling – for instance, Mott insulators with an odd number of spin-1/2 moments per crystalline unit cell – the celebrated Lieb-Schultz-Mattis (LSM) theorem and its generalizations put significant constraints on certain physical properties, which are manifest differently in different phases of matter. Examples are the so-called “odd” Z_2 gauge theories, which arise in systems at half-filling and have a net background Z_2 gauge charge in each crystalline unit cell. The Z_2 flux excitations transform as a projective representation of the lattice symmetries, which leads to lattice-symmetry-breaking-order (*e.g.* valence bond solid order) in proximate confining phases.

In this work, we studied how LSM constraints are manifest in fracton phases as a non-trivial action of lattice translation and $U(1)$ charge or spin symmetry on the restricted-mobility excitations [4]. This occurs in “odd” versions of the X-cube fracton model that we introduced and showed can arise in half-filled systems. We also studied the conventional symmetry-breaking orders that lie in proximity to these odd fracton phases.

Fractons from vector gauge theory and exotic higher-form symmetries. In our earlier work on coupled-layer constructions of the X-cube model [5], we showed how to obtain the X-cube fracton phase by coupling together more familiar degrees of freedom. This mechanism was dubbed “p-string condensation,” because particle-like excitations organize into extended strings, which then condense. After that work, it was an open question whether the many fracton phases

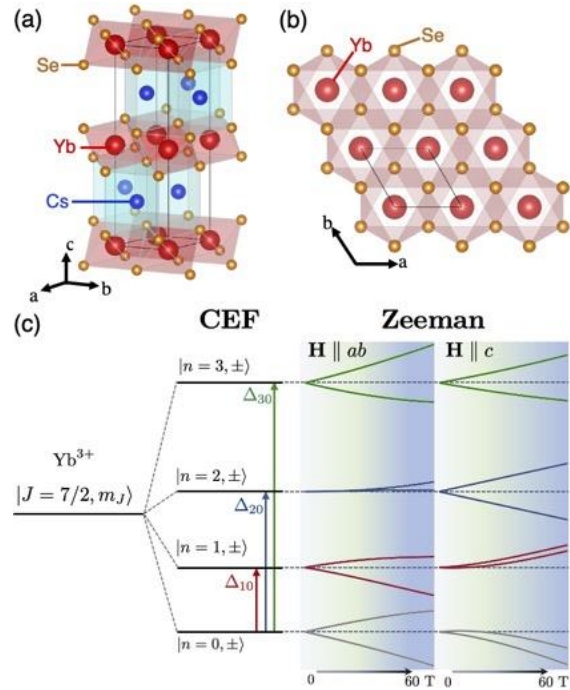
described by U(1) tensor gauge theories can be described in a similar way, by coupling together some more conventional degrees of freedom. In this work with Radzihovsky, we generalized the p-string condensation mechanism to certain U(1) tensor gauge theories, which we showed can be obtained by starting from some number of ordinary U(1) vector gauge theories, and condensing strings built from point-like excitations carrying the gauge charge [6]. In a later work, we went on to develop an understanding of p-string condensation mechanisms in terms of a breaking of exotic higher-form symmetries [7].

Extracting crystal electric field parameters from magnetization measurements. In magnetic materials where moments originate from partially filled $4f$ shells, an important ingredient in obtaining an effective spin Hamiltonian is a determination of the single-ion crystal electric field (CEF) Hamiltonian. This Hamiltonian depends on the angular momentum operator \mathbf{J} , and is parametrized by a set of Stevens operator coefficients allowed by the site symmetry. These CEF parameters are commonly determined by fitting to the single-ion energy spectrum as determined by inelastic neutron scattering. However, this is often a highly underdetermined fit, with fewer independent spectral gaps than CEF parameters, and more reliable methods for determining these parameters are desirable.

We provided theoretical support to Minhyea Lee’s group in a study of the triangular lattice delafossite CsYbSe_2 , where low-field magnetic susceptibility and high-field resonant torque magnetometry measurements were used to provide a reliable determination of CEF parameters for the $J=7/2$ Yb^{3+} ions, based on a Weiss mean-field analysis [8]. An important and apparently overlooked basic finding, of expected relevance to many $4f$ magnetic systems, is that quadratic corrections to the linear Zeeman effect do not simply give an additive van Vleck contribution to the susceptibility, but instead lead to a mean-field susceptibility that substantially differs from the conventional Curie-Weiss form.

Future Plans

Fracton phases. In addition to the current work in progress discussed under program scope, we plan to investigate certain non-abelian fracton models (the “cage-net” models we introduced in



Crystal structure of CsYbSe_2 and single-ion Yb^{3+} energy spectrum, based on CEF parameters determined in our work. The pronounced nonlinear Zeeman effect for c -axis applied field leads to correspondingly pronounced deviations of the mean-field c -axis susceptibility from the conventional Curie-Weiss form.

earlier work [9]) from the point of view of foliated fracton phases [10]. The latter point of view provides one of the few clear organizing principles so far in the study of fracton phases, but only applies to certain models, and it is important to extend its range of applicability as far as possible. While the cage-net models share many features in common with known foliated fracton phases, the behavior of the ground-state degeneracy with system size indicates that the usual foliated approach cannot apply. However, it appears that a non-trivial extension of this approach may apply to the cage-net models, which we plan to investigate.

4f and 5d materials. In addition to the current work in progress discussed under program scope, we plan to study in greater depth a problem of hybridization between acoustic phonons and spin-flip excitations, that arises generically in many *4f* insulators under applied magnetic field. While at low temperature this problem is simple and can be treated using quantum mechanical perturbation theory, it becomes a non-trivial many-body problem at intermediate temperatures, where the effect on thermodynamics and thermal transport is not clear. Quantum Monte Carlo simulations are one possible way forward to gain a handle on this problem.

References

1. D. T. Stephen, J. Garre-Rubio, A. Dua and D. J. Williamson, “Subsystem symmetry enriched topological order in three dimensions.” *Phys. Rev. Res.* **2**, 033331 (2020).
2. G. Cao, H. Zheng, H. Zhao, Y. Ni, C. A. Pocs, Y. Zhang, F. Ye, C. Hoffmann, X. Wang, M. Lee, M. Hermele and I. Kimchi, “Quantum liquid from strange frustration in the trimer magnet Ba₄Ir₃O₁₀.” *npj Quantum Materials* **5**, 26 (2020).
3. E. Lake and M. Hermele, “Subdimensional criticality: condensation of lineons and planons in the X-cube model.” arXiv:2107.09073, accepted in *Phys. Rev. B*.
4. M. Pretko, S. A. Parameswaran and M. Hermele, “Odd fracton theories, proximate orders, and parton constructions.” *Phys. Rev. B* **102**, 205106 (2020).
5. H. Ma, E. Lake, X. Chen and M. Hermele, “Fracton topological order via coupled layers.” *Phys. Rev. B* **95**, 245126 (2017).
6. L. Radzihovsky and M. Hermele, “Fractons from vector gauge theory.” *Phys. Rev. Lett.* **124**, 050402 (2020).
7. M. Qi, L. Radzihovsky and M. Hermele, “Fracton phases via exotic higher-form symmetry breaking.” *Ann. Phys.* **424**, 168360 (2021).
8. C. A. Pocs, P. E. Siegfried, J. Xing, A. S. Sefat, M. Hermele, B. Normand and M. Lee, “Systematic fitting of crystal-field levels and accurate extraction of quantum magnetic models in triangular-lattice delafossites.” arXiv:2109.09758, submitted to *Phys. Rev. X*.
9. A. Prem, S.-J. Huang, H. Song and M. Hermele, “Cage-net fracton models.” *Phys. Rev. X* **9**, 021010 (2019).
10. W. Shirley, K. Slagle, Z. Wang and X. Chen, “Fracton models on general three-dimensional manifolds.” *Phys. Rev. X* **8**, 031051 (2018).

Publications

1. S. Pai and A. Prem, “Topological States on Fractal Lattices.” *Phys. Rev. B* **100**, 155135 (2019).
2. S. Pai and M. Hermele, “Fracton fusion and statistics.” *Phys. Rev. B* **100**, 195136 (2019).
3. Z. Song, S.-J. Huang, Y. Qi, C. Fang and M. Hermele, “Topological states from topological crystals.” *Sci. Adv.* **5**, eaax2007 (2019).
4. S. Pai and M. Pretko, “Fractons from confinement in one dimension.” *Phys. Rev. Res.* **2**, 013094 (2020).
5. H. Song, C. Z. Xiong and S.-J. Huang, “Bosonic crystalline symmetry protected topological phases beyond the group cohomology proposal.” *Phys. Rev. B* **101**, 165129 (2020).
6. G. Cao, H. Zheng, H. Zhao, Y. Ni, C. A. Pocs, Y. Zhang, F. Ye, C. Hoffmann, X. Wang, M. Lee, M. Hermele and I. Kimchi, “Quantum liquid from strange frustration in the trimer magnet Ba₄Ir₃O₁₀.” *npj Quantum Materials* **5**, 26 (2020).
7. L. Radzihovsky and M. Hermele, “Fractons from vector gauge theory.” *Phys. Rev. Lett.* **124**, 050402 (2020).
8. V. Khemani, M. Hermele and R. M. Nandkishore, “Localization from Hilbert space shattering: From theory to physical realizations.” *Phys. Rev. B* **101**, 174204 (2020).
9. M. Pretko, S. A. Parameswaran and M. Hermele, “Odd fracton theories, proximate orders, and parton constructions.” *Phys. Rev. B* **102**, 205106 (2020).
10. M. Qi, L. Radzihovsky and M. Hermele, “Fracton phases via exotic higher-form symmetry breaking.” *Ann. Phys.* **424**, 168360 (2021).
11. E. Lake and M. Hermele, “Subdimensional criticality: condensation of lineons and planons in the X-cube model.” arXiv:2107.09073, accepted in *Phys. Rev. B*.
12. C. A. Pocs, P. E. Siegfried, J. Xing, A. S. Sefat, M. Hermele, B. Normand and M. Lee, “Systematic fitting of crystal-field levels and accurate extraction of quantum magnetic models in triangular-lattice delafossites.” arXiv:2109.09758, submitted to *Phys. Rev. X*.

Theory of Novel Superconductors

P.J. Hirschfeld (U. Florida Physics)

Program Scope

The grant explores novel aspects of unconventional superconductivity, applicable to iron-based systems, cuprates, ruthenates, and heavy fermion systems. Recent focus has been on the canonical unconventional superconductor Sr_2RuO_4 , long assumed to support a chiral p-wave ground state and of considerable potential interest for quantum computing. However, interest in this material has recently experienced a renaissance because of NMR measurements supporting a spin singlet pairing state[1]. Determining the true order parameter would be aided by a direct measurement of the gap structure, but Δ is so small that only STM-quasiparticle interference (QPI) is possible. But there are several mysteries in the STM experiments:

- Some STM experiments [2,3] do not detect a superconducting gap despite high energy resolution, others do[4,5]
- Both STM and ARPES (surface probes) [2,3,6] sometimes report reconstructed electronic structure
- QPI on both normal and superconducting state show only weak evidence of tunneling into d_{xy} band[2,4]

Here we investigate effects of surface octahedral rotation on QPI and nematic surface states, and show why the contribution of d_{xy} states to tunneling is suppressed everywhere except near van Hove singularity. We further calculate the QPI patterns to be expected in realistic (singlet) spin fluctuation pairing models.

Keywords:

Unconventional superconductivity

Correlated electron materials

Spin fluctuations

Recent Progress

- 1) *Nematic electronic structure of FeSe.* Spectroscopic probes have pointed out for some years that the expected Y electron-pocket of the Fermi surface of FeSe in its nematic state at low temperatures is “missing”. We proposed (Sprau et al, Science 2017) that the pocket was there, but could not be observed due to decoherence of the xz relative to the yz state, but others have suggested it could be a consequence of nematic order in the

absence of quasiparticle decoherence “lifting” the entire band away from the Fermi level. In this study we considered the effect of longer-range Coulomb interaction, expected to be larger in FeSe, on the low-energy electronic structure. We showed that interorbital nematic terms can in fact “lift” the Y-pocket entirely. However, the magnetic susceptibility calculated from this electronic structure was incompatible with experiment. We commented that the correlations invoked in the Sprau et al paper must be preserved, but the xz/yz asymmetry in the nematic phase could be relaxed somewhat.

- 2) *Bogoliubov Fermi surfaces (BFSs)* are topologically protected regions of zero energy excitations in a superconductor whose dimension equals that of the underlying normal state Fermi surface. Examples of Hamiltonians exhibiting this “ultranodal” phase are known to preserve charge-conjugation (C) and parity (P) but break time-reversal (T). We followed up on our Nature Communications study of spin-1/2 systems with BFSs with applications to Fe(Se,S) with a further examination of thermodynamic and electronic properties arising from the ultranodal state we predicted. In particular, we study the effect of a weak Zeeman field close to the topological transition and propose distinguishing features of BFSs using residual specific heat and tunneling conductance. Our calculation of the superfluid density in a toy multiband model indicated a large window of interband pairing strength where BFSs are stable with a positive superfluid density. We also presented additional signatures of BFSs in spin-polarized spectral weight and total magnetization measurements.
- 3) *Microscopic model of pair density wave.* We have recently studied a simple model of a superconductor with d-wave attraction and posed the question, under what circumstances is the homogeneous d-wave superconductor unstable to strong pairing fluctuations? Calculating the pair propagator for larger coupling, we find a 1st-order transition to a pair density wave state, and a fluctuating pair density wave state at higher temperatures. This state is quite reminiscent of underdoped cuprates. Our model may provide a simple platform in which properties of the fluctuating pair density wave can be easily calculated.

Future plans

The heavy fermion superconductor UTe_2 displays many of the classic signatures of a triplet superconductor, in NMR and the reentrant superconductivity observed in its phase diagram. It has been claimed to be proximate to a class of known ferromagnetic superconductors, suggesting that superconductivity is driven by ferromagnetic fluctuations. On the other hand, definitive neutron studies point to finite-momentum spin fluctuations, as is also observed in UPt_3 . This raises the quite general question of under what circumstances antiferromagnetic spin fluctuations can drive triplet superconductivity. Preliminary studies show that this can happen when the susceptibility is dominated by scattering vectors that do not connect opposite sides of the Fermi surface, and that UTe_2 may have a Fermi surface favorable for such an effect. We plan to

explore these effects, and those of spin-orbit coupling that drive the strong susceptibility anisotropy observed in UTe_2 .

We will continue our work on Sr_2RuO_4 , exploring 3D spin fluctuations, evolution of the spin fluctuation driven states found in earlier work below T_c , and a quantitative investigation of recent sound attenuation experiments that should provide useful information on the order parameter.

Our model for the Bogoliubov Fermi surface (BFS) transition in $FeSe,S$ appears to explain many aspects of experiments in that system near the nematic transition. We will pursue several related projects, including: a) nature of instability of the model in regime with negative superfluid density, in particular whether a modulated (pair density wave) phase is stable; b) relation of BFS to fluctuation effects visible in the superconducting transition of this of system; c) construction of microscopic model reproducing phenomenology, so that self-consistent results and T-dependence can be obtained.

References

- [1] A. Pustogow et al., *Nature* 574, 72 (2019); A. Chronister et al. *Proceedings of the National Academy of Sciences* 118 (2021).
- [2] Z. Wang et al., *Nature Physics* 13, 799 (2017).
- [3] C.A. Marques et al., arXiv:2005.00071; A. Kreisel et al, arXiv:2103.06188, , accepted for publication in *Nature Materials*.
- [4] I.A. Firmo, *Phys. Rev. B* 88, 134521 (2013).
- [5] R. Sharma, *Proceedings of the National Academy of Sciences* 117, 15222 (2020).
- [6]. C. Tamai, *Phys. Rev. X* 9, 021048 (2019).

Publications

- 1) "Bogoliubov Fermi Surfaces in Spin-1/2 Systems: Model Hamiltonians and Experimental Consequences", C. Setty, S. Bhattacharyya, Y. Cao, A. Kreisel and P.J. Hirschfeld, Phys. Rev. B 102, 064504 (2020).
- 2) "On the Remarkable Superconductivity of FeSe and its Close Cousins", A. Kreisel, P.J. Hirschfeld, and B.M. Andersen, Symmetry 12, 1402 (2020).
- 3) "Quasiparticle Interference near the van Hove singularity at the surface of Sr₂RuO₄", A. Kreisel, L. C. Rhodes, C. A. Marques, X. Kong, T. Berlijn, P. Wahl, and P. J. Hirschfeld, arXiv:2103.06188, submitted to npj-Quantum Materials.
- 4) "Inter-orbital nematicity and the origin of a single electron Fermi pocket in FeSe", D. Steffensen, A. Kreisel, P. J. Hirschfeld, B. M. Andersen, Phys. Rev. B 103, 054505 (2021).
- 5) "Theory of Strain-Induced Magnetic Order and Splitting of T_c and T_{TRSB} in Sr₂RuO₄", A. T. Rømer, A. Kreisel, I. M. Eremin, P. J. Hirschfeld, and B. M. Andersen, Phys. Rev. B 102, 054506 (2020).
- 6) "Pairing state of Sr₂RuO₄ in the presence of longer-range Coulomb interactions", A. T. Rømer, P. J. Hirschfeld, and B. M. Andersen, Phys. Rev. B 104, 064507 (2021).
- 7) "Superconductivity from Luttinger surfaces: Emergent Sachdev-Ye-Kitaev physics with infinite-body interactions", C. Setty Phys. Rev. B 103, 014501 (2020).
- 8) "Anharmonic phonon damping enhances the T_c of BCS-type superconductors". C. Setty, M. Baggioli, and A. Zaccane, Phys. Rev. B 102, 174506 (2021) .
- 9) "Analytical Description of the Effects of Pressure, Anharmonicity and Phonon Softening on the Superconducting T_c", Chandan Setty, Matteo Baggioli, Alessio Zaccane, Phys. Rev. B 103, 094519 (2021).
- 10) "Extracting correlation effects from momentum-resolved electron energy loss spectroscopy: Synergistic origin of the dispersion kink in Bi₂.1Sr_{1.9}CaCu₂O_{8+x}", E. W. Huang, K. Limtragool, C. Setty, A.A. Husain, M. Mitrano, P. Abbamonte, and P. W. Phillips, Phys. Rev. B 103, 035121 (2021).
- 11) "Superconducting gap-symmetry from Bogoliubov quasiparticle interference analysis on Sr₂RuO₄", Shinibali Bhattacharyya, R. Sharma, A. Rømer, B. M. Andersen, A. Kreisel, and P. J. Hirschfeld, arXiv:2109.10712, submitted to Phys. Rev. B.
- 12) "Ironing out the details of unconventional superconductivity", A. Coldea, H. Ding, R. Fernandes, I. Fisher, P.J. Hirschfeld, & G. Kotliar, invited review, arXiv: to be published in Nature.

Data Science Enabled Discovery of Superconductors

P.J. Hirschfeld (PI), J.A. Hamlin, G.R. Stewart (U. Florida Physics), R.G. Hennig (U. Florida Materials Sciences)

Program Scope

The recent discoveries of high-temperature superconductivity in hydrides renewed interest in the search for room temperature superconducting materials. One of the shortcomings of the hydride superconductors is the high pressure required to stabilize them. Metastable materials offer a promising route to synthesizing room temperature superconductors stable at ambient pressure. We have studied two different types of metastable superconducting materials,

- Nb₃Si - Metastable A15 superconducting phase at ambient pressure [1]
- WB2 - Superconductivity created by pressure-induced metastable planar defects [2]

A15 Nb₃Si is, until now, the only 'high' temperature superconductor produced at high pressure of over 100 GPa that was successfully brought back to room pressure conditions in a metastable condition. While the slow compression of tetragonal Nb₃Si up to 92 GPa showed no indications of the superconductivity characteristic of A15 Nb₃Si, the explosive compression up to 110 GPa produced 50%–70% of A15 with $T_c = 18$ K at ambient pressure. This implies that the accompanying high temperature of 1000°C caused by explosive compression is necessary to drive the reaction kinetics successfully. "Annealing" explosively formed A15 phase at room temperature for 39 years has no effect, demonstrating that slow kinetics can stabilize high-pressure metastable phases at ambient conditions over long times even for large driving forces of 90 meV/atom.

For WB2, high-pressure electrical resistivity measurements reveal that the mechanical deformation during compression induces superconductivity above 50 GPa with a maximum superconducting critical temperature of 17 K. Theoretical calculations show that electron-phonon mediated superconductivity originates from the formation of metastable stacking faults and twin boundaries. Synchrotron x-ray diffraction demonstrates that the abrupt appearance of superconductivity under pressure does not coincide with a structural transition but instead with the formation and percolation of mechanically-induced stacking faults and twin boundaries. The results identify an alternate route for designing superconducting materials.

Keywords:

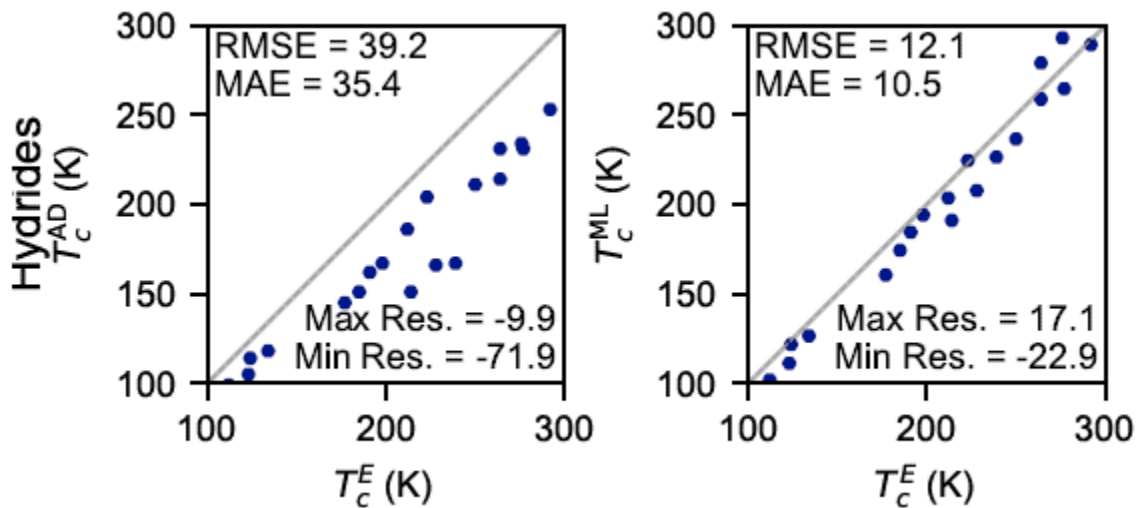
Superconductivity

Metastable materials

High pressure

Recent Progress

- **Teaching the machine Eliashberg theory** (Xie et al, submitted to Phys. Rev. B). The Eliashberg theory of superconductivity is the simplest set of equations that builds in the basic physics of conventional electron-phonon superconductors, including the retardation of the interaction as well as the effect of the Coulomb pseudopotential. Approximate closed form expressions for the critical temperature predicted by this theory, which depends essentially on the electron-phonon spectral function $\alpha^2F(\omega)$, were derived using α^2F for low- T_c superconductors by McMillan, and Allen and Dynes. We showed that modern machine learning techniques can substantially improve on these formulae, accounting for more general shapes of the α^2F function. Using symbolic regression and the sure independence screening and sparsifying operator (SISSO) framework, together with a database of artificially generated α^2F functions, ranging from multimodal Einstein-like models to calculated spectra of polyhydrides, as well as numerical solutions of the Eliashberg equations, we derive a formula for T_c that performs as well as Allen-Dynes for low- T_c superconductors, and substantially better for higher- T_c ones. Earlier work with a much smaller database of experimentally determined $\alpha^2F(\omega)$ moments appeared as Phys. Rev. B 100, 174513 (2019). An overview of some of these results was recently published in a special J. Phys-Cond. Mat. Issue as a ROADMAP contribution.



Predicted Allen-Dynes (AD) and machine-learned (ML) critical temperatures compared to the T_c predicted from a full solution to the Eliashberg equations (E). T_{cML} obtained by symbolic regression on a training set consisting of 30 low- T_c superconductors and thousands of artificially generated trimodal α^2F functions, and tested here against data for predicted superconducting hydrides.

- **High pressure study of low-Z superconductor Be₂₂Re** (under review at Phys. Rev. B)

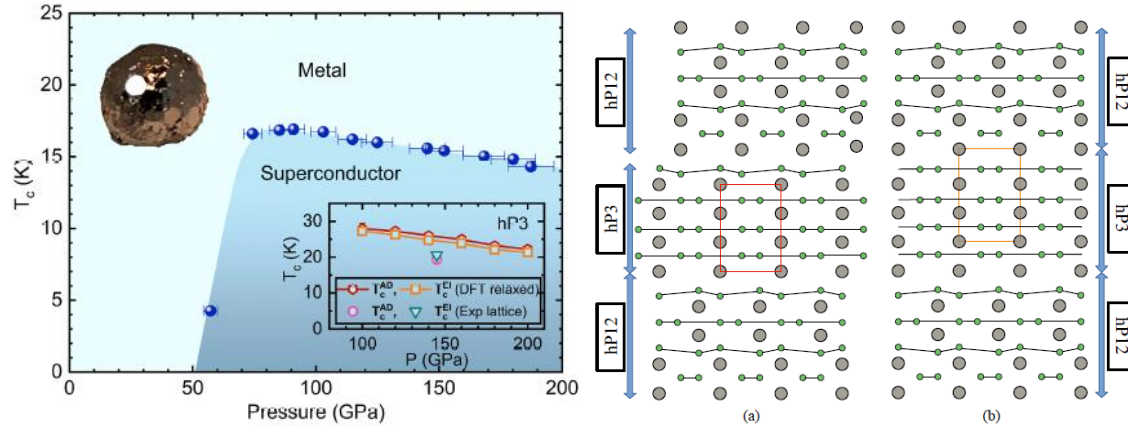
With $T_c \sim 9.6$ K, Be₂₂Re exhibits one of the highest critical temperatures among Be-rich compounds. In hopes of discovering an analog of clathrate structure superhydrides, we carried out a series of high-pressure electrical resistivity measurements on this compound to 30 GPa. The data show that the critical temperature T_c is suppressed gradually at a rate of $dT_c/dP = -0.05$ K/GPa. Using density functional theory (DFT) calculations of the electronic and phonon density of states (DOS) and the measured critical temperature, we estimated that the rapid increase in lattice stiffening in Be₂₂Re overwhelms a moderate increase in the electron-ion interaction with pressure, resulting in the decrease in T_c . High pressure x-ray diffraction measurements showed that the ambient pressure crystal structure of Be₂₂Re persists to at least 154 GPa.

- **Superconductivity of α and β Gallium** (Phys. Rev. B)

Elemental gallium can exist in several phases under ambient conditions. The stable α phase has a T_c of 0.9 K. By contrast, the T_c of the metastable β phase is around 6 K. There is great interest in understanding situations where long-lived metastable phases formed at ambient or high pressure might exhibit a higher T_c than their stable counterparts. The gallium phases represent a unique opportunity to study this problem theoretically to understand the enhancement from the low- T_c stable phase to the higher- T_c metastable phases. To understand the significant improvement in T_c in the β phase, we first calculated the electronic structure, phonon dispersion, and the electron-phonon coupling of gallium in the α and β phase. Next, we solved the Eliashberg equations to obtain the superconducting gaps and the transition temperatures. Using these results, we related the increased T_c in the β phase to structural differences between the phases that affect the electronic and phonon properties.

- **Creating superconductivity from metastable planar defects**

High-pressure electrical resistivity measurements reveal that the mechanical deformation of ultra-hard WB₂ during compression induces superconductivity above 50~GPa with a maximum superconducting critical temperature of 17~K at 90~GPa. Upon further compression up to 190~GPa, the T_c gradually decreases. Theoretical calculations show that electron-phonon mediated superconductivity originates from the formation of metastable stacking faults and twin boundaries that exhibit a local structure resembling MgB₂. X-ray diffraction measurements up to 145 GPa show that the ambient pressure hP12 structure persist up to this pressure, consistent with the formation of the planar defects with the MgB₂ structure above 50~GPa. Thus the abrupt appearance of superconductivity under pressure does not coincide with a structural transition but instead with the formation and percolation of mechanically-induced stacking faults and twin boundaries. The results identify an alternate route for designing superconducting materials.



Left: T_c vs. pressure for WB2 sample showing abrupt jump in T_c at ~ 50 GPa, but no change in crystal structure. Theoretical calculations for the electron-phonon T_c of all competitive structures show subKelvin results. Right: MgB₂ like structures at stacking faults and grain boundaries, with a predicted T_c of 20K.

Future Plans

We will develop a high-throughput framework for the data-mining of materials using the machine-learned analytic expression to estimate T_c , and select promising candidate materials for more expensive *ab initio* electron-phonon and Eliashberg calculations of the superconducting properties. Our aim is to design a scheme based entirely on DFT-based descriptors, but we will compare with earlier work on atomistic descriptors and with experimental databases. We will also investigate structural phase transformations under pressure using our genetic algorithm and machine-learning code GASP, focusing primarily on ternary hydrides and borides.

Work on hydrides will require a liquid hydrogen (less than 1 mg) loading system accommodating into high pressure diamond anvil cells, which are inserted inside the cryostat in the experimental setup to be built in the next months.

We will extend our symbolic regression work to study anisotropic Eliashberg equations, so that low-dimensional outliers like MgB₂ can be included. Finally, we will attempt to study the suppression of electron-phonon T_c due to spin fluctuations using *ab initio* methods, investigating a relatively cheap way of estimating fluctuations at wave vectors associated with strong susceptibility peaks suitable for incorporating in high-throughput studies.

References

- [1] J. Lim, J. Kim, A. C. Hire, Y. Quan, R. G. Hennig, P. J. Hirschfeld, J. J. Hamlin, and G. R. Stewart, *J. Phys. Condens. Matter* 33, 285705 (2021).
- [2] J. Lim, A. C. Hire, Y. Quan, J. Kim, S. R. Xie, R. S. Kumar, D. Popov, C. Park, R. J. Hemley, R. G. Hennig, P. J. Hirschfeld, G. R. Stewart, and J. J. Hamlin, arXiv:2109.11521.

Publications

- 1) "Functional Form of the Superconducting Critical Temperature from Machine Learning", S. R. Xie, G. R. Stewart, J. J. Hamlin, P. J. Hirschfeld, and R. G. Hennig, *Phys. Rev. B* 100, 174513 (2019).
- 2) "Be₅Pt: Properties of a novel pseudogapped semimetal", Fanfarillo et al, *Phys. Rev. B* 102, 155206 (2020).
- 3) "Probing the Origins of Superconductivity in Metastable A₁₅Nb₃Si", Jinhyuk Lim, Jungsoo Kim, Ajinkya Hire, Yundi Quan, R. G. Hennig, P. J. Hirschfeld, J. J. Hamlin, and G. R. Stewart, *J. Phys. Cond. Mat.* 33,285705 (2021).
- 4) "ROADMAP: Towards high-throughput superconductor discovery via machine learning" S. Xie, Y. Quan, A. Hire, L. Fanfarillo, G. R. Stewart, J. J. Hamlin, R. G. Hennig, and P. J. Hirschfeld, submitted to *J. Phys. Cond. Mat.* as contribution to special issue, "Designing Room Temperature Superconductors", *J. Phys.: Condens. Matter* in press <https://doi.org/10.1088/1361-648X/ac2864>.
- 5) "High pressure study of low-Z superconductor Be₂₂Re", J. Lim, A.C. Hire, Y. Quan, J. Kim, L. Fanfarillo, S.R. Xie, R.S. Kumar, R.J. Hemley, R.G. Hennig, P.J. Hirschfeld, G.R. Stewart and J.J. Hamlin, *Phys. Rev. B* 104, 064505 (2021).
- 6) "Machine learning of superconducting critical temperature from Eliashberg theory", Xie et al, accepted for publication in *Nature – Computational Materials*, arXiv:2106.05235.
- 7) "Superconductivity of α and β -gallium", Y. Quan, P.J. Hirschfeld and R. Hennig, *Phys. Rev. B* 104, 075117 (2021).
- 8) "Creating superconductivity in WB₂ through pressure-induced metastable planar defects", J. Lim, A. C. Hire, Y. Quan, J. S. Kim, S. R. Xie, R. S. Kumar, D. Popov, C. Park, R. J. Hemley, J. J. Hamlin, R. G. Hennig, P. J. Hirschfeld, and G. R. Stewart, submitted to *Nature Communications*, arXiv:2109.11521.

Nontrivial consequences of non-centrosymmetry in topological and trivial metals

Pavan Hosur, University of Houston

Program Scope

Symmetry plays a fundamental role in the physical properties of materials. For instance, piezoelectricity – the phenomenon that guarantees that quartz clocks tick at a constant rate – stems from the absence of a center of inversion at the microscopic level. Among *non-centrosymmetric* materials, namely, materials that lack an inversion center, metals are extremely rare despite being theoretically predicted over 50 years ago [1]. Over the past decade, however, fervent research on an exotic family of materials known as Weyl semimetals has paved a new and prolific route to non-centrosymmetric metals [2-8]. Inspired by this development, this project theoretically explores novel phenomena emerging from the interplay between non-centrosymmetry and metallicity and unlock their potential for the next generation of electronic devices.

First, we will study the effects of rotation and acceleration on electrons in 3D *chiral* metals – non-centrosymmetric metals that break all reflection symmetries besides lacking an inversion center and exhibit handedness. By doing so, we will unearth various phenomena that rely on an intrinsically quantum mechanical property of the electrons known as the Berry phase. One such phenomenon, well-studied in high-energy physics, is the chiral vortical effect, defined as an axial current that develops in a relativistic chiral fluid upon rotation [3]. In this project, we will explore, generalize and harness this effect in settings exclusive to solid-state physics and propose a series of scalable device designs that exploit connections between vortical effects and other electronic transport properties.

We will then turn to non-centrosymmetric metals that are also magnetic but lack Berry phases. Non-centrosymmetric, magnetic metals are extremely rare, but have been discovered recently [4]. These properties skew the energy-momentum relationship for the constituent electrons, and we will dub them *asymmetric metals*. Conventional metals rely on the absence of skewness for most of their physical properties such as their response to electromagnetic fields, behavior under disorder and their tendency to form superconductors. In asymmetric metals, the skewness immediately brings these properties under question. We will study how well 2D asymmetric metals can overcome disorder to retain their metallicity. When disorder is weak and the quantum nature of electrons is prominent, we predict striking signatures in magnetic field-dependent conduction. Parallely, we will show that asymmetric metals are a natural platform for certain exotic superconducting phenomena such as the spontaneous appearance of spatial modulations or persistent currents in the superconductor at equilibrium.

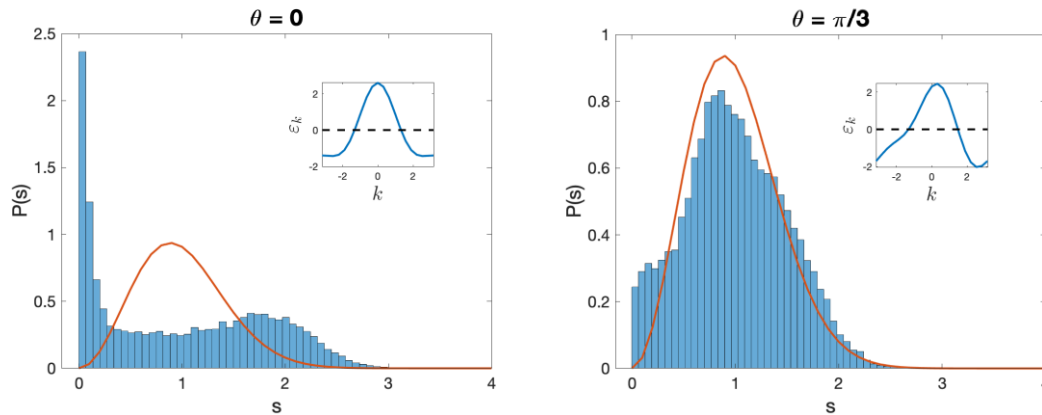
This project has the potential to strongly impact several areas of physics research. While the effects of rotation and acceleration on condensed matter systems have been extensively studied, their interplay with 3D chirality is less understood. We will establish a comprehensive theoretical framework for describing this interplay and sow the seeds for device applications based on non-inertial fluids. In addition, it will further strengthen the synergy between high-energy physics and condensed matter by providing table-top testbeds for studying accelerating and rotating 3D relativistic particles. We will also unearth fundamental physics of metals with regards to superconductivity and transport under disorder that had been missed, to the best of our knowledge, despite decades of research on metals. Presumably, these aspects received little attention due to the dearth of materials that realize asymmetric metals. The project, combined with the ongoing activity in Weyl semimetals and related materials, will boost the search for non-centrosymmetric metals including asymmetric metals.

Keywords: Chiral metals, vortical effects, asymmetric metals.

Recent Progress

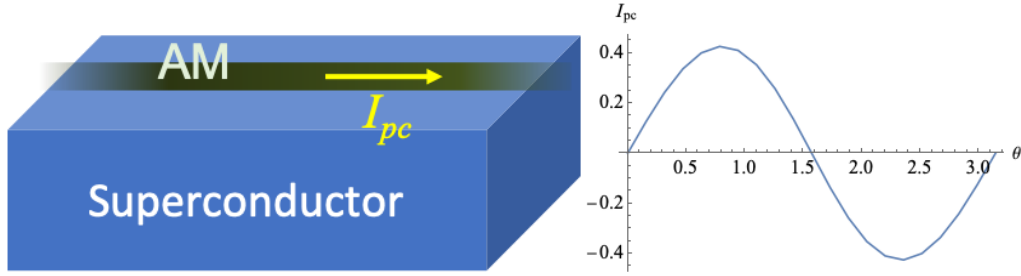
So far, we have obtained preliminary unpublished results on several aspects of the project:

1. We have studied the effect of rotation on single Weyl fermion. The chiral vortical effect predicts an axial current proportional to the angular velocity. We have discovered that the size of the current depends sensitively on the order of the $q \rightarrow 0$ and $\omega \rightarrow 0$ limits. Specifically, the current in the static limit ($\omega \rightarrow 0$ before $q \rightarrow 0$) is three times the current in the dc transport limit ($q \rightarrow 0$ before $\omega \rightarrow 0$).
2. We have found that 1D asymmetric metals (metals without inversion or time-reversal symmetry) exhibit Gaussian level statistics in the presence of disorder in regimes where the level statistics of symmetric metals are Poissonian.



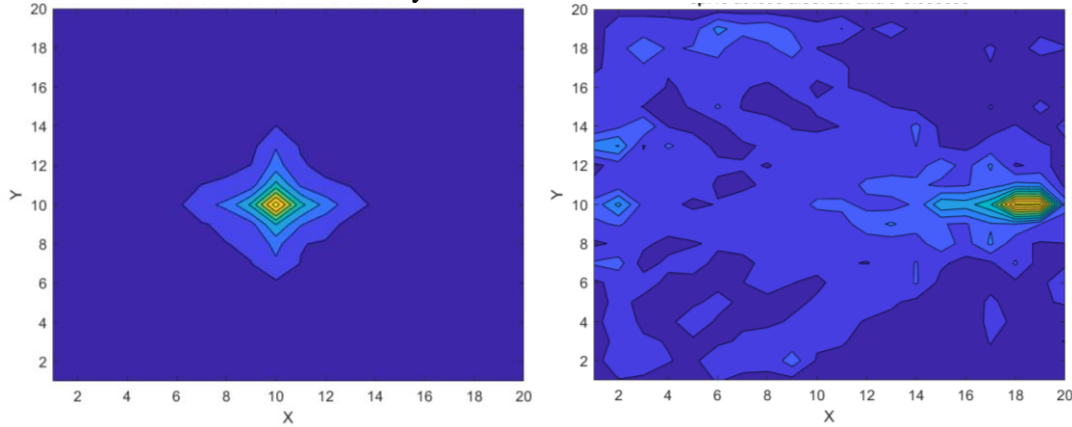
Distribution of level spacings for a disordered 1D chain (blue bars) compared to a Wigner-Dyson distribution (orange curve) for a symmetric (left) and an asymmetric (right) dispersion. The dispersion, shown inset, is given by $\epsilon_k = 2\cos k + 0.6\cos(2k - \theta)$, and is asymmetric for $\theta \neq 0, \pi$. Random chemical potential disorder, μ_i , is drawn uniformly from the interval $[-0.075, 0.075]$. The system size is $L = 1000$ and disorder average is performed over $n_{\text{dis}} = 30$ configurations.

3. We have found that 1D asymmetric metals proximity-coupled to an s-wave superconductors carry a non-zero supercurrent in the ground state.



Left: Depositing an asymmetric metal wire on a conventional superconductor will generate a persistent current I_{pc} , assuming periodic boundary conditions. Right: I_{pc} in arbitrary units vs θ assuming the same asymmetric dispersion as in Fig. 1., pairing $\Delta = 0.1$ and temperature $T = 1$.

4. We have also seen that an initially local electron in a disordered 2D asymmetric metal travels farther than it does in a symmetric 2D metal.



Probability density of an electron, initially at the center of the lattice, at time $t = 9.0$ for a symmetric metal (left) and an asymmetric metal (right). The dispersion is $\varepsilon_k = 2(\cos k_x + \cos k_y) + \cos(k_x + k_y + \theta) + \cos(k_x - k_y + \theta)$ with $\theta = 0$ (left) and $\theta = 5\pi/13$ (right).

Future Plans

In the future, we will build on the preliminary results mentioned above and tackle the problems described in the program scope in detailed manner. On one hand, we will describe responses to rotation and acceleration in general band structures and identify peculiar chiral and topological responses. We will also develop field theoretic and Boltzmann equation descriptions of transport under non-inertial driving forces and describe how the responses to rotation can be activated by electric field and temperature gradients for devices. On the other hand, we will investigate the localization and superconducting physics of asymmetric metals. We will use exact diagonalization to study the dependence of level statistics and quench dynamics on the band asymmetry and numerical solutions of mean field theory equations to explore Fulde-Ferrell-Larkin-Ovchinnikov superconductivity in these materials.

References

1. P. W. Anderson and E. I. Blount. Symmetry considerations on martensitic transformations: "ferroelectric" metals? *Phys. Rev. Lett.*, 14:217–219, Feb 1965.
2. H. Hodovanets et al., Single-crystal investigation of the proposed type-II Weyl semimetal CeAlGe. *Phys. Rev. B*, 98:245132, Dec 2018.
3. T. Suzuki et al., Singular angular magnetoresistance in a magnetic nodal semimetal. *Science*, 365(6451):377–381, 2019.
4. P. Puphal et al., Topological magnetic phase in the candidate Weyl semimetal CeAlGe. *Phys. Rev. Lett.*, 124:017202, Jan 2020.
5. K. Singh and K. Mukherjee. Spin–lattice relaxation phenomena in the magnetic state of a suggested Weyl semimetal CeAlGe. *Philosophical Magazine*, 100(13):1771–1787, 2020.
6. B. Meng et al., Large anomalous hall effect in ferromagnetic Weyl semimetal candidate PrAlGe. *APL Materials*, 7(5):051110, 2019.
7. D. Destraz et al., Magnetism and anomalous transport in the Weyl semimetal PrAlGe: possible route to axial gauge fields. *NPJ Quantum Materials*, 5(1):5, 2020.
8. D. S. Sanchez et al., Observation of Weyl fermions in a magnetic non-centrosymmetric crystal. *Nature Communications*, 11(1):3356, 2020.
9. A. Vilenkin. Parity nonconservation and rotating black holes. *Phys. Rev. Lett.*, 41:1575–1577, Nov 1978.
10. A. Vilenkin. Parity violating currents in thermal radiation. *Physics Letters B*, 80(1):150–152, 1978.
11. A. Vilenkin. Macroscopic parity-violating effects: Neutrino fluxes from rotating black holes and in rotating thermal radiation. *Phys. Rev. D*, 20:1807–1812, Oct 1979.
12. A. Vilenkin. Quantum field theory at finite temperature in a rotating system. *Phys. Rev. D*, 21:2260–2269, Apr 1980.
13. O. V. Rogachevsky et al., Chiral vortical effect and neutron asymmetries in heavy-ion collisions. *Phys. Rev. C*, 82:054910, Nov 2010.
14. R. Loganayagam and P. Surówka. Anomaly/transport in an Ideal Weyl gas. *Journal of High Energy Physics*, 2012(4):97, apr 2012.
15. M. A. Stephanov and Y. Yin. Chiral Kinetic Theory. *Phys. Rev. Lett.*, 109(16):162001, oct 2012.
16. J.-Y. Chen et al., Lorentz Invariance in Chiral Kinetic Theory. *Phys. Rev. Lett.*, 113(18):182302, oct 2014.
17. G. Prokhorov and O. Teryaev. Anomalous current from the covariant Wigner function. *Phys. Rev. D*, 97:076013, Apr 2018.
18. G. Y. Prokhorov et al., Axial current in rotating and accelerating medium. *Phys. Rev. D*, 98:071901, Oct 2018.
19. V. I. Zakharov and O. V. Teryaev. Quark-hadron duality in hydrodynamics: an example, 2018.
20. M. Stone and J. Kim. Mixed anomalies: Chiral vortical effect and the Sommerfeld expansion. *Phys. Rev. D*, 98:025012, Jul 2018.
21. G. Y. Prokhorov et al., Effects of rotation and acceleration in the axial current: density operator vs wigner function. *Journal of High Energy Physics*, 2019(2):146, 2019.

Publications No publications so far.

Van der Waals Reprogrammable Quantum Simulator

Benjamin M. Hunt (PI, Carnegie Mellon); Jeremy Levy (U. Pittsburgh); Patrick Irvin (U. Pittsburgh); Chang-Beom Eom (U. Wisconsin); Roman Engel-Herbert (Penn State); Erica Carlson (Purdue); Prineha Narang (Harvard), and Di Xiao (U. Washington)

Program Scope

Quantum materials are characterized by a high degree of coherence and entanglement among their constituent parts, which makes modelling on classic computers near-impossible. As a result, the development of novel quantum materials, such as high-Tc superconductors or materials that can carry certain types of topologically-robust quantum information, remains largely a trial-and-error endeavor. Here, we introduce a new path to the top-down design of quantum materials through the use of a unique quantum simulation platform, known as “van der Waals Reprogrammable Quantum Simulator”, or VR-QuSIM, which involves a van der Waals (vdW) material or heterostructure placed a few nanometers above the lanthanum aluminate-strontium titanate (LAO/STO) interface. The technique then enables sub-10-nm programming of a wide range of vdW materials by taking advantage of the ability to create conductive nanostructures in arbitrary patterns at LAO/STO interface. The VR-QuSIM platform has been enabled by a recent breakthrough: using an ultra-low-energy electron beam, the conductive nanostructures at the LAO/STO interface underneath the vdW layer can be written, erased, and rewritten without altering the vdW structure. The platform will harness both the astonishing variety of intrinsic material properties of vdW materials/heterostructures and the ability to create conductive patterns with arbitrary lattice symmetry, lateral length scale, and single-lattice-site controllable disorder to realize a vast array of simulated quantum materials.

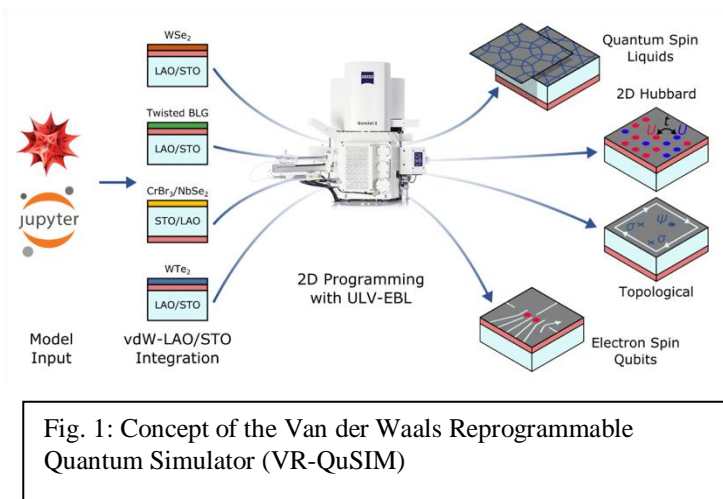


Fig. 1: Concept of the Van der Waals Reprogrammable Quantum Simulator (VR-QuSIM)

Keywords: quantum simulator, hybrid quantum system, two-dimensional materials, LAO/STO

Recent Progress

A new approach to programming the LAO/STO interface was recently established that uses ultra-low-voltage electron beam lithography (ULV-EBL) in place of conductive atomic force microscopy (c-AFM) lithography¹. This approach

overcomes all of the known limitations to the c-AFM approach: ULV-EBL is 10,000x faster and scalable, capable of creating sub-10-nm features over “canvases” exceeding 100 microns x 100 microns (~10⁸ superlattice sites). Electrically conducting areas can be inscribed into this heterostructure with sub-10-nm precision by locally inducing a 2DEG at the interface in a non-

volatile, reconfigurable fashion directly underneath vdW stacked layers. This approach represents a breakthrough in the programmability of van der Waals (vdW) materials, due to the reprogrammable control of conductivity in the LAO/STO layer. Figure 2 illustrates a recent key experiment performed by Levy and Hunt, demonstrating conductivity writing through a thick graphene layer encapsulated by hBN.

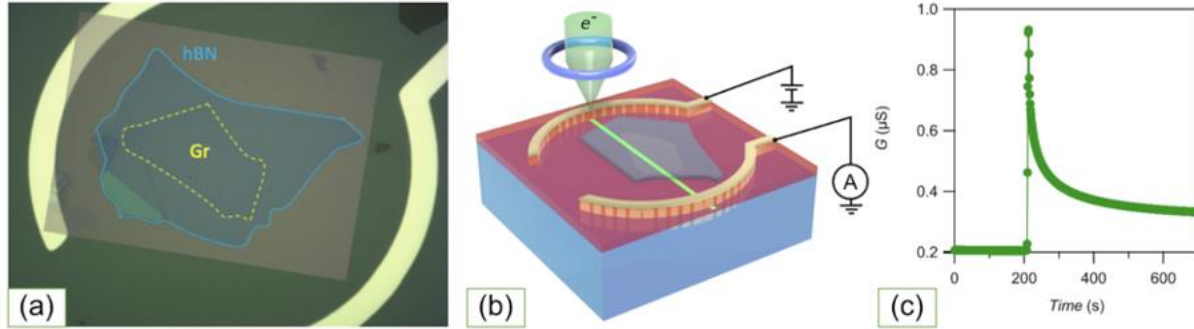


Fig. 2. Demonstration of ULV-EBL writing through graphene/(15-nm-thick hBN) heterostructure. (a) Optical image of test device with lithographically-defined electrodes wire bonded to a chip carrier. (b) Illustration showing how ULV-EBL beam creates a conductive nanowire at the LAO/STO interface. (c) In-situ monitoring of conductance as the ULV-EBL creates a conductive nanowire underneath the Gr/hBN

Future Plans

The overall goal of this project is to realize model Hamiltonians (e.g. 2D Hubbard model, 2D Kitaev honeycomb model) using superlattices programmed in the LAO/STO layer that are coupled to a two-dimensional van der Waals layer that possess specific desired properties, such as magnetism or spin-orbit coupling. In the first year of this project, on the experimental side, we plan to study LAO/STO superlattices of various lattice symmetries and lattice parameters with the vdW layer either monolayer or bilayer graphene (in which we would look for replica Dirac points), or monolayer WSe_2 (in which we would look for the signatures of the Hubbard model that have been seen in moiré superlattices^{2,3}). We will then move on to studying superlattices having symmetries that are not easily realized in the moiré superlattice platform. Other experimental targets in the first year include: the production of high-throughput canvases of MBE-grown STO on silicon; growth of transition-metal dichalcogenides on STO; and programming of LAO/STO membranes or inverted STO/LAO membranes. On the theory side of our program, we will pursue the realistic implementation of Hamiltonians in the VR-QuSIM platform using feedback from experiments about, for example, the strength and profile of the potential generated by the LAO/STO layer and felt by the vdW layer. We will also investigate the realization of spin models with tunable and directional exchange couplings in our platform using, e.g., the possibility of engineered spin-orbit coupling in 1D channels in the LAO/STO layer⁴.

References

1. Cen, C., Thiel, S., Mannhart, J. & Levy, J. Oxide Nanoelectronics on Demand. *Science* **323**, 1026–1030 (2009).
2. Tang, Y. *et al.* Simulation of Hubbard model physics in WSe₂/WS₂ moiré superlattices. *Nature* **579**, 353–358 (2020).
3. Regan, E. C. *et al.* Mott and generalized Wigner crystal states in WSe₂/WS₂ moiré superlattices. *Nature* **579**, 359–363 (2020).
4. Briggeman, M. *et al.* Engineered spin-orbit interactions in LaAlO₃/SrTiO₃-based 1D serpentine electron waveguides. *Sci. Adv.* **6**, eaba6337 (2020).

Publications

This is a new award in 2021.

Title: Quantitative Studies of the Fractional Quantum Hall Effect

PI: Jainendra Jain

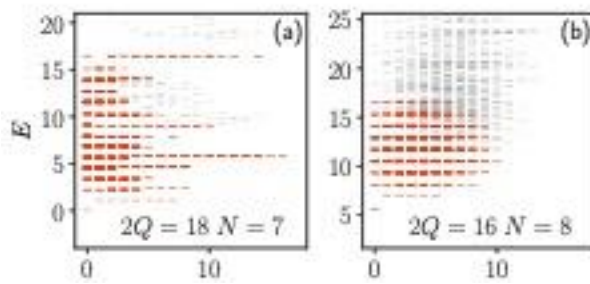
Affiliation: The Pennsylvania State University

Program Scope

The long-term objective of this DOE funded proposal is to strive toward a precise quantitative understanding of the fractional quantum Hall effect (FQHE). While tremendous progress has been made in this direction and the prominent observations are securely understood, the origin of certain delicate FQHE states still remains unsettled, and it is likely that quantitative studies combined with experiments will clarify their nature.

Exactly solvable model for strongly interacting electrons in the FQHE (Ref. iv in the list below): We have also been searching for exact Hamiltonians, i.e. parent Hamiltonians that will produce certain known FQHE wave functions as exact and unique ground states. Such a Hamiltonian has been known for the Laughlin $1/3$ state since Haldane's 1983 work [1], but we have failed to find such a Hamiltonian for the simplest non-Laughlin state, namely the lowest-Landau-level (LLL) projected $2/5$ state [2]. In the course of these studies, we began to consider another limit in which the interaction is infinitely large compared to the cyclotron energy. We have shown (iv) that for a particular choice of interaction, inspired by the physics of vortex attachment and defined in terms of Haldane's intra-LL and inter-LL pseudopotentials, this model can be solved for all finite energy states at arbitrary fillings less than $1/2$. Furthermore, its spectrum has an exact one-to-one correspondence with the spectrum of non-interacting fermions at an effective filling factor (see figure). In particular, it produces FQHE at filling fractions $n/(2n+1)$, which are precisely the prominently observed fractions. This model is not intended to capture the physics of Landau level mixing, but reproduces many topological properties correctly and, at least for small systems, is adiabatically connected to the Hamiltonian of electrons in the LLL interacting via the Coulomb interaction.

Keywords: Fractional quantum Hall effect, composite fermions, exactly solvable model.



This figure shows the spectrum of our model for 7 (8) electrons at $1/3$ ($2/5$) obtained by exact diagonalization in the spherical geometry. The eigenstates shown in orange exhibit a one-to-one correspondence with the states of non-interacting particles at filling factor $1/2$. The gray states are pushed to infinity with the interaction strength. From (iv).

Recent Progress

Here we provide the abstracts of several articles from the publication list below.

Anderson Localization in FQHE (i): The interplay between interaction and disorder-induced localization is of fundamental interest. This article addresses localization physics in the fractional quantum Hall state, where both interaction and disorder have nonperturbative consequences. We provide compelling theoretical evidence that the localization of a single quasiparticle of the fractional quantum Hall state at filling factor $\nu/(2\nu+1)$ has a striking *quantitative* correspondence to the localization of a single electron in the ν th Landau level. By analogy to the dramatic experimental manifestations of Anderson localization in integer quantum Hall effect, this leads to predictions in the fractional quantum Hall regime regarding the existence of extended states at a critical energy, and the nature of the divergence of the localization length as this energy is approached. Within a mean field approximation these results can be extended to situations where a finite density of quasiparticles is present.

BCS pairing of composite fermions (ii): Topological pairing of composite fermions has led to remarkable ideas, such as excitations obeying non-Abelian braid statistics and topological quantum computation. We construct a p-wave paired Bardeen-Cooper-Schrieffer (BCS) wave function for composite fermions in the torus geometry, which is a convenient geometry for formulating momentum space pairing as well as for revealing the underlying composite-fermion Fermi sea. Following the standard BCS approach, we minimize the Coulomb interaction energy at half filling in the lowest and the second Landau levels, which correspond to filling factors $1/2$ and $5/2$ in GaAs quantum wells, by optimizing two variational parameters that are analogous to the gap and the Debye cut-off energy of the BCS theory. Our results show no evidence for pairing at $1/2$ but a clear evidence for pairing at $5/2$. To a good approximation, the highest overlap between the exact Coulomb ground state at $5/2$ and the BCS state is obtained for parameters that minimize the energy of the latter, thereby providing support for the physics of composite-fermion pairing as the mechanism for the fractional quantum Hall effect. By similar methods, we look for but do not find an instability to s-wave pairing for a spin-singlet composite-fermion Fermi sea at half-filled lowest Landau level in a system where the Zeeman splitting has been set to zero.

Bloch ferromagnetism of composite fermions (viii): In 1929, Felix Bloch suggested that the paramagnetic Fermi sea of electrons should make a spontaneous transition to a fully magnetized state at very low densities, because the exchange energy gained by aligning the spins exceeds the enhancement in the kinetic energy. However, experimental realizations of this effect have been hard to implement. This experiment-theory collaboration reports the observation of an abrupt, interaction-driven transition to full magnetization, highly reminiscent of Bloch ferromagnetism. Our platform utilizes the two-dimensional Fermi sea of composite fermions near half-filling of the lowest Landau level. We measure the Fermi wavevector—which directly provides the spin polarization—and observe a sudden transition from a partially spin-polarized to a fully spin-

polarized ground state as we lower the density of the composite fermions. Our theoretical calculations that take Landau level mixing into account provide a semi-quantitative account of this phenomenon.

Hall effect for Dirac electrons in graphene exposed to an Abrikosov flux lattice (ix): The proposals for realizing exotic particles through coupling of quantum Hall effect to superconductivity involve spatially non-uniform magnetic fields. As a step toward that goal, we study, both theoretically and experimentally, a system of Dirac electrons exposed to an Abrikosov flux lattice. We theoretically find that non-uniform magnetic field causes a carrier-density dependent reduction of the Hall conductivity. Our studies show that this reduction originates from a rather subtle effect: a levitation of the Berry curvature within Landau levels broadened by the non-uniform magnetic field. Experimentally, we measure the magneto-transport in a monolayer graphene-hexagonal boron nitride - niobium diselenide (NbSe₂) heterostructure, and find a density-dependent reduction of the Hall resistivity of graphene as the temperature is lowered from above the superconducting critical temperature of NbSe₂, when the magnetic field is uniform, to below, where the magnetic field bunches into an Abrikosov flux lattice.

Zn superconductivity of composite bosons and the 7/3 FQHE (xiv): While the 1/3 state in the LLL was the first state to be understood, the origin of the 1/3 state in the second LL, i.e. the 7/3 state, is still not settled. Motivated by the parton construction, we consider the possibility of a new kind of emergent “superconductivity” in the 7/3 FQHE, which involves condensation of clusters of n composite bosons, which are electrons bound to three quantized vortices. Quantitative studies show that these states are at least as plausible as the Laughlin state. Many observable consequences of this physics are outlined.

Kohn-Sham theory of the FQHE (xvii): We formulate the Kohn-Sham equations for the FQHE by mapping the original electron problem into an auxiliary problem of composite fermions that experience a density dependent effective magnetic field. Self-consistent solutions of the Kohn-Sham equations demonstrate that our formulation captures not only configurations with nonuniform densities but also topological properties such as fractional charge and fractional braid statistics for the quasiparticles excitations. This method should enable a realistic modeling of the edge structure, the effect of disorder, spin physics, screening, and of fractional quantum Hall effect in mesoscopic devices.

Future Plans

We plan to explore the following problems in the immediate future:

Interplay between Landau levels and superconductivity: In collaboration with my colleague Chaoxing Liu and me, graduate student Jonathan Schirmer (supported by this grant) is studying what happens when we turn on nearest neighbor attractive interaction in a system of spin polarized electrons exposed to a uniform magnetic field. His preliminary calculations find a very rich phase diagram and show, surprisingly, that a skyrmions phase is preferred over a vortex

lattice phase for a range of parameters. This should give insight into realistic parameters for producing Majorana particles in this type of platform.

Interplay between composite fermions and superconducting correlations: We plan to explore how we can induce pairing of composite fermions by coupling a FQHE state or the $\frac{1}{2}$ Fermi sea to a superconductor. This problem is somewhat challenging, as it is not amenable to a mean field treatment, and also because the formation of composite fermions requires a repulsive interaction whereas superconductivity requires an attractive interaction.

Accurate calculation of excitation gaps: Excitation gaps of FQHE states are their most fundamental property, but an irritating discrepancy between the theoretically predicted and experimentally observed values has persisted. In recent years there has been a quantum jump in the sample quality at Princeton, which has enabled the most precise measurements of the gaps of various FQHE states, and in particular their dependence on the sample width. These experiments have motivated us to revisit the issue. Graduate student Tongzhou Zhao, who is supported by this DOE grant, is calculating the gaps by accurately including the effects of finite width (treated in an LDA approximation) and LL mixing (treated by fixed phase diffusion Monte Carlo). He will also estimate the error in trial wave function by comparing the results to exact diagonalization studies in finite systems. We hope that comparison with these state of the art theory numbers will give further insight into the effect of disorder on the gaps.

Extensions of the exactly solvable model: We will seek to extend the exactly solvable model described above in various directions. Inclusion of spin ought to be relatively straightforward. Implementation of the model in the torus geometry is far from obvious, as the relative angular momentum is not a good quantum number in this geometry. We will nonetheless look for at least an approximate implementation, as this can allow a discussion of mass anisotropy.

References

1. F.D.M. Haldane, PRL 51, 605 (1983).
2. G.J. Sreejith, M. Fremling, G.S. Jeon, J.K. Jain, PRB 98, 235139 (2018).

Publications during past two years (October 2019 – October 2021)

- (i) Anderson localization in fractional quantum Hall effect, S. Pu, G. J. Sreejith, J. K. Jain, arXiv:2109.00362.
- (ii) Bardeen-Cooper-Schrieffer pairing of composite fermions, A. Sharma, S. Pu, J.K. Jain, arXiv:2107.07628 (accepted in PRB).
- (iii) Composite anyons on a torus, S. Pu, J.K. Jain, PRB 104, 115135 (2021).

- (iv) Exactly solvable model for strongly interacting electrons in a magnetic field, A. Anand, J.K. Jain, G. J. Sreejith, PRL 126, 136601 (2021).
- (v) Crystalline Solutions of Kohn-Sham Equations in the Fractional Quantum Hall Effect, Y. Hu, Y. Ge, J.X. Zhang, J.K. Jain, PRB 104, 035122 (2021).
- (vi) Unconventional Zn parton states at $7/3$: Role of finite width, W.M. Faugno, T. Zhao, A.C. Balram, T. Jolicoeur, J.K. Jain, PRB 103, 085303 (2021).
- (vii) Kohn-Sham density functional theory of Abelian anyons, Y. Hu, G. Murthy, S. Rao, J.K. Jain, PRB 103, 035124 (2021).
- (viii) Bloch ferromagnetism of composite fermions, M.S. Hossain et al., Nature Physics 17, 48 (2021).
- (ix) Hall effect for Dirac electrons in graphene exposed to an Abrikosov flux lattice, J. Schirmer et al., Europhysics Lett. 132, 37002 (2020).
- (x) Interplay between fractional quantum Hall liquid and crystal phases at low filling, Z.W. Zuo et al. PRB 102, 075307 (2020).
- (xi) Non-Abelian fractional quantum Hall state at $3/7$ -filled Landau level, W.N. Faugno, J.K. Jain, A.C. Balram, Phys. Rev. Research 2, 033223 (2020).
- (xii) It's anyon's game: the race to quantum computation, J.K. Jain, Current Science 119, 430 (2020) (invited commentary).
- (xiii) Thirty Years of Composite Fermions and Beyond, in *Fractional Quantum Hall Effects: New Developments*, Editors B.I. Halperin and J.K. Jain, World Scientific, 2020 (book chapter).
- (xiv) Zn superconductivity of composite bosons and the $7/3$ fractional quantum Hall effect, A.C. Balram, J.K. Jain, M. Barkeshli, Phys. Rev. Research 2, 013349 (2020).
- (xv) Theoretical phase diagram of two-component composite fermions in double layer graphene, W.N. Faugno, A.C. Balram, A. Wojs, J.K. Jain, PRB 101, 085412 (2020).
- (xvi) Hall viscosity of composite fermions, S. Pu, M. Fremling, J.K. Jain, Phys. Rev. Research 2, 013139 (2020).
- (xvii) Kohn-Sham theory of the fractional quantum Hall effect, Y. Hu and J.K. Jain, Phys. Rev. Lett. 123, 176802 (2019).

Mapping and Manipulating Materials Phase Transformation Pathway

Duane D. Johnson (Ames Laboratory), William A. Shelton (LSU & Ames Laboratory), Prashant Singh and Andrey V. Smirnov (Ames Laboratory).

Program Scope

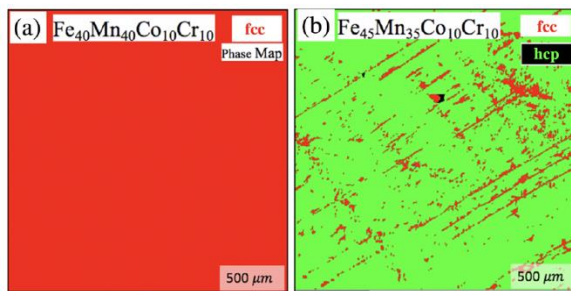
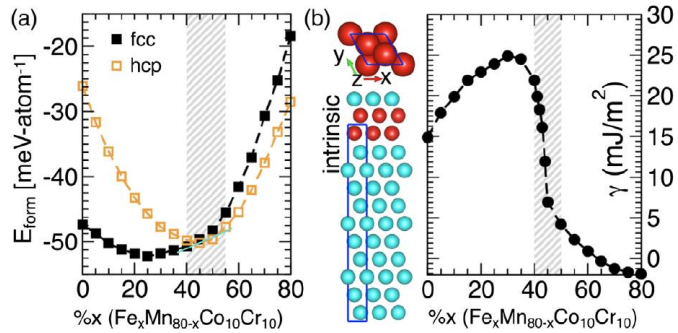
To design energy-relevant, complex, multicomponent materials and tailor their functionality, guide synthesis and characterization, we develop and apply unique electronic-structure-based, thermodynamic techniques to quantify stability by mapping *global solid-solid transformations* (e.g., competing long-range order, LRO) and *local structural instabilities* (e.g., competing short-range order, SRO), addressing doping, alloying, and disorder effects on key phenomena to control behavior of intriguing quantum materials. In particular, we are advancing thermodynamic linear-response theory to predict ordering in multicomponent systems arising from coupled electronic, chemical, magnetic, and structural effects to reveal directly the electronic origin and tailor properties, as well as directly guide experiments. Applications are on novel and responsive materials, e.g., complex intermetallics (e.g., high-entropy alloys), topological materials and iron-arsenide superconductors. Jointly, these innovative methods *uniquely assess global and local materials stability between competing structures and synthesis routes*, providing a direct means to *predict, understand, tailor, and interpret* properties in novel complex materials.

Keywords: Electronic-structure-based ordering, complex intermetallics, novel algorithms.

Recent Progress

- To enable materials discovery and to confirm results of KKR-CPA proper configurational averaging methods, our FWP developed a novel Hybrid Cuckoo Search optimization to generate models of high-entropy alloys 13,000 or more times faster than currently used methods, works for any short-range order any composition. The code is open-source.
 - ✓ Method was applied to arbitrary HEAs and revealed various correlations in refractory alloy systems. See *Nature Computational Science* **1**, 54-61 (2021).
 - ✓ The method was extended to surface high-entropy alloy configurations. It was applied in collaboration with Prof. Ye Xu at LSU to predict catalytic behavior with experimental confirmations. Without tuning, the electrode approached pure Pt. See *J. Phys. Chem. C* **125**, 17008-17018 (2021).
- To quantify and predict atomic order for any arbitrary solid-solution, KKR-CPA-based thermodynamic linear-response theory was extended to arbitrary crystal structures – providing a unique quantitative assessment of ordering in complex solid-solution alloys. (see pubs)
 - ✓ As experimentally confirmed at Argonne light source, discovered vacancy-mediated complex phase selection in refractory-based complex solid-solutions – creating a new beta-brass phase of tetrahedrally-order vacancy clusters. See *Acta Mater.* **194**, 540-546 (2020).
 - ✓ Reveals all incipient order in arbitrary high-entropy alloys, as exemplified in $\text{Ti}(0.25)\text{CrFeNiAl}(x)$ versus %Al. See *Acta Materialia* **189**, 248-254 (2020).

- ✓ Designing order-disorder transformations in high-entropy ferritic steels was presented as Prashant Singh's invited J. of Materials Research contribution of up-and-coming young research scientists. See, in press, *J. of Materials Research* (2021).
- ✓ We can directly explore chemical behavior in complex solid-solutions, where we revealed the electronic origin and control of TRansformation-Induced Phases (TWIP) or TWinning-Induced Phases (TWIP) transformations in Fe-Mn-Cr-Co alloys, as observed. See publication: *Phys. Rev. Lett.* **127**, 115704 (2021).



For $\text{Fe}_x\text{Mn}_{80-x}\text{Cr}_{10}\text{Co}_{10}$ **TOP** (a) formation energy and (b) intrinsic stacking fault energy. **BOTTOM** experimental (a) fcc phase map and (b) fcc-hcp mixed phase arising from TWIP transformation, as predicted in TOP calculations. SRO order was also predicted.

- A new formulation of Full-Potential (FP) Green's function KKR was developed using a "removed sphere method", requiring no multipolar expansions, no large L sums, and no Fast Fourier Transforms (FFTs). The method is being debugged numerically for KKR force code before publication. After which, some efforts for improved numerical efficiency will be made.

Future Plans

- These combined unique theory capabilities are directly applicable to many classes of quantum materials. At present, we are focusing on materials design of complex solid-solution alloys and physics-based design metrics, where we have linear correlators for strength and ductility to guide design of materials with particular properties. Three FWP papers are in draft stage.
- The KKR-CPA-based thermodynamic linear-response theory was extended to systems with arbitrary crystal structures and will be showcased in complex alloys with deformation. Paper currently being drafted for full FWP describing the full linear-response theory for general crystals with deformation.

- We plan to generalize the Hybrid Cuckoo Search algorithm to work for arbitrary supercell orientation and structures, so as to apply to surfaces and interfaces directly, which will be also made opensource to help the community. Currently recruiting new graduate student.
- The newly formulated FP-KKR, as fully tested, will be extended to address CPA (coherent potential approximation) and then applied to Arsenide superconductors where non-Fermi-liquid can be fully and quantitatively predicted, as will showcase.
- Mostly we will be publishing applications in novel quantum systems using our new and unique algorithms that provide quantitative predictions of material behavior and more directly unique design capabilities.

Publications

(Green are FWP post-docs, or Green* are FWP grad student; blue FWP PIs; bold other FWP PIs)

1. Prashant Singh, S. Picak, A. Sharma*, Y.I. Chumlyakov, R. Arroyave, I. Karaman, and Duane D. Johnson, “Martensitic phase transformation in Fe₄₀Mn₄₀Co₁₀Cr₁₀ high-entropy alloy,” *Phys. Rev. Lett.* **127**, 115704 (2021).
<https://doi.org/10.1103/PhysRevLett.127.115704>
2. Prashant Singh* and Duane D. Johnson, “Designing order-disorder transformation in high-entropy ferritic steels,” *J. of Materials Research* (2021), pg. 1-9. *In press*
<https://doi.org/10.1557/s43578-021-00336-w>
*Editor’s Invitation to Dr. Singh as a outstanding young research scientist, so restricted authorship.
3. Rahul Singh*, Aayush Sharma*, Prashant Singh, Ganesh Balasubramanian, and Duane D. Johnson, “Accelerating the computational modeling and design of high-entropy alloys,” *Nature Computational Science* **1**, 54-61 (2021). <https://doi.org/10.1038/s43588-020-00006-7>
4. Aayush Sharma*, Prashant Singh, Tanner Kirk, V.I. Levitas, P.K. Liaw, G. Balasubramanian, R. Arroyave, and Duane D. Johnson, “Pseudo-elastic deformation in Mo-based refractory multi-principal-element alloys,” *Acta Materialia* **220**, 117299 (2021).
<https://doi.org/10.1016/j.actamat.2021.117299>
5. Rahul Singh*, Prashant Singh, Aayush Sharma*, Onur Rauf Bingol, Aditya Balu, Ganesh Balasubramanian, Adarsh Krishnamurthy, Soumik Sarkar, and Duane D. Johnson, “Neural-networks model for force prediction in multi-principal-element alloys,” *Comput. Mater. Sci.* **198**, 110693 (2021). <https://doi.org/10.1016/j.commatsci.2021.110693>
6. Prashant Singh, Debashish Das, Duane D. Johnson, Raymundo Arroyave, and Aftab Alam, “Effect of Pd alloying on structural, electronic and magnetic properties of L1₀ FeNi,” *J. Phys. Condensed Matter* **33**, 154003 (2021). <https://doi.org/10.1088/1361-648X/abd1fb>
7. Frank McKay; Yuxin Fang; Orhan Kizilkaya; Prashant Singh; Duane D. Johnson; Amitava Roy; David Young; Phillip Sprunger; John Flake; William A. Shelton; Ye Xu, “CoCrFeNi high-entropy alloy as enhanced hydrogen evolution catalyst in acidic solution,” *J. Phys. Chem. C* **125**, 17008-17018 (2021). <https://pubs.acs.org/doi/10.1021/acs.jpcc.1c03646>
8. Rahul Singh*, Prashant Singh, Aayush Sharma*, Onur Rauf Bingol, Aditya Balu, Ganesh Balasubramanian, Adarsh Krishnamurthy, Soumik Sarkar, and Duane D. Johnson, “Neural-networks model for force prediction in multi-principal-element alloys,” *Comput. Mater. Sci.* **198**, 110693 (2021). [/10.1016/j.commatsci.2021.110693](https://doi.org/10.1016/j.commatsci.2021.110693) *FWP graduate students

9. Prashant Singh, A.V. Smirnov, A. Alam, and Duane D. Johnson, "First-principles prediction of incipient order in arbitrary high-entropy alloys: exemplified in $\text{Ti}_{0.25}\text{CrFeNiAl}_x$," *Acta Materialia* **189**, 248-254 (2020). [10.1016/j.actamat.2020.02.063](https://doi.org/10.1016/j.actamat.2020.02.063)
10. Prashant Singh, S. Thimmaiah, S. Gupta, Bryce Thoeny, **Pratik K. Ray**, A.V. Smirnov, Duane D. Johnson* and **M.J. Kramer**, "Vacancy-mediated complex phase selection in high entropy alloys," *Acta Mater.* **194**, 540-546 (2020). [10.1016/j.actamat.2020.04.063](https://doi.org/10.1016/j.actamat.2020.04.063)
11. Shengjie Zhang, Duane D. Johnson, William A. Shelton, and Ye Xu, "Hydrogen Adsorption on Ordered and Disordered Pt-Ni Alloys," *Topics in Catalysis* **63**, 714–727(2020). [10.1007/s11244-020-01338-4](https://doi.org/10.1007/s11244-020-01338-4)
12. H. Chen, N.A. Zarkevich, V.I. Levitas, Duane D. Johnson, X. Zhang, "Fifth-degree elastic potential for predictive stress-strain relations and elastic instabilities under large strain and complex loading in Si I," *npj Comput. Mater.* **6**: 115 (2020). [10.1038/s41524-020-00382-8](https://doi.org/10.1038/s41524-020-00382-8)

Collaborative FWP papers

13. Bryan Owens-Baird, Juliana P. S. Sousa, Yasmine Ziouani, Dmitri Petrovykh, N.A. Zarkevich, Duane D. Johnson, Yury V. Kolen'ko, **Kirill Kovnir**, "Crystallographic Facet Selective HER Catalysis: Exemplified in FeP and NiP_2 Single Crystals," *Chem. Sci.* **11**, 5007-5016 (2020), with Supplement. [10.1039/d0sc00676a](https://doi.org/10.1039/d0sc00676a)
14. A.K. Pathak, Yaroslav Mudryk, N.A. Zarkevich, Dominic H. Ryan, Duane D. Johnson, and **Vitalij K. Pecharsky**, "Extraordinarily strong magneto-responsiveness in phase-separated LaFe_2Si ," *Acta Materialia* **215**, 117083 (2021). [10.1016/j.actamat.2021.117083](https://doi.org/10.1016/j.actamat.2021.117083)
15. I. Hlova, Prashant Singh; Serhiy Malynych; Roman Gamernyk; Olexandr Dolotko; **Vitalij Pecharsky**; Duane D. Johnson; Raymundo Arroyave; A. Pathak; **Viktor Balema**, "Incommensurate Transition-Metal Dichalcogenides via Mechanochemical Reshuffling of Binary Precursors," *Nanoscale Adv.* **3**, 4065-4071 (2021). [10.1039/d1na00064k](https://doi.org/10.1039/d1na00064k)
16. A. Biswas, N.A. Zarkevich, Y. Mudryk, A.K. Pathak, **V. Balema**, Duane D. Johnson, **V.K. Pecharsky**, "Controlling magnetostructural transition and magnetocaloric effect in multi-component transition-metal-based materials," *J. Appl. Phys.* **129**, 193901 (2021). [10.1063/5.0044380](https://doi.org/10.1063/5.0044380)
17. Oleksandr Dolotko, Ihor Z. Hlova, Arjun K. Pathak, **Vitalij K. Pecharsky**, Prashant Singh, Duane D. Johnson, Brett W. Boote, Jingzhe Li, Emily A. Smith, Scott Carnahan, **Rossini, Aaron**, Lin Zhou, Ely Eastman, **Viktor P. Balema**, "Unprecedented Generation of 3D Heterostructures by Mechanical Disassembly and Re-ordering of Incommensurate Metal Chalcogenides," *Nature Commun.* **11**, 3005 (2020). [10.1038/s41467-020-16672-0](https://doi.org/10.1038/s41467-020-16672-0)
18. A. Marshal, Prashant Singh, Denis Music, S. Wolff-Goodrich, Simon Evertz, A. Schokel, Duane D. Johnson, G. Dehm, Christian Loebischer, and Jochem Schneider. "Effect of synthesis temperature on the phase formation of NiTiAlFeCr compositionally complex alloy thin films," *JALCOM* **854**, 155178 (2020). [/10.1016/j.jallcom.2020.155178](https://doi.org/10.1016/j.jallcom.2020.155178)
19. (in honor of Prof. Mookerjee who passed away. Singh and others were his graduate students) Sujoy Datta^c, Prashant Singh^c, D. Jana, C. B. Chaudhuri, Monaj K. Harbola, Duane D. Johnson, and Ahbijit Mookerjee, "Exploring the role of electronic structure on photo-catalytic behavior of carbon-nitride (C_3N_4) polymorphs," *Carbon* **168**, 125-134 (2020). [/10.1016/j.carbon.2020.04.008](https://doi.org/10.1016/j.carbon.2020.04.008)

Artificial intelligence and data science enabled predictive modeling of collective phenomena in strongly correlated quantum materials

PI: Steven Johnston (University of Tennessee, Knoxville). **Co-PIs:** Cristian Batista, Adrian Del Maestro, Jian Liu (University of Tennessee, Knoxville); Richard Scalettar (UC Davis); Ehsan Khatami (San Jose State University); Mark Dean (Brookhaven National Laboratory); Thomas Maier, Alan Tennant (Oak Ridge National Laboratory); Kipton Barros, Ying Wai Li (Los Alamos National Laboratory)

Program Scope: In strongly correlated quantum materials, the collective response of 10^{23} electrons and ions gives rise to a host of novel phenomena. Notable examples include metal-to-insulator transitions, colossal magnetoresistance, quantum magnetism and spin-liquid behavior, and high- T_c superconductivity, as well as topologically ordered states. These phenomena exhibit varying degrees of coherence and quantum entanglement and can revolutionize science and energy-related technologies. But to harness them, we must understand the microscopic mechanisms that drive and shape this collective behavior. This task, in turn, requires solving a quantum many-body problem, a grand challenge of the scientific community.

While density functional theory can predict materials properties while incorporating their full chemical complexity, it often fails to describe the collective phenomena induced by strong interactions. Therefore, the community's general strategy has been to identify minimal low-energy effective models that capture the essential physics of the problem but are simple enough to be solved using sophisticated many-body methods. While this strategy has been enormously successful in many cases, solving even the simplest effective models typically requires state-of-the-art computational methods. Achieving a comparable level of success for other materials will be challenging. In many instances, the correct effective models are not yet known. And when they are known, they are often too complex for current computational methods to tackle.

Our goal is to leverage advances in machine learning (ML), artificial intelligence (AI), and data science to advance and accelerate predictive modeling of correlated quantum materials and their collective phenomena. We will achieve this goal by developing state-of-the-art methods that utilize AI, ML, and data science to

- 1) generate and confirm novel low-energy effective many-body models for quantum materials;
- 2) accelerate model solutions for advanced non-perturbative computational methods; and
- 3) create end-to-end experiment and theory workflows that integrate these methods to accelerate discovery at user facilities like the *Spallation Neutron Source* or the *National Synchrotron Light Source II*.

Using these methods, we will study correlated systems hosting a mix of localized and delocalized excitations during the project's performance period. These systems are very challenging to study using conventional approaches and are highly relevant for energy-related applications. For example, we will address materials containing magnetic 4d, 5d, and 4f ions and correlated metals, iron-based and bismuthate superconductors, interfaces and artificial heterostructures, and materials with complex collective phenomena and nontrivial topological properties.

Keywords: Artificial intelligence, collective excitations, strongly correlated electrons.

Recent Progress: This is a new project; nevertheless, we have made progress in critical areas.

AI-assisted model extraction – We recently used ML methods to determine the correct low-energy effective model for a two-dimensional Kondo Lattice model (KLM) on a triangular lattice. For example, Fig. 1 compares the $T = 0$ Magnetic Field (H) – single ion anisotropy (D) phase diagrams obtained from the original Kondo Lattice Model (top) and the low-energy effective model derived by our ML powered-approach (bottom). The learned effective model was able to reproduce the phase diagram of the original KLM model, including the extended skyrmion crystal phase that is present even for zero single-ion anisotropy. However, here we were able to produce the phase diagram of the effective model in 1/100 of the time. In addition, we can compute the magnon dispersion on top of the ordered phases more efficiently, and can more easily investigate other effects beyond an applied magnetic field and single-ion anisotropy.

Accelerated Model Simulations – Our team members have implemented a hybrid Monte Carlo (HMC) algorithm for simulating *generic* electron-phonon (e-ph) coupled Hamiltonians with arbitrary lattice geometries, basis, and interactions. This implementation achieves *linear* scaling in the system size and temperature and can handle phonons in the adiabatic limit. We have recently deployed this code to study the bismuthate perovskites $\text{Ba}_{1-x}\text{K}_x\text{BiO}_3$ (BKBO) and $\text{BaPb}_x\text{Bi}_{1-x}\text{O}_3$, which host a high-temperature superconducting phase whose mechanism is still debated [1]. Our simulations consider the three-dimensional multi-orbital perovskite structure and include a Su-Schrieffer-Heeger (SSH)-type coupling to bond-stretching Bi-O optical phonons [2]. Figure 2,

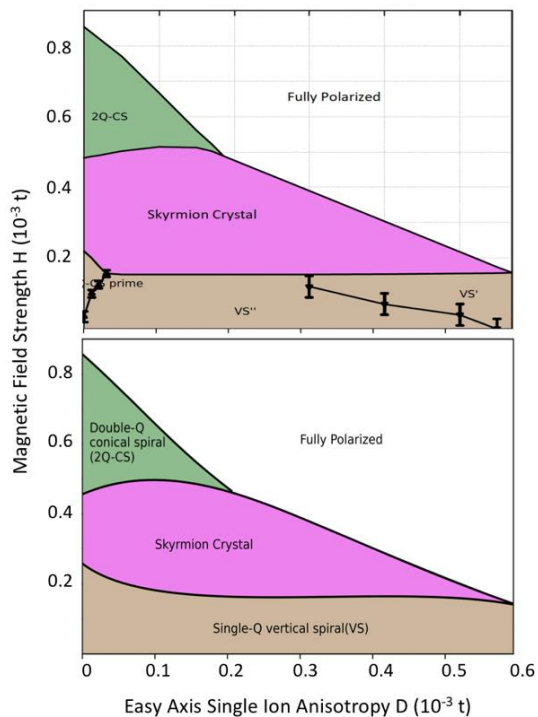
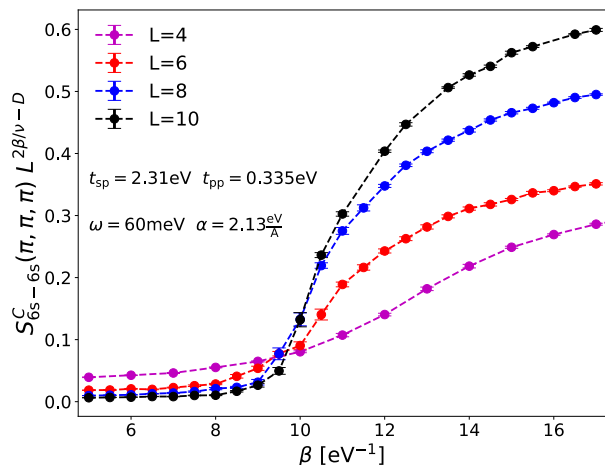


Figure 1: The $T = 0$ phase diagram of the 2D triangular lattice Kondo Lattice Model (KLM) for $n = 0.0586$ and $J/t = 0.5$. The bottom panel shows the phase diagram obtained by simulating a low-energy effective model learned from the simulation data for the high-energy KLM.

for example, shows the temperature dependence of the charge structure factor for parent compound ($x = 0$). BaBiO_3 undergoes a metal-insulator transition to a $\mathbf{Q} = (\pi, \pi, \pi)$ charge-density-wave phase at $T_{\text{CDW}} \sim 900$ K [1]. By performing simulations on large 3D clusters (upwards of 4000 orbitals), we obtain

Figure 2: A finite-size scaling analysis of the $\mathbf{Q} = (\pi, \pi, \pi)$ charge structure factor obtained from hybrid Monte Carlo simulations of a realistic 3D multi-orbital model of BaBiO_3 . The analysis assumes a 3D Ising universality class, and T_c is estimated from the crossing point of the curves.

$T_{\text{CDW}} \sim 1200$ K from a finite-size scaling analysis after adopting LDA-derived estimates for the strength of the e-ph interaction. Our results reveal that the SSH interaction is key to understanding the BKBO phase diagram. More importantly, they also demonstrate that it is now possible to obtain exact numerical solutions to material-specific electron-phonon models, which account for the full chemical complexity of the crystal.

Machine learning for analytic continuation – Our team currently has several implementations of analytic continuation algorithms at our disposal, including maximum entropy, stochastic optimization, and a recently developed AI-based approach [3]. More recently, our team members have developed a parameter-free genetic algorithm to generate the dynamic structure factor from imaginary time correlation functions, *Differential Evolution for Analytic Continuation*. This approach can be more efficient while achieving greater spectral fidelity compared to previous methods. It also eliminates fine-tuning of algorithmic control parameters by embedding them within the genome to be optimized for this evolutionary computation-based algorithm. Benchmarks have been performed for models where the exact dynamic structure factor is known and for quantum Monte Carlo (QMC) simulations of bulk ^4He at temperatures below the superfluid transition.

Future Plans: We will pursue multiple research thrusts in the coming year, each addressing our primary research aims and building on our preliminary results.

Effective Model Extraction – We will refine the hyperparameters of our ML algorithm and evaluate the robustness of the effective low-energy spin model against perturbations that we did not include in our training data set such as other types of anisotropy terms. We also plan to compare the low-energy excitation spectra (magnon bands) of the KLM to the predictions of the effective low-energy model. These tasks will help us understand the collective excitations of the KLM and help set the stage for extracting low-energy models from simulation data and inelastic neutron/x-ray scattering data.

Quantum Parallel Annealing – We have begun exploring which QMC parameters will be optimal to implement population annealing using a simple example of an asymmetric double-well in 1D. There are many choices here, such as mass, potential, interactions, imaginary time step, etc. The goal is to develop a generic framework to improve QMC sampling across the methods utilized in this project.

Machine Learning from QMC intermediate configurations – Using a worldline QMC, we have already obtained tens of thousands of configurations in the density basis for the 1D extended Fermi-Hubbard model. The data span a range of nearest-neighbor interactions strengths across the charge density wave (CDW)-spin density wave (SDW) transition line at a fixed local interaction strength and contain information about the spatial distribution of particles and their dynamics in the imaginary time dimension. We are also using DMRG (through the ITensor package) to sample configurations from much larger chains than are accessible to our worldline QMC algorithm. We are testing various ML algorithms using these data to see if any of them are sensitive to correlations developing in a narrow region of bond order phase in between the CDW and SDW phases. We will then assess how the ML model develops sensitivities to such a phase with a non-diagonal order parameter using intermediate data in the diagonal basis. Following

this, we plan to export similar configurations in the density basis from the DQMC for the Hubbard model using the method described in Ref. [4] and Green's functions and even raw auxiliary field configurations. These data sets should contain all the information about the simulation needed to explore unsupervised methods in the real-time analysis of data and detecting symmetry breaking.

Accelerated QMC simulations of interfaces – The physics of interfaces is essential both for technological applications and fundamental science. There has been considerable quantum simulation work on contact between a system with strong e-e interactions U and another “metallic” system with $U = 0$. Key issues include the nature of the inter-penetration of magnetic, insulating, and pairing behavior. Such geometries have been much less studied in correlated materials with strong e-ph interactions. We have begun a set of simulations to address how charge correlations cross the interface of a Holstein Hamiltonian and a metal. We have initially considered the case when both materials are half-filled. It will be interesting to investigate the materials with different electronic densities. The breaking of translation invariance by the interface places additional challenges on the simulation, necessitating the advanced computational methods under development in this project.

Spectral properties of correlated models – Finally, we plan to carry out several projects to understand the dynamical properties of several canonical correlated electron models and quantum materials. First, we will also use our HMC code to generate high-quality QMC data for benchmarking our analytic continuation methods for 2D and 3D Holstein and SSH models. This task will allow us to obtain robust results for the spectral properties of both models and perform a detailed comparative study of the spectral properties produced by the various methods. By deploying multiple complementary approaches, we will identify common features, thus providing greater confidence in the results. Finally, will use our AI-powered analytic continuation methods to study cuprate and nickelate superconductors in connection to experiments. For example, we will apply this technique to obtain the frequency-dependent gap function from QMC simulations of the single-band Hubbard model. We will also use these methods to compute the superconducting nickelates' collective spin and charge excitation spectrum from multi-band Hubbard models. We will then compare our results with existing inelastic neutron scattering data for the cuprates or new RIXS measurements conducted by our team at BNL in the case of the nickelates.

References

1. A.W. Sleight, *Physica C* **214**, 152-165 (2015).
2. S. Li and S. Johnston, *npj Quant. Mater.* **5**, 40 (2020).
3. X. Xie, F. Bao, T. Maier, and C. Webster. *Discrete & Continuous Dynamical Systems* (2021). Available at arXiv:1905.10430.
4. S. Humeniuk and Y. Wan, *Phys. Rev. B* **104**, 075155 (2021)

Publications:

1. N. John, A. Del Maestro, and B. Rosenow, *Robustness of helical edge states under edge reconstruction*. arXiv:2105.14763 (2021).

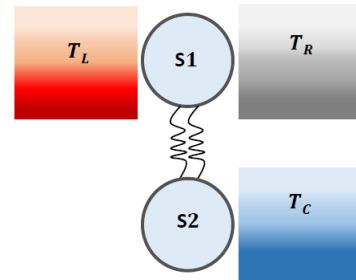
Solid State Quantum Refrigeration Superconducting, Absorption and Measurement Based

Andrew N. Jordan, University of Rochester & Chapman University

Program Scope

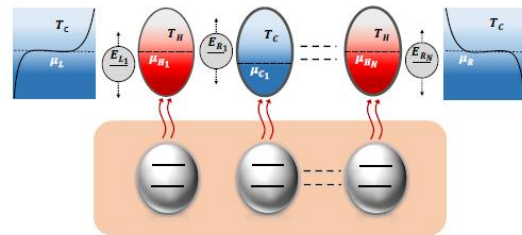
We have made extensive progress on the topics of absorption refrigerators in mesoscopic system, thermal control, as well as the stochastic analysis of mesoscopic heat engines in the past year.

Absorption refrigeration is where refrigeration is achieved by heating instead of work. We have investigated this effect in two different quantum setups: a minimal set up based on coupled qubits, and two non-linearly coupled resonators [1]. Considering ZZ interaction between the two qubits, we found the basic ingredients required to achieve cooling. Using local as well as global master equations, we observed that inclusion of XX-type term in the qubit-qubit coupling is detrimental to cooling. We compared the cooling effect obtained in the qubit case with that of non-linearly coupled resonators (multi-level system) where the ZZ interaction translates to a Kerr-type non-linearity. For small to intermediate strengths of non-linearity, we observe that multi-level quantum systems, for example qutrits, give better cooling effect compared to the qubits. We then applied Keldysh non-equilibrium Green's function formalism to go beyond first order sequential tunneling processes and study the effect of higher order processes on refrigeration. We find reduced cooling effect compared to the master equation calculations.



Schematic representation of the setup. The two systems S1 and S2 can either be qubits or resonators. The system S1 is connected to two baths L and R which are kept at temperatures T_L and T_R whereas the system S2 is coupled to the bath C which is kept at temperature T_C such that

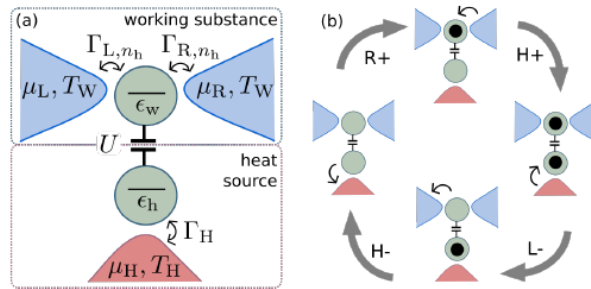
For the thermal control problem, we study a chain of alternating hot and cold electronic nanocavities - - connected to one another via resonant-tunneling quantum dots -- with the intent of achieving precise thermal control across the chain [2]. The problem is defined as specifying the control parameters in order to achieve a desired set of thermal currents in the system. For our system, this is accomplished by positioning the resonant quantum dots' energy levels such that a predetermined distribution of heat currents is realized across the chain in the steady state. The number of electrons in each cavity is conserved in the



We consider a series of electronic nanocavities connected to external reservoirs and coupled to each other via quantum dots with prescribed resonant energies. The cavities are exchanging energy in the form of heat with ancillary quantum systems.

steady state which constrains the cavities' chemical potentials. We determine these chemical potentials analytically in the linear response regime where the energy differences between the dots' resonant levels and the neighboring chemical potentials are much smaller than the thermal energy. In this regime, the thermal control problem can be solved exactly, while, in the general case, thermal control can only be achieved in a relative sense, that is, when one only preassigns the ratios between different heat currents. We apply our results to two different cases: We demonstrate that a "heat switch" can be easily realized with three coupled cavities, then we show that our linear response results can provide accurate results in situations with a large number of cavities.

A third recent project concerns the stochastic thermodynamic analysis of mesoscopic heat engines. We analyzed a steady-state thermoelectric engine, whose working substance consists of two capacitively coupled quantum dots [3]. One dot is tunnel-coupled to a hot reservoir serving as a heat source, the other one to two electrically biased reservoirs at a colder temperature, such that work is extracted under the form of a steady-state current against the bias. In single realizations of the dynamics of this steady-state engine autonomous, 4-stroke cycles can be identified. The cycles are purely stochastic, in contrast to mechanical autonomous engines which exhibit self-oscillations. In particular, these cycles fluctuate in direction and duration, and occur in competition with other spurious cycles. Using a stochastic thermodynamic approach, we quantify the cycle fluctuations and relate them to the entropy produced during individual cycles. We identify the cycle mainly responsible for the engine performance and quantify its statistics with tools from graph theory. We show that such stochastic cycles are made possible because the work extraction mechanism is itself stochastic instead of the periodic time dependence in the working-substance Hamiltonian which can be found in conventional mechanical engines. Our investigation brings new perspectives about the connection between cyclic and steady-state engines.



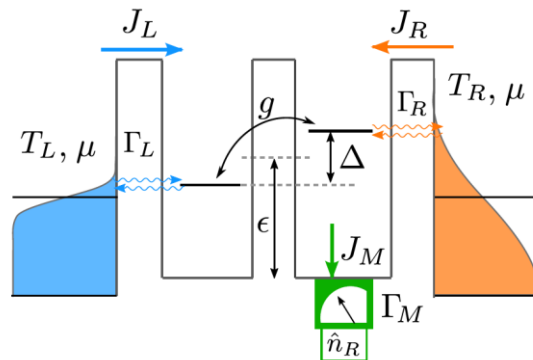
Schematic of a thermoelectric three-terminal engine that can be imagined as consisting of a heat source and a working substance. The double quantum dot contains a "work" and a "hot" dot which are capacitively coupled with coupling energy U . The dots are coupled to reservoirs. Importantly, the tunnel-coupling strengths can depend on the occupation of the dot, which is not involved in the tunneling process. (b) Example of a cycle in state space leading to power production. Tunneling transitions are labeled by the involved reservoir (L,R,H) and increase (+) or decrease (-) of dot occupations.

Keywords: Mesoscopic heat engines and refrigerators, stochastic thermodynamics, thermal control.

Recent Progress

We are making excellent progress on developing a fluxon-based refrigerator, as well as investigating measurement-based refrigeration in quantum dot systems. The fluxon-based refrigerator transports heat through the dissipative mechanism in superconductivity of a trapped magnetic vortex of flux. The system consists of a hot and cold reservoir, and a spatially changing magnetic field. The fluxons are trapped in a race-track like geometry. At the core of the fluxon is a collection of quasi-free electrons which can be transported from one side of the system to the other, analogous to a bucket of water. Electrical bias allows conversion of work to thermal cooling of the cold reservoir. We are currently investigating the statistical physics of fluxons to develop a thermodynamic model of an individual unit, that will go into the larger fridge system analysis.

We have also been developing a quantum measurement-based refrigerator. The basic idea here is to use quantum measurement as an energy resource. By monitoring select degrees of freedom, energy can be introduced or taken away from the system. The combination of measurement, and selective positioning of quantum levels in a quantum-dot based system, permits cooling of the cold reservoir. See figure below.



Schematic diagram of the system. Two quantum dots are tunnel-coupled as well as to two thermally biased leads. The charge in the right dot is continuously monitored. When the dots have a different charging energy as pictured, the measurement is able to induce a heat current against the thermal bias. In addition, the measurement extracts energy, continuously cooling down the system.

Future Plans

In this final year of the grant, we will be focusing on finishing the above projects, and also working on our proposed high temperature superconducting refrigerator.

References

- [1] Bibek Bhandari, Andrew N. Jordan, Minimal two-body quantum absorption refrigerator, *Phys. Rev. B* **104**, 075442 – Published 23 August 2021
- [2] Étienne Jussiau, Sreenath K. Manikandan, Bibek Bhandari, Andrew N. Jordan, Thermal control across a chain of electronic nanocavities, *Phys. Rev. B* **104**, 045414 – Published 16 July 2021
- [3] R David Mayrhofer, Cyril Elouard, Janine Splettstoesser, Andrew N Jordan, Stochastic Thermodynamic Cycles of a Mesoscopic Thermoelectric Engine, *Phys. Rev. B* **103**, 075404 – Published 2 February 2021

Publications (past 2 years)

- Cyril Elouard, George Thomas, Olivier Maillet, Jukka P. Pekola, Andrew N. Jordan, A quantum heat switch based on a driven qubit, *Phys. Rev. E* **102**, 030102(R) – Published 18 September 2020
- Jing Yang, Jen-Tsung Hsiang, Andrew N. Jordan, B. L. Hu, Nonequilibrium Steady State and Heat Transport in Nonlinear Open Quantum Systems: Stochastic Influence Action and Functional Perturbative Analysis, *Annals of Physics*, **421**, 168289 (2020)
- Jing Yang, Étienne Jussiau, Cyril Elouard, Karyn Le Hur, Andrew N. Jordan, Quantum system dynamics with a weakly nonlinear Josephson junction bath, *Phys. Rev. B* **103**, 085402 – Published 1 February 2021
- Sreenath K. Manikandan, Étienne Jussiau, Andrew N. Jordan, Autonomous quantum absorption refrigerators, *Phys. Rev. B* **102**, 235427 – Published 21 December 2020
- R David Mayrhofer, Cyril Elouard, Janine Splettstoesser, Andrew N Jordan, Stochastic Thermodynamic Cycles of a Mesoscopic Thermoelectric Engine, *Phys. Rev. B* **103**, 075404 – Published 2 February 2021
- Étienne Jussiau, Sreenath K. Manikandan, Bibek Bhandari, Andrew N. Jordan, Thermal control across a chain of electronic nanocavities, *Phys. Rev. B* **104**, 045414 – Published 16 July 2021
- Bibek Bhandari, Andrew N. Jordan, Minimal two-body quantum absorption refrigerator, *Phys. Rev. B* **104**, 075442 – Published 23 August 2021

Quantum Control and Tuning of Magnetic 2D van der Waals Heterostructures

PI: Liqin Ke, Ames Laboratory, Ames, IA 50011

Keywords: van der Waals materials, magnetic interaction, spin excitations, electron correlations

Program Scope

The recent development of magnetic two-dimensional (2D) van der Waals (vdW) materials has reignited interest in exploiting such systems as platforms for true 2D magnetism and for developing applications such as energy-efficient, ultra-compact, spin-based electronics [R1]. The goal of this project is to unravel the underlying magnetic mechanism in magnetic 2D vdW (m2DvdW) materials and identify effective strategies for controlling their properties by developing and applying novel theoretical tools, toward understanding experimentally observable phenomena.

Computational methods require accurate electronic-structure descriptions to achieve valuable predictions of the magnetic properties of m2DvdW materials. In 2D materials with open *d*- or *f*-shells, additional quantum confinement caused by the reduced dimensionality suppresses the screening and thus further enhance the electron correlation. Even in their bulk form, the reduced coordination number in quasi-2D lattices constrains the electron hopping, thereby increasing the role of the Coulomb interaction. The resulting enhancement of electron correlations directly affects exchange interactions and other properties. Thus, it is essential to adequately address the role of electron correlations in these systems in *ab initio* investigations.

Recent Progress

We have investigated the electronic structures, magnetic interactions, and spin excitations in various m2DvdW systems of bulk and multiple-layer forms. The electron-correlation effects beyond density functional theory (DFT) are included *via* the quasiparticle self-consistent *GW* (QSGW) method [R2], as incorporated through its effective one-particle potential, which consists of both on-site and off-site nonlocal parts. Calculations have been compared with various experiments such as inelastic neutron scattering (INS) and X-ray spectra. Furthermore, besides the *ab initio* methods, we also develop and apply a self-consistent renormalized spin-wave theory (SRSWT) to investigate of temperature-dependent phenomena in 2D materials. Finally, the PI is also developing a realistic tight-binding framework, interfacing with various *ab initio* codes, to compute and resolve spin-orbit-coupling-related properties, such as magnetocrystalline anisotropy [12], and other properties [9]. Selected progress is detailed below:

Role of nonlocality in exchange correlation for magnetic two-dimensional van der Waals materials [7]. In collaboration with Takao Kotani (Tottori University, Japan), we have investigated the effects of the nonlocal exchange-correlation on the electronic structures of magnetic 2D van der Waals materials by applying the QSGW method. Systems investigated include VI_3 , CrI_3 , CrGeTe_3 , and Fe_3GeTe_2 . QSGW provides a description of the nonlocal exchange-correlation term in the one-particle Hamiltonian. The nonlocal term is important not only as the U of DFT+ U but also for differentiating occupied and unoccupied states in semiconductors. QSGW correctly predicts the semiconducting states of VI_3 while DFT and G_0W_0 fail. The corresponding calculated bandgap values are within the range of reported experimental values for CrGeTe_3 and VI_3 and improved over DFT for CrI_3 . We also demonstrated that the

simplistic DFT+ U method could not completely mimic significant effects introduced by QSGW, suggesting the importance of a more elaborate treatment of electron correlations in these systems.

Electron correlation effects on exchange interactions and spin excitations in 2D van der Waals materials [1]. The PI, together with Mikhail I. Katsnelson (Radboud University, the Netherlands), is investigating the electron correlation effects on exchange interactions and spin excitations in 2D van der Waals materials. Despite significant effort, the nature of the magnetic interactions and the role of electron-correlation effects in magnetic two-dimensional (2D) van der Waals materials remains elusive. Using CrI_3 as a model system, we calculate the dynamic transverse spin susceptibility $\chi^+(\mathbf{q},)$ [R4] and directly compared it with the spinwave spectra measured by INS. The electronic structure calculated beyond DFT yields spin excitations consistent with INS measurements. Moreover, this approach identifies a new correlation-enhanced interlayer super-superexchange, which rotates the magnon Dirac lines off, and introduces a gap along the high-symmetry Γ -K-M path. This discovery provides a different perspective on the gap-opening mechanism observed in CrI_3 , which was previously associated with spin-orbit coupling through the Dzyaloshinskii–Moriya interaction or Kitaev interaction. Finally, we have also shown that the stacking-dependent magnetism in CrI_3 can be described correctly in a parameter-free fashion using our approach. Thus, our observation elucidates the critical role of electron correlations on the spin ordering and spin dynamics in magnetic van der Waals materials and

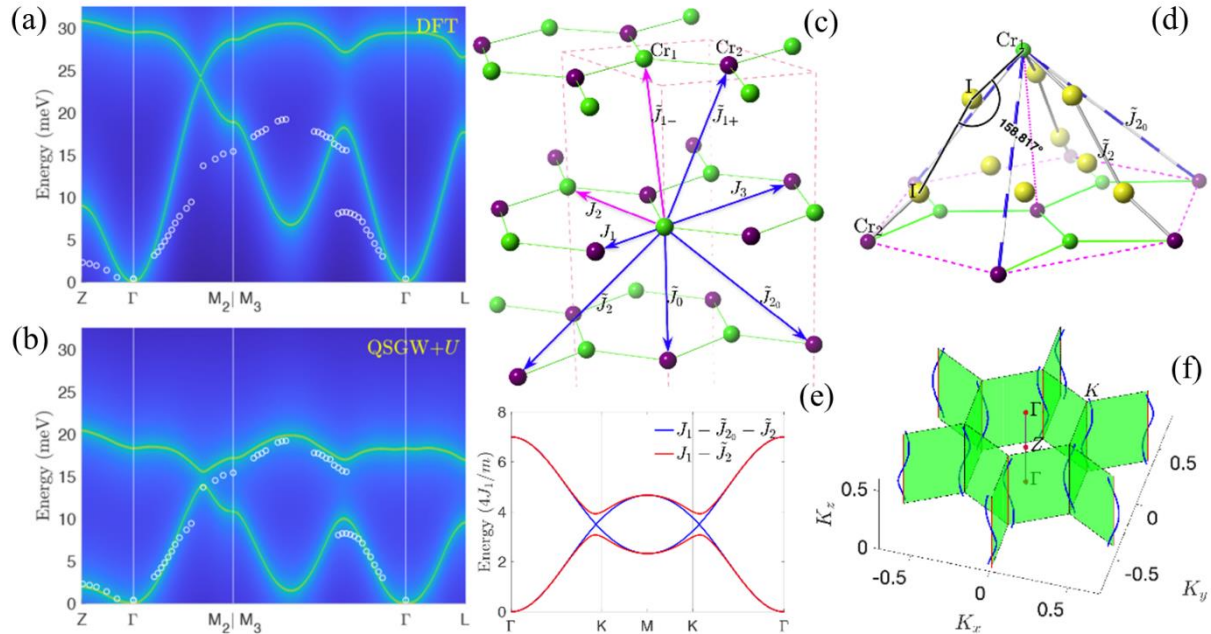


Figure 1: (a, b) Spinwave spectra in CrI_3 calculated within DFT and beyond DFT. Experimental SW energies are adopted from INS work [R3]. (c) Pair exchange parameters for the first few neighbors in R-CrI_3 . (c) Atomic configurations around the exchange paths correspond to a Cr-I-I-Cr super-superexchange coupling. (d) SW spectra along the Γ -K-M path with a gap induced by inter-layer super-superexchange coupling. (e) Dirac nodal lines, where the magnon bands cross, wind around the K-point and along the k_z direction.

demonstrates the necessity of explicit treatment of electron correlations in the broad family of 2D magnetic materials.

Self-consistently renormalized spin-wave theory of layered ferromagnets on the honeycomb lattice [2]. We are developing a self-consistent renormalized spin-wave theory to investigate the temperature-dependent phenomena in magnetic 2D materials. This method and code better link the intrinsic magnetic properties obtained in *ab initio* calculations with experimentally measured quantities such as critical temperatures in low-dimension magnetic systems. Compared to previous implementations, the SRSWT developed in our work is quite general and can be applied to systems with inequivalent sublattices. For example, this approach allows us to account for the physical difference of the surface and subsurface layers. We apply the SRSWT to two chromium-base layered materials $\text{Cr}_2\text{Ge}_2\text{Te}_6$ and CrI_3 . The two main outcomes of our analysis are the layer-resolved magnetization dependence on temperature and the temperature dependence of magnon dispersion. These dependences are observable in MOKE and neutron scattering experiments, respectively. Figure 2 outlines our results for monolayer and trilayer CrI_3 . Using the exchange parameters obtained in our *ab initio* investigation [1], the calculated critical temperatures agree well with experiments.

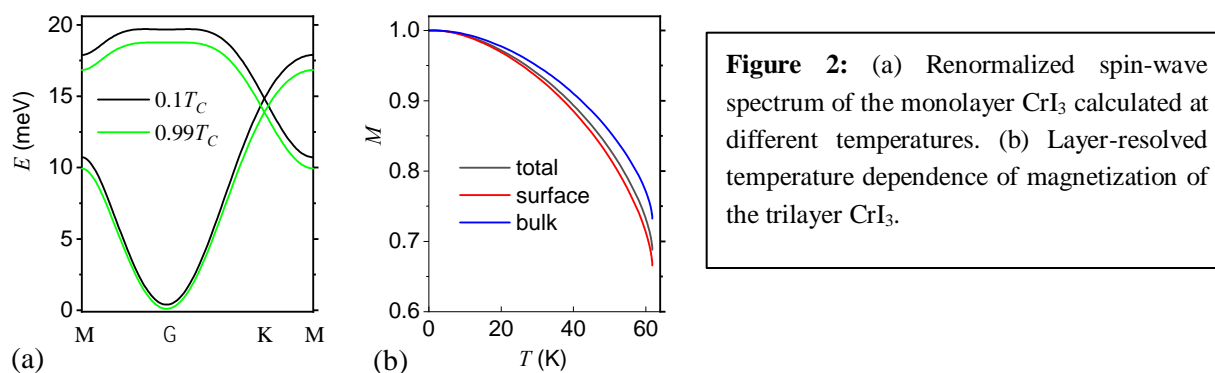


Figure 2: (a) Renormalized spin-wave spectrum of the monolayer CrI_3 calculated at different temperatures. (b) Layer-resolved temperature dependence of magnetization of the trilayer CrI_3 .

Future Plans

Continue to investigate the magnetic properties and their temperature dependence in Fe_3GeTe_2 -related m2dvdW metals. Fe_3GeTe_2 is one of the most promising m2DvdW materials with a much higher Curie temperature than the above-discussed m2DvdW semiconductors. Although the spin excitations have been measured using INS, the magnetism in Fe_3GeTe_2 is still not well understood. An accurate theoretical description of spin excitations is still lacking. Therefore, we are investigating the magnetic interactions and spin excitations in Fe_3GeTe_2 -related systems of various forms. Using our computational approach, the obtained preliminary results for bulk Fe_3GeTe_2 show a good agreement with experiments.

Investigate the effects of defects on magnetic properties in 2D van der Waals materials. 2D vdW materials such as Fe_3GeTe_2 and MnSb_2Te_4 often come with various degrees of disorder, such as vacancy and antisite defects. These defects can affect the magnetic interactions and excitations in vdW materials in a non-trivial way. They can even change the magnetic ground state, which affects the system's symmetry and topological electronic states in materials. We are extending our computational framework to address the disorder effects in 2D vdW materials. This may allow us to understand better the spin excitations measured experimentally and reveal the underlying defect-

driven magnetism, providing guidance to tune the magnetic properties and desired topological states.

Investigate the chiral magnetism in 2D systems and the interplay between magnetism and topological electronic states in newly emergent rare-earth magnetic quantum materials. In collaboration with Lin Zhou (Ames Laboratory), we plan to continue our joint experimental and theoretical effort to explore chiral magnetism [6, 9], focusing on the 2D-Skyrmion-lattice-formation kinetics in systems such as Fe_3GeTe_2 . Such studies can help us better understand the magnetic phase transitions and spin dynamics in 2D systems. In addition, we are also investigating the interplay between magnetism and electronic structures in newly emergent Kagome-lattice quantum materials such as RMn_6Sn_6 . This study may shed light on how to create and maintain robust magnetism in 2D materials with the help of rare earth elements.

References

- [R1] C. Gong, et al. "Discovery of intrinsic ferromagnetism in two-dimensional van der Waals crystals," *Nature* **546**, 265 (2017); Huang, B. et al. "Layer-dependent ferromagnetism in a van der Waals crystal down to the monolayer limit," *Nature* **546**, 270–273 (2017).
- [R2] M. van Schilfgaarde, T. Kotani, S. Faleev, Quasiparticle self-consistent GW theory. *Phys. Rev. Lett.* **96**, 226402 (2006).
- [R3] L. Chen, et al. "Topological spin excitations in honeycomb ferromagnet CrI_3 ," *Phys. Rev. X* **8**, 041028 (2018).
- [R4] T. Kotani, M. van Schilfgaarde, "Spin wave dispersion based on the quasiparticle self-consistent GW method: NiO , MnO and $\alpha\text{-MnAs}$," *J. Phys. Condens. Matter* **20**, 295214 (2008). Liqin Ke, M. van Schilfgaarde, J. Pulikkotil, T. Kotani, V. Antropov, "Low-energy coherent stoner-like excitations in CaFe_2As_2 ," *Phys. Rev. B Rapid Commun.* **83**, 060404 (2011).

Publications (2019-Aug. 2021)

- [1] Liqin Ke and Mikhail I. Katsnelson, "Electron correlation effects on exchange interactions and spin excitations in 2D van der Waals materials," *npj Computational Materials*, **7**(4):1–8, (2021).
- [2] V. V. Mkhitarian and Liqin Ke. Self-consistently renormalized spin-wave theory of layered ferromagnets on the honeycomb lattice. *Phys. Rev. B*, **104**, 064435 (2021).
- [3] Y. Lee, V. N. Antonov, B. N. Harmon, and Liqin Ke. "X-ray spectra in the magnetic van der Waals materials Fe_3GeTe_2 , CrI_3 , and CrGeTe_3 : A first-principles study," *Phys. Rev. B*, **103**, 134407, (2021).
- [4] Elijah Gordon, Vagharsh Mkhitarian, Haijun Zhao, Y. Lee, and Liqin Ke. "Magnetic interactions and spin excitations in van der Waals ferromagnet VI_3 ", *J. Phys. D: Appl. Phys.* **54**, 464001 (2021).
- [5] You Lai, Liqin Ke, Jiaqiang Yan, Ross D. McDonald, and Robert J. McQueeney. "Defect-driven ferrimagnetism and hidden magnetization in MnBi_2Te_4 ", *Phys. Rev. B*, **103**, 184429, Editors' Suggestions, (2021).
- [6] Tae-Hoon Kim, Haijun Zhao, Phuong-Vu Ong, Brandt Jensen, Baozhi Cui, Alexander H. King, Liqin Ke, Lin Zhou, "Kinetics of Magnetic Skyrmion Crystal Formation from the Conical Phase", *Nano Letters*, **21**(13):5547—5554 (2021).

- [7] Y. Lee, Takao Kotani, and Liqin Ke, “Role of nonlocality in exchange correlation for magnetic two-dimensional van der Waals materials.” *Phys. Rev. B*, **101**, 241409 (Rapid communications) (2020).
- [8] Bing Li, J-Q Yan, DM Pajerowski, Elijah Gordon, A-M Nedić, Y Sizyuk, Liqin Ke, Peter P Orth, David Vaknin, Robert J McQueeney, “Competing Magnetic Interactions in the Antiferromagnetic Topological Insulator MnBi_2Te_4 ”, *Phys. Rev. Lett.* **124**, 167204 (2020).
- [9] EI Timmons, S Teknowijoyo, M Kończykowski, O Cavani, MA Tanatar, Sunil Ghimire, Kyuil Cho, Yongbin Lee, Liqin Ke, Na Hyun Jo, SL Bud'ko, PC Canfield, Peter P Orth, Mathias S Scheurer, R Prozorov, “Electron irradiation effects on superconductivity in PdTe_2 : An application of a generalized Anderson theorem”, *Physical Review Research* **2**, 023140 (2020).
- [11] Tae-Hoon Kim, Haijun Zhao, Ben Xu, Brandt Jensen, Alexander H. King, Matthew J. Kramer, Liqin Ke, Lin Zhou, “Mechanisms of Skyrmion and Skyrmion crystal formation from the conical phase”, *Nano Lett.* **20**, **7**, 4731–4738 (2020).
- [10] W. H. Ji, L. Yin, W. M. Zhu, C. M. N. Kumar, C. Li, H.-F. Li, W. T. Jin, N. S. i, X. Sun, Y. Su, Th. Brückel, Y. Lee, B. N. Harmon, L. Ke, Z. W. Ouyang, Y. Xiao, “Non-collinear magnetic structure and anisotropic magnetoelastic coupling in cobalt pyrovanadate $\text{Co}_2\text{V}_2\text{O}_7$ ”, *Phys. Rev. B*, **100**, 134420 (2019).
- [12] Liqin Ke. Intersublattice magnetocrystalline anisotropy using a realistic tight-binding method based on maximally localized Wannier functions. *Physical Review B*, **99**, 054418 (2019).

Center for Predictive Simulation of Functional Materials

PI: P. R. C Kent, Oak Ridge National Laboratory

Co-PIs: A. Benali, A. Bhattacharya, O. Heinonen, Y. Luo, H. Shin, Argonne National Laboratory; R. Clay, L. Shulenburger, J. Townsend, Sandia National Laboratories; P. Ganesh, J. Krogel, H. N. Lee, Oak Ridge National Laboratory; L. Mitas, North Carolina State University; B. Rubenstein, Brown University

Program Scope

A central goal of condensed matter theory is to be able to understand, predict, and realize desired phenomena in specific, real materials. Successful theories should also be able to understand and help guide experimental efforts to realize novel phenomena. This is particularly challenging for materials with strong electronic correlations, van der Waals and spin-orbit interactions, including novel quantum materials that may host new quantum phases. The scope of the Center for Predictive Simulation of Functional Materials, is therefore *the development, validation, and distribution of external-parameter-free methods and open source codes to predict and understand the properties of functional materials, emphasizing those with strong electronic correlations, van der Waals and spin-orbit interactions*. The Center will take advantage of the imminent era of Exascale computing that will enable more challenging materials and phenomena to be studied, better linking with other theoretical methods, and many of the underlying uncertainties in the predictions to be quantified. Activities in the Center are focused on: (1) Developing validated and predictive methods, algorithms, and software for quantitative prediction of functional materials and analysis of their properties and underlying interactions. (2) Addressing how electronic charge, spin, and van der Waals interactions affect electronic structure as well as charge, magnetic, and topological order and how the insights can be used to design functional materials with desired properties and responses. (3) To facilitate direct use of these capabilities through the open source QMCPACK code and automated workflows on computers extending to the Exascale, and to facilitate validation, improvement, and upscaling of other electronic structure methods via curated databases. Key recent developments include the spin-orbit interaction, new methods for reducing dependence on input from other electronic structure methods, and a new scheme for obtaining atomic positions and structures of materials. Together these will enable studies of materials and phenomena involving both strong electronic correlations and spin-orbit effects.

Keywords: Quantum Materials, Theoretical Methods, Exascale

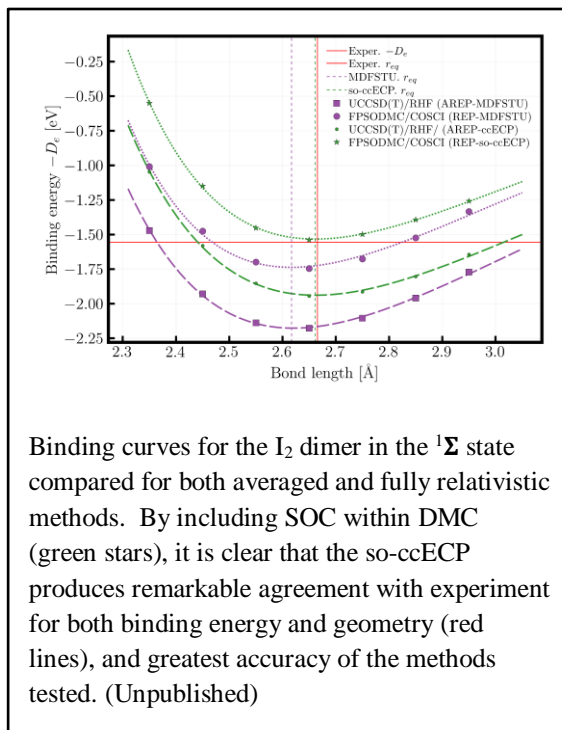
Recent Progress :

Recent methodological advances:

(1) We have implemented spinor wavefunctions, spin-orbit terms on the Hamiltonian, new relativistic effective core potentials, and trial wavefunction interfaces to DIRAC for quantum chemistry and Quantum ESPRESSO and RMG for solid-state calculations. This enables calculation of general materials and molecules incorporating spin-orbit. The source code is already available on the QMCPACK GitHub.

(2) Using a new geometry optimization scheme for quantum Monte Carlo (QMC) developed by this project, we showed that optical properties of 2D monolayer GeSe are strongly coupled to the underlying geometry and are not well-resolved with standard electronic structure methods[1]. This study is first time a non-trivial 2D materials geometry has been fully obtained within diffusion QMC (DMC). Specifically, the band gaps obtained withing DMC vary significantly between those computed at the fully optimized QMC geometry and those obtained from e.g. a DFT approximation. Accurate geometries are obtained for bulk GeSe where experimental data is available. The unexpected sensitivity of the electronic structure and optical properties may be present more widely in this class of materials and suggests potential applications.

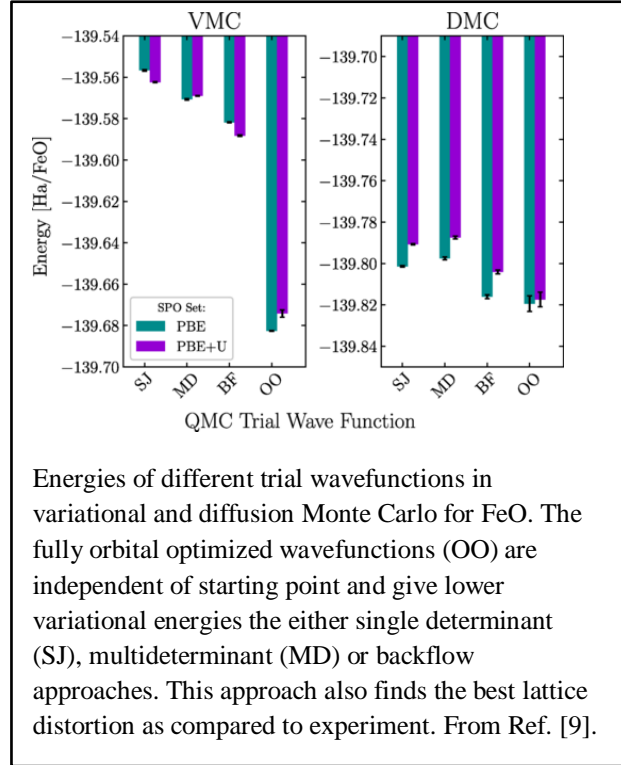
(3) We have made significant advances in understanding and improving on the treatment of the infamous Fermion sign problem in QMC calculations on real materials[7,8,9]. This is the source of the formal combinatorial scaling of solutions of the Schrodinger equation and also consequently a target of quantum computing methods. First, we have implemented procedures to generate and use large multideterminant expansions for the trial wavefunctions in both real space and auxiliary field QMC methods. Owing to improved algorithms these can now be efficiently evaluated. This is in principle a convergent approach, and it has enabled us to converge to near exact results both flavors of QMC methodology in simple primitive cells[7]. Second, in follow-up work we introduced new extrapolation procedures enabling us to obtain results in the thermodynamic limit in bulk carbon diamond[8]. Third, We also explored the potential of optimizing the nodes of simpler trial wavefunctions fully within QMC as a cheaper approach. For the case of the lattice distortion in antiferromagnetic FeO, this approach surprisingly delivered the most accurate results, outperforming more complex trial wavefunctions including backflow forms short determinant expansions. Due to this unexpected result, we are generalizing the implementation and will apply it more widely.



Several recent applications were focused on mechanisms for controlling the metal-insulator transition in VO₂:

(1) Origin of suppression of the metal-insulator transition in non-stoichiometric VO₂[5]: Rutile (R) phase VO₂ is a quintessential example of a strongly correlated bad metal, which undergoes a metal-insulator transition (MIT) concomitant with a structural transition to a V-V dimerized monoclinic (M1) phase below TMIT~340K. It has been experimentally shown that one can control this transition by doping VO₂. In particular, doping with oxygen vacancies (V_O) has been shown to completely suppress this MIT *without* any structural transition. We explain this suppression by elucidating the influence of oxygen vacancies on the electronic structure of the metallic R phase VO₂, explicitly treating strong electron-electron correlations using dynamical mean-field theory (DMFT) as well as diffusion quantum Monte Carlo (DMC). DMC calculations show a gap closure in the M1 phase when vacancies are present, suggesting that when vacancies are introduced in the high-temperature rutile phase, the dimerized insulating phase cannot be reached when temperature is lowered. Both DMFT and DMC calculations of nonstoichiometric metallic rutile phase shows that this tendency not to dimerize in the presence of vacancies is because VO's tend to change the V-3d filling away from its nominal half-filled value, with the $\epsilon\pi g$ orbitals competing with the otherwise dominant $a1g$ orbital. Loss of this near orbital polarization of the $a1g$ orbital is associated with a weakening of electron correlations, especially along the V-V dimerization direction. This removes a charge-density wave (CDW) instability along this direction above a critical doping concentration, which further suppresses the metal-insulator transition. Our study also suggests that the MIT is predominantly driven by a correlation-induced CDW instability along the V-V dimerization direction.

(2) Tuning the metal insulator transition in VO₂/TiO₂ superlattices by oxygen vacancy migration[10]: Oxygen defects are essential building blocks for designing functional oxides with remarkable properties, ranging from electrical and ionic conductivity to magnetism and ferroelectricity. We achieved tunable metal-insulator transitions (MIT) in oxide heterostructures by inducing interfacial oxygen vacancy migration. We chose the non-stoichiometric VO_{2- δ} as a model system due to its near room temperature MIT temperature. We found that depositing a TiO₂ capping layer on an epitaxial VO₂ thin film can effectively reduce the resistance of the insulating phase in VO₂. We systematically studied the TiO₂/VO₂ heterostructures by structural



and transport measurements, X-ray photoelectron spectroscopy, and ab initio calculations and found that oxygen vacancy migration from TiO_2 to VO_2 is responsible for the suppression of the MIT. DFT calculations validated by selected QMC calculations found that the preferred oxygen vacancy locations in these heterostructures are within the VO_2 . Our findings underscore the importance of the interfacial oxygen vacancy migration and redistribution in controlling the electronic structure and emergent functionality of the heterostructure, thereby providing an approach to designing oxide heterostructures for novel ionotronics and neuromorphic-computing.

Future Plans

Our immediate methodological plans involve the validation of the new spin-orbit capabilities on solid state materials. While these new capabilities have been validated for molecular systems, these will be the first real space quantum Monte Carlo calculations with spin orbit for periodic systems. In principle, strong electron correlations, van der Waals, charge and magnetism, as well as spin-orbit related effects should all be treatable simultaneously. We also aim to demonstrate starting point independent calculations for a wider range of materials, having shown that simple trial wavefunctions – when fully consistently optimized within QMC – can give surprisingly accurate results compared to experiment for systems such as FeO.

The above will be applied to a range of 2D, perovskite, and delafossite quantum materials where strong electron correlations, spin-orbit and (2D) van der Waals interactions are significant and are known to challenge established electronic structure methods and theories. Studies involving the latter two materials will be performed “in house” using specifically grown samples and characterization chosen to aid validation of the methodology. 2D materials will be studied through collaborations and existing literature and databases.

New releases of open source QMCPACK will be made incorporating the above capabilities. These will also be expanded in response to user requests from the wider community, particularly those received from other projects in the TCM program.

During 2022 we expect to run QMCPACK on DOE’s Exascale machines and intend to be ready for “day 1” of each machine that comes online. Besides enabling studies on materials with a much wider range of elements, the increased capability of these machines, combined with recent method developments, make it feasible to begin producing reference benchmark data for ranges of materials. We are soliciting input from the TCM community for the materials and properties that should be prioritized. Data will be made available through public databases such as a Materials Project Contribution.

In 2022 we will also hold an additional educational workshop on QMC methods and capabilities. At the time of writing in October 2021 we are just starting an 8 week virtual QMC workshop with over 250 registrants. An outcome of the 2021 workshop will be a “live” virtual machine containing QMCPACK and other electronic structure software to allow students and interested researchers to easily try out the methodology.

Selected Publications

1. “Optimized structure and electronic band gap of monolayer GeSe from quantum Monte Carlo methods”, H. Shin, J. T. Krogel, K. Gasperich, P. R. C. Kent, A. Benali, and O. Heinonen. *Physical Review Materials* **5** 024002 (2021).
<https://dx.doi.org/10.1103/PhysRevMaterials.5.024002>.
2. “Towards quantum Monte Carlo forces on heavier ions: scaling properties”, J. Tiihonen, R. C. Clay, and J. T. Krogel. *J. Chem. Phys.* **154** 204111 (2021).
<https://doi.org/10.1063/5.0052266> <https://arxiv.org/abs/2103.12782>.
3. “Cohesion and excitations of diamond structure silicon by quantum Monte Carlo: benchmarks and control of systematic biases”, A. Annaberdiyev, G. Wang, C. A. Melton, M. Chandler Bennett, and L. Mitas. *Phys. Rev. B* **103** 205206 (2021).
<https://doi.org/10.1103/PhysRevB.103.205206>
4. “Observation of an antiferromagnetic quantum critical point in high-purity LaNiO₃”, C. Liu, V. F. C. Humbert, T. M. Bretz-Sullivan, G. Wang, D. Hong, F. Wrobel, J. Zhang, J. D. Hoffman, J. E. Pearson, J. Samuel Jiang, C. Chang, A. Suslov, N. Mason, M. R. Norman & A. Bhattacharya. *Nature Communications* **11** 1402 (2020).
<https://doi.org/10.1038/s41467-020-15143-w>
5. “Doping a Bad Metal: Origin of Suppression of Metal-Insulator Transition in Non-Stoichiometric VO₂”, P. Ganesh, F. Lechermann, I. Kylanpaa, J. Krogel, P. R. C. Kent, and O. Heinonen, *Physical Review B* **101** 1155129 (2020).
<https://doi.org/10.1103/PhysRevB.101.155129>
6. “Doped NiO: the Mottness of a charge transfer insulator”, F. Wrobel, H. Park, C. Sohn, Haw-Wen Hsia, Jian-Min Zuo, H. Shin, H. N. Lee, P. Ganesh, A. Benali, P. R. C. Kent, O. Heinonen, and A. Bhattacharya. *Physical Review B* **101** 195128 (2020).
<https://doi.org/10.1103/PhysRevB.101.195128>
7. “Systematic Comparison and Cross-validation of Fixed-Node Diffusion Monte Carlo and Phaseless Auxiliary-Field Quantum Monte Carlo in Solids”, F. D. Malone, A. Benali, M. A. Morales, M. Caffarel, P. R. C. Kent, and L. Shulenburger. *Physical Review B Rapid Communications* **102** 161104 (2020). <https://doi.org/10.1103/PhysRevB.102.161104>
8. “Towards a Systematic Improvement of the Fixed-Node Approximation in Diffusion Monte Carlo for Solids – a case study in diamond”, A. Benali, K. Gasperich, K. D. Jordan, T. Applencourt, Y. Luo, C. Bennett, J. T. Krogel, L. Shulenburger, P. R. C. Kent, P.F. Loos, A. Scemama, and M. Caffarel. *J. Chem. Phys.* **153** 184111 (2020).
<https://doi.org/10.1063/5.0021036>
9. “Starting-point-independent quantum Monte Carlo calculations of iron oxide”, J. P. Townsend, R. C. Clay III, T. R. Mattsson, E. Neuscamman, L. Zhao, K. Esler, R. E. Cohen and L. Shulenburger. *Phys. Rev. B* **102** 155151 (2020). <https://doi.org/10.1103/PhysRevB.102.155151> .
10. “Metal-Insulator Transition Tuned by Oxygen Vacancy Migration across VO₂/TiO₂ interface”, Q. Lu, C. Sohn, G. Hu, X. Gao, M. F. Chisholm, I. Kylänpää, J. T. Krogel, P. R. C. Kent, O. Heinonen, P. Ganesh and H. N. Lee. *Scientific Reports* **10** 18554 (2020).
<https://doi.org/10.1038/s41598-020-75695-1> .
11. “Finite temperature auxiliary field quantum Monte Carlo in the canonical ensemble”, T. Shen, Y. Liu, Y. Yu, and B. M. Rubenstein. *J. Chem. Phys.* **153** 204108 (2020).
<https://doi.org/10.1063/5.0026606>

The Non-Equilibrium Quantum Frontier

Vedika Khemani, Stanford University

Program Scope

A confluence of theoretical and experimental advances has opened up a vast new territory of studying many-body phenomena in completely novel regimes: highly excited, quantum coherent, and *far from equilibrium*. In these settings, most well-established methods in quantum many-body theory do not apply. Our understanding of even fundamental questions of quantum statistical mechanics, such as whether or how isolated quantum systems can bring themselves to thermal equilibrium under their own dynamics - or fail to do so - is still nascent. From the perspective of condensed matter physics, an exciting new opportunity entails understanding the new kinds of emergent universal many-body phenomena that can arise once the strictures of equilibrium thermodynamics are relaxed. This research spans three broad research thrusts: (i) formulating and understanding the full range of 'dynamical universality classes', and the novel phase transitions between these; (ii) exploring new kinds of phenomena that may be realized out-of-equilibrium; and (iii) formulating new information theoretic approaches for studying many-body quantum dynamics. The current research described below focuses on novel dynamical phases of quantum entanglement in non-unitary quantum circuits in which quantum *measurements* play a central role. Such evolutions are natural for digital quantum simulators in the NISQ regime.

Keywords: non-unitary quantum dynamics, random circuits, quantum codes

Recent Progress

Entanglement phase transitions in measurement-only dynamics

“Monitored dynamics” *i.e.* unitary dynamics subject to repeated projective measurements can undergo an entanglement phase transition (EPT) as a function of the measurement rate [1,2]. The transition is between a disentangling area-law phase when measurements dominate, and an entangling volume-law phase at low measurement rate. This transition is generally understood in terms of a competition between the scrambling effects of unitary dynamics and the disentangling effects of measurements, and the volume law phase is understood as a “dynamically generated error correcting code” in which quantum information gets scrambled in non-local degrees of freedom and hidden from local measurements.

In [3], we showed that, surprisingly, EPTs are possible even in the absence of scrambling unitary dynamics, where they are best understood as arising from measurements alone. This motivated us to introduce *measurement-only models*, in which the "scrambling" and "un-scrambling" effects

driving the EPT are fundamentally intertwined and cannot be attributed to physically distinct processes. This gives a new type of an EPT driven by the frustration or non-commutativity of the measurement ensembles and is conceptually distinct from the EPT in hybrid unitary-projective circuits. The measurement ensembles can be enriched with symmetry and topology, and can be used to devise new *dynamical quantum codes* with similarities to prior work on topological quantum memories [4]. We explored the entanglement phase diagrams, critical points, and quantum code properties of some of these measurement-only models. We also introduced a measure of information spreading in dynamics with measurements and used it to demonstrate the emergence of a statistical light-cone, despite the non-locality inherent to quantum measurements.

Non-unitary dynamics via spacetime duality

A central hurdle with experimentally realizing the physics of monitored circuits is the *postselection problem*. The EPT in monitored circuits is only visible when considering pure states of individual quantum trajectories corresponding to specific sequences of measurement outcomes, and is invisible if these outcomes are averaged over, such as in a density matrix. However, due to the intrinsic randomness of quantum measurements, reproducing the same trajectory to produce the same output state (for experimental measurements) is exponentially hard in the space-time volume.

In [5], we proposed studying non-unitary circuits generated as the *spacetime dual* of unitary circuits (obtained by “flipping” a unitary gate sideways, thereby interchanging space and time directions). This is a duality transformation between space and time on one hand, and unitarity and non-unitarity on the other. Importantly, in spacetime dual circuits, non-unitarity manifests as a *forced* (rather than random) measurement in the flipped direction, thereby allowing a circumvention of the postselection barrier. We proposed a protocol that maps the purification dynamics of a mixed state under non-unitary evolution onto a particular correlation function in an associated unitary circuit, and which can be straightforwardly implemented on a digital quantum simulator.

In follow-up work in [6], we showed how spacetime duality can be used to realize steady state phases of non-unitary dynamics that exhibit a rich variety of behavior in their entanglement scaling with subsystem size -- from logarithmic to extensive *fractal*. We showed how these outcomes in spacetime dual non-unitary circuits relate to the growth of entanglement in time in the corresponding unitary circuits, and how they differ, through an exact mapping to a problem of unitary evolution with boundary decoherence, in which information gets “radiated away” from one edge of the system. In spacetime-duals of chaotic unitary circuits, this mapping allows us to uncover a non-thermal volume-law entangled phase with a logarithmic correction to the entropy distinct from other known examples. Most notably, we also find novel steady state phases with fractal entanglement scaling, $S(\ell) \sim \ell^\alpha$ with tunable $0 < \alpha < 1$ for subsystems of size ℓ in one dimension. These fractally entangled states add a qualitatively new entry to the families of many-

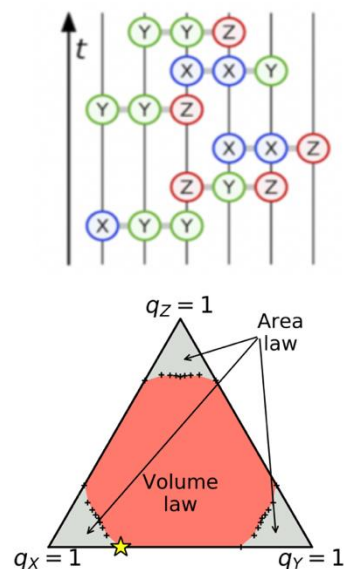


Figure 1: (top) A measurement-only circuit dynamics with measurements drawn from ensembles of three-site Pauli strings, with Pauli X/Y/Z operators drawn with probabilities $q_{x/y/z}$ respectively. (bottom): Entanglement phase diagram for these dynamics.

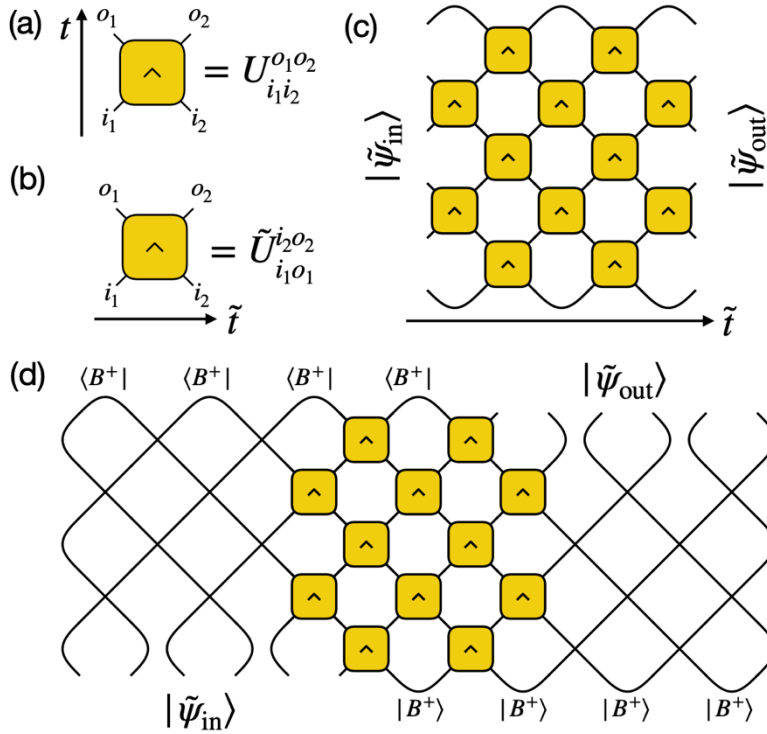


Figure 2: (a) A two-qubit unitary gate. Bottom legs are inputs, top legs are outputs. (b) If we follow the arrow of time sideways (left to right), the same object describes a non-unitary operation. (c) Spacetime dual of a brickwork unitary circuit: the non-unitary gates turn the input (at the left boundary) into the output state (at the right boundary). Both states exist on timelike surfaces. (d) The input and output states can be “teleported” to spacelike surfaces by employing ancillas initialized in a Bell pair state B^+ and SWAP gates.

body quantum states that have been studied as energy eigenstates or dynamical steady states, whose entropy almost always displays either area-law, volume-law or logarithmic scaling. We also presented an experimental protocol for preparing these novel steady states with only a very limited amount of postselection via a type of “teleportation” between spacelike and timelike slices of quantum circuits.

Future Plans

There are many directions to explore in the nascent domain of non-unitary dynamics. These include sharpening the connections between the EPTs we found and fault tolerance thresholds for error correction, and also to devise new types of codes inspired by dynamical phases. There are also many interesting future directions in understanding the nature of novel quantum critical points and different types of dynamical phases possible with non-unitary monitored evolutions, especially the interplay of “active” measurements and “passive” decoherence.

References

- [1] Quantum Zeno Effect and the Many-Body Entanglement Transition, Yaodong Li, Xiao Chen, Matthew P. A. Fisher, Phys. Rev. B 98, 205136 (2018)
- [2] Measurement Induced Phase Transitions in the Dynamics of Entanglement, Brian Skinner, Jonathan Ruhman, Adam Nahum, Phys. Rev. X 9, 031009 (2019)
- [3] Entanglement phase transitions in measurement-only dynamics, Matteo Ippoliti, Michael Gullans, Sarang Gopalakrishnan, David Huse, Vedika Khemani, Phys. Rev. X 11, 011030 (2021)
- [4] Topological quantum memory, Eric Dennis, Alexei Kitaev, Andrew Landahl and John Preskill, J. Math Phys. 43, 4452 (2002)
- [5] Postselection-free entanglement dynamics via spacetime duality, Matteo Ippoliti, Vedika Khemani, Phys. Rev. Lett. 126, 060501 (2021)
- [6] Fractal, logarithmic and volume-law entangled non-thermal steady states via spacetime duality, Matteo Ippoliti, Tibor Rakovszky, Vedika Khemani, arXiv:2103.06873

Publications

- [1] Entanglement phase transitions in measurement-only dynamics, Matteo Ippoliti, Michael Gullans, Sarang Gopalakrishnan, David Huse, Vedika Khemani, Phys. Rev. X 11, 011030 (2021)
- [2] Postselection-free entanglement dynamics via spacetime duality, Matteo Ippoliti, Vedika Khemani, Phys. Rev. Lett. 126, 060501 (2021)
- [3] Fractal, logarithmic and volume-law entangled non-thermal steady states via spacetime duality, Matteo Ippoliti, Tibor Rakovszky, Vedika Khemani, arXiv:2103.06873
- [4] Many-body physics in the NISQ era: quantum programming a discrete time crystal, Matteo Ippoliti, Kostyantyn Kechedzhi, Roderich Moessner, S. L. Sondhi, Vedika Khemani, PRX Quantum 2, 030346 (2021)
- [5] Topological and symmetry-enriched random quantum critical points, Carlos M. Duque, Hong-Ye Hu, Yi-Zhuang You, Vedika Khemani, Ruben Verresen, Romain Vasseur, Phys. Rev. B 103, 100207 (2021)
- [6] From tunnels to towers: quantum scars from Lie algebras and q-deformed Lie algebras, Nick O’Dea, Fiona Burnell, Anushya Chandran, Vedika Khemani, Phys. Rev. Research 2, 043305 (2020)

[7] Tri-unitary quantum circuits, Cheryne Jonay, Vedika Khemani, Matteo Ippoliti, Phys. Rev. Research 3, 043046 (2021)

[8] Avalanches and many-body resonances in many-body localized systems, Alan Morningstar, Luis Colmenarez, Vedika Khemani, David J. Luitz, David A. Huse, arXiv:2107.05642

[9] Perturbative instability towards delocalization at phase transitions between MBL phases, Sanjay Moudgalya, David Huse, Vedika Khemani, arXiv:2008.09113

Machine Learning Quantum Emergence

Eun-Ah Kim, Cornell University

Program Scope

Although the community’s access to ever-growing computational resources and creative algorithmic developments enables the generation of increasingly large volumes of data, a critical bottleneck remains the disconnect between quantities forming the basis of experimental discoveries and those attainable through computation. Another challenge lies in variational approaches’ non-trivial mappings between the ground state phase, wavefunctions, and the Hamiltonians. Variational techniques optimize within a given class of wave functions by referencing the target Hamiltonian. However, many wavefunctions can describe the same phase, and many Hamiltonians have the same ground state. All the while, the variational search is limited to the chosen class. The PI’s current research focuses on developing and adopting machine learning (ML) tools to address the data-driven challenges of strongly correlated quantum matter simulation.

Keywords: Machine Learning, Simulation Data

Recent Progress

Below are the highlights of recent progress reported in the following three papers: [1–3].

In Ref. [1], we probed the learning of artificial neural network (ANN) that has successfully obtained phase diagrams for three distinct topological quantum transitions using Quantum Loop Topography (QLT) we introduced earlier [4]. In particular, we revealed that ANN fused the neighboring Wilson loops of the corresponding Z_2 gauge theory to form larger Wilson loops to detect the Z_2 quantum spin liquid phase. This “interpretation” of the ANN’s learning allows us to use the QLT combined with a simple ANN (QLT+ANN) to confidently learn subtle features in simulated data.

In Ref. [2], we pursued the prime example of the disconnect between the experimental indicator of a state and what can

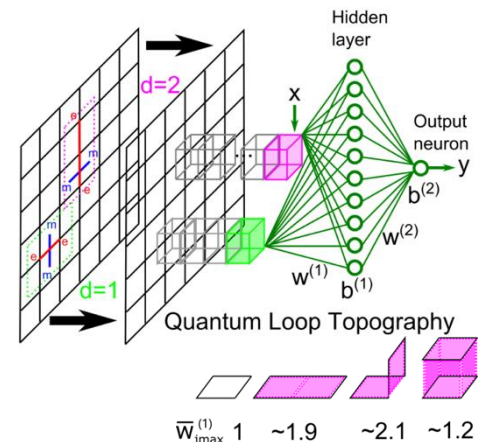


Figure 1. The QLT for Z_2 gauge theory and interpretation of the ANN’s learning revealing fusing of small Wilson loops [1].

be readily computed: non-Fermi liquid (NFL) transport. Specifically successfully extracted the NFL features from quantum Monte Carlo simulations of quantum critical phenomena of itinerant fermions coupled to antiferromagnetic spin-density wave and Ising-nematic order, using QLT+ ANN. The effort led to the profound computational evidence of a broad NFL fan that funnels into the antiferromagnetic spin density wave quantum critical point. Moreover, we established for the first time that new physics that is non-trivially encoded in voluminous computational data could be detected using unbiased machine-learning approaches.

In Ref.[3], we adopted the recently developed technique of Hamiltonian reconstruction for a comprehensive and meaningful analysis of ANN-based wavefunctions (see Figure 3). The severe compression of the entire information encoded in wavefunction into the single metric of variational energy costs significant information loss. Using Hamiltonian reconstruction, we revealed two different biases in the ANN-based variational framework that limits the framework from capturing the true ground state of the J_1 - J_2 model, a poster-child model for frustrated spin systems.

Future Plans

Building on the PI's recent success in tackling the data-driven challenges, the PI plans to study intertwined orders in quantum materials data using a holistic approach seeking synergy among ML, theory, and simulation. On the one hand, we will take the ML tools the PI developed to new and challenging problems. At the same time, the new physics of intertwined orders in moiré systems will be a natural target of studies, given rapid and exciting developments in the field. The PI plans to investigate new aspects of charge order or magnetism arising from the trigonal symmetry of the moiré systems in general. We will also study new phases that can arise from extended Wannier orbitals in magic-angle twisted bilayer graphene.

References

- [1] Y. Zhang, P. Ginsparg, and E.-A. Kim, *Interpreting Machine Learning of Topological Quantum Phase Transitions*, Phys. Rev. Research **2**, 023283 (2020).
- [2] G. Driskell, S. Lederer, C. Bauer, S. Trebst, and E.-A. Kim, *Identification of Non-Fermi Liquid Physics in a Quantum Critical Metal via Quantum Loop Topography*, Phys. Rev. Lett. **127**, 046601 (2021).

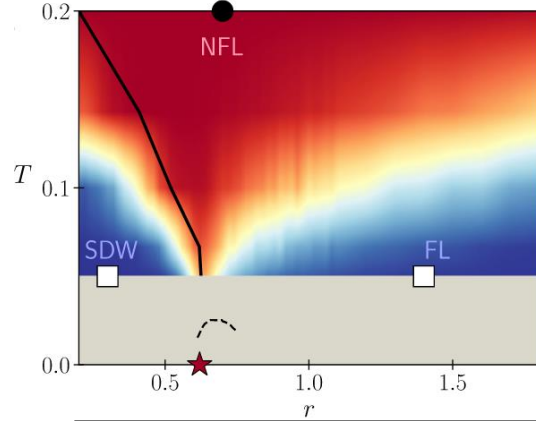


Figure 2. The output of neural networks trained to classify Fermi liquid (FL) and non-Fermi liquid regimes of the spin-density wave model [2].

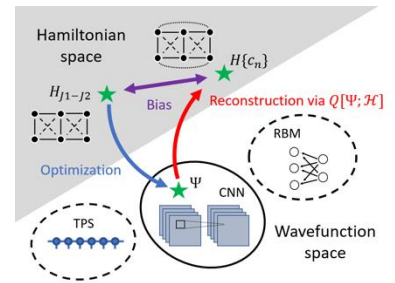


Figure 3. Hamiltonian reconstruction for variational studies[3].

- [3] K. Zhang, S. Lederer, K. Choo, T. Neupert, G. Carleo, and E.-A. Kim, *Hamiltonian Reconstruction as Metric for Variational Studies*, (2021).
- [4] Y. Zhang and E.-A. Kim, *Quantum Loop Topography for Machine Learning*, Phys. Rev. Lett. **118**, 216401 (2017).

Publications

- [1] M. Matty, Y. Zhang, Z. Papić, and E.-A. Kim, *Multifaceted Machine Learning of Competing Orders in Disordered Interacting Systems*, Phys. Rev. B **100**, 155141 (2019).
- [2] J. Venderley and E.-A. Kim, *Density Matrix Renormalization Group Study of Superconductivity in the Triangular Lattice Hubbard Model*, Phys. Rev. B **100**, 060506 (2019).
- [3] S. Ghosh, M. Matty, R. Baumbach, E. D. Bauer, K. A. Modic, A. Shekhter, J. A. Mydosh, E.-A. Kim, and B. J. Ramshaw, *One-Component Order Parameter in URu₂Si₂ Uncovered by Resonant Ultrasound Spectroscopy and Machine Learning*, Science Advances **6**, eaaz4074 (2020).
- [4] P. Cha, N. Wentzell, O. Parcollet, A. Georges, and E.-A. Kim, *Linear Resistivity and Sachdev-Ye-Kitaev (SYK) Spin Liquid Behavior in a Quantum Critical Metal with Spin-1/2 Fermions*, Proceedings of the National Academy of Sciences **117**, 18341 (2020).
- [5] J. Venderley, M. Matty, M. Krogstad, J. Ruff, G. Pleiss, V. Kishore, D. Mandrus, D. Phelan, L. Poudel, A. G. Wilson, K. Weinberger, P. Upreti, S. Rosenkranz, R. Osborn, and E.-A. Kim, *Harnessing Interpretable and Unsupervised Machine Learning to Address Big Data from Modern X-Ray Diffraction*, ArXiv: 2008.03275 [Cond-Mat.Str-El] (2020).
- [6] S. Lederer, E. Berg, and E.-A. Kim, *Tests of Nematic-Mediated Superconductivity Applied to Ba_{1-x}Sr_xNi₂As₂*, Phys. Rev. Research **2**, 023122 (2020).
- [7] Y. Zhang, P. Ginsparg, and E.-A. Kim, *Interpreting Machine Learning of Topological Quantum Phase Transitions*, Phys. Rev. Research **2**, 023283 (2020).
- [8] P. Cha, A. A. Patel, E. Gull, and E.-A. Kim, *Slope Invariant T-Linear Resistivity from Local Self-Energy*, Phys. Rev. Research **2**, 033434 (2020).
- [9] A. Hui, S. Lederer, V. Oganesyan, and E.-A. Kim, *Quantum Aspects of Hydrodynamic Transport from Weak Electron-Impurity Scattering*, Phys. Rev. B **101**, 121107 (2020).
- [10] G. Driskell, S. Lederer, C. Bauer, S. Trebst, and E.-A. Kim, *Identification of Non-Fermi Liquid Physics in a Quantum Critical Metal via Quantum Loop Topography*, Phys. Rev. Lett. **127**, 046601 (2021).
- [11] M. Matty, Y. Zhang, T. Senthil, and E.-A. Kim, *Entanglement Clustering for Ground-Stateable Quantum Many-Body States*, Phys. Rev. Research **3**, 023212 (2021).
- [12] Y. Zhou, D. N. Sheng, and E.-A. Kim, *Quantum Phases of Transition Metal Dichalcogenide Moiré Systems*, ArXiv:2105.07008 [Cond-Mat] (2021).
- [13] K. Zhang, S. Lederer, K. Choo, T. Neupert, G. Carleo, and E.-A. Kim, *Hamiltonian Reconstruction as Metric for Variational Studies*, ArXiv: 2102.00019 (2021).
- [14] K. Zhang, Y. Zhang, L. Fu, and E.-A. Kim, *Fractional Correlated Insulating States at $\nu = 1/3$ Filled Magic Angle Twisted Bilayer Graphene*, ArXiv:2105.13371 [Cond-Mat] (2021).
- [15] P. Cha, A. A. Patel, and E.-A. Kim, *Strange Metals from Melting Correlated Insulators in Twisted Bilayer Graphene*, ArXiv:2105.08069 [Cond-Mat] (2021).

Quantum probes of the materials origins of decoherence

V. Brar¹, J. Choy¹, J. Dubois², M. Eriksson¹, L. Faoro¹, M. Friesen¹,
S. Kolkowitz¹ (lead-PI), A. Levchenko¹, V. Lordi², R. McDermott¹, K. Ray², Y. Rosen²

¹*University of Wisconsin – Madison, Madison, WI, USA, 53706*

²*Lawrence Livermore National Laboratory, Livermore, CA, USA, 94550*

Program Scope

Our collaboration consists of parallel interrelated efforts to harness quantum probes to study and mitigate sources of materials-induced decoherence in three solid-state quantum systems: superconducting qubits, quantum dots, and crystal defects. The overarching goals of this project are to:

- Develop novel quantum probes to characterize sources of decoherence in quantum materials at previously inaccessible energy and length scales.
- Utilize novel quantum probes in close partnership with theoretical modeling to develop a deep understanding of the microscopic physical origins of decoherence in solid-state quantum systems.
- Leverage understanding of materials-induced decoherence to develop novel quantum materials, fabrication techniques, and surface treatments that can improve the coherence times of superconducting qubits, quantum dots, and crystal defects by more than one order of magnitude and result in corresponding improvements in gate fidelities and quantum sensor precision.

We use complementary quantum metrology tools including single spin magnetometry, spin-polarized scanning tunneling microscopy, Kelvin probe force microscopy, and qubit spectroscopy. In parallel we use theoretical modeling tools including DFT, Monte Carlo simulations, and other first-principles methods to simulate and predict the effect of microscopically observed defects on quantum devices. This cycle of measurement, growth, and theory enables systematic improvements in the materials used to fabricate solid state quantum systems.

Keywords: Quantum science, qubits, coherence

Recent Progress

We have established a high degree of collaboration across the two institutions, multiple experimental quantum platforms, and theoretical techniques comprising our efforts. We summarize our recent progress and results by subproject below.

Correlated noise in superconducting qubits. We performed experiments that reveal correlated phase-flip errors and bit-flip errors in multiqubit circuits (Fig. 1). The data are compatible with absorption in the qubit substrate of cosmic ray muons and gamma rays from low-level radioactivity in the laboratory. The impacts liberate of order 10^5 discrete charges, which diffuse over hundreds of microns, giving rise to correlated charge fluctuations in neighboring

qubits. As current approaches to error correction rely on the assumption that errors are not correlated, these results have major implications for proposed schemes for fault tolerant quantum computing. These results were published in *Nature* [1].

KPFM studies of charged defects in oxides used in semiconductor quantum dot qubits. We are studying charged defects in dielectric materials used in semiconducting qubits. By using cryogenic, UHV Kelvin probe microscopy (KPFM), the density, depth, and energy level of localized charges have been mapped on Al_2O_3 and HfO_2 films grown via ALD on Si wafers. We have developed new, comprehensive electrostatic modeling methods to accurately calculate the tip-sample interactions in our measurements, and from those models we can extract the depth and energy levels of the localized charges we have observed.

Charge noise measurements in Si-MOS-based quantum dots. We aim to correlate the KPFM experiments described in the above paragraph with charge noise measurements in MOS-based quantum dots. We have begun fabricating these devices, and measurements reveal mobility of order $1500 \text{ cm}^2/\text{Vs}$, which should rise after gas anneals. We also performed hybrid functional calculations to analyze electron and hole capture of dangling bond (DB)-type defects in $\text{Si}_x\text{Ge}_{1-x}$ as potential sources of charge noise in Si-based quantum dot devices. We analyzed compositional and strain dependence associated with the barrier and capping layers in different MOS and SiGe device designs, and evaluated thermodynamic and optical transitions, finding high plausibility for contributions to charge noise from DB defects. A manuscript was drafted detailing these results.

Decoherence in higher levels of superconducting qudits. We characterized the impact of charge noise on the higher levels of superconducting qudits. In tantalum transmons we were able to perform long spectroscopy which gives us unprecedented resolution on qudit frequency jumps. We have found that in this material the qudit seems to be experiencing stable charge points with a low barrier height that allows jumps between discrete states. A manuscript was drafted detailing these results.

Defect charge stability and control in diamond. We coordinated modeling and experimental efforts to evaluate the effect of diamond surface termination on the surface energy and the optical and spin properties of near-surface NV centers. We implemented various wet oxidizing processes. We then characterized the effects of these acid treatments on oxygen surface coverage and surface roughness. Our experimental explorations were performed alongside first-principles calculations of surface energies for different types of carbon-oxygen bonding and as a function of surface coverage (both of which are measured by x-ray photoelectron spectroscopy (XPS)). Carbon-fluorine and carbon-nitrogen bonding were also examined with hybrid density

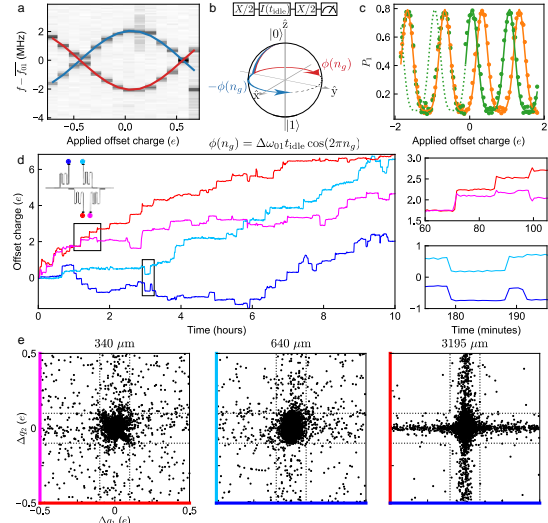


Figure 1 - Characterization of correlated charge fluctuations in superconducting qubits due to radiation impacts [1].

functional theory and a manuscript on these calculations is in preparation. In parallel, we developed and demonstrated a new technique for studying charge carrier transport and capture in diamond. These results were published in *Nano Letters*. In the process, we invented and filed a provisional patent for a new technique for super-resolution imaging and control in standard confocal microscopes using Airy disk diffraction patterns.

Fundamental sources of decoherence in diamond. We determined the ultimate limits to NV electronic spin coherence achievable at room temperature due to spin-phonon relaxation. We also performed a detailed theoretical analysis showing that Orbach-like relaxation from quasilocalized phonons are the dominant mechanism behind double quantum relaxation. These results were published in *PR Research*, and motivated measurements of the temperature dependence of the double quantum relaxation rate, which we are currently performing.

Probing origins of flux noise in superconducting qubits with NV centers, spin-polarized STM, and first-principles calculations. Atomic hydrogen has been identified in the literature as a probable flux noise source in superconducting qubits. Utilizing density functional theory calculations, we have found a mechanism for the formation of atomic hydrogen on near-fully hydroxylated Al_2O_3 surfaces. We also began first-principles simulations of Josephson junction (JJ) formation on the (431) Al surface. This surface is promising for reproducible and scalable ultra-thin JJ fabrication. We installed and commissioned a custom-build cryogenic confocal microscope at UW and implanted and processed diamond samples with shallow NV centers to perform measurements of flux noise emanating from superconducting interfaces.

Developing new scanned probe methods for imaging quasiparticle - potential interactions. We are developing new combined scanning-probe-microscopy (SPM) methodologies that can accurately extract the surface of potential of materials, and simultaneously image how quasiparticles in materials scatter off those potentials (Fig. 2). First, a circular quantum well was formed in a graphene/hBN device and the potential profile of the well was accurately measured using KPFM. Then a source-drain current was passed through a graphene/hBN sample while the electrochemical potential of the surface was measured using scanning tunneling potentiometry (STP). We used STP to map the flow of carriers around the pn junction at the edge of electrostatic barriers ‘drawn’ using the STM tip, where charge was injected into the hBN substrate to locally dope the graphene. By numerically solving the force balance equations, we show that the flow patterns were distinctly non-Ohmic and resembled either ballistic or viscous flow depending on the temperature. These measurements are a major step in imaging Fermi fluids near their quantum critical points. A manuscript detailing these results is under consideration at *Science* [2].

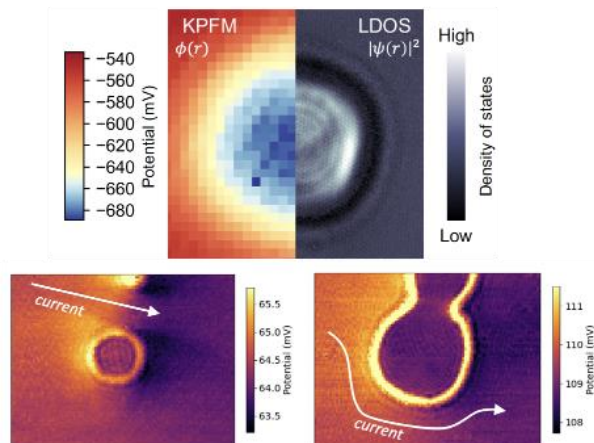


Figure 2 - KPFM/STM imaging of hydrodynamic flows in graphene [2].

Future Plans

KPFM studies of charged defects in oxides used in semiconductor quantum dot qubits: We will identify the specific charge defects we have observed in KPFM measurements by correlating their observed energy levels with the calculated (via DFT) energy levels of defects that have been predicted to occur in these materials. Based on these conclusions, we will develop and test methods for defect passivation.

Studies of TLS defects in oxides: We will measure two-level system characteristics on oxide materials starting with ALD deposited AlO_x . We will also leverage a recently developed LLNL capability to perform an unbiased search for TLS in computational models of amorphous materials. The TLS we find computationally can be compared with the energy level splittings and dipole moments/charges measured in experiment. We also will develop and explore a first-principles atomistic model of dipole fluctuators arising from coupled bistable charged defects.

Charge noise measurements in Si-MOS-based quantum dots: We plan to measure charge noise in full MOS quantum dots by monitoring the current on the edge of a Coulomb blockade peak. We anticipate characterizing both before and after forming gas anneals and to correlate results of these measurements with both the TLS and KPFM studies discussed above. We will perform hybrid density functional theory calculations of candidate defects to compare energy levels with measurements to help identify potential charge noise-causing defects.

Correlated noise in superconducting qubits. We will explore new qubit designs to protect against quasiparticle loss. In parallel, we will explore the impact of hBN passivation of qubit circuits on dephasing and dissipation.

Probing origins of flux noise in superconducting qubits with NV centers, spin-polarized STM, and first-principles calculations. We will develop flux noise mitigation strategies for the Al_2O_3 surface and simulate their effects. We will perform measurements of local magnetic flux noise near superconducting films and superconducting qubit devices using single NV centers and will use the experimental results to inform the theoretical modeling.

Defect charge stability and control in diamond. We will perform direct measurements of the electron affinity of oxidized diamond surfaces for comparison with surface energy calculations. Electron affinities and specific surface terminations will be correlated with measurements of spin coherence, charge stability, and photostability of near-surface NV centers.

Developing new scanned probe methods for imaging quasiparticle - potential interactions. We will use the KPFM potential correction methods we developed to more accurately quantify the charge in dielectric substrates used in semiconducting QIS devices. STP measurements will be performed using applied magnetic fields and with different barrier structures in order to image flow in the turbulent regime.

Part of this work was performed under the auspices of the U.S. Department of Energy by LLNL under Contract DE-AC52-07NA27344. LLNL-ABS-827449.

References

- 1) C. D. Wilen, et al., *Nature* **594**, 369 (2021).
- 2) Z.J. Krebs et al., *arxiv.2106.07212* (2021).

Publications

- 1) C. D. Wilen, S. Abdullah, N.A. Kurinsky, C. Stanford, L. Cardani, G. D'Imperio, C. Tomei, L. Faoro, L.B. Ioffe, C.H. Liu, A. Opremcak, B.G. Christensen, J. L. DuBois, and R. McDermott, *Nature* **594**, 369 (2021).
- 2) W.A. Behn, Z.J. Krebs, K.J. Smith, K.Watanabe, T.Taniguchi, and V.W. Brar, *Nano Letters* **21** (12) 5013–5020 (2021).
- 3) A. Gardill, I. Kemeny, M. C. Cambria, Y. Li, H. Dinani, A. Norambuena, J. R. Maze, V. Lordi, and S. Kolkowitz, *Nano Letters* **21** (16), 6960-6966 (2021).
- 4) M. C. Cambria, A. Gardill, Y. Li, A. Norambuena, J. R. Maze, and S. Kolkowitz, *Phys. Rev. Research* **3**, 013123 (2021).
- 5) M. Dzero, A. Levchenko, *Phys. Rev. B* **104**, L020508 (2021).
- 6) B.F. Bachman, Z.R. Jones, G.R. Jaffe, J. Salman, R. Wambold, Z. Yu, J.T. Choy, S.Kolkowitz, M.A. Eriksson, M.A. Kats, and R.J. Hamers, *Langmuir* **37** (30) 9222–9231 (2021).
- 7) A. Levchenko, T. Micklitz, *Journal of Experimental and Theoretical Physics*, **159**, 776 (2021).
- 8) V. Lordi and J. M. Nichol, *MRS Bulletin* **46**, 589–595 (2021).
- 9) L.V.H. Rodgers, L.B. Hughes, M. Xie, P.C. Maurer, S. Kolkowitz, A.C. Bleszynski Jayich, and N.P. de Leon, *MRS Bulletin*, **46**, 623–633 (2021).
- 10) G.R. Jaffe, K.J. Smith, K. Watanabe, T. Taniguchi, M.G. Lagally, M.A. Eriksson, and V.W. Brar, *arXiv:2103.07452* (2021).
- 11) Z.J. Krebs, W.A. Behn, S. Li, K.J. Smith, K. Watanabe, T. Taniguchi, A. Levchenko and V.W. Brar, *arxiv.2106.07212* (2021).
- 12) D.M. Tennant, L.A. Martinez, C.D. Wilen, R. McDermott, J. L DuBois, and Y. J. Rosen, *arXiv:2106.08406* (2021).
- 13) S. Li, M. Khodas, and A. Levchenko, *arXiv:2105.13384* (2021).
- 14) R.A. Wambold, Z. Yu, Y. Xiao, B. Bachman, G.R. Jaffe, S. Kolkowitz, J.T. Choy, M.A. Eriksson, R.J. Hamers and M.A. Kats, *Nanophotonics*, **10**, 393 (2020).
- 15) A. Gardill, M.C. Cambria, and S. Kolkowitz, *Phys. Rev. Applied*, **13**, 34010 (2020).
- 16) M. Khodas, M. Dzero, A. Levchenko, *Phys. Rev. B*, **102**, 184505 (2020).
- 17) K.R. Joshi, N.M. Nusran, M.A. Tanatar, K. Cho, S.L. Budko, P.C. Canfield, R.N. Fernandes, A. Levchenko, and R. Prozorov, *New Journal of Physics*, **22**, 53037 (2020).

Comscope: Center for Computational Design of Functional Strongly Correlated Materials and Theoretical Spectroscopy

PI: Gabriel Kotliar, Brookhaven National Lab and Rutgers University

Co-PIs: Robert Konik, Sangkook Choi, Mark Dean, Andrey Kutepov, Corey Melnick, Cedimir Petrovic (Brookhaven National Laboratory); Yongxin Yao (Ames Laboratory); Kipton Barros (Los Alamos National Laboratory); Martha Greenblatt, Kristjan Haule, Manish Parashar (Rutgers University); Gia-Wei Chern (Univ. of Virginia)

Program Scope

Prediction of material properties with minimal a priori experimental information has been a long-standing goal in condensed matter physics. Advances toward this goal are important not only for fundamental science, but also because of their impact on accelerating the development of new technologies of societal importance. Silicon and lithium-ion-based materials are well known examples of materials that have led to the proliferation of consumer hand-held devices.

For materials such as simple metals, semiconductors, and insulators, the basic theory is known. Fermi liquid theory provides a fundamental understanding of the excitation spectra. Powerful methods, such as practical implementations of density functional theory (DFT) formulated in the 1960's [1-3] provide accurate total energies. These, in turn, enabled the computation of phonon spectra, and of the relative energies of different structures enabling structural prediction, an area where recent progress was made using advanced DFT's [4]. DFT electronic energies enabled *ab initio* molecular dynamics [5] which, in turn, open new capabilities, as for example structural determination starting from random structures and non-equilibrium simulations.

The situation is very different in materials where correlations are important, and methods based on the band picture fail to describe the excitation spectra even qualitatively. For example, Mott insulators have a gap in the paramagnetic phase, while band theory predicts them to be metallic. The aim of our DOE BES Computational Materials Science Center, Comscope, is to design and produce methodologies and a computational platform that will do for strongly correlated materials what DFT has done for less correlated systems. Our ultimate vision sees a scientist being able to predict the properties of a correlated material in an *ab initio* theoretical framework without experimental input.

The tools that Comscope is building are predicated on combining dynamical mean field theory (DMFT) with first principles input and are developed to work on a range of computational platforms running the gamut from desktop workstations to leadership class machines. These tools are essential to realize our vision to develop a predictive theory of correlated materials in accordance with the Foundational challenges in predictive materials science discussed in the

DOE report Computational Materials Science and Chemistry: Accelerating Discovery and Innovation through Simulation-Based Engineering and Science.

Keywords: strongly correlated materials, *ab initio* dynamical mean field theory, theoretical spectroscopy

Recent Progress

We give a schematic overview of the connections between our codes in Figure 1. We have two main code packages, Comsuite and FlapwMBPT, that offer differing approaches to tackling the problem of computing the behavior of correlated materials. The first of these,

Comsuite (<https://www.bnl.gov/comscope/software/comsuite.php>), focuses on cases where correlations are primarily local, implementing three flavors of *ab initio* dynamical mean field theory in order of increasing computational complexity: LDA+RISB, LDA+DMFT, and GW+DMFT. Comsuite depends on FlapwMBPT for its LDA and GW capabilities and ComCTQMC for its quantum impurity solver. The second Green's function based code is FlapwMBPT (<https://www.bnl.gov/cmpmsd/FlapwMBPT/>). This is an all-electron LAPW basis first principle code that permits DFT, GW and GW+Vertex computations. FlapwMBPT not only provides a means to understand the effects of non-local interactions in correlated materials, it also serves as the platform on which Comsuite is built. EDRIXS and ComARPES are post-processing modules for Comsuite that allow the computation of the RIXS and ARPES response functions and so allow the user to directly connect to experiment.

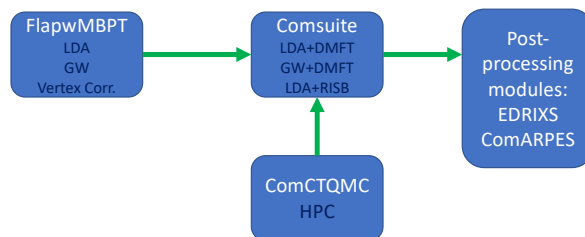


Figure 1. Overview of Comscope's codes.

Five key thrust of research progress in the past two years are i) Updates in The Softwares, ii) Readyng our Codes for Operation in a High Performance Environment; iii) Algorithmic and Methodological Development, iv) Validation of Codes and Methodologies, and v) Building Community. Below we summarize our main achievement in each thrusts

i) Updates in the Softwares. During the past two years, we updated FlapwMBPT, Comsuite, and ComCTQMC for their improved performances, new functionalities, and better user-interfaces. To name a few, ComCTQMC improved its GPU kernel enabling GPU acceleration by a factor of 225 times in the most difficult impurity problems tested and realized a dramatic reduction in the memory footprint on the GPUs. LDA+RISB part of Comsuite are now supported by machine learning (ML) aided solver. In the new released version of FlapwMBPT, vertex correction capabilities on top of GW calculation has been added. EDRIXS code has been released publicly (<https://github.com/NSLS-II/edrixs>). ComARPES packages, that connects to Comsuite and produces high-quality plots which can be directly compared with angle-resolved photoemission spectroscopy has been developed. We expect it to be released in the coming year.

ii) *Readying our Codes for Operation in a High Performance Environment.* A key thrust of our software development is preparing our codes to run at leadership class computational facilities. To this end Comscope has engaged in three activities. In the first, Comscope has optimized its LDA code within the FlapwMBPT package to better enable it to run in high performance settings. Here the goal is to use it in machine learning studies conducted on Sierra at LLNL aimed initially at understanding crystalline energies but ultimately at conducting large scale quantum molecular dynamic simulations. In the second, we have enabled key components of GW within FlapwMBPT to run with $O(N)$ scaling. This scaling matches that of the vertex correction calculations and so ensures that when FlapwMBPT is run in a high performance computation (HPC) environment it will not experience computational bottlenecks. Finally, we have achieved significant speedups (225x) in our continuous time quantum Monte Carlo (CTQMC) solver when run at Summit at ORNL as demonstrated in Fig. 2. This speedup underpinned successful INCITE and ALCC awards that have given Comscope over 0.5 million node hours on Summit (ORNL) and Theta (ANL).

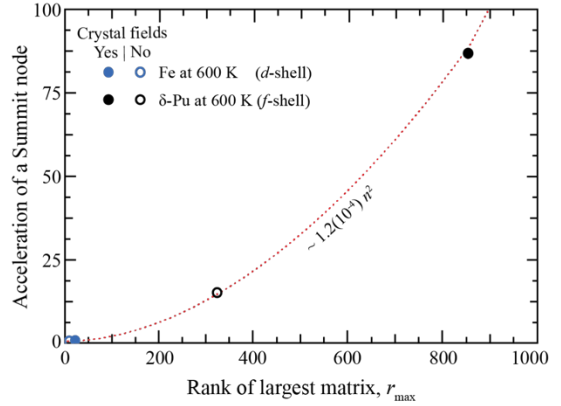


Figure 2. Acceleration of ComCTQMC by the six Volta GPUs on a Summit node for variations in the size of the impurity problem.

iii) *Algorithmic and Methodological Development.* In pushing forward the science of Green's function based methods, we have made several advancements in the past two years. In the first, we have extended our quantum molecular dynamics to enable it to study real materials in an *ab initio* setting. We have done detailed studies of the three-channel impurity physics expected to govern the behavior of Hund's metals in a DMFT setting and applied this understanding to superconductivity in the infinite-layered nickelates. And we have enabled our CTQMC solver to measure multi-point vertex correlation functions, a key step in building theoretical spectroscopy tools.

iv) *Validation of Codes and Methodologies.* The Comscope team developing scientific software tools has closely collaborated with a team of expert experimentalists. The focus has been on

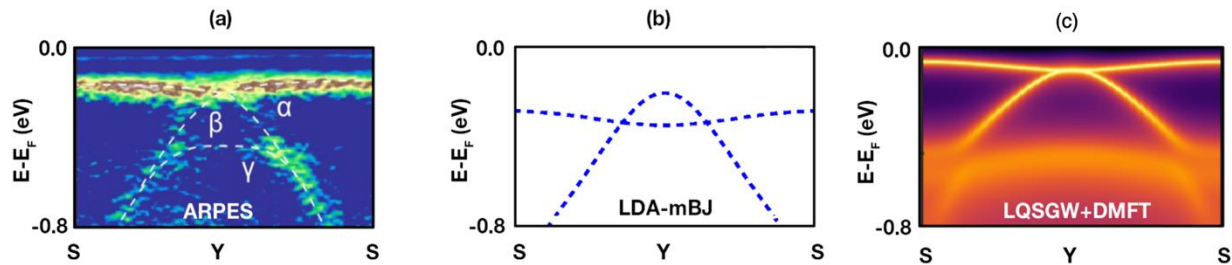


Figure 3. Bandstructure of FeSb2. From angle resolved photoemission spectroscopy (ARPES) there are three bands. Only LQSGW+DMFT shows three bands with the correct band topology.

strongly correlated thermoelectrics, in particular FeSb₂, the material which hosts a colossal thermopower of about 45 mV/K at 10 K. In the past two years, we have published the first angle-resolved photoemission experiments on this difficult-to-cleave material. We have also demonstrated that only GW+DMFT, our most computational expensive DMFT code, is capable of describing the measured correlated band structure as shown in Fig. 3. This provides both a validation test for this code module and a demonstration of why its development was necessary.

v) *Building Community*. In order to build a community of users, we have documented our codes, making them more user friendly by the addition of tutorials. This has achieved the goal of making the community more aware of new tools able to approach strongly correlated systems quantitatively. We are also teaching our codes. Comscope is holding a virtual school in the last week of June 2021 where our primary codes will be taught. 140+ students are registered to attend. The activities of Comscope are reported through the Center's website: <https://www.bnl.gov/comscope>.

Future Plans

In the next two years we plan to further develop our codes. In the next update of Comsuite, we will introduce the next step in *ab initio* methodology, fully self-consistent GW+EDMFT. This method addresses a limitation of our *ab initio* GW+DMFT currently in our software package, Comsuite: absence of bosonic self-consistency. Moreover, we can treat non-local correlations on all length scales diagrammatically and keep explicitly the frequency dependence of the non-local self-energy and polarizability. This is important as non-local electron correlations is at the heart of some of the most fascinating physical phenomena in quantum materials including high-temperature superconductivity and quantum criticality. We will also continue to improve our codes for running in a high performance environment. We will use the time won in our INCITE and ALCC awards to explore the physics of f-electron materials. And we will continue pushing methodological advances for strongly correlated system including the use of machine learning to enable our codes to run more efficiently.

References

- [1] Hohenberg, P. and W. Kohn, Physical Review, 1964. 136(3B): p. B864-B871.
- [2] Kohn, W. and L.J. Sham, Phys. Rev., 1964. 137(6A): p. 1697.
- [3] Kohn, W. and L.J. Sham, Physical Review, 1965. 140(4A): p. A1133-A1138.
- [4] Zhang, Y., et al., npj Computational Materials, 2018. 4(1): p. 1-6.
- [5] Car, R. and M. Parrinello, Phys Rev Lett, 1985. 55(22): p. 2471-2474.

Publications

- [1] Y.L.Wang, G.Fabbris, M.P.M.Dean, and G.Kotliar, “EDRIXS: An open source toolkit for simulating spectra of resonant inelastic x-ray scattering”, *Comp. Phys. Comm.* 243, 151 (2019).
- [2] S. Choi, P. Semon, B. Kang, A. Kutepov, and G. Kotliar, “ComDMFT: a Massively Parallel Computer Package for the Electronic Structure of Correlated-Electron systems” *Comp. Phys. Comm.* 244, 277
- [3] Low-Temperature Thermopower in CoSbS, Qianheng Du, Milinda Abeykoon, Yu Liu, G. Kotliar, C. Petrovic, *Phys. Rev. Lett.* 123, 076602 (2019)
- [4] Yu Liu, Lijun Wu, Xiao Tong, Jun Li, Jing Tao, Yimei Zhu and C. Petrovic. Thickness-dependent magnetic order in CrI3 single crystals. *Scientific Reports* 9, 13599 (2019).
- [5] Yu Liu, Jun Li, Jing Tao, Yimei Zhu and Cedomir Petrovic, Anisotropic magnetocaloric effect in Fe_{3-x}GeTe₂. *Scientific Reports* 9, 13233 (2019).
- [6] Y. Wang, E. Walter, S.-S. B. Lee, K. M. Stadler, J. von Delft, A. Weichselbaum, and G. Kotliar, Global phase diagram of a spin-orbital Kondo impurity model and the suppression of Fermi-liquid scale, *PRL* 124 134406 (2020).
- [7] S. Ryee, P. Sémon, M. J. Han, and S. Choi, “Nonlocal coulomb interaction and spin freezing crossover: a route to valence-skipping charge order”, *NPJ Quantum Materials*, 5, 19 (2020).
- [8] A. Kutepov, Self-consistent GW method: O(N) algorithm for the polarizability and the self energy, *Com. Phys. Comm.* 257, 107502 (2020).
- [9] Corey Melnick, Patrick Sémon, Kwangmin Yu, Nicholas D'Imperio, André-Marie Tremblay, Gabriel Kotliar, “Accelerated impurity solver for DMFT and its diagrammatic extensions” *Comp. Phys. Comm.* 267. 108075 (2021).
- [10] Hund physics landscape of two-orbital system, Siheon Ryee, Myung Joon Han, Sangkook Choi, *Phys. Rev. Lett.* 126, 206401 (2021).
- [11] Optical properties of the infinite-layer La_{1-x}Sr_xNiO₂ and hidden Hund's physics, Chang-Jong Kang, Gabriel Kotliar, *Phys. Rev. Lett.* 126, 127401 (2021).
- [12] K. Gilmore, J. Pelliciani, Y. Huang, J. J. Kas, M. Dantz, V. N. Strocov, S. Kasahara, Y. Matsuda, T. Das, T. Shibauchi, and T. Schmitt, Description of Resonant Inelastic X-Ray Scattering in Correlated Metals, *Phys. Rev. X* 11, 031013 (2021).
- [13] E. Walter, K. M. Stadler, S.-S. B. Lee, Y. Wang, G. Kotliar, A. Weichselbaum, and J. von Delft, Uncovering non-Fermi-liquid behavior in Hund metals: conformal field theory analysis of a SU(2) × SU(3) spin-orbital Kondo model, *Phys. Rev. X* 10, 031052 (2020).
- [14] Andrey Geondzhian, Alessia Sambri, Gabriella M. De Luca, Roberto Di Capua, Emiliano Di Gennaro, Davide Betto, Matteo Rossi, Ying Ying Peng, Roberto Fumagalli, Nicholas B. Brookes, Lucio Braicovich, Keith Gilmore, Giacomo Ghiringhelli, Marco Salluzzo, Large Polarons as key quasi-particles in SrTiO₃ and SrTiO₃-based heterostructures, *Phys. Rev. Lett.* 125, 126401 (2020).
- [15] Qianheng Du, Lijun Wu, Huibo Cao, Chang-Jong Kang, Christie Nelson, Gheorghe Lucian Pascut, Tiglet Besara, Kristjan Haule, Gabriel Kotliar, Igor Zaliznyak, Yimei Zhu, and Cedomir Petrovic, Vacancy defect control of colossal thermopower in FeSb₂, *npj Quantum Materials* volume 6, Article number: 13 (2021).
- [16] Tuning spin excitations in magnetic films by confinement, Jonathan Pelliciani, Sangjae Lee, Keith Gilmore, Jiemin Li, Yanhong Gu, Andi Barbour, Ignace Jarrige, Charles H. Ahn, Frederick J. Walker, Valentina Bisogni, *Nature Materials* volume 20, 188–193 (2021).

Spin currents in magnetic systems and heterostructures

Alexey Kovalev, Department of Physics and Astronomy, Nebraska Center for Materials and Nanoscience, University of Nebraska, Lincoln

Program Scope

The objectives of this project are to develop a theoretical description of spin currents and to use spin currents for detection of various quantum effects in magnetic systems. Quantum effects in what has recently been termed as *quantum materials* can be associated with quantum fluctuations, frustration, correlations, and entanglement. To better understand such quantum effects, this project will study how spin currents can be generated and further injected into quantum materials, searching for signatures associated with quantum fluctuations, correlations, and entanglement. Examples of spin current carriers are electrons, spin-triplet pairs, Bogoliubov quasiparticles, magnons, spin superfluids, spinons, etc. This project will also focus on possibilities of converting one type of spin current into another at interfaces. Such studies are important because they can uncover new physics associated with quantum materials and lead to applications requiring transmitting signals with minimal energy losses for information storage and processing. This research will provide deeper understanding of spin currents and their role in quantum materials and offer new principles for classical and even quantum information processing with low dissipation.

Keywords: Spin superfluids, magnons, magnetic interfaces.

Recent Progress

Magnon Landau Levels and Spin Responses in Antiferromagnets – the PI, in collaboration with Bo Li (graduate student) have studied gauge fields produced by gradients of the Dzyaloshinskii-Moriya interaction (DMI) and magnetic textures in ferromagnetic and antiferromagnetic insulators. We have shown that the gradient of DMI in antiferromagnet can lead to formation of topological insulator of AFM magnons and unconventional Hofstadter’s butterfly (see Figure 1). In such topological insulator, the magnon Landau levels induced by the inhomogeneous DMI exhibit relativistic physics described by the Klein-Gordon equation. We have shown that the van

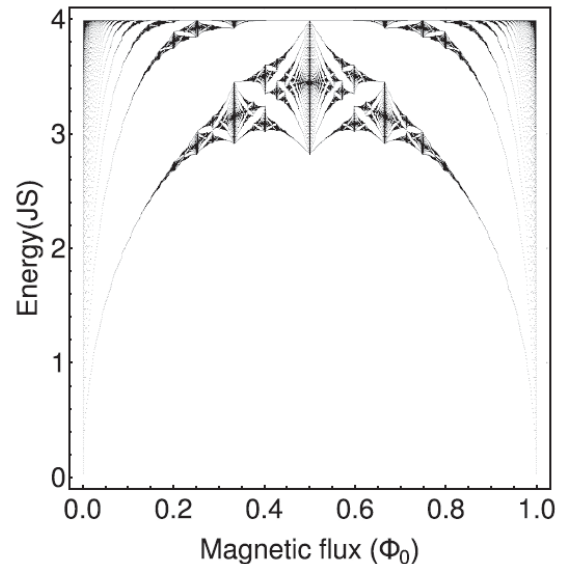


Figure 1: Hofstadter’s butterfly of the AFM magnons with uniform fictitious magnetic flux $\Phi = \frac{p}{q}\Phi_0$ per unit cell for $q = 1000$, Φ_0 is the flux quantum.

Have singularity in magnon density of states can lead to sign change of the topological Hall effect of magnons in ferromagnetic insulators. The gauge fields can be also produced by topological textures such as AFM skyrmion lattices and AFM square crystals of vortices and antivortices (see Figure 2). The spin Nernst response due to the formation of magnonic Landau levels have been compared for different mechanisms of gauge fields. The gauge fields produced by magnetic textures typically lead to formation of dispersive Landau levels. Our studies show that AFM insulators exhibit rich physics associated with topological magnon excitations and open many new possibilities for spin transport. The paper has been published in Physical Review Letters.

Spin superfluidity in noncollinear antiferromagnets – the PI, in collaboration with Bo Li (graduate student) have studied the spin superfluid transport in exchange interaction-dominated three-sublattice antiferromagnets. Magnetic insulators can transport spins in a regime in which the transport can be described as spin superfluidity. In easy-plane magnets, the spin is then transported over large distances by the coherent order parameter precession. The power-law decay of spin current can enable spin transport over longer distances compared to the diffusive regime. It has been determined that collinear antiferromagnetic insulators could provide a viable platform for realizing the spin superfluidity. In our work, we extend above analysis to noncollinear antiferromagnetic insulators. The system in the long-wavelength regime is described by an SO(3) invariant field theory. Additional corrections from Dzyaloshinskii-Moriya interactions or anisotropies can break the symmetry; however, the system still approximately holds a U(1)-rotation symmetry. Thus, the power-law spatial decay signature of spin superfluidity is identified in a nonlocal-measurement setup where the spin injection is described by the generalized spin-mixing conductance (see Figure 3). Our results suggest that three-sublattice systems with approximate in-plane anisotropy are promising for realizing spin superfluidity in noncollinear antiferromagnets. The paper has been published as PRB Letter.

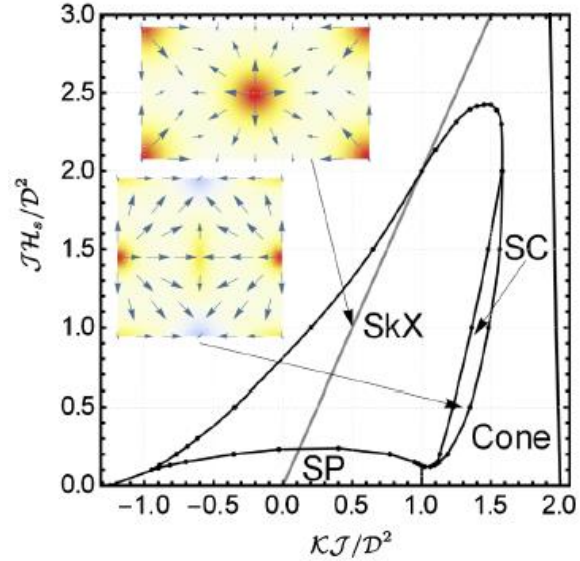


Figure 2: Zero temperature phase diagram of AFM with DMI. The axes correspond to the dimensionless staggered magnetic field and dimensionless effective anisotropy. This phase is taken over by the hexagonal skyrmion lattice (SkX), spiral (SP), cone phase, and the square crystal of vortices and antivortices (SC). The upper inset shows a hexagonal lattice unit cell with a skyrmion in the center. The lower inset shows a square crystal unit cell with an AFM antimeron-like structure in the center. Red and yellow correspond to the positive topological charge density and blue corresponds to the negative topological charge density.

Regular and in-plane skyrmions and antiskyrmions from boundary instabilities – the PI, in collaboration with Shane Sandhoefner (graduate student), Rabindra Nepal (graduate student), Aldo Raeliarijaona (postdoc) have studied skyrmion and antiskyrmion generation using magnetic field and charge current pulses. We have shown that the topological defects can be created at an edge of a system with Dzyaloshinskii-Moriya interaction (DMI) as well as at a boundary between regions with different DMI. We consider both perpendicular and in-plane (also known as magnetic bimerons)

versions of skyrmions and antiskyrmions (see Figure 4). We have shown that the magnetization twist in the vicinity of an edge or a boundary is described by a kink solution, the presence of which can instigate the generation of topological defects. The presence of the magnetization twist also leads to formation of magnon modes localized at the edge or boundary. We further study edge/boundary magnons analytically and numerically and demonstrate that under application of magnetic field and charge current

pulses the magnon modes localized near boundaries can develop instabilities leading to the formation of skyrmions or antiskyrmions. Due to the skyrmion and antiskyrmion Hall effects, a properly chosen current direction can push the topological defects away from the boundary, thus facilitating their generation. Realizations of antiskyrmions and in-plane (anti)skyrmions will require careful material engineering as the former can be realized in systems with D_{2d} or C_{2v} symmetry and the latter in systems with only mirror symmetry, M_x . Antiskyrmions have been realized in Heusler compounds. For in-plane skyrmions, proposed material candidates include $FeLa_3S_6$ and $Rb_6Fe_2O_5$. Systems based on magnetic heterostructures of different layered materials can in principle be engineered to realize various topological defects discussed in our work.

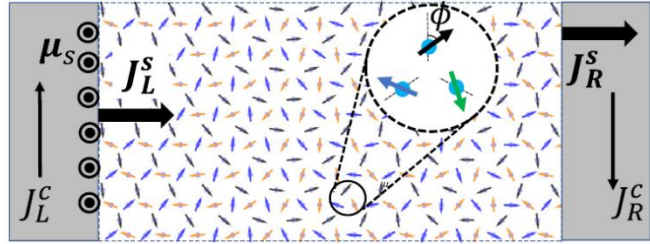


Figure 3: A nonlocal measurement setup containing normal metal/noncollinear antiferromagnet/normal metal heterostructure. A charge current in the left layer generates a spin accumulation μ_s via spin Hall effect, which injects a spin current into AFM layer. The spin current mediated by the collective modes in the middle layer passes the second interface by virtue of spin pumping effect. The pumped spin current is measured in the right layer via the inverse spin Hall effect.

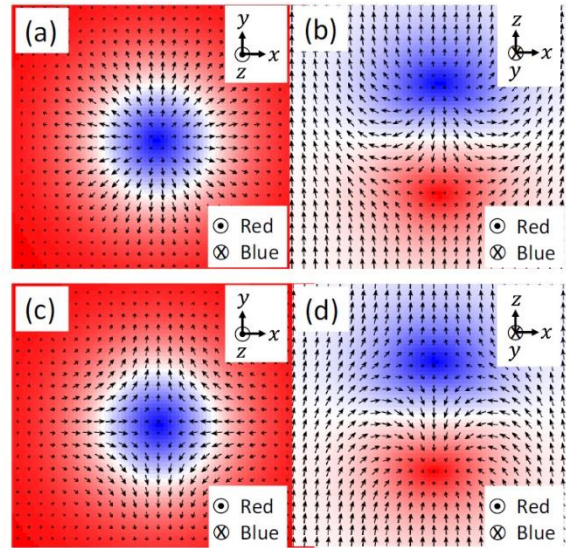


Figure 4: (a) Regular skyrmion, (b) in-plane skyrmion, (c) regular antiskyrmion, and (d) in-plane antiskyrmion, where the in-plane (anti)skyrmion is obtained from the regular (anti)skyrmion by sending x to x , y to z , and z to y .

The paper has been published in Physical Review B.

Future Plans

Spin superfluidity in insulating magnets – the PI will study signatures of BKT transition and its effect on spin superfluid transport. Magnetic systems with in-plane anisotropy and $U(1)$ symmetry in two dimensions do not have long range order. As a result, the conventional theory of spin superfluidity will only apply at $T = 0$ [1]. The PI is planning to develop numerical and possibly analytical approaches to study superfluid spin transport in insulating ferromagnets and antiferromagnets. This research is potentially important for realizing novel systems that can transport spins over long distances with almost no dissipation. Two dimensional materials such as van der Waals magnets are promising candidates for realizing above phenomena. We will also consider possibilities for realizing quantum phenomena in the context of hydrodynamic description of spin superfluidity, vorticity currents, and spin flows. Possible detection schemes relying on noise measurements will be considered.

Spin Hall currents and their conversion into torques in disordered magnetic systems with spin-orbit interactions – the PI will study analytically, and numerically novel mechanisms of spin-orbit torques. Recently, spin-orbit torques corresponding to higher order expansions in spherical harmonics [2] as well as those corresponding to lower symmetry attracted attention due to possible applications in magnetic memories and spin-torque oscillators. Starting from descriptions of spin currents, the PI will address various possibilities for realizing such spin-orbit torques, and their potential usefulness for magnetization reversal and dynamics.

Spin currents in superconductor/ferromagnet heterostructures with magnetic textures – the PI will study superconductor/ferromagnet hybrid structures when a magnetic texture, e.g., skyrmion, is present in the ferromagnetic layer. Of particular interest is the conversion of singlet Cooper pairs to triplet Cooper pairs which can result in a long-range spin current associated with the proximity effect in the ferromagnet [3]. We expect a very rich physics to arise due to interplay between the magnetization dynamics, processes at the interface, and spin flows.

References

- [1] Se Kwon Kim and Suk Bum Chung, “Transport signature of the magnetic Berezinskii-Kosterlitz-Thouless transition,” *SciPost Phys.* 10, 068 (2021).
- [2] K. D. Belashchenko, A. A. Kovalev, M. van Schilfgaarde, “Interfacial contributions to spin-orbit torque and magnetoresistance in ferromagnet/heavy-metal bilayers,” *Phys. Rev. B* 101, 020407(R) (2020).
- [3] S. Diesch, P. Machon, M. Wolz, C. Sürgers, D. Beckmann, W. Belzig, and E. Scheer, Creation of equal-spin triplet superconductivity at the Al/EuS interface, *Nature Communications* 9(1), 5248 (2018)

Publications

1. S. Sandhoefner, A. Raeliarijaona, R. Nepal, D. Snyder-Tinoco, A. A. Kovalev, “Regular and in-plane skyrmions and antiskyrmions from boundary instabilities,” *Phys. Rev. B* **104**, 064417 (2021).
2. W. Fang, A. Raeliarijaona, P-H. Chang, A. A. Kovalev, K. D. Belashchenko, “Spirals and skyrmions in antiferromagnetic triangular lattices,” *Phys. Rev. Materials* **5**, 054401 (2021).
3. B. Li, A. A. Kovalev, “Spin superfluidity in noncollinear antiferromagnets,” *Phys. Rev. B* **103**, L060406 (2021).
4. B. Li, A. A. Kovalev, “Magnon Landau Levels and Spin Responses in Antiferromagnets,” *Phys. Rev. Lett.* **125**, 257201 (2020).
5. G. G. Baez Flores, A. A. Kovalev, M. van Schilfgaarde, K. D. Belashchenko, “Generalized magnetoelectronic circuit theory and spin relaxation at interfaces in magnetic multilayers,” *Phys. Rev. B* **101**, 224405 (2020).
6. B. Li, S. Sandhoefner, A. A. Kovalev, “Intrinsic spin Nernst effect of magnons in a noncollinear antiferromagnet,” *Phys. Rev. Research* **2**, 013079 (2020).
7. K. D. Belashchenko, A. A. Kovalev, M. van Schilfgaarde, “Interfacial contributions to spin-orbit torque and magnetoresistance in ferromagnet/heavy-metal bilayers,” *Phys. Rev. B* **101**, 020407(R) (2020).
8. B. Li, A. Mook, A. Raeliarijaona, A. A. Kovalev, “Magnonic analog of the Edelstein effect in antiferromagnetic insulators,” *Phys. Rev. B* **101**, 024427 (2020).
9. S. Prabhakar, R. Nepal, R. Melnik, A. A. Kovalev, “Valley-dependent Lorentz force and Aharonov-Bohm phase in strained graphene p–n junction,” *Phys. Rev. B* **99**, 094111 (2019).
10. K. D. Belashchenko, A. A. Kovalev, M. van Schilfgaarde, “First-principles calculation of spin-orbit torque in a Co/Pt bilayer,” *Phys. Rev. Materials* **3**, 011401(R) (2019).
11. H. Takenaka, S. Sandhoefner, A. A. Kovalev, E. Y. Tsybal, “Magnetoelectric control of topological phases in graphene,” *Phys. Rev. B* **100**, 125156 (2019).

Correlated electronic structure and phase stability in real materials

Walter R. L. Lambrecht, Department of Physics, Case Western Reserve University

Program Scope

The focus of our current research over the last two years has been on topological aspects of antimonene, which is two-dimensional Sb in the honeycomb structure. This work was triggered by recent experimental advances in developing Sb and As as monolayer materials [1]. While free-standing Sb monolayers have a buckled honeycomb structure and are known to have a band gap, the flat honeycomb lattice can be realized on suitable substrates like Ag [2] which put the layer under tension. Our initial goal was to study the behavior of honeycomb Sb from the entirely flat case to the final buckled equilibrium form. In the process, we found a rich topological behavior from a nodal line semimetal for the flat case to merging Dirac cones, ending up in a gapped band structure. The edge states and effects of spin-orbit coupling were investigated at the different stages which involve two distinct topological phase transitions. The final buckled form still shows an isolated edge state, which was explained in terms of the topological concept of the “obstructed atomic limit” (OAL). Further investigation showed this system to be a higher order topological insulator exhibiting localized fractionalized corner states. Symmetry analysis shows that breaking the inversion symmetry using an electric field across the layer results in a metal to insulator transition of the edge states. This led to the concept of a topological quantum switch and to the formation of a domain wall soliton at the boundary between oppositely polarized domains. We proposed that this could lead to a novel way to make reconfigurable circuits. Finally, the physics of Dirac cone merging was studied in a broader context and shown to always lead to obstructed atomic limit insulators.

Keywords: topological band structure, antimonene, quantum electron transport

Recent Progress

Starting from density functional theory and quasiparticle self-consistent (QS) *GW* calculations of flat monolayer Sb, a tight-binding model and low energy models were developed for the behavior of the electrons near the Fermi surface. Full group-theoretical symmetry labeling was carried out to understand the band inversions that take place as function of gradually buckling the layers. Compared to graphene, three main differences apply to Sb in the flat honeycomb structure: (1) the atomic s and p valence levels are more separated than in C, (2) there is one additional valence electron and (3) spin-orbit coupling is stronger. The first of these leads to a clear separation of the s-derived band from the p-derived bands. The latter form symmetry decoupled bands from the p_z and p_x, p_y orbitals. Both of these form a Dirac cone at the

corner of the Brillouin zone K. The Fermi surface thus lies at the intersection of two warped Dirac cones, which turn out to be rotated by 60° relative to each other. Using the tight-binding model we were able to fully analytically explain how this leads to a nodal line semimetal with a Lissajous shaped nodal line, shown in Fig. 1. This unique energy band surface intersection was shown to lead to a change in sign in the Seebeck coefficient as function of angle as one switches from one cone to the other, in other words *goniopolarity*, or a dependence of the carrier type as function of angle. The conductivity and density of states at the Fermi level are also found to be very close to a van Hove singularity related to saddle point in the 2D band structure which should make the conductivity quite sensitive to the doping.

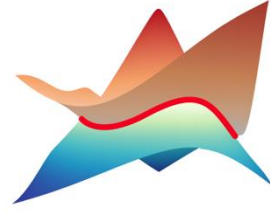


Fig. 1: Nodal line formed through the intersection of two rotated and warped Dirac cones.

Next, as we now allow the system to buckle slightly, the breaking of the horizontal mirror plane allows the coupling between the two Dirac cone energy surfaces, opening a gap at the nodal line, which, however, remains closed at six Dirac points surrounding each point K. These were found to be protected by a two-fold rotation symmetry in the plane. These Dirac points are not pinned but can move as the buckling increases. They are found to be alternately of opposite winding number and as the Dirac points approach each other along the K-M-K' line they annihilate in pairs at M, signaling a topological phase transition or band inversion taking place. Subsequently the remaining Dirac points move toward Γ and annihilate, at which point a full gap appears in the band structure. The Dirac points discussed are linked by edge states which were studied in finite width strips. The Dirac points open a gap when spin-orbit coupling is included, thus leading to a gapless topological crystalline insulator behavior. While a local gap opens, the gaps from one Dirac crossing are staggered in energy with respect to the other leading to a globally gapless state. For full details of the tight-binding models, group theory and QSGW results of the bands we refer the reader to Ref. [3], which also discusses the metastability of the flat vs. the buckled states of Sb and As and to what extent the monolayer Sb band structure states can still be recognized when placed against the background of the Ag substrate states.

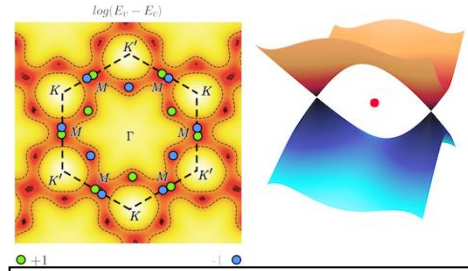


Fig. 2 Pairs of Dirac cones of opposite winding number annihilate at M as buckling of the layer increases or tensile strain is reduced.

Subsequently the remaining Dirac points move toward Γ and annihilate, at which point a full gap appears in the band structure. The Dirac points discussed are linked by edge states which were studied in finite width strips. The Dirac points open a gap when spin-orbit coupling is included, thus leading to a gapless topological crystalline insulator behavior. While a local gap opens, the gaps from one Dirac crossing are staggered in energy with respect to the other leading to a globally gapless state. For full details of the tight-binding models, group theory and QSGW results of the bands we refer the reader to Ref. [3], which also discusses the metastability of the flat vs. the buckled states of Sb and As and to what extent the monolayer Sb band structure states can still be recognized when placed against the background of the Ag substrate states.

The fully buckled gapped state was previously considered as being a trivial insulator in terms of its topology. However, calculations of finite width strips of the material, showed the persistence of an almost dispersion less edge state isolated in the gap (see Fig. 3). This can be explained in terms of the recently developed concept of the Obstructed Atomic Limit (OAL). This concept developed by Bradlyn et al. [4] refers to band manifolds which do allow a Wannier

function representation but one which cannot be smoothly reduced to atom-centered Wannier functions but rather consists of bond-centered Wannier functions. We showed that this is the case for the set of three mixed (p_x, p_y, p_z)-derived occupied bands in Sb and found that these bond centers form a kagome lattice, while the corresponding empty bands have Wannier functions centered at points opposite to the bond centers. These same bond centers also occur in the Kekulé lattice, which is a honeycomb lattice with alternating bond strengths. Using group-theoretical analysis we were able to show that these three lattices belong in the same topological class in terms of a symmetry indicator for Higher-Order Topological Insulators (HOTI). This places Sb in the class of S_6 quadrupole insulators which exhibit localized corner states with charge fractionalization. The existence of these corner charges was demonstrated explicitly using tight-binding models of finite size fragments with hexagonal symmetry and was also shown to be robust against disorder potential fluctuations as long as these remain in the interior of the nanoflake. These results were reported in [5].

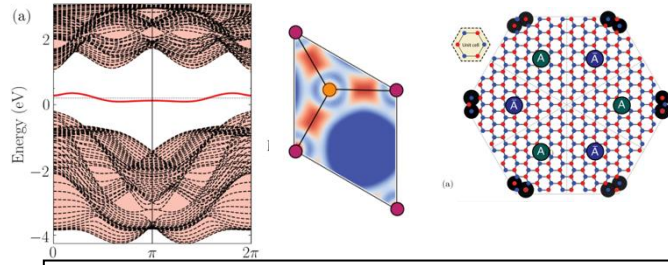


Fig. 3 Left: band structure of finite width strip of buckled Sb showing edge state, which is related to the OAL resulting from bond centered Wannier functions of the occupied bands shown in the center. The right shows the occurrence of corner localized charge fractionalized states for a hexagonal finite fragment.

The symmetry underlying the above higher order topological behavior is that of the D_{3d} group which has an S_6 operation and an

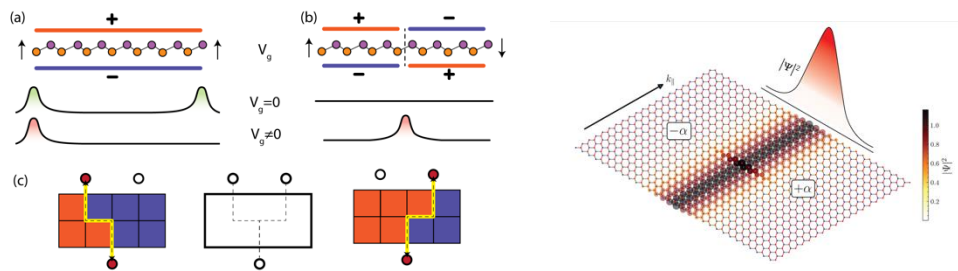


Fig. 4 Left: conceptual sketch of a quantum switch and reconfigurable circuit based on domain wall solitons (right) based on breaking of the inversion

inversion center. Breaking the inversion center reduces this symmetry to C_3 and gaps the edge and corner states found previously and hence leads to a metal to insulator transition. This symmetry breaking can be effectuated using an electric field across the layer as shown in Fig. 4. This symmetry breaking quantum switch operating on the edge states is well separated from the remaining bands and should require a voltage larger than the intrinsic band dispersion of the edge state which is dictated by next-nearest-neighbor interactions and therefore quite small. Furthermore, applying this inversion symmetry breaking in opposite ways in adjacent domains is shown to require a soliton-like domain wall state (see Fig. 4 right) extracted from either the valence or conduction band states. If this band becomes partially filled by doping, it can lead to a conducting path along the domain wall in an otherwise insulating 2D system. This could

potentially be exploited to create reconfigurable conducting path circuits. As explained in [6], this is closely related to a similar behavior in the Su-Schrieffer-Heeger model.

In a final paper, [7] we examined the physics of the Dirac cone annihilation in a broader context and showed that it always leads to an OAL situation.

Future Plans

In the coming year we plan to focus on other 2D systems, such as WSe₂ for which we have started carrying out Bethe-Salpeter-Equation calculations of the optical absorption as function of the distance between the layers. We also plan to return to oxide 2D systems such as V₂O₅ and MoO₃. In previous work, we found that the QSGW method strongly overestimates the band gap in these materials. One possible reason for this, which we discovered in LiCoO₂ is the formation of strongly bound excitons related to the flat bands in these systems. Finally, we plan to return to prior work done on some halide perovskites such as CsGeX₃ and RbGeX₃ with X a halogen which exhibit possible phase transitions between non-perovskite and perovskite structures accompanied by a large change in band gap and related to a ferroelectric to antiferroelectric alignment of GeX₃ dipoles.

References

- [1] P. Ares et al. *Adv. Mater.* **30**, 1703771 (2018)
- [2] Y. Shao et al. *Nano Lett.* **18**, 2133 (2018)
- [3] S. K. Radha and W. R. L. Lambrecht, *Phys. Rev. B* **102**, 235111 (2020)
- [4] B. Bradlyn et al. *Nature* **547**, 298 (2017)
- [5] S. K. Radha and W. R. L. Lambrecht, *Phys. Rev. B* **102**, 115104 (2020)
- [6] S. K. Radha and W. R. L. Lambrecht, *Phys. Rev. B* **102**, 245413 (2020)
- [7] S. K. Radha and W. R. L. Lambrecht, *Phys. Rev. B* **103**, 075435 (2021)

Publications

1. Topological obstructed atomic limit insulators by annihilating Dirac fermions, Santosh Kumar Radha and Walter R. L. Lambrecht, *Phys. Rev. B* 103, 075435 (2021)
2. Topological quantum switch and controllable one-dimensional conducting paths in antimonene facilitated by breaking the inversion symmetry, Santosh Kumar Radha and Walter R. L. Lambrecht, *Phys. Rev. B* 102, 245413 (2020)
3. Buckled honeycomb antimony: Higher order topological insulator and its relation to the Kekulé lattice, Santosh Kumar Radha and Walter R. L. Lambrecht, *Phys. Rev. B* 102, 115104 (2020)
4. Topological band structure transitions and goniopolar transport in honeycomb antimonene as a function of buckling, Santosh Kumar Radha and Walter R. L. Lambrecht, *Phys. Rev. B* 101, 235111 (2020)
5. Quasiparticle self-consistent GW band structure of CrN, Tawinan Cheiwchanchamnangij and Walter R. L. Lambrecht, *Phys. Rev. B* 101, 085103 (2020)
6. First-principles study of the phonon replicas in the photoluminescence spectrum of 4H-SiC, Sai Lyu and Walter R. L. Lambrecht, *Phys. Rev. B* 101, 045203 (2020)
7. Erratum: First-principles study of the phonon replicas in the photoluminescence spectrum of 4H-SiC [*Phys. Rev. B* 101, 045203 (2020)], Sai Lyu and Walter R. L. Lambrecht, *Phys. Rev. B* 102, 079904 (2020)

Strongly Correlated Electronic Systems: Local Moments and Conduction Electrons.

Patrick A. Lee, MIT.

Program Scope

Ultrashort laser pulses have become powerful tools to perturb materials, to probe the underlying excitations, and to create new phases. Among the recent developments, photo-induced superconducting-like responses in various strongly correlated materials are particularly interesting and surprising. This phenomenon is found in multiple species of cuprate high-temperature superconductors [1–4], K3C60 [5], and κ -(ET)2Cu[N(CN)2]Br [6]. In all of the works cited above, a pump laser induces transient superconducting-like responses at temperatures much higher than the equilibrium superconducting transition temperature. A key experimental finding is a $1/\omega$ imaginary part of the conductivity after the pump (Fig. 1(a)) [3–6], resembling the London equation of an equilibrium superconductor. In addition, κ -(ET)2Cu[N(CN)2]Br and K3C60 also show an emergent gap in the real part of the conductivity [5, 6] (Fig. 1(b)). This has been interpreted as the photo-induced superconducting gap.

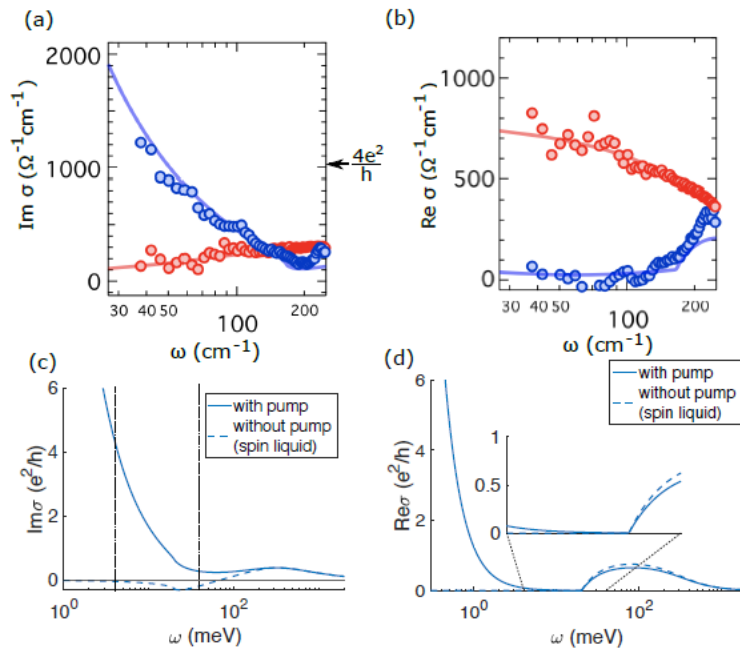


FIG. 1. (a-b) The measured real/imaginary part of the transient conductivity (blue dots) and the equilibrium conductivity (red dots) of the metallic sample κ -(ET)2Cu[N(CN)2]Br at 30K (reproduced from Fig.3 in Ref. [6]). The solid blue line in (a) is constant times $1/\omega$. The frequency is shown in log scale. To facilitate comparison with the vertical scale of the theory curves, the black arrow on the right of (a) indicates a conductance of $4e^2/h$ per (ET)2 layer. (c-d) Theoretical predictions [12] of the real/imaginary part of the conductivity

(per layer, in units of e^2/h) of a driven spin liquid (solid line) and a spin liquid in equilibrium (dashed line), where we have used $\Delta = 10\text{meV}$, $\rho_b = 3\text{meV}$, $\rho_f = 40\text{meV}$, and $\tau^{-1} = 1\text{meV}$. The dotted dashed lines in (c) and the inset of (d) represents the frequency range between 4meV and 40meV, comparable to the range shown in the experimental plot in (a-b).

Until now, it is still unclear what underlying mechanism produces the transient superconducting-like responses. Almost all existing theoretical attempts assume some form of superconducting fluctuations. It is commonly assumed that the pump either creates a quasi-static superconducting phase [3, 5, 6] or dynamically excite collective modes which exist because of superconducting fluctuations. [1, 2, 7] This assumption is reasonable for materials where superconducting fluctuations have been reported at relatively high temperatures. However, comparing the equilibrium properties with the transient response, we believe this scenario is unlikely to be the case for κ -(ET)₂Cu[N(CN)₂]Br. κ -(ET)₂Cu[N(CN)₂]Br is a layered material with a nearly isotropic triangular lattice; the low-energy physics is believed to be described by a single-band Hubbard model with one electron per unit cell. The conducting band comes from electron orbitals of the ET molecular dimers. This material is well-known to be close to a Mott transition. In fact, κ -(ET)₂Cu[N(CN)₂]Cl [8] and κ -(ET)₂Cu₂(CN)₃ [9], which have ET layers with slightly different lattice parameters, are Mott insulators. κ -(ET)₂Cu[N(CN)₂]Cl has an antiferromagnetic (AFM) order below 35K; κ -(ET)₂Cu₂(CN)₃ is a well-studied candidate as a spin liquid with spinon Fermi surface. Being close to the insulating phase, κ -(ET)₂Cu[N(CN)₂]Br behaves like an insulator in a broad temperature and frequency range, becoming metallic only at low temperature and frequency. The resistivity is very large at room temperature, rising with decreasing temperature and plunges rapidly around 60K [10]. Indeed, at 50K the real part of the AC conductivity does not show a Drude peak at all, but rises with increasing frequency [6]. The standard interpretation is that a coherent Fermi liquid onsets only at $T^* \sim 60$ K [6, 8]. The superconducting transition temperature is 12K in equilibrium, which is among the highest in the κ -ET family. The superconducting gap has not been measured from the optical conductivity. However, after the pump, both the ‘transition temperature’ and photo-induced ‘superconducting gap’ are much larger than the equilibrium energy scale of superconductivity. The photo-induced superconducting like response is observed up to 50K. At 15 to 30K, if we interpret half the optical gap (See Fig. 1(b)) as the induced ‘superconducting-gap’, it is 11meV \sim 130K, more than twice T^* [6]. It is hard to justify the existence of a quasi-static superconducting gap much larger than the coherent scale below which the electrons show metallic behavior. Some new point of view is called for. In a recent work, we propose a general mechanism for photo-induced superconducting-like response in materials with bosonic charge excitations [11]. In this proposal, the laser pulse creates particle-hole excitations of the boson; the density of the excitations grow exponentially at early time, inducing an AC conductivity just like ordinary superconductors, $\sigma(\omega) \propto i/\omega$, which we show is a consequence of Bose statistics. Here we show that in materials close to the Mott transition, our formalism can be applied to fractionalized charge e bosons that emerges due to electron fractionalization. [12]

Keywords: nonequilibrium superconductivity, Mott transition, pump-probe.

Recent Progress

We describe low energy physics of a spin liquid on the insulating side of the Mott transition by fractionalizing the electron into a spinon Fermi surface and bosons chargon. The charge dispersion is described by a relativistic boson shown in Fig. 2a. The upper branch represents the doubly occupied state (doublon) and the lower branch the empty state (holon). The pump drives transition between these branches. Unlike the more familiar case of driven fermions that results in hybridized Floquet bands, for bosons the hybridization is in the “horizontal” direction, resulting in a band of states with complex eigenvalues, i.e., these are capable of exponential growth. [12]

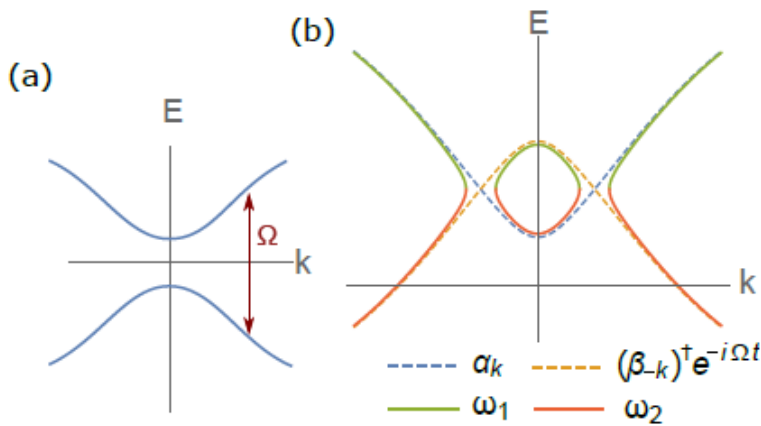


FIG. 2. (a) Sketch of the gapped bosonic particle and hole band (shown as negative energy for convenience) in a spin liquid. The periodic drive at frequency Ω resonantly generate particle-hole pairs. (b) Dispersion of a driven boson. The blue/orange dotted line represents the equilibrium dispersion $E_k/\Omega - E_k$. The solid lines represent the

dispersion under periodic drive. Near the crossings at $\Omega/2$, there is a region (forming a ring in the 2D B.Z.) where the eigen-frequencies are complex and the boson numbers grow exponentially.

In order to apply our theory to the pumped superconductor which is on the metallic side of the Mott transition, we take the point of view that in the Landau theory for the boson, the coefficient of the quadratic term can be driven from negative to positive when the boson population grows under the pump via the quartic term. Thus under the drive the superconductor can be pushed to the insulating side. We can now use the results obtained in our earlier publication [11] to compute the conductivity as measured by the probe field. The result is seen in Fig 1 c,d and matches the experimental data quite well.[12] It is important to note that the gap that emerges under pumping shown in fig. 1d is *not* a pairing gap, but an emergent Mott gap! This explains why the gap can be so much bigger than what can reasonably be expected from superconductivity in this material.

Future Plans

We have made a proposal to the experimentalists to apply the drive to the organic spin liquid materials. We will work on the theory as the experiment progresses. At the same time, we are working on understanding the data on high temperature superconductors, where it is more reasonable to think that pairing correlation persists to temperature much above T_c . The goal is to find the minimal set of assumptions which can explain the observed data.

Reference

- [1] S. Kaiser, C. R. Hunt, D. Nicoletti, W. Hu, I. Gierz, H. Y. Liu, M. Le Tacon, T. Loew, D. Haug, B. Keimer, and A. Cavalleri, *Phys. Rev. B* 89, 184516 (2014).
- [2] W. Hu, S. Kaiser, D. Nicoletti, C. R. Hunt, I. Gierz, M. C. Hoffmann, M. Le Tacon, T. Loew, B. Keimer, and A. Cavalleri, *Nature materials* 13, 705 (2014).
- [3] A. Cavalleri, *Contemporary Physics* 59, 31 (2018).
- [4] B. Liu, M. Först, M. Fechner, D. Nicoletti, J. Porras, T. Loew, B. Keimer, and A. Cavalleri, *Phys. Rev. X* 10, 011053 (2020).
- [5] M. Mitrano, A. Cantaluppi, D. Nicoletti, S. Kaiser, A. Perucchi, S. Lupi, P. Di Pietro, D. Pontiroli, M. Riccò, S. R. Clark, et al., *Nature* 530, 461 (2016).
- [6] M. Buzzi, D. Nicoletti, M. Fechner, N. Tancogne-Dejean, M. A. Sentef, A. Georges, T. Biesner, E. Uykur, M. Dressel, A. Henderson, T. Siegrist, J. A. Schlueter, K. Miyagawa, K. Kanoda, M.-S. Nam, A. Ardavan, J. Coulthard, J. Tindall, F. Schlawin, D. Jaksch, and A. Cavalleri, *Phys. Rev. X* 10, 031028 (2020).
- [7] M. H. Michael, A. von Hoegen, M. Fechner, M. Först, A. Cavalleri, and E. Demler, *Physical Review B* 102, 174505 (2020).
- [8] D. Faltermeier, J. Barz, M. Dumm, M. Dressel, N. Drichko, B. Petrov, V. Semkin, R. Vlasova, C. Mezière, and P. Batail, *Phys. Rev. B* 76, 165113 (2007).
- [9] T. Furukawa, K. Kobashi, Y. Kurosaki, K. Miyagawa, and K. Kanoda, *Nature communications* 9, 1 (2018).
- [10] M.-S. Nam, C. Mezière, P. Batail, L. Zorina, S. Simonov, and A. Ardavan, *Scientific reports* 3, 1 (2013).
- [11] Z. Dai and P. A. Lee, "Photo-induced superconducting like response in strongly correlated systems." *Phys. Rev. B* 104, 054512 (2021).
- [12] Dai, Zhehao, and Patrick A. Lee. "Superconducting-like response in driven systems near the Mott transition." *arXiv preprint arXiv:2106.08354*(2021).

Publications

1. Dai, Zhehao, T. Senthil, and Patrick A. Lee. "Modeling the pseudogap metallic state in cuprates: Quantum disordered pair density wave." *Physical Review B* 101, no. 6 (2020): 064502.
2. Chen, Chuan, Inti Sodemann, and Patrick A. Lee. "Competition of spinon Fermi surface and heavy Fermi liquid states from the periodic Anderson to the Hubbard model." *Physical Review B* 103, no. 8 (2021): 085128.
3. Lee, Patrick A. "Quantum oscillations in the activated conductivity in excitonic insulators: Possible application to monolayer WTe_2 ." *Physical Review B* 103, no. 4 (2021): L041101.
4. He, Wenyu and Patrick A. Lee, "Quantum Oscillation of Thermally Activated Conductivity in a Monolayer WTe_2 -like Excitonic Insulator." *Phys. Rev. B* 104, L041110 (2021)
5. Dai, Zhehao, and Patrick A. Lee. "Photo-induced superconducting-like response in strongly correlated systems." *Phys. Rev. B* 104, 054512 (2021).
6. Dai, Zhehao, and Patrick A. Lee. " Superconducting-like response in driven systems near the Mott transition." *arXiv preprint arXiv:2106.08354*(2021).
7. Lee, Patrick A. "Low temperature T -linear resistivity due to umklapp scattering from a critical mode." *Phys. Rev. B* 104, 035140 (2021).

Elucidating the Nature of Chiral and Topological Phonons in Materials for Energy Technologies

Lucas Lindsay, Oak Ridge National Laboratory

Program Scope

This project builds theoretical and numerical tools to predict and understand chiral and topological properties of phonons in condensed matter systems, particularly regarding interactions and transport. Impacts of chirality in biological systems have long been known and insights into electronic topologies are flourishing. However, topological bosonic systems are only now being explored for the potential zoo of novel quasiparticle behaviors and materials functionalities that they may support [1,2], and the role of structural and vibrational chirality in governing interactions and transport is little developed [3]. This project critically examines how structural symmetries and chirality determine quasiparticle angular momenta which underlie interactions, transport, and spectral observables via quantum interference conditions in non-symmorphic materials with complex unit cells. We also probe the relationship of chirality and other symmetry-constraints with the quasiparticle dynamics that determine protected band crossing behaviors and topologies. Building fundamental insights into chirality- and topologically-driven vibrational transport properties will open pathways to predicting and designing novel materials with targeted thermal functionalities for advanced thermal management applications.

Keywords: chiral/topological phonons, quasiparticle interactions, thermal transport.

Recent Progress

This project has made critical steps toward understanding chiral phonon dynamics in bulk materials with layered non-symmorphic ‘twisting’ of their lattice structures, thus demonstrating that quasiparticles in these systems carry angular momentum. **Figure 1** gives an example of a structurally twisted material, α -TeO₂, with a four-fold screw chiral symmetry ($\pi/2$ rotation with a $c/4$ translation; c being the lattice constant along the chiral axis) that gives rise to a variety of novel quasiparticle behaviors [4]. We build twist symmetry directly into the phonon dynamics using rotation operators and appropriate phase factors that relate the separate layers labeled by n_h [4,5]:

$$\bar{D}_l = D_{\alpha\beta}^{kk'}(q,l) = \frac{1}{\sqrt{m_k m_{k'}}} \sum_{\gamma h' p'} \Phi_{\alpha\gamma}^{0k,h'p'k'} S_{\gamma\beta}(\theta_{h'}) e^{iqR_{h'}} e^{il\theta_{h'}} \quad (1)$$

where m_k is the mass of the k^{th} atom, Greek subscripts designate Cartesian directions, h designates the layer, p designates the atom in the layer, S is a rotation operator, R_h and θ_h give the location of

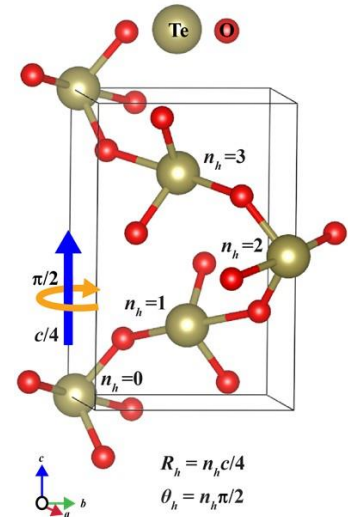


Figure 1: Structure of TeO₂. Each layer labeled by n_h is related by $c/4$ translation and $\pi/2$ rotation.

layer h along the chiral axis ($n_h c/4$ for α -TeO₂) and rotation of this layer about the axis ($n_h \pi/2$ for α -TeO₂), respectively, q is the continuous wavevector along the chiral axis, and l is an angular quantum number corresponding to the rotational phase about the chiral axis. This formalism elucidates the angular momentum quantum numbers that bands carry along chiral axes in non-symmorphic materials (**Fig. 2**). Similar formulations can be constructed for electronic bands from model Hamiltonians or Wannier projections derived from density functional theory (**Fig. 2**).

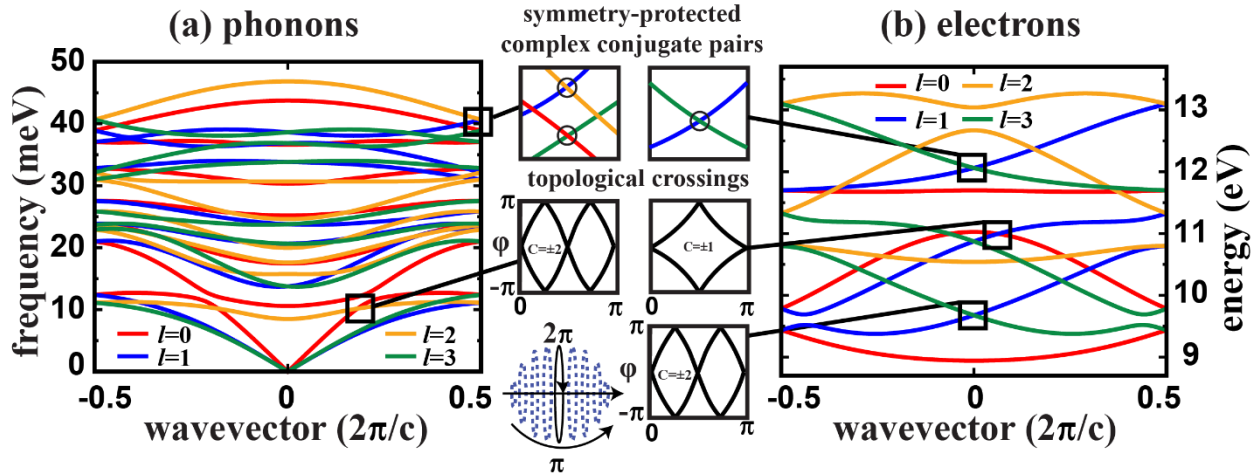


Figure 2: DFT-derived band structures for α -TeO₂ along the chiral c -axis for (a) phonons and (b) electrons. Band colors correspond to the angular momenta l [4]. The top two middle panels focus on symmetry-enforced crossings. The two middle panels and bottom panel show Berry phase winding and Chern classification (C) for different topological band crossings. The cartoon sphere demonstrates the Wilson loop method.

The twist dynamical description developed by this project brings to light a variety of novel quasiparticle band features, including, quantum phase interference conditions, symmetry-enforced band crossings and anti-crossings, and topological classifications [4].

First, we have demonstrated that the angular phase factor in **Eq. 1**, derived from the twist symmetry in a variety of non-symmorphic chiral and achiral materials, plays the role of an effective angular momentum for phonons that is conserved in interactions with other phonons, other quasiparticles (*e.g.*, Bloch electrons), and with external probes such as in neutron, x-ray, and Raman measurements. For example, we have used twist dynamics to understand unusual inelastic neutron scattering measurements on α -TeO₂ in terms of twist phase factors in the dynamical spectral function [4]. The angular momentum is particularly important when describing phonon-phonon and electron-phonon interactions from quantum perturbation theory, where quasiparticle operators that enter interaction matrix elements each carry an angular phase factor. When combined, terms that do not conserve the overall angular momentum (within a reciprocal lattice vector) have phase factors that are identically zero: conservation of angular momentum.

Second, quasiparticle band structures have a variety of protected band degeneracies at high symmetry Γ and zone boundary points in reciprocal space dictated by the twist dynamical matrices. Depending on the symmetry point, twist dynamical matrices for each l have complex conjugate partners, related by the rotational phase factor in **Eq. 1**. For instance, for phonons at $q=\pi/c$ in α -TeO₂, **Eq. 1** gives four dynamical matrices differing in phase by $e^{i\pi n_l/4} e^{i\pi n_l/2} = e^{i\pi n_l(l+1/2)/2}$: the phase factors for $l=\{0,1,2,3\}$ are $\{e^{i\pi n_l/4}, e^{i3\pi n_l/4}, e^{i5\pi n_l/4}, e^{i7\pi n_l/4}\}$. Since the phase factors multiply the same real terms in each Hermitian matrix, $e^{i\pi n_l/4} = e^{-i7\pi n_l/4}$ and $e^{i3\pi n_l/4} = e^{-i5\pi n_l/4}$ (note that $e^{\pm i2n_l\pi} = 1$), this gives $\bar{D}_{l=0} = \bar{D}_{l=3}^*$ and $\bar{D}_{l=1} = \bar{D}_{l=2}^*$, complex conjugate pairs with identical eigenvalues (*i.e.*, bands cross) and conjugate eigenvectors. This also ensures that each band has equal but opposite velocities at the high symmetry points.

Furthermore, bands of the same angular momentum do not cross as they are quantum systems with similar symmetry. We illustrated this behavior in a large unit cell semiconducting material, Ba₆Sn₆Se₁₃, which we demonstrated has a very low measured thermal conductivity and may be of interest for thermoelectric applications [6]. The low lattice thermal conductivity behavior arises in part due to low frequency optic bands that intermix with the heat-carrying acoustic modes with the same angular momentum, thus disrupting the band velocities for a portion of the Brillouin zone and reducing overall contributions to the thermal conductivity.

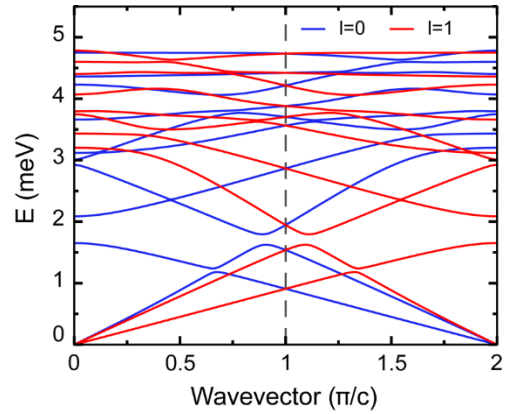


Figure 3: Low frequency dispersion of Ba₆Sn₆Se₁₃ - blue and red indicate different angular momenta l [6].

Thirdly, we correlate the crossing of bands with differing angular momenta along twist axes in chiral materials with non-trivial topological classifications. For instance, crossings within the Brillouin zone of $l=\{0,2\}$ electron and phonon bands in chiral α -TeO₂ have Chern number ± 2 as determined by the Wilson loop method and charting of the Berry phase in reciprocal space (see **Fig. 2**). Similarly, $l=\{0,1\}$ have Chern number ± 1 . We also demonstrated that Ba₆Sn₆Se₁₃ has non-trivial topological band crossings, a feature correlated with good thermoelectric performance.

We have also contributed to a number of collaborative works related to phonon interactions and transport (see publication list below), including examination of: non-local transport behaviors of relevance to ultrafast laser-based spectroscopies, phonon-mediated mechanical properties in MoS₂ and hBN microstructures, spectral dispersions of YbAl₃, and thermal transport in complex unit cell Te-based quaternary compounds.

Future Plans

We plan to critically examine symmetries and interactions in a wider range of materials and materials classes. For instance, we are applying the twist dynamics given by **Eq. 1** to non-

symmorphic chiral and achiral materials of different space groups and with varying numbers of twists. We will examine dynamical symmetries and cross-plane vibrations in twisted van der Waals layered systems with smaller twist angles. We are also exploring the modification of the twist dynamics for application to non-symmorphic materials whose layers are not twisted but simply translated by fractional lattice units, for example, as in candidate spin liquid α - RuCl_3 and layered cleavable magnet CrCl_3 . We are determining how neutrons probe these systems, as well as building insights into novel spectral features from polarized Raman and x-ray measurements.

We will also model the effects of twisting dynamics on phonon-quasiparticle interactions (other phonons, electrons, magnons) in bulk, one-dimensional (1D) chain systems, and superlattices, particularly as these relate to transport. The quasiparticle interactions governed by the symmetries described above directly affect transport constrained to lie along the twist axis, as occurs for single chain systems (*e.g.*, polymer chains) and nanotubes. In such cases, conservation of angular momentum provides an added constraint on phonon-phonon interactions, for example, and limits the thermal resistance. We are examining the thermal transport characteristics of a wide variety of 1D chain systems, their bulk quasi-1D counterparts, nanotubes, and nanowires. A major limitation of the twist dynamics in bulk materials is its applicability only along a 1D axis, whereas thermal conductivity calculations involve integrations over the full Brillouin zone. We plan to build further insights into the relationships of interatomic forces and symmetry constraints on interactions more generally throughout reciprocal space in bulk materials.

References

- [1] T. Zhang, Z. Song, A. Alexandradinata, H. Weng, C. Fang, L. Lu, and Z. Fang, “*Double-Weyl phonons in transition-metal monosilicides*,” *Phys. Rev. Lett.* **120**, 016401 (2018).
- [2] D. Malz, J. Knolle, and A. Nunnenkamp, “*Topological magnon amplification*,” *Nat. Commun.* **10**, 3973 (2019).
- [3] H. Zhu, J. Yi, M.-Y. Li, J. Xiao, L. Zhang, C.-W. Yang, R. A. Kaindl, L.-J. Li, Y. Wang, and X. Zhang, “*Observation of chiral phonons*,” *Science* **359**, 579 (2018).
- [4] R. Juneja, S. Thébaud, T. Pandey, C. A. Polanco, D. H. Moseley, M. E. Manley, Y. Q. Cheng, B. Winn, D. L. Abernathy, R. P. Hermann, and L. Lindsay, “*Quasiparticle twist dynamics in non-symmorphic materials*,” accepted for publication in *Mater. Today Phys.*
- [5] T. Pandey, C. A. Polanco, V. R. Cooper, D. S. Parker, and L. Lindsay, “*Symmetry-driven phonon chirality and transport in one-dimensional and bulk Ba_3N -derived materials*,” *Phys. Rev. B* **98**, 241405 (2018).
- [6] W. D. C. B. Gunatilleke, R. Juneja, O. P. Ojo, A. F. May, H. Wang, L. Lindsay, and G. S. Nolas, “*Intrinsic anharmonicity and thermal properties of ultralow thermal conductivity $\text{Ba}_6\text{Sn}_6\text{Se}_{13}$* ,” *Phys. Rev. Mater.* **5**, 085002 (2021).

Publications

- [1] W. D. C. B. Gunatilleke, R. Juneja, O. P. Ojo, A. F. May, H. Wang, L. Lindsay, and G. S. Nolas, “*Intrinsic anharmonicity and thermal properties of ultralow thermal conductivity $Ba_6Sn_6Se_{13}$* ,” Phys. Rev. Mater. **5**, 085002 (2021).
- [2] M. K. Zalalutdinov, J. T. Robinson, J. J. Fonseca, S. W. LaGasse, T. Pandey, L. R. Lindsay, T. L. Reinecke, D. M. Photiadis, J. C. Culbertson, C. D. Kresse, and B. H. Houston, “*Acoustic cavities in 2D heterostructures*,” Nat. Commun. **12**, 3267 (2021).
- [3] W. Shi, T. Pandey, L. Lindsay, and L. M. Woods, “*Vibrational properties and thermal transport in quaternary chalcogenides: The case of Te-based compositions*,” Phys. Rev. Mater. **5**, 045401 (2021).
- [4] L. Yin, R. Juneja, L. Lindsay, T. Pandey, and D. S. Parker, “*Semihard iron-based permanent-magnet materials*,” Phys. Rev. Appl. **15**, 024012 (2021).
- [5] A. D. Christianson, V. R. Fanelli, L. Lindsay, S. Mu, M. C. Rahn, D. G. Mazzone, A. H. Said, F. Ronning, E. D. Bauer, and J. M. Lawrence, “*Phonons, Q -dependent Kondo spin fluctuations, and 4f phonon resonance in $YbAl_3$* ,” Phys. Rev. B **102**, 205135 (2020).
- [6] Y. Kuang, L. Lindsay, Q. Wang, and L. He, “*Lattice chain theories for dynamics of acoustic flexural phonons in nonpolar nanomaterials*,” Phys. Rev. B **102**, 144301 (2020).
- [7] C. Hua and L. Lindsay, “*Space-time dependent thermal conductivity in nonlocal thermal transport*,” Phys. Rev. B **102**, 104310 (2020).

Theory of Materials Program

Steven G. Louie (Lead PI), Lawrence Berkeley National Laboratory and UC Berkeley

Marvin L. Cohen (co-PI), Lawrence Berkeley National Laboratory and UC Berkeley

Dung-Hai Lee (co-PI), Lawrence Berkeley National Laboratory and UC Berkeley

Jeffrey B. Neaton (co-PI), Lawrence Berkeley National Laboratory and UC Berkeley

Lin-Wang Wang (co-PI), Lawrence Berkeley National Laboratory

Program Scope

The main goal of this program is to explore, understand and compute material properties and behaviors through theory and modeling. Areas to be studied cover: new superconductors and mechanisms; excited-state properties of novel bulk as well as quasi two- and one-dimensional systems; theoretical and methodological developments; and symmetry and topological phases of matter. A variety of theoretical techniques are employed, ranging from first-principles electronic-structure calculations to new conceptual and computational frameworks suitable for complex materials/nanostructures and strongly interacting electron systems. Emphases are both to investigate realistic material systems employing microscopic first-principles approaches, including many-electron effects, as well as to study physically motivated model systems. Specific projects are carried out: 1) for the understanding and/or discovery of new phases and new classes of materials with novel properties; 2) for the excited-state (spectroscopic and transport) properties of materials and nanostructures which are critical to phenomena such as optical responses, photocatalysis, optoelectronic behaviors, etc. that are central to energy-conversion research and applications; and 3) for cutting-edge developments of new theoretical methods that would allow accurate and predictive calculations. The methods, concepts, and results obtained are anticipated to have broad benefit to the community. Close collaborations with experimentalists are maintained. The program moreover make use and interact strongly with unique resources at LBNL, including the National Energy Research Scientific Computing Center (NERSC), the Molecular Foundry, and the Advanced Light Source (ALS).

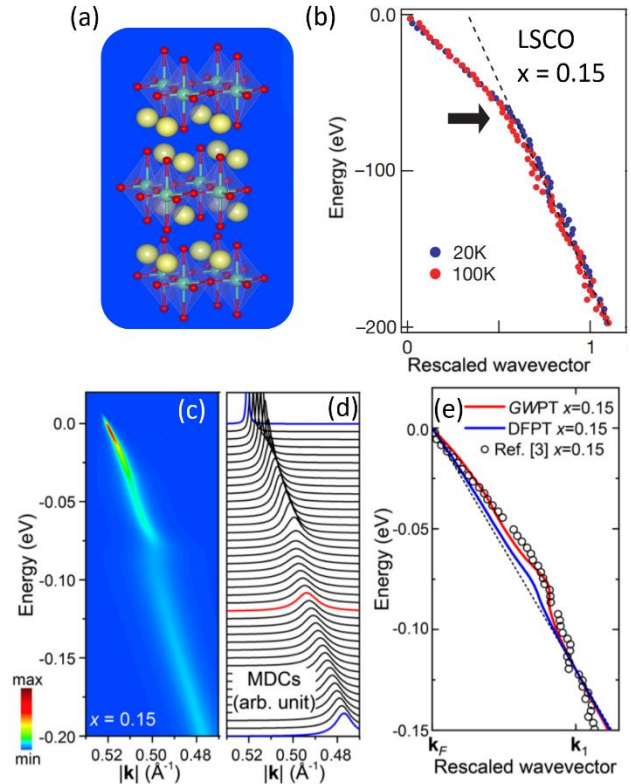
Keywords: Topological phases and phase transitions, two-dimensional materials, methods for correlated and complex materials

Recent Progress

Activities in the last two years covered advances on atomically thin two-dimensional (2D) crystals, topological phases and phase transitions, superconducting mechanisms, complex perovskites and oxides, strongly correlated systems, electron-phonon couplings, and new theoretical and computational methods. Twenty-nine (29) papers have been published

acknowledging this Program including publications in journals such as *Nature*, *Proc. Nat. Acad. Sci.*, *Phys. Rev. Letters*, *Angew. Chem. Int. Ed.*, *J. Am. Chem. Soc.*, among others. The team members have recognized with 4 awards. The work has led to formulation of new concepts, prediction of novel phenomena, and explanation of experiments for a range of materials. Some selected results are:

- *Ab initio* electron-phonon (e-ph) calculations using GW perturbation theory (GWPT) explain the origin of the observed kinks in angle-resolved photoemission spectra (ARPES) of high- T_c cuprates being due to correlation-enhanced electron-phonon coupling.
- Performed GW calculations on the band structure, core levels, and deformation potential (electron-phonon coupling) of monolayer FeSe, demonstrating the importance of electron self-energy corrections to these quantities. The results also justify a simple empirical +A approach, which was proposed to capture the renormalization of the electron-phonon interaction going beyond DFT in FeSe.
- First-principles calculations and analysis of the electron-phonon-induced self-energy in naphthalene crystals. Compute the zero-point renormalization and temperature dependence of the band gap, and the lifetimes of electronic states. The phonon renormalized GW band gap of 5 eV at room temperature is in good agreement with experiments, as well as the temperature-dependent mobilities of electrons and holes.
- Developed a natural orbital branching (NOB) scheme for time dependent density functional theory (TDDFT) simulation with wave function collapsing, enabling stochastic simulation using TDDFT.
- Using real-time time dependent density functional theory (rt-TDDFT), we have investigated several ultra-fast phase changes following an initial laser pulse excitation. It is found that, hot carrier cooling plays a significant role in order to predict the phase transition time and phase



(a) Structure of $\text{La}_{2-x}\text{Sr}_x\text{CuO}_4$ (LSCO). (b) ARPES data [A. Lanzara, et al, *Nature* **412**, 510 (2001)]. (c) *Ab initio* ARPES spectrum and (d) momentum distribution curves (MDC) of LSCO calculated with the GWPT method [Z. Li, G. Antonius, M. Wu, F.H. da Jornada, & S. G. Louie, *Phys. Rev. Lett.* **122**, 186402 (2019)]. (e) Comparison of theoretical results from GWPT method and standard density functional perturbation theory (DFPT) method with experimental data from A. Lanzara, et al.

recovery time. A Boltzmann factor is included to restore the detailed balance in rt-TDDFT, which makes it possible to describe hot carrier cooling.

- Developed a new scheme for charged defect image correction. In this formalism, there is no need to use the bulk dielectric constant, instead the dielectric constant is already included in the self-consistent calculations.
- Studied the microscopic mechanism for electronic device degradation due to the losing of H in Si-H bond. It is found that multi-electron process is important for breaking the Si-H bond.
- Developed a way to incorporate anharmonic effects in the nonradiative decay calculation formalism for the carrier dynamics in a bulk defect.
- Developed machine learning force field (ML-FF) methods, with linear fitting and neural network (NN); studied S alloy, carbon/Cu, carbon/SiC, and Al-H systems. The goal is to use ML-FF to study far from equilibrium systems.
- Used TDDFT to study laser induced ultrafast phase transitions in various systems (including IrTe₂, TaS₂/LaTe₃/TiSe₂ charge density wave phase change, In/Si(111) surface charge, VO₂ order/disorder change, bulk Si melting).
- Derived a new charge image correction formalism for charged defect calculations which, compared with previous intuition-based formalism, is more rigorous and converges faster.
- Achieved a proof that the boundary states of fermionic topological insulator and superconductors cannot be realized on a lattice having the dimension of the boundary.
- Developed a holographic theory of the topological phase transition between fermionic symmetry protected topological state.
- Showed that when geometric frustration inhibits the formation of charge density wave, strong electron-phonon interaction triggers high-temperature superconductivity.
- Achieved bosonization in two and three dimensions for strongly interacting fermion problems, such as the SU(2) gauge theory of the Mott insulator and the magic-angle twisted bilayer graphene.
- Studied the transport and electronic properties of novel energy materials, including halide and oxide perovskites, as well as organic semiconductors. Results include explaining an orthorhombic-to-cubic structural phase transition in (CH₃NH₃)PbI₃, and predicting that superlattices of La_{1/3}Sr_{2/3}FeO₃ (LSFO) are charge-order-driven ferroelectrics.
- Developed a new theory of phonon screening of excitons in semiconductors, which we applied to halide perovskites to understand their exciton binding energies.
- Discovered strong resonant excitons exhibiting a marked deviation from hydrogenic behavior in halide double perovskites whose nature depends sensitively on strong local field effects and chemical composition.
- Studied theoretically the nitrogen-terminated zigzag edges in an unconventional Bernal-stacked h-BN (AB-h-BN) that can be formed in a controlled fashion using a high-energy electron beam, showing that these “open” edges remain intact, enabling researchers potentially to investigate their edge states

- The observed metallization of hydrogen was examined and we proposed that it is caused by an electronic band structure effect rather than a structural transition.
- We show that there are errors in the analysis presented in the experimental paper reporting room-temperature high-pressure superconductivity by Snider et al. [2020 Nature 586 373–7], and with the correct analysis, the reported R vs. T data significantly deviate from the expected behavior. In particular, the extremely sharp change in resistance at the superconducting transition is not consistent with a strongly type II superconductor.

Future Plans

Planned activities are focused in: 1) reduced-dimensional systems, in particular quasi 1D and 2D materials; 2) excited-state properties of novel materials; 3) theoretical and methodological developments; 4) symmetry and topological phases; and 5) transport phenomena. Areas 1 & 4 concern with understanding and/or discovery of new phases and new classes of materials with novel properties. Areas 2 & 5 concern with excited-state (spectroscopic) and transport properties of materials and nanostructures. Area 3 concerns with developments of theoretical and computational methods that would allow accurate and predictive studies. Some selected projects include:

- Ab initio study of topological surface states in Bi_4Te_3 and topological invariants of its gaps.
- Role of electron-phonon coupling in iron-based superconductors and its doping dependence using GW perturbation theory.
- Ultrafast transition of intralayer exciton to interlayer exciton in MoS_2/WS_2 heterostructure.
- Novel exciton states and exciton spin dynamics induced by strong spin-orbital coupling in a two-dimensional topological insulator.
- Development of a new swapGW (self-consistent GW with appropriate polarizability) method, which provides a better description of quasiparticle excitations.
- Study of the impacts of phonons and chemical heterogeneity on the electronic structure and exciton binding energy of halide single and double perovskites.
- Development of a new framework based on ab initio Bethe-Salpeter equation approach for phonon-limited exciton diffusion in crystalline solids in both the band-like and hopping (exciton-polaron) regimes. We will apply this to singlets and triplets in acene crystals, as an initial application. We are also planning to perform *ab initio* calculations of novel Pb-free halide double perovskites.
- *Ab initio* calculation of the nature of excitons for Cs_2AgBX_6 , with $\text{B}=\text{Bi}$ and Sb , analyzing trends relative to simple models to better clarify its photophysics.
- Apply the new bosonization scheme to the physics of twisted bilayer graphene and spin liquid.
- Compute the optical and superconducting properties of candidate structural high-pressure phases of solid hydrogen, including the Cmca-12 , Cmca-4 and I41/amd-2 phases.
- Theoretical studies of low dimensional systems include one-dimensional chains and ultra-narrow nanoribbons which have been studied experimentally by encapsulation in nanotubes.

Selected Important Publications (out of 29 publications in the past two years)

1. W. H. Liu, J. W. Luo, S. S. Li, L. W. Wang, “Impurity diffusion induced dynamic electron donor in semiconductors”, *Phys. Rev. B* **100**, 165203 (2019).
2. Z.-X. Li, M. L. Cohen, and D.-H. Lee, “Enhancement of superconductivity by frustrating the charge order”, *Phys. Rev. B* **100**, 245105 (2019).
3. F. Brown-Altwater, G. Antonius, T. Rangel, M. Giantomassi, C. Draxl, X. Gonze, S. G. Louie, and J. B. Neaton, “Band gap renormalization, carrier mobilities, and the electron-phonon self-energy in crystalline naphthalene,” *Phys. Rev. B* **101**, 165102 (2020).
4. M. Weng, F. Pan, and L.W. Wang, “Wannier Koopmans method calculations for transition metal oxide band gaps” *npj Comp. Mat.* **6**, 33 (2020).
5. J.-H. Lee, A. Jaffe, Y. Lin, H. I. Karunadasa, and J. B. Neaton, “Origins of the Pressure-Induced Phase Transition and Metallization in the Halide Perovskite (CH₃NH₃)PbI₃”, *ACS Energy Lett.* **5**, 2174 (2020).
6. D. Y. Qiu, S. Coh, M. L. Cohen, and S. G. Louie, “Comparison of GW band structure to semiempirical approach for an FeSe monolayer,” *Phys. Rev. B* **101**, 235154 (2020).
7. L. Miao and L.W. Wang, “Liquid to crystal Si growth simulation using machine learning force field”, *J. Chem. Phys.* **153**, 074501 (2020).
8. S. Y. Park, K. M. Rabe, and J. B. Neaton, “Superlattice-induced ferroelectricity in charge-ordered La_{1/3}Sr_{2/3}FeO₃”, *Proc. Nat. Acad. Sci.* **116**, 23972 (2020).
9. L.W. Wang, “Natural Orbital Branching Scheme for Time-Dependent Density Functional Theory Nonadiabatic Simulations”, *J. Phys. Chem A* **124**, 9075 (2020).
10. M. Dogan, M. L. Cohen, “Magnetic multilayer edges in Bernal-stacked hexagonal boron nitride,” *Phys. Rev. B.* **102**, 155419 (2020).
11. M. Dogan, S. Oh and M. L. Cohen, “Observed metallization of hydrogen interpreted as a band structure effect”, *J. Phys. Condens. Matt.* **33**, 03LT01 (2020).
12. Z. Li, M. Wu, Y. H. Chan, and S. G. Louie, “Unmasking the Origin of Kinks in the Photoemission Spectra of Cuprate Superconductors”, *Phys. Rev. Lett.* **126**, 146401 (2021).
13. M. Dogan and M. L. Cohen, “Anomalous behavior in high-pressure carbonaceous sulfur hydride”, *Phys. C: Supercond. Appl* **583**, 1353851 (2021).
14. M. L. Aubrey, A. S. Valdez, M. R. Filip, B. A. Connor, K. P. Lindquist, J. B. Neaton, H. I. Karunadasa, “Directed assembly of layered perovskite heterostructures as single crystals” *Nature* **597**, 355 (2021)

Center for Computational Study of Excited-State Phenomena in Energy Materials

Steven G. Louie (lead PI), Lawrence Berkeley National Laboratory and UC Berkeley

Jeffrey B. Neaton (co-PI), Lawrence Berkeley National Laboratory and UC Berkeley

James R. Chelikowsky (co-PI), University of Texas, Austin

Jack R. Deslippe (co-PI), Lawrence Berkeley National Laboratory

Naomi S. Ginsberg (co-PI), Lawrence Berkeley National Laboratory and UC Berkeley

Felipe H. da Jornada (co-PI), Stanford University

Daniel Neuhauser (co-PI), UC Los Angeles

Diana Y. Qiu (co-PI), Yale University

Eran Rabani (co-PI), Lawrence Berkeley National Laboratory and UC Berkeley

Feng Wang (co-PI), Lawrence Berkeley National Laboratory and UC Berkeley

Chao Yang (co-PI), Lawrence Berkeley National Laboratory and UC Berkeley

Program Scope

The mission of the Center for Computational Study of Excited-State Phenomena in Energy Materials (C2SEPTEM) is to develop and implement new theories, methods, algorithms, and computer codes to explain and predict excited-state phenomena in materials. C2SEPTEM performs research on first-principles many-body perturbation theory and advanced algorithms, as well as their experimental validation and efficient implementation to high performance computers. Studies on quasiparticle excitations, optical spectra, trion and bi-exciton formation, exciton-exciton interactions, nonlinear optical processes, time-dependent phenomena, and more are carried out for bulk and reduced-dimensional systems. These phenomena are particularly important in processes of energy conversion, transport and storage. Existing ab initio methods and software, especially for multiple-particle correlated excitations and time-dependent electron phenomena incorporating essential electron-electron interactions, however have been under explored and hence limiting their studies in real materials. The work at C2SEPTEM (through a team of physical scientists, applied mathematicians and computational scientists) aims to fill this gap. In addition to expanding the frontiers of knowledge, an end product will be an integrated open-source software package, BerkeleyGW and associated codes, with capabilities (utilizing current petascale and future exascale high performance computers) to predict and understand a variety of excited-state phenomena from first principles. The research, based on equilibrium and nonequilibrium interacting multi-particle Green's function approach, are validated via

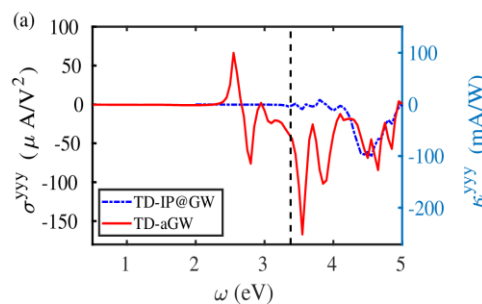
spectroscopic and other excited-state experiments. Software packages with new functionalities are regularly released to the community.

Keywords: Excited-state phenomena, computational materials science, novel methods and software deliverables

Recent Progress

Activities in the past two years cover development and release of high-performance software packages, novel theories for nonequilibrium dynamics, correlated multiparticle excitations, electron-phonon and exciton-phonon couplings, stochastic approaches, optical phenomena in two-dimensional (2D) materials, moiré heterostructures, defects, and advanced numerical algorithms. Twenty-seven (27) papers have been published in the past two years acknowledging this Program, including publications in journals such as *Nat. Materials*, *Nat. Commun.*, *Proc. Natl. Acad. Sci.*, *Phys. Rev. Letters*, *Nano Letters*, among others. The team members at C2SEPEM have been recognized with 6 significant awards. We have released new software versions -- BerkeleyGW 3.0 and StochasticGW 2.0, as well as made the NanoGW code released online. We organized the 7th BerkeleyGW Tutorial Workshop and 2021 Berkeley Excited State Conference, attracting over three hundred participants. The Center's efforts have led to formulation of new concepts/methods, prediction of novel phenomena, explanation of experiments for a range of materials, as well as strengthening the wide software users' and researchers' community. Some selected results include:

- Developed novel algorithms and code optimization leading to linear scaling of BerkeleyGW on CPU and CPU/GPU hybrid high performance computing systems for large-scale GW and GW-BSE calculations with thousands of atoms.
- Performed GW and GW-BSE studies of defects in a 10,968-electron system that scaled to 4,560 Summit nodes (27,360 GPU's, 99% of Summit computer) reaching speed of 106 Petaflop/s with time to solution of 10 minutes, resulting in the work being recognized as a 2020 ACM Gordon Bell Prize Finalist.
- Discovery of giant exciton-enhanced shift currents and direct current conduction with subbandgap photo excitations produced by many-electron interactions, using our newly developed time-dependent adiabatic GW (TD-aGW) approach for optical spectroscopies, pump-probe phenomena, and nonlinear optics.
- Development of ab initio quantum many-body theory and codes for 3- and 4-particle correlated excitations (biexcitons and trions, singlet exciton fission, etc.)
- Explained the origin of the observed kinks in the angle-resolved photoemission spectra of high Tc cuprates (a two-decade old puzzle) being due to correlation-enhanced electron-phonon interaction, using our GWPT method.



Excitonic effects strongly enhance shift current in monolayer GeS.

- Developed a subspace formalism for efficient solution of the Bethe-Salpeter equation for the optical properties of low dimensional materials.
- Verification of reproducibility of GW calculations performed through an international, multi-institutional study benchmarking G_0W_0 quasiparticle gaps in ZnO and TiO₂ across three different codes – BerkeleyGW, ABINIT, and Yambo – which is the first of its kind in solid-state systems.
- Showed that a simple chemical treatment of sulfur-vacancy defects in the transition metal dichalcogenide (TMD) 2D semiconductors allows one to control and increase carrier mobilities, and to increase photoluminescence by two orders of magnitude, suggesting a route for engineering defect properties in 2D materials, leading to tunable electronic properties.
- Demonstrated that excitons in organic-inorganic quantum wells are highly anisotropic and may be modified with changing chalcogen atoms in the material lattice, providing new design principles for engineering these complex emerging systems and their photophysics.
- Developed a reduced-order model to compress the two-time Green's function and an optimization procedure for updating the model during the time-evolution of the Green's function, as well as a dynamic mode decomposition (DMD) based approach to analyze and predict the off-diagonal elements of the two-time Green's function.
- Developed method and implemented code for exciton-phonon scattering to study exciton-phonon interactions in monolayer TMDs.
- Released BerkeleyGW 3.0 -- New releases include spinor formalism, finite momentum excitons within BSE, and broader support for mean-field starting points. (<https://berkeleygw.org/2021/05/27/berkeleygw-software-package-version-3-0-release/>)
- Developed codes for computing the magneto-optical properties of 2D magnets.
- Development of a range-separated stochastic resolution of identity for second-order Green's function theory to reduce the statistical error and bias.
- Application of a stochastic approach to study the optical properties of large 2-dimensional and nanotubular excitonic molecular aggregates.
- Performed *ab initio* study on the spectral properties of doped ZnO and SrTiO₃, revealing important polaron features which elucidate angle-resolved photoemission experiment.
- Computed the GW band structure of monolayer FeSe and justified a recent semiempirical approach for modeling the nonlocal and dynamical self-energy in this high-temperature superconducting system.
- Developed scalable implementation of polynomial filtering for density functional theory calculations in real-space pseudopotential codes.

Future Plans

Planned activities are focused in: 1) development of novel theories for excited-state phenomena in energy materials; 2) development of new computational algorithms and implementations to access new physics; 3) continuing to port existing high-performance software

packages to GPUs for exascale computing and maintain an active user community; and 4) applying developed new theories and methods to study optical and dynamics phenomena in two-dimensional materials and moiré heterostructures, defects, and molecular crystals, in close collaboration with experimental efforts. Some selected projects include:

- Further develop formalism and optimize code for correlated multiparticle excitations in materials using many-body perturbation theory techniques on the 3- and 4-particle Green's functions.
- Apply correlated multiparticle excitation approach to study trions and biexcitons in 1D (e.g., nanotubes and nanoribbons) and 2D (e.g., TMDs), in coordination with experimental efforts.
- Develop a linear response method for exciton-phonon interactions, combining results for electron-phonon interaction with exciton wavefunctions from GW-BSE calculations.
- Use exciton-phonon interactions to explore: phonon-mediated exciton transport in organic materials, phonon contribution to dielectric screening of excitons, exciton valley coherence times in TMDs, etc. Concurrent validation experiments are planned.
- Develop approaches to compute how carrier plasmons in TMDs affect exciton binding energy, exciton linewidth, and energy splitting between low-lying exciton and trion states.
- Further develop time-dependent GW (TD-GW) method for field-driven phenomena and pump-probe spectroscopies such as time-resolved angle-resolved photoemission spectroscopies (trARPES), nonlinear optics, field-driven phase transitions, etc.
- Perform GW-BSE calculations to elucidate the physical origin and nature of novel moiré excitons in TMD homo- and hetero-bilayers, in collaboration with experimental efforts.
- Explore phenomenon of exciton-enhanced spin shift current in 2D materials using TD-GW approach.
- Understand doping effects on exciton and trion binding energies in monolayer TMDs.
- Examine deep-level defects in semiconductors as candidates for realizing long-lived and photon-addressable qubits in quantum computing applications.
- Extend real-space codes to address problems in nucleation, solvation, and dielectric screening, as well as transfer of charged excitations to and from molecular species and interfaces.
- Developments of StochasticGW code: a) implantation to GPU and hybrid CPU/GPU computing systems, b) elimination of need for multiple single-particle orbitals, and c) implementation of sparse grid representations.
- Improve dynamic mode decomposition (DMD) based model order reduction methods and validate with more sophisticated models.
- Further optimize BerkeleyGW and StochasticGW components (post/pre-processing routines, optional code-paths, etc.) for HPC systems such as Perlmutter, Frontier and Aurora.
- Experimental probe of ultrafast spectroscopy of moiré phonon excitations and charge transfer dynamics in different TMD heterostructures and examine the twist angle dependence.

Selected Important Publications (out of 27 publication in the past two years)

1. W. Dou, M. Chen, T. Y. Takeshita, R. Baer, D. Neuhauser, and E. Rabani, "Range-Separated Stochastic Resolution of Identity: Formulation and Application to Second Order Green's Function Theory," *J. Chem. Phys.* **153**, 074113 (2020).
2. A. J. Lee, M. Chen, W. Li, D. Neuhauser, R. Baer, and E. Rabani, "Dopant levels in large nanocrystals using stochastic optimally tuned range-separated hybrid density functional theory." *Phys. Rev. B* **102**, 035112 (2020).
3. M. Del Ben, C. Yang, Z. Li, F. H. da Jornada, S. G. Louie, and J. Deslippe. "Accelerating Large-Scale Excited-State GW Calculations on Leadership HPC Systems," in SC20: International Conference for High Performance Computing, Networking, Storage and Analysis, pp. 1-11. IEEE, (2020).
4. T. Rangel, M. Del Ben, D. Varsano, G. Antonius, F. Bruneval, F. H. da Jornada, M. J. van Setten, O. K. Orhan, D. D. O'Regan, A. Canning, A. Ferretti, A. Marini, G. M. Rignanese, J. Deslippe, S. G. Louie, and J. B. Neaton, "Reproducibility in G_0W_0 calculations for solids," *Comput. Phys. Commun.* **255**, 107242 (2020).
5. K. H. Liou, C. Yang, and J.R. Chelikowsky, "Scalable implementation of polynomial filtering for density functional theory calculation in PARSEC," *Comp. Phys. Commun.* **254**, 107330 (2020).
6. S. G. Louie, Y. H. Chan, F. H. da Jornada, Z. Li and D. Y. Qiu, "Discovering and understanding materials through computation," *Nat. Mater.* **20**, 728 (2021).
7. D. Y. Qiu, F.H. da Jornada, and S. G. Louie, "Solving the Bethe-Salpeter equation on a subspace: Approximations and consequences for low-dimensional materials," *Phys. Rev. B* **103**, 045117 (2021).
8. M. Chen, D. Neuhauser, R. Baer, and E. Rabani, "Stochastic Density Functional Theory: Real- and Energy-Space Fragmentation for Noise Reduction," *J. Chem. Phys.* **154**, 204108 (2021).
9. K.H. Liou, A. Biller, L. Kronik, and J. R. Chelikowsky, "Space-Filling Curves for Real-Space Electronic Structure Calculations," *J. Chem. Theory Comput.* **17**, 4039 (2021).
10. Y.-H. Chan, D. Y. Qiu, F. H. da Felipe, and S. G. Louie, "Giant exciton-enhanced shift currents and direct current conduction with subbandgap photo excitations produced by many-electron interactions," *Proc. Natl. Acad. Sci. U.S.A.* **118**, e1906938118 (2021).

Non-Abelian quasiparticles and topological superconductivity for quantum information science

Yuli Lyanda-Geller, yuli@purdue.edu

Department of Physics and Astronomy, Purdue University, West Lafayette IN, 47907

Program Scope

The project goal is to uncover new non-Abelian effects and states with non-Abelian statistics. We concentrate on the leading candidate for generating topological superconductivity with parafermion quasiparticles, a system with a fractional quantum Hall effect spin transition at a $2/3$ filling of the ground Landau level. We find signatures of topological superconductivity in numerical modeling of proximity coupling of an s-type superconductor to the domain wall at the boundary between spin-polarized and un-polarized fractional quantum Hall liquids where helical fractional quantum Hall edge modes with opposite spin propagate in opposite directions. In the light of experimental results for measuring resistivity of the domain wall, different from expected for helical modes picture, we develop the effective theory approach for description of tunneling of Luttinger modes through the domain wall of a finite length, confirming viability of this setting for generating parafermions.

Keywords: Non-Abelian statistics, topological superconductivity, Luttinger liquid.

Recent Progress

In search for non-Abelian statistics and advancing the prospects for topological quantum computing, we have proposed that higher-order non-Abelian excitations, such as parafermions, may emerge in a system with fractional quantum Hall effect spin transitions. In the numerical modeling on the disc and torus, we found that counter-propagating modes with opposite spin polarization emerge on the boundary between electrostatically-controlled polarized and un-polarized regions of the fractional quantum Hall liquid. Effective theory consideration showed that these counter-propagating modes with opposite spin, i.e., the helical modes, are the lowest-lying modes when just edge-like states on the boundary are considered. Furthermore, numerical modeling in the torus configuration demonstrated that s-superconductors can be proximity-coupled to these helical modes, leading to topological superconductivity. For the fractional quantum Hall effect at $2/3$ filling of the ground Landau level, a six-level defect structure arises in the superconducting gap, signifying the emergence of parafermion excitations.

However, the resistivity of the domain wall on the boundary of polarized and un-polarized liquids, which follows from this picture of helical states, leads to a characteristic relation between the currents flowing in the system. Namely, the current propagating along the edge of the sample and the current diverted from the edge and propagating along the domain wall

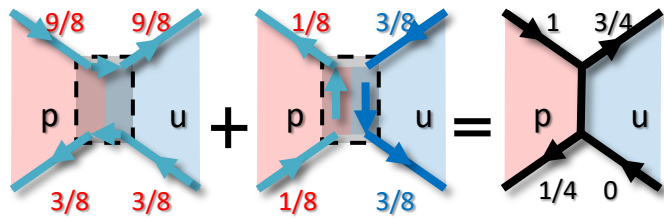
formed on the boundary between polarized and un-polarized quantum Hall liquids must be equal to each other. Surprisingly, the experimental measurements at small voltages and currents show that the current diverted by the domain wall is at most 11% of the current propagating along the edge of the sample, challenging our understanding of the system.

To address this challenge theoretically we considered scattering of Luttinger liquid modes by the domain wall. When we modeled the domain wall in an earlier work, we did not consider coupling of modes propagating in the domain wall with modes propagating along the edge of the sample. Torus and disc configurations allowed to exclude edge modes at the sample boundary in the numerical simulation of the domain wall. In the experiment, scattering of edge modes is crucial.

Our theoretical consideration of the system in the presence of both polarized and un-polarized fractional quantum Hall phases coexisting in a single two-dimensional layer required extension of the Wen K-matrix formalism and developing theory describing two phases simultaneously. Considering tunneling, we first assumed that it only occurs between the same-spin electron modes. For such spin-conserving tunneling, we consequently considered tunneling in several models. We started with considering tunneling through a triple junction connecting the current along the edge in the polarized phase, the current along the edge in the un-polarized phase, and the current propagating along the boundary between two phases along the domain wall. We made our calculations in the strong-coupling limit, for which the exact solution is known for tunneling of Luttinger modes through a point contact. Next, we modelled the domain wall as two triple junctions on the two opposite edges of the sample. We then further included scattering between modes propagating along the domain wall with the same spin within a segment connecting the two triple junctions. Finally, we extended our consideration to the domain wall of a finite length. Remarkably, incoming and outgoing currents for all these models coincide, due to properties of transfer matrices for Luttinger modes. We found that the edge channels in polarized and un-polarized phases are populated unequally, forming a number of down- and up-stream charge, spin and neutral modes. Remarkably, for spin-conserving tunneling the ratio of the current propagating along the domain wall and the current propagating along the edge equals $1/3$, three times less than in the naïve model. This, however, is still three times bigger than observed experimentally.

To understand this difference, we took into account the possibility of the effect of the dynamic nuclear spin polarization in a GaAs heterostructure that hosts our two dimensional electron liquid. The main mechanism of the nuclear spin polarization is the hyperfine coupling between electron and nuclear spins. On the quantum Hall plateaus, electron-nuclear spin flip processes are usually suppressed because of the large difference between the electron and nuclei spin splitting, preventing energy conservation in mutual spin-flip transitions. However, near the boundary between polarized and un-polarized phases, spin-up and spin-down electronic states are almost degenerate, opening the possibility of the effective hyperfine coupling and polarization of nuclear spins.

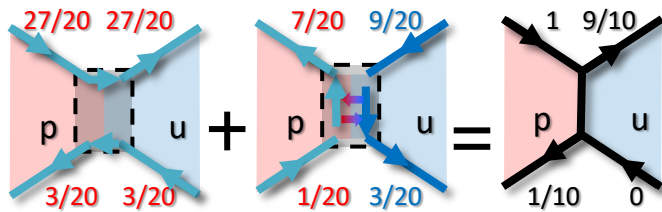
In order to take into account the electron nuclear hyperfine coupling on tunneling of the Luttinger modes, we developed the approach that allows for admixture of Luttinger modes with opposite spins. When such admixture is absent for spin-conserving processes, the results for tunneling can be conveniently expressed in terms of two kinds of modes. The first kind includes the quasiparticle modes with the same spin that propagate along the edge of the two-dimensional



Visualization of propagation of charge currents in the absence of nuclei-spin mediated electron spin flips across the boundary between polarized and un-polarized fractional quantum Hall liquid.

electron liquid and do not enter the domain wall. The second kind includes the quasiparticle modes with opposite spins that flow along the boundaries of the polarized and un-polarized electron liquids.

Scattering due to hyperfine interaction of electron and nuclear spins mixes the modes propagating along the domain wall. The mode travelling on the un-polarized side of the boundary, which is a superposition of a charge and a spin mode, and the mode travelling on the polarized side of the boundary, which is a superposition of a charge and a neutral mode, become coupled. We calculate the incoming and outgoing charge, spin and neutral currents in the presence of such spin admixture. The quasiparticle modes with the same spin still propagate along the edge of the two-dimensional electron liquid. However, the conservation of the total current results in the current redistribution between all modes. The ratio characterizing the domain wall charge current then becomes a function of the spin-flip probability and changes continuously between $1/3$ of the current along the edge for spin-conserving case and zero in the case when all spins are allowed to flip. Then all modes are reflected after multiple scattering inside the domain wall and, as a result, propagate along the edge. This explains the decrease of the current diverted through the domain wall with increase of the length of the boundary, which leads to increasing exposure to the hyperfine coupling of electron and nuclear spins that causes reflection of modes. In particular, for the probability of admixture equal to $3/4$, we calculate that the ratio of the current diverted through the domain wall to the current passing along the edge equals to 0.11, explaining the experimental result at small currents.



Propagation of charge currents in the presence of electron-nuclei spin flip mediated admixture of modes inside the domain wall on the boundary between polarized and un-polarized fractional quantum Hall liquid.

Furthermore, experimentalists were able to test that nuclei play considerable role in tunneling of electron modes. This was done by passing high current through the system. Passing high current results in the so-called Overhauser effect leading to sizable spin polarization of nuclear subsystem, which in turn reduces further electron-nuclear spin flip flops. Such reduction must decrease admixture of opposite spin modes inside the domain wall. Indeed, experiments measuring diverted current after nuclear spins were polarized by passing large currents showed the three-fold increase of the diverted current compared to that measured at small passing currents. This indicates formation of a bottleneck for spin flips due to Overhauser pumping of nuclei and a crossover from spin-non-conserving to almost spin-conserving transport.

As a result, our prediction of ratio $1/3$ of diverted current to current passing along the edge in spin-conserving tunneling theory was almost matched, confirming our understanding of the system. The results show that

- The boundary between polarized and un-polarized phases hosts counter-propagating modes with opposite spin-polarization.
- Preliminary nuclear spin pumping decreases mixture of these modes.

The next step is understanding superconducting proximity effect in the area at the boundary between two phases. Our preliminary considerations show that electron-nuclear spin interactions can potentially play an important role in emergence of parafermions in this setting. Experimental realization of the proximity coupling of an s-superconductor to the boundary area must lead to topological superconductivity with parafermion excitations.

Future Plans

We will further study the role of nuclei spins and the opportunities to control hyperfine interactions in order to generate parafermions. Crucial questions on theory of the superconducting proximity coupling to the fractional quantum Hall system will be addressed. We will investigate charge carrier holes system and will study Majorana fermions in the presence of superconducting proximity coupling in the region with electrostatic-gate induced crossing in a two-dimensional holes system, as well as study the role of crossings in magnetic field spectra in addition Coulomb spectra of quantum dots. Finally, investigation of superconducting proximity effects is underway for InAs/Al system, which is the breeding ground for Majorana fermions, where we will access the role of spin-orbit effects in magnetic field effects on Josephson currents and critical supercurrents in the system.

Publications

1. Wang, Y., Ponomarenko, V., Wan, Z. *et al.* Transport in helical Luttinger liquids in the fractional quantum Hall regime. *Nat. Commun.* **12**, 5312 (2021); <https://doi.org/10.1038/s41467-021-25631-2>
2. A.C. Keser, Y. Lyanda-Geller, O. P. Sushkov, Nonlinear quantum electrodynamics in Dirac materials, arXiv preprint arXiv:2101.09714
3. Y. B. Lyanda-Geller, V. Ponomarenko, Y. Wang, and L. P. Rokhinson "Engineering parafermions in helical Luttinger liquids" (Invited), Proc. SPIE 11805, Spintronics XIV, 1180515 (1 August 2021); <https://doi.org/10.1117/12.2595632>
4. J. Liang, G. Simion, and Y. Lyanda-Geller, Parafermions, induced edge states, and domain walls in fractional quantum Hall effect spin transitions, *Phys. Rev. B* **100**, 075155 (2019); <https://doi.org/10.1103/PhysRevB.100.075155>
5. Li, C. H., Qu, C., Niffenegger, R.J. *et al.* Spin current generation and relaxation in a quenched spin-orbit-coupled Bose-Einstein condensate. *Nat. Commun.* **10**, 375 (2019). <https://doi.org/10.1038/s41467-018-08119-4>

Materials for Ultra-Coherent, Mobile, Electron-Spin Qubits

S.A. Lyon (Princeton University), M.I. Dykman (Michigan State University), M.D. Henry (Sandia National Lab), E.A. Shaner (Sandia National Lab)

Program Scope

This project consists of joint experimental and theoretical research to understand how electrons bound the surface of superfluid helium can be used as qubits. Current theoretical work has shown how intersubband transitions of the electrons in a parallel magnetic field can be used as a tunable quantum simulator of many-body systems, and are similar to the optical excitation of color centers, such as an NV^- center in diamond. Coupling of the intersubband transition to the in-plane dynamics of the strongly correlated electron system is similar to the admixing of phonons to optical transitions in the color centers. Current experimental work has shown that high electron densities can be supported on thin helium films covering an ultrasmooth amorphous metallic electrode. The densities are in range where quantum effects are predicted to appear. High electron density structures are also being incorporated into measurements of the electron spin relaxation and coherence in these systems.

Keywords: electrons on helium, electron spin coherence, electron-electron interactions

Recent Progress

Theory: The major goal of the theoretical work is to establish the physics of electrons and electron spins on helium and to understand the spin coherence for moving electrons as well as for localized electrons. In addition to ripples, electron-electron interactions can lead to a nontrivial spin decoherence mechanism. In a nonuniform magnetic field electron-electron effects can admix in-plane excitations in the electron system to a spin transition. Recent work has discovered a new approach to understand the electron-electron interactions.

Electrons on the helium surface display sharp resonant absorption lines related to the transitions between the subbands of quantized motion transverse to the surface. A magnetic field parallel to the surface strongly affects the absorption spectrum. We have analyzed the spectra and have compared the results with experiment.¹ The initial suggestion that these spectra provide a valuable information about the dynamics of the electron system has been confirmed by a careful calculation. The results show that, indeed, the system of electrons on helium can serve as a quantum simulator of the many-

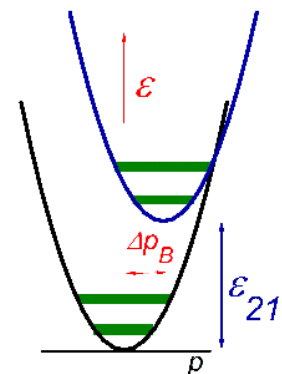


Figure 1. Energy spectrum of electrons in the two lowest subbands. The parabolas are shifted in momentum due to the in-plane magnetic field.

body systems. Of particular relevance is the possibility to simulate the optical spectra of the NV⁻ and other color centers in a broad range of temperatures, from the deeply quantum regime to room temperature.

We have shown that the electron absorption spectrum permits a direct characterization of the many-electron dynamics in the regime of the quantum nondegenerate electron liquid and a Wigner crystal. The parameters of the system can be varied over a broad range of temperatures. The shape of the in-plane excitation spectrum of the electron system is controlled by the magnetic field normal to the surface and also by the electron density.

The theoretical predictions on the shape of the spectrum and its dependence on the control parameters have been quantitatively confirmed by the experiment. The results are in full agreement, with no adjustable parameters, in a broad range of electron densities and temperatures, where the shape of the spectra changes dramatically.

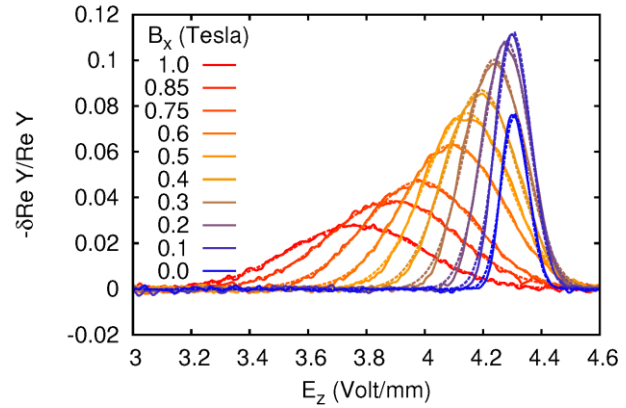


Figure 2. Calculated (dashed) and experimental (solid) relative intersubband absorption spectra of electrons coupled to a strongly correlated electron system in a perpendicular magnetic field ($B_z = 0.5$ T). The in-plane magnetic field, B_x , controls the coupling of the transition to the in-plane fluctuations of the electron system.

Experiment: The major experimental goal in this project is to understand the spin relaxation and decoherence dynamics of electrons bound to the surface of superfluid helium. In particular we expect these times to be long, and to be largely unaffected by transport (except the apparent loss of coherence if the electrons are transported in an inhomogeneous magnetic field). There are three details which make pulsed electron spin resonance experiments with these electrons difficult: (1) the electron densities are low (no more than $2 \times 10^9/\text{cm}^2$ on bulk He), which severely limits the signal; (2) the expected spin relaxation time (T_1) is long, which makes signal averaging difficult or impossible; and (3) if the diffusion of the electrons is unconstrained, the nonuniformity of the magnetic field will lead to an artificially short apparent T_2 .

An approach we have developed to circumvent these issues is to deposit a high density of electrons on a van der Waals film covering a metallic surface. The electron density on bulk helium is limited by a long-wavelength hydrodynamic instability, and higher densities can be supported on thin films. Previous experiments along these lines have been limited by the roughness of the underlying metal films, but we have developed ultra-smooth amorphous metal films. One such metal is an alloy of Ta, W, and Si. As shown in Fig. 3, we have used Kelvin probe (vibrating capacitor) measurements to monitor the electron density on the helium. The voltage offset between the two curves gives us a measure of the electron density by calculating

the resulting helium thickness using the known van der Waals constant of helium. As seen in the figure, this experiment produced an electron density of $10^{11}/\text{cm}^2$.

A density in the range of $10^{11}/\text{cm}^2$ is useful for the spin experiments, but also interesting in its own right. It has been a goal since the 1970s to achieve high enough electron densities on helium to reach a transition between the Wigner crystal (which forms here at zero magnetic field, unlike in semiconductor 2D systems) and a Fermi liquid. However, a definitive demonstration of a Fermi liquid has not been achieved. It has long been known that thin films of helium can in principle support high enough electron densities to reach degeneracy, as shown in the calculated phase diagram in Fig. 4, and our experimental situation is approximately that of the curve labeled $\delta=1$ (metallic substrate and $\sim 10\text{nm}$ helium film). Our current experiments are indicated by the red lines in Fig. 4. It would seem that we have reached the necessary conditions, but we must conduct transport experiments to determine the electron mobility. These transport experiments are currently underway. The mobility can be suppressed by both residual roughness on the metal surface and the formation of polarons (dimpling of the He surface). It may be possible to further reduce the surface roughness, and polarons are an interesting phenomena in their own right.

We have also measured electron densities approaching $10^{12}/\text{cm}^2$ in some experiments, but the electrons leak away on time scales of order minutes. If those densities can be stabilized, they might be particularly interesting, since the upper part of Fig. 4 near $T = 0$ corresponds to quantum melting of the Wigner crystal. It is unclear at this time whether observing quantum melting in these experiments will be possible.

These high electron density experiments are also a route to measuring the spin dynamics, as noted above. For the spin experiments we are working at 300 mK, since the calculations in Fig. 4 suggest that we will have a

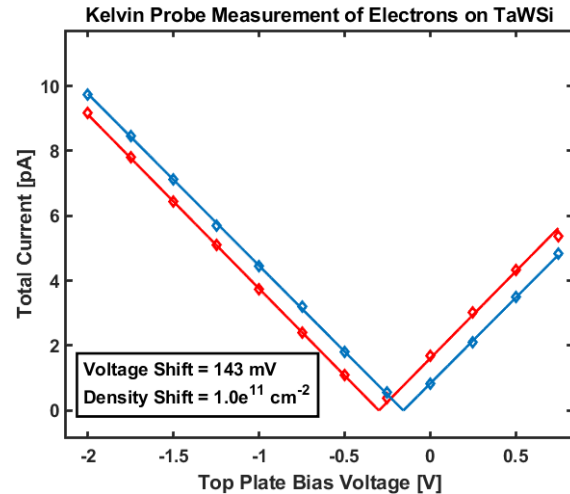


Figure 3. Measurement of the voltage shift in a Kelvin probe before (blue) and after (red) charging the surface of a van der Waals helium film covering an amorphous metallic electrode. The voltage shift corresponds to an electron density of about $10^{11}/\text{cm}^2$. The experimental temperature was 1.6K.

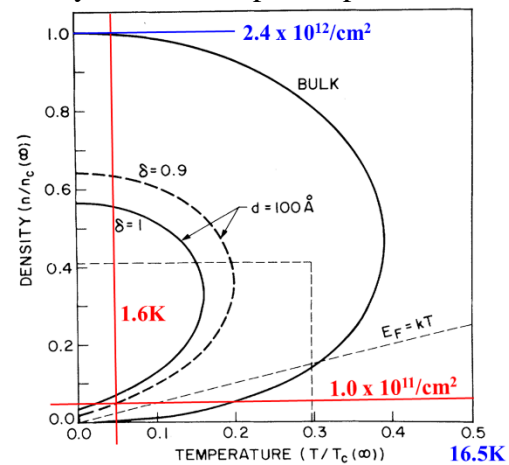


Figure 4. Calculated phase diagram for electrons on the surface of bulk helium (the rightmost solid curve) as well as on thin helium films covering a substrate. The experiments of Fig. 3 approximately correspond to the curve for $\delta = 1$, and the red lines are the experimental temperature and electron density from Fig. 3. The calculations are from ref. 2.

Wigner crystal. Crystallization will also promote the formation of polarons, reducing wave function overlap so that we can measure the pure spin properties. Somewhat lower densities (which leads to a thicker He film and expands the Wigner crystal region in Fig. 2) may be desirable to avoid overlap. The high electron densities will increase the signal in the electron spin resonance (ESR) experiments. At the same time the Wigner crystal will inhibit the diffusion of the electrons, and thus avoid the apparent decoherence which arises from motion in an inhomogeneous field. Also, the electrons are held very close to a normal metal where the Johnson noise currents are calculated to relax the electrons' spin in under a second (we adjust the superconducting transition temperature of the TaWSi to be low, which combined with the applied magnetic field for the ESR measurements ensures it is normal). Thus this arrangement promises to overcome the three major experimental hurdles discussed earlier. A complication is that the filament for depositing electrons must be kept outside the microwave resonator, to avoid reducing its Q-factor. Thus we have developed a mechanical arrangement to move the TaWSi coated sapphire substrate out of the resonator to deposit the electrons and then pull it into the resonator for the spin experiments at 300 mK. Those experiments are underway.

Future Plans

The theoretical work is aimed at developing the means for analyzing the effects of the coupling of electrons to ripplons and the electron-electron interactions on the electron spin dynamics. The immediate experimental plans are to use the high electron density structures in the spin resonance experiments, and to measure the electron transport properties on the thin He films above the amorphous metallic electrodes.

References

1. A. Chepelyanskiy, D. Konstantinov, and M. I. Dykman, "Many-Electron System on Helium and Color Center Spectroscopy," *Phys Rev Lett*, **127**, 016801 (2021).
2. F.M. Peeters and P.M. Platzman, "Electrons on Films of Helium: A Quantum Mechanical Two-Dimensional Fermion System," *Phys Rev Lett*, **50**, 2021 (1983).

Publications

1. K. Moskovtsev and M. I. Dykman, "Mobility of a spatially modulated electron liquid on the helium surface," *Phys Rev B*, **101**, 245435 (2020).
2. A. Chepelyanskiy, D. Konstantinov, and M. I. Dykman, "Many-Electron System on Helium and Color Center Spectroscopy," *Phys Rev Lett*, **127**, 016801 (2021).

Magnetism in Moiré Materials

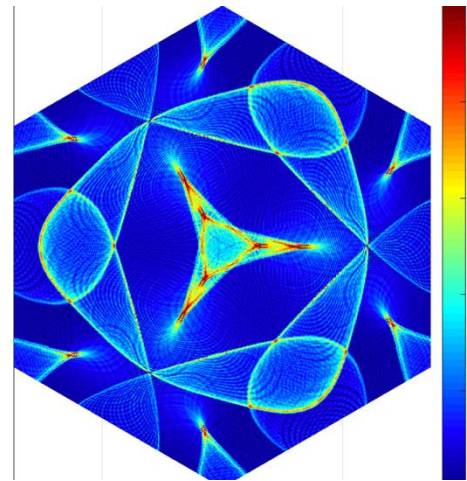
Allan H. MacDonald, University of Texas at Austin

Program Scope

I am working on three different projects related to magnetism in moiré materials:

i) I expect that itinerant electron ferromagnetism occurs in moiré materials, and wish to identify host materials and system parameters for which this order occurs at room temperature. The motivation for this work is the view that artificial gate-tuned two-dimensional ferromagnets that satisfy this criterion are very likely to be extremely valuable for technology if they can be realized, *i.e.* my motivation is a desire to find realistic applications of these materials. In current work, I have identified favorable conditions for ferromagnetism in TMD moiré materials and am working to estimate maximum T_c 's. These are limited by both by the size of the exchange splitting between majority and minority spins, and by the magnetic stiffness, with the former mechanism being dominant for very broad bands and the latter mechanism for narrow bands. My intuition is that the maximum possible T_c 's occur when these two bounds are comparable.

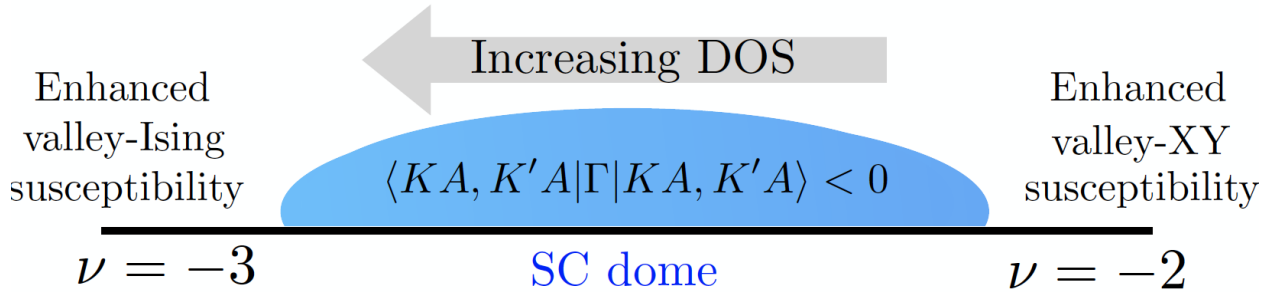
ii) The spin-valley order that is common in magic angle twisted bilayer graphene systems is a generalized form of ferromagnetism in which two-component electron spinors are replaced by four-component spin-valley systems. In regular ferromagnets, the order parameter is specified by three real numbers, normally partitioned as the magnitude and direction of the spin-magnetization vector. In MATBG, on the other hand, the order parameter is specified by up to fifteen parameters, which can be viewed as the eigenvalues and eigenvectors of the spin/valley density matrix. I believe that the phenomenology of flavor-symmetry-breaking in MATBG shows evidence of non-analytic corrections to Fermi liquid theory that generalize those that are important in standard itinerant electron magnetism, and that this new highly tunable example sheds additional light on these electron-electron interaction effects.



Momentum-dependence of low-energy particle-hole phase space in MATBG. Singularities at momenta that span the Fermi-surface are responsible for non-analytic corrections to Fermi liquid theory.

iii) I believe that spin-valley-sublattice fluctuations within the flat bands of MATBG are a likely origin of their superconductivity. I have generalized the paramagnon picture used previously to address the interplay between magnetism and fermion pairing in He and in metals, to the case of MATBG's spin-valley octet. The picture of superconductivity that results depends on one key observation related to the symmetries of the flat-band wavefunctions, namely that

superconductivity occurs when interactions between electrons on the same sublattice are attractive, even if interactions between electrons on opposite sublattices are strongly repulsive.



Superconducting dome in magic angle twisted bilayer graphene. Attractive interactions between electrons on the same sublattice are promoted by proximity to spontaneous sublattice polarization phase transitions. Because pairing between electrons on opposite sublattices is favored, proximity to valley-polarized phases near integer filling factors obstructs superconductivity.

The paramagnon theory of superconductivity provides an explanation for a number of aspects of the phenomenology of MATBG superconductivity.

i) *Influence of Boron-Nitride (hBN) Alignment*-- Aligned hBN induces a finite sublattice polarization in a graphene sheet, and weakens sublattice pseudospin fluctuations. Since all other contributions to the intrasublattice interaction are repulsive, the paramagnon theory predicts that superconductivity is suppressed by hBN alignment, in agreement with current experimental findings.

ii) *Coulomb screening*-- When MATBG devices are surrounded by nearby material that is conducting or has a large dielectric constant, insulating states at integer filling factors become less prominent in the phase diagram and superconductivity is found over a broader range of filling factors. Insulating states are understood in terms of exchange-splitting between bands associated with different flavor states that is larger than the flatband bandwidth. Since the exchange splittings are dominated by the Coulomb interaction, they are expected to be reduced by enhanced environmental screening. The reduction in insulating state gaps seen experimentally is therefore expected.

iii) *Particle-hole asymmetry of superconductivity*-- Experiment shows that the tendency toward valley polarization, which opposes superconductivity, is stronger for electron-doped than for hole-doped MATBG. This tendency is due in part to conduction bands that are less dispersive than the valence bands and have a different shape. It is quite likely that the normal state on the electron-doped side is a sublattice ferromagnet, and this is supported by the observation of the AHE over a wide range of filling factors in devices with and without aligned hBN.

Keywords: Moiré materials, itinerant electron magnetism, spintronics

Recent Progress

This project has started only recently. All progress is recent and described above.

Future Plans

I intend to continue research on all three aspects of this research.

Publications

1. “Exact Diagonalization for Magic-Angle Twisted Bilayer Graphene,” Pawel Potasz, Ming Xie, and A.H. MacDonald, *Phys. Rev. Lett.* **127**, 147203 (2021).

A new approach to the interacting phonon problem

Chris A. Marianetti

Columbia University, Department of Applied Physics and Applied Mathematics

Program Scope

There are two main goals of the proposed work: develop novel techniques *both* to compute the space group irreducible vibrational Hamiltonian of a crystal from a first-principles theory and to approximately solve the resulting quantum many-phonon problem. The central novelty of our methods is an unprecedented ability to trade off between efficiency and accuracy as dictated by the problem under consideration.

Our bundled irreducible derivative (BID) approach to computing phonons and their interactions results in the most efficient finite-displacement algorithm allowed by group theory[1], which facilitates the precise characterization of phonon and their interactions over all categories of crystals. An ongoing task is determining practical guidelines for executing BID, and when to incorporate our complementary lone irreducible derivative (LID) approach. A further development of our irreducible approaches is the incorporation of symmetrized strain derivatives of the space group irreducible derivatives at any order, which will allow us to efficiently handle constant pressure boundary conditions that are typically encountered in experiment. Alternatively, strain derivatives can be used as a critical test of the phonon interactions. Finally, we are concerned with characterizing anharmonic vibrational Hamiltonians over broad classes of materials, including the extraction of minimal models of anharmonicity.

Constructing the anharmonic vibrational Hamiltonian is the first step towards vibrational observables, but the resulting many-phonon problem must then be solved in some approximation. Our proposal is committed to implementing standard approaches to the many-phonon problem, such as diagrammatic perturbation theory, classical molecular dynamics, generalized Hartree-Fock, and many other techniques. Moreover, we are committed to developing new techniques which circumvent the shortcomings of existing methods. Our variational discrete action theory[2,3] (VDAT) is a powerful new way of formulating variational theories in an unbiased manner, which encompasses many existing simple theories (e.g. Hartree-Fock, Gutzwiller, etc), but also yields previously undiscovered approaches which are orders of magnitude faster for computing ground state properties as compared to state-of-the-art theories at a similar fidelity.

An equally important thrust of our proposal is the development of modular, open source, free software that implements our ideas for the broader community. The unique aspect of our software suite, *Principia Materia* (PM), is its group theoretical underpinning, which allows for both electrons and phonons to be treated in terms of irreducible representations of the space group. Both our BID and LID approaches for computing phonons and their interactions are

implemented in PM. Given that our methodology is more than an order of magnitude faster than popular finite displacement methods, we are confident that PM will rapidly acquire a large user base once released.

Keywords: Computing phonons and their interactions; variational approaches to the quantum many-body problem.

Recent Progress

An important recent development is the execution of our BID and LID approach for precisely and efficiently computing phonons in crystals with charge density waves (CDW), or soft phonon modes that are at least partially influenced by Fermi surface nesting. The computation of phonons in CDW crystals is typically sensitive to various aspects of the calculation, requiring a precise extrapolation of the discretization error of any finite displacement calculations, in addition to the proper convergence of any discretization involved in the other aspects of the first-principles calculation. We chose two crystals which have phase transition associate with soft modes: the shape memory alloy AuZn and the Kagome lattice material KV3Sb5.

AuZn has been faithfully studied in the literature using both density functional perturbation theory (DFPT) and finite displacement approaches[4]. Despite this rigorous effort, the authors still end up with results that are qualitatively wrong in at least one respect (see Figure 1, left panel). We computed the irreducible phonons using our LID approach, which can be thought of as the original frozen phonon approach, but it employs the smallest supercell allowed by group theory. While the method in the published literature used a single-supercell finite displacement approach in conjunction with a 6x6x6 supercell (i.e. multiplicity 216), our LID approach uses a series of supercells with multiplicities less than or equal to 6, which are a factor of 36 smaller. Given the scaling of plane wave DFT calculations, this computation speedup is dramatic. Most importantly, our phonons faithfully represent the curvature of the Born-Oppenheimer potential. The published results incorrectly predicts one of the acoustic modes to be soft (see gold line), which can be easily falsified by directly computing the elastic constants (see green lines).

The second CDW material that we addressed was the Kagome material KV3Sb5, which was only recently published[5]. Like any CDW material, the soft modes in this crystal should be anticipated to be sensitive. In this case, the authors chose to compute the phonons in a 3x3x2 supercell, which is a poor choice given that it is not commensurate with the experimentally observed wavevector of the CDW transition. As a result, the authors only indirectly study the soft mode via interpolation, and substantial errors can be observed (see Figure 1, panel b). The appreciable errors observed in AuZn and KV3Sb5 are more likely the rule than the exception, and our LID and BID approaches will clearly not only lead to massive computational speedups,

but also precise numerical results. In order to understand the subtle physics of these CDW materials, it is imperative to have qualitatively correct, precise results.

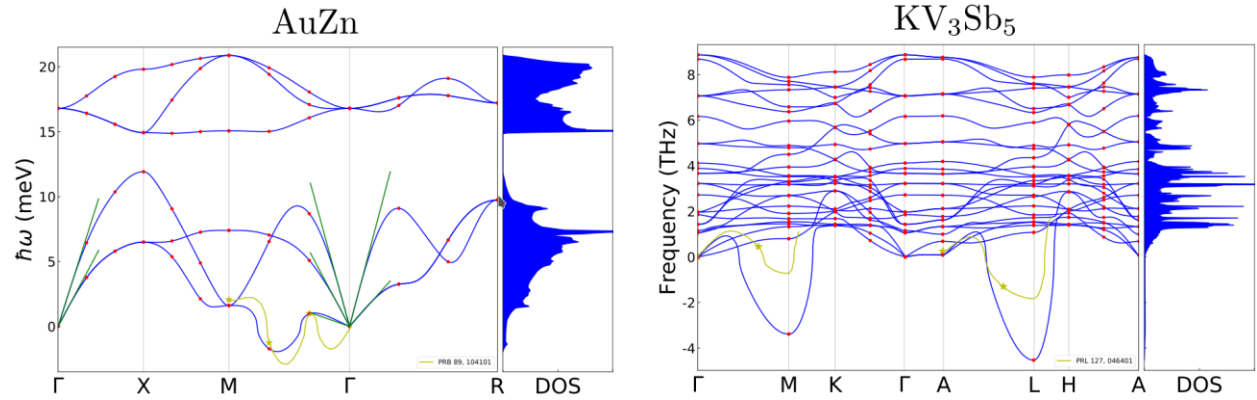


Figure 1: Phonons and corresponding DOS computed using the lone irreducible derivative approach with DFT for AuZn and KV3Sb5; direct numerical measurements are denoted with red points, while blue lines result from Fourier interpolation. Green lines are acoustic modes that are independently obtained by computing the irreducible elastic constants using the LID method for strain derivatives. Gold stars are finite displacement results from competing approaches in the literature, while gold lines are a Fourier interpolation (see legend for reference). (Left Panel) Phonons/DOS for the shape memory alloy AuZn. (Right Panel) Phonons/DOS for Kagome lattice material KV3Sb5.

In addition to making progress on demonstrating the power of our LID and BID approaches for computing phonons, we have also achieved important milestones for computing cubic and quartic phonon interactions in simple metals. We have computed the cubic phonon interactions in the face centered cubic metals Al, Cu, Au, and Ag; and quartic phonon interactions have been computed for Al. Additionally, cubic phonon interactions have been computed for the simple body centered cubic metals Li, Na, and K. The cubic phonon interactions were used to predict phonon line widths within perturbation theory, while the quartic interactions were used to predict line shifts within perturbation theory.

Another important development was the implementation of molecular dynamics using our space group irreducible derivatives, which we refer to as order N molecular dynamics (ONMD). ONMD is a powerful approach, yielding the numerically exact solution to the classical dynamics. When the simulation supercell is sufficiently large, the ONMD results must agree with the phonon line widths and shifts as predicted from classical perturbation theory. We have tested our ONMD in the case of Al, and we have found good agreement with classical perturbation theory at low temperatures. Studying the ONMD results at larger temperatures then allows one to examine the degradation of leading order perturbation theory, and determine which diagrams must be added.

One of our key developments in the past year was the formulation of the variational discrete action theory (VDAT)[2, 3]. VDAT consists of two core ideas: an ansatz for the many-body density matrix, denoted the sequential product density matrix (SPD), and a formalism for evaluating the SPD, denoted the discrete action theory (DAT). The SPD is inspired by the

Trotter-Suzuki decomposition, and is characterized by an integer N ; with $N=1$ recovering the generalized Hartree-Fock approximation, $N=2$ recovering the Gutzwiller approximation, and the limit of N going to infinity recovers the exact solution. The DAT gives rise to an “integer time” Green’s function, and a discrete framework which parallels usual many-body physics. VDAT is not only a different way of thinking, but we proved that it can dramatically outperform state of the art techniques for computing ground state properties in important canonical models of interacting electrons. VDAT will have a transformative effect when solving the multiband Hubbard model in the context of real materials, and it is equally applicable to interacting phonon problem.

Future Plans

The foundational goals of this proposal have been achieved, and now the most exciting phase begins. In the near term, we will begin to compute phonons in strongly correlated electron materials, including various iron pnictides, cuprates, and actinides. These calculations will likely involve DFT, DFT+U, hybrid functionals, and possibly DFT+DMFT. In terms of cubic and quartic phonon interactions, we will soon move to CDW crystals, where the anharmonicity is essential for predicting the CDW transition temperature, temperature dependent elastic constants, and other relevant observables. Our first candidate will likely be AuZn, given the cubic symmetry and a sufficient interest within the literature.

We will continue to implement traditional approaches to the many-phonon problem using our space group irreducible vibrational Hamiltonian. In particular, we will implement VDAT using $N=1$, which recovers the usual variational approach of Hooton. Additionally, we will implement classical Monte-Carlo to complement our ONMD.

Our final task in the near future is our first major software release. Our entire code suite, which is now more than 25,000 lines, was rewritten from the ground up during the past year. A substantial amount of work is still needed to polish the user interface, documentation, and tutorials such that the broader community can use it. A small group of test users has already been established outside Columbia, which will be critical to ensure other experts enjoy using our software.

References

1. L. Fu, M. Kornbluth, Z. Cheng, and C. A. Marianetti, Phys. Rev. B 100, 014303 (2019).
2. Z. Q. Cheng and C. A. Marianetti, Phys. Rev. Lett. 126, 206402 (2021).
3. Z. Q. Cheng and C. A. Marianetti, Phys. Rev. B 103, 195138 (2021).
4. L. Isaeva, P. Souvatzis, O. Eriksson, and J. C. Lashley, Phys. Rev. B 89, 104101 (2014).
5. H. X. Tan, Y. Z. Liu, Z. Q. Wang, and B. H. Yan, Phys. Rev. Lett. 127, 046401 (2021).

Publications

1. Z. Cheng and C. A. Marianetti, Variational discrete action theory, Phys. Rev. Lett. 126 206402 2021
2. Z. Cheng and C. A. Marianetti, Foundations of variational discrete action theory, Phys. Rev. B 103 195138 2021
3. E. B. Isaacs and C. A. Marianetti, Compositional phase stability of correlated electron materials within DFT+DMFT, Phys. Rev. B 102 045146 2020
4. Z. Cheng C. A. Marianetti, Off-shell effective energy theory: A unified treatment of the Hubbard model from $d=1$ to $d=\infty$, Phys. Rev. B 101 081105 2020

Less common topological phenomena in bulk materials

Igor I. Mazin, George Mason University

Program Scope

This project is about theoretical and computational investigation of different effects directly or indirectly related to topological properties of electron functions, largely based on non-trivial magnetic textures. The scope stays away from such actively studied topological phenomena like Dirac and Weyl points, Majorana fermions, topological insulators. The project started on 9/1/2020, that is, it's been active 13 month.

The principal directions of research are (1) less common magnetic structures (e.g., transverse conical spirals) and associated with them topological Hall effect (2) Frustrated magnetic orders and associated phenomena such as spin-liquid candidates, Mermin-Wagner fluctuations, toroidal moment orders, vector and scalar spin chirality, etc.

Keywords: Electronic structure, magnetism, magnetotransport

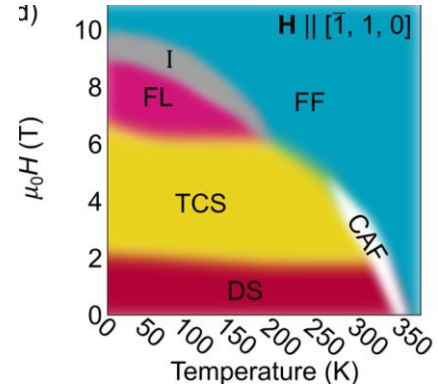
Recent Progress

(1) Time-reversal symmetry breaking without spatial inversion breaking, with and without spin-orbit coupling, and topological (in terms of the Berry phase topological properties) magnetotransport; computational design of such materials.

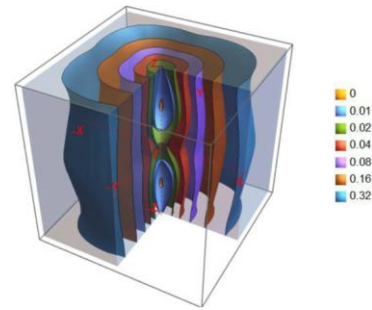
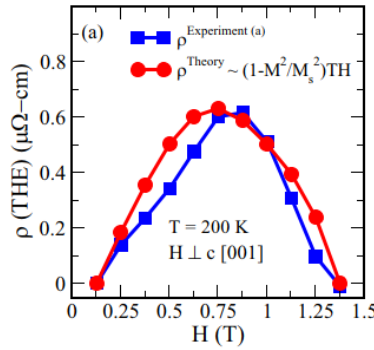
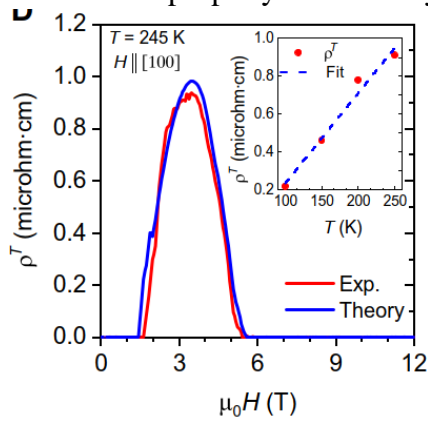
We have just published a paper entitled "Prediction of unconventional magnetism in doped FeSb_2 " [1]. There we predict that the well-known nonmagnetic semiconductor, FeSb_2 , under either hole (Cr) or electron doping, for specific concentration ranges, becomes a magnetic metal. The magnetism is unconventional, sharing antiferromagnetic (zero net magnetization, by symmetry) and ferromagnetic (nonzero spin-splitting of electronic bands, anomalous Hall response, and magneto-optical effects) properties. This magnetic state can be considered a third type of collinear magnets, besides the ferro(i)magnets and antiferromagnets. This state was recently dubbed *altermagnetism*. Symmetry constraints for such magnetism, which will serve as the basis for future computational materials search, have been derived. Effect of spin-orbit on the spin splitting and anomalous responses has been calculated, and it was shown that the predicted easy axis is favorable for anomalous properties. I am also proud of this paper because, in my opinion, it is as of now the most accessible description of the concept of altermagnetism.

(2) Topologically nontrivial magnetic states, such as combinations of different spiral states, with and without skyrmionic component.

I have published two papers on a double-spiral magnet, YMn_6Sn_6 , where I used first principle calculations and the mean-field theory to fully identify all magnetic phases as a function of temperature and external fields. My predictions have been fully confirmed by neutron scattering experiments. Further, I have developed a theory of scalar chirality driven by thermal fluctuations in a specific state, transverse conical spiral (TCS). This can be viewed as a dynamic skyrmionic liquid. The theory provides a quantitative explanation of the observed topological Hall effect (THE)[2,3]. After that, we have successfully applied this theory to another spin-spiral compound, Fe_3Ga_4 [4], where the interesting magnetic phase had been previously misidentified as a longitudinal spin density wave, but we have proved it is TCS. We then were able to explain the THE observed in this compound. Work on other materials where we believe one can observe this property is underway (see below).



Experimental phase diagram of YMn_6Sn_6 identifying the theoretically predicted phases DS (distorted spiral), TCS (transverse conical spiral) and FL (fan-like). TCS phase features the fluctuation-driven topological Hall effect.



Fluctuation-driven topological Hall effect in YMn_6Sn_6 (left) and Fe_3Ga_4 (right). Experiment fitted to our theoretical formula.

Calculated isoenergetic surfaces for helical spiral states in Fe_3Ga_4 .

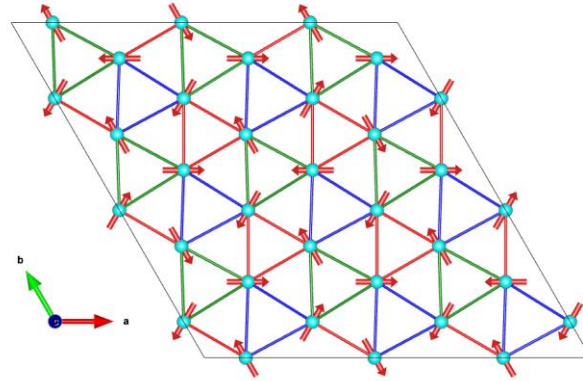
(3) Other nontrivial magnetic states

(a) We worked with experimentalists on a new magnetic material, BaCoSiO_4 . Using first principles calculations and the group theory, we identified the microscopic origin of the chiral (but not spiral) spin state, which turned out to be a

Chiral configuration	Left		mirror	Right	
Toroidal moment, \mathbf{t}	-	+	+	+	-
Vector chirality, ϵ	+	+	+	+	+
Scalar chirality, κ	+	-	+	+	-

Illustration of toroidicities and chiralities identified in BaCoSiO_4 .

consequence of a nontrivial hierarchy of magnetic interactions (which was predicted in our calculations, and confirmed). We furthermore found that, in addition, the material also hosts a toroidal order, which is coupled to the external field via the Dzyaloshinskii-Morya interactions, and can be tuned (as demonstrated experimentally) by moderate fields[5].



Magnetic unit cell of BaCoSiO4 at $H=0$ T. This order is fully explained by our calculations.

(b) I have been involved in a broad-scale investigation of a novel quasi-2D magnet AgRuO₃ with rather unusual properties, which we believe are driven by formation of specific molecular orbitals[6]

(c) The two papers above have been driven by our theory efforts at least as much as by the experiment. Regarding the next paper, Ref. 7, the collaboration was initiated Prof. Ni Ni who needed a microscopical explanation of the nontrivial magnetic phase diagram of the Sb-doped MnBi₄Te₇. This is a topological material in the conventional sense, but the nontrivial properties observed by Ni Ni turned out to be related not with this fact, but with unusual frustration and Mermin-Wagner fluctuation in this quasi-2D magnet. I generated a mean field theory of this phenomenon for this material, which was able to explain the observed phase transitions.

(d) I was finally able to finish a work, with experimentalists, on the magnetic dynamics of acatamite, an example of strongly coupled $S=1/2$ sawtooth chains, weakly coupled by frustrated inter-chain interactions. This paper has a long history, and initially was aimed to find elusive magnetization plateaus predicted for $S=1/2$ sawtooth chains. However, first principle calculations by H. Jeschke were not supporting the required parameter range. I joined the project at a later point, and was able to reconcile the calculations with the experiment using a proper mean field theory (our collaborators were able to confirm by direct quantum Monte Carlo that this is indeed a good approximation here). Part of this work was completed when I was supported by DOE[8].

Future Plans

I plan to continue research along the same lines as those outlined above. For the direction 1, my ultimate goal is to work out a protocol to predict new altermagnets through datamining. Isolated altermagnets will also be subject of studies, some of them are in work now, theoretically by myself and experimentally by my experimental colleagues. Yet another novel direction is altermagnetism driven by gating; we have preliminary results on two compounds with qualitatively different mechanisms of electro-altermagnetic coupling. For the direction 2, I am working in a very close contact with the experimental group of Prof. Ghimire at GMU. We have currently a paper under review about a topological (in the direct meaning of the word, i.e. Lifshits) transition

in YMn_6Sn_6 . We are also working together on anomalous Hall effect and magnetic interactions in TbMn_6Sn_6 . I am also planning to look for other potential candidate materials for the fluctuational topological Hall effect. In the moment I am mostly interested in a particular itinerant cycloidal magnet (and possibly unconventional superconductor under pressure), for which there is already experimental evidence for this particular (rather rare) type of magnetism, and of superconductivity, but no theory for either.

Publications

The numbered 13-month list of publications acknowledging this award

1. Prediction of unconventional magnetism in doped FeSb_2 , I. I. Mazin, K. Koepernik, M.D. Johannes, R. Gonzalez-Hernandez, L. Smejkal, PNAS **118**, e2108924118 (2021)
2. Competing magnetic phases and fluctuation-driven scalar spin chirality in the kagome metal YMn_6Sn_6 , N. J. Ghimire, R. L. Dally, L. Poudel, D. C. Jones, D. Michel, N. Thapa Magar, M. Bleuel, M. A. McGuire, J. S. Jiang, J. F. Mitchell, J. W. Lynn, I. I. Mazin. Sci. Adv. **6**, eabe2680 (2020)
3. Chiral properties of the zero-field spiral state and field-induced magnetic phases of the itinerant kagome metal YMn_6Sn_6 , R. L. Dally, D. Michel, P. Siegfried, I. I. Mazin, N. J. Ghimire, J. W. Lynn. Phys. Rev. B **103**, 094413 (2021)
4. Spin Spiral and Topological Hall Effect in Fe_3Ga_4 , M. Afshar, I. I. Mazin, Phys. Rev. B **104**, 094418 (2021)
5. Field-tunable toroidal moment in a chiral-lattice magnet. L. Ding, X. Xu, H. O. Jeschke, X. Bai, E. Feng, A. S. Alemany, J. Kim, F. Huang, Q. Zhang, X. Ding, N. Harrison, V. Zapf, D. Khomskii, I. I. Mazin, S.-W. Cheong, H. Cao. Nature Comm **12**, 5339 (2021)
6. Magnetic and electronic ordering phenomena in the $[\text{Ru}_2\text{O}_6]$ honeycomb lattice compound AgRuO_3 , W. Schnelle, B. E. Prasad, C. Felser, M. Jansen, E. V. Komleva, S. V. Streltsov, I. I. Mazin, D. Khalyavin, P. Manuel, S. Pal, D. V. S. Muthu, A. K. Sood, E. S. Klyushina, B. Lake, J.-C. Orain, H. Luetkens. Phys. Rev. B **103**, 214413 (2021)
7. $\text{Mn}(\text{Bi}_{1-x}\text{Sb}_x)_4\text{Te}_7$: tuning the magnetism and non-trivial band topology through antisite disorders, C. Hu, S.-W. Lien, E. Feng, S. Mackey, H.-J. Tien, I. I. Mazin, H. Cao, T.-R. Chang, and Ni Ni, Phys. Rev. B **104**, 054422 (2021)
8. Magnetization Process of Atacamite: A Case of Weakly Coupled $S=1/2$ Sawtooth Chains. L. Heinze, H. O. Jeschke, I. I. Mazin, A. Metavitsiadis, M. Reehuis, R. Feyerherm, J.-U. Hoffmann, M. Bartkowiak, O. Prokhnenko, A. U. B. Wolter, X. Ding, V. S. Zapf, C. Corvalán Moya, F. Weickert, M. Jaime, K. C. Rule, D. Menzel, R. Valentí, W. Brenig, and S. Süllo, Phys. Rev. Lett. **126**, 207201 (2021)

Structure and Electronic Properties of Dirac Materials

E.J. Mele, University of Pennsylvania

Program Scope: This project explores topological and quantum geometrical effects in the Bloch bands and response functions of patterned 1D and 2D lattice structures. The overall goal is to explore the geometrical characterization of nontrivial Bloch band manifolds, to connect this with their physical responses and to design/develop new structures that exploit these functionalities in applications. Systems of current interest include graphenes and their multilayers, nonlinear photonic lattices, and topological semimetals.

2. Keywords: 2D materials, van der Waals heterostructures, Nonlinear Optical Properties

Recent Progress

1. Quantum Geometry and Anomalous Electrodynamics in One Dimensional Graphene Bilayers

We proposed and analyzed the Dirac Harper model as a one-dimensional limit of a moire supercell material. We used the model to analyze flat band physics in graphene moire bilayers. Unlike 2D twisted bilayer graphene the DH model introduces a moire superlattice scale in one spatial dimension and retains lattice-scale periodicity in the orthogonal coordinate. This can be experimentally achieved by imposing a layer-antisymmetric shear strain on a graphene bilayer. Our work showed that this construction leads naturally to a spinorial extension of the well studied one dimensional Harper model describing electron motion on a long-period modulated lattice. The DH model contains a family of Hamiltonians parameterized by the conserved perpendicular crystal momentum. We discovered that the 1D model supports a manifold of narrow electronic bands near charge neutrality. The measure of states (per cell) in this manifold reproduces exactly the measure of low energy states in TBLG. Furthermore the DH model clearly identifies the origin of these bands which arise from nontrivial commutation relations between matrix-valued operators that represent in-plane and interlayer motion of the electrons

In a followup work we showed that electronic motion in the narrow bands of the DH model supports an unconventional quantum geometry. This is encoded in a new symplectic two-form distinct from the usual Berry curvature, which instead couples momentum and position degrees of freedom. We discovered that the experimental signature of this mixing is an anomalous response function by which an in-plane electric field drives a Hall-like (i.e. perpendicular) flow of a dipole current (importantly, not the charge current). We demonstrated that this is the intrinsic electric-dipole magnetic dipole coupling intrinsic to a chiral crystal structure. Furthermore the theory identifies a new reciprocity relation identifying responses to layer symmetric and antisymmetric electric fields.

2. Phase Fields in Low energy models for Twisted Bilayer Graphene. The interpretation of valley projected low energy models for narrow bands in TBLG remains a subject of an active discussion. In this work we show that the symmetries required in the low energy models can be constrained experimentally by analyzing the intensities of Bloch waves backscattered from localized scatterers.

Specifically we used a phase field analysis of the backscattered electron densities that directly measures the phase winding of the Bloch_wavefunctions at low energy and clearly identifies the active symmetries in the low energy models.

3. Boundary States from Periodic Magnetic and Pseudomagnetic Fields in Single Layer Graphene

In this work we examine the effects of zone folding produced by spatially periodic gauge fields in single layer graphene (SLG). We analyzed the spectral properties of SLG in the presence of periodic magnetic and pseudomagnetic fields. In both cases the Dirac cone of single layer graphene fractures into spectrally isolated manifolds of minibands separated by well developed gaps. For periodic magnetic fields the theory provides a realization of a class of Chern insulators where the total flux per unit cell is zero. This shows the expected distribution of topologically protected edge modes on all boundaries under open boundary conditions. By contrast for the pseudofield configuration, where the pseudofield arises from strain-coupling in the Dirac theory, time reversal symmetry is preserved and we discover instead a pattern of robust helical channels confined to a single edge.

Future Plans

1. Network Models for Moire Superlattices

A typical moire superlattice is a patterned 2D structure that uses twist/strain to produce a synthetic crystal on long spatial periods: 10-50 nm that vastly exceed the size of a primitive cell. Electrons moving in this background can be characterized as evolving through a family of slowly spatially varying local Bloch Hamiltonians $H(k,r)$ where r is the position in the moire cell and k is the locally conserved crystal momentum. Each $H(k,r)$ is a Hamiltonian for a short lattice periodic structure. We discovered that these local operators have a special symmetry: for each $H(k,r)$ on the energy isosurfaces there are special discrete directions where the “forward” and “backward” moving Bloch waves remain unmixed. The union of these directions properly defines a helical transport network: namely links that intersect at nodes where all the backscattering occurs. The situation is similar to the Chalker Coddington network for propagation on electrostatic equipotentials in the quantum Hall effect except that here the network is helical (forward and backward propagation occurs) not chiral.

Network models for TBLG have been considered previously in the literature (Kinderman (2018), Martin (2019), deBeule (2019)), but we find that there are essential differences between these ad-hoc models and our construction. We are working to refine this idea further. Of primary interest is the connection between the S matrix on this network and the flat band condition near charge neutrality. Specifically, we think we can use the scattering at the network nodes to identify a new mechanism for re-entrant band flattening in the small magic angle regime. Also our construction identifies an important intrinsic time scale in this problem: namely the propagation time $T = d/v$ where d is the mean length of a link and v is the Dirac velocity. This period can be tuned to match the period of a time-dependent external driving field (a’la Floquet) and may allow continuous tuning of a flat band condition even away from the structural magic angle.

2. Periodic Gauge Fields in Graphene: Phase Transitions

Our work on SLG in a periodic strain-induced pseudogauge field demonstrates that the Dirac bands fracture into miniband manifolds with well developed gaps between them. These gaps host robust boundary modes, but unlike the Chern insulator they are polar, i.e. they reside on a single crystallographic boundary and not its negate. Driving this system with circularly polarized light breaks time reversal symmetry and by using the Floquet-Magnus expansion can drive this to a Chern insulating state which must support protected modes on all boundaries. We will study the phase transition between these state and the valley selective gap closures that isolate them. The goal is to better understand the mechanism that leads to helical modes on a single boundary in the pseudofield case and the possibility of controlled switching between these limits.

3. Quantum Metric and Anomalous Second Harmonic Generation: Second harmonic generation is known as an intrinsic optical response of an inversion broken material. However, by higher order coupling to light (through electric quadrupole or magnetic dipole) an anomalous second harmonic signal can exist in inversion symmetric media, and such anomalous second harmonic processes have been observed. Ordinarily with the coherence length of the electronic states is small compared to an optical wavelength (atoms/molecules) this anomalous response is very weak. However in a band manifold this coherence length is the spread of the maximally localized Wannier function. This can be much larger, and in fact in obstructed band structures (Chern insulators) it can even diverge. We are developing this idea as a quantitative metric that can identify candidates for strong anomalous second harmonic generation. The work combines the geometric theory of the Fubini Study metric with an observed spectroscopic property.

Publications

1. V.T. Phong and E.J. Mele, "Boundary Modes from Periodic Magnetic and Pseudomagnetic Fields in Graphene ", Arxiv: 2108:08414
2. A. Timmel and E.J. Mele, "Anomalous Electrodynamics and Quantum Geometry in the Dirac Harper Model for a Graphene Bilayer ", *Physical Review B*, Volume 104, 075419, 2021.
3. J. Lu, L. He, Z. Addison, E.J. Mele, B. Zhen, "Floquet Topological Phases in One-Dimensional Nonlinear Photonic Crystals, ", *Physical Review Letters*, Volume 126, 113901, 2021.
4. L. Gao, Z. Addison, E.J. Mele, A.M. Rappe, "Intrinsic Fermi Surface Contribution to the Circular Photogalvanic Effect ", Arxiv:2011.06542 (to appear in *Physical Review Research (Letters)*, 2020)
5. V.T. Phong and E.J. Mele, "Obstruction and Interference in Low Energy Models for Twisted Bilayer Graphene ", *Physical Review Letters*, Volume 125, 176404, 2020.
6. A. Timmel and E. J. Mele, "Dirac Harper Theory for One Dimensional Moire Superlattices ", *Physical Review Letters*, Volume 125, 166803, 2020.

7. Z. Addison and E.J. Mele, "Nonlinear Time Domain Spectroscopy Near a Band Inversion ", *Physical Review B*, Volume 102, 115206, 2020.

8. B.F. Grosso and E.J. Mele, "Graphene Gets Bent ", *Physics Today*, Volume 73, 46, 2020.

9. L. He, Z. Addison, E.J. Mele, B Zhen, "Quadrupole Topological Photonic Crystals ", *Nature Communications*, Volume 11, s41467-020, 2020.

Metals and quantum materials with spin-orbit interactions by quantum Monte Carlo methods

Lubos Mitas, North Carolina State University, Raleigh, NC 27518

Program Scope

We develop quantum Monte Carlo (QMC) methods for many-body wave function calculations of condensed 2D, 3D and molecular materials with focus on capturing electron correlation effects with high fidelity. Our work is focused on three key directions: i) accurate construction of trial wave functions together with analysis and diminishing of fixed-node/phase errors; ii) control of finite size effects in periodic systems; iii) methods for treating spin-orbit effects in QMC.

Keywords: Quantum Monte Carlo; correlation energies; fixed-node/phase approximation.

Recent Progress

Finite sizes and band gap of LaScO₃ solid and related Si solid calculations [1,2]. In recent studies we have focused on two systems main goals: elimination of finite size effects and control of systematic errors in general and calculations of band gaps. The key system was scandate perovskite as well as Si solid [1-2]. The LaScO₃ perovskite proved to be challenging for traditional electronic structure approaches due to strong correlation effects resulting in inaccurate band gaps from DFT and *GW* methods when compared with existing experimental data. Besides calculating an accurate QMC band gap corrected for supercell size biases and in agreement with numerous experiments, we also predict the cohesive energy of the crystal using the standard fixed-node QMC without any empirical or nonvariational parameters. We show that promotion (optical) gap and fundamental gap agree with each other illustrating a clear absence of significant excitonic effects in the ideal crystal. We obtained these results in perfect consistency in two independent tracks that employ different basis sets (plane wave versus localized Gaussians), different codes for generating orbitals (QUANTUM ESPRESSO versus CRYSTAL), different QMC codes (QMCPACK versus QWALK) and different high-accuracy pseudopotentials (ccECPs versus Troullier-Martins) presenting the maturity and consistency of QMC methodology and tools for studies of strongly correlated problems. In related Si solid calculations, that complements and synergistically builds upon the scandate study, we have focused on the accuracy and systematic biases that affect characteristics such as the cohesion and the band gap. The results show that 64 and 216 atom supercells provide an excellent consistency for extrapolated energies per atom in the thermodynamic limit for ground, excited, and ionized states. We have calculated the ground state cohesion energy with both *systematic and statistical errors* below ≈ 0.05 eV, ie, we find that

$$E_{\text{coh}} = 4.683 \pm 0.05(\text{syst}) \pm 0.003(\text{stat}) \text{ eV.}$$

The Si crystal ground state exhibits a fixed-node error of only 1.3(2)% of the correlation energy, suggesting an unusually high accuracy of the corresponding single-reference trial wave function. We obtain a very good agreement between optical and quasiparticle gaps that affirms the marginal impact of excitonic effects. Our most accurate results for band gaps differ from the experiments by about 0.2 eV. This difference is assigned to a combination of residual finite-size and fixed-node errors. For the first time in QMC we have estimated the crystal Fermi level referenced to vacuum and that enabled us to calculate the edges of valence and conduction bands in agreement with experiments.

Fixed-node errors of excitations in Si_xH_y systems [3]. We present high-accuracy correlated calculations of small Si_xH_y molecular systems in both the ground and excited states. We employ quantum Monte Carlo (QMC) together with a variety of many-body wave function approaches based on basis set expansions. The calculations are carried out in a valence-only framework using recently derived correlation consistent effective core potentials. Our primary goal is to understand the fixed-node diffusion QMC errors in both the ground and excited states with single-reference trial wave functions. Using a combination of methods, we demonstrate the very high accuracy of the QMC atomization energies being within ≈ 0.07 eV or better when compared with essentially exact results. By employing proper choices for trial wave functions, we have found that the fixed-node QMC biases for total energies are remarkably uniform ranging between 1% and 3.5% with absolute values at most ≈ 0.2 eV across the systems and several types of excitations such as singlets and triplets as well as low-lying and Rydberg-like states. Our results further corroborate that Si systems, and presumably also related main group IV and V elements of the periodic table (Ge, Sn, etc), exhibit some of the lowest fixed-node biases found in valence-only electronic structure QMC calculations.

Fluorographene fundamental band gap: QMC and GW [4]. Fluorographene (FG) is a promising graphene-derived material with a large band gap. Currently existing predictions of its fundamental gap (Δ_f) and optical gap (Δ_{opt}) significantly vary when compared with experiment. We provide here an ultimate benchmark of Δ_f for FG by many-body GW and fixed-node diffusion Monte Carlo (FNDMC) methods. Both approaches independently arrive at $\Delta_f \approx 7.1 \pm 0.1$ eV. In addition, Bethe-Salpeter equation enabled us to determine the first exciton binding energy, $E_b = 1.92$ eV.

Weighted nodal domain averages and node nonlinearities [5,6]. We study the nodal properties of many-body eigenstates of stationary Schroedinger equation in order to elucidate their properties for quantum Monte Carlo calculations. In particular, we introduce weighted nodal domain averages that provide a new probe of nodal surfaces beyond the usual expectations. Particular choices for the weight function reveal, for example, that the difference between two arbitrary fermionic eigenvalues is given by the nodal hypersurface integrals normalized by overlaps with the bosonic ground state of the given Hamiltonian. In related study we investigate the impact of node nonlinearities combined with nonlocal operators such as pseudopotentials that could generate significant biases. We present illustrations how this can be addressed by improving the corresponding trial functions, more accurate Green's function and by using T-moves technique.

RuCl₃ layered material and spin-orbit effects. The current effort is devoted to the 2D layered RuCl₃ compound and we are in particular interested in impact of the spin-orbit on the fundamental properties such band structure, band gaps and cohesion. We have explored several types of trial wave functions based on orbitals from PBE0 with variable weight of the Fock exchange as well as from DFT+U approach. We find that both sets of orbitals give comparable results, however, with significant differences for the highest valence vs. the lowest conduction bands. This requires further study as well as particular effects stemming from the spin-orbit interaction – this is still in progress.

Future Plans

We plan to finalize:

- i) the current project on the layered ruthenate trichloride commented above;
- ii) pushing forward new approximations for trial wave functions using pair orbitals;
- iii) further develop approaches for the spin-orbit and optimization of Hamiltonians with effective core operators such as in related, synergistic projects [7-8].

References

- [1] C. A. Melton and L. Mitas, Many-body electronic structure of LaScO₃ by real-space quantum Monte Carlo, *Phys. Rev. B* **102**, 045103 (2020) Zhou, A. Scemama, G. Wang, A. Annaberdiyev, B. Kincaid, M. Caffarel, and L. Mitas, A quantum Monte Carlo study of systems with effective core potentials and node nonlinearities, arXiv:2109.08653
- [2] A. Annaberdiyev, G. Wang, C. A. Melton, M.C. Bennett, and L. Mitas, Cohesion and excitations of diamond-structure silicon by quantum Monte Carlo: Benchmarks and systematic biases, *Phys. Rev. B* **103**, 205206 (2021)
- [3] G. Wang, A. Annaberdiyev, and L. Mitas, Binding and excitations in SixHy molecular systems by quantum Monte Carlo, *J. Chem. Phys.*, **153**, 144303,(2020)
- [4] M. Dubecky, F. Karlicky, S. Minarik, and L. Mitas, Fundamental gap of fluorographene by many-body GW and fixed-node diffusion Monte Carlo methods, *J. Chem. Phys.*, **153**, 184706 (2020)
- [5] A. Annaberdiyev and L. Mitas, Weighted nodal domain averages of eigenstates for quantum Monte Carlo and beyond, arXiv:2109.01734
- [6] H. Zhou, A. Scemama, G. Wang, A. Annaberdiyev, B. Kincaid, M. Caffarel, and L. Mitas, A quantum Monte Carlo study of systems with effective core potentials and node nonlinearities, arXiv:2109.08653
- [7] C. Chandler Bennett, Fernando A. Reboredo, Lubos Mitas, and Jaron T. Krogel, High accuracy transition metal effective cores for many-body diffusion Monte Carlo, submitted to *JCTC*, (2021)
- [8] E. B. Isaacs, H. Shin, A. Annaberdiyev, C. Wolverton, L. Mitas, O. Heinonen, Assessing the accuracy of compound formation energies with quantum Monte Carlo, submitted to *Phys. Rev. Mat.* (2021)

Publications

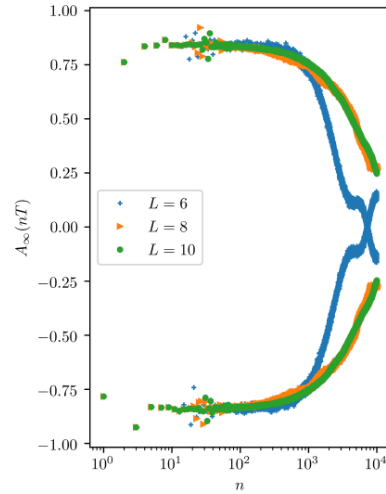
1. C. A. Melton and L. Mitas, Many-body electronic structure of LaScO₃ by real-space quantum Monte Carlo, *Phys. Rev. B* **102**, 045103 (2020)
<https://doi.org/10.1103/PhysRevB.102.045103>
2. G. Wang, A. Annaberdiyev, and L. Mitas, Binding and excitations in SixHy molecular systems by quantum Monte Carlo, *J. Chem. Phys.*, **153**, 144303,(2020);
<https://doi.org/10.1063/5.0022814>
3. M. Dubecky, F. Karlicky, S. Minarik, and L. Mitas, Fundamental gap of fluorographene by many-body GW and fixed-node diffusion Monte Carlo methods, *J. Chem. Phys.*, **153**, 184706 (2020); <https://doi.org/10.1063/5.0030952>
4. H. Zhou, A. Scemama, G. Wang, A. Annaberdiyev, B. Kincaid, M. Caffarel, and L. Mitas, A quantum Monte Carlo study of systems with effective core potentials and node nonlinearities, arXiv:2109.08653, <https://arxiv.org/abs/2109.08653>
5. A. Annaberdiyev and L. Mitas, Weighted nodal domain averages of eigenstates for quantum Monte Carlo and beyond, arXiv:2109.01734, <https://arxiv.org/abs/2109.01734>

Nonequilibrium Phenomena in Topological Insulators

Aditi Mitra, New York University

Program Scope

Floquet spin chains have been a venue for understanding topological states of matter that are qualitatively different from their static counterparts by, for example, hosting π edge modes that show stable period-doubled dynamics. However, the stability of these edge modes to interactions has traditionally required the system to be many-body localized in order to suppress heating. In contrast, here we show that even in the absence of disorder, and in the presence of bulk heating, π edge modes are long lived. Their lifetime is extracted from exact diagonalization and is found to be non-perturbative in the interaction strength. A tunneling estimate for the lifetime is obtained by mapping the stroboscopic time-evolution to dynamics of a single particle in Krylov subspace. In this subspace, the π edge mode manifests as the quasi-stable edge mode of an inhomogeneous Su-Schrieffer-Heeger model whose dimerization vanishes in the bulk of the Krylov chain.



Keywords: Topological Insulators, Floquet systems, Majorana modes, Krylov methods.

Recent Progress

Integrable Floquet spin chains are known to host strong zero and π modes which are boundary operators that respectively commute and anticommute with the Floquet unitary generating stroboscopic time-evolution, in addition to anticommuting with a discrete symmetry of the Floquet unitary. Thus, the existence of strong modes imply a characteristic pairing structure of the full spectrum. Weak interactions modify the strong modes to almost strong modes that almost commute or anticommute with the Floquet unitary. Manifestations of strong and almost strong modes are presented in two different Krylov subspaces. One is a Krylov subspace obtained from a Lanczos iteration that maps the Heisenberg time-evolution generated by the Floquet Hamiltonian onto dynamics of a single particle on a fictitious chain with nearest neighbor hopping. The second is a Krylov subspace obtained from the Arnoldi iteration that maps the Heisenberg time-evolution generated directly by the Floquet unitary onto dynamics of a single particle on a fictitious chain with longer range hopping. While the former Krylov subspace is sensitive to the branch of the logarithm of the Floquet unitary, the latter obtained from the Arnoldi scheme is not. The effective single particle models obtained in the two Krylov subspaces are discussed, and the topological properties of the Krylov chain that ensure

stable 0 and π modes at the boundaries are highlighted. The role of interactions is discussed. Expressions for the lifetime of the almost strong modes are derived in terms of the parameters of the Krylov subspace and are compared with exact diagonalization.

Future Plans

Going forward the PI plans to further develop Krylov subspace methods to study lifetime of quasi-stable edge modes. The PI is currently studying the lifetime when 0 and π edge modes exist together. She plans to also study parafermionic spin chains, exploring how parafermions appear in Krylov subspace, and investigating how interactions affect the lifetime of the parafermions. Besides 1D systems, the PI plans to study topological phenomena in two dimensions such as the appearance of orbital magnetization in periodically driven graphene and periodically driven twisted bilayer systems.

References

1. Daniel J. Yates, Alexander G. Abanov, and Aditi Mitra, Long-lived π edge modes of interacting and disorder-free Floquet spin chains, Invited contribution to Communications Physics, Nature Portfolio (in review), arXiv:2105.13766.

Publications

1. Daniel J. Yates and Aditi Mitra, Strong and almost strong modes of Floquet spin chains in Krylov subspaces, Phys. Rev. B (in review), arXiv:2105.13246.
2. Daniel J. Yates, Alexander G. Abanov, and Aditi Mitra, Long-lived π edge modes of interacting and disorder-free Floquet spin chains, Invited contribution to Communications Physics, Nature Portfolio (in review), arXiv:2105.13766.
3. Daniel J. Yates, Alexander G. Abanov, and Aditi Mitra, Dynamics of almost strong edge modes in spin chains away from integrability, Phys. Rev. B 102, 195419 (2020).
4. Daniel J. Yates, Alexander G. Abanov, and Aditi Mitra, Lifetime of almost strong edge mode operators in one dimensional, interacting, symmetry protected topological phases, Phys. Rev. Lett. 124, 206803 (2020).
5. Daniel J. Yates, Fabian H. L. Essler, and Aditi Mitra, Almost strong (0, π) edge modes in clean, interacting 1D Floquet systems, Phys. Rev. B 99, 205419 (2019).
6. Dillon T. Liu, Javad Shabani, and Aditi Mitra, Floquet Majorana zero and π modes in planar Josephson junctions, Phys. Rev. B 99, 094303 (2019).

Localization in Energy Materials

Juana Moreno, Louisiana State University

Program Scope

We develop a real space cluster extension of the typical medium theory (cluster-TMT) to study Anderson localization. The cluster-TMT extends the single-site typical medium theory to a multiple-site cluster theory in real space. Applying the developed method to the 3D Anderson model with a box disorder distribution, we demonstrate that the cluster-TMT successfully captures the localization phenomena in all disorder regimes. Our method obtains the correct critical disorder strength for the Anderson localization in 3D, and systematically recovers the re-entrance behavior of the mobility edge. From a general perspective, our developed methodology offers the potential to study Anderson localization at surfaces within quantum embedding theory. This opens the door to studying the interplay between topology and Anderson localization from first principles.

Keywords: Anderson Localization; Typical Medium, Cluster Mean Field Theory

Recent Progress

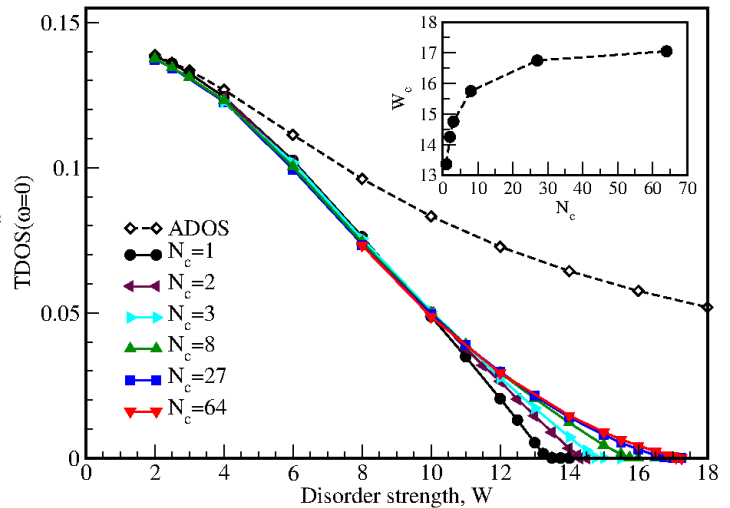
The presence of random disorder in materials is the norm rather than the exception. The seminal work by Anderson in 1957 [1] pointed out that the scattering of charge carriers from impurities may inhibit their propagation through the disordered media leading to the spatial confinement of carriers, a phenomenon known as Anderson localization. To model disorder, Anderson proposed a simplified model of electrons hopping among lattice sites being subjected to static scattering processes on locally disordered centers. The stochastic character of the problem is encoded into the on-site energies considered random variables distributed according to a chosen probability distribution. The local density of states (LDOS) turns out to be an important quantity which characterizes the disordered system.

A proper modeling in such cases can be constructed based on effective medium theories. Among them the single site effective medium methods, such as the coherent potential approximation (CPA) [2-4] or the typical medium theory (TMT) [5], proved to be simple and transparent theories that are able to capture important features of the disorder effects in electron systems. Common to these two methods is the mapping of the lattice problem into an impurity placed in a self-consistently determined effective medium. In both methods the measured quantity is the disorder averaged Green's function, however in CPA the Green's function is linearly (algebraically) averaged, while in the TMT the geometric average of the LDOS is used. This difference in disorder averaging defines the average and the typical effective media, respectively.

The key accomplishment of the present study is the development of a cluster mean field theory for the description of Anderson localization. The developed cluster version is based on a real-

space approach, and presents an alternative to the existing momentum space version of TMDCA [6,7]. To demonstrate the validity of the method, we apply it to the three dimensional Anderson model with box disorder distribution, and reproduce the full phase diagram and the critical disorder strength, W_c , for the metal-insulator transition. The cluster mean field theory we designed is an extension of the local single site typical medium theory. The developed real space cluster extension method incorporates the spatial non-local effects systemically, therefore the re-entrance behavior of the 3D Anderson model is recovered. We find that cluster extensions of TMT are necessary to properly capture the non-local effects in the Anderson transition. Quantitatively our results are in good agreement with the existing data in the literature. In particular, we find that the converged cluster value of $W_c \sim 17.05$ is superior to the value of 13.4 provided by single site TMT calculations. We demonstrate that non-local spatial correlations are significant in 3D Anderson model, and hence going beyond a single site approximation is necessary to properly describe the metal-insulator transition. Unlike the single site TMT, the present real-space cluster computation captures the re-entrance behavior driven by non-local multiple scattering effects which are missing in local approximations [8, 5, 9, 10]. Also just like the TMDCA, the real space cluster-TMT allows for a computationally efficient treatment of the non-local effects in Anderson localization. In addition however, the real-space cluster TMT opens the door to treating problems with open boundary conditions, which offers the possibility to study the localization of surface states. One potential application of this capability would be the search for a materials realization of the topological Anderson insulator [11] via first principles calculations. Also, the presented formalism being a real space cluster opens venues for easier embedding with ab initio Green's function electronic structure methods, which offer a more natural approach to disordered real materials, including high entropy alloys and disordered metals [12-14].

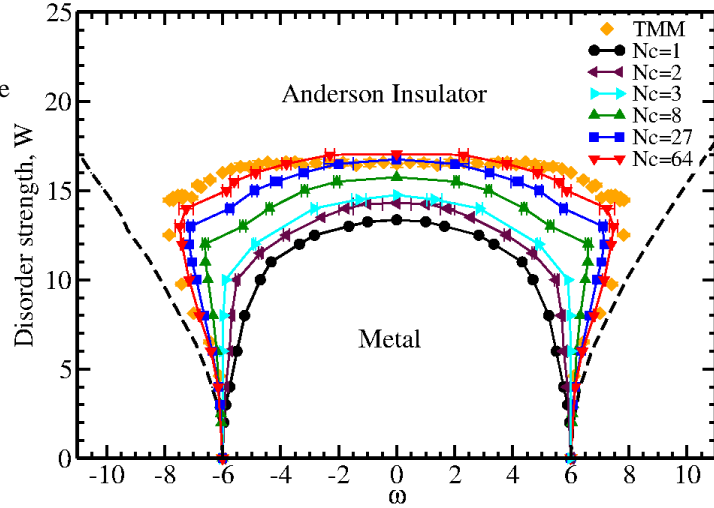
Fig. 1. The typical density of states (solid lines) at the band center, $\text{TDOS}(\omega=0)$, as a function of disorder strength W calculated for different cluster sizes $N_c=1, 2, 3, 8, 27, 64$. The ADOS($\omega=0$) as a function of disorder strength is obtained for $N_c=4^3$ (dashed line). Inset: the cluster size N_c dependence of the critical disorder strength W_c determined from the vanishing $\text{TDOS}(\omega=0)$.



We consider the evolution of the critical disorder strength W_c for the Anderson transition as a function of the cluster size N_c . In Fig. 1 we plot $\text{TDOS}(\omega=0)$ as a function of disorder strength W for several cluster sizes. For $N_c=1$ (the local TMT case), the critical disorder is $W_c \sim 13.4$. Since TMT is a mean field theory, it is expected that the critical disorder strength is underestimated and thus it is lower than the exact value. As the cluster size N_c increases, more spatial fluctuations are taken into account, which improves the value of W_c .

With increasing N_c , the W_c converges quickly to $W_c \sim 17.05$ (see inset of Fig. 1), which is in good agreement with the values of W_c reported in the literature [15]. Also notice that unlike the TDOS, the ADOS($\omega=0$) (shown by the dashed line in Fig. 1) remains finite as the disorder strength increases, indicating that it can not be used as an order parameter for the Anderson transition, and hence the typical medium treatment is needed.

Fig. 2. Disorder strength W vs frequency ω phase diagram of the 3D Anderson model obtained from cluster-TMT calculations. The mobility edge boundaries (solid lines) are obtained for $N_c=1, 2, 3, 8, 27, 64$ cluster sizes. Dashed line mark the band edges obtained from the ADOS(ω). The transfer matrix method (TMM) mobility edge boundaries are taken from Ref. [16].



Finally, in Fig. 2, we present the disorder strength W vs. frequency ω phase diagram. Here we plot the cluster size N_c dependence of the mobility edge boundaries at different disorder strengths W obtained by our real space cluster-TMT formalism. In addition, we also show the band edges, which are defined by the frequencies at which $\text{ADOS}(\omega=0)=0$. As we discussed above a signature of the cluster mean field theory is the re-entrance at high energy. At $N_c > 1$, the mobility edge boundaries first expand and then retract back with increasing W . As Fig. 2 displays such re-entrance behavior is missing in the single site ($N_c=1$) TMT case, and is recovered for $N_c > 1$ clusters. This indicates that non-local spatial correlations and multiple-scattering effects in the Anderson transition are important, and capturing such effects requires the usage of finite cluster methods. To benchmark our results even further, we also present the mobility edge trajectories obtained from the highly accurate transfer matrix method (TMM) [6]. For $N_c=4^3$, the cluster-TMT results are already rather close to those of the TMM. These results demonstrate that our cluster-TMT method can be used to successfully describe the electron localization in the 3D Anderson model.

Future Plans

Furthermore, while the cluster TMT in this study has been restricted to periodic boundary conditions, the same methodology can be used to simulate Anderson localization in surfaces. This will be relevant for example to unraveling the role of disorder in topological materials [11,17]. Another interesting topic is to combine this approach with the multiple scattering theory [18], and the locally self-consistent multiple scattering method [19] for the study of materials with random disorder.

References

- [1] Anderson, P.W., Phys. Rev. 1958, 109, 1492–1505.
- [2] Soven, P., Phys. Rev. 1967, 156, 809–813.
- [3] Shiba, H. A., Prog. Theor. Phys. 1971, 46, 77.
- [4] Zhang, Y.; Östlin, A.; Terletska, H.; Bauernfeind, D.; Tam, K.M.; Evertz, H.G.; Byczuk, K.; Vollhardt, D.; Chioncel, L., Phys. Rev. B 2021, 104, 045127.
- [5] Dobrosavljevic, V.; Pastor, A.A.; Nikolic, B.K., EPL 2003, 62, 76.
- [6] Terletska, H.; Zhang, Y.; Tam, K.M.; Berlijn, T.; Chioncel, L.; Vidhyadhiraja, N.; Jarrell, M., Applied Sciences 2018, 8, 2401.
- [7] Terletska, H. et al., Annals of Physics 2021, p. 168454.
- [8] John, S., Phys. Rev. Lett. 1984, 53, 2169–2172.
- [9] Byczuk, K.; Hofstetter, W.; Vollhardt, D., International Journal of Modern Physics B 2010, 24, 1727–1755.
- [10] Bulka, B.; Kramer, B.; MacKinnon, A.Z., Phys. B Condensed Matter 1985, 60, 13–17.
- [11] Li, J.; Chu, R.L.; Jain, J. K.; Shen, S.Q., Phys. Rev. Lett. 2009, 102, 136806.
- [12] Zhang, Y.; Nelson, R.; Siddiqui, E.; Tam, K.M.; Yu, U.; Berlijn, T.; Ku, W.; Vidhyadhiraja, N.S.; Moreno, J.; Jarrell, M., Rev. B 2016, 94, 224208.
- [13] Zhang, Y.; Nelson, R.; Tam, K.M.; Ku, W.; Yu, U.; Vidhyadhiraja, N.S.; Terletska, H.; Moreno, J.; Jarrell, M.; Berlijn, T., Phys. Rev. B 2018, 98, 174204.
- [14] Östlin, A.; Zhang, Y.; Terletska, H.; Beiușeanu, F.; Popescu, V.; Byczuk, K.; Vitos, L.; Jarrell, M.; Vollhardt, D.; Chioncel, L., Phys. Rev. B 2020, 101, 014210.
- [15] MacKinnon, A.; Kramer, B., Z., Phys. B Condensed Matter 1983, 53, 1–13.
- [16] Ekuma, C.E.; Terletska, H.; Tam, K.M.; Meng, Z.Y.; Moreno, J.; Jarrell, M., Phys. Rev. B 2014, 89, 081107.
- [17] Roy, B.; Slager, R.J.; Juricic, V., Phys. Rev. X 2018, 8, 031076.
- [18] Terletska, H.; Zhang, Y.; Chioncel, L.; Vollhardt, D.; Jarrell, M., Phys. Rev. B 2017, 95, 134204.

[19] Zhang, Y.; Terletska, H.; Tam, K.M.; Wang, Y.; Eisenbach, M.; Chioncel, L.; Jarrell, M., Phys. Rev. B 2019, 100, 054205.

Publications

- 1.** Locally self-consistent embedding approach for disordered electronic systems, Yi Zhang, Hanna Terletska, Ka Ming Tam, Yang Wang, Markus Eisenbach, Liviu Chioncel, Mark Jarrell, Phys. Rev. B 100, 054205 (2019).
- 2.** Ab initio typical medium theory for substitutional disorder, A. Ostlin, Y. Zhang, H. Terletska, F. Beiușeanu, V. Popescu, K. Byczuk, L. Vitos, M. Jarrell, D. Vollhardt, L. Chioncel, Phys. Rev. B 101, 014210 (2020).
- 3.** Interatomic Potential in a Simple Dense Neural Network Representation, Ka-Ming Tam, Nicholas Walker, Samuel Kellar, and Mark Jarrell, arXiv:1911.01365 (2019).
- 4.** Neural Network Solver for Small Quantum Clusters, Nicholas Walker, Samuel Kellar, Yi Zhang, Ka-Ming Tam, arXiv:2008.12331 (2020).
- 5.** Beyond Quantum Cluster Theories: Multiscale Approaches for Strongly Correlated Systems, Herbert F. Fotso, Ka-Ming Tam, Juana Moreno, arXiv:2011.05522 (2020).
- 6.** Application of the Locally Self-Consistent Embedding Approach to the Anderson Model with Non-Uniform Random Distributions, K.-M.Tam, Y. Zhang, H. Terletska, Y. Wang, M. Eisenbach, L.Chioncel, J. Moreno, Annals of Physics, 168480 (2021).
- 7.** Non-local corrections to the typical medium theory of Anderson localization, H. Terletska, A. Moilanen, K.-M. Tam, Y. Zhang, Y. Wang, M.Eisenbach, N. S. Vidhyadhiraja, L. Chioncel, J. Moreno, Annals of Physics, 168454 (2021).
- 8.** Real-space Quantum Cluster formulation for the Typical Medium Theory of Anderson Localization, Ka-Ming Tam, Hanna Terletska, Tom Berlijn, Liviu Chioncel, Juana Moreno, arXiv:2109.14267, submitted for publication
- 9.** Application of Variational Autoencoder to Detect Critical Points of Anisotropic Classical Model, Anshumitra Baul, Nicholas Walker, Juana Moreno, and Ka-Ming Tam, submitted for publication
- 10.** Quantum Convolutional Neural Network as a Classifier for Many-Body Wavefunctions from the Quantum Variational Eigensolver, Nathaniel Wrobel, Anshumitra Baul, Juana Moreno, and Ka-Ming Tam, submitted for publication

Non-Equilibrium Physics at the Nanoscale

Principal investigator: Dirk K. Morr

Department of Physics, University of Illinois at Chicago, IL 60607

Program Scope

The goal of this program is to discover and understand novel non-equilibrium phenomena at the nanoscale. In particular, this program investigates the question of how non-equilibrium phenomena can provide novel insight into the nature of complex strongly correlated or topological phases. Recently, the PI has focused on developing novel approaches to the quantum engineering of topological superconductors, and the ensuing Majorana modes. As the non-Abelian braiding statistics of Majorana modes are a crucial element in the realization of topological qubits, the PI has developed novel non-equilibrium techniques to study in real space and time the topological nature and braiding properties of Majorana modes.

Keywords: topological superconductors, Majorana zero modes, non-equilibrium manipulation of quantum states

Recent Progress

Topological Superconductivity in Skyrmion Lattices

Atomic manipulation and interface engineering techniques have provided an intriguing approach to custom-designing topological superconductors and the ensuing Majorana zero modes, representing a paradigm for the realization of topological quantum computing and topology-based devices. Magnet-superconductor hybrid (MSH) systems have proven to be experimentally suitable to quantum engineer topological superconductivity through the control of both the complex structure of its magnetic layer and the interface properties of the superconducting surface. We demonstrated [1] that two-dimensional MSH systems containing a magnetic skyrmion lattice provide an unprecedented ability to control the emergence of topological phases. By changing the skyrmion radius, which can be achieved experimentally through an external magnetic field, we showed that it is possible to tune the MSH system between different topological superconducting phases, as characterized by the topological invariant, the Chern number (see Fig.1). This, in turn, allows us one (i) to study the transitions between topological and trivial phases, and visualize these transitions using scanning tunneling spectroscopy, and (ii)

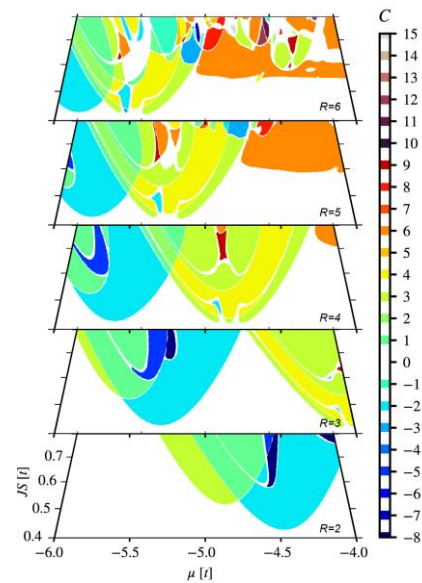


Fig.1 Topological phase diagram of an MSH system with a skyrmion lattice for different skyrmion radii.

to explore the unique properties of topological phases that directly reflect the topological invariant that describes them. Moreover, we demonstrated that in such MSH systems, Josephson scanning tunneling spectroscopy can be employed to visualize not only the spatial structure of the superconducting s-wave order parameter, which is modified by the presence of skyrmions, but

also that of the induced spin-triplet correlations, with the latter being a crucial aspect underlying the emergence of topological superconductivity.

Origin of topological surface superconductivity in $\text{FeSe}_{1-x}\text{Te}_x$

$\text{FeSe}_{0.45}\text{Te}_{0.55}$ has attracted significant interest over the last 3 years as it is the first unconventional (iron-based) high-temperature superconductor in which experiments have provided strong evidence for the existence of topological surface superconductivity. Topological superconductors are of great importance as they represent a new paradigm for the realization of topological quantum computing using the non-Abelian braiding statistics of Majorana zero modes. The evidence for the existence of topological superconductivity in $\text{FeSe}_{0.45}\text{Te}_{0.55}$ includes by now the observation of a surface Dirac cone, of Majorana zero modes (MZMs) in vortex cores, and at the end of line defects in monolayer $\text{FeSe}_{0.45}\text{Te}_{0.55}$ and of Majorana edge modes near domain walls. The microscopic origin of topological superconductivity in $\text{FeSe}_{0.45}\text{Te}_{0.55}$, however, has remained an open question. This origin was initially proposed to arise from a band-inversion involving the bulk p_z and d_{xz} -bands -- rendering $\text{FeSe}_{0.45}\text{Te}_{0.55}$ a 3D topological insulator -- and the gapping of the ensuing surface Dirac cone by proximity induced superconductivity (the 3DTI mechanism). A series of recent ARPES and quantum sensing experiments, however, have cast serious doubt on the validity of this proposal. In particular, these experiments have reported strong evidence for the existence of ferromagnetism on the surface of $\text{FeSe}_{0.45}\text{Te}_{0.55}$. However, already weak surface ferromagnetism can destroy the topological phase arising from the 3DTI mechanism, raising the question of whether a different mechanism might be responsible for the emergence of topological surface superconductivity and the ensuing Majorana modes in $\text{FeSe}_{0.45}\text{Te}_{0.55}$.

We answered this question [2,3] by proposing a different microscopic explanation for the experimentally observed topological surface superconductivity in $\text{FeSe}_{0.45}\text{Te}_{0.55}$. Specifically, we showed that the ferromagnetism observed experimentally is a key element in the emergence of topological superconductivity when combined with two other essential properties of $\text{FeSe}_{0.45}\text{Te}_{0.55}$: its superconducting gap of s_{\pm} -wave symmetry and strong Rashba spin-orbit interaction. We demonstrated that the interplay of these three physical properties gives rise to robust topological surface superconductivity in $\text{FeSe}_{0.45}\text{Te}_{0.55}$, characterized by a Z topological invariant, the Chern

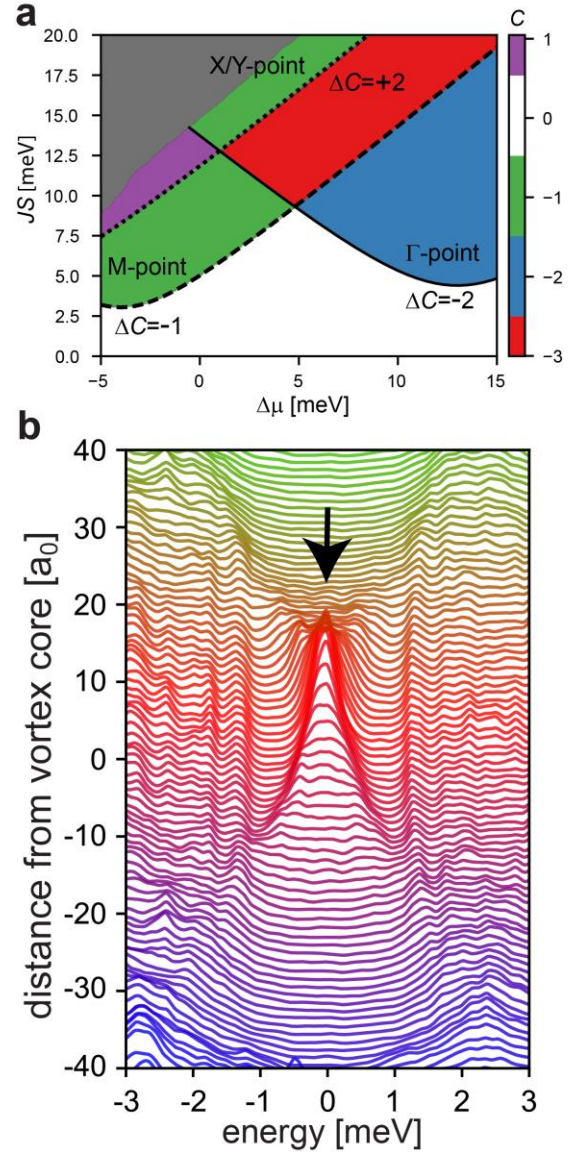


Fig.2 **a** Topological phase diagram. **b** Line cut of the LDOS through the vortex core. Black arrow indicates the position of the MZM

number (see Fig.2a). Moreover, our proposal explains the experimental observations of Majorana zero modes in vortex cores (see Fig.2b) and at the end of line defects, as well as the emergence of dispersive Majorana edge modes along domain walls. In addition, we propose a novel experimental signature, the presence or absence of supercurrents along domain walls, which can distinguish topological Majorana modes from trivial in-gap states and can be imaged via scanning superconducting quantum interference device.

Non-equilibrium manipulation of YSR states and the braiding of Majorana modes in topological superconductors

The experimental advances in developing non-equilibrium pump-probe and periodic driving techniques have opened unprecedented opportunities to manipulate correlated and topological matter at the nanoscale. Of particular interest is here the question of whether these non-equilibrium techniques can be employed for the braiding of Majorana modes, one of the crucial steps in the creation of quantum gates and the realization of topological quantum computing. To investigate this question, we have developed two new theoretical formalisms, based on the Keldysh formalism and path-integral formalism to study the real time and real space dynamics of quantum systems. We recently employed this formalism to investigate the non-equilibrium manipulation and emergence of Yu-Shiba-Rusinov (YSR) states in *s*-wave superconductors. Specifically, we studied the time evolution of the electronic structure and of the YSR states when the moments of two magnetic impurities residing on nearest neighbor sites are rotated from a parallel to an antiparallel alignment. When the moments are parallel, their YSR states hybridize, leading to the emergence of four YSR peaks in the LDOS, while the YSR states do not hybridize for antiparallel alignment, yielding two degenerate sets of YSR states [see Fig.3(a)]. To characterize the time-evolution of the electronic structure, we computed the time-dependent differential conductance, dI/dV measured in scanning tunneling spectroscopy (STS) experiments, as well as the non-equilibrium analogue of the density of states, $N_{NEQ}(E, t)$. In Fig.3(b), we present the time-evolution of $N_{NEQ}(E, t)$ when the moments are rotated from a parallel to an antiparallel alignment over a time scale indicated by the yellow arrow.

Similar to the equilibrium case, we demonstrated that $dI/dV \sim N_{NEQ}(E, t)$ allowing for the exploration of these non-equilibrium transitions using STS experiments. Moreover, we showed that this formalism can be used to induce phase-transitions in time through an externally driven precession of the impurity spins. These results are the first step towards a real-time study of Majorana modes and their braiding in topological superconductors.

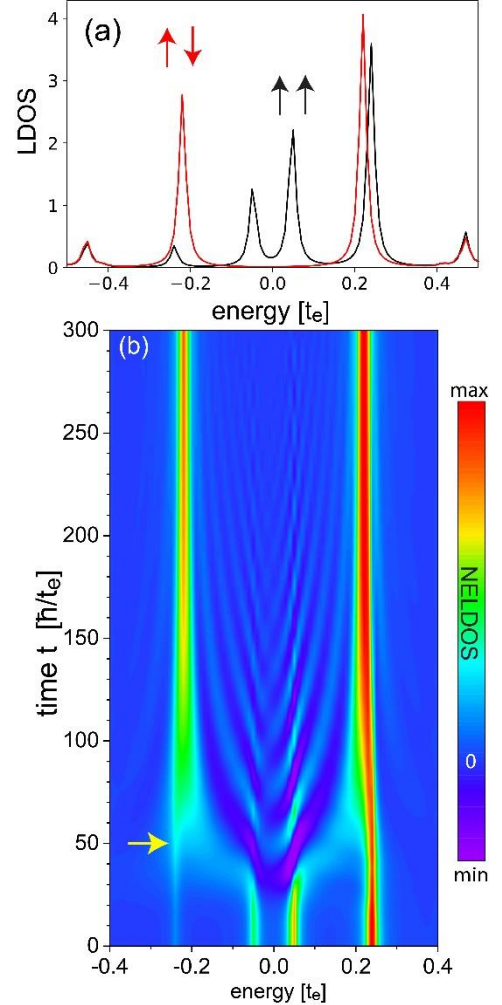


Fig.3 (a) LDOS for parallel and antiparallel alignment of impurity moments. (b) Time-evolution of $N_{NEQ}(E, t)$ when the moments are rotated from parallel to antiparallel alignment

Topological superconductivity induced by a triple-q magnetic structure

We demonstrated [4] that the recently discovered triple-q ($3\mathbf{q}$) magnetic structure, when embedded in a magnet-superconductor hybrid system, gives rise to the emergence of topological superconductivity. We investigated the structure of chiral Majorana edge modes at domain walls, and showed that they can be distinguished from trivial in-gap modes through the spatial distribution of the induced supercurrents. Finally, we showed that topological superconductivity in $3\mathbf{q}$ MSH systems is a robust phenomenon that does not depend on the relative alignment of the magnetic and superconducting layers, or on the presence of electronic degrees of freedom in the magnetic layer.

Identifying Majorana zero modes in magnet-superconductor hybrid systems: a first principle approach

Magnet-superconductor hybrid systems represent one of the most promising platforms to host Majorana zero modes (MZMs). While modeling of one-dimensional chain MSH geometries usually predicts point-like bound states at the chain ends, recent STS experiments on the putative topological system Mn/Nb reported qualitatively different signatures in the local density of states. To address this apparent discrepancy, we used density functional theory to derive an effective 80-band superconducting tight-binding model for a Mn chains on superconducting Nb [5]. While we find that this system is topological over nearly all of parameter space, it exhibits an abundance of unconventional MZM features. In particular, the MZM are spatially extended over much of the chain, and most strikingly, exhibit a drastic accumulation of spectral weight on sites next to the magnetic chain. These features are observed in STS experiments on chains up to 52 Mn atoms deposited on a Nb substrate, widening the range of spatial and spectral features that allow us to identify MZMs experimentally.

Future Plans

The theoretical formalism we developed to study the real time and real space dynamics of quantum systems, will be employed to study the braiding of Majorana modes in magnet-superconductor hybrid structures. Indeed, in preliminary studies, we successfully simulated the time-dependent braiding of Majorana modes in one-dimensional MSH networks located on the surface of a two-dimensional s -wave superconductor. To this end, we developed a protocol to spatially move Majorana modes which is based on the rotation of magnetic moments via ESR techniques. As a next step in this project, we will study how the specific form of the braiding protocol and in particular the characteristic time scales involved, affect the fidelity of the braiding process. This study will allow us to identify the most efficient braiding protocol that ensures the fidelity of the braiding process. The insight gained from this study will subsequently be employed to study the real time and real space implementation of Clifford gates.

Publications (November 2019 – October 2021)

- [1] *Topological superconductivity in skyrmion lattices*, E. Mascot, J. Bedow, M. Graham, S. Rachel and D. K. Morr, npj Quant Mat. 6,6 (2021).
- [2] *Origin of Topological Surface Superconductivity in $FeSe_{0.45}Te_{0.55}$* , E. Mascot, S. Cocklin, M. Graham, M. Mashkooi, S. Rachel, and D. K. Morr, arXiv:2102.05116, submitted to Commun. Physics.
- [3] *Shot-noise and differential conductance as signatures of putative topological superconductivity in $FeSe_{0.45}Te_{0.55}$* , K.H Wong, E. Mascot, V. Madhavan, D.J. Van Harlingen, and D. K. Morr, arXiv:2110.02238, submitted to Phys. Rev. B Letters.
- [4] *Topological superconductivity induced by a triple- \mathbf{q} magnetic structure*, J. Bedow, E. Mascot, T. Posske, G. S. Uhrig, R. Wiesendanger, S. Rachel, and D. K. Morr, Phys. Rev. B 102, 180504(R) (2020).
- [5] *Majorana modes with side features in magnet-superconductor hybrid systems*, D. Crawford, E. Mascot, M. Shimizu, L. Schneider, P. Beck, J. Wiebe, R. Wiesendanger, H. O. Jeschke, D. K. Morr, and S. Rachel, arXiv:2109.06894, submitted to Nat. Phys.
- [6] *Nature of the spin resonance mode in $CeCoIn_5$* , Y. Song, W. Wang, J. Van Dyke, N. Pouse, S. Ran, D. Yazici, A. Schneidewind, P. Cermak, Y. Qiu, M. B. Maple, D.K. Morr, and P. Dai, Commun. Phys. **3**, 98 (2020).
- [7] *High-Temperature Majorana Fermions in Magnet-Superconductor Hybrid Systems*, D. Crawford, E. Mascot, D. K. Morr, and S. Rachel, Phys. Rev. B. **101**, 174510 (2020).
- [8] *Evidence for dispersing 1D Majorana channels in an iron-based superconductor*, Z. Wang, J. O. Rodriguez, M. Graham, G. D. Gu, T. Hughes, D.K. Morr, and V. Madhavan, Science **367**, 104 (2020).
- [9] *Imaging emergent heavy Dirac fermions of a topological Kondo insulator*, H. Pirie, Y. Liu, A. Soumyanarayanan, P. Chen, Y. He, M.M. Yee, P.F.S. Rosa, J.D. Thompson, D.-J. Kim, Z. Fisk, X. Wang, J. Paglione, D. K. Morr, M. H. Hamidian, and J. E. Hoffman, Nat. Phys. **16**, 52 (2020).
- [10] *Quantum Engineered Kondo Lattices*, J. Figgins, L. S. Mattos, W. Mar, Y.-T. Chen, H. C. Manoharan, and D.K. Morr, Nat. Commun. **10**, 5588 (2019).
- [11] *Stability of Disordered Topological Superconducting Phases in Magnet--Superconductor Hybrid Systems*, E. Mascot, C. Agrahar, S. Rachel and D.K. Morr, Phys. Rev. B **100**, 235102 (2019).
- [12] *Dimensional Tuning of Majorana Fermions and the Real Space Counting of the Chern Number*, E. Mascot, S. Cocklin, S. Rachel, and D.K. Morr, Phys. Rev. B **100**, 184510 (2019).

Duality and Strongly Interacting Systems

Michael Mulligan, University of California, Riverside

Program Scope

The broad goal of my current research is to develop and improve our theoretical frameworks for understanding non-Fermi liquid states of matter, with a particular attention on those states that occur in 2d. One focus is to use duality to study anomalous low-temperature metallic behavior that is observed in a variety of quasi-2d materials, such as the 2d electron gas or thin superconducting films. The relevant quantum field theory dualities provide effective descriptions with invariances that appear to be emergent symmetries in the electron systems of primary interest. The fundamental question concerns the existence and universal characterization of the metallic ground state in the presence of interactions and quenched disorder. Other theoretical approaches to non-Fermi liquid states of matter that we may consider include the study of the $d = \infty$ limit in non-Fermi liquid continuum effective theories, such as a Fermi sea coupled to a gapless boson; the study of transport and stability of metallic states formed from a lattice of SYK dots; and anisotropic 2d Fermi systems arising from coupled 1d Luttinger liquids. A complementary research direction is the study of multipartite entanglement (using, e.g., the entanglement negativity, an entanglement measure in mixed quantum states) in manybody quantum systems.

Keywords: non-Fermi liquid states of matter; quantum field theory duality; entanglement in manybody systems

Recent Progress

Here we discuss our recent work [P3] studying edge-state transport of the anti-Pfaffian quantum Hall state.

The nature of the quantum Hall ground state at filling fraction $\nu = 5/2$ has been the subject of debate since its discovery in 1987 [R1]. Numerical studies favor either the Moore-Read Pfaffian [R2, R3] or its particle-hole conjugate, the anti-Pfaffian state [R4, R5], both of which host quasiparticles with non-Abelian statistics. Quantum point contact tunneling experiments are consistent with both non-Abelian and Abelian candidate states, while the observation of neutral upstream modes are only consistent with the possibility of a non-Abelian quantum Hall state.

The thermal Hall conductance K provides a sensitive probe of the topological order of a quantum Hall state [R6, R7]: K/T (measured in units of $\kappa_0 = \pi^2 k_B^2 / 3h$ at temperature T) equals the difference of the right and left central charges, i.e., the chiral central charge $c_- = c_R - c_L$, of the edge-state theory. (For an Abelian state, such as the Laughlin state at $\nu = 1/3$, the chiral central charge is an integer equal to the difference of the number of right and left moving chiral

edge modes.) Consequently, the recent measurement of Banerjee et al. [R8] that finds $K/T \approx 2.5\kappa_0$ is strong evidence for a non-Abelian quantum Hall state.

At first sight, this result supports the possible realization of the particle-hole symmetric Pfaffian (PH-Pfaffian) state [R9, R10], which has $c_- = 5/2$. The realization of this state has been argued to rely on the presence of quenched disorder, inevitably present in any real system, but challenging to incorporate into numerics. Thus far, the theoretical conditions for the realization of the PH Pfaffian have been found to be rather restrictive [R11, R12, R13].

Simon [R14] has proposed an alternative interpretation: The Banerjee et al. experiment [R8] may not directly reflect the bulk topological order; instead $K/T \approx 2.5\kappa_0$ may be due to suppressed thermal equilibration relative to charge equilibration of anti-Pfaffian edge-state modes. If true, this would help to alleviate the tension between prior numerical studies and the recent experimental one. This proposal is based on the fact that the theoretical thermal Hall conductance result [R6, R7] assumes complete equilibration of the different edge channels. If, for example, there's no equilibration between right and left edge modes, then $K/T = (c_R + c_L)\kappa_0$. If the edge modes partially equilibrate with one another, then $(c_R - c_L)\kappa_0 \leq K/T \leq (c_R + c_L)\kappa_0$.

The Pfaffian state has three bosonic edge modes and one Majorana fermion edge mode, all moving “downstream” in the same direction along the edge. The resulting edge-state, which produces $K/T = 7/2\kappa_0$, is therefore

not consistent with [R8]. On the other hand, the anti-Pfaffian edge state, pictured in Fig. 1, has three “downstream” bosonic modes, one “upstream” bosonic mode, and one “upstream” Majorana fermion mode.

Simon’s observation [R14] is that depending on the degree of equilibration between edge modes, K/T of the anti-Pfaffian state can take any value between $3/2\kappa_0$ and $9/2\kappa_0$. Interestingly (and confusingly!), this idea requires partial thermal equilibration simultaneous with full charge equilibration to be consistent with experiment [R8].

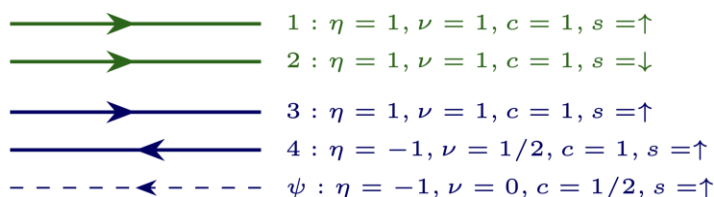


Figure 1. Edge modes of the anti-Pfaffian state at $\nu = 5/2$, in the absence of edge reconstruction. Here, $\eta = \pm 1$ denotes the chirality of the mode; ν is the charge carried by the mode; c is the central charge of the mode so that $c_- = \sum_i \eta_i c_i$ and $c_R + c_L = \sum_i c_i$; and s is the spin of the mode. Green indicates integer edge modes of the filled lowest Landau levels, while the blue indicates anti-Pfaffian edge modes of the half-filled second Landau level.

In [P3], we extended previous studies [R14, R15, R16] of the role of equilibration in anti-Pfaffian edge-state transport. We considered the two-terminal electrical and thermal Hall conductances in the setup shown in Fig. 2. We assumed electron tunneling between different edge modes, induced by short-range disorder along the edge, serves to equilibrate the edge modes.

Tunneling between the spin-up and spin-down integer lowest Landau level edge modes (shown in green in Fig. 1), an effect not considered in prior analyses due to an assumed suppressed spin-orbit coupling, plays a prominent role in our scenario. In the presence of a strong Coulomb interaction, two candidate low-energy effective edge-state theories emerge. These candidate states enjoy an approximate spin symmetry between lowest Landau level edge modes that can suppress thermal equilibration while simultaneously allowing complete charge equilibration over a range of experimentally-relevant temperatures. Analysis of the kinetic equations for low-temperature transport with respect to model parameters characterizing the edge-mode interactions shows that only one of these phases is realistic without fine-tuning (see Fig. 3). The quantum point-contact tunneling conductance in this phase scales with temperature as $G_{tun} \sim T^{2g-2}$ with $g \sim 3/10$. The electrical and thermal Hall

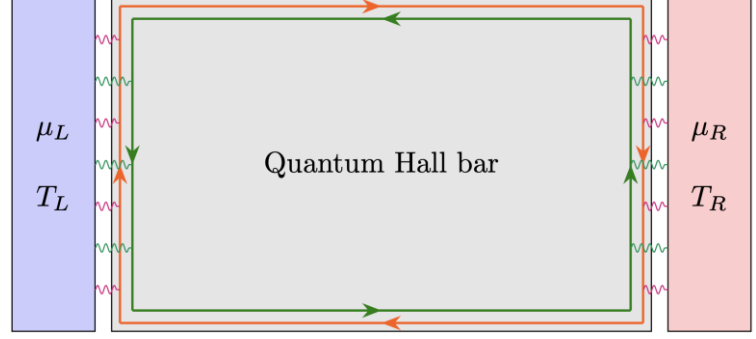


Figure 2. Quantum Hall bar geometry depicting (for simplicity) two counter-propagating edge modes. The wiggly lines represent tunnelings between the left (right) contact at chemical potential μ_L (μ_R) and temperature T_L (T_R) and the edge modes. Edge-state interactions are assumed to occur along the top and bottom edges.

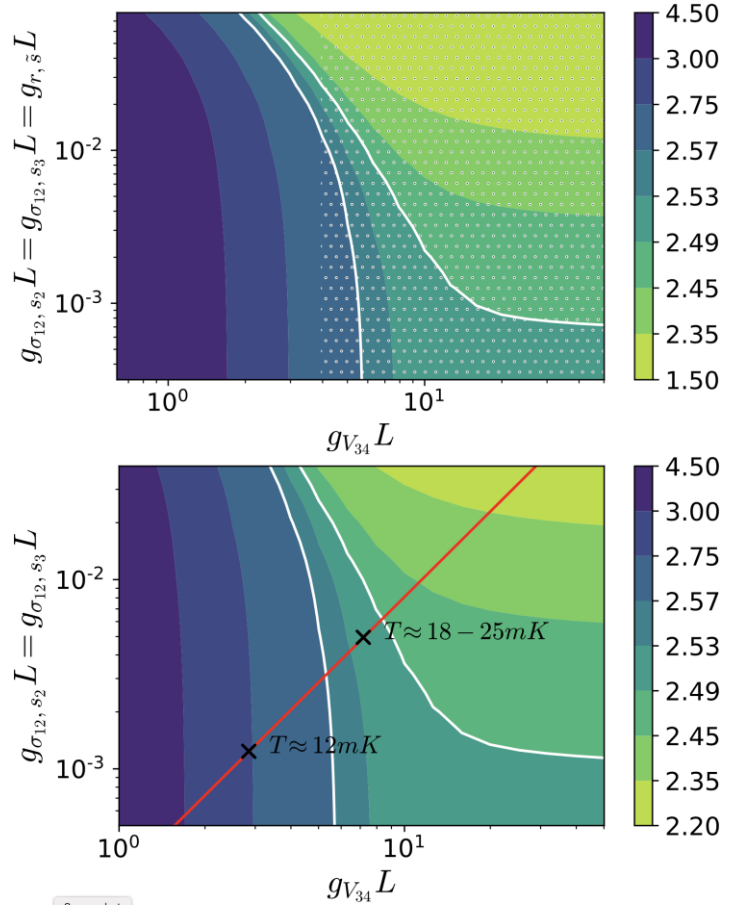


Figure 3. Contour plots of K/T (in units of κ_0) as a function of model parameters g_x and edge length L . Regions within the white contours have experimentally-consistent K ; hatched points (in the top figure) have consistent electrical Hall conductance. The red line (in the lower figure) represents the expected behavior of the system upon a lowering of the temperature.

conductances are expected to be decreasing functions of increasing temperature in the vicinity of the experimentally probed temperatures $T \approx 18 - 25mK$.

Future Plans

In [P3], we assumed specific boundary conditions for how the edge modes were thermally coupled to the contacts. It would be interesting to study other boundary conditions to better understand the role of the coupling to the heat reservoirs on the measured thermal Hall conductance, analogous to the analysis of the effect of the coupling to the charge reservoirs on the electrical Hall conductance in [R17].

Future plans, unrelated to [P1], include the study of the symmetries of the chiral Fermi metal [R18] and possible interacting generalizations. This chiral 2d state consists of coupled 1d chiral fermions, imagined as arising from nearby edges of stacked integer quantum Hall states. The chirality of the resulting 2d free fermion state allows it to avoid localization in the presence of quenched disorder. Interestingly, this state possesses a “hidden” nonlocal $SU(N)$ symmetry with $N \rightarrow \infty$, associated to conservation of each point of the Fermi surface. Here, N equals the number of 1d chiral fermion wires. The chiral $U(N)$ Wess-Zumino-Witten model at level $k = 1$ is an alternative representation of this 2d state. It would be interesting if the $SU(N)$ symmetry persists for $k > 1$. Such states may be nontrivial examples of ersatz Fermi liquids [R19].

In [P5], we used the entanglement negativity to study how multipartite entanglement constrains the real-space structure of the ground-state wave functions of the Laughlin and Moore-Read states at $\nu = 1/m$. We showed that a combination of entanglement negativities, calculated with respect to specific cylinder and torus geometries, determines a necessary condition for when a topological state can be disentangled, i.e., factorized into a tensor product of states defined on cylinder subregions. This condition, which requires the ground state to lie in a definite topological sector, is sufficient for the Laughlin state. On the other hand, we find that a general Moore-Read ground state cannot be disentangled even when the disentangling condition holds. It would be interesting to find an entanglement measure that provides a sufficient condition for whether the Moore-Read state (or a more general (2+1)d topological state) can be disentangled.

References

[R1] R. Willett, J. P. Eisenstein, H. L. Stormer, D. C. Tsui, A. C. Gossard, and J. H. English, Phys. Rev. Lett. **59**, 1776 (1987).

[R2] G. Moore and N. Read, Nuclear Physics B **360**, 362 (1991).

[R3] N. Read and D. Green, Phys. Rev. B **61**, 10267 (2000).

[R4] M. Levin, B. I. Halperin, and B. Rosenow, Phys. Rev. Lett. **99**, 236806 (2007).

- [R5] S.-S. Lee, S. Ryu, C. Nayak, and M. P. A. Fisher, Phys. Rev. Lett. **99**, 236807 (2007).
- [R6] C. L. Kane and M. P. A. Fisher, Phys. Rev. B **55**, 15832 (1997).
- [R7] A. Cappelli, M. Huerta, and G. R. Zemba, Nucl. Phys. B **636**, 568 (2002).
- [R8] M. Banerjee, M. Heiblum, V. Umansky, D. E. Feldman, Y. Oreg, and A. Stern, Nature (London) **559**, 205 (2018).
- [R9] D. T. Son, Phys. Rev. X **5**, 031027 (2015).
- [R10] P. T. Zucker and D. E. Feldman, Phys. Rev. Lett. **117**, 096802 (2016).
- [R11] C. Wang, A. Vishwanath, and B. I. Halperin, Phys. Rev. B **98**, 045112 (2018).
- [R12] D. F. Mross, Y. Oreg, A. Stern, G. Margalit, and M. Heiblum, Phys. Rev. Lett. **121**, 026801 (2018).
- [R13] B. Lian and J. Wang, Phys. Rev. B **97**, 165124 (2018).
- [R14] S. H. Simon, Phys. Rev. B **97**, 121406(R) (2018).
- [R15] K. K. W. Ma and D. E. Feldman, Phys. Rev. B **99**, 085309 (2019).
- [R16] S. H. Simon and B. Rosenow, Phys. Rev. Lett. **124**, 126801 (2020).
- [R17] C. de C. Chamon and E. Fradkin, Phys. Rev. B **56**, 2012 (1997).
- [R18] L. Balents and M. P. A. Fisher, Phys. Rev. Lett. **76**, 2782 (1996).
- [R19] D. V. Else, R. Thorngren, and T. Senthil, arXiv:2007.07896 (2020).

Publications

- [P1] A. Mitra and M. Mulligan, Phys. Rev. B **100**, 165122 (2019).
- [P2] C.-J. Lee and M. Mulligan, Phys. Rev. Research **2**, 023303 (2020).
- [P3] H. Asasi and M. Mulligan, Phys. Rev. B **102**, 205104 (2020).
- [P4] C.-J. Lee, P. Kumar, and M. Mulligan, Phys. Rev. B **104**, 125119 (2021).
- [P5] P. K. Lim, H. Asasi, J. C. Y. Teo, and M. Mulligan, Phys. Rev. B **104**, 115155 (2021).

Fractons and beyond

Rahul Nandkishore, University of Colorado Boulder

Program Scope

The funded research is focused on exploring fracton phases of quantum matter, and consists of three major thrusts. The first thrust uses fractons as inspiration to explore many body quantum dynamics with constraints, and leverages the PI's expertise in non-equilibrium and dynamical phases. The key goals are to explore the rich quantum dynamics of fracton phases, and to understand what are the general principles for 'designing' lattice models with ultra-slow dynamics (which may serve as arbitrarily good memories for quantum information). The second thrust investigates the thermodynamics of fracton phases at non-zero charge density complete with their interplay with disorder (material heterogeneity). This thrust aims to discover new phases in the fractonic setting with no analog in conventional condensed matter systems, and to understand also their stability (or lack thereof) to disorder, which will inevitably be present in laboratory realizations. The third thrust is concerned with the search for fractons in real materials, and makes connections in particular to frustrated magnetism. Key problems include identifying crisp experimental diagnostics of fracton phases, and also identifying candidate materials that might realize such phases.

Keywords: fracton dynamics, experimental diagnostics of fracton physics

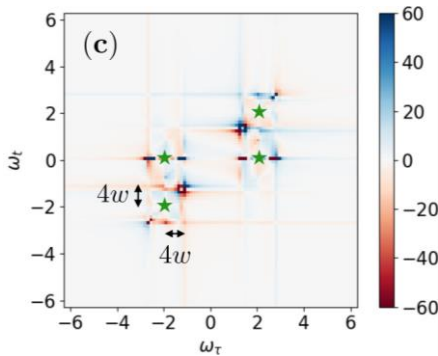
Recent Progress

DOE support has enabled the completion of three major projects. Two of these are published and the third is on arXiv and under review. One published project explains how *gapped* spin liquid phases (both conventional spin liquids and 'fracton' spin liquids) may be unambiguously identified in (non-linear) spectroscopic experiments. The manuscript on arXiv/under review explains how certain *gapless* fracton phases 'of type II' may be spectroscopically identified experimentally. Both address an important open problem that was a key focus of the proposal: viz. the experimental characterization of fracton phases. Another manuscript explores how quantum information may be protected using 'higher form symmetries,' which are closely related to the subsystem symmetries inherent in many descriptions of fracton phases. This addresses a different problem that was also a key part of the proposal viz. the identification of new 'fracton inspired' lattice models capable of protecting quantum information. I discuss these three completed projects in more detail below.

- 1. Spectroscopic fingerprints of gapped quantum spin liquids, both conventional and fractonic.** Rahul M. Nandkishore, Wonjune Choi and Yong Baek Kim, *Phys. Rev. Research* **3**, 013254 (2021)

The proposal is concerned with *fracton* phases, which are exotic types of spin liquid phases where the elementary excitations have restricted mobility. However, an important question pertaining to fracton phases is still open: if we had an experimental realization of a fracton phase, how would we know? Thus, identifying signatures by which fracton phases might be experimentally *characterized* was a key portion of the proposal.

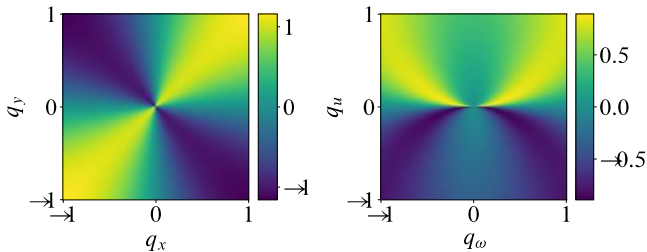
Fracton phases come in two types: type I (which contain ‘subdimensional’ excitations able to move in certain directions, but not others), and ‘type II’ (where non-trivial excitations are fully immobile). The phases can further be subdivided into *gapped* phases (where the ground state is separated from the rest of the spectrum by an energy gap), and *gapless* phases, where excited states exist (in the thermodynamic limit) at energies arbitrarily close to the ground state. Prior work by the PI had identified characteristic signatures of *gapless, type I* fracton phases in neutron scattering [1]. However, how to diagnose *gapped* fracton phases was still an open question. Furthermore, unambiguous experimental diagnosis even of *conventional* gapped spin liquids is a longstanding and famously challenging problem.



Two dimensional Fourier transform of the imaginary part of the non-linear susceptibility for the Ising spin liquid. This contains fingerprints of deconfinement. Similar fingerprints arise in fracton phases, and are not limited to solvable points.

In this work, carried out in collaboration with a group at the University of Toronto, I explained how *gapped type I* fracton phases may be unambiguously characterized experimentally. As a bonus, the method of characterization also works for conventional gapped spin liquids. The method of characterization uses the rapidly developing experimental tool of *multidimensional coherent* (nonlinear) *spectroscopy*. In this technique, one ‘hits’ the sample with two distinct ‘pump’ pulses, with a time delay between them, and then examines the nonlinear response. We explained how gapped spin liquids, both conventional and (type I) fractonic, have characteristic fingerprints in the response thereby obtained. Results are specifically worked out for the Kitaev toric code and the X-cube model, which are paradigmatic examples of conventional gapped spin liquids, and gapped type I fracton phases respectively. Results are presented both at the exactly solvable points, and for small perturbations about the solvable points.

2. Spectroscopic signatures of type II gapless fracton phases. Oliver Hart and Rahul Nandkishore, arXiv: 2106.15631



Characteristic pinch point structure for conventional U(1) spin liquids (left) contrasted with gapless type II fracton spin liquids (right). The ‘parabolic’ contours on the right are fingerprints of type II fracton behavior.

This project tackles the same basic problem as the first project viz. identification of crisp experimental fingerprints of fracton phases, but this time focusing on the exotic type II fracton phases. Specifically, we explained how gapless type II fracton phases, such as the U(1) Haah code, may be identified spectroscopically. Our analysis makes use of the ‘multipole gauge theory’

description of type II fracton phases, which exhibits ultraviolet-infrared (UV-IR) mixing. We show that neutron scattering experiments on gapless type II fracton phases should generically exhibit pinch points in the structure factor, with distinctive parabolic contours as a result of UV-IR mixing. This distinctive pinch point structure provides a clean diagnostic of type II fracton phases. We also identify distinctive signatures of the (3+1)-D U(1) Haah code in the low temperature specific heat.

3. Symmetry protected self correcting quantum memory in three space dimensions. Charles Stahl and Rahul Nandkishore, *Phys. Rev. B* **103**, 235112 (2021)

Another major objective of the proposal was to identify new fracton inspired routes to realizing lattice models with long relaxation times, capable of protecting quantum information. Indeed, whether self-correcting quantum memories can exist at nonzero temperature in a physically reasonable setting remains a great open problem. It has recently been argued [2] that symmetry-protected topological (SPT) systems in three space dimensions subject to a strong constraint—that the quantum dynamics respect a *1-form symmetry* (closely related to the ‘subsystem symmetries’ that show up in fracton phases)—realize such a quantum memory. We illustrate how this works in Walker-Wang codes, which provide a specific realization of these desiderata. In this setting we show that it is sufficient for the 1-form symmetry to be enforced on a subvolume of the system. This strongly suggests that the SPT character of the state is not essential. We confirm this by constructing an explicit example with a *trivial* (paramagnetic) bulk that realizes a self-correcting quantum memory. We therefore show that the enforcement of a 1-form symmetry on a measure-zero subvolume of a three-dimensional system can be sufficient to stabilize a self-correcting quantum memory at nonzero temperature.

Future Plans

I plan to continue working on the problems detailed in the proposal. We've already made substantial progress in the course of the past year, and I am optimistic that I will be able to make substantial further progress over the next year. Specific problems that I am currently working on include:

1. Exploring the dynamics of fracton systems. Specific lines of attack include:
 - (a) Generalizing the notion of ‘Hilbert space shattering’ which I previously developed for type I fracton systems (*Phys. Rev. B* 101, 174204(2020)) to type II fracton systems
 - (b) Exploring settings in which ‘higher form’ symmetries can emerge naturally, and hence yield slow dynamics
 - (c) Combining ‘fracton like’ quantum codes with Michnicki's notion of ‘welding’ (*Phys. Rev. Lett.* 113, 130501 (2014)) to yield new highly protected quantum memories
2. Exploring the thermodynamics of fracton phases. Specific lines of attack include

- (a) Obtaining Mermin-Wagner theorems for the spontaneous breaking of 'multipolar symmetries,' which naturally arise in the context of fractonic systems.
 - (a) Generalizing Imry-Ma type theorems to systems with 'multipole conservation laws' (such as arise in fracton systems, and in non-fractonic systems in fractonic dynamical universality classes), as a stepping stone to a general understanding of the stability of fracton phases to disorder.
 - (b) Exploring the stability of type II fracton orders to quenched disorder
3. Searching for material realizations of fracton physics . Specific lines of attack include
- (a) Identifying crisp experimental fingerprints for gapped type II fracton phases
 - (b) Developing a phenomenology of fracton systems 'enriched' by spin SU(2) symmetry, and hence searching for possible fracton phases that may have been discovered but overlooked in old studies of spin glasses (with collaborators Michael Hermele and Itamar Kimchi), and
 - (c) Searching for manifestations of 'Hilbert space shattering' in the context of elasticity theory, motivated by fracton elasticity duality (with collaborator Leo Radzihovsky).

References

- 1) A. Prem, S. Vijay, Y.Z. Chou, M. Pretko and R.M. Nandkishore, *Phys. Rev. B* **98**, 165140 (2018)].
- 2) S. Roberts and S. D. Bartlett, *Phys. Rev. X* **10**, 031041 (2020)

Publications

1. **Spectroscopic fingerprints of gapped quantum spin liquids, both conventional and fractonic.** Rahul M. Nandkishore, Wonjune Choi and Yong-Baek Kim, *Phys. Rev. Research* **3**, 013254 (2021)
2. **Symmetry-protected self-correction quantum memory in three space dimensions.** Charles Stahl and Rahul Nandkishore, *Phys. Rev. B* **103**, 235112 (2021)
3. **Experimental signatures of gapless type II fracton phases.** Oliver Hart and Rahul Nandkishore, arXiv: 2106.15631 (under review)

Controlling reversible phase transitions in rare-earth nickelates for novel memory devices

Principal Investigator: Badri Narayanan (University of Louisville)

Collaborators: Dillon Fong (Materials Science Division, Argonne National Laboratory), Subramanian Sankaranarayanan (Center for Nanoscale Materials, Argonne National Laboratory)

Program Scope

Resistive switching in strongly correlated oxides is lucrative for emerging applications in neuromorphic computing, and densely scaled non-volatile memory. Colossal changes in electrical conductance (up to 7 orders of magnitude) can be achieved in rare-earth nickelates by introducing oxygen vacancies; via a combination of crystal field splitting, and filling-controlled Mott-Hubbard electron-electron correlations in the Ni $3d$ orbitals. More importantly, resistance states can be manipulated by controlling the spatial distribution of oxygen vacancies, which can migrate under applied bias. Nevertheless, the promise of using defect-driven Mott transitions in these emergent materials for a new paradigm in energy-efficient computing is far from being realized. Most of the challenges thwarting progress stem from a lack of fundamental understanding of the dynamical processes that determine transport of oxygen vacancies, and spatiotemporal evolution of oxygen vacancies (and other extended defects) over nano-to-mesoscopic length/timescales under applied electric field. The goal of this research program is to address this knowledge gap by using a combination of density functional theory (DFT) calculation, *ab initio*/classical molecular dynamics (AIMD/CMD) simulations using accurate interatomic models developed machine learning (ML) methods, precision synthesis, and multi-modal X-ray imaging experiments. The synthesis and characterization experiments are performed by collaborators at Argonne National Laboratory. Such an integrated approach offers to elucidate the correlations between subtle structural distortion and oxidation states; treat localized charge carriers; describe defect/ion transport in the presence of electric field; and, in turn, greatly advance the current understanding of microstructural evolution in rare-earth nickelates under applied bias. The fundamental knowledge gained from this work will enable precise control over hierarchical defect structures and unravel new routes to manipulate resistance states in rare-earth nickelates. This, in turn, will accelerate design of novel neuromorphic devices with prescribed set of neural functionalities, and high-speed densely-scaled resistive random access memory (RRAM) technologies.

Keywords: Strongly correlated oxides, resistive switching, defect dynamics for neuromorphic computing

Recent Progress

The project started on September 1, 2020. In the first year, we made significant progress in (a) understanding the correlations between local structure, electronic properties, magnetic ordering, and transport barriers for OVs in oxygen deficient rare-earth nickelates (RNiO_3), (b) developed a deep neural network based classical interatomic potential for SmNiO_3 (representative nickelate) to investigate bond and charge disproportionation at various temperatures, and (c) demonstrated how spatio-temporal evolution of oxygen vacancies in WO_{3-x} can be controlled via carefully designed electrode geometries to reduce stochastic nature of conducting channels in memristors, and in turn,

enhance their reliability. Below, we briefly describe the key results obtained in each of these directions:

1. Migration of oxygen vacancies in oxygen-deficient rare-earth nickelate: Introduction of oxygen vacancies (OVs) into the lattice of $RNiO_3$ leads to a formation of a range of different Ni-centered polyhedral shapes, including square pyramidal (NiO_5), square planar or distorted tetrahedron (NiO_4), and trigonal planar (NiO_3). AIMD simulations on a representative oxygen-deficient rare-earth nickelate, $SmNiO_{3-\delta}$ showed that OVs migrate by hopping between neighboring O sites within a NiO_x polyhedron, regardless of local OV concentration or their spatial distribution. However, the activation barrier for OV migration (as determined by DFT+ U based nudged elastic band calculations)[1, 2] is strongly controlled by (a) presence of different NiO_x polyhedra, (b) magnetic ordering, and (c) spatial distribution of OVs (Figure 1). OV migration within 3D-shaped polyhedron (i.e., square pyramidal) is associated with a higher activation barrier as compared to 2D shapes (such as square-planar) due to lower space in the inter-polyhedral region available for OV migration. Interestingly, although OV migration is restricted to a specific NiO_x polyhedron, the shapes of other NiO_x polyhedra in the vicinity of the migrating OV significantly impact its kinetics (Figure 1 (b,c)). For instance, increasing the number of 2D square planar NiO_4 (at higher δ) in the local neighborhood drastically slows down OV migration within a square pyramid NiO_5 . This increase in barrier is found to be strongly correlated with decreasing average magnetic moment of Ni (Figure 1c). Magnetic ordering of the crystal also has a strong influence on the activation barrier, with A-AFM showing fastest OV migration kinetics (Fig. 1d) – once again, correlated with high average magnetic moment of Ni atoms. More importantly, at any composition, several distinct spatial distributions of OVs can co-exist; with dramatically different

OV transport kinetics. Figure 1e shows two OV configurations at $\delta = 0.125$ with different OV-OV separation distances that are energetically close to each other (within 5 meV/atom). The OV migration barrier is significantly lower (~14%) when the OVs are in proximity ($d_1 = 2.5 \text{ \AA}$) as compared to when they are far apart ($d_2 = 6.5 \text{ \AA}$). This reduction is directly related to difference in shape of the NiO_x polyhedron containing the OV hop; at $d_1 = 2.5 \text{ \AA}$, the OV hops within a 2D square planar NiO_4 ,

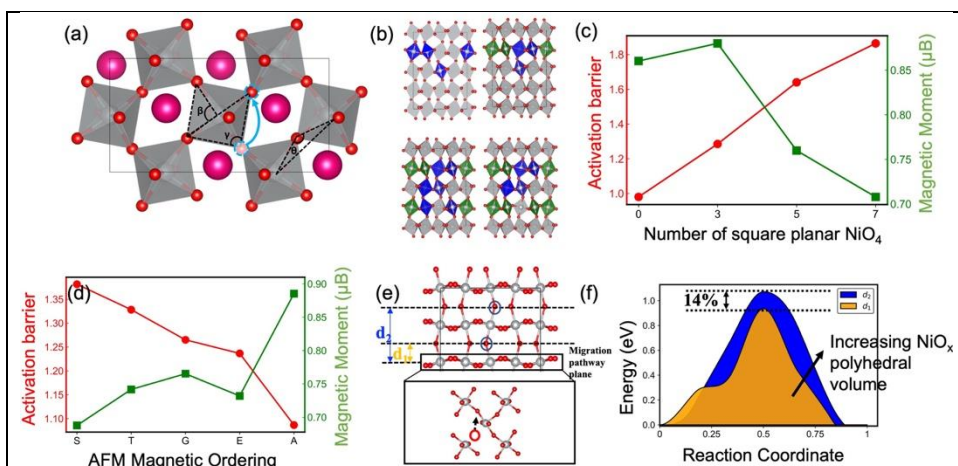


Figure 1. DFT + U investigation of migration of OVs in oxygen deficient $SmNiO_{3-\delta}$. (a) Crystal structure of pristine $SmNiO_3$ showing a corner-sharing network of NiO_6 octahedra (gray); a typical pathway for OV migration is shown by cyan arrow. (b) Schematic atomic images showing varying amounts of different NiO_x polyhedral, namely square pyramid (blue) and square-planar (green) at different levels of oxygen deficiency. (c) Variation in OV migration barrier and average magnetic moment of Ni with number of square planar NiO_4 , (d) Variation in OV migration barrier in $SmNiO_{2.9375}$ and average magnetic moment of Ni at different magnetic ordering. Spatial distribution of OVs strongly influence the OV migration barrier. Two representative configurations with different OV separation in $SmNiO_{2.875}$ are shown in panel (e) and the energy landscape of migrating OV in each case is shown in panel (f).

which affords higher inter-polyhedral space than at $d_2 = 6.5 \text{ \AA}$, wherein, OV hops within a 3D square pyramid NiO_5 . In addition, distortions of RNiO_3 lattice is directly related to size of the rare-earth cation (R); lower size of R induces low lattice distortion, which in turn, is associated with higher OV migration barrier due to low inter-polyhedral space available for OV migration.

2. Machine learning classical interatomic potential for pristine rare-earth nickelate: Atomic-scale interaction models are urgently needed to investigate the dynamical processes underlying the spatiotemporal evolution of oxygen vacancies (and other extended defects) over nano-to-mesoscopic length/timescales. To address this urgent need, we employ deep learning neural networks (DNNs) to train a model for SmNiO_3 as a representative of the rare earth nickelates. The data sets for the training were generated from AIMD simulations at several representative temperatures; the number of training sets were reduced by using active learning approaches.[3] The DNN architecture consisted of 3 layers with 400 nodes each. The local structure was represented by the symmetry functions implemented in the smooth version of the DeePMD-kit.[4] Our newly developed DNN predicts the atomic forces within 0.5 meV/\AA , and Ni-charges within $0.01e$ of the DFT+ U calculations. Our newly developed DNN models accurately predict the Ni-O bond disproportionation, observed as two distinct volumes of NiO_6 octahedra, ($\sim 9.7 \text{ \AA}^3$ and $\sim 11.5 \text{ \AA}^3$) at low temperature (insulator phase), as well as collapse of this heterogeneity (i.e., one single type of NiO_6 octahedra $\sim 10.5 \text{ \AA}^3$) at high temperature (metal phase) (Figure 2(a,b)). The DNN model also accurately describes the concomitant charge disproportionation between Ni atoms (Figure 2(c,d)). This newly developed model provides a route to access long-time dynamics in RNiO_3 , which has not been possible till date.

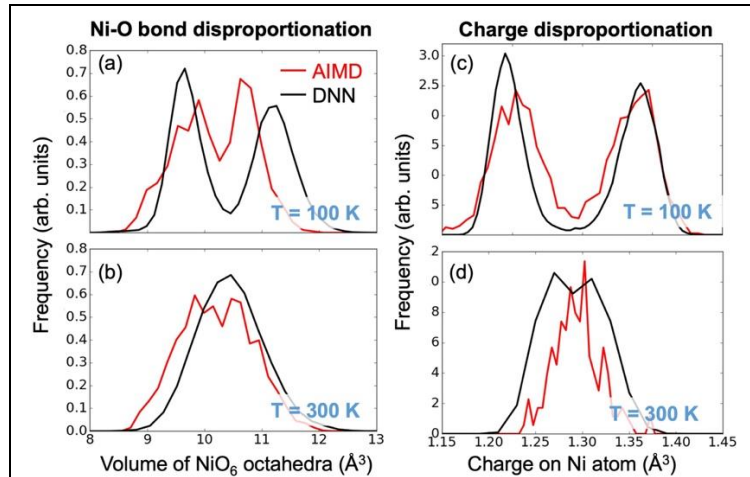
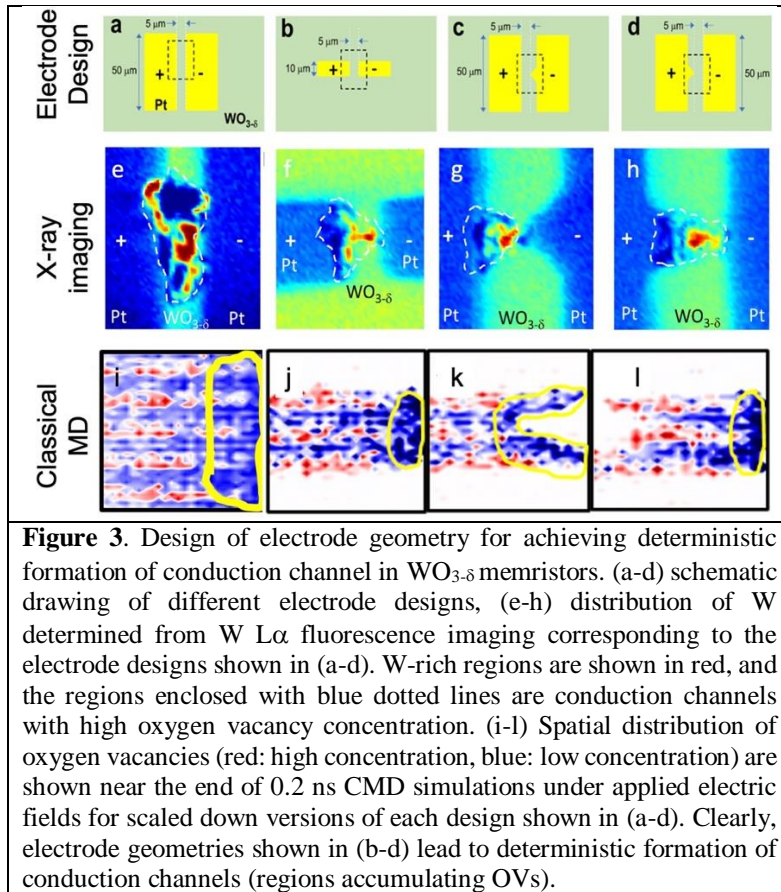


Figure 2. Deep neural network model for SmNiO_3 developed using data from AIMD simulations. Distribution of (a,b) volume of NiO_6 octahedra, and (c,d) charges on Ni atoms over a 500 ps NVT trajectory obtained using DNN based classical molecular dynamics at 100 K (panels (a,c)), and 300 K (panels (b,d)). We have also provided distributions obtained from 50 ps long AIMD simulations for comparison.

Our newly developed DNN predicts the atomic forces within 0.5 meV/\AA , and Ni-charges within $0.01e$ of the DFT+ U calculations. Our newly developed DNN models accurately predict the Ni-O bond disproportionation, observed as two distinct volumes of NiO_6 octahedra, ($\sim 9.7 \text{ \AA}^3$ and $\sim 11.5 \text{ \AA}^3$) at low temperature (insulator phase), as well as collapse of this heterogeneity (i.e., one single type of NiO_6 octahedra $\sim 10.5 \text{ \AA}^3$) at high temperature (metal phase) (Figure 2(a,b)). The DNN model also accurately describes the concomitant charge disproportionation between Ni atoms (Figure 2(c,d)). This newly developed model provides a route to access long-time dynamics in RNiO_3 , which has not been possible till date.

3. Understanding deterministic Formation of Conduction Channel in Memristive Devices via classical molecular simulations: One of the biggest roadblocks thwarting commercialization of memristors is the large variability in their performance from device-to-device and cycle-to-cycle. This variability is mainly due to the highly stochastic nature of the formation of conduction channels. Both the location and resistivity of these channels that form via re-distribution of OVs (under applied electric field) can vary widely across devices and operating cycles in the devices. Using a combination of classical MD (CMD) simulations and multi-modal X-ray imaging (at Argonne), we found that conduction channels can be formed deterministically via careful design of the electrode. Instead of the widely used vertical geometry, we have introduced a planar device geometry that allowed us full spatial access of the conduction channel. Our CMD simulations show that the electrode shape can control the application of the electric field on a specific area and thereby can control the migration of the oxygen vacancies and consequent formation of the



conduction channel; these results are supported by multi-modal X-ray imaging (Figure 3). In our CMD simulations, we used scaled-down version of the electrode geometries used to fabricate the memristor devices at Argonne. Specifically, we investigated defect re-distribution in crystalline $\text{WO}_{2.7}$ (composition from experiment). We then selectively applied the electric field to mimic the specific electrode geometry as shown in the Figure 3(a-d). Our CMD simulations showed that in regions where electric field is applied, the OVs selectively migrate to the cathode (negative electrode). These O-deficient regions constitute the conduction channels that form in the memristor during operation. Clearly, the constraining the electric field to specific regions via careful design of the electrode

drastically reduces the stochastic nature of the formation of conduction channels and enhances the reliability of these devices.

Future Work

We will extend our DNN model to accurately describe energies, atomic forces, and atomic charges for oxygen-deficient SmNiO_3 . Once the DNN model is well trained for both pristine and defects, we will employ CMD simulations to identify atomic-scale mechanisms that govern (a) spatiotemporal evolution of defect structure, formation of grain boundaries/extended defects, and (b) evolution of nano-scale domains (with different resistivity) under applied bias; as well as (c) hysteresis effects, and relaxation dynamics during repeated cycles of alternating forward and reverse bias.

References

1. Zuo, F., et al., *Habituation based synaptic plasticity and organismic learning in a quantum perovskite*. Nature Communications, 2017. **8**.
2. Zhang, Z., et al., *Perovskite nickelates as electric-field sensors in salt water*. Nature, 2017. **553**: p. 68.
3. Patra, T.K., et al., *A coarse-grained deep neural network model for liquid water*. Applied Physics Letters, 2019. **115**(19): p. 193101.
4. Wang, H., et al., *DeePMD-kit: A deep learning package for many-body potential energy representation and molecular dynamics*. Computer Physics Communications, 2018. **228**: p. 178-184.

Publications

- 1) R. Pidathala, D. Bhagat and B. Narayanan. *Ab initio* investigation of formation and migration of oxygen vacancies in oxygen-deficient samarium nickelate. *Manuscript under preparation*.
- 2) M. Galib and B. Narayanan, Machine learning interatomic potentials for rare-earth nickelates. *Manuscript under preparation*
- 3) H. Liu, M.Galib, Y. Dong, T. Loeffler, Z. Cai, L. Stan, H. Zhou, S. Sankaranarayanan, B. Narayanan, and D. Fong. Deterministic Formation of Conduction Channel in Memristive Devices. *Manuscript under preparation*

Correlations and Dynamics in Quantum Materials

Olle Heinonen (ANL), Peter Littlewood (UC/ANL), Ivar Martin (ANL), Kostya Matveev (ANL), Michael Norman – lead PI (ANL), Hyowon Park (UIC/ANL)

Program Scope

Our multi-faceted condensed matter theory research program has the overarching goal of understanding how interactions, dimensionality and topology lead to new equilibrium or metastable phases, and exploiting this to propose new materials with desired properties. One key focus is on the understanding of novel phenomena and electronic phases in transition metal oxides and related materials, including the influence of structural and magnetic fluctuations, phonons, spin-orbit, orbital degrees of freedom, chemical doping, and defects. Another key focus is on topological properties and dynamics of magnets, artificial spin ices, multiferroics and superconductors, including driven systems, along with electrical and thermal transport in quantum wires and low carrier density materials.

Keywords: strongly correlated materials, low dimensional systems, topological matter

Recent Progress

Scar states in a system of interacting chiral fermions - We have studied the energy spectrum of a system of interacting chiral fermions, such as those at the edge of a quantum Hall droplet. We found that as a function of interaction strength, the levels near the upper edge of the spectrum intersect each other. This results in a novel mechanism of formation of quantum many-body scars in the system. Our analytical theory and numerical calculations show that states of bosonic nature, that are native to the strong interaction regime, penetrate the region of weak interactions dominated by fermionic many-body states. We have suggested a way to observe the scar states in a properly gated quantum Hall droplet.

First-principles study of magnetic states and the anomalous Hall conductivity of $M\text{Nb}_3\text{S}_6$ ($M=\text{Co}, \text{Fe}, \text{Mn}, \text{Ni}$) - Inspired by the observation of the extremely large anomalous Hall effect in the absence of applied magnetic fields or uniform magnetization in CoNb_3S_6 [Nature Commun. 9, 3280 (2018)], we performed first-principles study of this and related materials of the $M\text{Nb}_3\text{S}_6$ type with different transition metal M ions to determine their magnetic orders and their anomalous Hall conductivity (AHC). We found that non-coplanar antiferromagnetic ordering is favored relative to collinear or coplanar order in the case of $M=\text{Co}, \text{Fe}$ and Ni , while ferromagnetic ordering is favored in MnNb_3S_6 . The AHC in these materials with non-coplanar spin ordering can reach about e^2/h per crystalline layer, while being negligible for coplanar and collinear cases. We also find that the AHC depends sensitively on doping and reaches a maximum for weak to intermediate values of the local spin exchange fields. Our AHC results are consistent with the reported Hall measurements in CoNb_3S_6 and suggest the possibility of a similarly large anomalous Hall effect in related materials.

Nematic order driven by superconducting correlations - The interplay of nematicity and superconductivity has been observed in a wide variety of quantum materials. To explore this

interplay, we considered a 2D array of nematogens, local droplets with Z3 nematicity, coupled to a network of Josephson junction wires. Using finite temperature classical Monte Carlo simulations, we elucidated the phase diagram of this model and showed that the development of superconducting correlations and the directional delocalization of Cooper pairs can promote nematogen ordering, resulting in long-range nematic order. We obtained transport properties of our model within an effective resistor network picture. We discussed this in the context of the 2D electron gas at a (111) KTaO₃ interface and the doped topological insulators M_xBi₂Se₃ (M=Nb, Cu). In related work, based on ARPES data, we have modeled the surface electronic structure of (111) KTO using both tight binding and k-p schemes. The (111) surface gives rise to a quasi-1D electronic structure that leads to pronounced nesting peaks in the susceptibility. For the case of magnetic order (likely induced by the EuO that is at the other side of the interface), we predict this takes the form of a single-Q spin density wave (magnetic stripe state) stabilized by spin-orbit effects from the Ta ions, which in turn can explain the large transport anisotropy that is observed in experiment. From the k-p analysis, we find significant magnetic octupolar correlations that mix with the magnetic dipolar ones.

Floquet vortex states induced by light carrying orbital angular momentum - We proposed a scheme to create an electronic Floquet vortex state by irradiating a 2D semiconductor with the laser light carrying non-zero orbital angular momentum. We analytically and numerically studied the properties of the Floquet vortex states, with the methods analogous to the ones previously applied to the analysis of superconducting vortex states. We showed that such Floquet vortex states are similar to superconducting vortex states, and they exhibit a wide range of tunability. To illustrate the potential utility of such tunability, we showed how such states could be used for quantum state engineering.

Quasiparticle energy relaxation in one dimension - We have studied how the long-range nature of the Coulomb interaction affects relaxation of 1D fermions. We discovered that unlike higher-dimensional systems, in 1D the relaxation of energetic quasiparticles *increases* rapidly at low energies, as the inverse 6th power of energy. Similarly, for thermal quasiparticles, the relaxation becomes more efficient at low temperatures, where it grows as the inverse square of the temperature. These results suggest that unlike most other systems, a 1D Fermi gas with Coulomb interactions equilibrates most rapidly at low temperatures.

Thermal transport through a defect in a one-dimensional conductor - We have studied thermal transport through a 1D electron system with a single strong defect. We found a novel mechanism of energy transport via hopping of 1D plasmons. The energy current through a 1D system connecting two leads with different temperatures was found to be a difference of the contributions of each lead that scale as a power of the respective temperature. The power is either two or four, depending on whether the Coulomb interactions are screened by a gate. Our results are in good agreement with experiments on carbon nanotubes.

Layered nickelates - In the reduced trilayer nickelates, La₄Ni₃O₈ and Pr₄Ni₃O₈, we have shown via DFT+DMFT simulations that its many-body electronic structure is similar to infinite layer nickelates when compared at the same nominal doping. Moreover, these materials are closer than cuprates to being Mott-Hubbard like, with strong correlations only evident for the Ni 3d x²-y² orbitals. We have also done extensive simulations of x-ray absorption and resonant inelastic x-ray scattering on the reduced trilayer nickelates to compare to data taken at the APS and NSLS-II. The data exhibit d-d excitations along with a pronounced fluorescence line that is a signature

of mixing of the Ni 3d x^2-y^2 orbitals with oxygen 2p orbitals. This has been further confirmed by simulations of O K edge spectra taken at NSLS-II, that indicate that the charge transfer energy, Δ , is of order the Coulomb repulsion energy, U , meaning these materials are intermediate between cuprates ($\Delta < U$) and pure Mott-Hubbard materials (with $\Delta > U$). We have also modeled the magnon excitations of the stripe phase, and found that they are consistent with a large superexchange of 70 meV, again placing these materials intermediate in behavior between other layered nickelates like La_2NiO_4 and cuprates.

Leggett modes associated with crystallographic phase transitions - Higgs and Goldstone modes, well known in high energy physics, have been realized in a number of condensed matter physics contexts, including superconductivity, magnetism and structural phase transitions. We have demonstrated that the Leggett mode, a collective mode observed in multi-band superconductors, also has an analog in crystallographic phase transitions. Such structural Leggett modes can occur in the phase channel as in the original work of Leggett. That is, they are antiphase Goldstone modes (anti-phasons). In addition, a new collective mode can also occur in the amplitude channel, an out-of phase (antiphase) Higgs mode, that should be observable in multi-band superconductors as well. We illustrated the existence and properties of these structural Leggett modes using the example of the pyrochlore relaxor ferroelectric, $\text{Cd}_2\text{Nb}_2\text{O}_7$.

Computing the charge susceptibility in rare-earth tellurides - This project is designed to understand the nature of the CDW state in RTe_3 , with phonon softening near the CDW wavevector indicating the importance of electron-phonon interactions. Although DFT band structures in these materials match with experimental ARPES spectra, the charge susceptibility we computed from DFT does not reproduce the CDW wavevector. We have studied the electron-phonon self-energy effect on the CDW peak positions of tellurides with different rare-earth ions and found that the local electron-phonon interaction can modify the CDW peak location.

Future Plans

Topological frequency conversion - We will investigate a Weyl semimetal irradiated by two electromagnetic modes with distinct frequencies. Under suitable driving, each electron near the Weyl node can transfer energy from one mode to the other at a universal rate of Planck's constant multiplied by the product of the frequencies of the modes. Due to the macroscopic number of electrons involved, the power of conversion can be very large (of order 10^{12} W/cm³). This effect may be used for optical amplification, and terahertz (THz) generation.

Exploring a link between time crystals and many-body scars in long-range interacting systems - A time crystal is a non-equilibrium state of matter which spontaneously breaks time translation symmetry. While the existence of time crystals has been theoretically and experimentally established in periodically driven systems, resulting in a spontaneous breaking of a discrete Z_2 symmetry, we plan to investigate the possibility of a *continuous* time crystal, which has been proposed to occur in undriven, energy-conserving systems exhibiting prethermalization. Such systems are characterized by an exponentially long regime where thermalization is delayed, allowing the system to order and display long-lived oscillations of its order parameter, with the frequency set by the chemical potential.

Interplay between topological protected valley and quantum Hall edge transport - The quantum Hall regime in bilayer graphene hosts a variety of topological correlated states stemming from an eight-fold near-degeneracy of the zeroth Landau level. Some of these states break valley symmetry and correspond to some type of quantum valley Hall states. Generally, these do not yield dissipationless transport due to intervalley scattering at the device edges, which localizes the edge modes. On the other hand, bilayer graphene can contain distinct structural domains, separated by domain walls forming “internal edges”, which are only weakly affected by intervalley scattering. Motivated by recent experimental work, we will study the interplay between transport via the sample edges and domain walls within the manifold of the zeroth Landau level.

Spectral function of electrons at the quantum Hall edge - We will evaluate the spectral function, which can be probed in experiments involving tunneling between edges of two parallel integer quantum Hall systems. At occupation fraction of 1, we expect no power-law renormalization of the tunneling rate typical of Luttinger liquids. The spectral function is expected to have a form of a broadened peak. We will study the width and the shape of the peak as a function of energy.

Viscosity of the one-dimensional Fermi gas - We plan to study the bulk viscosity of a gas of interacting 1D fermions with non-quadratic dispersion. This case describes particles on a lattice. Near the bottom of the spectrum, the dispersion is almost quadratic, which is known to suppress the bulk viscosity. Thus, we will account for interaction effects on quasiparticle energies. In addition, in a certain range of frequencies, 1D systems behave as superfluids. Their viscous properties are described by three viscosity coefficients, which will be separately evaluated.

Layered nickelates – In cuprates, Pr behaves in a mixed valent fashion, leading for instance to dramatically different behavior in $\text{PrBa}_2\text{Cu}_3\text{O}_7$ than in other RBCO materials (R a rare earth). Similarly, for low valence nickelates, $\text{Pr}_4\text{Ni}_3\text{O}_8$ is metallic, whereas $\text{La}_4\text{Ni}_3\text{O}_8$ is a stripe ordered insulator, indicating the possibility that Pr is mixed valent in order to move the effective hole doping (relative to d^9) away from $1/3$. To address whether Pr is mixed valent in these reduced (low valence) nickelates, we plan to perform DFT, DFT+U and DMFT calculations including the 4f electrons of the Pr ions.

Superconducting electron gas in KTaO_3 –Recent experimental work by Bhattacharya on (111) KTaO_3 finds that both the mean-field T_{BCS} and the Kosterlitz-Thouless temperature T_{BKT} scale linearly with carrier density. This implies that one has anti-adiabatic pairing ($E_{\text{F}} < \omega_{\text{D}}$) due to coupling to high energy LO modes. On the other hand, T_{c} is an order of magnitude larger than that found in SrTiO_3 , indicating that coupling of the electrons to the low energy soft TO mode is stronger for KTO, likely due to the much larger spin-orbit coupling of Ta relative to Ti. A microscopic theory of this is challenging given the fact that the TO and LO modes span two orders of magnitude in energy, with the Fermi energy having an intermediate energy scale. This is further complicated by the presence of spin-orbit coupling and Rashba, necessary for coupling to the low energy TO mode. Moreover, T_{c} is very low on the (001) surface compared to the (110) and (111) surfaces. We plan to tackle this problem taking into account the full frequency dependence of the pairing interaction in the presence of a small Fermi energy, along with a surface/interface orientation dependent Rashba coupling.

Select Publications (2020-2021)

1. A. S. Botana and M. R. Norman, Similarities and differences between LaNiO_2 and CaCuO_2 and implications for superconductivity, *Phys. Rev. X* 10, 011024 (2020).
2. J. Karp, A. S. Botana, M. R. Norman, H. Park, M. Zingl and A. Millis, Many-body electronic structure of NdNiO_2 and CaCuO_2 , *Phys. Rev. X* 10, 021061 (2020).
3. J. Karp, A. Hampel, M. Zingl, A. S. Botana, H. Park, M. R. Norman, and A. J. Millis, Comparative many-body study of $\text{Pr}_4\text{Ni}_3\text{O}_8$ and NdNiO_2 , *Phys. Rev. B* 102, 245130 (2020).
4. C. Broholm, R. J. Cava, S. A. Kivelson, D. G. Nocera, M. R. Norman and T. Senthil, Quantum Spin Liquids, *Science* 367, eaay0668 (2020).
5. M. R. Norman, Crystal structure of the inversion-breaking metal $\text{Cd}_2\text{Re}_2\text{O}_7$, *Phys. Rev. B* 101, 045117 (2020).
6. Hyowon Park, Ravindra Nanguneri, and Anh T. Ngo, DFT+DMFT study of spin-charge-lattice coupling in covalent LaCoO_3 , *Phys. Rev. B* 101, 195125 (2020).
7. W. DeGottardi and K. A. Matveev, Viscous Properties of a Degenerate One-Dimensional Fermi Gas, *Phys. Rev. Lett.* 125, 076601 (2020).
8. K. A. Matveev, Sound in a system of chiral one-dimensional fermions, *Phys. Rev. B* 102, 155401 (2020).
9. I Martin, Moiré superconductivity, *Annals of Physics* 417, 168118 (2020).
10. K Agarwal and I Martin, Dynamical Enhancement of Symmetries in Many-Body Systems, *Phys. Rev. Lett.* 125, 080602 (2020).
11. I. Martin and K. Agarwal, Double Braiding Majoranas for Quantum Computing and Hamiltonian Engineering, *PRX Quantum* 1, 020324 (2020).
12. F. Nathan, G. Refael, M. S. Rudner, and I. Martin, Quantum frequency locking and down conversion in a driven qubit-cavity system, *Physical Review Research* 2, 043411 (2020).
13. E. Iacocca, S. Gliga, and O. Heinonen, Tailoring spin wave channels in a reconfigurable artificial spin ice, *Phys. Rev. Applied* 13, 044047 (2020).
14. S. Gliga, E. Iacocca, and O. G. Heinonen, Dynamics of reconfigurable spin ice: towards magnonic functional materials, *APL Materials* 8, 040911 (2020).
15. P. Villar Arribi, A. Paramakanti, and M. R. Norman, A striped electron fluid on (111) KTaO_3 , *Phys. Rev. B* 103, 035115 (2021).
16. G. Chaudhary, A. H. MacDonald and M. R. Norman, Quantum Hall Superconductivity from Moiré Landau Levels, *Phys. Rev. Research* 3, 033260 (2021).
17. X. Liao, V. Singh and H. Park, Oxygen vacancy induced site-selective Mott transition in LaNiO_3 , *Phys. Rev. B* 103, 085110 (2021).
18. Z. Ristivojevic and K. A. Matveev, Quasiparticle energy relaxation in a gas of one-dimensional fermions with Coulomb interaction, *Phys. Rev. Lett.* 127, 086803 (2021).
19. Q. N. Meier, D. Hickox-Young, G. Laurita, N. A. Spaldin, J. M. Rondinelli and M. R. Norman, Leggett Modes Accompanying Crystallographic Phase Transitions, arXiv:2107.11332, submitted, *Phys. Rev. X*.
20. I. Martin and K. A. Matveev, Scar states in a system of interacting chiral fermions, arXiv:2109.06220, submitted, *Phys. Rev. B*.
21. O. Heinonen, R. A. Heinonen, H. Park, Magnetic ground states and spin waves of a model for $(\text{TM})\text{Nb}_3\text{S}_6$, $\text{TM}=\text{Co, Fe, Ni}$, arXiv:2109.13837, submitted, *Phys. Rev. Materials*.

Center for Nonperturbative Studies of Functional Materials Under Nonequilibrium Conditions

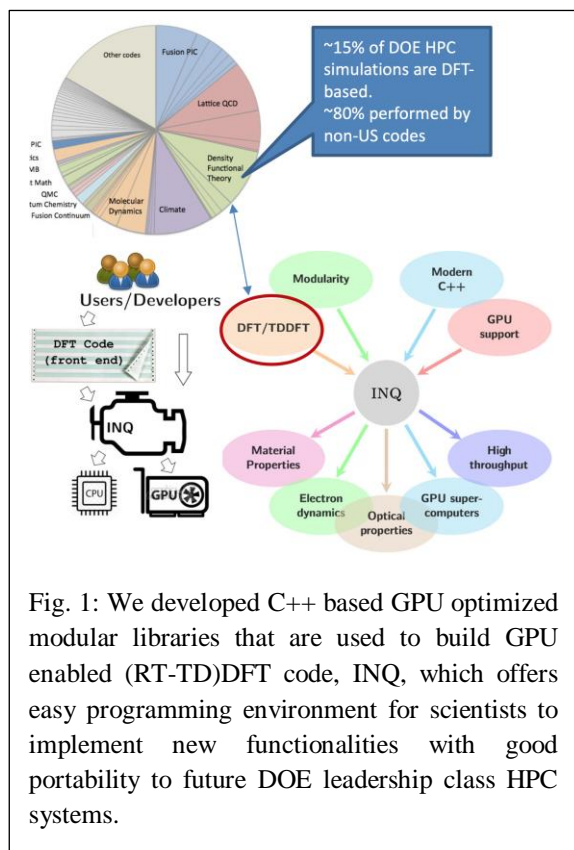
Tadashi Ogitsu¹, Xavier Andrade¹, Alfredo Correa¹, Liang Z. Tan², David Prendergast², C. D. Pemmaraju³, and Aaron M. Lindenberg^{3,4}

¹Lawrence Livermore National Laboratory, ²Lawrence Berkeley National Laboratory, ³SLAC National Accelerator Laboratory, ⁴Stanford University

Program Scope

The development of quantum mechanics in the early 20th century led to a paradigm shift in materials science and engineering that resulted in, for example, the invention of semiconductor devices. The emergence of Density Functional Theory (DFT) together with breakthroughs in algorithms [1,2] and rapid increases in computer performance contributed significantly to the success of modern electronic structure theory. In addition, cross-validation of theory with state-of-art experiments, such as angle resolved photo emission spectroscopy, played a key role in advancing the use of DFT, as it was found to have an optimal balance of accuracy and computational expense. However, progress in the 20th century was mostly limited to describing time-independent quantum mechanical problems. Towards the end of the century, time-dependent versions of DFT (TDDFT) began to emerge [3] and together with the progress in ultrafast experimental techniques and continued advancements in high performance computing (HPC), we

are now positioned to probe into phenomena that require the use of the time-dependent version of the Schrödinger equation, where spin, electronic, and ionic degree of freedoms evolve in a coupled manner.



In this context, the DOE CMS Software Center for Nonperturbative Studies of Functional Materials under Nonequilibrium Conditions (NPNEQ) was launched in September 2019 with the initial goal of developing and distributing an open source real-time TDDFT (RT-TDDFT) code optimized for the current and future DOE Leadership Class HPC systems such as Sierra (LLNL: 125 petaflops, active from 2018), El Capitan (LLNL: 1.5 exaflops, 2023), Perlmutter (NERSC: 64 petaflops, phase I active from June 2021), Summit (200 petaflops, active from 2018), Frontier (ORNL, 1.5 exaflops, 2023), Aurora (ANL, 1 exaflops, 2021).

While our software development platform github/gitlab offers elaborate functionality for developing and testing software, the workflow is

specific to the software and must be drafted by the software developers. Accordingly, we are developing a workflow specific to the INQ code including automated tests performed over multiple HPC systems, which is described in a document accessible through the repository. Also, the users/programmers guides of INQ software will be published.

Our project URL: <https://sc-programs.llnl.gov/npneq>

Download INQ: <https://gitlab.com/npneq/inq>

Keywords: Real-Time Time Dependent-Functional-Theory, GPU computing, Nonequilibrium physics.

Recent Progress

As of June 2021, the RT-TDDFT software named INQ has been successfully implemented and released with all of the functions necessary for calculating ground state electronic structure and time propagation. Rigorous tests for scientific research such as reproducibility of relevant physical quantities have been performed based on comparisons with well established DFT (QE/Qbox) and TDDFT (Octopus/Qb@ll) codes. Optimization on GPU-based architectures has been successfully carried out together with a MPI parallel implementation, where software design, development and testing efforts were closely coordinated through extensive online meetings. INQ has achieved excellent parallel performance using multiple GPUs with standard DFT (GGA) based on the band parallelization scheme. See Figures 2 and 3 for scaling and validation results. A comprehensive report describing the INQ code and its future extension plans has been summarized and submitted to a peer reviewed journal (our publication list [1]).

Current GPU-ready (TD)DFT codes focus on delivering GPU parallel performance for specific types of simulations, such as hybrid exchange-correlation (BigDFT)[4], GW calculations (VASP) [5,6], and CCSD (NWChem) [7]. These calculations intrinsically have a high arithmetic intensity, or k-point parallelization [9, 10] and fewer communication requirements compared to band or grid parallelization strategies. (TD)DFT simulations of realistic materials and systems often require large system sizes in order to account for factors such as defects, impurities, and interfaces. To address the length-scales required for these types of calculations, band and grid parallel schemes are more important than parallelization over k-points in minimizing time to solution. At the time of this writing, only the real space GGA (TD)DFT codes [11, 12] have taken full advantage of the computing power of parallel GPU-type architectures, which suggests that a lack of sufficient interconnect bandwidth in the current HPC platforms may pose a significant challenge to codes that are based on parallel 3D FFT routines, as 3D FFT are known to require high memory and interconnect bandwidth [13].

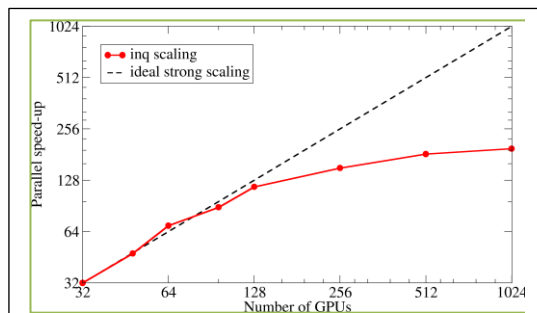
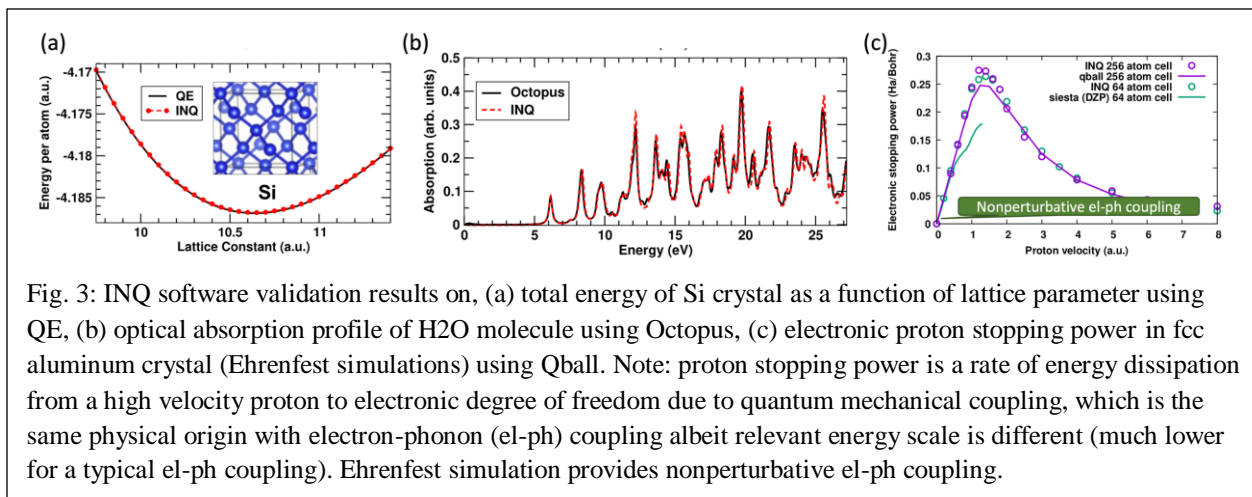


Fig. 2: Speed up of TDDFT simulation as a function of number of GPUs on Lassen at LLNL. The system is 1024 aluminum atoms in a supercell.



Our software development strategy is comprehensive and aims to facilitate advancement of theory by highly programmable design. As such, scientists who are not expert programmers can use our software to implement newly developed theories and algorithms with ease, which will expand the user community and extend the functionality of INQ. Also, our code design focuses on retaining flexibility to accommodate the rapidly evolving HPC system architectures as well as the development of the RT-TDDFT theory itself.

Future Plans

Our future software development plan will prioritize further optimization of INQ for current and next generation DOE Leadership Class HPC systems, such as Lassen/Sierra at LLNL (IBM-Nvidia), El Capitan at LLNL (HPE-AMD), Summit at ORNL (IBM-Nvidia), Frontier at ORNL (HPE-AMD), Aurora at ANL (Intel), Perlmutter at NERSC (HPE-AMD/Nvidia), as well as implementations of functionalities that are necessary for quantum functional materials research. See Fig. 4 for more details and timeline. We will simultaneously conduct regular outreach activities. Please contact Tadashi Ogitsu (ogitsu1@llnl.gov) for more information.

	FY21	FY22		FY23			
INQ	CPU+GPU+MPI opt.	Adopting to AMD/Intel GPUs					
	Fast hybrid exc-corr	Spiral Boundary Condition		Electric/magnetic field			
	Spin-Orbit Coupling	Beyond Ehrenfest		Nuclear spin			
Outreach	CCMS/ TMF Users Meeting	Benasque TDDFT (TBD)		CCMS	CECAM (TBD)		CCMS

Fig. 4: INQ software development and outreach plan for FY21-FY23. Note: CCMS is Computational Chemistry and Materials Science summer school annually held at Lawrence Livermore National Laboratory.

References

1. James W Cooley and John W Tukey, “An algorithm for the machine calculation of complex Fourier series”, *Mathematics of computation* **19**, 297 (1965).
2. Jose Luies Martins and Marvin L. Cohen, “Diagonalization of large matrices in pseudopotential band-structure calculations: Dual-space formalism”. *Phys. Rev. B* **37**, 6134 (1988).
3. Erich Runge and E. K. U. Gross, “Density-Functional Theory for Time-Dependent Systems”, *Phys. Rev. Lett.* **52**, 997 (1984).
4. Laura E Ratcliff et al., “Affordable and accurate large-scale hybrid-functional calculations on GPU-accelerated supercomputers”, *Journal of Physics: Condensed Matter* **30**, 95901 (2018).
5. Mohamed Hacene et al., “Accelerating VASP electronic structure calculations using graphic processing units”, *Journal of Computational Chemistry* **33**, 2581 (2012).
6. Maxwell Hutchinson and Michael Widom, “VASP on a GPU: Application to exact-exchange calculations of the stability of elemental boron”, *Computer Physics Communications* **183**, 1422 (2012).
7. Kiran Bhaskaran-Nair et al., “Noniterative multireference coupled cluster methods on heterogeneous CPU–GPU systems”, *Journal of Chemical Theory and Computation* **9**, 1949 (2013).
8. Paolo Giannozzi et al., “Quantum ESPRESSO toward the exascale”, *The Journal of Chemical Physics* **152**, 154105 (2020).
9. Joshua Romero et al., “A performance study of Quantum ESPRESSO’s PWscf code on multi-core and GPU systems”, *International Workshop on Performance Modeling, Benchmarking and Simulation of High Performance Computer Systems*. Springer. 2017, pp. 67–87.
10. Joshua Romero et al., “A performance study of Quantum ESPRESSO’s PWscf code on multi-core and GPU systems”, *International Workshop on Performance Modeling, Benchmarking and Simulation of High Performance Computer Systems*. Springer. 2017, pp. 67–87.
11. Xavier Andrade et al., “Time-dependent density-functional theory in massively parallel computer architectures: the octopus project”, *Journal of Physics: Condensed Matter* **24**, 233202 (2012).
12. Xavier Andrade and Alán Aspuru-Guzik, “Real-space density functional theory on graphical processing units: computational approach and comparison to gaussian basis set methods”, *Journal of chemical theory and computation* **9**, 4360 (2013).
13. Alan Ayala et al. “heFFTe: Highly Efficient FFT for Exascale”, *Computational Science – ICCS 2020*. Ed. by Valeria V. Krzhizhanovskaya et al. Cham: Springer International Publishing, 2020, pp. 262–275.

Publications

1. Xavier Andrade, Chaitanya Das Pemmaraju, **Alexy Kartsev**, Liang Z. Tan, **Sangeeta Rajpurohit**, Jun Xiao, Aaron Lindenberg, Tadashi Ogitsu, and Alfredo Correa, "INQ, a modern GPU-accelerated computational framework for (time-dependent) density functional theory", <https://doi.org/10.1021/acs.jctc.1c00562>.
2. **Sangeeta Rajpurohit**, C. Das Pemmeraju, Tadashi Ogitsu, and Liang Z. Tan, "A non-perturbative study of bulk photovoltaic effect enhanced by an optically induced phase transition", submitted on May 24, 2021, <https://arxiv.org/abs/2105.11310>.
3. Tyler J. Smart, Hiroyuki Takenaka, Tuan Anh Pham, Liang Z. Tan, Jin Z. Zhang, Tadashi Ogitsu, and Yuan Ping, "Enhancing Defect Tolerance with Ligands at the Surface of Lead Halide Perovskites", *J. Phys. Chem. Lett.* **12**, 6299 (2021).
4. Jorge Kohanoff, Alfredo Correa, Gleb Gribakin, Conrad Johnston, and Andres Saul, "Radioactive decay of ^{90}Sr in cement: a non-equilibrium first-principles investigation", *Euro. Phys. J. D* **75**, 248 (2021).
5. Khalid M. Siddiqui, Daniel B. Durham, Frederick Cropp, Colin Ophus, **Sangeeta Rajpurohit**, Yanglin Zhu, Johan D. Carlström, Camille Stavrakas, Zhiqiang Mao, Archana Raja, Pietro Musumeci, Liang Z. Tan, Andrew M. Minor, Daniele Filippetto, and Robert A. Kaindl, "Ultrafast optical melting of trimer superstructure in layered $1\text{T}'\text{-TaTe}_2$ ", *Comm. Phys.* **4**, 152 (2021).
6. M.-F. Lin, N. Singh, S. Liang, M. Mo, J.P.F. Nunes, K. Ledbetter, J. Yang, M. Kozina, S. Weathersby, X. Shen, A.A. Cordones, T.J.A. Wolf, C.D. Pemmaraju, M. Ihme, and X.J. Wang, "Imaging the short-lived hydroxyl-hydronium pair in ionized water", *Science* **374**, 92 (2021).
7. **Sangeeta Rajpurohit**, Liang Z. Tan, Christian Jooss, and P. E. Blöchl, "Ultrafast spin-nematic and ferroelectric phase transitions induced by femtosecond light pulses", *Phys. Rev. B* **102**, 174430-6 (2020).
8. Edwin E. Quashie, Rafi Ullah, Xavier Andrade, and Alfredo A. Correa, "Effect of chemical disorder on the electronic stopping of solid solution alloys", *Acta Mater.* **196**, 576-583 (2020).
9. Jun Xiao, Ying Wang, Hua Wang, C. D. Pemmaraju, Siqi Wang, Philipp Muscher, Edbert J. Sie, Clara M. Nyby, Thomas P. Devereaux, Xiaofeng Qian, Xiang Zhang and Aaron M. Lindenberg, "Berry curvature memory through electrically driven stacking transitions", *Nature Physics* **16**, 1028-1034 (2020).
10. Luke McClintock, Rui Xiao, Yasen Hou, Clinton Gibson, Henry Clark Travaglini, David Abramovitch, Liang Z. Tan, Ramazan Tugrul Senger, Yongping Fu, Song Jin, and Dong Yu, "Temperature and Gate Dependence of Carrier Diffusion in Single Crystal Methylammonium Lead Iodide Perovskite Microstructures", *J. Phys. Chem. Lett.* **11**, 1000-1006 (2020).

For concreteness, let us focus now on the Raman spectroscopy of optical phonons [4,6], and particularly on the salient Fano line shape, which arises when the phonon resonance peak couples to the magnetic continuum [4,6,7]. In the experimental studies of the candidate material alpha-RuCl₃ [8-12], schematically shown in Figure 1, the pronounced temperature and field dependence of Fano lineshape indicated rich information about the underlying spin liquid phase that awaits exploration. However, a clear theoretical description of the Raman scattering in the Kitaev spin-phonon coupled system was up to now still missing, mainly due to the lack of proper description of spin-phonon and spin-photon couplings. In Ref. [4], we used the symmetry approach and developed a theoretical description of the Raman spectroscopy in the spin-phonon coupled Kitaev system. We showed that it can provide intriguing observable signatures of fractionalized excitations characteristic of the underlying spin liquid phase. In particular, we obtain the explicit form of the phonon modes and construct the coupling Hamiltonians based on D_{3d} symmetry. We then systematically computed the Raman intensity (Fig.2(a-c)) and showed that the spin-phonon coupling renormalizes phonon propagators. In particular, the spin-phonon interaction leads to the Raman vertex renormalization due to the final-state interactions that generate the salient Fano lineshape. We found that the temperature evolution of the Fano lineshape displays two crossovers (Fig.2(d-f)), and the low temperature crossover shows pronounced magnetic field dependence. We thus identify the observable effect of the Majorana fermions and the Z₂ gauge fluxes encoded in the Fano lineshape. Our results explained most of the phonon Raman scattering in the candidate material alpha-RuCl₃.

We believe that our findings on the spin-phonon effects in the Kitaev materials are important for several reasons. Firstly, the results are important for the ongoing hunt for quantum spin liquids. We present a new way for the characterization and identification of such phases through their coupling to phonons. Secondly, we provide a theoretical framework to calculate corresponding experimental observables which will allow to account for the potential experimental findings and not only in Kitaev materials. Thirdly, the community interested in these results is very large and very broad, combining

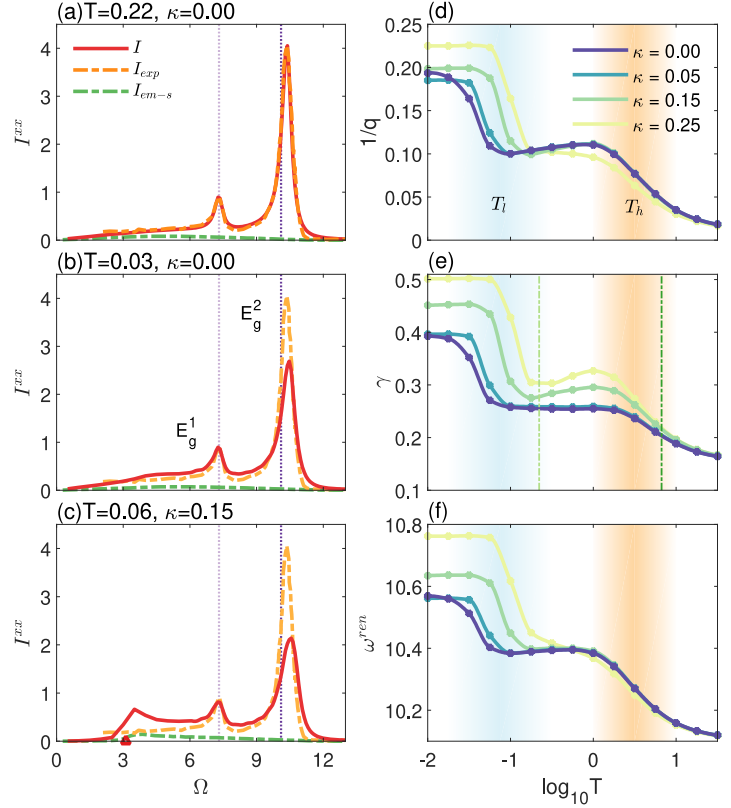


Figure 2: Panels (a-c): The frequency dependence of MC simulated Raman intensity $I(\Omega)$ at different temperatures T and three-spin interaction term strengths κ , corresponding to various average flux densities. $I_{exp}(\Omega)$ is the experimental Raman spectrum in the xx geometry scattering [8] obtained at $T=0.22$ and $\kappa=0$. By fitting computed curve $I(\Omega)$ to the experimental intensity $I_{exp}(\Omega)$, the best-fit parameters of the theory can be obtained. Panels (d-e): The temperature dependence of the E_g^2 peak curve parameters obtained from the Lorentzian fitting: $1/q$, γ and ω^{ren} . T_1 and T_h are two crossover temperatures.

researchers – theorists and experimentalists alike – working in the field of quantum magnetism. Finally, this is a timely contribution to a very active and rapidly developing field.

Future Plans

Future plans include the continuation of the exploration of the spin-phonon coupling in other quantum spin liquids. Now we are studying the phonon dynamics in the Kitaev model on the hyperhoneycomb lattice. We already derived the Majorana fermion-phonon coupling vertices using the symmetry considerations. We will use these vertices to compute phonon attenuation, phonon conductivity, phonon viscosity, and phonon Hall effect in this three-dimensional Kitaev spin liquid. We expect that the attenuation rate due to the decay of a phonon into a pair of Majorana fermions will be linear in temperature due to the vanishing density of states at the vicinity of the nodal line and, thus, will be the dominant one compared with the sound attenuation due to phonon-phonon interactions that in the three-dimensional system scales as T^4 . Our preliminary results, indicate that due to the presence of the nodal line in the low-energy Majorana fermion spectrum, the scattering of the acoustic phonons on the Majorana fermions is stronger for the hyperhoneycomb lattice than for the honeycomb lattice.

Other immediate research plan is to fully understand the magnetic Raman scattering data in beta-Li₂IrO₃ obtained by the group of K. Burch from Boston College. Our preliminary results show that a distinctive, one-magnon low-energy peak in the ac polarization channel observed by them comes from the non-Loudon-Fleury terms, which we recently analyzed in Ref. [13]. We also plan to analyze optical phonon modes observed in this compound.

References

- [1] A. Kitaev, *Annals of Physics* 321, 2 (2006).
- [2] M. Ye, R. M. Fernandes, and N. B. Perkins, *Physical Review Research* 2, 033180 (2020).
- [3] K. Feng, M. Ye, and N. B. Perkins, *Phys. Rev. B* 103, 214416 (2021).
- [4] K. Feng, S. Swarup, and N. B. Perkins, arxiv:2108.08878.
- [5] A. Metavitsiadis and W. Brenig, *Physical Review B* 101, 035103 (2020).
- [6] A. Metavitsiadis, W. Natori, J. Knolle, and W. Brenig, arXiv preprint arXiv:2103.09828 (2021).
- [7] J. Knolle, G.-W. Chern, D. Kovrizhin, R. Moessner, and N. Perkins, *Physical review letters* 113, 187201 (2014).
- [8] L. J. Sandilands, Y. Tian, K. W. Plumb, Y.-J. Kim, and K. S. Burch, *Physical review letters* 114, 147201 (2015).
- [9] G. Li, X. Chen, Y. Gan, F. Li, M. Yan, F. Ye, S. Pei, Y. Zhang, L. Wang, H. Su, et al., *Physical Review Materials* 3, 023601 (2019).
- [10] D. Wulferding, Y. Choi, S.-H. Do, C. H. Lee, P. Lemmens, C. Faugeras, Y. Gallais, and K.-Y. Choi, *Nature communications* 11, 1 (2020).
- [11] A. Sahasrabudhe, D. A. S. Kaib, S. Reschke, R. German, T. C. Koethe, J. Buhot, D. Kamenskyi, C. Hickey, P. Becker, V. Tsurkan, A. Loidl, S. H. Do, K. Y. Choi, M. Grüninger, S. M. Winter, Z. Wang, R. Valenti, and P. H. M. van Loosdrecht, *Phys. Rev. B* 101, 140410(2020).
- [12] D. Lin, K. Ran, H. Zheng, J. Xu, L. Gao, J. Wen, S.-L. Yu, J.-X. Li, and X. Xi, *Physical Review B* 101, 045419 (2020).
- [13] Yang Yang, Mengqun Li, Ioannis Rousochatzakis, Natalia B. Perkins, arxiv:2108.08878 (accepted in PRB).

Publications

- [1] M. Ye, R. M. Fernandes, and N. B. Perkins, *Physical Review Research* 2, 033180 (2020).
- [2] K. Feng, M. Ye, and N. B. Perkins, *Phys. Rev. B* 103, 214416 (2021).
- [3] K. Feng, S. Swarup, and N. B. Perkins, arxiv:2108.08878 (submitted to PRL).
- [4] Yang Yang, Mengqun Li, Ioannis Rousochatzakis, Natalia B. Perkins, arxiv:2108.08878 (accepted in PRB).
- [5] Alejandro Ruiz, Nicholas P. Breznay, Mengqun Li, Ioannis Rousochatzakis, Anthony Allen, Isaac Zinda, Vikram Nagarajan, Gilbert Lopez, Mary H. Upton, Jungho Kim, Ayman H. Said, Xian-Rong Huang, Thomas Gog, Diego Casa, Robert J. Birgeneau, Jake D. Koralek, James G. Analytis, Natalia B. Perkins, Alex Frano, *Phys. Rev. B* 103, 184404 (2021).
- [6] Yang Yang, Natalia B. Perkins, Fulya Koç, Chi-Huei Lin, Ioannis Rousochatzakis, *Phys. Rev. Research* 2, 033217 (2020).
- [7] Mengqun Li, Ioannis Rousochatzakis, Natalia B. Perkins, *Physical Review Research* 2, 033328 (2020).
- [8] Mengqun Li, Ioannis Rousochatzakis, Natalia B. Perkins, *Physical Review Research* 2, 033328 (2020).
- [9] Aysel Shiraliev, Artem Prokoshin, Natalia B. Perkins, *Low Temperature Physics* 47 (2021), (in production).

Materials Project

PI: Kristin Persson

Co-PIs: Mark Asta (LBNL), Shreyas Cholia (LBNL), Daryl Chrzan (UC Berkeley), Gerbrand Ceder (LBNL), Geoffroy Hautier (Dartmouth), Peter Khalifah (Stony Brook), Sinead Griffin (LBNL), Anubhav Jain (LBNL), Lane Martin (LBNL), Jeffrey Neaton (LBNL), Shyue Ping Ong (UCSD)

Program Scope

Materials discovery and development is a key innovation driver for new technologies and markets, and an essential part of the drive to a renewable energy future. The goal of the Materials Project (online at <https://www.materialsproject.org/>) is to accelerate materials discovery and education through advanced scientific computing and innovative design tools. High-throughput calculations, state-of-the-art electronic structure methods as well as novel datamining algorithms for electronic, magnetic, elastic, defect, and finite temperature property predictions will be combined with existing capabilities at the Materials Project for tens of thousands of materials to yield an unparalleled materials design environment. In addition, the Materials Project is facilitating collaboration and data sharing amongst the research community through user-contributed data platforms and engaging in computational to experimental materials design in the applications of ferroelectrics, piezoelectrics, and more. Furthermore, the Project is developing new methods to calculate a variety of materials properties efficiently and accurately, such as high-temperature properties of materials, defect properties, and electron transport properties. We envision that the combination of data, new methods, software tools, machine learning and computation at a massive scale will change the manner by which functional materials are designed.

Keywords: Theory-driven materials design, materials databases and informatics, high-throughput calculations and method development

Recent Progress

Overview / community database and web site / outreach

The Materials Project's (MP) online database of materials properties (www.materialsproject.org) currently has > 210,000 users, and more than 10,000 unique visitors come on to the site every day. We recently pre-released a completely new website with an improved user interface, additional features, infrastructure changes for extensibility. Three brand new apps were released (Synthesis Explorer, Catalysis Explorer, MOF Explorer) and XANES/EXAFS data added for >50,000 compounds. Furthermore, three database updates were released.

The MP database is now officially recognized as a PuRE data resource. The MPContribs platform for external user data has 34 data sets (109,000 structures, 386,000 tables, 68,000

attachments in 240,000 total contributions). Key data partnerships with the Open Catalyst Project, NSLS-II and ALS light sources, and the NOMAD consortium were established. MP is also OSTI's largest data provider with 145k DOIs requested to date, with machine learning used to generate DOI metadata. The "Matbench" platform to benchmark community machine learning algorithms integrated into MPContribs.

Recently, MP launched a monthly seminar series (1400 registrants) with invited speakers demonstrating usage of MP data and tools. Furthermore, the MP annual workshop (virtual) was held with interactive tutorials and hosted 100 participants. An MP lecture and hands-on tutorial was given at the DCMS Materials 4.0 Summer School and MP was featured on the MongoDB podcast.

Method development / new software packages

MP has continued to work on translating theoretical methods from the "single calculation" mode to a high-throughput mode, and pioneering new ways to perform fast and accurate calculations for materials design. For example, MP developed and benchmarked workflows for R2SCAN for all classes of inorganic materials on Materials Project, allowing for higher accuracy calculations at low cost. It is also developing an improved defect workflow that makes use of a fast implementation of hybrid-DFT in the CP2K software – mixing benefits of localized and plane wave basis sets. MP is also developing formal extensions to the cluster expansion methodology to deal with highly complex materials with large number of components. MP is also working on automatic transport computations from full electron-phonon computations & other models. A new energy correction framework was developed for more accurate reaction energies and estimates of error in formation energy predictions[1].

MP has also continued developing codes and methods for use by the community. We recently developed an open-source code, iFermi, for Fermi surface generation and analysis. We developed a pymatgen tool for automatically plotting f^* diagrams which can sensitively distinguish different defect types in structures refined from powder diffraction data series. We released a new workflow for calculating topological properties of materials in both centrosymmetric and non-centrosymmetric cases. We also released a workflow for automatic Hubbard U and Hund J values using the linear response methodology including possibility of applying Hubbard corrections on a

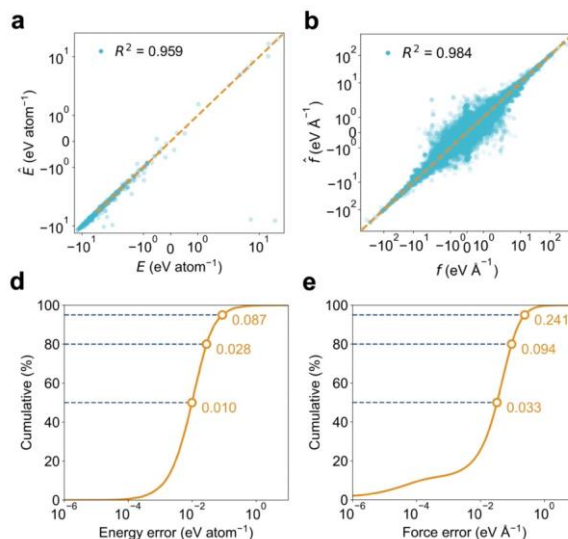


Figure 1 The GUFF model prediction results (y axis) compared to DFT (x axis) on unseen test data for energies (a+d), forces (b+e). Stress plots omitted for conciseness.

per-site basis for improved workflows for magnetic properties. We developed a new coordination environment algorithm which is currently used by many in the community. Finally, we built a robust engine for solving powder diffraction patterns of complex structures[2].

Machine learning

MP recently helped develop a new graph-based ML model, GUFF, that can learn energies (scalar), forces (rank-1 tensor), and stresses (rank-2 tensor) jointly and self-consistently. The ML model can perform structural relaxation, phonon calculations, molecular dynamics, elasticity calculations, etc., for all materials (see Figure 1). It also helped develop a framework (AtomSets) to perform transfer learning to help researchers use materials data of different sizes for training ML models. We also trained a neural network model our phonon database to predict vibrational entropy of materials. Synthesis information was integrated into the Materials Project by using text-mining of 5 million research papers to extract codified solid-state synthesis recipes as part of the Synthesis Explorer App. Finally, the Matbench framework was integrated into the Materials Project for benchmarking machine learning algorithms developed by the community.

New materials discovery

A promising ferroelectric derived previously through high-throughput computational search was subjected to additional calculations and experimental verification. Here, we synthesized epitaxial $\text{Pb}_{1-x}\text{Sr}_x\text{HfO}_3$ ($x = 0, 0.05, 0.15, 0.25, 0.5, 0.75, 1$) thin films across a range of temperatures, oxygen partial pressures, substrates, laser fluences, etc. to explore this system. $\text{Pb}_{0.5}\text{Sr}_{0.5}\text{HfO}_3$ was found to exhibit the highest E_B (5.12 MV/cm; three-times the value of 1.23 MV/cm for PbHfO_3), a 6% increase in the η values (from 91% for PbHfO_3 to 97%), a 2.7-times increase in U_r (from 21 J/cm³ for PbHfO_3 to 77 J/cm³), and a 10⁶-times improvement in fatigue endurance at $E_B = 1.23$ MV/cm. This performance places $\text{Pb}_{0.5}\text{Sr}_{0.5}\text{HfO}_3$ among the most promising antiferroelectrics for such applications[3].

The work above motivated a further study of $\text{PbHf}_{1-x}\text{Ti}_x\text{O}_3$ ($0 < x < 1$) as epitaxial thin films with a potential morphotropic phase boundary for high dielectric and piezoelectric response. We observed an enhancement of dielectric permittivity near the $x = 0.5$ composition as expected; current collaboration are attempting to clarify the theoretical understanding of the result.

Experimentally investigated piezoelectric response in novel computationally designed compound $\text{Sr}_2\text{Nb}_{2-2x}\text{V}_{2x}\text{O}_7$, predicted by theory (Persson) to exist and have piezoelectric properties. The films were successfully synthesized at $\text{Sr}_2\text{Nb}_{2-2x}\text{V}_{2x}\text{O}_7$ ($x = 0, 0.05, 0.1$) compositions which were found to exhibit robust ferroelectric

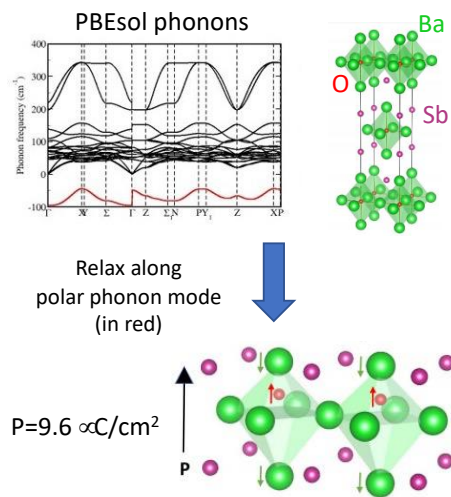


Figure 2 Identification of unstable polar phonons leading to a ferroelectric phase in $\text{Ba}_4\text{Sb}_2\text{O}$

properties upon being annealed in an oxygen-rich atmosphere at temperatures as high as 1175°C. Piezoelectric characterization will be conducted in the future using equipment due to arrive soon.

We developed a method to search for ferroelectrics using unstable phonons developed and applied to the Materials Project phonon database. Discovery of a new family of anti-ferroelectric and ferroelectric materials (A_4Sb_2O , see Figure 2) which includes a magnetoelectric multiferroic Eu_4Sb_2O [4]. We also performed a high-throughput search for magnetic and topological materials, computationally identifying several unknown oxides that may exhibit these properties.

Future Plans

In the next phase we will release next-generation Materials Project web site, with improved functionality for users as well as improved stability due to cloud-based architecture. We will improve accuracy of all stable and nearly stable binary and ternary MP compounds using the R2SCAN functional, release a database of electron and phonon properties, and deliver a cluster expansion framework for metal alloys and multi-component solid solutions. We will further develop the universal force field, improve its accuracy using larger, more accurate and more diverse data sets. Follow-ups to joint computational-experimental design projects such as the $PbHf_{1-x}Ti_xO_3$ ($0 < x < 1$), $LuGaO_3$, and $Sr_2Nb_{2-2x}V_{2x}O_7$ will be pursued for greater theoretical understanding and experimental performance.

References

1. A. Wang, R. Kingsbury, M. McDermott, A. Jain, S.P. Ong, S. Dwaraknath, K.A. Persson. “A Framework for Quantifying Uncertainty in DFT Energy Corrections,” *Sci. Rep.* **11** (1), 15496 (2021). DOI: 10.1038/s41598-021-94550-5
2. Mattei, J. Dagdelen, M. Bianchini, A. Ganose, A. Jain, E. Suard, F. Fauth, C. Masquelier, L. Croguennec, G. Ceder, K. A. Persson, and P. Khalifah, “Enumeration as a tool for structure solution – a materials genomic approach to solving the cation-ordered structure of $Na_3V_2(PO_4)_2F_3$ ”, *Chem. Mater.*, **32**, 20, 8981–8992 (2020) DOI: 10.1021/acs.chemmater.0c03190
3. M. Acharya, E. Banyas, M. Ramesh, Y. Jiang, A. Fernandez, A. Dasgupta, H. Ling, B. Hanrahan, K. A. Persson, J. B. Neaton, L. W. Martin, “Exploring the $PB1-xSrxHfO_3$ System and Potential for High Capacitive Energy Storage Density and Efficiency”, *Adv. Mater.* 2021 (in press). DOI: 10.1002/adma.202105967.
4. Markov, L. Alaerts, H. Pereira Coutada Miranda, G. Petretto, W. Chen, J. George, E. Bousquet, P. Ghosez, G.-M. Rignanese, and G. Hautier “Ferroelectricity and multiferroicity in anti-Ruddlesden-Popper structures”, *Proc. Natl. Acad. Sci. U.S.A.*, **118**, e2026020118 (2021). DOI: 10.1073/pnas.2026020118

Publications

1. J. M. Munro, K. Latimer, M. K. Horton, S. Dwaraknath, and **K. A. Persson**. "An improved symmetry-based approach to reciprocal space path selection in band structure calculations", npj Comput. Mater. **6**, 1–6 (2020) DOI: [10.1038/s41524-020-00383-7](https://doi.org/10.1038/s41524-020-00383-7)
2. H. Zheng, X. Li, R. Tran, C. Chen, M. Horton, D. Winston, **K.A. Persson**, **S.P. Ong**. "Grain Boundary Properties of Elemental Metals", Acta Materialia, **186**, 40-49 (2020) DOI: [10.1016/j.actamat.2019.12.030](https://doi.org/10.1016/j.actamat.2019.12.030)
3. T. E. Smidt, S. A. Mack, S. E. Reyes-Lillo, **A. Jain**, and **J. B. Neaton**, "An automatically curated first-principles database of ferroelectrics", Sci. Data **7**, 72 (2020) DOI: [10.1038/s41597-020-0407-9](https://doi.org/10.1038/s41597-020-0407-9)
4. M. Acharya, S. Mack, A. Fernandez, J. Kim, H. Wang, K. Eriguchi, D. Meyers, V. Gopalan, **J. B. Neaton**, and **L. W. Martin**, "Searching for New Ferroelectric Materials Using High-Throughput Databases: An Experimental Perspective on BiAlO₃ and BiInO₃", Chem. Mater. **32**, 7274 (2020) DOI: [10.1021/acs.chemmater.0c01770](https://doi.org/10.1021/acs.chemmater.0c01770)
5. J. Kim, M. Acharya, S. Saremi, G. Velarde, E. Parsonnet, P. Donahue, A. Qualls, D. Garcia, **L. W. Martin**, "Ultra-high capacitive energy density in ion-bombard relaxor ferroelectric films", Science **369**, 81-84 (2020). DOI: [10.1126/science.abb0631](https://doi.org/10.1126/science.abb0631)
6. Mattei, J. Dagdelen, M. Bianchini, A. Ganose, **A. Jain**, E. Suard, F. Fauth, C. Masquelier, L. Croguennec, **G. Ceder**, **K. A. Persson**, and **P. Khalifah**, "Enumeration as a tool for structure solution – a materials genomic approach to solving the cation-ordered structure of Na₃V₂(PO₄)₂F₃", Chem. Mater., **32**, 20, 8981–8992 (2020) DOI: [10.1021/acs.chemmater.0c03190](https://doi.org/10.1021/acs.chemmater.0c03190)
7. C.J. Bartel, A. Trewartha, Q. Wang, A. Dunn, **A. Jain**, **G. Ceder**. "A critical examination of compound stability predictions from machine-learned formation energies", npj Comput. Mater. **6**, 97 (2020) DOI: [10.1038/s41524-020-00362-y](https://doi.org/10.1038/s41524-020-00362-y)
8. M. Acharya, E. Banyas, M. Ramesh, Y. Jiang, A. Fernandez, A. Dasgupta, H. Ling, B. Hanrahan, K. A. Persson, J. B. Neaton, L. W. Martin, "Exploring the PB_{1-x}Sr_xHfO₃ System and Potential for High Capacitive Energy Storage Density and Efficiency", Adv. Mater. 2021 (in press). DOI: [10.1002/adma.202105967](https://doi.org/10.1002/adma.202105967).
9. A. M. Ganose, A.J. Searle, A. Jain and S.M Griffin. "iFermi: A Fermi surface analysis and manipulation tool", J. Open Source Softw. , **6**(59), 3089 (2021). DOI: [10.21105/joss.03089](https://doi.org/10.21105/joss.03089)
10. M. Markov, L. Alaerts, H. Pereira Coutada Miranda, G. Petretto, W. Chen, J. George, E. Bousquet, P. Ghosez, G.-M. Rignanese, and G. Hautier "Ferroelectricity and multiferroicity in anti-Ruddlesden-Popper structures", Proc. Natl. Acad. Sci. U.S.A., **118**, e2026020118 (2021). DOI: [10.1073/pnas.2026020118](https://doi.org/10.1073/pnas.2026020118)
11. C. Chen, Y.X. Zuo, W.K. Ye, X.G. Li, S.P. Ong. "Learning Properties of Ordered and Disordered Materials from Multi-Fidelity Data", Nat. Comput. Sci. **1**, 46-53 (2021). DOI: [10.1038/s43588-020-00002-x](https://doi.org/10.1038/s43588-020-00002-x)
12. M.L.H. Chandrappa, Z.Y. Zhu, D.P. Fenning, S.P. Ong. "Correlated Octahedral Rotation and Organic Cation Reorientation Assist Halide Ion Migration in Lead Halide Perovskites," Chem. Mater. **33** (12), 4672-4678 (2021). DOI: [10.1021/acs.chemmater.1c01175](https://doi.org/10.1021/acs.chemmater.1c01175)

Complex (anti)ferroic oxides: statics and dynamics at finite temperatures

Inna Ponomareva, University of South Florida

Program Scope

Perovskites that exhibit ferroic, antiferroic, multiferroic or relaxor properties are of extreme fundamental and technological importance. Fundamentally such materials are very attractive because they exhibit delicate energy competitions which result in appearance of some spontaneous property (magnetization, electric polarization or strain) or a particular type of ordering. Technologically they are in the heart of numerous applications. A few examples include memory applications, pyroelectric sensors, pressure sensors, capacitors, optical communications, ultrasonic motors, phase-array radars, ultrasound imaging and actuators, thermistors, filters, light detectors, high-power microwave devices, and many others. While this area has been dominated by inorganic perovskites for many years, very recently organic-inorganic perovskites have emerged as a potential very attractive alternative to their inorganic counterparts. Despite the very special role of ferroic perovskites many of their unique properties remain rather poorly understood. Some examples include statics and dynamics of ferroics that exhibit phase competition and/or frustration due to disrupted dipolar interactions, elusive dynamics associated with metastable phases and nonequilibrium conditions including its manifestation at the nanoscale, and the nature of ferroelectricity and phase transitions in hybrid perovskites. Such lack of understanding critically hinders both scientific and technological progress and requires timely attention. *The ultimate goal of this project is to achieve a fundamental understanding of statics and dynamics of perovskites that exhibit ferroic, antiferroic, multiferroic or relaxor properties at both macro- and nano-scales through state-of-the-art computer simulations.*

Keywords: Complex ferroics at finite temperatures, methodological developments for finite-temperature simulations

Recent Progress

Insights into hybrid organic-inorganic perovskites ferroics. Piezoelectrics are critical functional components of many practical applications such as sensors, ultrasonic transducers, actuators, medical imaging, and telecommunications. So far, the best performing piezoelectrics are ferroelectric ceramics, many of which are toxic, heavy, hard, and cost-ineffective. Recently, a groundbreaking discovery of extraordinarily large piezoelectric coefficients in the family of organic-inorganic perovskites gave a hope for a cheaper, environmentally friendly, inexpensive, lightweight, and flexible alternative. However, the origin of such a response in organic-inorganic ferroelectrics whose spontaneous polarization is an order of magnitude smaller than for inorganic counterparts remains unclear. We employed first-principles simulations to predict that the mechanism associated with large piezoelectric constants is of extrinsic origin and associated with switching between the stable phase and a previously overlooked energetically competitive metastable phase that can be stabilized by the external stress. The phase switching changes the polarization direction (see Fig.1) and therefore produces a large piezoelectric response

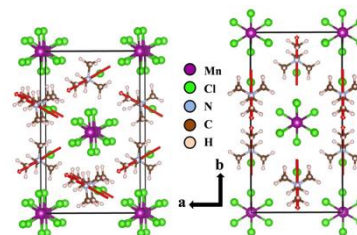


Fig.1: The ground state (left panel) and the metastable phase (right panel) of hybrid perovskite. The red arrows give the direction of the molecular dipole moment.

similar to $\text{PbZr}_{1-x}\text{Ti}_x\text{O}_3$ near the morphotropic phase boundary. The existence of such metastable phases is likely to manifest as the dynamical molecular disorder above the Curie temperature and therefore could be intrinsic to the entire family of organic-inorganic ferroelectrics with such disorder.

Our next focus is the electronic structure of the hybrids and its tunability. We used density functional theory calculations to predict Rashba-Dresselhaus spin-splitting in the valence band of Cd-based hybrid perovskites. Interestingly, the splitting is not necessarily sensitive to the polarization of the material but to the organic molecule itself which opens a way to its chemical tunability through the choice of the molecule. This is indeed confirmed in computations. Further chemical tunability of spin-splitting is possible through substitution of Cl in the CdCl_3 chains as the valence band was found to originate from Cl-Cl weakly bonding orbitals. For example, substitution of Cl with Br in TMCM- CdCl_3 resulted in ten times increase of spin-splitting. Furthermore, the spin-polarization in these materials give origin to persistent spin textures which are coupled to the polarization direction, and, therefore can be controlled by the electric field (see Fig.2). This is promising for spintronics applications.

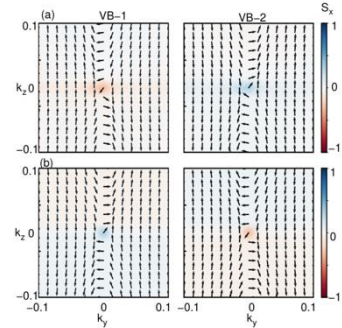


Fig.2: Spin textures in TMCM- CdCl_3 for two opposite polarization directions.

Another interesting tunability aspect is the role of hydrostatic pressure on the various properties of hybrid organic-inorganic perovskites. This aspect was investigated in TMCM- CdCl_3 and TMCM- MnCl_3 with the help of density functional theory simulations. Computations predict (1) the (co)existence of multiple competing phases with different polarizations and band gaps tunable by the pressure; (2) the presence of two regions of structural response to pressure and their atomistic origin; (3) increase of spontaneous polarization of up to 18% driven by the significant volume decrease under pressure; and (iv) 36% decrease in the band gap of TMCM- MnCl_3 and 10% increase in the band gap of TMCM- CdCl_3 under 10 GPa.

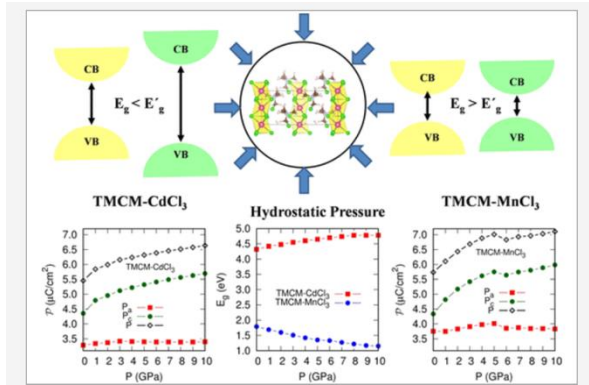


Fig.3: Illustration of different properties tunability in hybrid organic-inorganic perovskites by hydrostatic pressure.

Insights into inorganic perovskites ferroics.

PbZrO_3 is regarded as the first antiferroelectric and currently is under intense reexamination. We developed a multiscale approach that combines classical and first-principles density functional theory-based simulations to explore polar phases in this material. Application of this approach to PbZrO_3 predicted three polar phases, none of which is the common $R3c$. The lowest-energy polar phase Cc is metastable at 0 K but can be stabilized by

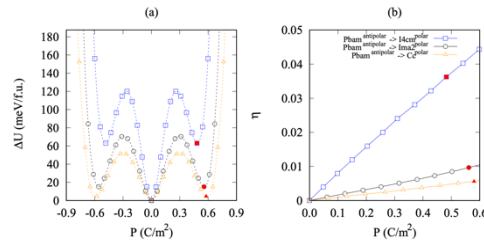


Fig.4: Dependence of the energy (a) and strain (b) on the polarization in PbZrO_3 . The red points indicate the location of energy minima.

application of electric field. Its structural and polarization response to the electric field is in good agreement with experimental data from. The other two phases are $I_{ma}2$ and $I4cm$ of orthorhombic and tetragonal symmetry, respectively, and predicted to stabilize at finite temperatures and under application of larger electric fields. These two phases exhibit very large strain which is of technological significance.

Future Plans

The future plans include (i) development, implementation and application of computational methodology to extend the present study of hybrid organic-inorganic perovskites to finite-temperatures; (ii) applications of the recently developed computational methodologies for inorganic perovskites to provide an insight into puzzling and controversial experimental data (this part will be done in collaboration with experimental groups; (iii) to continue development, implementation and applications of non-equilibrium methodologies to study energy converting properties of ferroics.

Publications

1. “Chemically and electrically tunable spin-polarizations in ferroelectric Cd-based hybrid organic-inorganic perovskites”, Ravi Kashikar, P.S. Ghosh, S. Lisenkov, B.R.K. Nanda, and I. Ponomareva, submitted (2021).
2. “Tunability of structure, polarization and band gap of high T_C organic-inorganic ferroelectrics by hydrostatic pressure: first-principles study”, P.S. Ghosh, J. Doherty, S. Lisenkov, and I. Ponomareva, *J. Phys. Chem. C* **125**, 16296 (2021).
3. “Structural, electrical, and electromechanical properties of inverse hybrid perovskites from first-principles: The case of $(CH_3NH_3)_3OI$ ”, M. Kingsland, P. S. Ghosh, S. Lisenkov, and I. Ponomareva, *J. Phys. Chem. C*, **125** 8794 (2021).
4. “ $Ba(Ti_{1-x}Zr_x)O_3$ relaxors: dynamic ferroelectrics at gigahertz”, S. Lisenkov, A. Ladera and I. Ponomareva, *Phys. Rev. B*, **102** 224109 (2020).
5. “Phase switching as the origin of large piezoelectric response in organic-inorganic perovskites: A first-principles-study”, P. S. Ghosh, S. Lisenkov, and I. Ponomareva, *Phys. Rev. Lett.*, **125** 207601 (2020).
6. “Negative capacitance regime in ferroelectrics demystified from non-equilibrium Molecular Dynamics”, K.A. Lynch and I. Ponomareva, *Phys. Rev. B*, **102** 134101 (2020).
7. “Prediction of high strain polar phases in antiferroelectric $PbZrO_3$ from multiscale approach”, S. Lisenkov, Yulian Yao, Nazanin Bassiri-Gharb, and I. Ponomareva, *Phys. Rev. B*, **102** 104101 (2020).
8. “Comparative Study of Minnesota Functionals Performance on Ferroelectric $BaTiO_3$ and $PbTiO_3$ ”, M. Kingsland, K.A. Lynch, S. Lisenkov, Xiao He, and I. Ponomareva, *Phys. Rev. Materials* **4**, 073802, (2020).

9. “Role of depolarization in the polarization reversal in ferroelectrics”, M. Kingsland, Z. G. Fthenakis, and I. Ponomareva, Phys. Rev. B, **024114**(2019).
10. “Phase evolution in the ferroelectric relaxor Ba(Ti_{1-x}Zr_x)O₃ from atomistic simulations”, C. Mentzer, S. Lisenkov, Z. G. Fthenakis and I. Ponomareva, Phys. Rev. B **99**, 064111 (2019).

First Principles Approach to Exciton Transport in Energy Materials

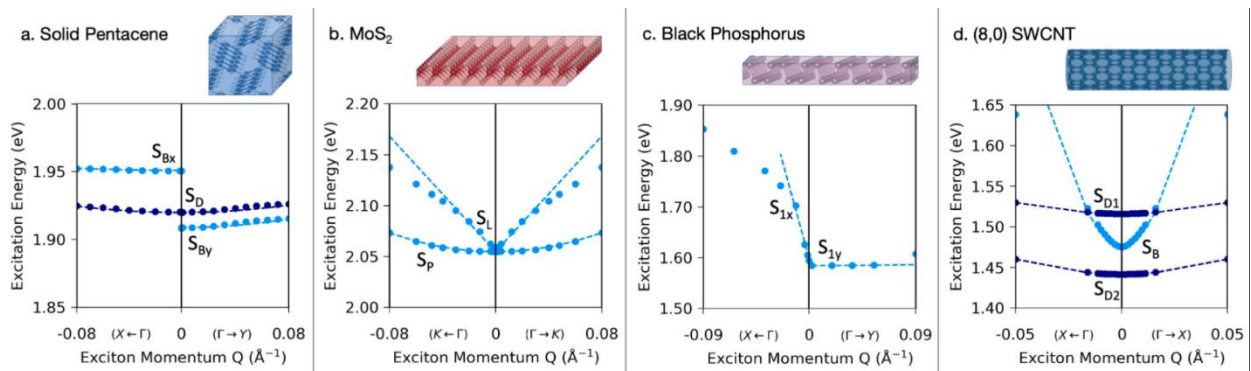
Diana Qiu, Yale University

Program Scope

This project aims to develop and apply a range of first-principles methods based on the GW plus Bethe Salpeter (GW-BSE) equation approach to understand exciton dynamics in materials of interest for optoelectronics, energy harvesting and energy transport. The proposed work is broadly organized under three objectives that address exciton dynamics in the ballistic, diffusive, and intermediate regimes. The first objective is to understand how features of crystal symmetry and dimensionality manifest in exciton dynamics through band-like exciton transport. The second objective is to understand the role of exciton-phonon interactions in exciton dynamics by developing and performing predictive calculations of exciton-phonon relaxation and decoherence times. The third objective is to model exciton diffusion processes by parametrizing a Boltzmann-like equation for exciton transport from ab initio calculations. The materials we will focus on include 1) monolayer transition metal dichalcogenides (TMDs), which exhibit exceptionally strong light-matter coupling and spin-momentum locking, 2) layered metal organic hybrid halide perovskites, which are promising materials for photovoltaics and broadband light emitting diodes (LEDs), and 3) topological insulators (TIs). The methods we employ build on the ab initio GW plus Bethe Salpeter equation (GW-BSE) approach.

Keywords: exciton dynamics, electronic structure methods, exciton diffusion

Recent Progress



Exciton bandstructures for spin $S=0$ excitons. Dots are GW-BSE results. Dashed lines show the fit to a model Hamiltonian. (a) Solid pentacene, with two exciton bands that are dipole-allowed (S_B , light blue) and dipole-forbidden (S_D , dark blue); (b) monolayer MoS₂ with excitons with linear (S_L) and parabolic (S_P) dispersion; (c) monolayer black phosphorus with a dipole-allowed exciton with linear dispersion along the Γ to X direction; and (d) (8,0) single-walled carbon nanotube, showing a non-parabolic low-lying exciton that is dipole-allowed (S_B , light blue) and two nearby dark parabolic exciton bands (S_{D1} and S_{D2} , dark blue).

This project began in July of 2021. In the first stage of the project, we have derived a general theory for exciton bandstructure connecting both *ab initio* and model Hamiltonian approaches. We show that contrary to common assumption, the exciton bandstructure contains non-analytical discontinuities---a feature which is impossible to obtain from the underlying electronic bandstructure alone. These discontinuities are purely quantum phenomena, arising from the exchange scattering of electron-hole pairs. We show that the degree of these discontinuities depends on the materials' symmetry and dimensionality, with jump discontinuities occurring in 3D and different orders of removable discontinuities in 2D and 1D. Moreover, we derive a general rule for understanding how the degree and number of discontinuities in the band structure changes with layer number and degeneracy.

We connect these features in the exciton bandstructure to the early stages of exciton dynamics, radiative lifetimes, and diffusion constants, in good correspondence with recent experimental observations. This analysis reveals that the discontinuities in the bandstructure can lead to ultrafast exciton transport in the quasi-ballistic regime and unexpected nodal structure in the exciton density. So far, we focus only on the early stages of exciton transport prior to decoherence and thermalization. However, our results suggest that these initial stages nonetheless establish a non-trivial initial distribution of excitons, prior to diffusion. Thus, measured exciton diffusion patterns at later timescale may be influenced by the underlying exciton bandstructure [1].

Future Plans

In the next stage of the project, we will continue to study ballistic energy transport in materials of interest for energy, quantum information and optoelectronic applications. Here, we plan to study the extent to which exciton interactions can mix bulk and surface states in topological insulators (TIs) and look at the ballistic transport of chiral excitons in TIs. We also plan to calculate the exciton bandstructure in the Ruddelsden-Popper series of layered perovskites, where we expect asymmetric dispersion along the in-plane and out-of-plane directions to lead to different exciton velocities. Towards this goal, we have recently developed new screening models that allow us to account for disorder in the perovskite structure at greatly reduced computational cost.

Beyond the ballistic regime, the next major goal of this project is to calculate exciton-phonon interactions and develop models for exciton diffusion. Here, we will follow the work of Antonius and Louie [2] and Chen, Sangalli and Bernardi [3] to calculate the exciton-phonon self energy to first order within *ab initio* many body perturbation theory. We will apply this approach to calculate exciton-phonon relaxation times as a function of exciton momentum in perovskites, two-dimensional layered materials and heterostructures, and TIs and develop models of exciton diffusion in these systems.

References

- [1] D. Y. Qiu*, G. Cohen, D. Nochvoka, S. Refaely-Abramson, Nano Letters 21, 7644-7650 (2021).
- [2] G. Antonius and S.G. Louie, S. G., arXiv:1705.04245 (2017).
- [3] H.Y. Chen, SD. angalli, M. Bernardi, Phys. Rev. Lett. 125, 107401 (2020).

Publications

D. Y. Qiu*, G. Cohen, D. Nochvoka, S. Refaely-Abramson, Nano Letters 21, 7644-7650 (2021).

Emergent properties of highly correlated electron materials

Srinivas Raghu, Stanford University, Photon Sciences division, SLAC National Accelerator Laboratory, Stanford CA 94305.

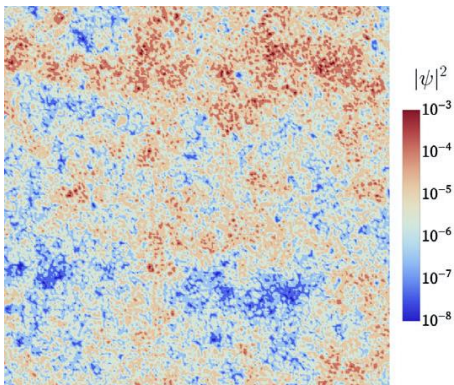
Program Scope

The main focus of the PI's current program has been on universal behavior of quantum matter stemming from the effects of topology, electron-electron interactions and quenched randomness. The PI has taken a multifarious approach, attempting to "triangulate" complex phenomena using a diverse toolset, ranging from numerical studies of model Hamiltonians, to analytic studies of asymptotic behavior of quantum systems, and phenomenology to tackle experimental observations head on. Specific topics of investigation include, 1) developing new approaches to quantum Hall to insulator transitions based on dual representations that take into account interaction and disorder effects[1,2], 2) studying the fate of the two dimensional electron gas near a magnetic instabilities in the presence of quenched disorder[3], 3) Uncovering pairing symmetries of unconventional superconductors such as the recently discovered nickelate family[4] and heavy fermion systems such as UTe_2 , and 4) phenomenological studies of superconductivity in doped quantum paraelectrics[5,6], such as niobium-doped $SrTiO_3$.

Keywords: Quantum criticality, quantum transport, unconventional superconductivity.

Recent Progress

1) Dual representation of quantum Hall transitions: numerical and analytical results



Composite fermion multifractal behavior at criticality, is identical to the electrons at the critical point.

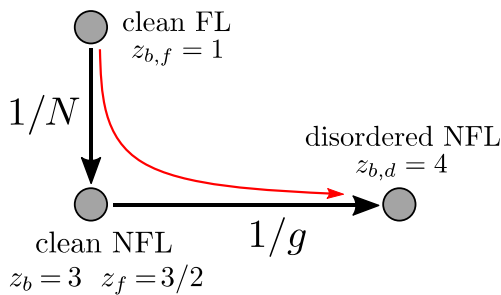
Despite decades of intense investigation, key aspects of these archetypal family of quantum critical points remain poorly understood. The reason is that the problem involves electrons in Landau levels, with singular interactions and disorder effects: there are no small parameters and numerical tools suffer with the inability to tackle interactions. Without interactions, even the most basic properties, such as 1) the observation of a finite DC resistivity at finite temperature, 2) non-trivial dynamical scaling laws, and 3) a systematic comparison between integer and fractional quantum Hall transitions continue to defy theoretical explanation.

To help rectify some of these shortcomings, the PI has developed alternate frameworks for describing quantum Hall

transitions that work directly in dual representations of fermionic vortices, known as composite fermions[1,2]. The representations so far have proven most fruitful in that they enable a systematic statistical mechanics based approach to the problem, including “mean-field” and fluctuational corrections. They offer several distinctive advantages over previous studies based directly in the electron representation. For example, they naturally allow for a non-zero dc resistance at finite temperature, since composite fermions, unlike non-interacting electrons in a Landau levels have are delocalized states over a range of energies. They provide an elegant mean-field perspective in which the composite fermions themselves undergo quantum Hall to insulator transitions, and lead to identical critical exponents as studied in electron coordinates based on network models (we have developed and thoroughly studied dual network models based on composite fermions). The dual formulation directly enables you to see why the dynamical critical exponent $z=1$ when gauge fluctuations are taken into account. Finally, the dual approach shows explicitly that transitions involving integer and abelian fractional quantum Hall transitions are in the same universality class, which previously remained understood only at the conjectural level. In the future, we aim to obtain the specific heat exponent of the transition in the presence of both interactions and randomness using the dual representation.

2) Interaction induced metallicity in a 2d non-Fermi liquid with disorder

The interplay of disorder and interactions in two-dimensions has been studied for decades. The paradigmatic approach involves starting with a clean Fermi liquid and adding perturbatively, the effects of disorder and interactions. In a seminal set of papers by Finkel’stein and co-workers, a renormalization group (RG) description of the interplay of disorder and



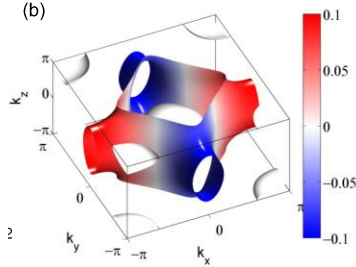
Schematic RG flows for a disordered 2d electron system near a ferromagnetic instability. The intermediate clean NFL fixed point is unstable to disorder and ultimately leads to a dirty fixed point with dynamical exponent $z = 4$.

interactions in the vicinity of a clean Fermi liquid fixed point was presented. Metallic behavior was found in this study to occur as the RG flows runaway to strong coupling while marking the onset of a magnetic ordering tendency. In [3] we revisited this problem by considering instead a different hierarchy of scales, namely one where interaction effects due to soft magnetic fluctuations near a ferromagnetic instability set in more strongly before the effects of quenched disorder. As a result, diffusive motion of charge was inherited from a non-Fermi liquid metal and displayed a distinct dynamical scaling exponent.

We then analyzed the interplay between this ‘anomalous’ diffusion propagator and the critical fluctuations associated with magnetism. We discovered an asymptotically exact solution corresponding to a perfect conductor, with weak logarithmic divergence of the tunneling density of states, as well as with heat capacity $C(T) \sim \sqrt{T}$. The theory in the vicinity of the metallic behavior remained well-controlled due to the asymptotic decoupling between the magnetic fluctuations and the diffusive charge motion.

We are currently investigating the effects of enhanced superconductivity and weak-localization effects near our solution for the dirty metallic critical point.

3) *Robust d-wave symmetry of infinite layer nickelate superconductors*



d-wave gap function shown on the Fermi surface obtained from *ab initio* calculations.

Motivated by the recent breakthrough of the observation of superconductivity in the infinite layer nickelates, the PI has recently undertaken a theoretical study aiming to uncover the most likely pairing scenario in this intriguing family of materials[4]. Instead of making simple-minded comparisons to cuprate superconductors, we decided to study the nickelate materials as distinct in their own right. We began by using electronic structure calculations (LDA + GGA) to obtain the dominant contributions to the states near the Fermi level (such calculations were demonstrated first by W. Pickett). We found a quasi-two dimensional Fermi surface composed of the Nickel d-electrons as well as a more three-

dimensional Fermi surface made of the rare earth electrons. We then went further than previous studies, to obtain the dominant superconducting instabilities in this system using a variety of techniques, from controlled weak-coupling theories based on superconductivity from repulsive interactions, to physically-motivated calculations taking into account Mott physics, namely slave boson mean-field theory. In all cases, we found a robust feature that the dominant pairing tendency was in the B1g dx²-y² channel.

4) *Superconductivity in doped quantum paraelectrics*

A variety of materials, such as doped SrTiO₃, PbTe, and KTa₃ exhibit superconductivity in the dilute limit in the vicinity of incipient ferroelectricity. A variety of mechanisms have been proposed including exotic “anti-adiabatic” pairing mechanisms in which the phonon frequency exceeds the Fermi energy, effectively inverting the hierarchy of energy scales. Other exotic proposals include pairing mediated by 2 transverse optic (TO) phonons, the soft modes associated with ferroelectricity. This mechanism is notable for involving 2 phonons rather than one, in mediating interactions in the pairing channel. Motivated by recent tunneling studies [5], we constructed a theory which involved superconductivity mediated by an adiabatic TO phonon, in conjunction with spin-orbit coupling, which enabled pairing by single rather than 2 phonons[6]. Our theory naturally accounts for a superconducting dome in the vicinity of extreme dilute concentrations. Our theoretical approach of extracting pairing mechanisms from planar tunneling spectroscopy can be generalized fruitfully to other materials exhibiting superconductivity on the verge of a ferroelectric quantum critical point.

Future Plans

Strange insulators

The PI has started numerical studies of interaction effects on Anderson insulators. Using extensive DMRG simulations on Hubbard chains and ladders, he will uncover the novel spin physics that results in the Anderson insulator phase as a consequence of interactions. Such spin physics definitely play a role in the proximate metal and may likely inform the nature of metal insulator transitions with disorder and interactions. The PI will also study Hall response of such insulators using physically motivated mean-field like approximations and DMRG simulations in ladders. This program, if successful, would greatly enhance our understanding of the insulating state in the presence of both interactions and disorder.

Superconductivity and weak-localization effects near 2D metallic critical points

Following up on his recent paper [], the PI will consider effects of superconductivity and weak-localization to study the role of singular interactions, non-Fermi liquid behavior, superconductivity and quenched randomness in the vicinity of ferromagnetic and nematic quantum critical points, both of which have been observed in a variety of materials ranging from heavy fermion systems to iron-based superconductors. The PI will obtain controlled solutions revealing superconductivity enhanced by disorder and quantum critical fluctuations. The PI will also explore whether such frameworks can provide a controlled description of superconductor-insulator transitions in a metallic system.

Superconducting phenomenology in correlated electron materials

The PI has maintained an interest in unconventional superconductivity in a variety of materials. He plans to continue pursuing phenomenological questions involving these systems. A prime example includes the exciting spin-triplet superconductor candidate UTe₂, which exhibits an intriguing reentrant superconducting behavior in the presence of an external magnetic field. The PI will construct phenomenological descriptions of how such reentrant behavior may be understood in a vastly simplified effective description. Another example is superconductivity in the infinite layer nickelate family. In close collaboration with his colleague Harold Hwang, the PI plans on devoting efforts towards explaining ongoing experimental developments in this exciting new family of (likely unconventional) superconductors.

References

Put the numbered list of references here using this font (Times New Roman 12 pt).

[1] P. Kumar, P. Nosov and S. Raghu, arXiv:2006.11862.

[2] K. Huang, S. Raghu, and P. Kumar, Phys. Rev. Lett. **126**, 056802 (2021) [Editor's selection].

- [3] P. Nosov, I. Burmistrov, S. Raghu, Phys. Rev. Lett. 125, 256604 (2020).
- [4] X. Wu et al., Phys. Rev. B 101, 060504(R) (2020).
- [5] H. Yoon et al, arXiv:2106.10802.
- [6] Y. Yu, H. Hwang, S. Raghu, S.-B. Chung, arXiv:2110.03710.

Publications (Selected)

- [1] *Theory of superconductivity in doped quantum paraelectrics*, Y. Yu, H. Hwang, S. Raghu, S.-B. Chung, arXiv:2110.03710.
- [2] *Majorana fermion arcs and the local density of states of UTe_2* , Y. Yu, V. Madhavan, S. Raghu, arXiv:2107.04621.
- [3] *The Hubbard Model*, D. Arovas, E. Berg, S. Kivelson, S. Raghu, Ann. Rev. CMP, In press.
- [4] *Numerical study of a dual representation of the integer quantum Hall transition*, K. Huang, S. Raghu, P. Kumar, Phys. Rev. Lett. 126, 056802 (2021) [Editor's suggestion].
- [5] *Interaction-induced metallicity in a two-dimensional disordered non-Fermi liquid*, P. Nosov, I. Burmistrov, S. Raghu, Phys. Rev. Lett. 125, 256604 (2020).
- [6] *3D Network model for strong topological insulator transitions*, J. Son, S. Raghu, Phys. Rev. B 104, 125142 (2021).
- [7] *Interaction effects on quantum Hall transitions: dynamical scaling laws and superuniversality*, P. Kumar, P. Nosov, S. Raghu, arXiv:2006.11862.
- [8] *Robust dx^2-y^2 wave superconductivity of infinite-layer nickelates*, X. Wu, D. Sante, T. Schwemmer, W. Hanke, H. Hwang, S. Raghu, R. Thomale, Phys. Rev. B 101, 060504R (2020)

Theoretical and Computational Studies of Excitations in Functional Nanomaterials

PI: Talat S. Rahman, Department of Physics, University of Central Florida, Orlando, FL

Program Scope

The overarching goal of this project (DE-FG02-07ER46354) is to understand, explain, and predict striking equilibrium and *non-equilibrium* properties of novel materials, with special attention to their response to *ultrafast* probes, through application of reliable computational and theoretical techniques. While for most systems calculations of ground state electronic structure and the excitation spectra (equilibrium properties) with methods beyond density functional theory (DFT) reveal information on novel properties of the low dimensional materials, deeper insights into the impact of electron correlations, electron-phonon scattering and other multi-excitation processes in excited state dynamics are obtained from calculations in the non-equilibrium regime, in response to ultrafast probes. For the latter purpose, we have developed a density matrix based time dependent density functional theory (DM-TDDFT) code.¹ In addition to absorption and emission spectra, we calculate the characteristics of quasiparticle (excitons, trions, biexcitons) and collective (plasmons) excitations. To unveil the role of electron correlation, particularly through response to ultrafast probes, we have developed techniques based on dynamical mean field theory (DMFT) and TDDFT through which we have provided rationale for experimental observations such as the femto-second range demagnetization of Ni² and insulator to metal transition in VO₂.³ Some of the questions we address are: what are the signatures of electron correlations in the observed ultrafast charge dynamics in the Mott insulator VO₂? What causes spin flipping in Ni leading to its ultrafast demagnetization? What role does electron-phonon coupling play in photoluminescence in bilayer MoS₂? What is the effect of hydrogenation on excitons in single layer MoS₂? How do excited charges and spins relax after laser pulse perturbation? What is the effect of nonadiabaticity (memory) on charge dynamics? What is the rationale for the observed exotic phases in twisted bilayers of WSe₂? The proposed projects aim at answering the above questions and more through rationalization of experimental observations and validation of predictions using robust methods.

Keywords: Excitations in novel materials, excited state charge and spin dynamics, ultrafast response of novel functional materials.

Recent Progress

1. Effect of H adsorption on excitons in single layer MoS₂⁴

One way to tune the novel optical and chemical properties of single layer MoS₂ is through exposure to hydrogen. To obtain microscopic insights into the process, we have calculated the excitation spectrum of single-layer MoS₂ at several hydrogen coverages, using the DM-TDDFT approach to find that the fully hydrogenated system is metallic, while at lower

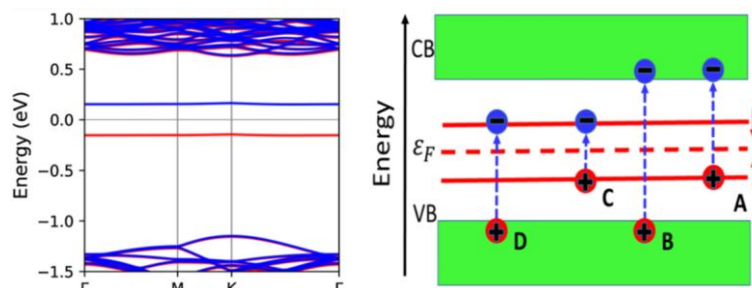


Fig. 1 (Left) DFT (PBE) bands for spin-up (red) and spin-down (blue) electrons of hydrogenated MoS₂ at 1/25 coverage. Fermi energy is 0 eV. (Right) Schematic representation of possible excitonic states in the hydrogenated system.

coverages the spectrum consists of spin-polarized partially filled localized mid-gap states (see Fig. 1). The calculated absorption spectrum of the system reveals standard excitonic peaks corresponding to the bound valence-band hole and conduction-band electron, as well as excitonic peaks that involve the mid-gap states that are produced on hydrogen adsorption.

Table 1 Calculated exciton binding energies in meV and corresponding dipole strengths, for two hydrogen coverages. The dipole strengths are in units of the “standard” excitonic state formed by the valence hole and conduction electron. Two type of long range XC kernels have been used in the calculations: Slater and LR. Details can be found in Ref. [4].

Exciton	1/25 Coverage			1/9 Coverage		
	Slater	LR	Strength	Slater	LR	Strength
A	-63.708	-61.346	0.05	-2.406	-1.885	5
B	-57.016	-57.009	1	-1.126	-0.679	1
C	-82.592	-97.578	47	-26.771	-40.25	27
D	-57.043	-57.053	0.1	-1.054	-0.834	6

Importantly, the emission spectrum of the hydrogenated system is in the infra-red range (the peak is at $\sim 0.15\text{eV}$), while in the pristine system it is in the visible. The quench of the visible photoluminescence in single-layer MoS_2 after hydrogenation agrees with experimental observations. Furthermore, the binding energies of the excitons (Table 1) of the hydrogenated system are found to be relatively large (few tens of meV), making their experimental detection facile and suggesting hydrogenation as a knob for tuning the optical properties of single-layer MoS_2 . Moreover, we find hydrogenation to suppress visible light photoluminescence, in agreement with experimental observations.

2. Ultrafast charge dynamics and photoluminescence in bilayer MoS_2 ⁵

While single layer MoS_2 has a direct band gap, its bilayer has an indirect band gap ($\sim 1.5\text{ eV}$ in our calculations). Yet, the photoluminescence spectrum of the bilayer displays two peaks: one corresponding to the indirect band gap and the other to the direct band gap of the single layer ($\sim 1.9\text{ eV}$). Our examination of the interplay of ultrafast charge dynamics and electron-phonon interaction in bilayer MoS_2 , as summarized in Fig. 2, shows that while the initial accumulation of excited charge occurs around the Q point of the two-dimensional Brillouin zone, emission takes place predominantly through two pathways: direct charge recombination at the K point, and indirect phonon-assisted recombination of electrons at the K valley and holes at the Γ hill of the Brillouin zone.

The evidence comes from the calculated momentum-resolved density of the pumped charges excited from the two top valence bands (v1 and v2 in Fig. 2) to the two lowest conduction bands (c1 and c2 in Fig. 2) in the presence of a 100 fs pulse of an electric field of magnitude $1\text{V}/\text{\AA}$. The time dependence of the excited charge density at the k-points (Fig. 2) corresponding to the total pumped charges plotted in Fig. 3 show that the occupancies at most k-points begin to decrease after 200 fs, just as electron-phonon coupling starts to play a role in scattering electrons out of the Q valley into the K valley. The originally highest-

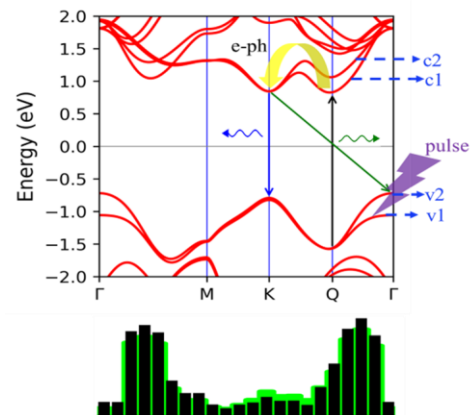


Fig. 2 **Top:** Schematics of excitation and recombination processes in bilayer MoS_2 that lead to photoluminescence. **Bottom:** excited charge accumulation at Brillouin zone k-points immediately after external perturbation (black) and after phonon dynamics set in (green).

populated Q-valley thus gets significantly depopulated, in contrast to that at the K-valley. The “final” excited charge density at different k-points is shown in the bottom of Fig. 2) (green columns). This electron relaxation due to electron-phonon

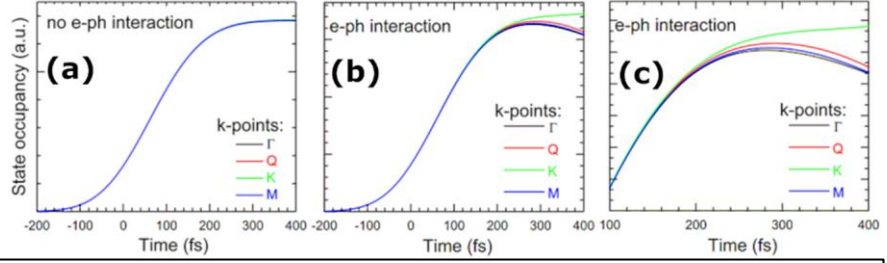


Fig. 3 Time dependent occupancies of conduction band at Γ , Q, K and M points of Brillouin zone: (a) No electron-phonon interaction and (b) with electron-phonon interactions. In (c) zoomed long-time occupancies from (b) are shown.

interaction is represented schematically in the top panel of Fig. 2. The energy required to move an electron from Q to K valley of the conduction band is ~ 40 meV, which we find to be the effective (average) phonon energy. We thus conclude that electron-phonon coupling is the main source of depopulation of excited state occupancies at points other than the K valley. At the K point, the major contribution to electron-phonon coupling arises from the low frequency longitudinal acoustic modes which do not affect the occupancy of the excited state. Our results reveal the importance of ultrafast charge dynamics in understanding the photoluminescence of a few-layer transition-metal dichalcogenide.

3. Isotope effect on electronic bandgap and exciton binding energy in 1L MoS₂

We have carried out DM-TDDFT + many body calculations to understand an interesting trend in the observed isotope effect (in collaboration with the experimental group of Geohegan et al. at ORNL) in single layer (1L) MoS₂, namely the unexpected red shift of the PL peak with increasing Mo isotope mass corresponding to an increase in the exciton binding energy.

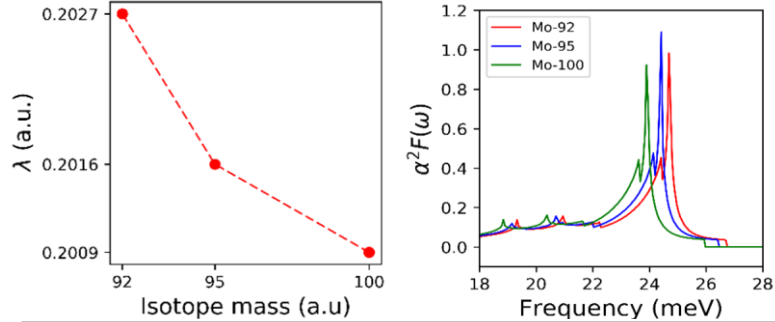


Fig. 4 Modes of the Eliashberg function (left) and the PL spectrum (right) of 2L MoS₂. The lower- (higher-) energy peak corresponds to indirect (direct) emission.

As expected, our DFT results for the electron-phonon interaction parameter and Eliashberg function (Fig. 4) demonstrate

a $\frac{1}{\sqrt{M}}$ dependence. A similar trend is found for bandgap changes for the three Mo isotopes (Table 2). On the other hand, quite unexpectedly but in agreement with experimental data, we do not find such $M^{-1/2}$ dependence for the exciton binding energy. Instead, in

single-layer MoS₂ the exciton binding energy *increases* with *increasing* isotope mass (Table 3). We trace this anomaly in the isotope effect (on the exciton binding energy) to the unusually large frequency-dependence of the electron self-energy dynamical term that arises from exciton-phonon

Table 2 Electron-phonon coupling constant, band gap, band gap shift, partial contribution to band gap shift from electron (e) and hole (h) bands for the three Mo isotopes.

Isotope	λ	gap (eV)	Δ	Δ_e	Δ_h
92	0.2027	1.588	-0.067	-0.029	-0.038
95	0.2016	1.591	-0.064	-0.027	-0.037
100	0.2009	1.594	-0.061	-0.0265	-0.0345

interaction corresponding to the absorption and emission of phonons by excitons that modify the average energy of the exciton. Such an energy change can be expected for systems with exciton binding energies as large as that found in transition-metal dichalcogenides, but not in standard semiconductors, for which the term in question is small (since exciton binding energies are smaller than phonon frequencies).

Table 3 The bandgap, exciton binding energy with relative contribution of the dynamical and static Fan electron self-energy terms and the positions of the PL peaks for the three Mo isotopes.

Mo Isotope	Bandgap (eV)	Exciton binding energy (eV)	Fan term: dynamic part	Fan term: static part	PL peak (eV)	PL peak (sciss.) (eV)
92	1.588	0.562	0.063	0.019	1.027	1.809
95	1.591	0.571	0.071	0.020	1.016	1.800
100	1.594	0.578	0.077	0.021	1.006	1.790

Future Plans

Our future plans include continuation of examination of the response of novel and strongly correlated materials to ultrafast probes. Two systems are currently being studied: WeSe_2 bilayers and V_2O_3 . For WeSe_2 bilayers the effort focuses on understanding the characteristics of excitons, biexcitons and trions as affected by electron-phonon interactions. We have developed a code based on the Casida equation approach to calculate the exciton binding energies, absorption spectrum and excitation transition map with TDDFT and applied it to 1L WSe_2 . To the best of our knowledge, this is the first calculation of TDDFT excitation transition map for solids (beyond finite systems). Future work will also include the intriguing case of twisted bilayers. For V_2O_3 we have obtained preliminary results for the excitation spectra using our DFT+DMFT code. Calculations of the electron susceptibility will next help construct the exchange correlation functional with appropriate inclusion of electron correlations and memory effects that we found so essential for elucidating excited state charge dynamics of these materials and their response to ultrafast probes. The effort will be further facilitated by our recent derivation of the nonadiabatic TDDFT XC potentials for strongly correlated materials in the limits of strong and weak correlations from the nonequilibrium electron self-energy, using Sham-Schlüter equation approach. We are also finalizing the manuscript on the excitations and absorption spectrum of pristine and defected laden single layer h -BN for which our TDDFT (RBO XC kernel) analysis reveals the exciton peak at $\sim 5.5\text{eV}$, for both systems, above the defect states thus establishing that the single photon emission emanates from the defect state (N or B vacancy) not the excitonic one.

References

1. V. Turkowski, N.U. Din, and T.S. Rahman, "Time-Dependent Density-Functional Theory and Excitons in Bulk and Two-Dimensional Semiconductors," *Computation* **5**, 39 (2017).
2. S.R. Acharya, V. Turkowski, G.P. Zhang, and T.S. Rahman, "Ultrafast Electron Correlations and Memory Effects at Work: Femtosecond Demagnetization in Ni," *Physical Review Letters* **125**, 017202 (2020).
3. J.M. Galicia-Hernandez, V. Turkowski, G. Hernandez-Cocoletzi, and T.S. Rahman, "Electron correlations and memory effects in ultrafast electron and hole dynamics in VO_2 ," *Journal of Physics: Condensed Matter* **32**, 20LT01 (2020).
4. N.U. Din, V. Turkowski, and T.S. Rahman, "Excited states in hydrogenated single-layer MoS_2 ," *Journal of Physics: Condensed Matter* **33**, 33 075201 (2020).
5. N.U. Din, V. Turkowski, and T.S. Rahman, "Ultrafast charge dynamics and photoluminescence in bilayer MoS_2 ," *2D Materials* **8**, 025018 (2021).

Publications

1. K.M. Conley, N. Nayyar, T.P. Rossi, M. Kuisma, V. Turkowski, M.J. Puska, and T.S. Rahman, "Plasmon Excitations in Mixed Metallic Nanoarrays," *ACS Nano* **13**, 5344-5355 (2019). DOI:10.1021/acsnano.8b09826
2. S.R. Acharya, V. Turkowski, G.P. Zhang, and T.S. Rahman, "Ultrafast Electron Correlations and Memory Effects at Work: Femtosecond Demagnetization in Ni," *Physical Review Letters* **125**, 017202 (2020). DOI:10.1103/PhysRevLett.125.017202
3. B.T. Blue, G.G. Jernigan, D. Le, J.J. Fonseca, S.D. Lough, J.E. Thompson, D.D. Smalley, T.S. Rahman, J.T. Robinson, and M. Ishigami, "Metallicity of 2H-MoS₂ induced by Au hybridization," *2D Materials* **7**, 025021 (2020). DOI:10.1088/2053-1583/ab6d34
4. H.-T. Chang, A. Guggenmos, S.K. Cushing, Y. Cui, N.U. Din, S.R. Acharya, I.J. Porter, U. Kleineberg, V. Turkowski, and T.S. Rahman, "Electron Thermalization and Relaxation in Laser-Heated Nickel by Few-Femtosecond Core-Level Transient Absorption Spectroscopy," *Phys Rev B* **103**, 064305 (2021)
5. K.M. Conley, N. Nayyar, T.P. Rossi, M. Kuisma, V. Turkowski, M.J. Puska, and T.S. Rahman, "Plasmon excitations in chemically heterogeneous nanoarrays," *Physical Review B* **101**, 235132 (2020). <https://dx.doi.org/10.1103/PhysRevB.101.235132>
6. N.U. Din, V. Turkowski, and T.S. Rahman, "Ultrafast charge dynamics and photoluminescence in bilayer MoS₂," *2D Materials* **8**, 025018 (2021).
7. N.U. Din, V. Turkowski, and T.S. Rahman, "Excited states in hydrogenated single-layer MoS₂," *Journal of Physics: Condensed Matter* **33**, 33 075201 (2020).
8. J.M. Galicia-Hernandez, V. Turkowski, G. Hernandez-Cocolezzi, and T.S. Rahman, "Electron correlations and memory effects in ultrafast electron and hole dynamics in VO₂," *Journal of Physics: Condensed Matter* **32**, 20LT01 (2020).
9. K.A.M.H. Siddiquee, R. Munir, C. Dissanayake, X. Hu, S. Yadav, Y. Takano, E.S. Choi, D. Le, T.S. Rahman, and Y. Nakajima, "Fermi surfaces of topological semimetal CaSn₃ probed by de Haas van Alphen oscillations," *J. Phys.: Condens. Matter* **33**, 17LT01 (2021).
10. N. S. Vorobeva, A. Lipatov, A. Torres, J. Dai, J. Abourahma, D. Le, A. Dhingra, S. J. Gilbert, P. V. Galiy, T. M. Nenchuk, D. S. Muratov, T. S. Rahman, X. C. Zeng, P. A. Dowben, and A. Sinitskii, "Anisotropic Properties of Quasi-1D In₄Se₃: Mechanical Exfoliation, Electronic Transport, and Polarization-Dependent Photoresponse," *Adv. Funct. Mater.* **2021**, 2106459. <https://doi.org/10.1002/adfm.202106459>
11. V. Turkowski, "Dynamical Mean-Field Theory for Strongly Correlated Materials" (Springer, Cham Switzerland, 2021).
12. B. Barman, A. Linn, A. O'Beirne, J. Holleman, C. Garcia, V. Mapara, J. Reno, S. McGill, V. Turkowski, D. Karaiskaj, D. Hilton, "Nanoscale Control of Superradiant Emission in a High-mobility Two-dimensional Electron Gas", submitted to *Nano Letters* (2021).
13. V. Turkowski and T. S. Rahman, "Nonadiabatic exchange-correlation potential for strongly correlated materials in the weak- and strong-interaction limits," submitted 2021.
14. J. Shi, D. Le, V. Turkowski, N. Ud Din, T. Jiang, Q. Gu, T. S. Rahman, "Thickness dependence of superconductivity of FeSe films," submitted 2021.
15. M. Alcántara Ortigoza and T.S. Rahman, "A closer look at how symmetry constraints and the spin-orbit coupling shape the electronic structure of Bi(111)," arXiv:2011.14879.
16. J.M.G. Hernandez, V. Turkowski, G.H. Cocoletz, and T.S. Rahman, "Spatially non-homogeneous metallization of VO₂: a TDDFT+DMFT analysis," arXiv:2011.14864.

Ab initio Prediction of Novel Optoelectronic Properties for Topological Materials

Andrew M. Rappe, Department of Chemistry, University of Pennsylvania

Program Scope

As the need for cleaner, safer, and more sustainable energy grows, it is imperative to search for alternatives to traditional energy sources such as fossil fuels and nuclear reactors. To this end, significant research has been conducted to cultivate the optoelectronic properties of materials since the excitation of electrons with light could in principle provide ample electricity from sunlight. However, even though significant progress has been made in generating electricity from the traditional photovoltaic effect, the high cost of manufacturing and the pollution generated in the fabrication process limits its wide application. In addition, the traditional photovoltaic effect has intrinsic limits that keep the maximum conversion efficiency to be 33.7%. Therefore, we are motivated to investigate more unconventional optoelectronic properties in novel materials, trying to understand their physics and exploring the possibility of using them in energy applications.

Under DOE support, we have developed multiple *ab initio* approaches that can allow for the prediction of the bulk photovoltaic effect (BPVE) in various real materials. The BPVE is a nonlinear optoelectronic property that can generate electricity without a traditional p-n junction, which will greatly simplify the solar cell geometry and thus the manufacturing process [1]. More importantly, such effect has been shown to possess the potential of exceeding the intrinsic limit of traditional photovoltaic effects, promising for higher-efficiency solar cells [2]. Previously, we have developed an *ab initio* approach to calculate the shift current contribution to BPVE, which can explain part of the experimentally observed BPVE photocurrent. In this reporting period, we addressed another important contribution to BPVE, ballistic current, and formulated a first principles theory that enables the prediction of ballistic current in real systems. The developed theories can help us better understand the physical mechanisms of BPVE and propose strategies to enhance the photocurrent. As an example, we have proposed a strategy to increase the photocurrent in monolayer MoS₂ by ten times via an electric-field-driven polar distortion.

Meanwhile, emerging materials with topologically nontrivial phases can have huge potential in optoelectronic applications [3,4]. Distinct from normal (topologically trivial) materials, topologically nontrivial materials are characterized by a topological index and band structure features that cannot be removed by adiabatic (small) deformation of the Hamiltonian. As a result, optoelectronic response in topological materials can be robust, and it can also have huge change during the topological phase transition due to the rapidly changing band characters [5]. To explore the possibility of using a newly discovered topological semimetal, CoSi, in optoelectronics, we performed first principles calculations on its optical conductivity and related different features in experimental optical conductivity of CoSi to the nontrivial topology in band structures. We expect this work can help interpret further optical and transport phenomenon in

other types of chiral multifold semimetals, paving the way of bringing them into real-world applications.

Keywords: optoelectronics, topology, first principles

Recent Progress

1. Ballistic Current From First Principles Calculations [P1, P2].

To calculate ballistic current from first principles, we used a perturbative approach to derive a formula for the ballistic current resulting from the intrinsic electron-phonon scattering in a form amenable to first-principles calculation. We then implemented the theory and calculate the phonon ballistic current of the prototypical BPVE material BaTiO₃ using quantum-mechanical density functional theory. The magnitude of the ballistic current is comparable to that of the shift current, and the total spectrum (shift plus ballistic) agrees well with the experimentally measured photocurrents. Furthermore, we show that the ballistic current is sensitive to structural change, which could benefit future photovoltaic materials design.

To take into account more scattering mechanisms that could lead to asymmetric carrier generation, we also consider the contribution from electron-hole interaction. We demonstrate two approaches that enable the ab initio calculation of the ballistic current originating from the electron-hole interaction in semiconductors. Still using BaTiO₃ as an example, we show clearly that for it the asymmetric scattering from electron-hole interaction is less appreciable than that from electron-phonon interaction. Meanwhile, we also performed the calculation on monolayer MoS₂, a material that is predicted to have large excitonic effect, and showed that the increase of current is mainly from the larger relaxation time instead of the asymmetric carrier generation rate. Thus, our calculations indicate that more scattering processes in addition to electron-phonon and electron-hole need to be included to further the BPVE theory. Application-wise, our approaches build up a venue for predicting and designing materials with larger ballistic current due to electron-hole interactions.

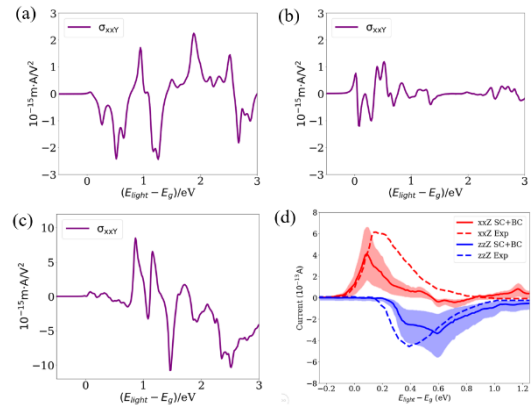
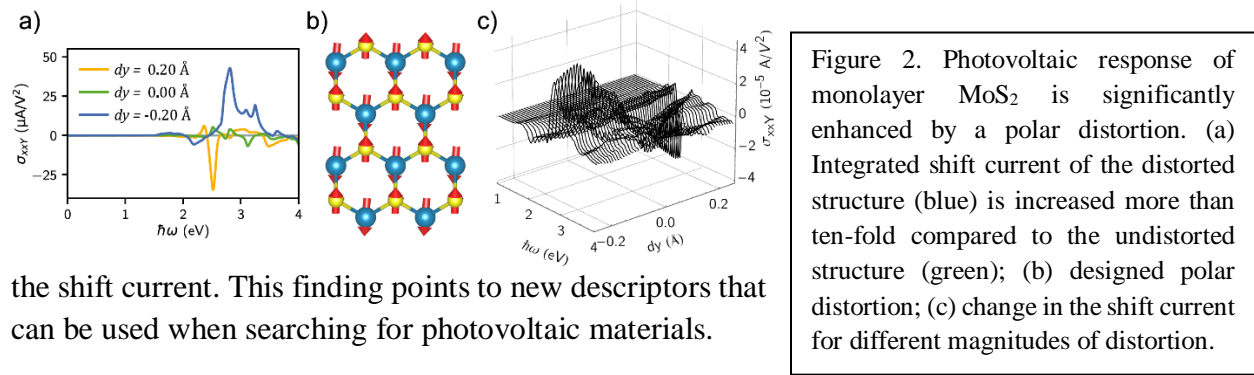


Figure 1. Ballistic current with various mechanisms and the comparison with shift current. (a) Exciton ballistic current using perturbative approach for MoS₂. (b) Exciton ballistic current using diagrammatic approach for MoS₂. (c) Shift current for MoS₂. Note that both approaches calculating exciton ballistic current give same order of magnitude and qualitatively similar features, and they are both smaller than shift current. (d) Phonon ballistic current combined with shift current comparing against experimental BPVE photocurrent of BaTiO₃. The combined theoretical photocurrent explains most of the experimental photocurrent.

2. Large bulk piezophotovoltaic effect of monolayer 2H-MoS₂ [P3].

To demonstrate the capability of our first principles BPVE theories in guiding materials design, we explored the possible routes of enhancing the BPVE photocurrent in monolayer 2H-MoS₂. Many studies have shown that the shift current can be engineered through mechanical strain and strain gradients, and our recent work complements this by showing that structural distortions driven by electric field can also be used to tune the response. We outline an automated method to design distortions that enhance the shift current response in the transition metal dichalcogenide MoS₂ and use it to discover a distortion that couples with the material polarization and dramatically enhances the shift current. This polar distortion, which can be driven by a static electric field via the converse piezoelectric effect, increases the integrated shift current more than ten-fold. Further analysis of this distortion shows that the momentum-space distributions of the shift vector (a quantity measuring the real space displacement of wave packets on excitation) and the transition intensity shows that the overlap of these quantities—not just their magnitude—is vital to increasing



the shift current. This finding points to new descriptors that can be used when searching for photovoltaic materials.

3. Optical signatures of multifold fermions in the chiral topological semimetal CoSi [P4].

To explore topologically nontrivial materials and its potential in optoelectronic applications, we performed first-principles calculations on the optical conductivity of CoSi, a newly discovered multifold topological semimetal that hosts multifold topological degeneracies at the Γ and R points in the Brillouin zone. We constructed the Hamiltonian based on maximally localized Wannier functions and calculated the optical conductivity using Kubo's formula.

Firstly, to understand the linearity of conductivity at low frequency (< 0.1 eV), we constructed a linear $k \cdot p$ model describing the threefold topological fermion at Γ point. This model predicts that the conductivity is linear to photon frequency, and the slope is proportional to the Fermi velocity. The analytic conductivity agrees with that obtained from first-principles calculations and from experiments, indicating that only the threefold topological node contributes to the optical conductivity at low frequency. Secondly, in the $k \cdot p$ model where all electronic bands are not curved, we do not observe the dip structure present in the DFT-calculated optical conductivity spectrum (~ 0.25 eV). The dip structure is associated with the middle band curving

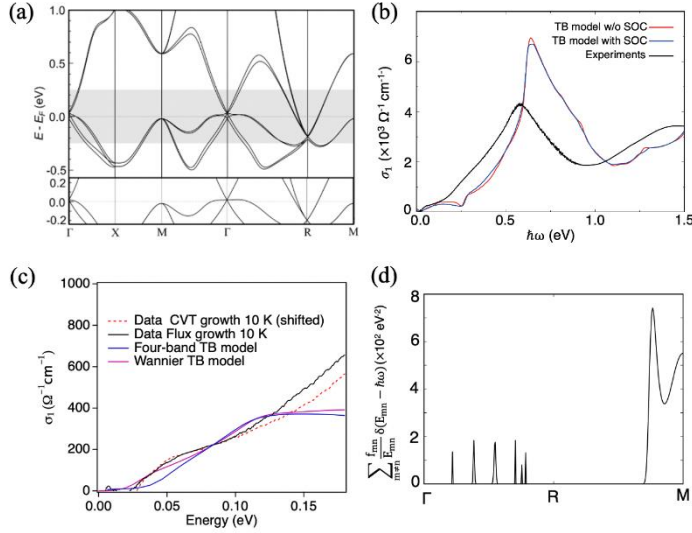


Figure 3. (a) The calculated band structure of CoSi, with the inset (bottom) calculated without spin-orbit coupling effect; (b) Calculated and experimental optical conductivity; (c) The comparison between low-energy experimental optical conductivity and theoretical conductivity calculated using Wannier functions and linear $k \cdot p$ model; (d) The delta function (energy-matching criterion) for optical transitions along high-symmetry lines.

down below the Fermi level away from Γ point; the allowed optical transition changes from low-to-middle band transition to middle-to-high band transition, where the latter occurs at a higher photon frequency. This switching causes the dip structure. Finally, we analyzed the contributions to the main peak at around 0.6 eV. We focused on the product of velocity matrix elements and delta function (the energy-matching criteria), and found out that the transitions between electronic bands near M point mainly contribute to the peak, since the energy difference between these bands are the most close to 0.6 eV.

To sum up, we analyzed the contributions from different topological fermions to the optical conductivity at

different frequencies and provided a way to resolve them using the optical conductivity spectrum.

Future Plans

With regard to exploiting BPVE in energy applications, the prediction of a more than ten-fold increase in shift current response demonstrates the benefits of novel materials design strategies, as the enhancement from this electric field-driven distortion is much larger than that accessible through strain alone. Further work is needed to uncover how the converse piezophotovoltaic effect can be used to tune the behavior of novel sensing devices. In particular, monolayer materials can be stacked into heterostructures with exciting new properties. Incorporating ferroelectric monolayers into such heterostructures is a promising direction that could reliably but flexibly manipulate the photovoltaic properties of a device.

To discover and assess more topologically nontrivial materials for optoelectronics, we plan to extend the above analysis for CoSi to different materials and different optical phenomena. For example, we can consider other multifold topological semimetals, including RhSi and FeGe, and nodal line semimetals where the band-touching points are extended to band-touching lines. Furthermore, we can analyze the novel nonlinear optical responses of this class of topological materials, such as shift current, injection current, and surface-state (Fermi arcs) induced responses, because CoSi has the longest Fermi arcs among known topological materials.

References

- [1] V. I. Belinicher and B. I. Sturman, The photogalvanic effect in media lacking a center of symmetry. *Sov. Phys. Usp.* **23**, 199 (1980)
- [2] J. E. Spanier, V. M. Fridkin, A. M. Rappe, A. R. Akbashev, A. Polemi, Y. Qi, Z. Gu, S. M. Young, C. J. Hawley, D. Imbrenda, G. Xiao, A. L. Bennett-Jackson, and C. L. Johnson, Power conversion efficiency exceeding the Shockley–Queisser limit in a ferroelectric insulator. *Nature Photonics* **10**, 611 (2016).
- [3] F. de Juan, A. G. Grushin, T. Morimoto, and J. E. Moore, Quantized circular photogalvanic effect in Weyl semimetals. *Nature communications* **8**, 1, (2017).
- [4] G. Chang, J. X. Yin, T. Neupert, D. S. Sanchez, I. Belopolski, S. S. Zhang, T. A. Cochran, Z. Cheng, M. C. Hsu, S. M. Huang, and B. Lian, Unconventional photocurrents from surface Fermi arcs in topological chiral semimetals. *Physical Review Letters*, **124**, 166404 (2020).
- [5] L. Z. Tan and A. M. Rappe, Enhancement of the bulk photovoltaic effect in topological insulators. *Physical Review Letters*, **16**, 237402 (2016).

Publications (21 publications in total. Only showing selected ones.)

- [P1] Z. Dai, A. M. Schankler, L. Gao, L. Z. Tan, and A. M. Rappe, Phonon-Assisted Ballistic Current from First-Principles Calculations. *Physical Review Letters*, **126**, 177403 (2021).
- [P2] Z. Dai and A. M. Rappe, First Principles Calculation of Ballistic Current from Electron-Hole Interaction. *arXiv:2102.12004* (2021).
- [P3] A. M. Schankler, L. Gao, and A. M. Rappe, Large Bulk Piezophotovoltaic Effect of Monolayer 2H-MoS₂. *The Journal of Physical Chemistry Letters*, **12**, 1244 (2021).
- [P4] B. Xu, Z. Fang, M. Á. Sánchez-Martínez, J. W. Venderbos, Z. Ni, T. Qiu, K. Manna, K. Wang, J. Paglione, C. Bernhard, C. Felser, E. J. Mele, A. G. Grushin, A. M. Rappe, and L. Wu, Optical signatures of multifold fermions in the chiral topological semimetal CoSi. *Proceedings of the National Academy of Sciences*, **117**, 27104. (2020)
- [P5] A. M. Burger, L. Gao, R. Agarwal, A. Aprelev, J. E. Spanier, A. M. Rappe and V.M. Fridkin, Shift photovoltaic current and magnetically induced bulk photocurrent in piezoelectric sillenite crystals. *Physical Review B*, **102**, 081113 (2020).
- [P6] R. Fei, L. Z. Tan and A. M. Rappe, Shift-current bulk photovoltaic effect influenced by quasiparticle and exciton. *Physical Review B*, **101**, 045104 (2020).
- [P7] X. Li, T. Qiu, J. Zhang, E. Baldini, J. Lu, A. M. Rappe and K. A. Nelson, Terahertz field-induced ferroelectricity in quantum paraelectric SrTiO₃. *Science*, **364**, 1079 (2019).
- [P8] Z. Ji, G. Liu, Z. Addison, W. Liu, P. Yu, H. Gao, Z. Liu, A. M. Rappe, C. L. Kane, E. J. Mele and R. Agarwal, Spatially dispersive circular photogalvanic effect in a Weyl semimetal. *Nature materials*, **18**, 955 (2019).
- [P9] H. Gao, J. W. Venderbos, Y. Kim and A. M. Rappe, Topological semimetals from first principles. *Annual Review of Materials Research*, **49**, 153 (2019).
- [P10] T. Qiu, L. Kronik and A. M. Rappe, General Approach for Reducing Continuous Translational Symmetry Errors in Finite Difference Real-Space Calculations. *Journal of Chemical Theory and Computation*, **16**, 4327 (2020).
- [P11] L. Z. Tan and A. M. Rappe, Upper limit on shift current generation in extended systems. *Physical Review B*, **100**, 085102 (2019).

Advanced theoretical and computational methods for quantum materials

PI: F.A. Reboredo, co-PI M.-H. Du, M. Eisenbach, J. Krogel and M. Yoon
Oak Ridge National Laboratory

Program Scope

The development of the theoretical/computational approach is key to achieve the accuracy required to predict new materials with competitive degrees of freedom. Accurate theory for complex quantum materials demands the description of all competitive effects of comparable magnitude with similar detail. In this project we focus on theoretical-computational studies using *ab initio* based approaches and high-performance supercomputers. Our overarching goal is to predict novel quantum materials and to understand the impact of defects, dopants and interfaces on the properties of quantum materials with improved first-principles-based theory and computational approaches. This goal will be addressed by the following three specific aims: (1) Understand the impact of electronic correlation and localized defects on heterostructures, layered materials, and bulk systems, (2) Identify the changes in the ground state magnetic properties of materials induced by local and global symmetry breaking, and (3) Understand the interplay of topological properties with electronic correlation, magnetism, dopants and symmetry. We will apply and develop many-body approaches based on quantum Monte Carlo techniques (QMC) and large-scale state-of-the-art density functional theory (DFT) simulations. Computationally assisted discovery methods based on machine learning will be developed to generate effective models and to predict novel quantum materials that are accessible through experimental synthesis and characterization approaches. This set of complementary techniques will allow us to have a comprehensive picture of materials systems across different energy and length scales involved in the experimental program supported by MSED BES DOE at ORNL.

Keywords: Magnetism, Topology and Correlation

Recent Progress

Nanostructured correlated materials: We have used many-body *ab-initio* methods to understand theoretically how magnetism is controlled by strain.(3) In general, there is a competition between exchange, that favors single occupied electronic orbitals, and crystal field splitting, that favors double occupation. In LaCoO_3 , crystalline field and exchange energies almost balance each other. The six electrons at the d orbital of Co can occupy the t_{2g} and e_g multiplets in configurations with a total spin that varies (0, 1, or 2), but with similar energy. Experiment finds that the bulk material is not magnetic.

Attempts to control the total spin of Co via strain-induced tuning of the crystalline field observed i) the emergence of magnetism with strain [1-3] and ii) the spontaneous occurrence of a lateral modulation of the lattice perpendicular to the growth direction [4]. These discoveries generated a debate in the literature on both the mechanism that caused the lateral modulation and the induced magnetism. One line of thought argued in favor of departures of the stoichiometry, in particular the potential ordering of oxygen vacancies [5]. Another interpretation argued in favor of a purely electronic/magnetic mechanism within the stoichiometric configuration [4]. Alternative state-of-the-art approximations of DFT supported either mechanism depending on the choice of density functional [4,5].

Our DMC calculations found that i) a magnetic moment appears in the Co atoms in the strained samples and ii) the lowest energy configuration of the Co spin result in a ferrimagnetic configuration (see Figure 1). However, not every experimental observation is accounted by our DMC calculations. Our calculations, in divergence with the experimental consensus, find that there is a net magnetic moment on Co in the bulk. Thus far we have been using the simplest formulation of DMC, a Slater/Jastrow single determinant approach. This simplified approach has seldom failed to describe the qualitative ground state.

First-principles discovery of new magnetic Weyl semimetals with high thermodynamic stability:

Using DFT combined with an evolutionary algorithm we identified new Weyl phases of Co-based shandite and alloys, $\text{Co}_3\text{MM}'\text{X}_2$ ($\text{M}/\text{M}'=\text{Ge}, \text{Sn}, \text{Pb}, \text{X}=\text{S}, \text{Se}, \text{Te}$) with high thermodynamic stability (10). Our theoretical modeling, which combined first-principles DFT and tight-binding approaches, revealed the origin of the nodal lines of Co-based shandites and further identified two novel topological phases of alloys such as $\text{Co}_3\text{SnPbS}_2$. The $\text{Co}_3\text{SnPbS}_2$ alloy exhibits two distinguished

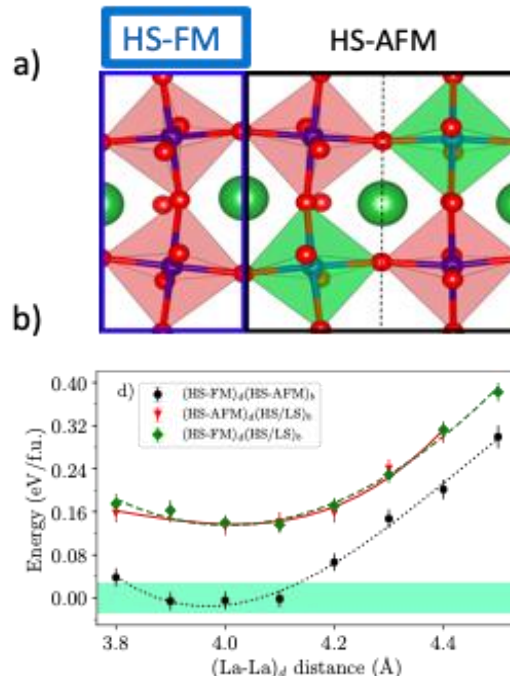


Figure 1: a) Laterally modulated unit cell of epitaxial LaCoO_3 . Blue (black) means compressed (expanded). b) (black squares) Energy of the ground state in (a) as a function of the La-La distance in the expanded region relative to the uniform high-spin AFM phase (green bar).

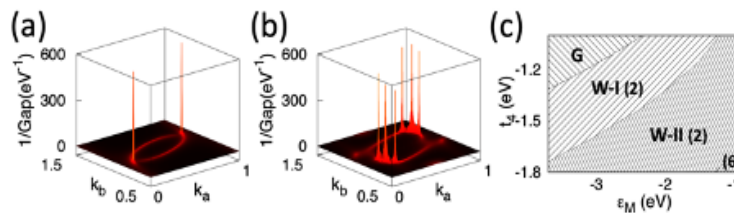


Figure 2: Inverse gap structures identify the number of Weyl points. For example, a pair of Weyl points (a) in $k_b=k_c$ mirror plane and three pairs of Weyls points (b) in the mirror plane with different parameters are identified. (c) The phase diagram where G, W-I, and W-II stand for compounds with local gaps along the nodal lines, type I, and II Weyl semimetals, respectively; and the numbers in parentheses indicate the number of Weyl points.

topological phases, depending on the relative positions of the Sn and Pb atoms: a three-dimensional quantum anomalous Hall phase and an MWSM phase with anomalous Hall conductivity ($\sim 1290 \text{ W}^{-1}\text{cm}^{-1}$) that is larger than that of $\text{Co}_2\text{Sn}_2\text{S}_2$, the first material confirmed as an MWSM in recent experiments [6]. We also for the first time reported the topological transition between different Weyl phases with changing metal dopants. In addition, we revealed a microscopic mechanism of the origination of Weyl fermions in Co-based shandite structures and proposed new MWSMs with high thermal stability for experimental synthesis.

Novel defect-tuning strategy for topological surface conduction: Novel defect control and chemical doping strategies are discovered to suppress the detrimental bulk conduction in the antiferromagnetic topological insulators MnBi_2Te_4 and MnBi_4Te_7 (4). This project combines theory (Du, Cooper, Eisenbach) with experimental synthesis and transport measurements by (Yan). MnBi_2Te_4 is the first topological insulator discovered with an intrinsic magnetic ordering. A topological insulator should have an insulating bulk and a conductive surface. A high defect density is a major obstacle in observing topological quantum states, such as quantum anomalous Hall effect and axion insulator states, because the defects give rise to bulk metallic conductivity, which prevents the measurement of quantum transport through the topological surface state. Density functional theory calculations of defect and dopant properties in MnBi_2Te_4 and MnBi_4Te_7 , combined with carrier statistics calculations, provide understanding of the main defect formation mechanism, which is intimately related to the internal strain in these layered materials. This novel understanding enabled us to design strategies for tuning bulk conductivity by precisely controlling defects and dopants. We further proposed a new acceptor dopant, Na, and specific growth conditions to minimize bulk conductivity for the measurement of quantum transport through topological surface states.

Future Plans: A few examples of current and immediate research are listed below. Please contact for discussions/collaborations.

Intrinsic magnetic topological insulators (Mn-Bi-Te family):

- New mechanism controlling magnetic properties by magnetoelectric coupling (manuscript to be submitted)—Du, Reboredo, Yoon
- Use of different stoichiometries for controlling topological properties—Du, Yoon, Reboredo (in collaboration with Cooper FWP and McGuire FWP)
- Defect and dopant long-range magnetic interactions—Eisenbach, Du, Yoon, Reboredo (in collaboration with McGuire FWP and Lee FWP)

Magnetic Weyl semimetals, Shandites (Co-X-S [X=Sn, I, Pb, Sb, ...] family):

- Obtaining accurate U values based on QMC for magnetic properties—Krogel, Reboredo, Yoon
- Role of defects and dopants on topological properties and magnetic interactions —Yoon, Eisenbach, Du, Krogel, Reboredo (in collaboration with McGuire FWP and CNMS [Z. Gai])

Quantum materials with versatile properties—delafossites (PdCoO_2 , PdCrO_2 , CuCrO_2):

- High-throughput DFT and machine learning for structure exploration and engineering topological, magnetic, and electronic properties—Yoon, Reboredo, Du, Krogel, Eisenbach
- Optical properties and functional plasmonic polaritons in PdCoO_2 —Du, Yoon, Reboredo (in collaboration with Lee and Kalinin FWPs)
- Growth mechanism—the role of defects, interfaces, and charge transfer—Yoon, Reboredo (in collaboration with Lee FWP)

Correlated physics and defect phenomena:

- Single-photon emission in qubit candidates—Krogel, Du, Yoon, Reboredo (in collaboration with Jesse FWP, Lawrie FWP, Xiao FWP)
- Defects in highly correlated materials—Reboredo, Krogel (in collaboration with Kent CMS, latest advances of QMCPACK for large systems being used)
- Auxiliary boson DMC method for excited states—Reboredo, Krogel Kent

References (In [] in main text)

- [1]M. A. Korotin, S. Y. Ezhov, I. V. Solovyev, V. I. Anisimov, D. I. Khomskii, and G. A. Sawatzky, Intermediate-spin state and properties of LaCoO_3 , *Physical Review B* 54, 5309 (1996).
- [2]J. M. Rondinelli and N. A. Spaldin, Structural effects on the spin-state transition in epitaxially strained LaCoO_3 films, *Physical Review B* 79, 054409 (2009).
- [3]H. Seo, A. Posadas, and A. A. Demkov, Strain-driven spin-state transition and superexchange interaction in LaCoO_3 : Ab initio study, *Physical Review B* 86, 014430 (2012).
- [4]J.-H. Kwon, W. S. Choi, Y.-K. Kwon, R. Jung, J.-M. Zuo, H. N. Lee, and M. Kim, Nanoscale Spin-State Ordering in LaCoO_3 Epitaxial Thin Films, *Chemistry of Materials* 26, 2496 (2014).
- [5]N. Biškup, J. Salafranca, V. Mehta, M. P. Oxley, Y. Suzuki, S. J. Pennycook, S. T. Pantelides, and M. Varela, Insulating Ferromagnetic $\text{LaCoO}_{3-\delta}$ Films: A Phase Induced by Ordering of Oxygen Vacancies, *Physical Review Letters* 112, 087202 (2014).
- [6]E. Liu *et al.*, Giant anomalous Hall effect in a ferromagnetic kagome-lattice semimetal, *Nature Physics* 14, 1125 (2018).

Recent Selected Publications (In () in main text)

- 1) K. Saritas, W. Ming, M.-H. Du, and F. A. Reboredo, Excitation energies of localized correlated defects via quantum Monte Carlo: A case study on Mn⁴⁺ doped phosphors, *J. Phys. Chem. Lett.* **10**, 67 (2019).
- 2) S. Mu, J. Yin, G. D. Samolyuk, S. Wimmer, Z. Pei, M. Eisenbach, S. Mankovsky, H. Ebert, G. M. Stocks, Hidden Mn magnetic-moment disorder and its influence on the physical properties of medium-entropy NiCoMn solid solution alloys, *Phys. Rev. Mat.* **3**, 014411 (2019).
- 3) K. Saritas, J. T. Krogel, S. Okamoto, H. N. Lee, and F. A. Reboredo, Structural, electronic, and magnetic properties of bulk and epitaxial LaCoO₃ through diffusion Monte Carlo, *Phys. Rev. Mater.* **3**, 124414 (2019).
- 4) M.-H. Du, J. Yan, V. R. Cooper, and M. Eisenbach, Tuning Fermi levels in intrinsic antiferromagnetic topological insulators MnBi₂Te₄ and MnBi₄Te₇ by defect engineering and chemical doping, *Adv. Funct. Mater.* 2006516 (2020).
- 5) J. A. Santana, J. T. Krogel, S. Okamoto, and F. A. Reboredo, Electron confinement and magnetism of (LaTiO₃)₁/(SrTiO₃)₅ heterostructure: A diffusion quantum Monte Carlo, *J. Chem. Theory Comput.* **16**(1), 643 (2020).
- 6) J. T. Krogel and F. A. Reboredo, Hybridizing pseudo-Hamiltonians and non-local pseudopotentials in diffusion Monte Carlo, *J. Chem. Phys.* **153**, 104111 (2020).
- 7) J. Zhang, X. Liu, S. Bi, J. Yin, G. Zhang, and M. Eisenbach, Robust data-driven approach for predicting the configurational energy of high entropy alloys, *Mater. Des.* **185**, 108247 (2020).
- 8) L. Zhang, C. Park, and M. Yoon, Quantum phase engineering of two-dimensional post-transition metals by substrates: Toward a high-temperature quantum anomalous Hall insulator, *Nano Lett.* **20**(10), 7186 (2020).
- 9) X. Liu, J. Zhang, J. Yin, S. Bi, M. Eisenbach, Y. Wang, Monte Carlo simulation of order-disorder transition in refractory high entropy alloys: a data driven approach, *Computational Material Science* **187**, 110135 (2021).
- 10) T. Ichibha, A. L. Dzubak, J. T. Krogel, V. R. Cooper, and F. A. Reboredo, CrI₃ revisited with a many-body ab initio theoretical approach, *Phys Rev Mat.* **5**, 064006 (2021)
- 11) W. Luo, Y. Nakamura, J. Park, and M. Yoon, Cobalt-Based Magnetic Weyl Semimetals with high-Thermodynamic Stabilities, *npj Comp. Mater.* **7**, 2 (2021).
- 12) K. M. Roccapiore, Q. Zou, L. Zhang, R. Xue, J. Yan, M. Ziatdinov, M. Fu, D. G. Mandrus, M. Yoon, B. G. Sumpter, Z. Gai, and S. V. Kalinin, Revealing the Chemical Bonding in Adatom Arrays via Machine Learning of Hyperspectral Scanning Tunneling Spectroscopy Data. *ACS Nano* **15**, 11806 (2021).
- 13) C. Liu, Y.-C. Lin, M. Yoon, Y. Yu, A. A. Puretzky, C. M. Rouleau, M. F. Chisholm, K. Xiao, G. Eres, D. B. Geohegan, and G. Duscher, Understanding Substrate-Guided Assembly in van der Waals Epitaxy by In Situ Laser Crystallization within a TEM, *ACS Nano* **15**, 8638 (2021).
- 14) A. F. May, M.-H. Du, V. Cooper, and M. A. McGuire, Tuning the magnetic ground state of the van der Waals metal Fe₅GeTe₂, *Phys. Rev. Mater.* **4**, 074008 (2020).
- 15) W. R. Meier, M.-H. Du, S. Okamoto, N. Mohana, A. F. May, M. A. McGuire, C. A. Bridges, G. D. Samolyuk, and B. C. Sales, Flat bands in the CoSn-type compounds, *Phys. Rev. B* **102**, 075148 (2020).
- 16) Yuto Ishii, G. Sala, M. B. Stone, V. O. Garlea, S. Calder, Jie Chen, Hiroyuki K. Yoshida, Shuhei Fukuoka, Jiaqiang Yan, Clarina dela Cruz, Mao-Hua Du, David S. Parker, Hao Zhang, C. Batista, Kazunari Yamaura, and A. D. Christianson, “Magnetic properties of the Shastry-Sutherland lattice material BaNd₂ZnO₅”, *Phys. Rev. Mater.* **5**, 064418 (2021).

New Developments in the Theory of Excited States and X-ray Spectra

Principal investigators: J. J. Rehr and J. J. Kas, Department of Physics, University of Washington, Seattle, WA 98195-1560

Project Scope

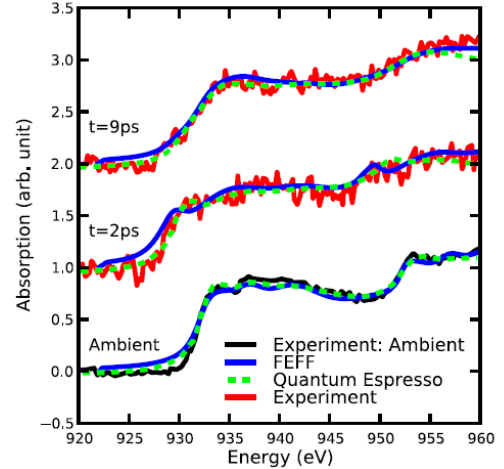
The search for general theories of electronic structure beyond the independent particle approximation continues to be a major challenge in theoretical condensed matter physics. Needed are theoretical tools that are applicable over a broad range of energy, time, distance, and temperature scales. Our research pursues several developments in the theory of excited-state electronic structure and dynamic response to meet this challenge, in particular the treatment of finite temperature and time-dependence. Going beyond the usual wave-function approach of quantum theory, our approach is based on modern cumulant Green's function methods which are exceptionally well suited for this research. The synergism between theory, computation and experiment made possible by our research enhances scientific understanding and creates opportunities for innovations in materials and energy science and in many other fields.

Keywords: x-ray spectra, excited states, cumulant Green's function, finite-temperature

Recent Progress

Excited states and x-ray spectra at finite-temperature - A major focus of our current project is the extension of modern Green's function methods for calculating and understanding excited states at finite temperature (FT), up to the warm dense matter (WDM) regime where the temperature T is of order the Fermi temperature $T_F \sim 10^5$ K. Understanding matter in extreme conditions is an important challenge in many fields, ranging from plasma- and astrophysics to inertial confinement fusion. An important focus of our work is on FT x-ray spectroscopy, with XFEL sources such as the LCLS. A significant advance of our recent research was the development of a FT cumulant Green's function approach for excited state and thermodynamic properties [1]. This method provides an alternative to FT density functional theory (DFT) or quantum Monte Carlo (QMC) methods, which are not well suited for calculations of excited state properties. In this approach, the Green's function $G(t)$ is calculated in the time-domain $G(t) = G_0(t) \exp[C(t)]$ and many-body effects beyond the independent particle approximation are embedded in the cumulant $C(t)$. As at $T=0$, the leading cumulant $C(t)$ is linear in the screened Coulomb interaction and no more difficult to calculate than Hedin's GW self-energy. Our approach yielded results for the homogeneous electron gas over a wide range of densities and temperatures [1]. Remarkably, exchange-correlation energies $\epsilon_{xc}(T)$ and potentials $v_{xc}(T)$ were found to be in good agreement (typically within a few percent) of existing theories such as path integral Monte-Carlo. Moreover, our approach also yields an interpretation of the exchange and correlation contributions to thermodynamic quantities such as energy, entropy, pressure, and specific heat, including spin-dependence up to the WDM regime. The FT exchange-correlation

energy and potential were found to vary weakly with temperature at low $T \ll T_F$, and cross over from exchange- to correlation-dominated behavior at high T . We also found that a simple quasiparticle approximation for the spectral function gave efficient and fairly accurate results. These advances have been incorporated into the real-space Green's function (RSGF) approach used in the FEFF10 code of our group [2]. Using a two-temperature model to describe the time-evolution of the electronic $T_e(t)$ and lattice temperatures T_L , we obtain good agreement with experiment: the figure at the right shows the time-resolved L-edge XAS of Cu following laser excitation at 2 ps ($T_e = 10,200$ K) and 9 ps ($T_e = 6000$ K) time-delay calculated with FEFF10.



Real-time approaches for excitations in x-ray spectra – A second key effort of our research is the development of a real-time time-dependent DFT (RT-TDDFT) approach to calculate and interpret plasmon satellites and charge-transfer excitations in x-ray spectra [5,6]. These losses give rise to the satellites observed in XPS and XAS. We have shown that these intrinsic losses due to the sudden creation of the core-hole can be calculated accurately using an RT-TDDFT generalization of the Langreth linear-response cumulant. Recent applications have treated these effects in transition metal oxides and sulfides probed by XPS, resonant Auger, and XAS, using a combination of the real-time cumulant and the Bethe-Salpeter equation. Analysis of the experimental and theoretical data demonstrates the charge transfer character of the excitations, and the interplay with the underlying electronic structure of the materials. Another application is the simulation of an ultra-fast pump-probe XAS of an FeMgO heterostructure; a preliminary account is given in [7]. In this system the Fe layers absorb the pump energy, raising T_e within a fraction of a picosecond. We have modeled the electronic structure and XAS of this system with our FT spin-dependent version of FEFF using a two-temperature model for the electron- and lattice-temperature dependence, and a Curie-Weiss model for the magnetization of the iron layers. Another application was a unified real-time approach to the exciton cumulant; a preliminary account is given in [8]. This approach extends our previous work on the particle-hole cumulant and includes intrinsic, extrinsic and interference effects on equal footing. The particle-hole cumulant is again related to the valence density response to the sudden appearance of the core-hole. This core-hole response function can be interpreted in terms of a quasi-bosonic excitation spectrum consistent with the satellite spectrum in the core-hole spectral function. Our approach has also been used in a definitive study of satellites in ARPES to analyze extrinsic and intrinsic losses [8], as part of our long-term collaboration with the Reining group at the Ecole Polytechnique (Paris). Finally we have collaborated in the development of non-linear cumulant Green's function methods [9].

Next-generation spectroscopy codes and applications – A significant product of our research over the past three decades is the development of spectroscopy codes such as FEFF, which are in use worldwide to analyze x-ray spectra. Beginning in 2022, the FEFF-project theory and code development will be carried out at the Theory Institute for Materials and Energy Spectroscopies

(TIMES), of which we are co-investigators. For example, the extension to FEFF10 was developed at TIMES with the addition of the theoretical developments discussed above [10]. A significant application is the use of FEFF for automated calculations of L-edge XAS for a large subset of the structures present in the Materials Project data-base [11].

Future plans

At the next stage, we plan to pursue a number of topics related to FT Green's function developments. For example, an improvement to the finite temperature cumulant will be carried out by adding local field corrections and self-consistency. In addition, we plan to investigate the addition of non-linear corrections to the cumulant, and their effect on the spectral function. These additions will likely improve the FT-DFT functionals calculated. Second, we will continue our investigations of real-time-approaches for x-ray spectra. These include the development of the integrated real-time approach to the particle-hole cumulant to replace the previous approximation for the interference term, and extensions to the approach for time-dependent and pulsed x-ray sources. These plans will be continued at TIMES following the conclusion of the current award in 2022.

References

- [1] Kas, J. J., Blanton, T. D. & Rehr, J. J. Exchange-correlation contributions to thermodynamic properties of the homogeneous electron gas from a cumulant Green's function approach. *Phys. Rev. B* **100**, 195144, NOV 2019. <http://dx.doi.org/10.1103/PhysRevB.100.195144>.
- [2] Tun S. Tan, J. J. Kas, and J. J. Rehr, Real-space Green's function approach for x-ray spectra at high temperature, *Phys. Rev. B* **104**, 035144 JUL 2021. <https://doi.org/10.1103/PhysRevB.104.035144>
- [3] Cumulant expansion of the exciton Green's function: A unified approach for many-body intrinsic, extrinsic, and interference effects in XAS, APS March Meeting 2020.
- [4] Kas, J.J.; Vila, F.D.; Pemmaraju, C.D. Tan, T.S.; Rehr, J.J. Advanced calculations of X-ray spectroscopies with FEFF10 and Corvus. *J. Synchrotron Rad.* (in press, 2021).
- [5] Woicik, J. C. et al. Charge-transfer satellites and chemical bonding in photoemission and x-ray absorption of SrTiO₃ and rutile TiO₂: Experiment and first-principles theory with general application to spectroscopic analysis. *Phys. Rev. B* **101**, 245119, Jun 2020. <http://dx.doi.org/10.1103/PhysRevB.101.245119>.
- [6] Woicik, J. C. et al. Core hole processes in x-ray absorption and photoemission by resonant Auger-electron spectroscopy and first-principles theory. *Phys. Rev. B* **101**, 245105, JUN 2020. <http://dx.doi.org/10.1103/PhysRevB.101.245105>
- [7] Tan, T. S. and Rehr, J. J. and Kas, J. J. Finite temperature full multiple scattering calculation of ultrafast x-ray absorption spectroscopy, APS March Meeting 2020.

[8] Zhou, J. S. et al., Dispersing and non-dispersing satellites in the photoemission spectra of aluminum, *Proc. Nat. Acad. of Sci.* **117**, 28596 JUN 2020.
www.pnas.org/cgi/doi/10.1073/pnas.2012625117

[9] Tzavala, M., Kas, J. J., Reining, L. & Rehr, J. J. Nonlinear response in the cumulant expansion for core-hole photoemission. *Phys. Rev. Research* **2**, 033147, JUL 2020.
[10.1103/PhysRevResearch.2.033147](https://doi.org/10.1103/PhysRevResearch.2.033147)

[10] Kas, J.J.; Vila, F.D.; Pemmaraju, C.D. Tan, T.S.; Rehr, J.J., Advanced calculations of X-ray spectroscopies with FEFF10 and Corvus, *J. Synchrotron Rad.* (in press, 2021).

[11] Y. Chen. *et al.* Database of ab initio L-edge X-ray absorption near edge structure. *Sci Data* **8**, 153 (2021). <https://doi.org/10.1038/s41597-021-00936-5>

Publications

[1] Tun S. Tan, J. J. Kas, and J. J. Rehr, Real-space Green's function approach for x-ray spectra at high temperature, *Phys. Rev. B* **104**, 035144 JUL 2020.
<https://doi.org/10.1103/PhysRevB.104.035144>

[2] Kas, J.J.; Vila, F.D.; Pemmaraju, C.D. Tan, T.S.; Rehr, J.J., Advanced calculations of X-ray spectroscopies with FEFF10 and Corvus, *J. Synchrotron Rad.* (in press, 2021);
arXiv:2106.13334v1 [cond-mat.mtrl-sci].

Applications of Nickelate perovskites for neuromorphic computing from electronic structure and Machine Learning

PI: Aldo H. Romero

Affiliation: West Virginia University

Program Scope

As stated in Murphy's law, at this age in technology we are met with a bottleneck for improving computational speed and storage. Neuromorphic Computing, a method that closely follows the inner workings of the human brain, may be the solution in overcoming this limitation. In this arena, the metal to insulator (MIT) transition present in strongly correlated materials (SCM) is crucial in designing materials for neuromorphic applications, as they show great sensibility to small environment changes. Controlling external stimuli such as electric fields and oxygen vacancies enable the tuning of the MIT which opens the possibility of modeling materials into switching devices [1, 2, 3]. Nickelate perovskites are ideal candidates for materials displaying MIT behavior due to the nature of their structure, a NiO_6^{3-} octahedra linked at their corners with a R^{3+} cation, where $\text{R}=\{\text{La, Sm, Gd, Lu, Nd}\}$. The transitions stem from the interaction between the Ni-3d and O-2p manifested in the Ni-O-Ni bond, sensitive to its length and angle changes [4, 5, 6]. Such sensitivities in nickelate perovskites result in tunable responses in electrical conductivity and optical response allowing their use in adaptive hardware that could mimic organismic response to environmental changes. However, the switching phenomenon occurs at length scales elusive to usual electronic structure methods. This can be overcome by employing classical force fields trained with energies and forces obtained with electronic structure methods. As the go-to electronic structure method density functional theory (DFT) fails for correlated materials, more accurate forces and energies are obtained with dynamical mean field theory (DMFT) method through our in-house DMFTwDFT framework [7]. The neural network force field trained with the BLAST package [8] is then able to simulate molecular dynamics (MD) of large systems at long time scales, properly emulating required device scales. Further investigations are carried out to understand the effect of strain, proton doping, external electric fields, grain formation and vacancy presence and migration on the MIT. Active learning methods are used to generate data where training data is insufficient.

Keywords: neuromorphic computing, machine learning, strongly correlated materials

Recent Progress

We performed preliminary studies on controlling MIT in SCM's through means of a combination of DFT and DMFT to accurately probe the elusive properties of correlated materials. As the initial step in investigating the MIT, our in-house DMFTwDFT framework provided DMFT total energies of various strongly correlated bulk SmNiO_3 and GdNiO_3 configurations mimicking a Boltzmann distribution at a finite temperature that was used to train

an atomic interaction potential based on artificial neural networks (ANNs). Our preliminary results indicate very good correlation between the DMFT energies, and the total energy predicted by the machine learning model as shown in Fig. 1.

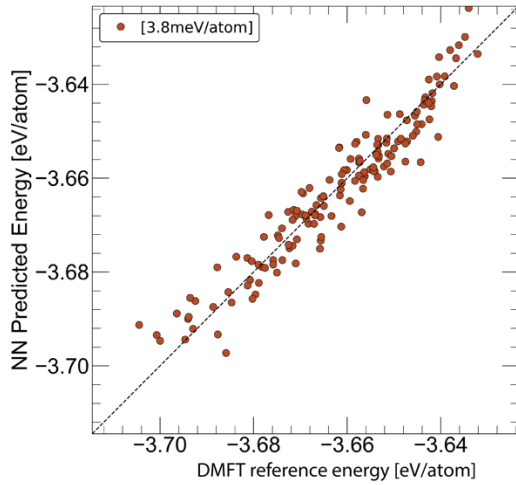


Figure 1: Validation results of the energy obtained from DMFT calculations of SmNiO₃

Future Plans

As our next step, we introduce external stimuli to manipulate the presence of oxygen vacancies in order to tune the MIT and incorporate that for training the machine learning model. Moreover, we also study the oxygen vacancy diffusion energy barrier through means of Nudged Elastic Band (NEB) analysis and DMFT to characterize the energy profile to see how vacancy migration may affect the MIT. Due to the crystal symmetries in both systems, we need to consider different reaction paths, which are first computed by means of DFT+U and energetically characterized with DMFT. As elastic properties are one of the properties that can affect the electronic response in neuromorphic materials, we have also developed a methodology that calculates elastic constants from energy obtained from DMFT calculations through the energy-strain relationship (to second and third order). These configurations are also fed to the NN potential. This is being improved to include the stress-strain relationship which provides more accurate predictions. The relation between the deformation and the energy obtained from DMFT allow us to describe how vacancies can create distortions which impact the electronic properties. The process would be repeated for other nickelate perovskite materials.

References

1. R. Zhang, Q. Fu, C. Yin, C. Li, X. Chen, G. Qian, C. Lu, S. Yuan, X. Zhao, and H. Tao, "Understanding of metal-insulator transition in VO_2 based on experimental and theoretical investigations of magnetic features," *Scientific reports*, vol. 8, no. 1, p. 17093, 2018.

2. M. Imada, A. Fujimori, and Y. Tokura, "Metal-insulator transitions," *Reviews of modern physics*, vol. 70, no. 4, p. 1039, 1998.
3. R. Kukreja, N. Hua, J. Ruby, A. Barbour, W. Hu, C. Mazzoli, S. Wilkins, E. E. Fullerton, and O. G. Shpyrko, "Orbital domain dynamics in magnetite below the Verwey transition," *Physical review letters*, vol. 121, no. 17, p. 177601, 2018.
4. G. Catalan, "Progress in perovskite nickelate research," *Phase Transitions*, vol. 81, no. 7-8, pp. 729–749, 2008.
5. J. Shi, Y. Zhou, and S. Ramanathan, "Colossal resistance switching and band gap modulation in a perovskite nickelate by electron doping," *Nature communications*, vol. 5, p. 4860, 2014.
6. S. J. Allen, A. J. Hauser, E. Mikheev, J. Y. Zhang, N. E. Moreno, J. Son, D. G. Ouellette, J. Kally, A. Kozhanov, L. Balents, et al., "Gaps and pseudogaps in perovskite rare earth nickelates," *APL materials*, vol. 3, no. 6, p. 062503, 2015.
7. Singh, V., Herath, U., Wah, B., Liao, X., Romero, A. H. & Park, H. DMFTwDFT: An Open-Source Code Combining Dynamical Mean Field Theory with Various Density Functional Theory Packages. *Computer Physics Communications*, 107778, 2021.
8. Henry Chan, Badri Narayanan, Mathew J Cherukara, Fatih G Sen, Kiran Sasikumar, Stephen K Gray, Maria KY Chan, and Subramanian KRS Sankaranarayanan. "Machine Learning Classical Interatomic Potentials for Molecular Dynamics from First-Principles Training Data". In: *The Journal of Physical Chemistry C* 123.12, 2019.

Publications

1. Pedram Tavazde, Reese Boucher, Guillermo Avendaño-Franco, Keenan X. Kocan, David S. Mebane, Wilfredo Ibarra-Hernandez, Matthew B Johnson, and Aldo H. Romero, Bayesian Calibration assisted by Markov Chain Monte Carlo sampling of the parameter space in DFT+ U: Applications on simple Fe compounds, accepted *NPJ Computational Physics* (2021).
2. Viviana Dovale-Farelo, Pedram Tavazde, Matthieu J. Verstraete, Alejandro Bautista-Hernandez, and Aldo H. Romero, Exploring the Elastic and Electronic properties of Chromium Molybdenum Diboride alloys, *J. Alloys and Compounds*, 866, 158885 (2021).
3. Mina Aziziha, Saeed Akbarshahi, Suresh Pittala, Sayandeep Ghosh, Rishamli Sooriyagoda, Aldo H. Romero, Subhash Thota, Alan D. Bristow, Mohindar S. Seehra, and Matthew B. Johnson, Experimental and Computational Studies of the Optical Properties of $\text{CuAl}_{1-x}\text{Fe}_x\text{O}_2$, accepted in *J. Phys. Chem. C* 125 (6), 3577-3583 (2021).
4. Logan Lang, Adam Payne, Irais Valencia Jaime, Matthieu J. Verstraete, Alejandro Bautista-Hernandez, and Aldo H. Romero, Assessing Nickel Titanium Binary Systems using Structural Search Methods and Ab Initio Calculations, *J. Chem. Phys. C* 125, 2, 1578–1591 (2021).

Optoelectronic properties of bent two-dimensional materials from first-principles methods combined with machine learning

Adrienn Ruzsinszky, Temple University

Program Scope

A material's interaction with light is highly relevant in the design of nanoelectronic devices such as photodiodes, solar cells, photocatalytic cells, phototransistors, and photodetectors. The interaction of a material with light can be altered by mechanical deformation.

Due to their reduced dimensionality, two-dimensional (2D) materials (e.g., transition metal dichalcogenides or TMDs) exhibit an extraordinary optical response [1] in comparison with bulk counterparts, as has been shown early via the examples of graphene and 2D MoS₂. In addition, spatial confinement and reduced dielectric screening of 2D materials causes strong Coulomb interactions that allow more stable exciton formation with large binding energy and oscillator strength compared to bulk crystals, also enhancing their optical properties. Spectacular optical properties have opened opportunities for exploration of 2D materials for use as absorbers, reflectors, and modulators in optical nanodevices such as photodiodes, solar cells, photocatalytic cells, phototransistors, and photodetectors.

Fine tuning of the optical properties can be achieved by external strain that alters the electronic structure. Since large homogeneous uniaxial or biaxial strains are relatively harder to realize in practical devices, local nonuniform strains (LNS), by wrinkling, indentation and interface conforming, have been explored recently. Mechanical bending can provide effective LNS on nanoribbons, as shown by Yu et al in 2016 [2] on the bending effects for MoS₂ and phosphorene nanoribbons. It was found that the bending induced shifting of edge bands and the charge localization of top valence bands can mitigate or remove the Fermi-level pinning and change the conductivity both along and perpendicular to the width direction of doped nanoribbons.

Optical properties strongly depend on band gaps, therefore any alteration in the band structure results in a changed optical response of the material. The impact of bending is not yet explored. Since edge band positions in band structures and edge band gaps are important for the optical absorption of nanoribbons, it is appealing to show how the edge bands will evolve with bending for varied widths of nanoribbons and how this will modify the optical properties.

The goal of this project is to assess the impact of mechanical bending of two-dimensional transition metal dichalcogenides on their optoelectronic properties, using first-principles methods. These first-principles approximations will be largely built upon GW, GW+BSE [3] and time-dependent density functional theory (TDDFT) with recent nonlocal exchange-correlation kernels [4,5]. These kernels can yield an accurate and computationally efficient optical response in a certain range of band gaps that occur in the semiconductors considered in the project. The low dimensionality of the materials is a stringent test for the methodology applied in the project. The applied approaches are expected to reveal a large number and diverse character of bound excitons in quasi-one-dimensional nanoribbons, suggesting potential applications to electronics utilizing inter- and intraexcitonic processes.

Keywords: low-dimensional materials, optical response, many-body approximations

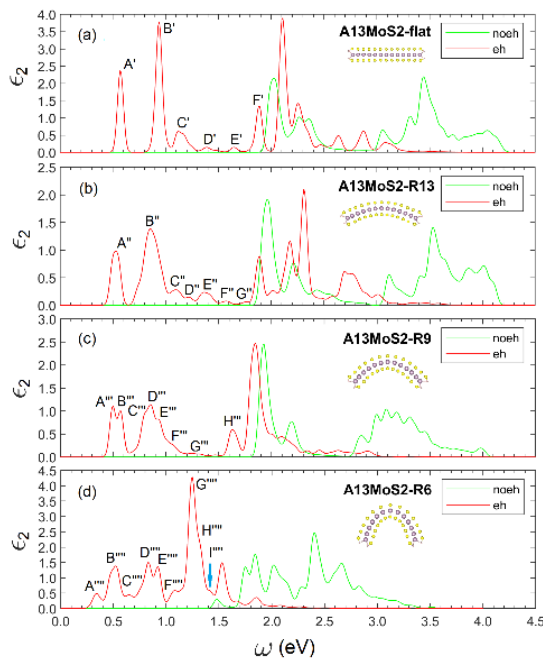
Recent Progress

In the past year we have established and tested novel density functional approximations and the many-body GW+BSE method on the electronic and optical properties of bent nanoribbons. Among these methods the TASK and modified TASK (mTASK) non-empirical meta-GGA density functional approximations deliver accuracy for fundamental band gaps that competes with the accuracy of the popular HSE06 screened hybrid functional [1']. mTASK is cheaper than hybrids and opens great opportunities to replace more expensive methods for band gap estimation. mTASK is the modified version of TASK with enhanced non-locality more suitable for the reduced screening of low-dimensional materials.

We have revealed the large role of the edge states within nanoribbons [2']. We have demonstrated that the more delocalized bulk band states have a very different behavior than the more localized edge states under bending.

The complex strain patterns in the bent nanoribbons control the varying features of band gaps. We have made a link between the complex strain pattern in the nanoribbon and the resulting optical responses. The complex strain patterns in the bent nanoribbons control the varying features of band gaps. Those features will result in varying exciton formations and optical properties. We find that there are two critical bending curvatures κ_{c1} and κ_{c2} with $\kappa_{c1} < \kappa_{c2}$, with very different behavior of the edge and non-edge band gaps with the bending curvature below and beyond κ_{c1} and κ_{c2} .

In addition, we have found a relation between the edge and non-edge band gaps and the periodicity of the nanoribbon as well as the quantum confinement [2'].



The optical absorption spectra of A12MoS₂ nanoribbon under different curvature radii from GW+BSE calculations.

We have found that bending generally induces more exciton states and they contribute to controllable optical absorptions [2']. The induced excitons are related to the bands near the gap and the subtle changes of these bands with bending.

Future Plans

GW+BSE calculations are expensive. Yang et al. in 2015 [6] have replaced the dielectric matrix of BSE by a simple screening constant related to the dielectric function in the spirit of hybrid calculations based on the inverse static dielectric function. This approximation is called the screened exact-exchange approximation (SXX) with accurate exciton binding energies for bulk solids. In our work we started testing this method to show to what extent we can reproduce the BSE exciton binding energies and optical absorption spectra by SXX.

We are working to extend the TDDFT linear-response scheme to two-dimensional materials. TDDFT with recent exchange-correlation kernels can deliver accurate exciton binding energies or optical spectra with more favorable computational scaling than the expensive GW+BSE approximation. We are exploring two different routes. The first approach is to construct a truncation scheme that prevents the harmful Coulomb interaction of replica supercells. Another approach to be explored is to replace the three-dimensional static dielectric function within the closed form of the bootstrap exchange-correlation kernel of S. Sharma et al, 2011 [7]. This latter approach opens the way to circumvent the truncation scheme.

We think that the relatively large and tunable singlet-triplet splitting can make the nanoribbon system suitable for quantum information applications. By identifying ground-state triplet excitons in nanoribbons, it is feasible to optically excite the system from one triplet state to another. Furthermore, the intersystem crossing in the MoS₂ system is realizable by bending, as evidenced by the phosphorescence application of an MoS₂ quantum dot.

References

- [1] M.M. Ugeda, A.J. Bradley, S.-F. Shi, F.H. da Jornada, Y. Zhang, D.Y. Qiu, W. Ruan, S.-K. Mo, Z. Hussain, Shen, Z.-X.; et al. Giant bandgap renormalization and excitonic effects in a monolayer transition metal dichalcogenide semiconductor, *Nat. Mater.* **13**, 1091 (2014)
- [2] L. Yu, A. Ruzsinszky and J.P. Perdew, Bending Two-Dimensional Materials To Control Charge Localization and Fermi-Level Shift, *Nano Lett.* **16**, 2444 (2016)
- [3] M. Rohlfing and S.G. Louie, Electron-hole excitations and optical spectra from first principles, *Phys. Rev. B* **62**, 4927 (2000)
- [4] C.A. Ullrich, *Time-Dependent Density-Functional Theory: Concepts and Applications* (Oxford University Press, Oxford, 2012)
- [5] A. Ruzsinszky, N.K. Nepal, J.M. Pitarke, J.P. Perdew, Constraint-based wave vector and frequency dependent exchange-correlation kernel of the uniform electron gas, *Phys. Rev. B* **101**, 245135 (2020)

[6] Z.H. Yang, F. Sottile, C. Ullrich, Simple screened exact-exchange approach for excitonic properties in solids, *Phys. Rev. B* **92**, 035202 (2015)

[7] S. Sharma, J.K. Dewhurst, A. Sanna, E.K.U. Gross, Bootstrap approximation for the exchange-correlation kernel of time-dependent density-functional theory, *Phys. Rev. Lett.* **107**, 186401 (2011)

Publications

[1'] B. Neupane, H. Tang, N.K. Nepal, S. Adhikari, A. Ruzsinszky, Opening band gaps of low-dimensional materials at the meta-GGA level of density functional approximations, *Phys. Rev. Materials*, 5, 063803 (2021)

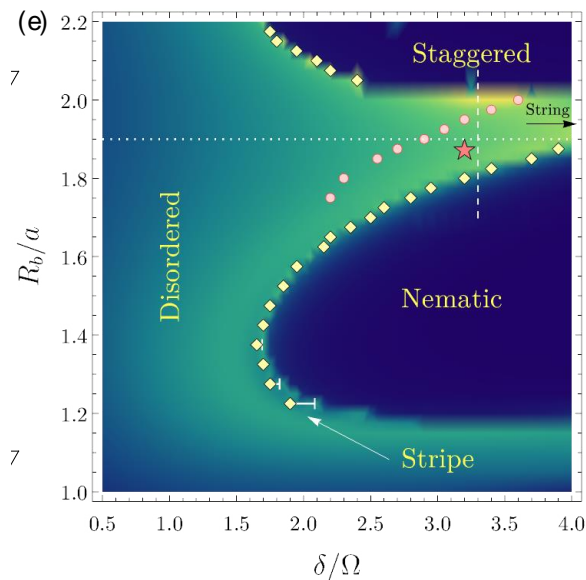
[2'] H. Tang, B. Neupane, S. Neupane, S. Ruan, N.K. Nepal, A. Ruzsinszky, Tunable band gaps and optical absorption properties of bent MoS₂ nanoribbons, submitted, arXiv:2109.04551.

Quantum Simulation of Correlated Quantum Matter

Subir Sachdev, Harvard University

Program Scope

There have been remarkable advances in the experimental study of ultracold atoms trapped in optical tweezer arrays and laser pumped to Rydberg states. The interplay between the Rydberg blockade and the laser pumping leads to a quantum many-body system described by a model of hard-core bosons proposed by the P.I. [1]. We have extended the theoretical study of such models to two-dimensional arrays [2,3] and found rich possibilities for novel quantum phases and phase transitions, many of which have already been explored in experiments by the Lukin group at Harvard [4,5]. On the square lattice [2], we predicted high a complex phase diagram with several density wave order, and an Ising quantum critical point for the onset of checkerboard order. These results have been experimental confirmed [4], along with the first study of the strongly-coupled Ising critical point in 2+1 dimensions. On the kagome lattice [3], along with density-wave orders, we found a novel liquid regime with no observable density-wave order despite a high density of Rydberg excitations. We argued that this regime (denoted by the orange star in the figure) contains one or more Z_2 spin liquid phases, in which the Rydberg excitation operator creates a pair of topological 'vison' excitations (the Z_2 spin liquid is the long-sought gapped resonating valence bond state, containing the same set of topological anyon



excitations as the toric code (which was discovered later)). Evidence for the density wave states, and the spin liquid coherence in a closely related kagome configurations has recently been reported [5]. It is clear that a new frontier is opening up in the experimental and theoretical study of quantum many-body states with site-specific probes, and we intend to continue theoretical research to explore this frontier.

Theoretical phase diagram of Rydberg atoms on the kagome lattice, as a function of detuning for different blockade radius R_b

Keywords: Spin liquids, Rydberg atom arrays, strongly-coupled quantum criticality

Recent Progress

In collaboration with the group of Zi-Yang Meng at the University of Hong Kong, we have been numerically studying a variety of quantum dimer models on different lattices. These dimer models are careful truncations of the hard-core boson model [1], and allow exploration of larger system sizes. Such system sizes are needed to distinguish between the rich possibilities for different spin liquid phases, density wave orders, and the disordered phase.

Future Plans

We will explore parton theories of the possible phases of the hard-boson models [1]. Different parton constructions are possible for the same model, and their excitations are related by self-dualities of the spin liquid. We will study these duality relations, and so obtain a better understanding of the topological excitations of the spin liquid, and how to best study them in the experimentally.

References

1. P. Fendley, K. Sengupta, and S. Sachdev, *Physical Review B* **69**, 075106 (2004).
2. Complex density wave orders and quantum phase transitions in a model of square-lattice Rydberg atom arrays, R. Samajdar, Wen Wei Ho, H. Pichler, M. D. Lukin, and S. Sachdev, *Physical Review Letters* **124**, 103601 (2020).
3. Quantum phases of Rydberg atoms on a kagome lattice, R. Samajdar, Wen Wei Ho, H. Pichler, M. D. Lukin, and S. Sachdev, *Proceedings of the National Academy of Sciences* **118**, e2015785118 (2021).
4. Quantum Phases of Matter on a 256-Atom Programmable Quantum Simulator, S. Ebadi, Tout T. Wang, H. Levine, A. Keesling, G. Semeghini, A. Omran, D. Bluvstein, R. Samajdar, H. Pichler, Wen Wei Ho, Soonwon Choi, S. Sachdev, M. Greiner, V. Vuletic, and M. D. Lukin, *Nature* **595**, 227 (2021).
5. Probing Topological Spin Liquids on a Programmable Quantum Simulator, G. Semeghini, H. Levine, A. Keesling, S. Ebadi, Tout T. Wang, D. Bluvstein, R. Verresen, H. Pichler, M. Kalinowski, R. Samajdar, A. Omran, S. Sachdev, A. Vishwanath, M. Greiner, V. Vuletic, M. D. Lukin, arXiv:2104.04119; *Science*, to appear.

Publications

1. Theory of a Planckian metal, A. A. Patel and S. Sachdev, *Physical Review Letters* **123**, 066601 (2019).
2. Complex density wave orders and quantum phase transitions in a model of square-lattice Rydberg atom arrays, R. Samajdar, Wen Wei Ho, H. Pichler, M. D. Lukin, and S. Sachdev, *Physical Review Letters* **124**, 103601 (2020)

3. Notes on the complex Sachdev-Ye-Kitaev model, Yingfei Gu, A. Kitaev, S. Sachdev, and G. Tarnopolsky, *Journal of High Energy Physics* 02 (2020) 157
4. Thermoelectric power of Sachdev-Ye-Kitaev islands: Probing Bekenstein-Hawking entropy in quantum matter experiments, A. Kruchkov, A. A. Patel, Philip Kim, and S. Sachdev, *Physical Review B* **101**, 205148 (2020).
5. Spectral form factors of clean and random quantum Ising chains, Nivedita, H. Shackleton, and S. Sachdev, *Physical Review E* **101**, 042136 (2020).
6. Metal-insulator transition in a random Hubbard model, G. Tarnopolsky, Chenyuan Li, D.G. Joshi, and S. Sachdev, *Physical Review B* **101**, 205106 (2020).
7. Linear in temperature resistivity in the limit of zero temperature from the time reparameterization soft mode, Haoyu Guo, Yingfei Gu, and S. Sachdev, *Annals of Physics* **418**, 168202 (2020).
8. Quantum phases of Rydberg atoms on a kagome lattice, R. Samajdar, Wen Wei Ho, H. Pichler, M. D. Lukin, and S. Sachdev, *Proceedings of the National Academy of Sciences* **118**, e2015785118 (2021).
9. Excitation spectra of quantum matter without quasiparticles I: Sachdev-Ye-Kitaev models, M. Tikhonovskaya, Haoyu Guo, S. Sachdev, and G. Tarnopolsky, *Physical Review B* **103**, 075141 (2020).
10. Quantum Phases of Matter on a 256-Atom Programmable Quantum Simulator, S. Ebadi, Tout T. Wang, H. Levine, A. Keesling, G. Semeghini, A. Omran, D. Bluvstein, R. Samajdar, H. Pichler, Wen Wei Ho, Soonwon Choi, S. Sachdev, M. Greiner, V. Vuletic, and M. D. Lukin, *Nature* **595**, 227 (2021).
11. Excitation spectra of quantum matter without quasiparticles II: random t - J models, M. Tikhonovskaya, Haoyu Guo, S. Sachdev, and G. Tarnopolsky, *Physical Review B* **103**, 075142 (2020)
12. Probing Topological Spin Liquids on a Programmable Quantum Simulator, G. Semeghini, H. Levine, A. Keesling, S. Ebadi, Tout T. Wang, D. Bluvstein, R. Verresen, H. Pichler, M. Kalinowski, R. Samajdar, A. Omran, S. Sachdev, A. Vishwanath, M. Greiner, V. Vuletic, M. D. Lukin, arXiv:2104.04119; *Science*, to appear.
13. Sachdev-Ye-Kitaev Models and Beyond: A Window into Non-Fermi Liquids, D. Chowdhury, A. Georges, O. Parcollet, and S. Sachdev, arXiv:2109.05037, to be submitted to *Reviews of Modern Physics*.

Quantum Simulations of the Interplay of Charge Density Wave, Magnetic, and Pairing Correlations

Richard Scalettar, University of California, Davis

Program Scope

Understanding the competition, and possible cooperation, of different low temperature ordered phases in strongly correlated electron systems is one of the core endeavors of condensed matter physics. The quintessential example is the cuprates, where a Mott insulating Néel phase at half-filling dominates over superconductivity, yet residual antiferromagnetic fluctuations are widely believed to be necessary to provide the ‘pairing glue’ upon doping. The presence of additional charge stripes and nematic patterns provides further richness to the problem. In this extended abstract we describe aspects of recent progress [1] on a new idea in quantum simulation methodology to examine thermal and quantum critical points in such strongly correlated electron models. We also summarize future plans to examine the nature of charge density wave transitions in multi-orbital electron-phonon systems.

Keywords: Quantum Simulations, Magnetism, Exotic Superconductivity

Recent Progress

The “sign problem” (SP)[2] is the fundamental limitation to simulations of strongly correlated materials in nuclear matter[3], quantum chemistry[4], condensed matter physics[5], and quantum chromodynamics[6]. We have recently shown that the SP in determinant quantum Monte Carlo (DQMC) is quantitatively linked to quantum critical behavior in several fundamental models of condensed matter physics, including the spinful and spinless Hubbard Hamiltonians on a honeycomb lattice and the ionic Hubbard Hamiltonian, both of whose critical properties are relatively well understood. We then proposed a reinterpretation of the low average sign for the Hubbard model on the square lattice when away from half-filling, an important open problem in condensed matter physics, in terms of the onset of pseudogap behavior and exotic superconductivity. Here we will focus just on the first case: the semimetal to antiferromagnetic Mott insulator (AFMI) of Dirac fermions in the honeycomb-Hubbard model. However, as our work in [1] demonstrates, our new approach charts a path for exploiting the average sign in QMC simulations to understand a broad variety of quantum critical behavior.

We examine the SP within the context of one of the most powerful and general quantum simulation approaches- Auxiliary Field Quantum Monte Carlo (AFQMC). In AFQMC, the trace over fermionic degrees of freedom is done for all species (i.e. all spin and orbital indices α). If there is no hybridization between different α , each trace gives an individual determinant. In some situations, particle-hole, time-reversal, or other symmetries impose a relation between the determinants for different α , and as a consequence the negative determinants always come in pairs. Low temperature (ground-state) properties can be accessed in such ‘sign problem free’ cases. If such a partnering does not occur, a reasonable rule of thumb is that the average sign $\langle \mathcal{S} \rangle$ is sufficiently bounded away from zero with measurements that exhibit sufficiently small error bars for $T \gtrsim W/20 - W/40$, at intermediate interaction strengths. The

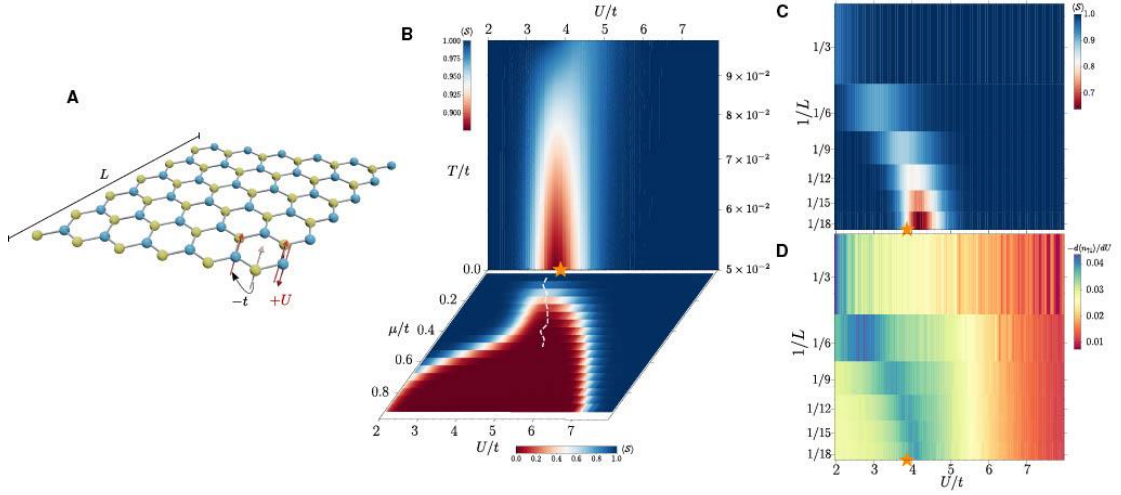


Figure 1. **The SU(2) Hubbard model on the honeycomb lattice.** (A) Cartoon depicting a honeycomb lattice with $N = 2L^2$ sites ($L = 6$ here), accompanied by the relevant terms in \hat{H} . (B) Contour plot of the average $\langle \mathcal{S} \rangle$ in the $T/t(\mu/t)$ vs U/t in the upper (lower) panel. Here $L = 9$ and $\mu/t = 0.1$ ($T/t = 1/20$) in the upper (lower) panel. (C) The average sign extrapolated with the linear system size L , using $T/t = 1/20$ and $\mu/t = 0.1$. (D) Similar extrapolation as in C, but displaying a local quantity (the derivative of the double occupancy), which is an indicator of the QCP. In all panels with data, the prediction for the ground-state phase transition occurring at $U_c/t = 3.869$ [7] is depicted by a star marker.

DQMC methodology [8] we use here is a specific implementation of AFQMC.

We describe results [1] for the Hubbard Hamiltonian,

$$\hat{H} = - \sum_{\langle ij \rangle \sigma} t_{ij} (\hat{c}_{i\sigma}^\dagger \hat{c}_{j\sigma} + \hat{c}_{j\sigma}^\dagger \hat{c}_{i\sigma}) - \sum_{i\sigma} \mu_i \hat{n}_{i\sigma} + U \sum_i (\hat{n}_{i\uparrow} - \frac{1}{2})(\hat{n}_{i\downarrow} - \frac{1}{2})$$

We provide detailed results when $\langle i, j \rangle$ are near-neighbor sites on a honeycomb lattice, with $t_{ij} = t$. In such a geometry (Fig. 1A), the $U = 0$ Hubbard Hamiltonian has a semi-metallic density of states which vanishes linearly at $E = 0$. Its dispersion relation $E(\mathbf{k})$ has Dirac points in the vicinity of which the kinetic energy varies linearly with momentum. Unlike the square lattice that displays AF order for all $U \neq 0$, the honeycomb Hubbard model at $T \rightarrow 0$ remains a semimetal for small nonzero U , turning to an AF insulator only for U exceeding a critical U_c [7]. The upper panel of Fig. 1B gives $\langle \mathcal{S} \rangle$ in the $U - T$ plane. By introducing a small non-zero $\mu = 0.1$, we can induce a SP which begins to develop at $T/t \sim 0.1$. As T is lowered further the average sign deviates from $\langle \mathcal{S} \rangle = 1$ in a relatively narrow window of U/t close to the known U_c . We show $\langle \mathcal{S} \rangle$ on the $U - \mu$ plane at fixed $T/t = 0.05$ in the lower panel of Fig. 1B. For large μ the sign is small for a broad swath of interaction values. As μ decreases this region pinches down until it terminates close to U_c ; the dashed white line displays the minimum $\langle \mathcal{S} \rangle$ in the relevant range. In both panels, the behavior of the average sign outlines the quantum critical fan that extends above the QCP.

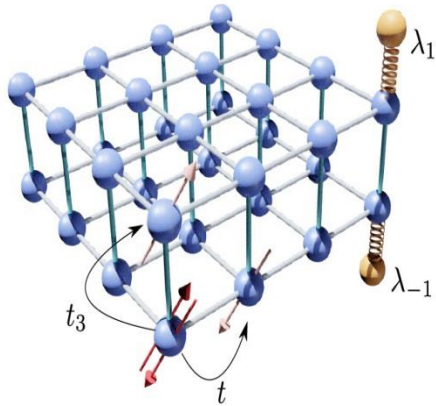


Figure 2. Sketch of a Holstein Hamiltonian with intralayer hopping t and interlayer hopping t_3 between sheets $l = +1$ and $l = -1$. The coupling λ to the phonon degrees of freedom λ_l is only drawn in a pair of sites for clarity, but is present at every site. We will consider cases when $\lambda_{+1} \neq \lambda_{-1}$

Figure 1C shows a finite size extrapolation of $\langle \mathcal{S} \rangle$ in the $1/L - U$ plane, where L is the linear lattice size. Just as $\langle \mathcal{S} \rangle$ worsens with increasing β , it is also known to deviate increasingly from $\langle \mathcal{S} \rangle = 1$ with growing L . What these data further indicate is that the extrapolation $L \rightarrow \infty$ clearly reveals U_c in the presence of a small chemical potential. For comparison to the evolution of $\langle \mathcal{S} \rangle$, Fig. 1D shows one example, the rate of change of the double occupancy D , again in the $1/L - U$ plane. A peak in $-dD/dU$ indicates where local moments $\langle m^2 \rangle$ are growing most rapidly. The similarity between Figs. 1C and 1D emphasizes how $\langle \mathcal{S} \rangle$ is tracking the physics of the model in a way remarkably similar to $\langle m^2 \rangle$.

We have described here only the first of several situations in which we have been able to quantify a connection between critical behavior and the sign problem. We have also demonstrated that the average sign undergoes an abrupt drop at the band-insulator to antiferromagnetic insulator transition, at a semimetal to charge insulator transition, and that it also may yield insight into the strange metal/d-wave pairing phase of the square lattice Hubbard model [1].

Future Plans

Much attention has been focused in the condensed matter community over the last several decades on layered materials, cuprate superconductors [9] and bilayer graphene [10] being prominent examples. From a theoretical perspective, bilayer materials offer an opportunity to explore the competition between the formation of long range order at weak interlayer coupling and collections of independent local degrees of freedom in the limit of strong interlayer coupling. Computational studies have lent considerable insight into these phenomena, including quantitative values for the quantum critical points [11] separating antiferromagnetic and singlet phases at zero temperature.

Our future plans include investigations of analogous questions concerning bilayer (multi-orbital) systems in which the fermions interact with phonon degrees of freedom rather than via direct electron-electron correlations. We will use DQMC simulations of the multi-band Holstein model (Fig. 2) at half-filling. We plan to address whether interband hybridization t_3 can destroy CDW order and, if so, the quantitative value of the associated quantum critical point; the value of the critical temperature T_c at any thermal transitions; and, in a situation where the

electron-phonon energy scales in the two bands are very different, can CDW order in one band coexist with metallic behavior in the other?

References

- [1] R. Mondaini, S. Tarat, and R. T. Scalettar, Quantum critical points and the sign problem, arXiv preprint arXiv:2108.08974 (2021).
- [2] M. Troyer and U.-J. Wiese, Computational complexity and fundamental limitations to fermionic quantum Monte Carlo simulations, *Phys. Rev. Lett.* 94, 170201 (2005).
- [3] J. Carlson, S. Gandolfi, F. Pederiva, S. C. Pieper, R. Schiavilla, K. Schmidt, and R. Wiringa, Quantum Monte Carlo methods for nuclear physics, *Rev. Mod. Phys.* 87, 1067 (2015).
- [4] R. Needs, M. Towler, N. Drummond, P. López Ríos, and J. Trail, Variational and diffusion quantum Monte Carlo calculations with the CASINO code, *J. Chem. Phys.* 152, 154106 (2020).
- [5] W. Foulkes, L. Mitas, R. Needs, and G. Rajagopal, Quantum Monte Carlo simulations of solids, *Rev. Mod. Phys.* 73, 33 (2001).
- [6] T. Degrand and C. DeTar, *Lattice Methods for Quantum Chromodynamics* (World Scientific, 2006).
- [7] S. Sorella, Y. Otsuka, and S. Yunoki, Absence of a spin liquid phase in the Hubbard model on the honeycomb lattice, *Sci. Rep.* 2, 992 (2012).
- [8] R. Blankenbecler, D. Scalapino, and R. Sugar, Monte Carlo calculations of coupled boson-fermion systems. I, *Phys. Rev. D* 24, 2278 (1981).
- [9] M. Vojta, Lattice symmetry breaking in cuprate superconductors: stripes, nematics, and superconductivity, *Advances in Physics* 58, 699 (2009).
- [10] E. McCann and M. Koshino, The electronic properties of bilayer graphene, *Rep. Prog. Phys.* 76, 056503 (2013).
- [11] A. W. Sandvik and D. J. Scalapino, Order-disorder transition in a two-layer quantum antiferromagnet, *Phys. Rev. Lett.* 72, 2777 (1994).

Publications Acknowledging DOE DE-SC0014671

1. “Self-Organized Bosonic Domain Walls”, X. Zhu, S. Dong, Y. Lin, R. Mondaini, H. Guo, S. Feng, and R.T. Scalettar, Phys. Rev. R2, 013085 (2020).
2. “Charge Density Waves on a half-filled Decorated Honeycomb Lattice”, C. Feng, H.M. Guo, and R.T. Scalettar, Phys. Rev. B101, 205103 (2020).
3. “Charge Density Wave and Superconductivity in the Disordered Holstein Model”, B. Xiao, N.C. Costa, E. Khatami, G.G. Batrouni, and R.T. Scalettar, Phys. Rev. B103, L060501(2020).
4. “Dynamical resilience to disorder: the dilute Hubbard model on the Lieb lattice”, L. Oliveira-Lima, N.C. Costa, J. Pimentel de Lima, R.T. Scalettar, and R.R. dos Santos, Phys. Rev. B101, 165109 (2020).
5. “Charge-Density Wave Order on a π -flux Square Lattice”, Y. Zhang, H. Guo, and R.T. Scalettar, Phys. Rev. B101, 205139 (2020).
6. “Visualizing strange metallic correlations in the two-dimensional Fermi-Hubbard model with artificial intelligence”, E. Khatami, E. Guardado-Sanshez, B.M. Spar, J.F. Carrasquilla, W.S. Bakr, and R.T. Scalettar, Phys. Rev. A102, 033326 (2020).
7. “Hybridization effect on the X-ray absorption spectra for actinide materials: Application to PuB_4 ”, W-T. Chiu, R.M. Tutchton, G. Resta, T-H. Lee, E.D. Bauer, F. Ronning, R.T. Scalettar, and J-X. Zhu, Phys. Rev. B102, 085150 (2020).
8. “Langevin Simulations of the Half-Filled Cubic Holstein Model”, B. Cohen-Stead, K. Barros, Z.Y. Meng, C. Chen, and R.T. Scalettar, Phys. Rev. B102, 161108(R) (2020).
9. “Quantum Monte Carlo Simulations of the 2D Su-Schrieffer-Heeger Model”, B. Xing, W-T. Chiu, D. Poletti, R.T. Scalettar, and G.G. Batrouni, Phys. Rev. Lett. 126, 017601(2020).
10. “Magnetoresistance effects in a spin-fermion model for multilayers,” S. Tarat, J. Li, R.T. Scalettar, and R. Mondaini, Phys. Rev. B102, 094423 (2020).
11. “Thermodynamics and magnetism in the 2D-3D crossover of the Hubbard model,” E. Ibarra-García-Padilla, R. Mukherjee, R.G. Hulet, K.R.A. Hazzard, T. Paiva, R.T. Scalettar, Phys. Rev. A102, 033340 (2020).
12. “Antiferromagnetic transitions of Dirac fermions in three dimensions,” Y. Huang, H. Guo, J. Maciejko, R.T. Scalettar, and S. Feng, Phys. Rev. B102, 155152 (2020).
13. “Interplay of Flat Electronic Bands with Holstein Phonons”, C. Feng and R.T. Scalettar, Phys. Rev. B102, 235152 (2020).
14. “Superconductivity and charge density wave order in the 2D Holstein model”, O. Bradley, G.G. Batrouni, and R.T. Scalettar, Phys. Rev. B103, 235104 (2021).
15. “Quantum Monte Carlo study of an anharmonic Holstein model”, G. Paleari, F. Hébert, B. Cohen-Stead, K. Barros, R. Scalettar, and G. Batrouni Phys. Rev. B103, 195117 (2021).
16. “Magnetic properties of alternating Hubbard ladders” K. Essalah, A. Benali, A. Abdelwahab, E. Jeckelmann, and R.T. Scalettar, Phys. Rev. B103, 165127 (2021).

Holographic quantum simulation of strongly correlated electron systems

Shyam Shankar, University of Texas at Austin (Principal Investigator)

Andrew Potter, University of Texas at Austin (Co-Investigator)

Program Scope

Predicting the ground-state, low-energy excitations, and dynamical response of correlated electronic and magnetic systems are central tasks for computational materials science. Unfortunately, exact classical numerical computation is infeasible even for simplified models, and approximation methods do not produce accurate results for many problems. Quantum computers promise to be able to perform accurate materials simulation at significantly reduced computational cost. However, standard quantum simulation algorithms for implementing these tasks require thousands of qubits with high-fidelity control to outperform classical computers, which is out of reach for near-term quantum hardware [1].

In this project, we will develop new “holographic” quantum simulation algorithms and co-designed superconducting quantum processors and apply them to various problems related to understanding the physics of strongly correlated electron systems. Our goal is to show that this co-designed hardware and software can demonstrate quantum advantage over classical simulations by efficiently using the resources of moderate-size, noisy quantum processors. Holographic simulation [2] uses a compressed quantum tensor network state (qTNS) representation along with mid-circuit measurement and qubit reuse to encode the quantum state of the material using far fewer qubits than quantum degrees of freedom in the material. The qTNS representation thus greatly reduces the barrier to building quantum hardware that can solve scientific and technologically important problems, by allowing small scale quantum processors to simulate large scale complex material models. qTNS methods are also expected to reduce the impact of noise and errors – key obstacles to performing precise calculations with existing hardware. Whereas early demonstrations of holographic qTNS methods relied on qubit arrays [2–4], we will achieve a substantial increase in hardware efficiency by using a circuit quantum electrodynamics (cQED) system [5] with an array of superconducting cavities to act as multi-level memory “qudits” coupled to a small number of “processor” superconducting qubits. This co-designed approach should result in quantum advantage with far fewer physical devices than qubit-only platforms running traditional quantum simulation algorithms.

We will apply our algorithms and hardware to three specific simulation tasks that fall within the broad umbrella of unraveling the physics of strongly correlated electron systems (SCES): (1) holographic preparation of ground- and thermal- states of correlated magnetic and electronic systems including quasi-2d frustrated-spin, Fermi-Hubbard, and fractional quantum Hall (FQH) systems, (2) holographic-simulation of long-time out-of-equilibrium dynamics, and (3) holographic analogs of embedding methods such as dynamical mean-field theory (DMFT) and density-matrix embedding theory (DMET) to solve systems with complex structure or long-range

interactions. These tasks are prototypes for the kinds of material simulation problems, such as the simulation of multiferroic materials, perovskite photovoltaics and high-temperature superconductors, that tax the capabilities of the most powerful classical supercomputers. Our work will substantially reduce the size and fidelity requirements for quantum simulation of realistic materials and devices, bringing practical quantum material simulations closer to the capabilities of near-term hardware.

Keywords: Quantum simulation, superconducting quantum circuits, tensor network methods

Recent Progress

On the experimental side, we have designed an initial prototype of a superconducting quantum processor, described in Fig. 1, consisting of a 3-dimensional coaxial cavity machined from ultra-high-purity aluminum, into which is placed a sapphire chip with a lithographically defined transmon qubit. The cavity acts as the quantum memory for storing the holographically encoded qTNS, while the transmon acts as the processor qubit in the holographic simulation. We have conducted simulations using commercial electromagnetic solvers and open-source quantum circuit solvers to extract relevant Hamiltonian parameters of the processor such as the dispersive shift between the transmon and the cavity. The designed dispersive shift of ~ 2 MHz sets the time-scale for qubit-cavity unitary operations. We have also designed nearly-quantum-limited microwave amplifiers which are crucial for fast, high-fidelity readout of the processor qubit.

On the theoretical side, we have constructed a classical simulation framework to simulate the operation of a single qubit-cavity pair. Early investigations show that quantum optimal control techniques [6] can be used effectively construct control wave-forms to synthesize complex quantum states of correlated electron and spin systems in qTNS form using experimentally realistic capabilities. The ability to prepare a classically-constructed qTNS approximation to a correlated-electronic state will serve as an important stepping stone to “seed” the variational optimization of highly-entangled states beyond classical reach, or to prepare correlated initial states for quantum dynamics simulations (which quickly generate highly-

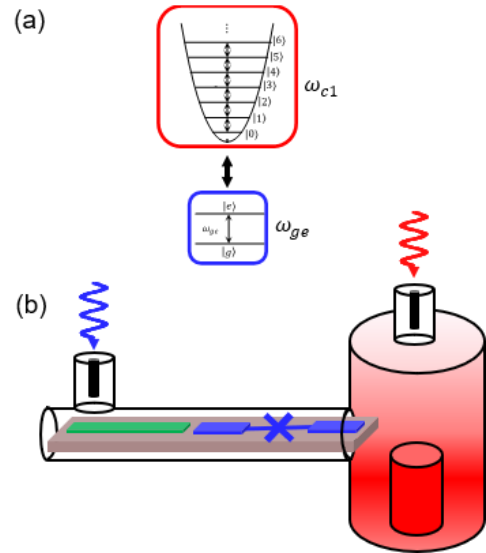


Fig. 1 Initial prototype of superconducting quantum processor (a) Energy levels of a harmonic oscillator (red) coupled to a single transmon qubit (dark blue). The lowest $D \sim 10$ levels of oscillator store the bond-space of the holographically encoded qTNS, while the transmon acts as the processor qubit (b) Schematic of physical implementation. A coaxial post cavity (red), realizes the oscillator mode with frequency, ω_{c1} . A transmon qubit (frequency ω_{ge} , dark blue) and auxiliary readout resonator (dark green) are lithographically defined on a sapphire chip and coupled to one end of the post cavity. Drives are applied to coaxial ports to control the state of the qubit and oscillator.

entangled states beyond reach of classical computers, even when the starting quantum state is only moderately entangled).

Future Plans

Our short-term experimental research goal is to fabricate and characterize the 1-transmon/1-cavity device referred above. We hope to achieve long coherence times ($T_2 > 10 \mu\text{s}$ for the transmon, $T_1 > 100\mu\text{s}$ for the cavity), and correspondingly high gate fidelity ($> 99\%$ for the transmon, $> 90\%$ for the cavity) and measurement fidelity ($\sim 99\%$).

In parallel we will continue to develop simulation capabilities to model realistic methods of noise and open-systems dynamics, to critically assess their impact on planned experimental demonstrations. Further, we plan to scale the classical simulations to tackle multiple cavity modes, and to integrate our cQED simulation framework with state-of-the-art classical tensor network software tools in order to facilitate exploration of new holographic qTNS algorithmic capabilities for variationally preparing ground- and thermal states of correlated electronic systems and simulating non-equilibrium dynamics. A key goal will be to identify optimization heuristics that can be successfully scaled to control a complex quantum processor with multiple interacting qubits and cavities.

Once we have completed initial characterization of the quantum hardware, we plan to demonstrate holographic preparation of the fractional quantum Hall state of a system of interacting electrons in a strong magnetic field. We will benchmark the state fidelity against exact solutions.

References

- [1] S. McArdle, S. Endo, A. Aspuru-Guzik, S. C. Benjamin, and X. Yuan, *Quantum Computational Chemistry*, Rev. Mod. Phys. **92**, 015003 (2020).
- [2] M. Foss-Feig, D. Hayes, J. M. Dreiling, C. Figgatt, J. P. Gaebler, S. A. Moses, J. M. Pino, and A. C. Potter, *Holographic Quantum Algorithms for Simulating Correlated Spin Systems*, Phys. Rev. Research **3**, 033002 (2021).
- [3] M. Foss-Feig, S. Ragole, A. Potter, J. Dreiling, C. Figgatt, J. Gaebler, A. Hall, S. Moses, J. Pino, B. Spaun, B. Neyenhuis, and D. Hayes, *Entanglement from Tensor Networks on a Trapped-Ion QCCD Quantum Computer*, ArXiv:2104.11235 [Cond-Mat, Physics:Quant-Ph] (2021).

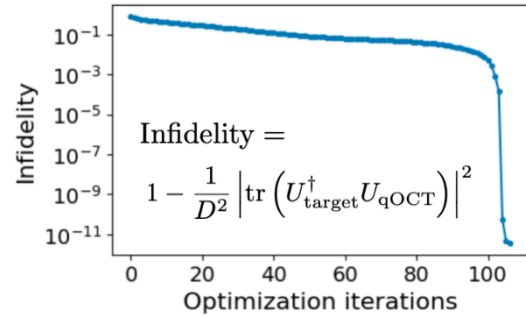


Fig. 2 Classical simulation results. Demonstration of quantum optimal control techniques to synthesize control wave-forms for qubit and cavity drives that implement a desired target unitary operation U_{target} , U_{target} represents a tensor of a TNS representation of a correlated electron state. Shown here, is the convergence of the synthesized unitary U_{qOCT} to the target one with number of optimization iterations, for the preparation of a tensor for a Laughlin fractional quantum Hall wave-function of interacting electrons in a strong magnetic field. The simulation was conducted on a cylindrical geometry, using a single qubit-cavity pair, and operating $D=10$ levels of the cavity mode.

- [4] E. Chertkov, J. Bohnet, D. Francois, J. Gaebler, D. Gresh, A. Hankin, K. Lee, R. Tobey, D. Hayes, B. Neyenhuis, R. Stutz, A. C. Potter, and M. Foss-Feig, *Holographic Dynamics Simulations with a Trapped Ion Quantum Computer*, ArXiv:2105.09324 [Cond-Mat, Physics:Quant-Ph] (2021).
- [5] A. Blais, S. M. Girvin, and W. D. Oliver, *Quantum Information Processing and Quantum Optics with Circuit Quantum Electrodynamics*, Nature Physics **16**, 3 (2020).
- [6] R. W. Heeres, P. Reinhold, N. Ofek, L. Frunzio, L. Jiang, M. H. Devoret, and R. J. Schoelkopf, *Implementing a Universal Gate Set on a Logical Qubit Encoded in an Oscillator*, Nature Communications **8**, 1 (2017).

Publications

None

First-Principles Understanding of Optical Excitations within Low-Dimensional Materials

PI: Sahar Sharifzadeh

Department of Electrical & Computer Engineering, Boston University, Boston, MA 02215

Keywords: two-dimensional materials; excitons; defects in two-dimensional semiconductors

Project Scope

The objective of this project is to utilize first-principles computational approaches to understand optical excitations within two-dimensional monolayers and heterostructures, with the ultimate goal of designing new materials by modifying the chemical and physical structure on the nanoscale. In 2D heterostructures, the nature and movement of the exciton is determined to a large extent by the electron-electron and electron-phonon strengths within individual monolayers, as well as the coupling between layers, all of which in turn depend on chemistry, solid-state screening properties, and quantum confinement. Controlling the nature and migration properties of excitons requires an understanding of the complex relationship between electrons, phonons, defects, disorder, and dynamics. The aim of this project is to determine, by analysis of highly accurate density functional theory (DFT) and many-body perturbation theory (MBPT) calculations, how these complexities can be decomposed into simple, tunable parameters.

The specific goals of this project are to 1) understand electron conductivity, absorption and transparency of monolayer semiconductors and metals; 2) develop a theory of excitons near defects in low dimensions, including the role of phonons; and 3) understand the influence of inter-layer interactions in multi-layer materials and heterostructures.

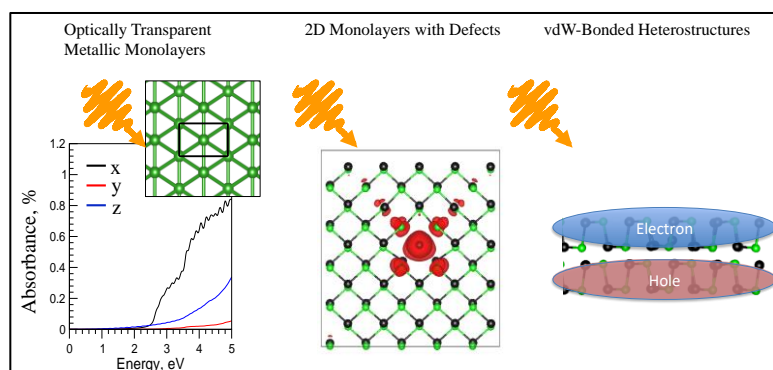


Figure 1: A schematic of the Project Scope. Left: electron-phonon and electron-electron interactions within monolayer boron; approximated structure (right) and calculated absorption (left) are shown. Center: excitonic effects in the presence of defects; an excited state within monolayer semiconductor GeSe with the introduction of a single Se vacancy is shown. Right: Intralayer interactions and charge-transfer excitations within 2D heterostructures.

Recent Progress

I. Localized excitons near defects in bulk and monolayer semiconductors

Point defects can be present naturally in semiconductors or can be introduced intentionally to achieve desired properties [1]. In order to mitigate the deleterious effects of point defects and control the desired properties, it is necessary to understand the relationship between the individual defect and its structural and electronic impact on a specific material. We have studied the influence of point defects on the excitonic properties of bulk GaN, a technologically important light emitting material [2]; and 2D GeSe, a promising monolayer material for optoelectronics [3].

Point defects in Bulk GaN: We performed time-dependent density functional theory (TDDFT) calculations of pristine and with-defect GaN using a promising optimally tuned hybrid (OT-RSH) functional that has been shown to produce GW/BSE quality results for pristine semiconductors but had not been applied to defective systems previously. We determined that (TD) OT-RSH was able to reproduce MBPT within the GW/BSE approximation. Moreover, given the reduced computational cost associated with this method, we were able to study a series of defects relevant to the well-known yellow luminescence problem within GaN. We determined that the carbon interstitial is a potential candidate for yellow luminescence, in agreement with recent measurements (see Figure 2) [10]. We are now investigating the optical properties to probe whether Cr can be a color center defect in GaN [Mansouri, Lewis, Sharifzadeh, in preparation].

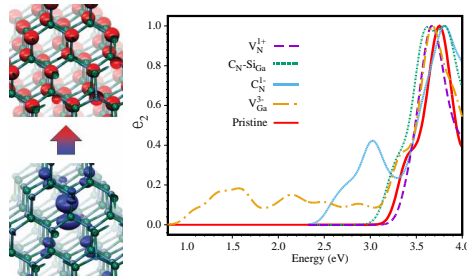


Figure 2: The optical absorption spectrum of likely defects in bulk GaN as calculated by TD-RSH. The top shows an example of a defect to bulk transition from the C substitutional defect. Figure from Ref. 10.

Point defects in monolayer Germanium Selenide (GeSe): GeSe, a van der Waals-bonded layered semiconductor with promising optoelectronic applications, including photosensing and photocatalysis [3]. We first developed an a technique to extract the Bohr radius from GW/BSE and quantify localization of the Wannier-Mott exciton in the presence of the defect [8]. We applied this approach to GeSe with selenium vacancy in the -2 charge state in order to understand exciton localization. We found that the vacancy induces in-gap “trap states” that strongly localize the electron and hole density and result in a sharp optical absorption peak below the predicted pristine optical gap. Analysis of the exciton wavefunction envelope function indicated that the presence of the defect also results in a localized exciton wavefunction, with a Bohr radius of 0.5 nm, a factor of four smaller than the Bohr radius of pristine GeSe. These results demonstrate the strong perturbation of electronic properties due to defects, indicating that defects should be considered in the context of material design [11].

II. Electron-phonon interactions in 2D and layered materials

Exciton-phonon interactions in monolayer GeSe: We studied the optical absorption and excitonic properties of monolayer GeSe in the presence of phonons within GW/BSE coupled to the special displacement method [6], which approximates the role of finite-temperature phonons via an independent particle approximation. We determined that the optical gap is reduced and the exciton wavefunction is distorted at room temperature due to the presence of optical phonons at energies near 100 cm^{-1} . This work demonstrated that the combination of many-body perturbation theory and special displacements offers a new, computationally tractable route to investigate electron-phonon couplings in excitonic spectra, band gap renormalization, and the nature of phonons that couple to the exciton [14].

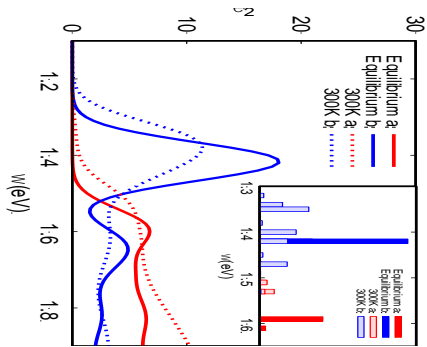
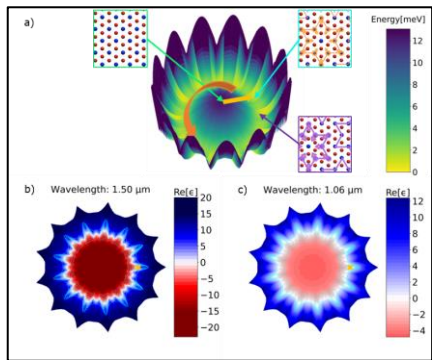


Figure 3: Imaginary component of the dielectric function calculated within GW/BSE for monolayer GeSe at $T = 0 \text{ K}$ with no zero-point motion (labeled as equilibrium) and at $T = 300 \text{ K}$, for light polarized along the a (zigzag) and b (armchair) direction. The inset shows the square of the transition dipole moment for both polarization directions at equilibrium and $T = 300 \text{ K}$. Figure from Ref. 14.

Light-induced dynamical phase transition in 1T-TaS₂: For 1T-TaS₂, a commensurate charge density wave layered material, the presence of light can lead to a transient displacement of atoms from the low-symmetry insulating to the high-symmetry metallic phase [7]. In our study, we applied (time-dependent) density functional theory and the nudged elastic band method to describe the potential energy surface and dielectric constant associated with atomic displacement along the order parameters of the phase transition. Specifically, our method maps the dielectric properties along the Higgs and Goldstone modes associated with the charge density wave (see Figure 4). We show that small displacements of atoms lead to a large change in the dielectric constant along the Higgs coordinate, resulting in large optomechanical coupling. Additionally, we derived a classical model to describe the light-induced dynamics in this material, and examined the possibility of using near- and mid-infrared illumination to generate regular orbits of the material internal

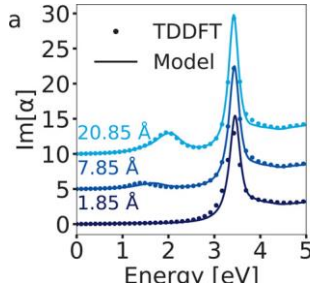


coordinates along regions of large dielectric contrast. Using this model, we predict that the non-linear optical response of charge density wave materials can be deterministically controlled by illumination protocols [16].

Figure 4: a) Total energy of 1T-TaS₂ with respect to the Higgs and Goldstone coordinates. The range of displacement along the radial coordinate is 1.30 \AA and the energy is indicated per TaS₂. b) and c) show the corresponding real part of the in-plane dielectric function at two different excitation wavelengths. Figure from Ref. 16.

III. Microscopy theory of plasmons on substrate-supported borophene

We have calculated the plasmonic properties of two-dimensional boron (borophene), a metallic monolayer material, on and near metallic substrates using linear response time-dependent DFT. By simulating borophene-on-substrate systems for a range of borophene-substrate distances, we determined that at equilibrium the borophene plasmons are quenched due to the large polarizability of the substrate but that the borophene plasmons can be recovered as the distance with the substrate



is increased. Furthermore, we developed a simple electrodynamic, one-parameter model that describes the plasmonic interactions between any bulk substrate and 2D plasmonic material with a single fitting parameter. This insight into the borophene-substrate system allowed us to develop a model that can be applied to a general 2D-substrate plasmonic systems [9].

Figure 5: The coupled response of borophene on silver at various separations from TDDFT calculations of the total system (dots) and from a classical model (lines). The distance shown is with respect to the metal image plane (d_z). Figure from Ref. 9.

Future Plans

Our studies have demonstrated that the use of state-of-the-art computational tools combined with analysis techniques developed by us, including first-principles-informed semiclassical models, allow for a new understanding of electronic excitations in 2D and layered materials. In the future, we will additionally incorporate the role of spins for the study of magnetic MXene materials such as the antiferromagnetic layered material, NiPS3 [14], and will continue to apply the developed approach to a more diverse set of monolayers, bilayers, and bulk van der Waals bonded materials.

References

1. Queisser and Haller, “Defects in Semiconductors: Some Fatal, Some Vital” *Science* **281** 5379 (1998)
2. M. a. Reshchikov and H. Morkoc, “Luminescence properties of defects in GaN” *J. Appl. Phys.* **97**, 061301 (2005).
3. X. Lv, W. Wei, Q. Sun, F. Li, B. Huang, and Y. Dai, “Two dimensional germanium monochalcogenides for photocatalytic water splitting with high carrier mobility,” *Appl. Catal., B* **217**, 275 (2017).
4. F. Zimmermann, G. Gartner, H. Strater, C. Roder, M. Barchuk, D. Bastin, P. Hofmann, M. Krupinski, T. Mikolajick, J. Heitmann, and F.C. Beyer, “Green coloring of gan single crystals introduced by cr impurity,” *Journal of Luminescence*, **207** 507 (2019).
5. W.F. Koehl, B. Diler, S.J. Whiteley, A. Bourassa, N.T. Son, E. Janzén, and D.D. Awschalom, “Resonant optical spectroscopy and coherent control of Cr⁴⁺ spin ensembles in SiC and GaN” *Phys. Rev. B* **95**, 035207 (2017).
6. M. Zacharias and F. Giustino, “Theory of the special displacement method for electronic structure calculations at finite temperature,” *Phys. Rev. Research* **2**, 013357 (2020).
7. M. Eichberger, H. Schäfer, M. Krumova, *et al.*, “Snapshots of cooperative atomic motions in the optical suppression of charge density waves,” *Nature* **468**, 799 (2010).

Publications (October 2019 – October 2021)

8. D.K. Lewis and S. Sharifzadeh, “Defect-Induced Exciton Localization in Bulk Gallium Nitride from Many-Body Perturbation Theory,” *Physical Review Materials* **3**, 114601 (2019).
9. A. Haldar, C.L. Cortes, P. Darancet, and S. Sharifzadeh, “Microscopic Theory of Plasmons in Substrate-Supported Borophene,” *Nano Letters* **20**, 2986 (2020).
10. D.K. Lewis, A. Ramasubramaniam, S. Sharifzadeh, “Tuned and Screened Range-Separated Hybrid Density Functional Theory for Describing Electronic and Optical Properties of Defective Gallium Nitride,” *Physical Review Materials* **4**, 063803 (2020).
11. A. Cohen, D. K. Lewis, T. Huang, S. Sharifzadeh, “Localized Excitons in Defective Monolayer Germanium Selenide,” *Physical Review Materials* **4**, 076002 (2020).
12. M. Alaghemandi, L. Salehi, P. Samolis, B.T. Trachtenberg, A. Turnali, M.Y. Sander, and S. Sharifzadeh, “Atomic Understanding of Structural Deformations upon Ablation of Graphene,” *Nano Select*, **1** (2021).
13. X. Wang, J. Cao, Z. Lu, A. Cohen, H. Kitadai, T. Li, M. Wilson, C. Hung Lui, D. Smirnov, S. Sharifzadeh, and X. Ling, “Spin-Induced Linear Polarization of Excitonic Emission in Antiferromagnetic van der Waals Crystals,” *Nature Materials* **20** 964 (2021).
14. T.A. Huang, M. Zacharias, D.K. Lewis, F. Giustino, and S. Sharifzadeh, “Exciton-Phonon Interactions in Monolayer Germanium Selenide from First-Principles,” *J. Physical Chemistry Letters* **12**, 3802 (2021).
15. D.K. Lewis and S. Sharifzadeh, “Modeling Excited-States of Point Defects in Materials from Many-body Perturbation Theory,” *ACS Materials Letters* (Review article) **3**, 862 (2021).
16. A. Haldar, C.L. Cortes, S.K Gray, S. Sharifzadeh, P.T. Darancet, “Giant Optomechanical Coupling in the Charge Density Wave State of Tantalum Disulfide,” under revision (arXiv:2105.08874v2).

Theoretical studies in very strongly correlated matter

B Sriram Shastry, Physics Department, UCSC, Santa Cruz, CA 95064

Program Scope

This abstract describes two recent projects calculating (a) The normal state resistivity of the single-layer hole or electron doped cuprate superconductors [P-3] and (b) the emergence of the superconducting state in the 2-d single layer t-J model [P-1]. The basic methodology for these calculations is the extremely correlated fermi liquid (ECFL) theory developed for this purpose [1,2]. The ECFL theory has been earlier benchmarked successfully against existing methods for strong coupling problems.

Keywords: (I) Analytical solutions for strong coupling models (II) T- dependent resistivity in cuprates (III) The mechanism of superconductivity in cuprates

Recent Progress

Resistivity of single layer cuprates: In the paper [P-3] the resistivity of the 2-d t-J model describing single layer cuprates is calculated using the extremely correlated fermi liquid theory. The resistivity of the cuprates and other strongly correlated systems has been the subject of intense research in the last two decades. The main characteristics of these works is that the resistivity in the a-b plane is 2-5 orders of magnitude less than that along the c-axis, and the T dependence of resistivity is almost linear above the superconducting transition temperature. Of particular interest is the detailed and systematic study of the resistivity over a large range of densities and T, on single layer cuprates LSCO, BSLCO [3] and NCCO [4]. These display quasi-linear (for hole doped), and quadratic (for electron doped) T dependences, and our goal is to see whether theory can reproduce the observed complexity of data. Our theory has a small quasiparticle weight Z and a low effective Fermi temperature scale, so that one expects a quadratic in T resistivity at very low T, followed by other regimes. This is unlike a class of competing non-fermi liquid type theories, where the resistivity is linear over the entire T range. It is of great interest to see which of the two types of theories are supported by the data sets, since interpreting resistivity data over limited ranges of T (or density) can be quite misleading. For example the body of data [3] shows a variety of T dependences, for different ranges of density and temperature.

The ECFL theory gives quite accurate spectral functions of electrons in the t-J model in 2-dimensions at any density and T as functions of the parameters of the model, which are taken to be the nearest neighbor hopping t, the next nearest hopping t', and the exchange energy J. A weak momentum dependence of the self energy in our calculations can be used to justify the simplest version of Kubo's formula, which combines two spectral functions to give the

resistivity. With hopping parameter ratio t'/t given by the photoemission determined shape of the Fermi surface, and exchange J given from insulating state Raman studies, the theoretical resistivity is calculated in terms of a dimensionless resistivity $\bar{\rho}$ which is a function of the displayed dimensionless variables $\rho = R_{vK} c_0 \bar{\rho}(t'/t, J/t, kT/t, \delta)$, where c_0 is the measured separation between two layers, $R_{vK} = 25813\Omega$, and δ the concentration of charge carriers measured from half filling. This implies that the choice of a single free parameter t fixes the resistivity on an absolute scale, and hence the comparison can be quite meaningful. The impurity resistivity can be accounted for by assuming that it is additive to the inelastic processes. In the case of electron doped cuprates, experimental determination of the impurity contribution is possible and leads to very accurate (absolute scale) inelastic resistivity to check against theory.

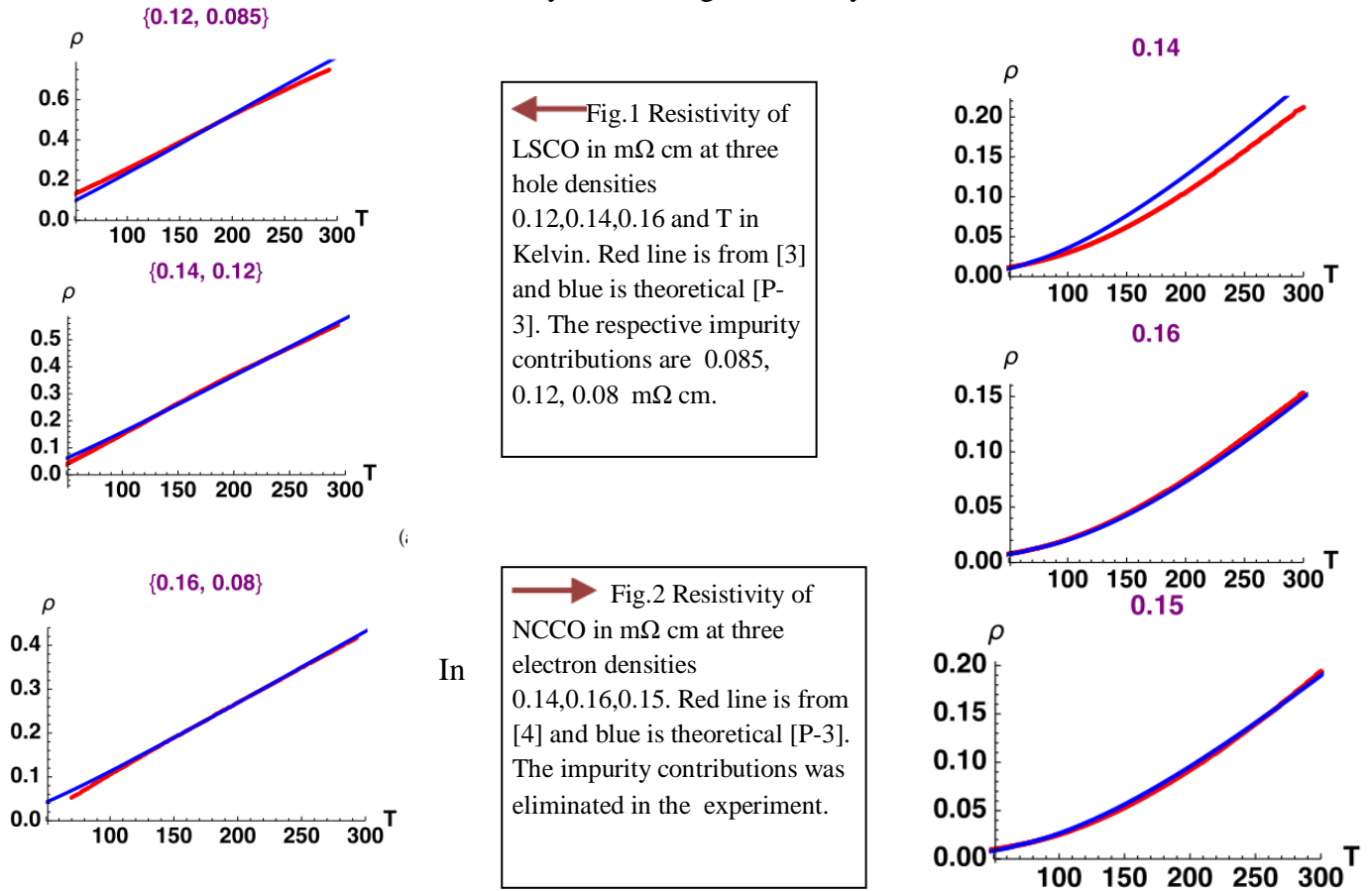


Fig.1 we show the comparison between theory and experiment for the hole doped LSCO system, where we chose $t'/t=-0.2$ and $t=0.9$ eV, $J=0.17$ t. Similarly in In Fig.2 we show the comparison between theory and experiment for the electron doped NCCO system, where we chose $t'/t=0.2$ and $t=0.9$ eV, $J=0.17$ t. We see a remarkably close agreement between theory and experiment in both cases. The crucial role played by the sign of t'/t is further explored in [9].

Superconductivity and strong correlations: In [P-1] the extremely correlated fermions was applied to the problem of superconductivity in the t-J model. The key point about this approach is that it does not introduce extra degrees of freedoms (such as slave particles etc), and works directly with the given problem of two component electrons with a strong local interaction. In the t-J model studies, the Hubbard U is eliminated in favor of a superexchange interaction

$$\frac{J}{2} \sum_{ij} (\vec{S}_i \cdot \vec{S}_j - \frac{1}{4} n_i n_j),$$

while electron hops are carried out always respecting the Gutzwiller constraint of single occupancy. The theory first establishes exact coupled (functional differential) equations for both the normal and anomalous (Go`rkov-Nambu type) Greens functions in this constrained problem. It then proceeds by carrying out a systematic expansion in two small variables, the J/t ratio and a parameter λ that controls the fraction of doubly occupied sites. The first important outcome of this new formalism is an equation for the d-wave order parameter $\Delta^*(p)$ in terms of the Greens functions, where strong correlations are built in systematically. To leading order in the the two small parameters it is $\Delta^*(k) = kT \sum_{pn} J(k - p) \Delta^*(p) g_0(p, -i\omega_n) \mathbf{G}(p, i\omega_n)$ where g_0, \mathbf{G} are the non-interacting and full Greens functions.

From this equation Tc can be found by ignoring superconducting order in \mathbf{G} , and using a strongly correlated Greens function. For the latter we used a flexible model spectral function of the type found in most theories of strong correlation, from the original Gutzwiller-Brinkman-Rice theory to the modern era, it consists of a flat background plus a delta function quasiparticle peak with a weight Z, and an effective mass m^* . The Mott-Hubbard physics enters through these parameters, in particular Z vanishes as we approach half filling. The great advantage of this approach is that we can find a explicit solution for Tc, consisting of a BCS type formula

renormalized by the physics of strong correlations: $k_B T_c \sim 1.134 W_0 \times \sqrt{m/m^*} \times e^{-\frac{1}{g_{eff}}}$, where $2W_0$ is the electron band-width, and $g_{eff} = \frac{2Z}{(1+m/m^*)} \{J_{eff} \Psi(\mu_0) n(\mu_0)\}$, where n is the band

density of states, \square is the d-wavefunction averaged over the fermi surface $\Psi =$

$$\frac{1}{n(\mu_0)} \sum_p \{ \cos(p_x) - \cos(p_y) \}^2 \delta(\epsilon_p - \mu_0) \quad \text{and} \quad J_{eff} = \frac{J}{1 - \log_4 \Psi n(\mu_0)}$$

is the exchange, renormalized by the background. This formula is for d-wave symmetry which easily defeats other symmetries for typical band parameters. We see that the Mott-Hubbard localization leads to a suppression of g_{eff} and hence has a drastic effect on superconductivity. The d-wavefunction is maximized with a suitable shape of the fermi surface, and gives clearcut predictions for maximizing Tc. The optimum Tc turns out to be a few hundred K and is

depressed by two orders of magnitude from the typical value for uncorrelated version of this model.

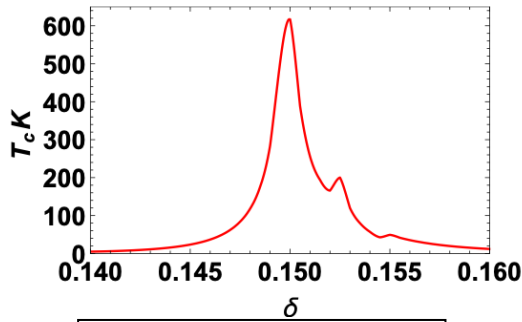


Fig.3 The phase diagram for superconductivity using hopping parameters $t'/t=-0.159$, $t''/t=0.01$, $t=0.45$ eV, and $J=0.3 t$

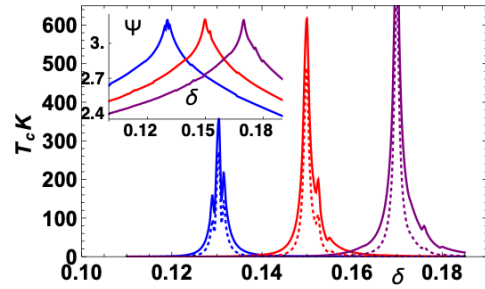


Fig.4 The peak density and T_c can be varied by changing t'/t . The correspond (l-r) to $t'/t=-0.18,-0.14,-0.16$ The inset tracks the d-wavefunction at these parameters.

Future Plans

The ideas developed in the above presentation will be applied using microscopic spectral functions, leading to detailed solutions of the pairing equations and hence the superconducting state properties. The PI is currently making progress on incorporating long ranged Coulomb interaction terms in the t-J model, in order to describe the momentum resolved electron scattering experiments (MEELS) of P. Abbamonte and colleagues [5].

References

- [1] B. S. Shastry, arXiv:1102.2858 (2011), Phys. Rev. Letts. 107, 056403 (2011).
- [2] B. S. Shastry, Phys. Rev. B 87, 125124 (2013); Ann. Phys. 343, 164-199 (2014).
- [3] Y. Ando *et. al.* Phys. Rev. Letts. **93**, 267001 (2004).
- [4] T. Sarkar, R. L. Greene and S. D. Sarma, Phys. Rev. B **98**, 224503 (2018).
- [5] M. Mitranoa *et. al.*, PNAS 115, 5392 (2018).

Publications in the 2 year period 2019-2021

P-1) Extremely Correlated Superconductors, B Sriram Shastry, arXiv:2102.08395; Annals of Physics, 168614 (2021); <https://doi.org/10.1016/j.aop.2021.168614>

P-2) Generalized Toeplitz-Hankel matrices and their application to a layered electron gas, O. Narayan and B. Sriram Shastry, J. Phys. A **54**, 175201 (2021); DOI: <https://doi.org/10.1088/1751-8121/abee67>

P-3) Aspects of the Normal State Resistivity of Cuprate Superconductors, B. Sriram Shastry and Peizhi Mai, arXiv:1911.09119; Phys. Rev. B **101**,115121(2020); DOI: <https://doi.org/10.1103/PhysRevB.101.115121>

P-4) Theory of anisotropic elastoresistivity of 2-D extremely strongly correlated metals, Michael Arciniaga, Peizhi Mai and B Sriram Shastry, arXiv:1909.06471; Phys. Rev. B **101**, 245149 (2020); DOI: <https://doi.org/10.1103/PhysRevB.101.245149>

Fractional topological states in disorder quantum Hall and graphene based superlattice systems

PI name: Dong-Ning Sheng

Affiliation: California State Univ. Northridge

Program Scope

The project involves theoretical (numerical) study of the fractionalized topological states in disordered quantum Hall and graphene based superlattice systems. We aim to make significant contribution in solving strongly correlated systems and provide fundamental understanding for emerging topological states in such systems. By advancing the state of art density matrix renormalization group (DMRG) method for such systems, we search, identify and uncover new topological states in fractional quantum Hall and Moire superlattice systems through tuning experimental relevant parameters. Our work is aiming to provide answers for the mechanism of the emergence of new quantum phases of interacting systems, reveal the nature of the new states, explain experimental results, and predict new experimental observations. We have made important progress in the following areas: (i) Providing fundamental understanding for disorder effect in topological states, quantum Hall interface, and non-Abelian fractional quantum Hall effects; (ii) Identifying and characterizing correlated insulating states and quantum phase transitions in twisted graphene and other superlattice systems; (iii) Identifying and characterizing spin liquids and quantum phase transitions of interacting systems.

Keywords: Topological states of matter; strongly interacting systems; density matrix renormalization group.

Recent Progress

SU(4) chiral spin liquid and quantized dipole Hall effect in moir`e bilayers--We study the correlated insulating phases in an interacting SU(4) Hubbard model¹, which captures the key physics of Moir`e bilayer systems formed by twisting two sheets of TMD to an angle close to 180^o, i.e. twisted AB stacked transition metal dichalcogenide (TMD) homo-bilayer with orbits carrying both spin and pseudospin (valley) degrees of freedom. We perform DMRG studies of the SU(4) spin model obtained in the limit of large repulsion for integer band fillings $\nu=1, 3$. We retain terms in the t/U expansion up to t^3/U^2 order, that generates nearest-neighbor Heisenberg exchange J , as well as an additional three spin ring-exchange term K . As shown in Fig. 1, for filling $\nu=3$, when increasing K , we identify three different phases: a spin stripe phase, an SU(4)₁ chiral spin liquid (CSL) and a decoupled one dimensional chain phase. The CSL phase exists at intermediate coupling window $11.3 < U/t < 22.9$, which is much wider than the one for the CSL in the one-band Hubbard model on triangular lattice. The layer pseudospin carries an electric dipole moment in z direction, thus the CSL is really a dipole-spin liquid, with quantum fluctuations in both the electric and magnetic moments. We simulate the spin Hall conductivity matrix (Chern number matrix) in DMRG by doing adiabatic flux insertion, which provides smoking gun evidence for the CSL that

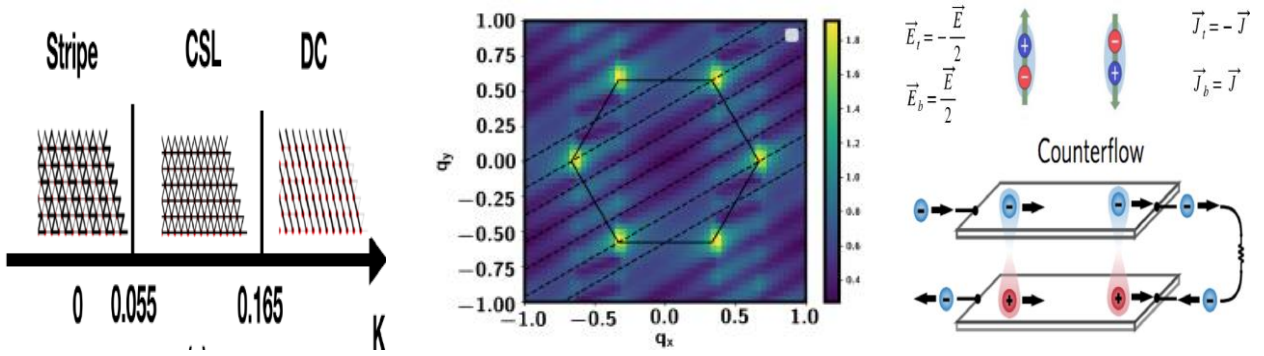


Fig.1 Left: Phase diagram for SU4 Hubbard model of TMD bilayer at filling number $\nu=1$. Middle: Super-solid phase for an imbalanced filling number. Right: Experimental detection of the chiral spin liquid.

could be measured experimentally in counter-flow Hall transport. For filling $\nu=1$ with the opposite sign of K , the spin stripe phase survives to very large K . We also predict two exciton supersolid phases with inter-layer coherence at imbalanced filling under displacement field. Interestingly, the system can simulate an SU(2) Bose-Einstein-condensation (BEC) by injecting inter-layer excitons into the magnetically ordered Mott insulator at the layer polarized limit. Smoking gun evidences of these phases can be obtained by measuring the longitudinal pseudo-spin transport in the counter-flow channel.

Quantum phases of transition metal dichalcogenide (TMD) Moir'e systems--Recent experiments on hetero-bilayer TMD systems are exciting in that they manifest a relatively simple model system of an extended Hubbard model on a triangular lattice. We explore the nature of quantum phases² and metal insulator transitions to different Mott states using the DMRG method. Specifically, we explore the phase space with varying on-site Hubbard interaction U , and the further-range Coulomb interaction, both are tunable in experiments. We find competition between Fermi fluid, chiral spin liquid, spin density wave, and charge density wave. In particular, our finding of the optimal further-range interactions for the chiral correlation presents a favorable possibility for experimental detecting of the chiral spin liquid.

Doped Mott Insulators in the Triangular Lattice Hubbard Model

A central issue in the physics of strongly correlated materials is the nature of the correlated phases that emerge on doping a Mott insulator. Given its relevance to the high temperature cuprate superconductors, much efforts have been devoted to doped Mott insulators in the square lattice Hubbard Model. However, the analogous problem on the triangular lattice is equally interesting and likely to exhibit new and distinct physics due to magnetic frustration and the absence of nesting and particle-hole symmetry in the minimal models. We have investigated the evolution of the Mott insulators in the triangular lattice Hubbard model, as a function of hole doping in both the

intermediate and strong coupling limits. Using the advanced DMRG method, at light hole doping, we find a significant difference between strong and intermediate couplings³. Notably, at intermediate coupling an unusual metallic state emerges, with short ranged spin correlations but long ranged spin-chirality order. Moreover, no clear Fermi surface or wave-vector is observed, this chiral metal also exhibits staggered loop current, which breaks the translational symmetry. These features disappear on increasing interaction strength or on further doping. At strong coupling, the 120 degrees magnetic order of the insulating magnet persists for light doping, which produces hole pockets with a well defined Fermi surface. On further doping around 10%~20%, the spin density wave (SDW) order and coherent hole Fermi pockets are found at both strong and intermediate couplings. At even higher doping larger than 20%, the SDW order is suppressed and the spin-singlet Cooper pair correlations are simultaneously enhanced. We interpret this as the onset of superconductivity on suppressing magnetic order.

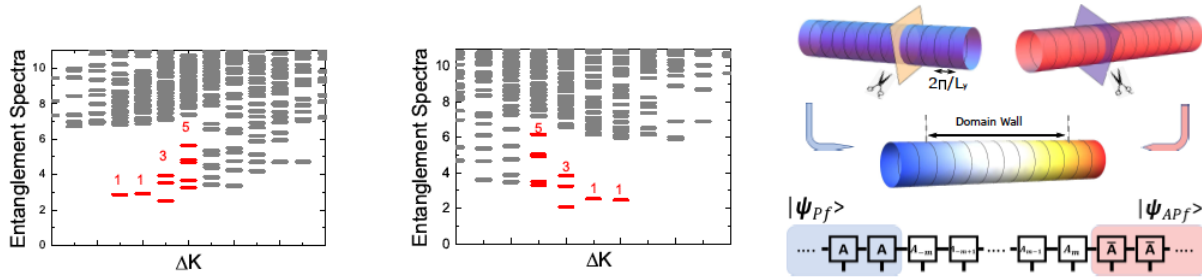


Fig.2. Interface between two non-Abelian (Pf and APf) states on the cylinder geometry. Typical entanglement spectra for gapped Pf (left) and APf (middle) states. We first cut the Pf (APf) state into two halves, and glue the left part of Pf and right part of APf together, which creates an interface of Pf and APf states.

Topological interface between 5/2 Pfaffian and anti-Pfaffian state--Another exciting direction explored in the research is the interface⁴ effect between two non-Abelian topological states of matter. By developing the state-of-the-art DMRG simulations, we have studied the interface between the PF and APF states, which is created by connecting two infinite DMRG solutions for PF and APF together using cut-and-glue method as illustrated in Fig.2. Through optimizing the interface in the middle of the infinite cylinder, we obtain the ground state and identify the topological nature of the interface. We find that the counter-propagating charge modes are fully gapped out and only neutral modes survive around the Pf-APf interface. Furthermore, an intrinsic electric dipole moment emerges at the interface with a topological origin, whose formation is to counter-balance the mismatch of guiding-center Hall viscosity of bulk PF and APF states. In addition, the PF-APF domain wall hosts an intricate structure, which is overlooked in the effective edge theories. It makes the domain wall energetically favorable in the presence of an electric field due to its coupling with the dipole moments. These results imply that the formation of a dipole moment could be helpful to stabilize the PF-APF puddle state in experimental conditions.

Future Plans

We will study the physics of doped Mott insulators by considering realistic model Hamiltonians realized by different Moiré superlattice systems. We will search and discover different unconventional superconducting or other correlated states and make concrete predictions for experimental discovery of topological superconductivity in such systems. Furthermore, we will develop numerical methods to target properties of excited states and dynamic response functions in these strongly correlated systems.

References

1. Ya-Hui Zhang, D. N. Sheng, Ashvin Vishwanath, *An $SU(4)$ chiral spin liquid and quantized dipole Hall effect in moiré bilayers*, arXiv:2103.09825, submitted to Phys. Rev. Lett.
2. Yiqing Zhou, D. N. Sheng, Eun-Ah Kim, *Quantum Phases of Transition Metal Dichalcogenide Moiré Systems*, arXiv:2105.07008, submitted to Phys. Rev. Lett.
3. Zheng Zhu, D. N. Sheng, Ashvin Vishwanath, *Doped Mott Insulators in the Triangular Lattice Hubbard Model*, arXiv:2007.11963, submitted to Phys. Rev. Lett.
4. W. Zhu, D. N. Sheng, and Kun Yang, *Topological Interface between Pfaffian and Anti-Pfaffian Order in $\nu = 5/2$ Quantum Hall Effect*, Phys. Rev. Lett. 125, 146802 (2020).

Publications

1. Ya-Hui Zhang, D. N. Sheng, Ashvin Vishwanath, *An $SU(4)$ chiral spin liquid and quantized dipole Hall effect in moiré bilayers*, arXiv:2103.09825, submitted to Phys. Rev. Lett.
2. Zheng Zhu, D. N. Sheng, Ashvin Vishwanath, *Doped Mott Insulators in the Triangular Lattice Hubbard Model*, arXiv:2007.11963, submitted to Phys. Rev. Lett.
3. W. Zhu, D. N. Sheng, and Kun Yang, *Topological Interface between Pfaffian and Anti-Pfaffian Order in $\nu = 5/2$ Quantum Hall Effect*, Phys. Rev. Lett. 125, 146802 (2020).
4. Zheng Zhu, Zheng-Yu Weng, and D. N. Sheng, *Magnetic field induced spin liquids in $S = 1$ Kitaev honeycomb model*, Phys. Rev. Research 2, 022047(R), (2020).
5. Zheng Zhu, D. N. Sheng, and Inti Sodemann, *Widely Tunable Quantum Phase Transition from Moore-Read to Composite Fermi Liquid in Bilayer Graphene*, Phys. Rev. Lett. 124, 097604 (2020).
6. D. N. Sheng and Liang Fu, *Thermoelectric response and entropy of fractional quantum Hall systems*, Phys. Rev. B 101, 241101(R), (2020).
7. Yixuan Huang, D. N. Sheng, and C. S. Ting, *Coupled dimer and bond-order-wave order in the quarter-filled one-dimensional Kondo lattice model*, Phys. Rev. B 102, 245143 (2020).
8. Tian-Sheng Zeng, D. N. Sheng, and W. Zhu, *Continuous phase transition between bosonic integer quantum Hall liquid and a trivial insulator: Evidence for deconfined quantum criticality*, Phys. Rev. B 101, 035138, (2020).
9. Yiqing Zhou, D. N. Sheng, Eun-Ah Kim, *Quantum Phases of Transition Metal Dichalcogenide Moiré Systems*, arXiv:2105.07008, submitted to Phys. Rev. Lett.
10. Huan-Da Ren, Tian-Yu Xiong, Han-Qing Wu, D. N. Sheng, Shou-Shu Gong, *Characterizing random-singlet state in two-dimensional frustrated quantum magnets and implications for the double perovskite $Sr_2CuTe_{1-x}W_xO_6$* , arXiv:2004.02128, submitted to Phys. Rev. Lett.

Electron Correlations, Bad-Metal Behavior and Unconventional Superconductivity

Principal Investigator: Qimiao Si, Rice University

Program Scope

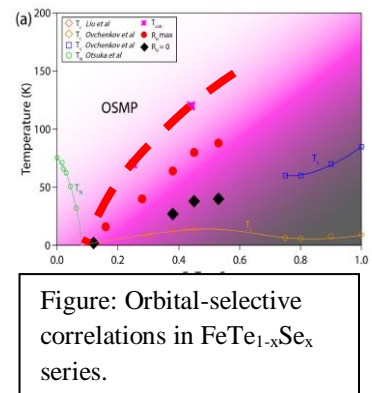
This project aims to deepen our understanding of electron correlations, bad-metal behavior, and their connections with electronic orders and superconductivity in the Fe-based superconductors (FeSCs) [1] and correlated moiré systems. One direction is to study orbital selectivity in the normal state of the FeSCs, especially its interplay with electronic orders. Another direction is to investigate orbital-selective superconductivity in the iron-based systems. The third direction is to explore the effects of electron correlations in the correlated moiré systems. Here, our focus will be on the nature of the correlated insulators and the role of nematic correlations in the phase diagram, both of which will set the stage to elucidate the mechanism for superconductivity in these systems. Overall, the proposed projects will shed light on the multi-orbital correlations and superconductivity in several strongly correlated systems and, in general, help elucidate the fundamental physics of quantum materials that may have impact on the development of future quantum technology.

Keywords: Correlated electrons, unconventional superconductivity, quantum phase transitions

Recent Progress (primarily 2020-2021)

Topic #1 -- Orbital-selective correlations in iron-based systems

1.A Orbital-selective Mott transition in iron chalcogenides. One major open question is how to realize an orbital-selective Mott transition at low temperature. A particularly fruitful way of probing this is through a Fermi-surface reconstruction. For the Fe-chalcogenides, we have shown [P10] a surprisingly important role played by $d(z_2)$ orbitals. We find that the localization of the $d(xy)$ orbital is manifested as the destruction of a gap of the symmetry-allowed hybridization with the $d(z_2)$ orbital near the X point. We worked with the ARPES group of my colleague Ming Yi to observe this effect! Our theoretical work has opened up an entirely new means of probing orbital-selective localization-delocalization physics, a notion that comes into play in a wide array of systems –even likely in the hole-doped high T_c cuprates too.



1.B Orbital-selective Mott transition in iron pnictides. One important question is about the extent to which electron correlations in the iron pnictides are orbital selective. We recently considered the case of LiFeAs [P9], and analyzed a multi-orbital Hubbard model for this compound using the

U(1) slave spin method that we developed in earlier work. We find the system to be close to an orbital-selective Mott phase at low temperatures and driven into it with increasing temperature. Importantly, we demonstrate a new mechanism for a large change in the size of the Fermi surface, namely, orbital selectivity of the energy-level renormalization cooperating with that of the quasiparticle spectral weight. Our results reveal a remarkable degree of universality out of the seemingly complex multiorbital building blocks across a broad range of strongly correlated superconductors.

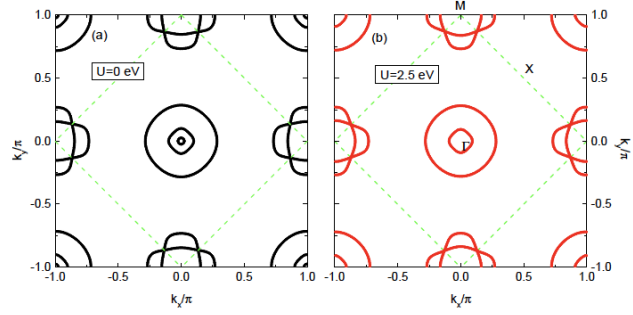


Figure: The orbital-selective correlations in LiFeAs remove the innermost hole pocket and reduce the other pockets.

Topic #2 -- Orbital-selective superconductivity in iron-based systems

2. Recent experiments in multiband Fe-based have challenged the long-held dichotomy between simple s- and d-wave spin-singlet pairing states. We have advanced time-reversal-invariant irreducible pairings that go beyond the standard spin-singlet pairing functions through a matrix structure in the band/orbital space [P1]. We consider the τ_3 multiorbital superconducting state for Fe-chalcogenide superconductors. This state, corresponding to a d + d intra- and inter-band pairing, is shown to contrast with the more familiar d + id state in a way analogous to how the B-phase of ^3He superfluid differs from its A-phase counterpart. This analogy not only establishes the naturalness of the novel multi-orbital pairing state, but also inspires a way to construct similar type of pairing states in other classes of multi-orbital superconductors, including when spin-orbit coupling is strong.

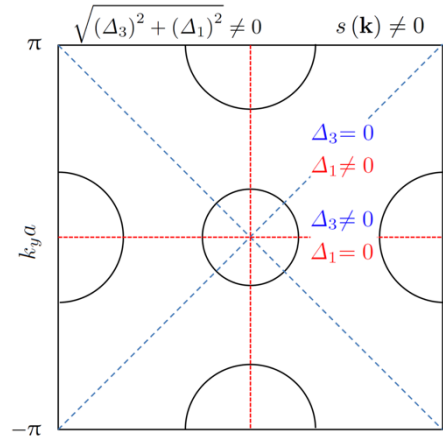


Figure: Addition in quadrature of the pairing components makes the d+d pairing fully gapped.

Topic #3 -- Nematic correlations in iron-based systems

3.A Since its discovery, Fe-based superconductivity has been known to develop near an antiferromagnetic order, but this paradigm fails in the iron chalcogenide FeSe, whose single-layer version holds the record for the highest superconducting transition temperature in the iron-based superconductors. We propose [P11] that the phase diagram of FeSe under pressure could be qualitatively described by a quantum spin model with highly frustrated interactions. We implement both the site-factorized wave-function analysis and the large-scale density matrix renormalization group (DMRG) in cylinders to study the spin-1 bilinear-biquadratic model on the square lattice, and identify quantum transitions from the well-known $(\pi, 0)$ antiferromagnetic state to an exotic $(\pi, 0)$ antiferroquadrupolar order, either directly or through a $(\pi/2, \pi)$ antiferromagnetic state. These

many phases, while distinct, are all nematic. We also discuss our theoretical ground-state phase diagram for the understanding of the experimentally determined low-temperature phase diagram in pressurized FeSe. Our results suggest that superconductivity in a wide range of iron-based materials has a common origin in the antiferromagnetic correlations of strongly correlated multi-orbital electrons.

3.B While it is commonly assumed that nematic order represents a broken rotational symmetry, for the FeSCs, we find that it is profitable to use a broken mirror symmetry to characterize the nematic order. Remarkable, the general considerations lead us to a new type of nematic order, which is B_{2g} and is driven by incommensurate magnetic fluctuations. We proposed B_{2g} and its cousin A_{2g} nematic orders as the origin of some recent new experimental observations in the heavily hole-doped and very strongly correlated regime of the Ba122 iron pnictides.

Topic #4 -- Multi-orbital physics in other correlated systems

Strong correlations with multiple orbitals are playing an important role in several newly discovered superconductors.

4.A Nickelate: The recent discovery of superconductivity in Sr-doped NdNiO₂ raised the issue of multi-orbital correlations in this infinite-layer nickelate. We have investigated [P12] superconductivity in the trilayer member of the same series (R₄Ni₃O₈) using a combination of first-principles and t–J model calculations. R₄Ni₃O₈ compounds resemble cuprates more than RNiO₂ materials in that only Ni-d(x²-y²) bands cross the Fermi level, they exhibit a largely reduced charge transfer energy, and as a consequence superexchange interactions are significantly enhanced. We find that the superconducting instability in doped R₄Ni₃O₈ compounds is considerably stronger with a maximum gap about four times larger than that in Sr_{0.2}Nd_{0.8}NiO₂.

4.B The new candidate-chiral-p-wave superconductor: UTe₂ has been argued as a spin-triplet superconductor, potentially hosting Majorana fermions important for quantum computation. We have constructed new pairing states [P2] taking into account their orbital structure, and raised the exciting possibility of antiferromagnetic correlations driving spin-triplet pairing.

Topic #5 -- Electron correlations in moiré flat bands

5. Graphene moiré bands represent a new setting for correlation effects. Strikingly, the strength of electron correlations is now understood to be comparable to the bandwidth, making it a tunable play ground to elucidate the physics of intermediately correlated bad metals or the nearby (what we term) “fragile insulators”. In [P14], we develop a variational Monte Carlo method for this systems. Using the method, we carry out the first non-perturbative calculations that are suitable for this intermediate correlation regime. We advance the notion of a fragile insulator, a correlation-driven insulating state that is on the verge of a delocalization transition into a bad metal. We realize such a fragile insulator and demonstrate a nematic order in this state

as well as in the nearby bad metal regime. Our results are consistent with the observed electronic anisotropy and provide a natural understanding of what happens when the insulator is tuned into a bad metal. We propose the fragile insulator and the accompanying bad metal as competing states at integer fillings that analogously anchor the overall phase diagram of the correlated moiré systems and beyond.

Future Plans

Our plan for the coming year includes:

Orbital selectivity in the normal state of the FeSCs, especially its interplay with electronic orders. We plan to study the orbital-selective Mott regime of FeTe, as evidenced by our work during Y1 (publications P10), and its interplay with antiferromagnetic and nematic order.

Orbital-selective superconductivity in the iron-based systems. Our work during Y1 (publications P1) has opened up several important directions of future study on this topic. In particular, we plan to address the evolution of the pairing state in the overall phase diagram of FeTe_{1-x}Sex and LiFeAs. The potential interplay between the bulk topological multi-band electronic states and the topological aspects of the superconductivity will be explored.

Frustrated magnetism and spin dynamics in nematic FeSe. In working with the experimental group of my colleague Pengcheng Dai, we have very recently uncovered high energy dispersive spin excitations in the fully detwinned nematic FeSe. Preliminary results (see Y1 publication P6). This work opens an avenue for fresh new insights on the enigmatic mechanism for the nematic order in FeSe. We will explore the role of frustrated magnetism and, in particular, antiferroquadratic order and its interplay with nematicity. This work promises to shed much new light on the overarching understanding of the relevant low-energy electronic degrees of freedom and the basic building blocks of the electronic orders across the FeSCs.

Orbital-selective correlations and superconductivity in UTe₂. As I have observed in an invited review being jointly prepared with Nigel Hussey on FeSCs for Physics Today, FeSCs, even they are as complex and as challenging as any teenager, are beginning to impart some of their new-found wisdom on a slew of emerging superconductors that appear to share similar traits. A case in point is UTe₂, which is a promising candidate for topological superconductor. Our preliminary work in Y1 (publication P2) has uncovered evidence for the important role of multiorbital pairing. We plan to pursue this thread on this and related issues.

References

1. Q. Si, R. Yu and E. Abrahams, *High Temperature Superconductivity in Iron Pnictides and Chalcogenides*, Nature Reviews Materials **1**, 16017 (2016).

Publications (selected, focused on 2020-2021):

- P1. E. M. Nica and Qimiao Si, *Multiorbital singlet pairing and $d+d$ superconductivity*, NPJ Quantum Materials **6**, 3 (2021).
- P2. C. Duan et al., E. M. Nica, Q. Si, P. C. Dai, *Resonance from antiferromagnetic spin fluctuations for superconductivity in UTe_2* , Nature, to appear (2021).
- P3. S. Paschen, Q. Si, *The many faces (phases) of strong correlations*, Europhysics News (EPN) **52/4**, 30-32 (2021).
- P4. R. Yu, H. Hu, E. M. Nica, J.-X. Zhu, Q. Si, *Orbital selectivity in electron correlations and superconducting pairing of iron-based superconductors*, Front. Phys. **9**, 978347 (2021).
- P5. E. M. Nica, Q. Si, O. Erten, *Matrix-pairing states in the alkaline Fe-selenide superconductors: exotic Josephson junctions*, arXiv:2108.05442.
- P6. X. Y. Lu et al., R. Yu, Q. Si, P. C. Dai, T. Schmitt, *Spin-excitation anisotropy in the nematic state of detwinned $FeSe$* , arXiv:2108.04484.
- P7. C. Setty, H. Hu, L. Chen, Q. Si, *Electron correlations and T -breaking density wave order in a Z_2 kagome metal*, arXiv:2105.15204.
- P8. C. Mielke III et al., Q. Si, ..., Z. Guguchia, *Time-reversal symmetry-breaking charge order in a correlated kagome superconductor*, arXiv:2106.13443.
- P9. H. H. Lin, R. Yu, J.-X. Zhu, Q. Si, *Orbital-selective correlations and renormalized electronic structure in $LiFeAs$* , arXiv:2101.05598.
- P10. J. W. Huang, et al., Q. Si, R. J. Birgeneau, M. Yi, *Non-thermal Emergence of an Orbital-Selective Mott Phase in $FeTe_{1-x}Se_x$* , arXiv:2010.13913.
- P11. W. J. Hu, H.-H. Lai, S.-S. Gong, R. Yu, E. Dagotto, and Q. Si, *Quantum Transitions of Nematic Phases in a spin- $S=1$ Bilinear-Biquadratic Model and Their Implications for $FeSe$* , Phys. Rev. Research **2**, 023359 (2020).
- P12. E. M. Nica, ..., Q. Si, A. S. Botana, O. Erten, *Theoretical investigation of superconductivity in trilayer square-planar nickelates*, Phys. Rev. B **102**, 020504 (2020)
- P13. C. R. Duan, et al., Q. Si, P. C. Dai, *Incommensurate Spin Fluctuations in the Spin-triplet Superconductor Candidate UTe_2* , Phys. Rev. Lett. **125**, 237003 (2020).
- P14. L. Chen, H. Hu, Q. Si, *Fragile insulator and electronic nematicity in a graphene moiré system*, Nat. Comm. submitted; arXiv:2007.06086.

Frontiers in Magnetic Materials

David J. Singh, University of Missouri

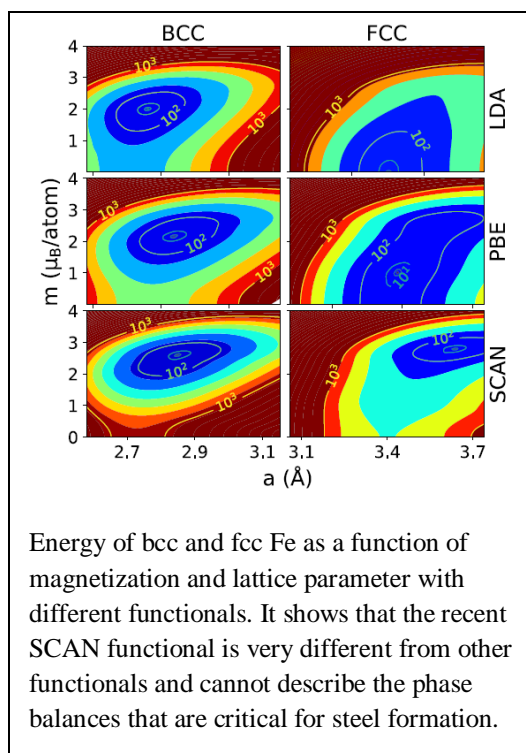
Program Scope

Magnetism is crucial to many modern technologies, a driver for condensed matter physics research and one of the most remarkable and diverse properties of matter. We use materials specific theory, primarily density functional theory to understand properties of magnetic materials, predict new materials and to explore novel phenomena associated with magnetism, including quantum critical systems and superconductivity near magnetism. We also assess density functionals in the context of magnetism, following our discovery that recently developed functionals have serious problems in treating standard magnetic materials such as Fe. We are devising test cases and mapping out the behavior of functionals which may eventually lead to more universal functionals. We used analogies with thermoelectrics to identify semiconductors that can become ferromagnetic with doping, including a material that may exhibit a novel gate controllable magnetic quantum critical state and a material that may be a new magnetic semiconductor with relatively low-level doping. Additionally, we built on insights into the interplay of A-site disorder and ferroelectric properties in perovskites from our prior DOE supported work, to help understand anomalous measurements on nanostructured niobate films leading to a demonstration of giant piezoelectric effects, published in Science along with the 2021 Charles Hatchett Award. In another collaboration with experiment, we showed mechanisms as well as signatures leading to identification of room temperature ferromagnetism in ultrathin CrTe₂ films.

Keywords: Magnetic Materials, Superconductivity near Magnetism, Quantum Critical Materials.

Recent Progress

Accurate benchmarked density functionals are important for progress in materials and condensed matter. We discovered that a recent advanced meta-GGA functional (SCAN) that is widely used was unable to describe the phase balances underlying steel – a vitally important technological material. We showed that this was a consequence of overestimation of magnetic energies (see Figure). We then did a series of benchmark calculations, and found that the key issue is over-localization in itinerant systems,

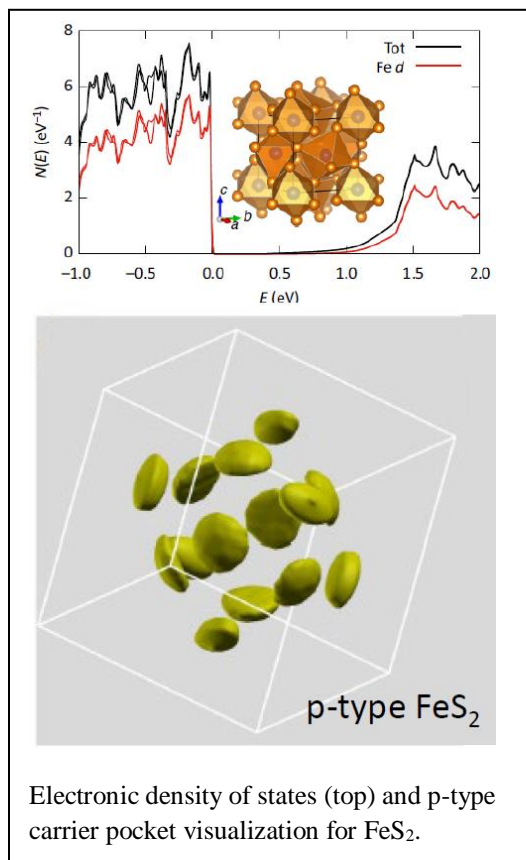


leading to similar overestimation of magnetic moments and magnetic energies. For example, we found that graphene is incorrectly predicted to be an antiferromagnetic semiconductor rather than a Dirac semimetal in SCAN calculations. The challenge of simultaneously treating localized and delocalized electronic systems remains. While the meta-GGA rung of Jacob's ladder shows great promise, SCAN does not yet provide a universal density functional, and the quest for such a functional and strategies for finding one is open. Our identification of the degree of localization as a key issue for the development of meta-GGA functionals is expected to be useful for this.

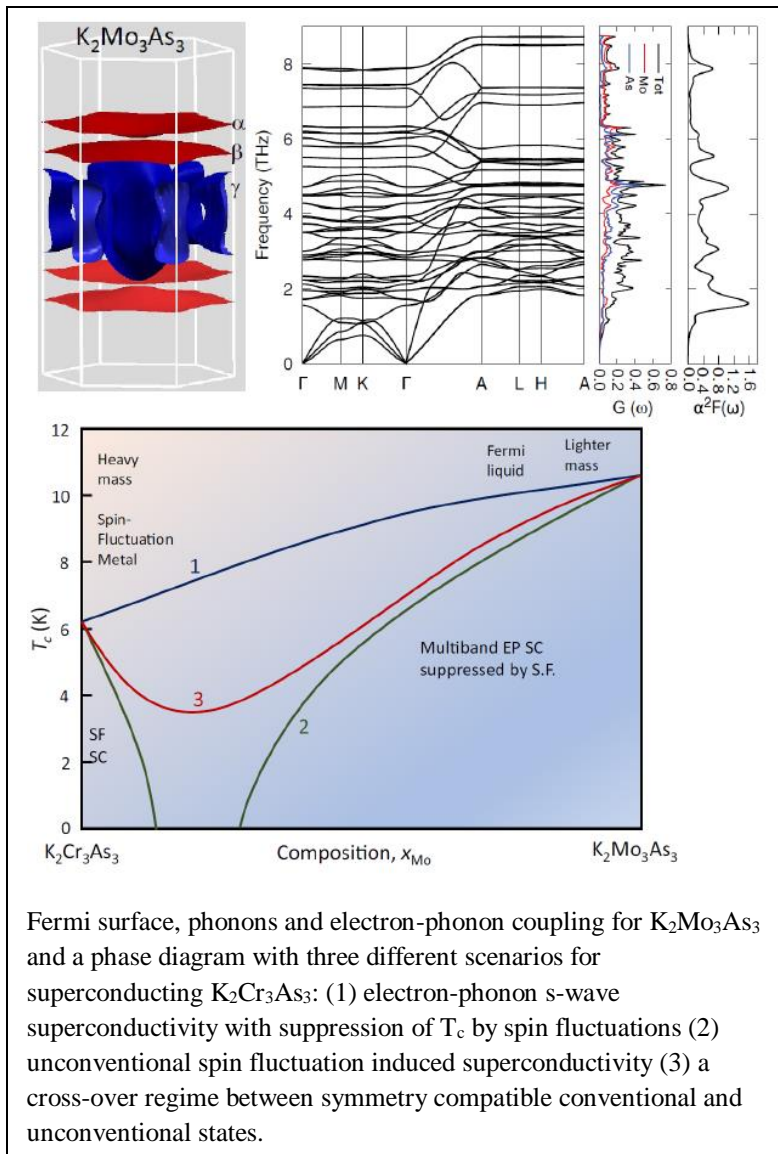
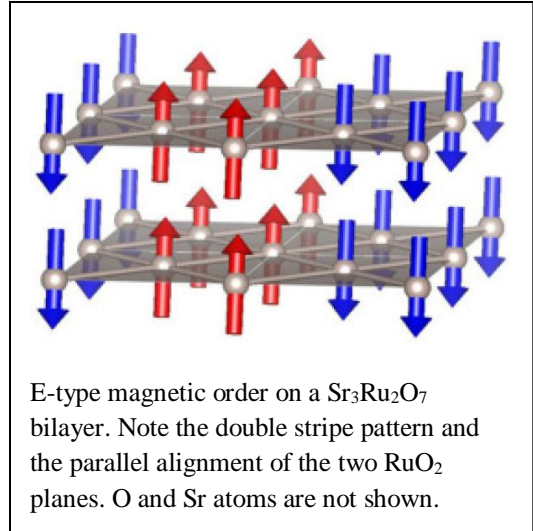
Magnetic semiconductors are critically needed to enable spintronic devices. However, existing materials are deficient both in terms of their semiconductor properties and their magnetic ordering. The traditional approach involves doping a semiconductor with magnetic impurities, as in Mn-doped GaAs. We identified a different approach based on itinerant electron physics, specifically doping a non-magnetic semiconductor with ordinary dopants to achieve a Stoner instability. This requires resolution of a conundrum – the Stoner instability requires a very high band edge density of states. However, mobility requires a low effective mass, inconsistent with this. We recognized that a very similar conundrum occurs in thermoelectrics, where high thermopower associated with heavy mass is required at the same time as conductivity, associated with light mass. This is resolved by recognizing that in complex non-parabolic band structures, different effective masses enter different quantities, so that it is

possible to have high density of states effective mass and low transport effective mass. We searched for non-magnetic semiconductors with this type of band feature and identified binary and ternary compounds. One new finding is that pyrite FeS_2 can become a ferromagnetic semiconductor if doped p-type. This is due to the complex band structure shown by the many anisotropic complex shaped carrier pockets with p-type doping (See Figure). Another is that marcasite FeAs_2 is a useful material for exploring low carrier density magnetic quantum criticality as the quantum critical point may be accessible by electrostatic gating.

Quantum criticality in both low carrier density systems, where it has been little explored so far, and in large Fermi surface metals is a topic of great interest. It is thought to play a key role in phase diagrams of unconventional superconductors, and also to lead to unusual ground states such as nematic electron systems. $\text{Sr}_3\text{Ru}_2\text{O}_7$ is a well-studied but still poorly understood example. It is closely related to the ferromagnetic 4d oxide, SrRuO_3 and the unconventional



superconductor, Sr_2RuO_4 . $\text{Sr}_3\text{Ru}_2\text{O}_7$ is noteworthy in showing an exceptionally large renormalization of the ground state due to spin fluctuations and a metamagnetic quantum critical state with emergence of a poorly understood nematic. A key issue is the nature of the spin fluctuations, and in particular whether there is an antiferromagnetic state that competes with ferromagnetism. We did an exhaustive search of possible competing orders using first principles calculations, including tests with different functionals. We found a close competition between a complex E-type order (See Figure) and ferromagnetism, with other possible orders much less



avored. We also found that among all the orders studied only the E-type order gives a large conductivity anisotropy. This suggests a possible connection to the nematicity, since conductivity anisotropy is a key signature of the nematic state in $\text{Sr}_3\text{Ru}_2\text{O}_7$.

Superconductivity near magnetism is of long-standing interest in condensed matter. Examples include cuprates, Sr_2RuO_4 , and Fe-based superconductors. Recently, a new family of pnictide superconductors exemplified by $\text{K}_2\text{Cr}_3\text{As}_3$ was discovered. These superconductors are chemically related to the Fe-based superconductors, but structurally very distinct, in particular having 1D non-centrosymmetric metal-pnictide nanowire-based structures. Both DFT calculations and experiments show signatures of magnetism in these compounds. The compounds also

show anomalously high upper critical fields, which can be a signature of unconventional superconductivity. However, $\text{K}_2\text{Cr}_3\text{As}_3$ is an extraordinarily complex material, with both chemical instabilities and as we showed complex structural distortions. These predictions were confirmed by neutron scattering experiments done at ORNL. However, these still not fully characterized distortions make first principles studies of superconducting mechanisms difficult since both electron-phonon calculations and magnetic calculations depend on these details. Fortunately, the Mo system, $\text{K}_2\text{Mo}_3\text{As}_3$ exists and has similar superconducting properties to $\text{K}_2\text{Cr}_3\text{As}_3$ including an anomalous upper critical field. Importantly, unlike the Cr system, $\text{K}_2\text{Mo}_3\text{As}_3$ is stable in its ideal high-symmetry structure. We did extensive first principles calculations seeking magnetic states as well as phonon and electron-phonon calculations. We did not find magnetic instabilities, and in fact find that $\text{K}_2\text{Mo}_3\text{As}_3$ is far from a ferromagnetic instability, which is thought to be the main character of spin fluctuations in $\text{K}_2\text{Cr}_3\text{As}_3$. On the other hand, we did find superconductivity from electron-phonon calculations, with properties including the critical temperature in good accord with existing experiments. The calculations also provided an explanation for the exceptional upper critical field of this material. Specifically, we find very different coupling on different sheets of Fermi surface leading to multigap superconductivity. This suggests tunneling experiments. Additionally, it provides an experimentally based method to sort out the nature of superconductivity in $\text{K}_2\text{Cr}_3\text{As}_3$ as it constrains the shape of the phase diagram. This is illustrated in the Figure, which also shows results of electron phonon calculations and the Fermi surface.

Future Plans

We will develop a test set of magnetic materials useful for benchmarking the performance of advanced density functionals. The characteristic feature of this set of tests is to identify materials where different functionals yield different magnetic tendencies in ways that affect ground state properties. Fe discussed above is one example. We will search for and characterize materials near magnetic quantum critical points (QCPs), using the fact that strong quantum spin fluctuations near QCPs renormalize ground state properties and specifically that the interplay of moment formation and chemical bonding, can lead to substantial changes in bond lengths. High-quality structural information available in databases facilitates use of this search criterion. We will continue investigations of superconductivity near magnetism, including both materials with two gap superconductivity and materials thought to have unconventional superconducting symmetries, perhaps due to spin-fluctuation induced pairing. We will search for new low carrier density ferromagnets based on itinerant models. We will particularly emphasize materials with unusual combinations of properties such as high spin polarization and low transport effective mass.

This work will push the limits of extreme magnetic behavior in materials, specifically through the finding of novel quantum phases related to spin fluctuations, new magnetic materials with exceptional properties and potentially the discovery of materials that manifest new and unanticipated quantum electronic phases of matter.

Publications (partial list):

1. X. Zhang, Q. Lu, W. Liu, W. Niu, J. Sun, J. Cook, M. Vaninger, P.F. Miceli, D.J. Singh, S.W. Lian, T.R. Chang, X. He, J. Du, L. He, R. Zhang, G. Bian and Y. Xu, “Room-temperature intrinsic ferromagnetism in epitaxial CrTe₂ ultrathin films”, *Nature Comm.* **12**, 2492 (2021).
2. B.H. Lei and D.J. Singh, “Ferromagnetism in a Semiconductor with Mobile Carriers via Low-Level Nonmagnetic Doping”, *Phys. Rev. Appl.* **15**, 044036 (2021).
3. H. Yao, C. Chen, W. Xue, F. Bai, F. Cao, Y. Lan, X. Liu, Y. Wang, D.J. Singh and Q. Zhang, “Vacancy ordering induced topological electronic transition in bulk Eu₂ZnSb₂”, *Science Adv.* **7**, eabd6162 (2021).
4. B.H. Lei and D.J. Singh, “Multigap electron-phonon superconductivity in the quasi-one-dimensional pnictide K₂Mo₃As₃”, *Phys. Rev. B* **103**, 094512 (2021).
5. G. Qin, W. Ren, D.J. Singh and B.H. Lei, “Disorder and Itinerant Magnetism in Full Heusler Pd₂TiIn”, *Chin. Phys. Lett.* **38**, 017102 (2021).
6. A. Putatunda, G. Qin, W. Ren and D.J. Singh, “Competing magnetic orders in quantum critical Sr₃Ru₂O₇”, *Phys. Rev. B* **102**, 014442 (2020).
7. B.H. Lei, Y. Fu, Z. Feng and D.J. Singh, “Quantum critical point and ferromagnetic semiconducting behavior in p-type FeAs₂”, *Phys. Rev. B* **101**, 020404 (R) (2020).
8. G. Qin, W. Ren and D.J. Singh, “Interplay of local moment and itinerant magnetism in cobalt-based Heusler ferromagnets: Co₂TiSi, Co₂MnSi and Co₂FeSi”, *Phys. Rev. B* **101**, 014427 (2020).
9. A.R.M. Iasir, T. Lombardi, Q. Lu, A.M. Mofrad, M. Vaninger, X. Zhang and D.J. Singh, “Electronic and magnetic properties of perovskite selenite and tellurite compounds: CoSeO₃, NiSeO₃, CoTeO₃ and NiTeO₃”, *Phys. Rev. B* **101**, 045107 (2020).
10. H. Liu, H. Wu, K.P. Ong, T. Yang, P. Yang, P.K. Das, X. Chi, Y. Zhang, C. Diao, W.K.A. Wong, E.P. Chew, Y.F. Chen, C.K.I. Tan, A. Rusydi, M.B.H. Breese, D.J. Singh, L.Q. Chen, S.J. Pennycook and K. Yao, “Giant piezoelectricity in oxide thin films with nanopillar structure”, *Science* **369**, 292 (2020).
11. F. Tran, G. Baudesson, J. Carrete, G.K.H. Madsen, P. Blaha, K. Schwarz and D.J. Singh, “Shortcomings of meta-GGA functionals when describing magnetism”, *Phys. Rev. B* **102**, 024407 (2020).
12. J. Neu, D. Graf, K. Wei, A. Gaiser, Y. Xin, Y. Lai, T.E. Albrecht-Schmitt, R. Baumbach, D.J. Singh and T. Siegrist, “Superstructures and superconductivity linked with Pd intercalation in Nb₂Pd_xSe₅”, *Chem. Mater.* **32**, 8361 (2020).
13. Y. Zhang, W. Zhang and D.J. Singh, “Localization in the SCAN meta-generalized gradient approximation functional leading to broken symmetry ground states for graphene and benzene”, *Phys. Chem. Chem. Phys.* **22**, 19585 (2020).
14. Z. Feng, Y. Fu, Y. Zhang and D.J. Singh, “Characterization of rattling in relation to thermal conductivity: ordered half-Heusler semiconductors”, *Phys. Rev. B* **101**, 064301 (2020).

Late stages in the ordering of magnetic Skyrmion lattices

Principal Investigator: Uwe C. Täuber (tauber@vt.edu)
Co-Principal Investigator: Michel Pleimling (pleim@vt.edu)
Department of Physics (MC 0435), Virginia Tech
Robeson Hall, 850 West Campus Drive, Blacksburg, Virginia 24061

Keywords: skyrmions, Magnus force, non-equilibrium relaxation, ordering, magnetic strip

Project Scope

This project aims at understanding relaxation processes of magnetic skyrmions in different systems. Magnetic skyrmions have been of great interest in the last decade as a potential candidate for both information storage and logic devices. Magnetic skyrmions are small topological defects that can be produced in a number of materials and are generally stabilized by strong spin-orbit coupling. The behavior of magnetic skyrmions has been intensively explored in the last few years. We had previously explored the effect of the Magnus force on the relaxation of magnetic skyrmions [1]. Recently we examined the late stages of ordering in these systems when very few imperfections remain in the lattice [2]. The effect of both the Magnus force and thermal fluctuation were examined. We utilize a coarse-grained particle-like representation of the dynamics of magnetic skyrmions in terms of stochastic equations of motion to probe their relaxation features and gain a comprehensive understanding of the interplay between the crucial Magnus force, the repulsive skyrmion-skyrmion interactions, and thermal as well as non-equilibrium fluctuations in disordered magnetic films. We also explore how these topological defects interact when confined on a thin magnetic strip.

Recent Progress

Late stage relaxation of magnetic skyrmions

We have conducted a detailed investigation into the late stages of ordering for magnetic skyrmions [2]. To conduct this research, a Langevin molecular dynamics program was used based on the coarse grain particle model previously derived [3]. Magnetic skyrmion lattices, due to the repulsive skyrmion-skyrmion interaction, want to form a triangular lattice. To measure the order of the lattice we used a Voronoi tessellation algorithm and counted the number of sides for each cell. Events were then defined as a change to the total number of six sided cells present in the system. When there were a few defects left in the lattice of skyrmions, the events become rare and can be separated by long periods. The events are binned to obtain smooth curves to build histograms that can be used to explore the behavior of the rare events in the late stages of ordering. The resulting histograms are then plotted as a function of time that an event occurs and also as a function of the difference in time of two consecutive events. The system we used to

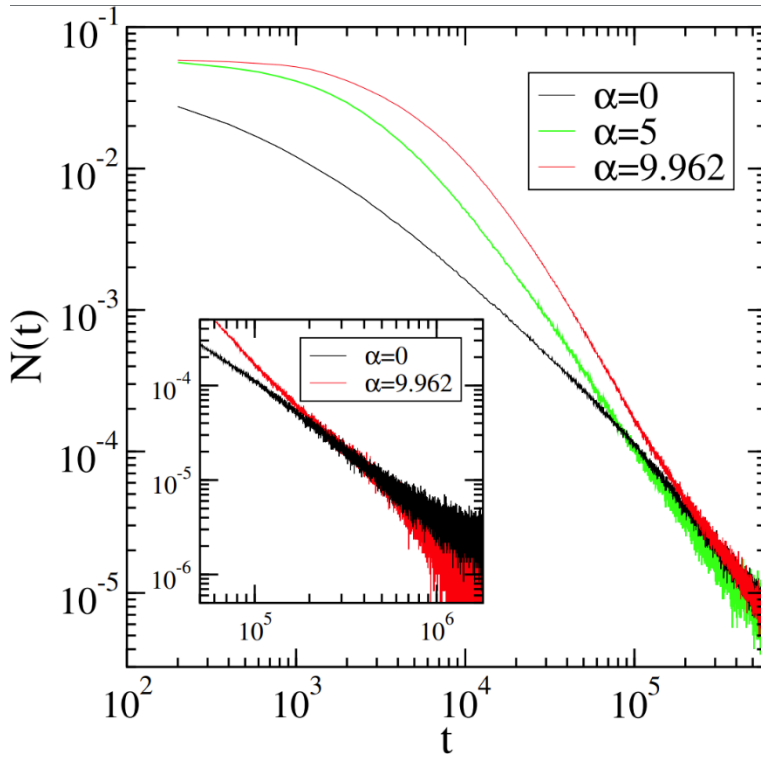


Fig. 1 Number N of events per skyrmion as a function of the number of time steps t since preparation of the system in a disordered initial state. Data are shown for different strengths of the Magnus force α . The inset highlights that with Magnus force the long-time algebraic decay is governed by a different exponent than without this force. From [2].

examine these effects was free of any repulsive or attractive pins. Initially, the systems were prepared in a disordered state with constant skyrmion density across runs. The only constraint for the initial positions of the skyrmions was that no two skyrmions overlapped, as this is an assumption made by the particle model. The histograms showed different dynamic regimes as the system evolved. Of particular interest were the algebraic tails that were similar to other processes with rare events. We showed that similar to earlier time regimes, for the relaxation of the lattice at later time regimes, in the absence of thermal noise, the Magnus force led to faster relaxation of the system. This can be seen in Figure 1. This figure shows the histogram of the events as a function of time, where α denotes the ratio of the Magnus coefficient to the dampening coefficient. It can be seen in the figure that as the Magnus force is increased, the algebraic tails, when plotted, decay faster. This was also

seen to be the case in the pair correlation function, and the resulting correlation length obtained from this data. Interestingly, when the histograms were plotted as a function of the difference in time, almost the entire curve showed algebraic decay.

In this work, the system was also examined for cases where $T > 0$. Thermal fluctuations of varying size were added to better understand the effect of thermal noise on these processes (see Figure 2). It has been previously shown that when thermal noise is added to these systems, the Magnus force enhances the disorder in the system. We show that when a large Magnus force is present, for small values of noise, the algebraic tails are largely unaffected. When the noise level is increased even further, the presence of the Magnus force leads to additional fluctuations that prohibits the ordering of the lattice. In addition, the number of events is constant through time,

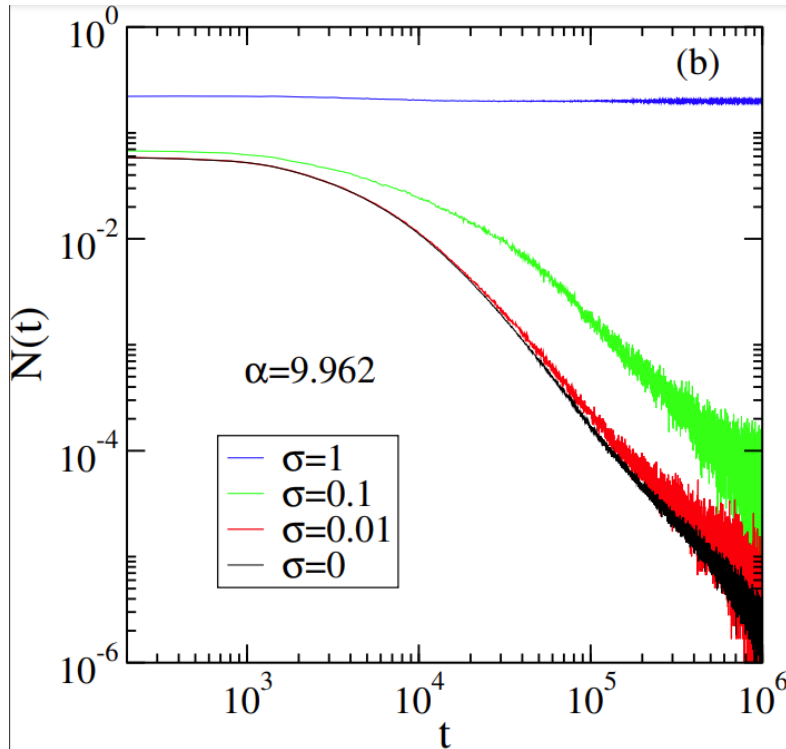


Fig. 2: Number N of events per skyrmion as a function of the number of time steps t for various strengths of the thermal noise. With a Magnus force of strength $\alpha = 9.962$. Other system parameters are set at $L = 72$ and $\lambda = 7\xi$. The data are the average of at least 1,000 independent runs. From [2].

leading to the conclusion that the lattice has, in effect, melted. When there is no Magnus force present, low levels of noise see a similar effect as when a Magnus force is present, but at high noise levels, the system still shows a decay in the number of events as a function of time.

Future Plans

Relaxation of skyrmions in a channel

Until recently [4], no works had examined this particle model with many skyrmions confined to a channel. This geometry is of great interest, given the proposed applications for magnetic skyrmions. We are planning [5] on examining the behavior of skyrmions in this specific

geometry. We plan on examining how the relaxation of the skyrmions differs when the lattice is confined to these tracks that have repulsive potentials near the walls that can be overcome, leading to annihilation of the skyrmions. The form of the potential will be based on the work [6]. To do this, we will similarly start with a disordered system, again similarly constrained by no overlapping skyrmions. We will also work in a regime without pinning or attractive defects in the system, and with no thermal noise. To understand the behavior of skyrmions in the system, a driving force will be applied that is parallel to the walls of this channel. In presence of a Magnus force this will cause the skyrmions to be biased to one side of the channel as the Magnus force deflects them due to the drive. Initially, we will examine qualitatively the distribution of the skyrmions for different widths of the channel. We then plan on measuring the average nearest neighbor distance to be able to quantify when the system has reached a quasi-steady state. This will be characterized by the average nearest neighbor distance becoming constant in time. We also plan on examining how a periodic drive might affect the ordering of the system, due to the applicability of this in potential applications (Figure 3 shows first results from an exploratory study). We expect that these periodic drives, where the drive is switching off for substantially long enough times, will cause the system to reach a new steady. Skyrmions will be further from

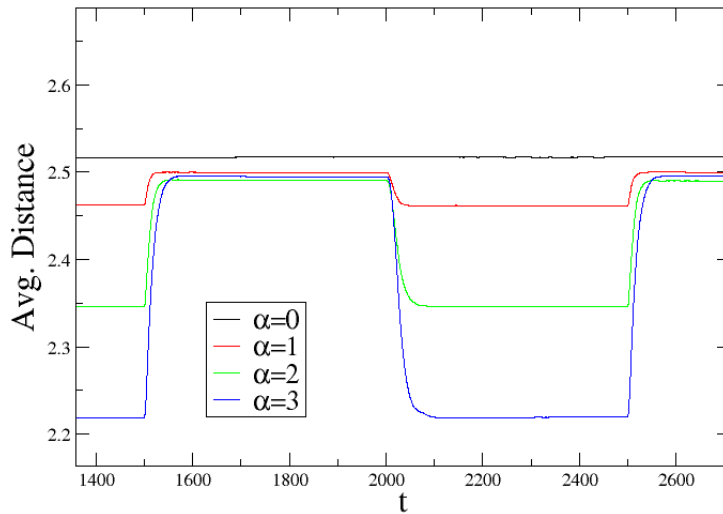


Fig. 3: The average distance in between nearest neighbor skyrmions with a slow periodic drive. The system is 100 by 10 skyrmion radii, prepared initially with 100 skyrmions. The drive is on/off for 50,000 for integration timesteps with a step value of $dt=0.01$. This was done for 400 independent realizations.

the potential walls and the drive is not forcing them to congregate to one side of the system. First results indicate that the Magnus force has the opposite effect on the relaxation of this system when compared to a non-driven system prepared in some initially disordered state. This means that the correlations that are formed result in the Magnus force slowing down the relaxation of the system when the drive is switched off and on.

References

1. B. L. Brown, U. C. Täuber, and M. Pleimling, *Effect of the Magnus force on skyrmion relaxation dynamics*, Phys. Rev. B **97**, 020405(R) (2018).
2. J. Stidham and M. Pleimling, *Late stages in the ordering of magnetic skyrmion lattices*, Phys. Rev. B **102**, 144434 (2020).
3. S.-Z. Lin, C. Reichhardt, C. D. Batista, and A. Saxena, *Particle model for Skyrmions in metallic chiral magnets: Dynamics, pinning, and creep*, Phys. Rev. B **87**, 214419 (2013).
4. A. K.C. Tan, P. Ho, J. Lourebam, L. Huang, H. K. Tan, C. J.O. Reichhardt, C. Reichhardt, and A. Soumyanarayanan, *Visualizing the Strongly Reshaped Skyrmion Hall Effect in Multilayer Wire Devices*, Nat. Commun. **12**, 4252 (2021).
5. J. Stidham and M. Pleimling, in progress.
6. N. Nagaosa and Y. Tokura, *Topological properties and dynamics of magnetic Skyrmions*, Nature Nanotech **8**, 899–911 (2013).

Publications (August 2019 - July 2021)

1. B. L. Brown, and U. C. Täuber, and M. Pleimling, *Skyrmion relaxation dynamics in the presence of quenched disorder*, Phys. Rev. B **100**, 024410 (2019).
2. H. Chaturvedi, U. Dobramysl, M. Pleimling, and U. C. Täuber, *Critical scaling and aging near the flux line depinning transition*, Phys. Rev. B **101**, 024515 (2020).
3. J. Stidham and M. Pleimling, *Late stages in the ordering of magnetic skyrmion lattices*, Phys. Rev. B **102**, 144434 (2020).

Unconventional metals in strongly correlated systems

T. Senthil, Massachusetts Institute of Technology

Program Scope

Unconventional metals that depart from the textbook paradigm of fermi liquid theory are increasingly commonly found in many materials but yet they remain amongst the most mysterious. The research program supported by this award seeks to develop a foundation for understanding these `strange' metals. The approach taken by the PI is multi-pronged. First he will pursue obtaining new (or strengthening existing) general model-independent constraints on such non-fermi liquid metals that follow from general principles like symmetry and its realization and are independent of the detailed Hamiltonian. Second, he will construct specific microscopic models to see how these constraints are realized in concrete situations. Third he will seek implications of these general constraints for experiments, and develop a phenomenological understanding of experiments. Finally he will use the insights developed from experiments to refine the general theoretical understanding and the construction of microscopic models.

Keywords: 1. Strange metal transport

2. Non-fermi liquids

Recent Progress

In his recent work, the PI obtained general constraints[1] on the emergent low energy symmetries of any clean (i.e lattice translation invariant) strange metal. These constraints may be viewed as a generalization of the Luttinger theorem of ordinary Fermi liquids. Many, if not all, non-Fermi liquids will have the same realization of emergent symmetry as a Fermi liquid (even though they could have very different dynamics). Such phases - dubbed ersatz Fermi liquids - share some (but not all) universal properties with Fermi liquids. In [2,3] he discussed the implications for understanding the strange metal physics observed in experiments. Combined with a few experimental observations, these general model-independent considerations lead to concrete predictions about a class of strange metals. The most striking of these is a divergent susceptibility of an observable that has the same symmetries as the loop current order parameter.

Future Plans

The PI is currently studying concrete theoretical models that illustrate the general ideas developed in his previous work. An interesting model is one that describes the quantum critical point associated with the onset of loop current order in a metal. In the near future he hopes to apply the insights gained from this and previous studies to obtain general results on magnetotransport, thermal conductivity and thermoelectric effects in clean strange metals.

References

1. Non-Fermi liquids as ersatz Fermi liquids: general constraints on compressible metals, Dominic V. Else, Ryan Thorngren, T. Senthil, Phys. Rev. X 11, 021005 (2021).
2. Strange metals as ersatz Fermi liquids, Dominic V. Else, T. Senthil, Phys. Rev. Lett. 127, 086601 (2021).
3. Critical drag as a mechanism for resistivity, Dominic Else, T. Senthil, <https://arxiv.org/abs/2106.15623>

Publications

1. Critical drag as a mechanism for resistivity, Dominic Else, T. Senthil, <https://arxiv.org/abs/2106.15623>
2. Strange metals as ersatz Fermi liquids, Dominic V. Else, T. Senthil, Phys. Rev. Lett. 127, 086601 (2021).
3. Non-Fermi liquids as ersatz Fermi liquids: general constraints on compressible metals, Dominic V. Else, Ryan Thorngren, T. Senthil, Phys. Rev. X 11, 021005 (2021).
4. Bose-Luttinger Liquids, Ethan Lake, T. Senthil, Ashvin Vishwanath, Phys. Rev. B 104, 014517 (2021)
5. Entanglement Clustering for ground-stateable quantum many-body states, Michael Matty, Yi Zhang, T. Senthil, Eun-Ah Kim, Phys. Rev. Research 3, 023212 (2021).
6. Exciton-mediated coherent magnon generation in a van-der-Waals antiferromagnet, Carina A. Belvin, Edoardo Baldini, Ilkem Ozge Ozel, Dan Mao, Hoi Chun Po, Clifford J. Allington, Suhan Son, Beom Hyun Kim, Jonghyeon Kim, Jae Hoon Kim, Je-Geun Park T. Senthil, Nuh Gedik, Nature Communications 12, 4837 (2021).
7. Slow scrambling and hidden integrability in a random rotor model, Dan Mao, Debanjan Chowdhury, T. Senthil, Phys. Rev. B 102, 094306 (2020).

8. Modeling the pseudogap metallic state in cuprates: quantum disordered pair density wave, Zhehao Dai, T. Senthil, Patrick A. Lee, *Phys. Rev. B* 101, 064502 (2020).
9. Strange metal in magic-angle graphene with near Planckian dissipation, Yuan Cao, Debanjan Chowdhury, Daniel Rodan-Legrain, Oriol Rubies-Bigordà, Kenji Watanabe, Takashi Taniguchi, T. Senthil, Pablo Jarillo-Herrero, *Phys. Rev. Lett.* 124, 076801 (2020).
10. Faithful Tight-binding Models and Fragile Topology of Magic-angle Bilayer Graphene, Hoi Chun Po, Liujun Zou, T. Senthil, Ashvin Vishwanath, *Phys. Rev. B* 99, 195455 (2019).
11. Landau Level Degeneracy in Twisted Bilayer Graphene: Role of Symmetry Breaking, Ya-Hui Zhang, Hoi Chun Po, T. Senthil, *Phys. Rev. B* 100, 125104 (2019).
- 12.. Spectroscopy signatures of tunable electron correlation in a trilayer graphene/hBN Moire superlattice, Jixian Yang, Guorui Chen, Qihang Zhang, Ya-Hui Zhang, Lili Jiang, Bosai Lyu, Hongyuan Li, Kenji Watanabe, Takashi Taniguchi, Zhiwen Shi, T. Senthil, Yuanbo Zhang, Feng Wang, Long Ju (under review in *Science*)

Orbital-free Quantum Simulation Methods for Applications to Warm Dense Matter

Principal Investigator: Samuel B. Trickey, Dept. of Physics, Univ. Florida, Gainesville FL 32611-8435 co-PI: J.W. Dufty (Physics, Univ. Florida)

Program Scope

From basic theory, we construct innovative methods for predictive simulation of highly challenging materials systems. That includes both extreme state conditions (high pressure P and temperature T) and complicated aggregates of very large molecular constituents. Extreme P , T occur in giant planet interiors and in the state trajectory of inertial confinement fusion. Intricate condensed phases of very large molecules show up in hydrogen storage, magnetic materials, and myriad other emerging materials-based technologies.

A remarkable, un-anticipated very recent outcome is our discovery [Publication 1] of *qualitatively incorrect* predictions of a continuous liquid-liquid phase transition (LLPT) in dense hydrogen from a highly touted machine-learning potential (MLP)[1].

A little background is needed. Ab initio molecular dynamics (AIMD) currently is the best practice for treating extreme condensed systems. In AIMD, the ions follow classical dynamics with Born-Oppenheimer forces from quantum electrons. Cost-accuracy balance makes free-energy density functional theory (DFT) [2] the best choice for the quantum part. That implicates development of reliable free-energy exchange-correlation (XC) functionals with proper $T=0$ K limits. We have played a leading role in that work. To accelerate AIMD-DFT, we also develop orbital-free DFT non-interacting functionals. See Recent Progress, below. Such development necessitates extensive ordinary AIMD-DFT calculations.

Ref. [1] raised a serious issue of methodological impact on predicted materials physics. The hydrogen LLPT is an insulator-to-metal conversion via dissociation of H_2 to atomic H. Ref. [1] claims that the LLPT is a continuous transition, contrary to all previous AIMD-DFT and coupled-electron-ion Monte Carlo results (see citations in Publ. 1). It claims that those calculations are flawed because of finite-size effects (small numbers of atoms) that drive the spurious formation of defective solid regions. It also claims the MLP trained on $\approx 39,000$ small systems (108 atoms) and 1,800 larger ones (512 atoms) drives MD reliably at much larger system sizes (up through 1,728 atoms) for longer times to surmount those limitations.

In Publ. 1 we showed that in fact the MLP-MD fails to reproduce the AIMD-DFT it is supposed to mimic for systems up through 2048 atoms. Fig. 1 shows the H density as a function of T at $P=250$ GPa. For 256, 512, and 2048 atoms, the AIMD-DFT results are the same – an abrupt jump at the LLPT. The MLP-MD density curve for 1728 atoms is smooth. This is typical of the MLP-DFT. The MLP is not a faithful replica of the underlying DFT. Its outcomes suggest a faulty smooth interpolation between the two phases.

Our large system results are fully consistent with our previous LLPT findings and prior literature. In Publ. 3 we did very thorough AIMD-DFT calculations of the LLPT for both H and D that had the novel methodological feature of completely consistent usage of the SCAN [3] and de-orbitalized SCAN [4] XC functionals. We also had done path integral MD to assess nuclear quantum effects and their dependence on methodology (Publ. 3, 6); see below. Everything is

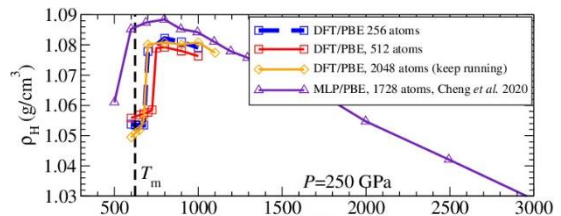


Fig. 1. H density as function of T at 250 GPa..

consistent with the conclusion that the LLPT is sharp and first order. *Finding: The MLP-MD results in Ref. [1] are wrong. This is a strong cautionary note regarding recent enthusiasm for unfettered use of ML techniques.*

Keywords: free energy density functional theory, orbital-free density functional theory, matter under extreme conditions

Recent Progress

Since project inception, we have worked to bring free-energy DFT to the point of real applicability with a sound formal basis (i.e. non-empirical functionals with proper finite-T behavior and proper T=0K limits). We produced the first purely Monte-Carlo-based local-spin-density approximation (LSDA) XC free-energy functional \mathcal{F}_{xc} [5] (analogous with the T=0K Perdew-Zunger LSDA) and the first internally consistent generalized gradient approximation (GGA) \mathcal{F}_{xc} [6].

Simulation of matter *in extremis* also stimulates demand for an AIMD version that scales linearly with the number of occupied states (i.e., system size and/or T), *irrespective of system state* instead of the nominal cubic scaling of ordinary Kohn-Sham AIMD. Orbital-free DFT (OF-DFT) in principle meets that demand. It adds the need for accurate approximations for the non-interacting free energy \mathcal{F}_s (at T=0K, the KS kinetic energy \mathcal{T}_s). Thus, we produced the first pseudo-potential adapted non-interacting free energy \mathcal{F}_s (LKT-F) (Publ. 7) and innovated by deorbitalizing ground-state meta-GGA XC functionals usable in OF-DFT calculations, i.e. linear-scaling meta-GGA [4].

Progress, however, was hampered by the Covid-19 pandemic, including lack of in-person discussions and having the newest postdoctoral working from Washington state for several months.

Challenging Physical System Examples - Regarding the Hydrogen LLPT mentioned above, Fig. 2, from Publ. 3 shows the DC conductivity (upper) and HOMO-LUMO gap (lower) as a function of T for two densities from AIMD-DFT (“BOMD” in the figure) and path-integral MD (PIMD) to estimate nuclear quantum effects (NQEs). The horizontal line at 2,000 Siemen/cm indicates a widely used criterion for transition to conduction. NQEs lower the predicted transition and sharpen it. Not shown (space constraints) is the detailed study in Publ. 3 showing that consistent use of the formally best-justified meta-GGA XC functional, SCAN [3], and its de-orbitalized counterpart SCAN-L [4] provide better agreement with experiment than all previous DFT studies. Conductivity calculations were done with our previously published Kubo-Greenwood code, KGEC [7].

Almost concurrently, in Publ. 6 we examined NQEs on the equation of state and the radial distribution functions for two-temperature H systems. Those had ion and electron temperatures $300 \leq T_i \leq 14610\text{K}$, $T_e = 20, 50, \text{ and } 100 \text{ kK}$ respectively. Such transient out-of-equilibrium, steady-state systems are achievable in laser experiments. We showed that OF-DFT with our LKT-F \mathcal{F}_s (Publ. 7) and corrKSDT LSDA XC free energy [5] agreed reasonably with conventional KS AIMD. Then we did OF-DFT-PIMD and found NQEs to be meaningful in the two-T case for the ratio of the ionic thermal de Broglie wavelength to the ionic Wigner-Seitz radius $\lambda_{\text{ion}} / (2 r_{s,\text{ion}}) \geq 0.3$.

Warm dense systems commonly are immersed in substantial magnetic fields. That is little-treated in WDM studies. Our strategic focus on OF-DFT has led us to de-orbitalization of advanced

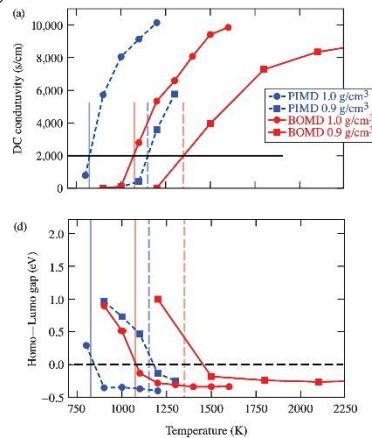


Fig. 2 *H* conductivity (upper) and HOMO-LUMO gap as function of *T*.

meta-GGA \mathcal{F}_{xc} [4]. It provides a unique perspective on predicted magnetization, since the orbital dependence can be isolated. In [Publ. 10](#) we used that advantage to diagnose the cause of SCAN over-magnetizing elemental $3d$ elemental solids. We found that the misbehavior arises from a peculiarity of the SCAN switching function which de-orbitalization mitigates unintentionally.

Innovative Functionals – We constructed the aforementioned LKT-F ([Publ. 7](#)) non-interacting free-energy functional \mathcal{F}_s to satisfy important constraints when pseudo-densities (not natural Coulombic densities) are used, the case in almost all simulations. [Publ. 7](#) showed both how to do the finite-T generalization of our earlier LKT (T=0K) [8] and that LKT-F is superior to other one-point KEDFs.

OF-DFT also drives us to continue to try to squeeze as much as possible out of GGA XC approximations and their finite-T generalizations. Three papers examined that challenge, including a non-separable functional (XC together), [Publ. 4](#); correction of electron affinities, [Publ. 8](#); and a GGA with nearly correct X asymptotics and a derivative discontinuity estimate, [Publ. 12](#). Then, in [Publ. 9](#), we did numerical tests of the limitations of a regularization for the SCAN XC functional, a matter of importance for computational stability and for de-orbitalization (for OF-DFT).

Theoretical Foundations Understanding the relationship of free-energy DFT with the microscopic origins of macroscopic continuum dynamics continues to be of importance both because of the possibility of novel approximations and as a corrective to some of the recently popular “quantum hydrodynamics” phenomenological treatment. In [Publ. 5](#) we used results from non-equilibrium statistical mechanics to construct an exact generalized hydrodynamics representation. [Publ. 2](#) investigated consequences of local pressure definitions from thermodynamics and mechanics, again both of intrinsic interest and of interest because of the use of local (one-point) approximations in DFT applications.

In [Publ. 11](#), we also presented a critical analysis of free-energy representations from quantum Monte Carlo calculations on the homogeneous electron gas (HEG). Detailed numerical comparisons show that some criticisms of corrKSDT \mathcal{F}_{xc} are unfounded. In fact, the two published representations are indistinguishable. More importantly, we showed that the HEG specific heats associated with both of the representations exhibit unphysical behavior for $0.1 \leq T/T_{\text{Fermi}} \leq 1$, $r_s \geq 10$. Additional QMC data is needed for that regime, followed, we speculated, by refined fitting forms.

Future Plans

The PI, with M. Pavanello (Rutgers), Wenhui Mi (Jilin University), and Kai Luo (Nanjing University of Science and Technology, formerly of our group), is completing a massive review (144 pages of manuscript text, 642 references) of ground state OF-DFT for *Chemical Reviews*. The review includes thorough treatment of the construction of both one-point and two-point kinetic energy density functionals (KEDFs), the constraints they satisfy and their limitations, algorithms and numerical techniques for solving the OF-DFT variational problem, and selected application examples from recent literature. Progress on ground-state KEDFs is important in its own right for T=0K AIMD but also important because such KEDFs are the T=0K limit for \mathcal{F}_s approximations. Completion is expected before the end of calendar 2021.

We have resumed (after COVID-19 interruption) work to extend our r^2 SCAN-L mGGA ground-state XC functional [9] into a free-energy functional \mathcal{F}_{xc} . That extension utilizes formulations developed earlier in this project [10]. The result will be the most sophisticated \mathcal{F}_{xc} extant. The primary remaining difficulty is the instability of algorithms in the Profess 3.0 code [11] for functionals with $\nabla^2 n$ dependence such as r^2 SCAN-L. Demonstration calculations on the H LLPT problem and on some warm dense system such as Al will follow, along with code patches release.

We will complete and publish a study of extending uniform density scaling [12] to two-point KEDFs that is well along. A key finding is that density-independent kernels such as those of Wang-Teter type, do not scale correctly.

As to other theoretical underpinnings, the co-PI is leading an effort to extend to $T > 0\text{K}$ the time-dependent DFT (tdDFT) formulation of Ruggenthaler et al. [13] The fixed-point analysis that seemingly solves the non-analytic potential problem in the original Runge-Gross tdDFT appears to go through essentially unchanged upon converting from pure to ensemble states. However, that preserves the so-far unresolved difficulty with the $T = 0\text{K}$ proof, namely that the fixed-point scheme itself is not fully justified. Apparently, only essentially trivial solutions for the key differential equation in the $T=0\text{K}$ case are known.

We still need to extend the corrKSDT LSDA XC functional (recall above) to fully polarized systems and include additional quantum Monte Carlo data [14,15] for low r_s . This is collaborative work with V.V. Karasiev (U. Rochester). Completion is dependent upon his time commitments. The same is true for ongoing support of the KGEC code (see above), an unresolved issue.

References

Note: Refs. 4-8, 10, and the second entry in 12 are work from this project in prior reporting periods

- [1] B. Cheng, G. Mazzola, C.J. Pickard, and M. Ceriotti, *Nature* **585**, 217-220 (2020)
- [2] N.D. Mermin, *Phys. Rev.* **137**, A1441 (1965)
- [3] J. Sun, A. Ruzsinszky, and J. P. Perdew, *Phys. Rev. Lett.* **115**, 036402 (2015)
- [4] D. Mejía-Rodríguez and S.B. Trickey, *Phys. Rev. B* **98**, 115161 (2018)
- [5] V.V. Karasiev, T. Sjöstrom, J.W. Dufty, and S.B. Trickey, *Phys. Rev. Lett.* **112**, 076403 (2014)
- [6] V.V. Karasiev, J. W. Dufty, and S.B. Trickey. *Phys. Rev. Lett.* **120**, 076401 (2018)
- [7] L. Calderín, V.V. Karasiev, and S.B. Trickey, *Comput. Phys. Commun.* **221**, 118 (2017); arXiv 1707.08437
- [8] Kai Luo, V.V. Karasiev, and S.B. Trickey, *Phys. Rev. B* **98**, 041111(R) (2018); arXiv 1806.05205
- [9] D. Mejía-Rodríguez and S.B. Trickey, *Phys. Rev. B* **102**, 121109(R) (2020); arXiv 2008.12420
- [10] V.V. Karasiev, Travis Sjöstrom, and S.B. Trickey, *Phys. Rev. B* **86**, 115101 (2012).
- [11] M. Chen, J. Xia, C. Huang, J.M. Dieterich, L. Hung, I. Shin, and E.A. Carter, *Computer Phys. Commun.* **190**, 228 (2015)
- [12] M. Levy and J. P. Perdew, *Phys. Rev. A* **32**, 2010 (1985); J.W. Dufty and S.B. Trickey, *Phys. Rev. B* **84**, 125118 (2011)
- [13] M. Ruggenthaler, M. Penz, and R. van Leeuwen, *J. Phys. Condens. Matter* **27**, 203202 (2015)
- [14] T. Dornheim, S. Groth, T. Sjöstrom, F.D. Malone, W.M.C. Foulkes, and M. Bonitz, *Phys. Rev. Lett.* **117**, 156403 (2016)
- [15] S. Groth, T. Dornheim, T. Sjöstrom, F.D. Malone, W.M.C. Foulkes, and M. Bonitz, *Phys. Rev. Lett.* **119**, 135001 (2017)

Publications (2019– present)

All publications, codes, and other software are available from <http://www.qtp.ufl.edu/ofdft>

- [1] “On the Liquid - liquid Transition of Dense Hydrogen”, Valentin V. Karasiev, Joshua Hinz, S.X. Hu, and S.B. Trickey, *Nature*, submitted 26 Dec. 2020; accepted 12 Aug. 2021; arXiv 2012.13835
- [2] “Local Pressure for Inhomogeneous Fluids”, James Dufty, Jeffrey Wrighton, and Kai Luo [AICHE Journal, **67**, e17323 [9 pp] (2021); arXiv 2008.11709
- [3] “Fully Consistent Density Functional Theory Determination of the Insulator-Metal Transition Boundary in Warm Dense Hydrogen”, Joshua Hinz, Valentin V. Karasiev, S.X. Hu, Mohamed Zaghoo, Daniel Mejía-Rodríguez, S.B. Trickey, and L. Calderín, *Phys. Rev. Res.* **2**, 032065(R) [7 pp] (2020); arXiv 2002.05594v2
- [4] “Generalized Gradient Approximations with Local Parameters”, Angel Albavera-Mata, Karla Botello-Mancilla, S. B. Trickey, José; L. Gázquez, and Alberto Vela, *Phys. Rev. B* **102**, 035129 [11 pp] (2020)
- [5] “Generalized Hydrodynamics Revisited”, J. Dufty, Kai Luo, and J. Wrighton. *Phys. Rev. Res.* **2**, 023036 [19 pp] (2020); arXiv 2002.01549
- [6] “Two-temperature Warm Dense Hydrogen as a Test of Quantum Protons Driven by Orbital-free Density Functional Theory Electronic Forces”, Dongdong Kang, K. Luo, K. Runge, and S.B. Trickey, *Matter Radiat. Extremes* **5**, 064403 [12 pp] (2020)
- [7] “Towards Accurate Orbital-free Simulations: a Generalized Gradient Approximation for the Non-interacting Free-energy Density Functional”, K. Luo, V.V. Karasiev, and S.B. Trickey [Phys. Rev. B **101**, 075116 [9 pp] (2020); arXiv 2001.10602
- [8] “Negative Electron Affinities and Derivative Discontinuity Contribution from a Generalized Gradient Approximation Exchange Functional”, J. Carmona-Espíndola, J.L. Gázquez, Alberto Vela, and S.B. Trickey, *J. Phys. Chem. A* **124**, 1334-1342 (2020)
- [9] “Comment on ‘Regularized SCAN functional’” [J. Chem. Phys. **150**,161101 (2019)], Daniel Mejía-Rodríguez and S.B. Trickey, *J. Chem. Phys.* **151**, 207101 [2 pp] (2019)
- [10] “Analysis of Over-magnetization of Elemental Transition Metal Solids from the SCAN Density Functional”, Daniel Mejía-Rodríguez and S.B. Trickey, *Phys. Rev. B* **100**, 041113(R) [5 pp] (2019); arXiv 1905.01292
- [11] “Status of Free-energy Representations for the Homogeneous Electron Gas”, V.V. Karasiev, S.B. Trickey, and J.W. Dufty, *Phys. Rev. B* **99**, 195134 [8 pp] (2019)
- [12] “Generalized Gradient Approximation Exchange Functional with Near-best-semilocal Performance”, J. Carmona-Espíndola, J.L. Gázquez, Alberto Vela, and S.B. Trickey, *J. Chem. Theory Comput.* **15**, 303-310 (2019)

Interaction and Transport Effects in Driven Magnetic and Topological Materials

Wang-Kong Tse

Department of Physics and Astronomy

University of Alabama

Program Scope

The scope of this program encompasses investigations of fundamental non-equilibrium effects arising from magnetic, transport and interaction-induced phenomena in periodically-driven low-dimensional materials and structures. Electronic band structures are known to become renormalized both on or off resonance under irradiation, with the renormalized bands occupied by a non-equilibrium distribution of photon-dressed electrons. One can tailor the parameters of driving field to design the system Hamiltonian to achieve the desired responses in the illuminated material. We have made considerable progress along the following directions: indirect exchange interaction between impurity spins, photo-modulated electron screening of charged impurities, photo-induced Hall transport, and strong-field magneto-optical effects.

Keywords: Non-Equilibrium, Light-Matter Interaction, Floquet Dynamics

Recent Progress

(1). Dynamically Tunable Indirect Exchange Interaction. We have investigated [1] the indirect exchange interaction between impurity spins that is mediated by two-dimensional electron systems irradiated by a periodic driving field. An important motivation is to explore the conditions for which such a spin-spin interaction can be dynamically tuned by the parameters of the driving field. We have examined the non-equilibrium steady state regime established under both resonant and off-resonant illumination. In the off-resonant regime, we have focused on graphene irradiated by a high-frequency circularly polarized light. To study the time-averaged exchange interaction modulated by light, we have developed a non-equilibrium theory for Ruderman-Kittel-Kasuya-Yosida (RKKY) interaction using the Floquet-Keldysh Green's function formalism. By achieving a control of the Fermi surface through a dynamical gating effect by light, we have found that the

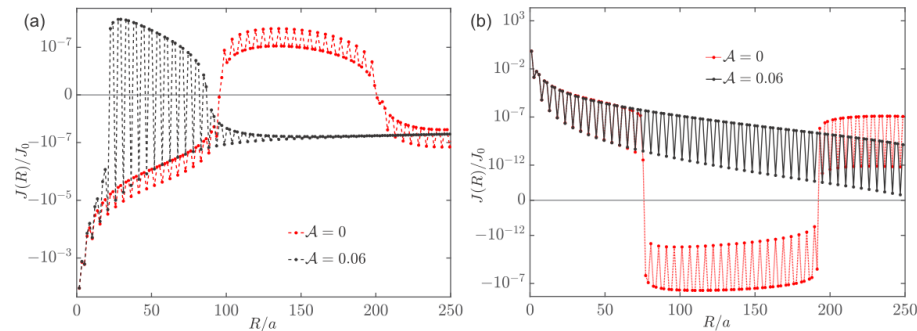


Fig.1: Time-averaged RKKY coupling as a function of distance for impurities situated on the same (left) and different (right) sublattice sites [1].

RKKY interaction can be tuned extensively including sign changes between ferromagnetic or anti-ferromagnetic coupling (Fig.1).

We have also studied [2] the case for resonant irradiation in 2D electron systems (2DESs), describable by a single parabolic band. The time-averaged spin susceptibility is found to exhibit multiple non-equilibrium Kohn anomalies that reflect photon-assisted scatterings between nested Fermi surfaces. To model the scenario of a 2D ferromagnet-metal-ferromagnet lateral heterostructure, we studied the time-averaged exchange interaction between two impurity spin chains. The exchange interaction displays RKKY oscillations with multiple spatial periods that are tunable by the laser field. By increasing the light-matter coupling, the optically induced energy shift exceeds the Fermi level, the oscillatory behavior is suppressed and the exchange interaction becomes purely ferromagnetic characterized by a fast spatial decay. Taken together, our investigations and findings for graphene and 2DES unravel the workings of Floquet-driven dynamical control of indirect exchange interactions in both off-resonant and resonant regimes.

(2). Periodically-Driven Screening of Charged Impurities. As another manifestation of the physics presented above, we have investigated [3] the effects on the screening response of a charged impurity in a 2DES under a Floquet drive. Using Floquet-Keldysh formalism we have formulated the time-averaged polarization function and dielectric function. Up to second-order light-matter coupling, we have obtained analytic results for the momentum dependence of these quantities, and elucidated the non-analyticity of the emergent non-equilibrium Kohn anomalies. The screened impurity potential exhibits Friedel oscillations with multiple spatial periods induced by photon-assisted scatterings (Fig.2). Increasing the Floquet drive so that the optically induced

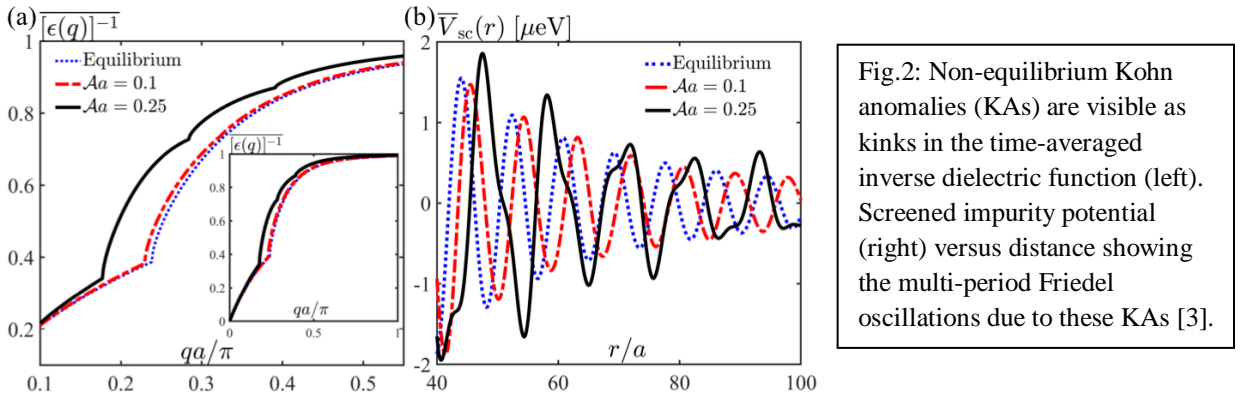


Fig.2: Non-equilibrium Kohn anomalies (KAs) are visible as kinks in the time-averaged inverse dielectric function (left). Screened impurity potential (right) versus distance showing the multi-period Friedel oscillations due to these KAs [3].

energy shift the Fermi level suppresses the Friedel oscillations and the time-averaged impurity potential becomes largely unscreened. Our results open up the intriguing possibility of Floquet engineering of Coulomb interactions and screening response in a many-body electron system.

(3). Photo-induced Geometric Transport. We have investigated [4] the anomalous Hall effect in 2D transition-metal dichalcogenides (TMDs) irradiated by a circularly polarized resonant pump field. Using the rotating wave approximation, we have analytically obtained the non-equilibrium steady-state solution of the density matrix kinetic equation and numerically calculated the

longitudinal and Hall photovoltaic transport in the TMD MoS₂. In the previous literature, an oversimplified picture is often used as a starting point of calculations, where the Fermi levels are simply taken to be unbalanced at different valleys under illumination. We do not adopt this assumption but instead opt to base our formulation on first principles. Putting both photon-induced band renormalization and non-equilibrium kinetic effects on an equal footing, this approach has allowed us to unveil the nuances in the actual physical picture underlying the phenomenon that were often missed in the previous literature.

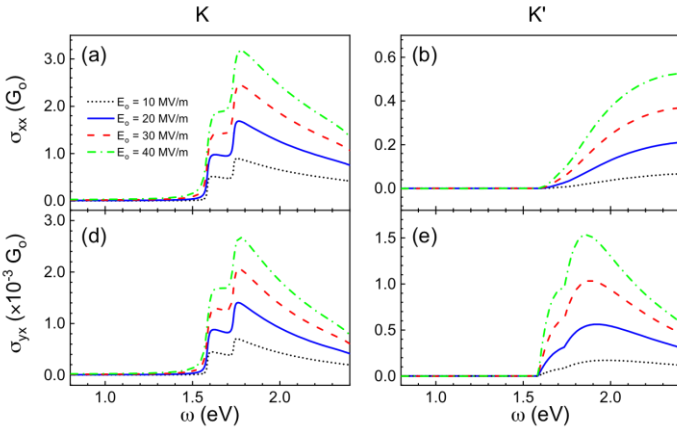


Fig.3: Time-averaged longitudinal [panels a and (b)] and anomalous Hall conductivities [panels (d) and (e)] as a function of pump field frequency, showing that both valleys contribute to the Hall conductivity with the same sign [4].

Our results show that the photon dressed electrons are excited to occupy a ring of resonant states in the vicinity of the induced dynamical gap. In the photovoltaic effect, these photon-dressed electrons are the carriers that contribute to the transport under an in-plane electric field. Our calculated anomalous Hall conductivity shows resonant enhancement features for optical frequencies reaching the transition energies between band edges of the same spin. Moreover, the geometric origin of the photo-induced anomalous Hall effect arises from light-induced interband coherence, rather than the interband coherence inherently present in the equilibrium band structure.

(4). Linear and Nonlinear Magneto-Optical Effects. We have recently revealed a previously overlooked effect of particle-hole asymmetry in certain topological insulators in the interpretation of magneto-optical Landau level (LL) spectroscopy data. In collaboration with experimental

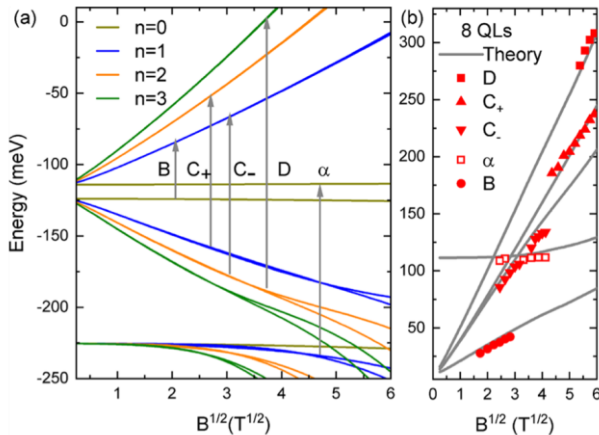


Fig.4: Calculated surface and bulk Landau levels for magnetic fields up to 36 T (left panel). Comparison of the theoretical transition energies show good agreement with experimental data (right panel) [5].

groups including those from Pennsylvania State University and National High Magnetic Field Laboratory, we have theoretically elucidated the observed LL structures in Sb_2Te_3 films at high magnetic fields. Taking into account the effects of thin film confinement, electron-hole asymmetry and Zeeman splitting without any fitting parameter, our approach yields results that closely agree with the measured data. Our work particularly highlights the oft neglected effects of electron-hole asymmetry in understanding surface-to-bulk LL transitions in topological insulators. This work is published in Refs. [5]-[6]. Current work includes investigation of the magneto-optical effects in topological insulators in the nonlinear regime.

Future Plans

We will generalize our non-equilibrium exchange coupling theory to address the regime of strong impurity scattering under irradiation. We will also continue to investigate interlayer exchange coupling to elucidate the interplay between magnetism and light-matter coupling under periodic driving conditions. One important aspect in non-equilibrium materials is electron-electron interaction effects. We will carry out diagrammatic perturbation theory to address various facets of electronic interaction effects in van der Waals heterostructures driven by a periodic driving field. Finally, we plan to continue investigating the nonlinear dynamic transport phenomena, including photocurrents and nonlinear optical conductivities using a two-pronged approach of diagrammatic perturbation theory and Floquet formalism.

References

1. M. Ke and W.-K. Tse, *Non-equilibrium RKKY interaction in irradiated graphene*, Phys. Rev. Research 2, 033228 (2020).
2. M. M. Asmar and W.-K. Tse, *Floquet Control of Indirect Exchange Interaction in Periodically Driven Two-Dimensional Electron Systems*, arXiv:2003.14383 (2020).
3. M. M. Asmar and W.-K. Tse, *Impurity Screening and Friedel Oscillations in Floquet-driven Two-dimensional Metals*, arXiv:2105.12269 (2021).
4. P. X. Nguyen and W.-K. Tse, *Photoinduced anomalous Hall effect in two-dimensional transition metal dichalcogenides*, Phys. Rev. B 103, 125420 (2021).
5. Y. Jiang, M. M. Asmar, X. Han, M. Ozerov, D. Smirnov, M. Salehi, S. Oh, Z. Jiang, W.-K. Tse, L. Wu, *Electron-Hole Asymmetry of Surface States in Topological Insulator Sb_2Te_3 Thin Films Revealed by Magneto-Infrared Spectroscopy*, Nano Lett. 2020, 20, 6, 4588–4593.
6. G. Gupta, M. M. Asmar, and W.-K. Tse, *Particle-hole asymmetry and quantum confinement effects on the magneto-optical response of topological insulator thin-films*, arxiv:2105.12275 (2021).

Publications

1. M. Ke and W.-K. Tse, *Non-equilibrium RKKY interaction in irradiated graphene*, Phys. Rev. Research 2, 033228 (2020).
2. M. M. Asmar and W.-K. Tse, *Floquet Control of Indirect Exchange Interaction in Periodically Driven Two-Dimensional Electron Systems*, arXiv:2003.14383 (2020).
3. M. M. Asmar and W.-K. Tse, *Impurity Screening and Friedel Oscillations in Floquet-driven Two-dimensional Metals*, arXiv:2105.12269 (2021).
4. P. X. Nguyen and W.-K. Tse, *Photoinduced anomalous Hall effect in two-dimensional transition metal dichalcogenides*, Phys. Rev. B 103, 125420 (2021).
5. Y. Jiang, M. M. Asmar, X. Han, M. Ozerov, D. Smirnov, M. Salehi, S. Oh, Z. Jiang, W.-K. Tse, L. Wu, *Electron–Hole Asymmetry of Surface States in Topological Insulator Sb₂Te₃ Thin Films Revealed by Magneto-Infrared Spectroscopy*, Nano Lett. 2020, 20, 6, 4588–4593.
6. G. Gupta, M. M. Asmar, and W.-K. Tse, *Particle-hole asymmetry and quantum confinement effects on the magneto-optical response of topological insulator thin-films*, arxiv:2105.12275 (2021).
7. J. Zeng, T. Hou, Z. Qiao, and W.-K. Tse, *Finite-size effects in the dynamical conductivity and Faraday effect of quantum anomalous Hall insulators*, Phys. Rev. B 100, 205408 (2019).

Nonequilibrium thermodynamics in magnetic nanostructures

Yaroslav Tserkovnyak (University of California, Los Angeles)

Keywords: Spin superfluidity, nonequilibrium topological textures, quantum entanglement dynamics

Program Scope

Quantum materials with strong spin correlations and/or magnetic order provide a rich playground for collective out-of-equilibrium phenomena driven by entropic forces. The latter can most simply be established by applying a temperature gradient to the system of interest. More generally, ensembles of mobile degrees of freedom can be biased to sustain gradients in their conjugate thermodynamic potentials, setting a stage for nonequilibrium thermodynamics. The ensuing cooperative phenomena, which, while generally dissipating energy, can give rise to striking emergent behavior not present in equilibrium. Quantum-mechanical degrees of freedom, such as electron spin, have proven to be invaluable to this end, as a medium that can intertwine different physical constituents forming coupled dynamics as well as transfer energy between them in a desired fashion.

The progress in this project is fueled by the versatility of the overarching phenomenologies of nonequilibrium thermodynamics as well as a growing availability of spin-active materials for constructing novel hybrid structures and devices. Much of our focus has progressively shifted towards insulating materials, with minimal dissipation, particularly at lower temperatures, while still exhibiting robust transport based on the motion of collective spin-carrying quasiparticles or topological spin-texture configurations. This allows us to explore unusual, sometimes seemingly hidden, transport properties, with a delicate interplay between the coarse-grained flows carried by the itinerant degrees of freedom and the coherent dynamics of the parent materials. We now appreciate that the pertinent flows may not only be associated with some local (pseudo)spin degrees of freedom, but also nonlocal topological textures that can be carried by dynamic distortions in the background order. The unifying principles based on the overall change in entropy and the thermodynamic forces that drive the collective dynamics, both coherent and incoherent, are still applicable and useful, however.

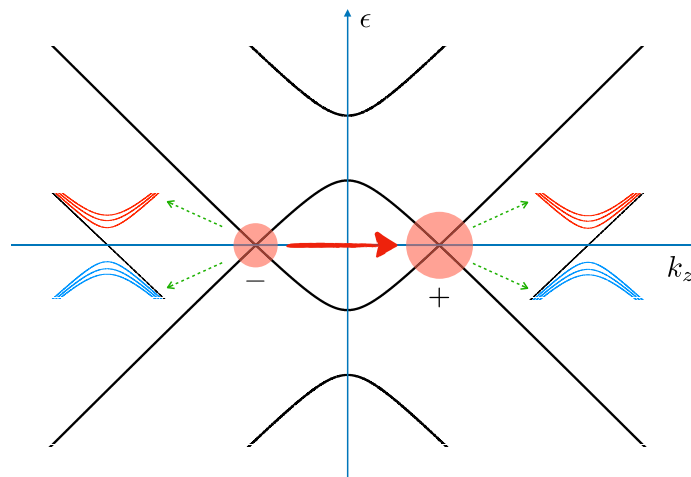
We are currently pursuing three research directions, which are mutually related and evolve from the prior work: (i) Incoherently pumped collective dynamics in noncollinear and other complex spin systems, (ii) Novel phenomena and circuits based on energy exchange with topological charge flows, and (iii) Multiple quantum-sensor integration with magnetic (nano)structures and quantum entanglement propagation out-of-equilibrium. Motivated in part by recent experimental progress, in the first of these topics, we are extending our efforts to magnetic materials where nuclear spin dynamics becomes prominent at lower temperatures, while electronic degrees of freedom essentially freeze out. In addition, we will develop further the understanding of noncollinear and frustrated magnets, and will venture to study and exploit the fascinating interplay of spin and valley

degrees of freedom in magnetic Weyl semimetals. In the second thrust, we are aiming to study hydrodynamic cross-coupling effects between the fluxes of conserved topological “charges” associated with spin textures (such as vortices and hedgehogs), on the one hand, and conventional thermoelectric or spintronic flows, on the other. We will propose higher-level circuit and device concepts, in order to validate and utilize these ideas. Finally, in the third research topic, we will study quantum-information flow between a complex quantum material and multiple quantum-impurity sensors assembled on its surface. A particular focus here will be on (thermo)dynamic manipulations of the substrate material, whose ensuing (nonequilibrium) quantum correlations are both imprinted on and probed by the appropriately tailored quantum sensors.

Recent Progress

Here, I will touch upon three highlights from the most recent work. The full publication list for the work supported by this Award is appended below, for the last two years.

In Ref. [6], we studied *Magnetic Dynamics with Weyl Fermions*. Transport of charge and valley (axial) degrees of freedom coupled to order-parameter dynamics in magnetic Weyl semimetals is investigated here in the framework of nonequilibrium thermodynamics. In addition to the established valley-related transport anomalies that are rooted in band-structure topology, we construct dissipative couplings between the three dynamic constituents of the system driven out of

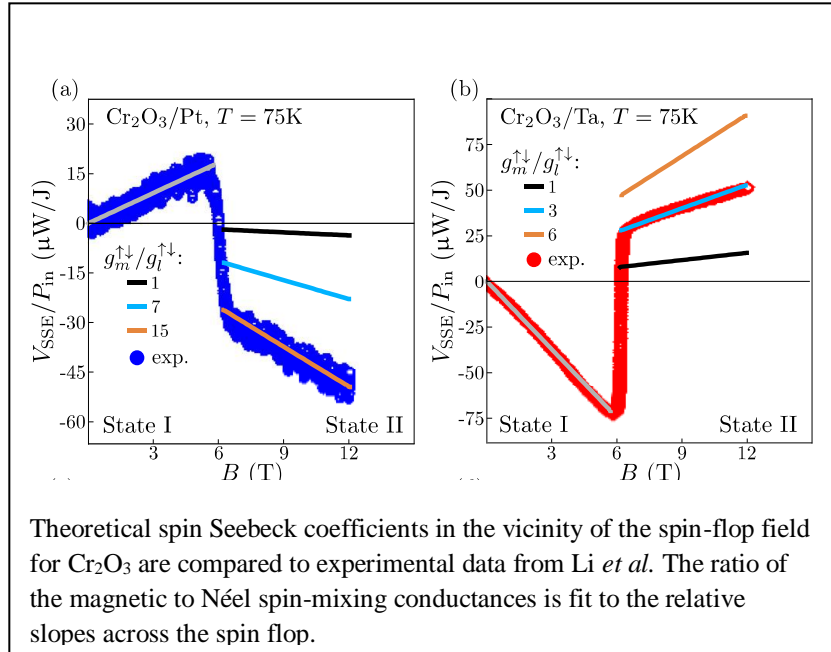


Two linearly-dispersing (nondegenerate) Weyl points in a four-band model with magnetism. The solid circles at the \pm Weyl points schematically designate the corresponding (valley-dependent) chemical potentials. The red arrow depicts the quantized Berry flux between the Weyl points. The zoom-out insets flanking the Weyl points show the Landau-level dispersions in the presence of a magnetic field along the z axis. Spectral flow along the zeroth Landau levels governs the chiral anomaly, which controls the coupled charge-valley dynamics, while the magnetic modulation of the Weyl-point positions in momentum space governs the valley-spin gauge coupling. Putting these together, the valley degree of freedom mediates a plethora of dynamic magnetoelectric phenomena, enriching the phenomenology and control of magnetic dynamics.

equilibrium by electromagnetic perturbations. We show how the valley degree of freedom mediates an effective coupling between the charge and magnetic sectors of the system, through a combination of the chiral anomaly, on the electric side, and the Onsager-paired valley torque and pumping, on the magnetic side. This work complements previous studies of magnetic Weyl semimetals by a more systematic analysis of collective dissipation. We discuss several concrete examples of the valley-mediated current-driven magnetic instabilities and charge pumping, and extend the theory to the antiferromagnetic case.

Ref. [10] resulted from a theory-experiment collaboration between UCLA and UC Riverside. Motivated by their experimental work, we developed a low-temperature, long-wavelength theory for the *interfacial spin Seebeck effect (SSE) in easy-axis antiferromagnets*. The field-induced spin-flop (SF) transition of Néel order is associated with a qualitative change in SSE behavior: Below SF, there are two spin carriers with opposite magnetic moments, with the carriers polarized along the field forming a majority magnon band. Above SF, the low-energy, ferromagnetic-like mode has magnetic moment opposite the field. This results in a sign change of the SSE across SF, which

agrees with recent measurements on Cr₂O₃/Pt and Cr₂O₃/Ta devices [Li *et al.*, Nature 578, 70 (2020)]. In our theory, SSE is due to a Néel spin current below SF and a magnetic spin current above SF. Using the ratio of the associated Néel to magnetic spin-mixing conductances as a single constant fitting parameter, we reproduce the field dependence of the experimental data and partially the temperature dependence of the relative SSE jump across SF.

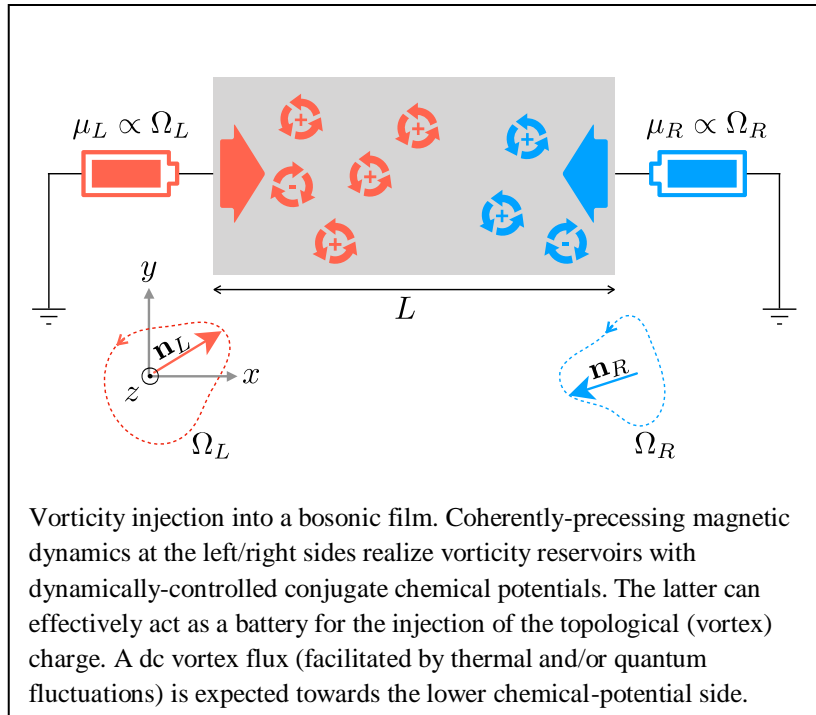


Finally, Ref. [13] is conceptual proposal for realizing *quantum vorticity (hydro)dynamics* on a general two-dimensional bosonic lattice (or a magnetic film). In the classical limit of a bosonic condensate, it reduces to conserved plasma-like vortex-antivortex dynamics. The nonlocal topological character of the vorticity flows is reflected in the bulk-edge correspondence dictated by the Stokes theorem. This is exploited to establish physical boundary conditions that realize, in the coarse-grained thermodynamic limit, an effective chemical-potential bias of vorticity. A Kubo formula is derived for the vorticity conductivity, which could be measured in a suggested practical device, in terms of quantum vorticity-flux correlators of the original lattice model. As an

illustrative example, we discuss the superfluidity of vorticity, exploiting the particle-vortex duality at a bosonic superfluid-insulator transition.

Future Plans

In the future work, we plan to advance our efforts on nonequilibrium thermodynamics of complex spin systems, with diverse microscopic constituents spanning a broad range of energy and lengthscales. Of particular interest to us will be the interplay of topological texture flows and quantum correlations, arising in response to thermodynamic biases.



Specifically, bolstered by the recent advances in understanding and controlling the coupled spin and energy transfer in complex magnetic materials and structures, I plan to focus on the following three thrusts over the coming years:

- Incoherently pumped collective dynamics in noncollinear and other complex spin systems
- Novel phenomena and circuits based on energy exchange with topological charge flows
- Multiple quantum-sensor integration with magnetic (nano)structures and quantum entanglement propagation out-of-equilibrium

Publications (October 2019 – September 2021)

1. T. Kikkawa, D. Reitz, H. Ito, T. Makiuchi, T. Sugimoto, K. Tsunekawa, S. Daimon, K. Oyanagi, R. Ramos, S. Takahashi, Y. Shiomi, Y. Tserkovnyak, and E. Saitoh, *Observation of Nuclear-Spin Seebeck Effect*, Nature Comm. **12**, 4356 (2021)
2. K. An, R. Kohno, N. Thiery, D. Reitz, L. Vila, V. V. Naletov, N. Beaulieu, J. Ben Youssef, G. de Loubens, Y. Tserkovnyak, and O. Klein, *Short-Range Thermal Magnon Diffusion in Magnetic Garnet*, Phys. Rev. B **103**, 174432 (2021)
3. T. Schneider, D. Hill, A. K'akay, K. Lenz, J. Lindner, J. Fassbender, P. Upadhyaya, Y. Liu, K. Wang, Y. Tserkovnyak, I. N. Krivorotov, and I. Barsukov, *Self-Stabilizing Exchange-Mediated Spin Transport*, Phys. Rev. B **103**, 144412 (2021)

4. H. Ochoa, R. Zarzuela, and Y. Tserkovnyak, *Self-Induced Spin-Orbit Torques in Metallic Ferromagnets*, J. Magn. Magn. Mater. **538**, 168262 (2021)
5. M. Tanhayi Ahari and Y. Tserkovnyak, *Superconductivity-Enhanced Spin Pumping: Role of Andreev Resonances*, Phys. Rev. B Lett. **103**, L100406 (2021)
6. Y. Tserkovnyak, *Magnetic Dynamics with Weyl Fermions*, Phys. Rev. B **103**, 064409 (2021)
7. Y. Tserkovnyak, E. Maniv, and J. Analytis, *Collective Spin Dynamics under Dissipative Spin Hall Torque*, Appl. Phys. Lett. **118**, 032406 (2021)
8. D. Jones, J. Zou, S. Zhang, and Y. Tserkovnyak, *Energy Storage in Magnetic Textures Driven by Vorticity Flow*, Phys. Rev. B (Rap. Comm.) **102**, 140411(R) (2020)
9. H. Zhang, M. J. H. Ku, F. Casola, C. H. Du, T. van der Sar, M. C. Onbasli, C. A. Ross, Y. Tserkovnyak, A. Yacoby, and R. L. Walsworth, *Spin-Torque Oscillation in a Magnetic Insulator Probed by a Single-Spin Sensor*, Phys. Rev. B **102**, 024404 (2020)
10. D. Reitz, J. Li, W. Yuan, J. Shi, and Y. Tserkovnyak, *Spin Seebeck Effect near the Antiferromagnetic Spin-Flop Transition*, Phys. Rev. B (Rap. Comm.) **102**, 020408(R) (2020)
11. T. Moriyama, K. Hayashi, K. Yamada, M. Shima, Y. Ohya, Y. Tserkovnyak, and T. Ono, *Enhanced Antiferromagnetic Resonance Linewidth in NiO/Pt and NiO/Pd*, Phys. Rev. B (Rap. Comm.) **101**, 060402(R) (2020)
12. P. Shen, Y. Tserkovnyak, and S. K. Kim, *Driving a Magnetized Domain Wall in an Antiferromagnet by Magnons*, J. Appl. Phys. **127**, 223905 (2020)
13. Y. Tserkovnyak and J. Zou, *Quantum Hydrodynamics of Vorticity*, Phys. Rev. Res. **1**, 033071 (2019) (Editors' Suggestion)

Condensed Matter Theory

Alexei Tsvelik, Robert Konik, Weiguo Yin, Andreas Weichselbaum, Laura Classen,
Brookhaven National Laboratory

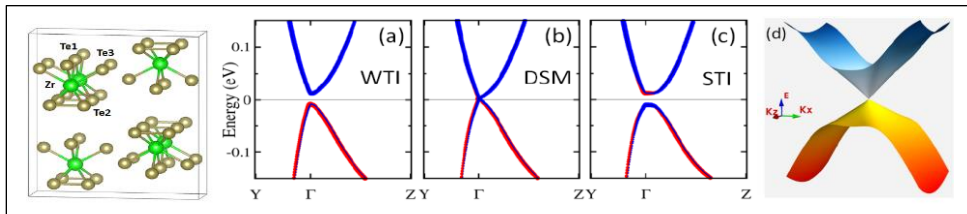
Program Scope

The unifying theme of the project is the study of condensed matter systems whose parameters can be engineered and thus tuned in a controlled manner. Current examples include:

- Laser pulse driven transition in the topological material ZrTe_5 , where the lattice deformations excited by the pulse drive the system from being a strong to a weak topological insulator.
- Various strongly correlated states obtained by changing the twist angle in bilayer graphene.
- Research in anomalous thermalization explores possibilities of obtaining long living mesoscopic states in low dimensional magnets.

Keywords: Topological insulators, twisted bilayer graphene, thermalization

Dynamically Induced Topological Phase Transitions in ZrTe_5 [1,2]: Electron states at the tip of the Dirac cone in Dirac/Weyl materials have relaxation times at least an order of magnitude greater than optical phonons. Hence, we have suggested the use of ultrafast generation and photoexcitation of certain phonon modes to induce topological phase transitions and to control topological states for energy and information applications.



Combined density-functional theory and effective Hamiltonian analysis of the electronic band structure and topology of ZrTe_5 predicts (1) topological phase transitions via various combinations of A_g Raman optical phonon modes and (2) Weyl modes of opposite chirality propagating along photoinduced domain boundaries. With lattice displacements experimentally determined by ultrafast electron diffraction, these calculations reveal how a transient Dirac semimetal state is photoinduced in ZrTe_5 .

Simulating exotic phases of matter with bond-directed interactions with arrays of Majorana-Cooper pair boxes (MCB): It is predicted that when

certain conditions are met the Bogolyubov quasiparticles in a semiconducting wire proximitized with a superconductor become Majorana fermions and the boundary of such device contains zero energy Majorana bound states [3]. Such a mesoscopic device is called an MCB. It is suggested [4] that since three zero modes comprise spin $1/2$, one can make networks of MCB's in order to

The evolution of the band structure of ZrTe_5 (pictured on the left) for three different values of the normal coordinate Q corresponding to the A_g -27 Raman-active phonon mode reveals the three following phases: (a) a weak topological insulator, (b) a Dirac semimetal, and (c) a strong topological insulator. The red (blue) dots show the weights of the Te_3 (Te_2) $5p$ orbitals. Fig. (d) shows the spectrum at the transition point.

engineer quantum magnets, in particular to simulate various exotic states of matter such as the famous Kitaev spin liquid model with all of its generalizations including to Kondo lattices and various spin models with three-spin interactions.

Higher Symmetries in Bilayer Graphene (TGB) and Transition Metal Dichalcogenides (TMD): Condensed matter systems consisting of several weakly coupled layers are easily manipulated by changing the twist angle between the layers, substrate engineering and gating. The experiments on bilayer and trilayer graphene reveal an extremely rich phase diagram containing alternating superconducting and insulating ground-states. Our publications (two examples are given below) consider yet unexplored opportunities for discovering ever more exotic states of matter.

The multivalley character of the electronic spectrum in hetero-bilayer TMD's make them unique platforms for the realization of new types of topological superconductivity such as one with a *chiral g-wave* order parameter with winding number $N=4$ and with clear experimental signatures including distinct quantum Hall features [5].

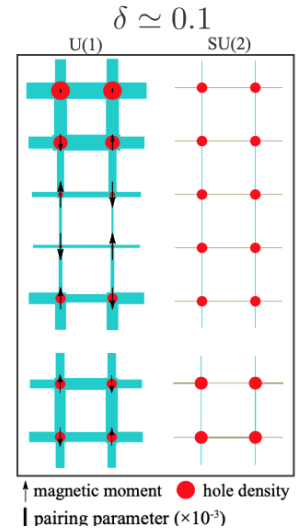
Experiments on small angle TBG reveal the existence of a triangular network of domain walls separating areas with different stacking. Each wall contains two pairs of counterpropagating modes. It is suggested [6] that by placing the chemical potential in the bulk gap one may emulate stripe-ordered phases in $\text{La}_{1.875}\text{Ba}_{0.125}\text{CuO}_4$ where a reliable microscopic description is not yet available. Hence the experimental research on the TBG, where such descriptions exists, may provide a useful check for the ideas determining our understanding of the cuprates. Our theory suggests that the Coulomb interaction in TBG leads to the formation of a Luther-Emery liquid in domain walls with the formation of superconducting pairs and the subsequent establishment of global phase coherence by Josephson tunneling between the walls.

Anomalous thermalization in correlated systems: A fundamental problem in non-equilibrium correlated materials physics that our FWP is addressing is how to create metastable states that are long lived and have useful functionalities. This theme is found, for example, in our work on light-induced topological phase transitions in ZrTe_5 . An allied question to the creation of metastable states is under what conditions are anomalous patterns of thermalization present in a correlated system. If a system does not thermalize or it does so only slowly, it is much more likely to be able support long-lived states with perhaps novel functionality. Here we have identified principles by which a strongly correlated will not thermalize. One principle that we have found promoting anomalous thermalization is long ranged confinement. Such confinement, most famously, exists between quarks and is induced by the color force. However, such confinement also exists in quantum Ising-like spin chains where the confinement is induced by the application of a longitudinal magnetic field. We have shown that this type of confinement leads to the violation of the eigenstate thermalization hypothesis, a fundamental principle by which a quantum system is meant to thermalize [7]. More recently confinement and anomalous thermalization has been seen in quantum simulators formed by trapped ions [8].

In our work in this area, we have also demonstrated a phenomena that we have termed many-body dynamical localization, showing that a lack of thermalization can survive even in the presence of many-body interactions. The quantum kicked rotor system is a textbook example of a system where the energy saturates after a finite number of kicks. A natural question to ask here is whether this localization in energy can survive the presence of many-body interaction. Here we shown the

answer is yes [9] by providing evidence that for systems that are Luttinger liquids that dynamical localization can persist, at the very least, for exponentially long times.

Understanding stripe superconductivity using iPEPs: Since the BNL-led discovery of the unusual 2D superconductivity in the cuprate LBCO [10], the Condensed Matter Theory FWP has been actively involved in this research (see [6] and also [11,12]). Ref. [13] presents the results for the t-J model on a square lattice obtained with the use of infinite projected entangled pair states (iPEPS). At small doping, multiple orders, such as antiferromagnetic order, stripe order and superconducting order, are intertwined or compete with each other. We analyze the role of spin symmetry at small doping by either imposing SU(2) spin symmetry or its U(1) subgroup in the iPEPS ansatz, thereby excluding or allowing spontaneous spin-symmetry breaking respectively in the thermodynamic limit. From a detailed comparison of our simulations, we provide evidence that stripe order is favored by long-range antiferromagnetic order. In contrast, for the case of the SU(2) iPEPS, which enforces a spin-singlet state, we find a uniform charge distribution that favors d-wave singlet pairing.



Future Plans

1. To continue working on topological phase transitions (TPT), including further exploring properties of phonon-induced phases, in particular the nonlinear anomalous Quantum Hall effect in ZrTe_5 (A. Tsvelik, W. Yin, Q. Li), as well as possible realization of magnetocaloric TPT in $(\text{Cr,Fe})\text{Cr}_2\text{Te}_4$ (W. Yin, M. Abeykoon, S. Guchhait of Howard University).
2. As a continuation of our broad effort in understanding of non-equilibrium systems, we will study the non-equilibrium evolution of the Renyi entropies in continuum systems admitting confinement. This evolution provides one measure of thermalization. As part of this, we will develop the field theoretic tools to do so. (R. Konik, P. Calabrese of SISSA).
3. To continue studies of the unusual 2D superconductivity and ultra-quantum metal in the striped-ordered LBCO (A. Tsvelik, J. Tranquada, Q. Li, A. Weichselbaum, R. Konik).
4. Spin liquids with active orbital degrees of freedom may give rise to new physical phenomena such as *fractionalized order* (a concept developed by A. Tsvelik and P. Coleman from Rutgers University). The work in this direction will also include exploration of the material candidates for such liquids, such as $\text{Ru}(\text{P,As,Sb})$, etc. (W. Yin, Tsvelik, E. Bozin, C. Petrovic)
5. The generic framework of tensor networks covers a wide spectrum of powerful non-perturbative algorithms with prominent examples being the numerical renormalization group, the density matrix renormalization group, thermal tensor networks or iPEPS. It requires at its heart a powerful tensor library. For this we use the QSpace tensor library that allows us to fully exploit non-abelian symmetries in a generic fashion. We will work towards making QSpace v4.0 open source (current version is QSpace v3.2) (A. Weichselbaum).

References

1. "Topological phase transition and phonon-space Dirac topology surfaces in ZrTe₅", N. Aryal, X. Jin, Q. Li, A. M. Tsvelik, W. Yin, Phys. Rev. Lett. **126**, 016401 (2021).
2. "Photoinduced Dirac semimetal in ZrTe₅", T. Konstantinova, L. Wu, W.-G. Yin, J. Tao, G. D. Gu, X. J. Wang, J. Yang, I. A. Zaliznyak, Y. Zhu, NPJ Quantum Materials **5**, 80 (2020).
3. "Majorana Fermions and a Topological Phase Transition in Semiconductor-Superconductor Heterostructures", R. M. Lutchyn, J. D. Sau, S. D. Sarma, Phys. Rev. Lett **105**, 077001 (2010).
4. "Simulating exotic phases of matter with bond-directed interactions with arrays of Majorana-Cooper pair boxes", A. M. Tsvelik, Phys. Rev. Lett. **125**, 197202 (2020).
5. "N=4 chiral superconductivity in moire transition metal dichalcogenides", M. M. Scherer, D. M. Kennes, L. Classen, arXiv: 2108.11406.
6. E. Konig, P. Coleman, A. M. Tsvelik, "Spin magnetometry as a probe of stripe superconductivity in twisted bilayer graphene", Phys. Rev. B **102**, 104514 (2020).
7. "Nonthermal States Arising from Confinement in One and Two Dimensions", A. J. A. James, R. M. Konik, N. J. Robinson, Phys. Rev. Lett. **122**, 130603 (2019).
8. "Quantum coherence confined", R. Konik, Nature Physics **17**, 669 (2021); "Domain-wall confinement and dynamics in a quantum simulator", W. Tan et al., Nature Physics **17**, 742 (2021).
9. "Many-body Dynamical Localization in a Kicked Lieb-Liniger Gas", C. Rylands, E. B. Rosenbaum, V. Galitski, R. Konik, Phys. Rev. Lett. **124**, 155302 (2020).
10. "Two-dimensional superconducting fluctuations in stripe-ordered La_{1.875}Ba_{0.125}CuO₄, Q. Li, M. Hucker, A. M. Tsvelik, G. D. Gu and J. M. Tranquada, Phys. Rev. Lett **99**, 067001 (2007).
11. "Deconstructing a stripe-ordered superconductor with a magnetic field", Y. Li, P. G. Baity, J. Terzic, Dragana Popovic, G. D. Gu, A. M. Tsvelik, J. M. Tranquada, Science Advances, **5**, no. 6, eaav7686, (2019).
12. "How magnetic field can transform a superconductor into a Bose metal", Tianhao Ren and A. M. Tsvelik, New J. Phys. **22**, 103021 (2020).
13. "iPEPS study of spin symmetry in the doped t-J model", J.-W. Li, B. Brugnolo, A. Weichselbaum, and J. von Delft, Phys. Rev. B **103**, 075127 (2021).

Publications

1. "How magnetic field can transform a superconductor into a Bose metal", Tianhao Ren and A. M. Tsvelik, *New J. Phys.* **22**, 103021 (2020).
2. "Simulating exotic phases of matter with bond-directed interactions with arrays of Majorana-Cooper pair boxes", A. M. Tsvelik, *Phys. Rev. Lett.* **125**, 197202 (2020).
3. "Topological phase transition and phonon-space Dirac topology surfaces in ZrTe5", N. Aryal, X. Jin, Q. Li, A. M. Tsvelik, W. Yin, *Phys. Rev. Lett.* **126**, 016401 (2021).
4. "Photoinduced Dirac semimetal in ZrTe5", T. Konstantinova, L. Wu, W.G. Yin, J. Tao, G. D. Gu, X.J. Wang, J. Yang, I. A. Zaliznyak, Y. Zhu, *NPJ Quantum Materials* **5**, 80 (2020).
5. "Time-reversal symmetry breaking in the Fe-Chalcogenide superconductors", N. Zaki, J. R. Rameau, G. Gu, A. Tsvelik, P. D. Johnson, and Congjun Wu, *PNAS* **118**, e2007241118 (2021).
6. "Many-body Dynamical Localization in a Kicked Lieb-Liniger Gas", C. Rylands, E. B. Rosenbaum, V. Galitski, R. Konik, *Phys. Rev. Lett.* **124**, 155302 (2020).
7. N. J. Robinson, P. D. Johnson, T. M. Rice, A. M. Tsvelik, "Anomalies in the pseudogap phase of the cuprates: Competing ground states and the role of umklapp scattering", *Reports in Progress in Physics*, **82**, 126501 (Dec. 2019).
8. A. E. Feiguin, A. M. Tsvelik, Weiguo Yin, and E. S. Bozin, "Quantum liquid with strong orbital fluctuations: the case of the pyroxene family," *Phys. Rev. Lett.* **123**, 237204 (2019).
9. A. M. Tsvelik, R. M. Konik, N. V. Prokofev, I. S. Tupitsyn, "Resonant Inelastic X-Ray Scattering in Metals: A Diagrammatic Approach", *Phys. Rev. Research* **1**, 033093 (2019).
10. R. J. Koch, R. Sinclair, M. T. McDonnell, R. Yu, M. Abeykoon, M. G. Tucker, A. M. Tsvelik, S. J. L. Billinge, H. D. Zhou, W.-G. Yin, and E. S. Bozin, "Dual Orbital Degeneracy Lifting in a Strongly Correlated Electron System," *Phys. Rev. Lett.* **126**, 186402 (2021).
11. E. S. Bozin, W.-G. Yin, R. J. Koch, M. Abeykoon, Y. S. Hor, H. Zheng, H. C. Lei, C. Petrovic, J. F. Mitchell, and S. J. L. Billinge, "Local orbital degeneracy lifting as a precursor to an orbital-selective Peierls transition," *Nature Communications* **10**, 3638 (2019).
12. A. Weichselbaum, W. Yin, A. M. Tsvelik, "Dimerization and spin-decoupling in two-leg Heisenberg ladder with frustrated trimer rungs," *Phys. Rev. B* **103**, 125120 (2021).
13. Andreas Weichselbaum, "X-symbols for non-Abelian symmetries in tensor networks", *Phys. Rev. Research* **2**, 023385 (2020).
14. E. J. Sturm, M. R. Carbone, Deyu Lu, A. Weichselbaum, and R. M. Konik, "Predicting impurity spectral functions using machine learning", *Phys. Rev. B* **103**, 245118 (2021).
15. K. M. Stadler, G. Kotliar, S.-S. B. Lee, A. Weichselbaum, and J. von Delft, "Differentiating Hund from Mott physics in a three-band Hubbard-Hund model: Temperature dependence of spectral, transport, and thermodynamic properties", *Phys. Rev. B* **104**, 115107 (2021).

Time-dependent density-functional approaches for spin-dependent nonequilibrium phenomena

Carsten A. Ullrich

Department of Physics and Astronomy, University of Missouri, Columbia, MO 65211

Project Scope

The objective of this research is to develop new approaches for spin-dependent nonequilibrium phenomena in quantum materials, and to apply these methods in linear response and in the real-time nonlinear regime. This work is motivated by a growing interest in noncollinear magnetism in systems of interacting electrons, occurring in the ground state, during spin-wave excitations, or driven by strong, ultrafast fields. The standard density-functional approaches for noncollinear magnetism, the local spin-density and generalized gradient approximations, assume a local spin quantization axis for the exchange-correlation (xc) functional. This does not produce any xc magnetic torques, thus missing an important aspect of magnetization dynamics. The PI will develop a new class of orbital-dependent xc functionals for noncollinear magnetism by generalizing the local Slater exchange and the Singwi-Tosi-Land-Sjölander (STLS) method for the case of general mixed two-component spinor wave functions. These new functionals will be applied to the following situations. *1. Spin waves in 2D materials.* We will extend our prior work under DOE support, where we studied 2D electron systems in the presence of Rashba and Dresselhaus spin-orbit coupling. We will calculate spin-wave dispersions with noncollinear Slater and STLS and compare with experimental data from inelastic light scattering, and study spin waves in graphene and related 2D topological materials. *2. Strongly driven Hubbard dimers.* We will solve the time-dependent Kohn-Sham equation for two electrons in a Hubbard dimer driven by noncollinear magnetic fields, testing the Slater and STLS xc magnetic fields and torques by comparison with exact benchmark results from the two-body Schrödinger equation. *3. Ab initio noncollinear spin dynamics.* We will implement our new xc functionals for noncollinear magnetism in the open source codes Abinit and Octopus. We will calculate the magnetization of typical noncollinear materials such as lattices of Cr atoms. With Octopus, we will simulate the ultrafast magnetization dynamics of small Fe or Cr clusters and of magnetic molecules, in particular graphene fragments. The proposed research will have fundamental and practical impact in the area of noncollinear magnetic phenomena in a broad spectrum of materials in and out of equilibrium.

Keywords:

Density-functional theory for noncollinear magnetism, spin waves in graphene, magnetic torques in the Hubbard model

Recent Progress

In spin-polarized itinerant electron systems, collective spin-wave modes arise from dynamical exchange and correlation (xc) effects. We here consider *spin waves in doped paramagnetic graphene* with adjustable Zeeman-type band splitting [1]. The spin waves are described using time-dependent spin-density-functional response theory, treating dynamical xc effects within the

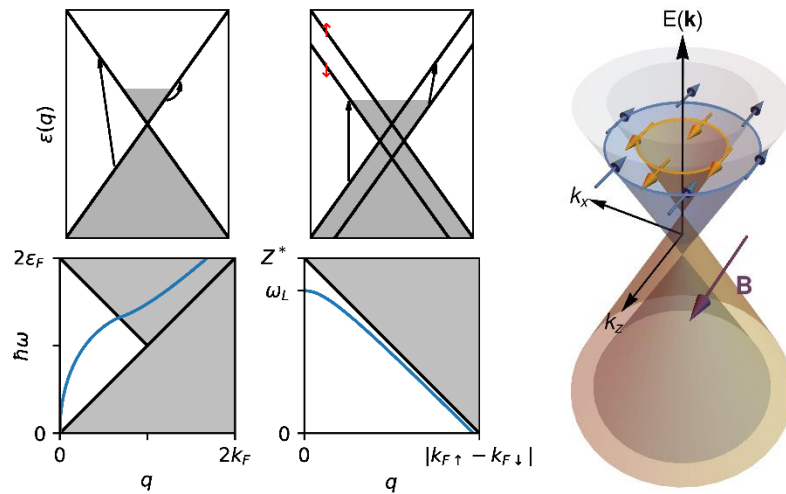


Fig.1. Left: spin-conserving single-particle transitions and plasmon dispersion in graphene. Middle: spin-flip single-particle transitions and spin-wave dispersion in doped graphene with Zeeman splitting. Right: spin-split Dirac cone, showing the Fermi surfaces of minority and majority spins.

Slater and STLS approximations. We obtain spin-wave dispersions and spin stiffnesses as a function of doping and spin polarization, and discuss prospects for their experimental observation.

The basic physics is shown in Fig. 1, which compares spin-conserving and spin-flip excitations in doped graphene close to the Dirac point. The

Dirac cone is assumed to be Zeeman split by an in-plane magnetic field, leading to a spin polarized Dirac fermion gas.

Plasmons in graphene have been well studied in the literature, but spin waves have so far not received much attention. The motivation for the present study is two-fold. First, from a theoretical and computational perspective, spin waves in graphene pose an interesting challenge. The formation of spin waves is due to electronic many-body effects beyond the random-phase approximation (RPA), mainly exchange, but also correlation. In the ab initio treatment of magnons in ferromagnets, one uses standard exchange-correlation functionals such as the LSDA; however, these are not applicable here, since the homogeneous electron gas is not an appropriate reference system for Dirac fermions. To avoid this problem, we here use orbital-based xc functionals, notably the Slater and STLS (Singwi-Tosi-Land-Sjölander) approximations [2]. We recently generalized these approximations to noncollinear spin systems [3,4].

Secondly, spin waves in graphene are potentially of interest as a way to encode and transmit quantum information (this field of research is known as magnonics). Spin lifetimes in graphene are known to be long, and graphene has been intensely studied in the context of spintronics [5]. Therefore, it is of interest to calculate spin-wave dispersions in graphene, and we expect our work to stimulate further theoretical and experimental research.

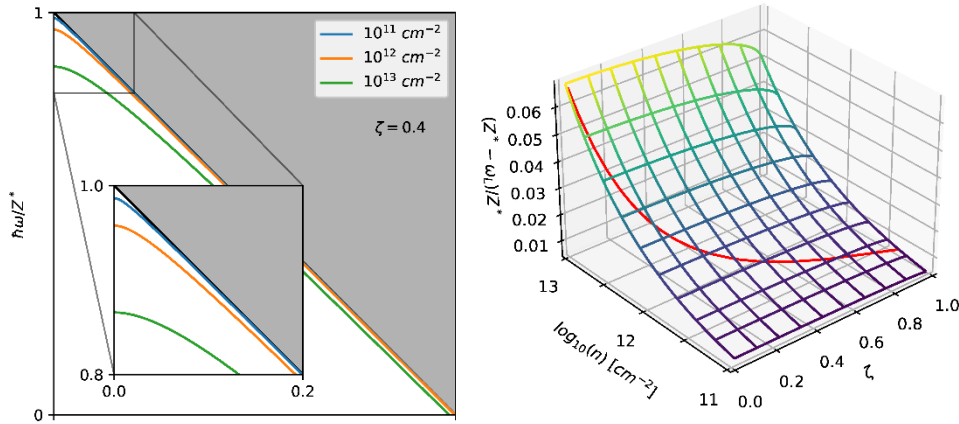


Fig.2. Left: Spin-wave dispersions in graphene for various doping concentrations and spin polarization 0.4. Right: Offset of the Larmor frequency ω_L with respect to the effective Zeeman energy Z^* . The red line indicates where the offset is 0.5 meV.

In Fig. 2, we show calculated spin-wave dispersions for a given spin polarization of 0.4. If the system is sufficiently strongly doped, the dispersion is well separated from the spin-flip continuum, which means that the spin wave should have a sufficiently long lifetime to be experimentally observable. The quantity $Z^* - \omega_L$ determines how well the spin wave is separated from the spin-flip continuum; values of 0.5 meV or larger indicate that the spin wave is well enough defined and sufficiently long-lived to be experimentally observable.

This work has recently been submitted to Physical Review B [1].

Future Plans

Exchange-correlation magnetic torques and spin dynamics. The PI has developed a density-functional formalism for noncollinear spin using orbital-dependent exchange-correlation functionals. In earlier work [3,4], the formalism was benchmarked for small Hubbard systems. It is now planned to extend this work into the time domain and to show that exchange-correlation torques play an important role in the precessional dynamics of magnetic moments. This will again be done using small Hubbard systems. Preliminary results show that the effect is particularly pronounced in systems showing magnetic frustration (such as Hubbard trimers, mimicking Cr₃).

Ab-initio (TD)DFT for noncollinear magnetism. In collaboration with Dr. Nicolas Tancogne-Dejean from the Max-Planck-Institute of Structure and Dynamics of Matter, Hamburg, Germany, we are developing a novel type of exchange-correlation functional for (TD)DFT for noncollinear magnetism. The functional is derived from the noncollinear Slater approximation and takes the form of a meta-GGA. In contrast with standard DFT approximations, our new functional accounts for xc torques, while being fully U(1) and SU(2) gauge invariant. The functional will be implemented into the Octopus code [6], and will be tested for the magnetic structure of Cr₃ clusters and the ultrafast demagnetization of bulk Ni.

References

1. M. J. Anderson, F. Perez, and C. A. Ullrich, *Spin waves in doped graphene: a time-dependent spin-density-functional approach to collective excitations in paramagnetic two-dimensional Dirac fermion gases*, submitted to Phys. Rev. B (arXiv:2110.00045)
2. K. S. Singwi, M. P. Tosi, H. R. Land, and A. Sjölander, *Electron correlation at metallic densities*, Phys. Rev. **170**, 589 (1968)
3. C. A. Ullrich, *Density-functional theory for systems with noncollinear spin: orbital-dependent exchange-correlation functionals and their application to the Hubbard dimer*, Phys. Rev. B **98**, 035140 (2018)
4. E. A. Pluhar III and C. A. Ullrich, *Exchange-correlation magnetic fields in spin-density-functional theory*, Phys. Rev. B **100**, 125135 (2019)
5. W. Han, R. K. Kawakami, M. Gmitra and J. Fabian, *Graphene spintronics*, Nature Nanotech. 9, **794** (2014)
6. N. Tancogne-Dejean et al., *Octopus, a computational framework for exploring light-driven phenomena and quantum dynamics in extended and finite systems*, J. Chem. Phys. **152**, 124119 (2020)

Publications (2018-2021)

1. S. Karimi, C. A. Ullrich, I. D'Amico, and F. Perez, *Spin-helix Larmor mode*, Sci. Rep. **8**, 3470 (2018)
2. C. A. Ullrich, *Density-functional theory for systems with noncollinear spin: orbital-dependent exchange-correlation functionals and their application to the Hubbard dimer*, Phys. Rev. B **98**, 035140 (2018) (Editors' Suggestion)
3. I. D'Amico, F. Perez, and C. A. Ullrich, *Topical Review: Chirality and dissipation of spin modes in two-dimensional electron liquids*, J. Phys. D: Appl. Phys. **52**, 203001 (2019)
4. C. A. Ullrich, *(Spin-)density-functional theory for open-shell systems: exact magnetization density functional for the half-filled Hubbard trimer*, Phys. Rev. A **100**, 012516 (2019)
5. E. A. Pluhar III and C. A. Ullrich, *Exchange-correlation magnetic fields in spin-density-functional theory*, Phys. Rev. B **100**, 125135 (2019)
6. S. Yesudhas, M. V. Morrell, M. J. Anderson, C. A. Ullrich, C. Kenney-Benson, Y. Xing, and S. Guha, *Pressure-induced phase changes in cesium lead bromide perovskite nanocrystals with and without Ruddlesden-Popper faults*, Chem. Mater. **32**, 785 (2020)
7. R. Butler, R. Burns, D. Babaian, M. J. Anderson, C. A. Ullrich, M. V. Morrell, Y. Xing, J. Lee, P. Yu, and S. Guha, *Weak magnetic field-dependent optical properties of lead bromide, perovskites*, submitted to Phys. Rev. Materials
8. M. J. Anderson, F. Perez, and C. A. Ullrich, *Spin waves in doped graphene: a time-dependent spin-density-functional approach to collective excitations in paramagnetic two-dimensional Dirac fermion gases*, submitted to Phys. Rev. B (arXiv:2110.00045)

***Ab initio* theory of unconventional superconductivity**

Mark van Schilfgaarde (PI)
Co-PIs: Stephan Lany and Dimitar Pashov
National Renewable Energy Laboratory

Program Scope

In this program we will apply and extend a Green's-function-based, *ab initio* theoretical framework for unconventional superconductivity (UCS) within the Questaal electronic structure package.⁽¹⁻⁴⁾ UCS are the archetype laboratory for exotic states and quantum phenomena in condensed matter systems, and have wide application as magnets, in metrology, superconducting electronics and spintronics, and quantum computation. Yet the origins of UCS remain one of the outstanding unsolved problems in theoretical condensed matter physics today. The Hubbard model, which forms the basis of most of our understanding, has provided much insight, but theories must rely on model assumptions and lack predictive power.

Our basic framework is a new, high-fidelity four-tier Green's function theory implemented in the past few years, to complement traditional model approaches. We show that in many cases it already comes close to meeting the exacting requirements of a high-fidelity description applicable at all relevant energy scales. Some examples are given in Recent Progress, below.

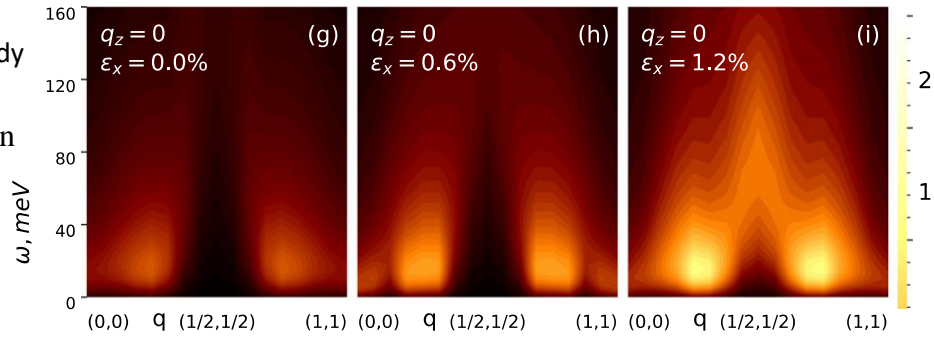
With further developments, this approach can offer new insight into different kinds of UCS beyond the reach of model descriptions. The project has three focus areas: first to study selected Hund's metals, overdoped Mott and nearly ferromagnetic superconductors with a focus on questions where materials-specific information is important, such as the role of disorder. Among the cuprates, we focus on the overdoped regime because it is likely that the underdoped regime has significant nonlocality in the self-energy driven by long range spin fluctuations, which our theory is not yet equipped to address (see Future Plans). Second, we will advance the existing theory in several ways to make it feasible to answer these questions *ab initio*. Third, we plan a dissemination and outreach component of this community code, to encourage its use in the broader scientific community.

Keywords: unconventional superconductivity; strongly correlated materials; *ab initio* theory.

Recent Progress

The theory has provided a microscopic description of Sr_2RuO_4 , showing the competition between spin singlet and spin triplet superconductivity,^(3,4) and how susceptibility becomes more concentrated with tensile strain until it reaches a critical strain at the Lifshitz transition, causing the critical temperature T_C to peak there before the susceptibility becomes incoherent on the other side of the transition. In another system, FeSe, the theory provided a good, parameter-free description of the spin susceptibility in bulk material, and also superconductivity including its instability to an s^+/s^- ground state, the corresponding T_C . Moreover the theory was also applied to

monolayer-FeSe/SrTiO₃. The study was also used to show the difference between it and bulk FeSe, and why T_c dramatically increases in the latter case, as has been observed experimentally. We could also trace the underlying reasons for the dramatic shift: the proximity of the d_{xy} state to the Fermi level together with the extraordinary



Imaginary part of the dynamic spin susceptibility $\chi^m(\mathbf{q};\omega)$ are shown in the Cartesian xy plane for different strains ε_x in Sr_2RuO_4 . The unstrained compound shows a spin fluctuation spectrum strongly peaked at $\mathbf{q} = (0.3, 0.3)$ in the plane (units $2\pi/a$). At $\varepsilon_x = 0$ (panel *g*), χ^m is nearly independent of q_z , but it begins to depend on it for $\varepsilon_x > 0$. With increasing strain, spin fluctuations become more coherent and strongly peaked, reaching a zenith at $\varepsilon_x^* = 0.6\%$ (panel *h*), where critical temperature (T_c) is maximum. For $\varepsilon_x > \varepsilon_x^*$, this peak becomes more diffuse (panel *i*). See Refs (3,4) for further details and discussion about instabilities to ordered magnetic states.

dependence of T_c on the Hund's parameter J , and in turn the variation of J with the environment.⁽⁵⁾ For another pair of systems, LaFe_2As_2 and CaFe_2As_2 , each possessing uncollapsed and collapsed tetragonal phases, the theory was able to explain what caused T_c to change so dramatically between the two phases, and how the ground state is affected by competition between superconductivity and antiferromagnetism.⁽⁶⁾

Future Plans

Our primary objective is to survey known superconductors, test where the theory can provide an adequate explanation of UCS, whether it can uncover trends, e.g. with doping or structural changes, find similarities and differences among different materials classes, and make some assessment of the theory's capabilities and its limits. We will attempt to reduce the full calculations to the key features that are responsible for superconductivity, to gain intuitive insight into the trends and driving forces for UCS. We will also consider other manifestations of strong correlations, e.g. the role of electron phonon interaction and optical conductivity, and the connection between them and superconductivity.

We also plan to advance formal development with a focus on adding low-order diagrammatic terms to include nonlocal contributions to the spin self-energy. This we plan to accomplish by considering dual Trilex diagrams. Our project also has a component in using quantum computers to solve the embedding problem. While the classical Continuous Time Monte Carlo method has been very effective, it has challenges reaching the low superconducting transition temperatures.

A main alternative, exact diagonalization is limited in the number of degrees of freedom it can manage on classical computers, a limit that quantum computers can potentially extend.

References

- ⁽¹⁾ Dimitar Pashov, Swagata Acharya, Walter R. L. Lambrecht, Jerome Jackson, Kirill D. Belashchenko, Athanasios Chantis, Francois Jamet, Mark van Schilfgaarde, *Questaal: a package of electronic structure methods based on the linear muffin-tin orbital technique*, Comp. Phys. Comm 249, 107065 (2020).
- ⁽²⁾ Swagata Acharya, Cedric Weber, Evgeny Plekhanov, Dimitar Pashov, A Taraphder, Mark van Schilfgaarde, *"Metal-insulator transition in copper oxides induced by apex displacements,"* Phys. Rev. X 8, 021038 (2018)
- ⁽³⁾ Swagata Acharya, Dimitar Pashov, Cedric Weber, Hyowon Park, Lorenzo Sponza, Mark van Schilfgaarde, *Maximization of T_C via Conspired Even-Parity Spin and Charge Collective Excitations in Strained Sr_2RuO_4* , Communications Physics 2, 163 (2019).
- ⁽⁴⁾ Swagata Acharya, Dimitar Pashov, Elena Chachkarova, Mark van Schilfgaarde, and Cedric Weber, *Electronic structure correspondence of singlet-triplet scale separation in strained Sr_2RuO_4* , Appl. Sci. 11, 508 (2021).
- ⁽⁵⁾ Swagata Acharya, Dimitar Pashov, Francois Jamet, Mark van Schilfgaarde, *Electronic Origin of T_c in Bulk and Monolayer $FeSe$* , Symmetry 13, 169 (2021)
- ⁽⁶⁾ Swagata Acharya, Dimitar Pashov, Francois Jamet, and Mark van Schilfgaarde, *Controlling T_c through Band Structure and Correlation Engineering in Collapsed and Uncollapsed Phases of Iron Arsenides*, Phys. Rev. Lett. 124, 237001 (2020)

Publications

No publications that reference this program to date.

Quantum criticality and topology in non-equilibrium systems

Romain Vasseur, University of Massachusetts, Amherst

Program Scope

Non-equilibrium systems can host new phases and phenomena with no equilibrium counterpart, and could also enable robust ways to build quantum memory devices to store and manipulate quantum information in a coherent manner. These phases and phenomena are inherently dynamical: they are described not by changes in the arrangement or structure of the constituent particles, but instead marked by sharp distinctions in how the particles move and exchange energy or quantum information. The discovery of robust non-equilibrium phases raises many fundamental questions: Can we develop a systematic theory of states of matter and of dynamical transitions between such states? How can such states be realized and probed experimentally? This research explores the emergence of topological phases and quantum criticality (two cornerstones of modern condensed matter physics in equilibrium) in such non-equilibrium quantum systems. The current research reported below focuses on dynamical phases and phase transitions in a broad class of quantum spin chains that show anomalous transport properties. Such transitions occur solely in the dynamical transport properties of those systems, and are not visible in equilibrium thermodynamical observables.

Keywords: quantum spin chains, spin transport, anomalous diffusion

Recent Progress

Kinetic theory of spin superdiffusion in isotropic spin chains

Finite temperature spin transport in a broad class of isotropic quantum spin chains – including spin-1/2 Heisenberg magnets -- was recently observed to be “superdiffusive”: spin is transported via a process that is faster than diffusion, the expected behavior. This surprising anomalous transport property was first uncovered numerically [1], and was also observed experimentally in the past year in neutron scattering experiments on the one-dimensional Heisenberg antiferromagnet KCuF_3 [2], and using quantum microscopy techniques [3]. We proposed a recent theory of this elusive phenomenon in terms of “giant magnon”

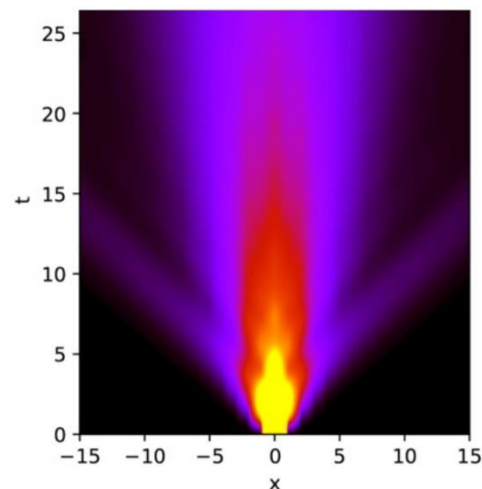


Figure 1: Structure Factor of the XXZ spin chain near the Heisenberg point, showing ballistic magnons coexisting with broad superdiffusive features [7].

quasiparticles that are dressed by interactions [1',2']. We identified the quasiparticles responsible for superdiffusion as soft, Goldstone-like modes, stabilized by the integrability of the Heisenberg spin chain [3']. We developed a generalized hydrodynamic theory [4,5] of transport in such spin chains, that allowed us to compute the finite-temperature spin structure factor of anisotropic XXZ spin chains in the hydrodynamic regime (low frequency and momenta) for the first time, uncovering a broad regime of anomalous relaxation properties [4'].

Superuniversality of superdiffusion

This property of superdiffusive transport turns out to be quite universal [5'], and is also present in the Fermi-Hubbard model [6'], spin ladders, SU(N) magnets or in multi-component Fermi gases. We recently explained this “superuniversality” using a general quasiparticle picture combined with non-Abelian symmetries [5']. All those systems have in common being at or close to some special integrable limit, and have isotropic spin rotation symmetries (in general, non-Abelian symmetry groups). We showed that superdiffusive transport holds regardless of the symmetry group, local degrees of freedom, Lorentz invariance, or particular realization of microscopic interactions for this class of systems.

Hydrodynamics of integrability breaking

In one dimension, many paradigmatic models of quantum many-body physics—such as the Hubbard, Heisenberg, and Lieb-Liniger models—are integrable. These models approximately describe experiments in quasi-one-dimensional systems. Integrable systems have infinitely many conserved quantities, which spread ballistically in general, and stable quasiparticle excitations.

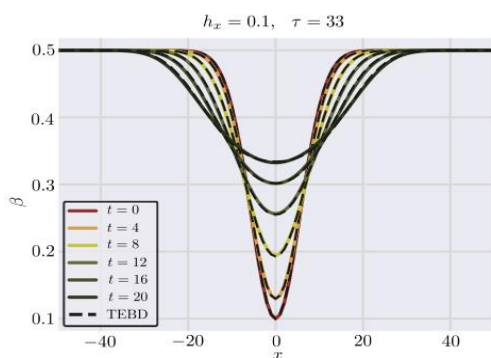


Figure 2: Inverse temperature $1/T(x,t)$ profiles in the XXZ spin chain with staggered transverse fields breaking integrability, for different times, showing energy transport. The numerical data is in very good agreement with the Boltzmann approach [11].

When integrability is broken, only a few of these conserved quantities survive. The remaining conserved quantities are generically transported diffusively, corresponding to the familiar Fick’s or Fourier’s laws for particle or heat transport, respectively. We have recently proposed a hydrodynamical framework to describe this crossover between generalized to conventional hydrodynamics in nearly integrable systems [7',8']. We have also proposed a generalized relaxation time approximation that turned out to be remarkably accurate to capture the crossover between ballistic and diffusive hydrodynamics in strongly-interacting systems close to integrability. This generalizes the Boltzmann equation formalism to strongly interacting systems, using the underlying quasiparticles of integrable systems. This

formalism can be applied to describe quantitatively the non-equilibrium dynamics of interacting one-dimensional Bose gases, and heat transport in quantum spin chains near integrability.

Future Plans

We are currently working on deriving the emergence of this anomalous hydrodynamic theory in large N theories using field theory techniques. While those results should apply to describe transport from generic initial states after a short localization time scales, recent experiments on the XXZ spin chain with spin helix initial states have uncovered a breath of different relaxation properties [6,7] that my group is also currently working on.

A different direction related to transport in quantum spin chain is to address non-linear response properties. Most conventional experimental probes of many-body systems, from spectroscopy to transport, operate in the linear-response regime. Despite its many successes, linear response has its limitations as a probe of correlated quantum matter. For example, many different mechanisms — of varying levels of interest — give rise to incoherent spectral continua, and cannot be differentiated on the basis of linear-response data. Recently, various experimental probes of nonlinear response have been developed, including pump-probe spectroscopy and multidimensional coherent spectroscopy in condensed-matter settings. Despite a flurry of recent work, the theoretical toolbox for addressing nonlinear response in generic interacting quantum many-body systems is primitive, with few exact results beyond free theories and those that reduce to ensembles of two-level systems. We have been working on developing new hydrodynamic approaches to study non-linear response functions in quantum spin chains (Ising chains and Heisenberg magnets in particular). The anomalous superdiffusion properties reported above are related to intrinsically nonperturbative regimes of the nonlinear response, which we are investigating.

References

- [1] M Ljubotina, M Žnidarič, T Prosen, Nature communications 8 (1), 1-6 (2017)
- [2] A Scheie et al, Nature Physics 17 (6), 726-730 (2021).
- [3] D. Wei et al, “Quantum gas microscopy of Kardar-Parisi-Zhang superdiffusion”, [arXiv:2107.00038](https://arxiv.org/abs/2107.00038).
- [4] Bruno Bertini, Mario Collura, Jacopo De Nardis, and Maurizio Fagotti, “Transport in Out-of-Equilibrium XXZ Chains: Exact Profiles of Charges and Currents”, Phys. Rev. Lett. **117**, 207201 (2016).
- [5] Olalla A. Castro-Alvaredo, Benjamin Doyon, and Takato Yoshimura, “Emergent Hydrodynamics in Integrable Quantum Systems Out of Equilibrium”, Phys. Rev. X **6**, 041065 (2016).

[6] S. Hild et al, Phys. Rev. Lett. 113, 147205 (2014).

[7] N. Jepsen et al, Nature 588, 403-407 (2020).

Relevant Publications

[1'] Kinetic Theory of Spin Diffusion and Superdiffusion in XXZ Spin Chains, S. Gopalakrishnan and R. Vasseur, Phys. Rev. Lett. **122**, 127202 (2019).

[2'] Anomalous low-frequency conductivity in easy-plane XXZ spin chains, U. Agrawal, S. Gopalakrishnan, R. Vasseur and B. Ware, Phys. Rev. B **101**, 224415 (2020).

[3'] Superdiffusion from emergent classical solitons in quantum spin chains, J. De Nardis, S. Gopalakrishnan, E. Ilievski and R. Vasseur, Phys. Rev. Lett. **125**, 070601 (2020).

[4'] Anomalous relaxation and the high-temperature structure factor of XXZ spin chains, S. Gopalakrishnan, R. Vasseur, and B. Ware, Proceedings of the National Academy of Sciences **116** (33) 16250-16255 (2019).

[5'] Superuniversality of Superdiffusion, E. Ilievski, J. De Nardis, S. Gopalakrishnan, R. Vasseur, and B. Ware, Phys. Rev. X **11**, 031023 (2021).

[6'] Spin crossovers and superdiffusion in the one-dimensional Hubbard model, M. Fava, B. Ware, S. Gopalakrishnan, R. Vasseur and S. Parameswaran, Phys. Rev. B **102**, 115121 (2020).

[7'] Diffusive hydrodynamics from integrability breaking, A.J. Friedman, S. Gopalakrishnan and R. Vasseur, Phys. Rev. B **101**, 180302(R) (2020).

[8'] Hydrodynamics of nonintegrable systems from a relaxation-time approximation, J. Lopez-Piqueres, B. Ware, S. Gopalakrishnan and R. Vasseur, Phys. Rev. B **103**, L060302 (2021).

Other DOE supported publications since October 2019:

[9'] Local integrals of motion and the quasiperiodic many-body localization transition, H. Singh, B. Ware, R. Vasseur & S. Gopalakrishnan, Phys. Rev. B **103**, L220201 (2021).

[10'] Topological and symmetry-enriched random quantum critical points, C.M. Duque, H.-Y. Hu, Y.-Z. You, V. Khemani, R. Verresen, and R. Vasseur, Phys. Rev. B **103**, L100207 (2021).

[11'] Perturbative instability of nonergodic phases in non-Abelian quantum chains, B. Ware, D. Abanin, and R. Vasseur, Phys. Rev. B **103**, 094203 (2021).

[12'] Distinguishing localization from chaos: challenges in finite-size systems, D.A Abanin, J.H. Bardarson, G.De Tomasi, S. Gopalakrishnan, V. Khemani, S.A. Parameswaran, F. Pollmann, A.C. Potter, M. Serbyn and R. Vasseur, Annals of Physics **427**,168415 (2021).

- [13'] Superuniversality from disorder at two-dimensional topological phase transitions, B. Kang, S.A. Parameswaran, A.C. Potter, R. Vasseur and S. Gazit, Phys. Rev. B **102**, 224204 (2020).
- [14'] Quantum Criticality in the 2D Quasiperiodic Potts Model, U. Agrawal, S. Gopalakrishnan and R. Vasseur, Phys. Rev. Lett. **125**, 265702 (2020).
- [15'] Mean-field entanglement transitions in random tree tensor networks, J. Lopez-Piqueres, B. Ware and R. Vasseur, Phys. Rev. B **102**, 064202 (2020).
- [16'] Universality and quantum criticality in quasiperiodic spin chains, U. Agrawal, S. Gopalakrishnan and R. Vasseur, Nature Communications **11**, 2225 (2020).
- [17'] Measurement-induced criticality in random quantum circuits, C-M. Jian, Y-Z. You, R. Vasseur and A.W.W. Ludwig, Phys. Rev. B **101**, 104302 (2020).
- [18'] Integrable Many-Body Quantum Floquet-Thouless Pumps, A.J. Friedman, S. Gopalakrishnan and R. Vasseur, Phys. Rev. Lett. **123**, 170603 (2019).
- [19'] Entanglement transitions from holographic random tensor networks, R. Vasseur, A.C. Potter, Y-Z. You and A.W.W. Ludwig, Phys. Rev. B **100**, 134203 (2019).

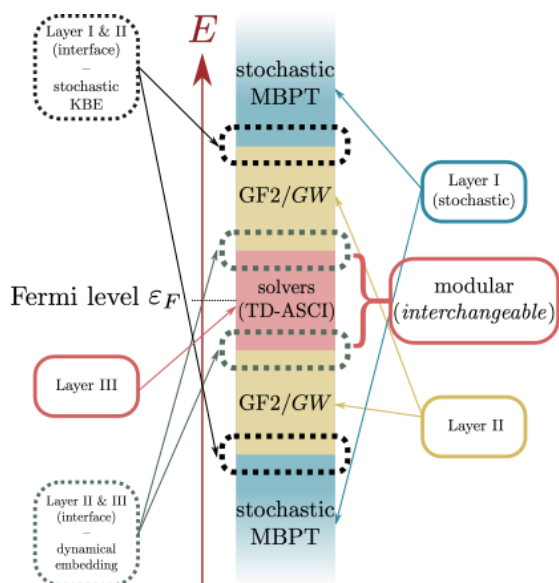
Real-time dynamics of driven correlated electrons in quantum materials

Vojtech Vitek (UC Santa Barbara), Khaled Ibrahim (LBNL), Gabriel Kotliar (Rutgers), Lin Lin (LBNL), Daniel Neuhauser (UC Los Angeles), K. Birgitta Whaley (UC Berkeley), Chao Yang (LBNL), Dominika Zgid (U Michigan)

Program Scope

Non-equilibrium strong field effects are at the forefront of the development of new materials with applications ranging from femtosecond state switching in traditional optoelectronic devices to novel quantum information platforms. Control of quantum states and their couplings to the environment is a new frontier in fundamental and applied physics, chemistry, and engineering. Future development, enhancement, and use of these systems hinges upon understanding and accurately predicting the dynamics of the individual electronic states under non-equilibrium conditions.

The interdisciplinary Partnership with SciDAC-5 institutes FASTMath and RAPIDS2 develops a multiscale framework to capture non-equilibrium dynamics. The new computational paradigm will directly overcome many of the limitations that hinder the simulations of realistic and practically relevant energy and quantum materials out-of-equilibrium. Crucially, the proposed methodology is based on state-of-the-art first-principles quantum theory.



Schematics of the embedding scheme employing time-dependent stochastic (Layer I) and deterministic (Layer II) many-body techniques with modular explicitly correlated many-body solvers (Layer III).

This project tackles the computational hurdle by developing novel numerical techniques and combine them with neural network approaches and efficient (i.e., resource lean) embedding. The unique framework is based on connecting stochastic (Layer I), deterministic (Layer II), and explicitly correlated (Layer III) methods. The most extensive part of the calculation (Layer I) is accomplished using the many-body perturbation theory relying on a statistical sampling of single-particle states and operators. This revolutionary stochastic approach enables treating systems with thousands of atoms. Layer II is based on an accurate deterministic implementation which provides a necessary transition to Layer III treated by (numerically exact) many-body calculations (i.e., beyond the perturbation theory).

The framework exploits the capabilities of DOE's flagship computing architectures and addresses the non-equilibrium properties of systems with thousands of atoms. The new suite of

tools will enable studying time-dependent problems that are at least two orders of magnitude larger in spatial and temporal dimensions than those treatable by the most advanced present algorithms.

The wide collaboration among experts from multiple fields enables extensive validation and verification on bulk semiconductors and insulators, ranging from molecules and conventional (3D periodic) phases to correlated 2D low dimensional materials, which exhibit novel excited-state phenomena. The practical calculations will investigate both the efficiency of the embedding as well as the time evolution of the quantum states (and associated numerical stability of the mathematical treatments).

This Partnership will produce efficient and scalable open-source software, computational tools, and practical procedures available to the research community. The results will impact a wide range of areas in physics, chemistry, materials science, and applied mathematics. Novel tools will enable a direct connection between theory, computations, and ultrafast experimental techniques characterizing of transient quantum properties. In particular, this Partnership will facilitate research on systems for quantum information and sensing, photonics, and ultrafast electronics.

Keywords: Simulation of quasiparticle excitations; Embedding methods; Real-time quantum dynamics

Recent Progress

The scientific Partnership has been successfully initiated in August 2021 and led to new collaborations among the PIs. The research tasks in the individual groups are aligned with various goals of the proposal ranging from optimal representation of the quantum embedding to efficient treatment of the non-equilibrium phenomena. The Partnership leverages the complementary expertise offered by the domain scientists (describing electronic structure and its time evolution in realistic systems), mathematicians (developing new computational tools with reduced computational needs), and computational scientists (optimizing the algorithms for HPC).

In the early period of this research, we initiated regular meetings of all PIs and created focus groups working on (i) reduction of computational burden (CPU time and memory) for treating large scale systems, (ii) optimization of the real-space and real-time algorithms for HPC, (iii) development of deterministic equilibrium finite temperature embedding in the stochastic algorithms and its verification, (iv) development of time-evolution algorithms for explicitly correlated methods (time-dependent adaptive selected configuration interaction – TD-ASCI) related reduced-order models for solving Kadanoff-Baym equations.

Future Plans

The Partnership has outlined three main goals: (i) Development of an embedding framework relying on a combination of stochastic and deterministic methods for simulating out-of-equilibrium phenomena, e.g., in time-resolved photoemission and pump-probe spectroscopy.

(ii) Development of modular computational tools (codes, libraries, and algorithms). (iii) Development of efficient computational toolkit with performance portability optimized for present and near-future exascale high-performance computers and tackling up to 100,000 electrons.

In the immediate future, the team plans to: **(i)** reduce the computational cost of large scale simulations in Layer I via introduction of Orthogonalized Projector-Augmented Waves (OPAW), reducing finite-size errors via advanced convergence schemes in momentum space, and optimization of memory usage and communication. **(ii)** develop and apply correlated self-consistent embedding in Layer I to describe excited states in large periodic systems that are inaccessible by conventional approaches (e.g., hexagonal oxide perovskites with large unit cells such as SrIrO₃, BaRuO₃, or twisted bilayer graphene). **(iii)** employ TD-ASCI with smooth time evolution with intermittent re-selection of core determinants for the many-body state expansion. We will explore CASSCF approaches to enable larger size bath calculations for improved calculation of bulk spectroscopic properties. **(iv)** develop efficient approximations to the non-equilibrium time-evolution memory kernel via trained recurrent neural network self-energy interpolation. We will identify a hierarchy of model problems with increasing levels of complexity to test and verify our approaches. **(v)** Optimize the GPU implementation of tensor contraction engine for computing Kadanoff-Baym equations and data movement between GPUs within and across nodes for Perlmutter, focusing on improving the CSPACER runtime. We will create a custom-optimized implementation for Cray Shasta interconnect to improve solver scalability.

References

None (Partnership initiated in August 2021)

Publications

None (Partnership initiated in August 2021)

Exploratory Development of Theoretical Methods

Cai-Zhuang Wang, Vladimir Antropov, Yongxin Yao, Kai-Ming Ho and Feng Zhang
Ames Laboratory, Ames, IA 50011

Program Scope

The scope of this FWP is to develop new theories and computational methods to solve challenging basic science problems to significantly advance the mission of Department of Energy's Basic Energy Science and Ames Laboratory. We focus on developing computationally efficient first-principles theories and computational methods for accurate calculation of correlated-electron materials without using adjustable Coulomb interaction U and J parameters. These methods aim to treat the energetic stability, electronic structure, and magnetism in an equal footing for correlated materials containing both localized and itinerant electrons so that fundamental physics and chemistry of rare earth (RE) materials can be correctly described and predicted. We also integrate the advances in machine learning (ML) and data science with the state-of-the-art materials modeling and simulation algorithms to develop robust ML-guided feedback frameworks to dramatically accelerate the design and discovery of novel materials with desirable structures and functionalities for energy applications. Our researches will provide strong leverage supports to achieving the scientific goals in the strategic plans of Ames Laboratory and its Division of Materials Science and Engineering. Moreover, since the key scientific problems to be tackled are the grand challenge problems faced by DOE-BES and by the condensed matter physics and materials science communities, advances in our research also will have lasting impacts on advancing the fundamental sciences and materials design and discovery.

Keywords: Correlated Materials; First-principles methods; Machine learning; Materials discovery.

Recent Progress

In the last two years, this FWP has been working on: (a) First-principles theories and computational methods for calculating the total energy and electronic structures of correlated-electron materials; (b) New and improved *ab initio* methods for description and prediction of spin fluctuations, spin correlations, and spin dynamics in quantum materials; and (c) Efficient and accurate algorithms and computational tools for predicting the structures and phase stabilities at both zero Kelvin and finite temperatures. Some highlights of the recent accomplishments are given below.

CMRT and computational code for correlated electron materials. An efficient correlation matrix renormalization theory (CMRT) and computational code for studying correlated electron systems have been developed [1]. The CMRT is based on Gutzwiller wave function but efficiently incorporates electron correlation effects into self-consistent *ab initio* calculations without using adjustable Coulombic U and J parameters. Moreover, the computational speed of the CMRT is similar to minimal basis Hartree-Fock calculations which is very efficient for correlated materials. The CMRT has also been successfully applied to address the volume collapse problem in *fcc* Ce [2] as can be seen from Fig. 1. This is the first truly accurate *ab initio* calculation of *f* electron materials without using U and J parameters. Our development of the CMRT enable accurate *ab initio* predictions of the structures, energies, and the electronic properties of real correlated materials, especially those containing *f* electrons.

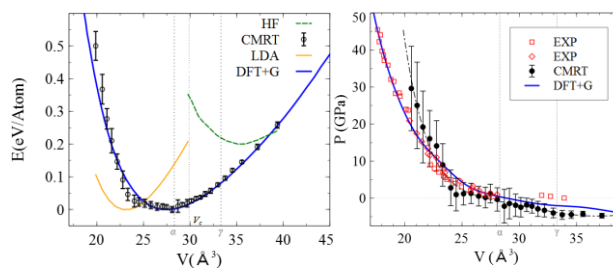


Fig. 1 (a) Energy-volume curves for *fcc* Ce from CMRT are compared with those from DFT+Gutzwiller (DFT+G), LDA, and Hartree-Fock (HF). (b) Pressure as the function of volume for *fcc* Ce from CMRT, DFT+G and experiment.

Treating electron correlations beyond Gutzwiller approximation. We have also been developing new theories and computational codes to calculate the total energy and electronic properties of correlated electron systems based on Gutzwiller wavefunction but without relying on the commonly used Gutzwiller approximation. One of the recent advances is the development of Gutzwiller conjugate gradient minimization (GCGM) method which describes electron correlations with higher accuracy. Application of the GCGM to 1-band one dimensional (1D) and two-dimensional (2D) Hubbard models yields accurate results comparable to exact solutions by auxiliary-field quantum Monte Carlo (AFQMC) or density matrix renormalization group (DMRG) methods as shown in Fig. 2, while being 10-100 times faster [3,4].

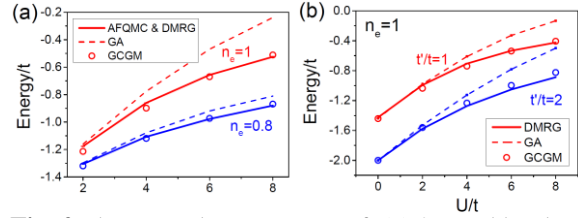


Fig. 2 The ground state energy of (a) 2D Hubbard model and (b) 2-leg Hubbard ladder vs U/t . n_e is electron filling with $n_e = 1$ being half filled. GCGM results compare well with AFQMC or DMRG results.

Prediction of novel highly responsive material with spin fluctuation induced superconductivity. By using the adaptive genetic algorithm developed from this FWP, we predict an energetically and dynamically stable FeNiB_2 compound [5]. We show that the *ab initio* inclusion of spin fluctuations drastically changes the magnetic state and the antiferromagnetic (AFM) spin fluctuations in the discovered FeNiB_2 , leading to the possible appearance of spin mediated superconductivity. The FeNiB_2 compound exhibits a highly responsive state, as the magnetic moment of its ferromagnetic (FM) and AFM states are very sensitive to external perturbations such as volume contraction. This highly responsive state is also characterized by a high level of spin fluctuations which strongly influence possible magnetic long- and short-range orders. Our calculation demonstrates the capability to predict a very elusive property such as spin-induced superconductivity in complex quantum materials, by the combination of the methods development for efficient novel material discovery and accurate description of spin fluctuations.

Machine learning (ML) assisted materials discovery and synthesis. Understanding the relationship between the undercooled liquid and stable/metastable phases which form is a long-standing challenge in materials synthesis. Knowledge about the local orders in the liquid and glass and their relationship to the structure of crystalline phases is vital to understanding the phase selection and transformation upon rapid solidification. We have developed interatomic potentials based on neural-network machine learning (ML) approach to assist reliable molecular dynamics (MD) simulation and analysis to address this long-standing challenge in complex materials. For example, an accurate ML potential developed from this FWP for Al-Tb system enables us to perform reliable MD simulations for non-crystalline phases and genetic algorithm search for new crystalline phases [6,7]. Such studies gain useful insights into the structures and the mechanisms of phase selection and phase transformations where RE element plays an important role in the formation and stability of the intermetallic compounds. In Fig. 3 we show that the 3661 and 15551 SRO motifs centered at Tb atoms in $\text{Al}_{90}\text{Tb}_{10}$ glass are consistent with building blocks of metastable crystalline structures in the nearby compounds.

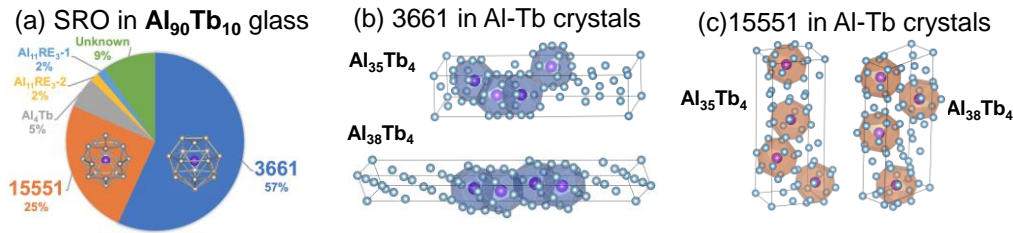


Fig. 3 (a) The 3661 and 15551 motifs are the dominate SRO structures in $\text{Al}_{90}\text{Tb}_{10}$ glass. Metastable crystalline structures in the nearby compounds incorporate (b) 3661 and (c) 15551 as building blocks.

Future Plans

We will further develop ab initio theories and computational methods without commonly used U and J parameters to describe correlated-electron materials, especially those containing 4f electrons, with desired accuracy and fast computational speed. Many physical properties of correlated electron materials are governed by the interplay and transformation between itinerant and localized electronic states. It remains a great challenge to develop *ab initio* theory and corresponding computational methods to accurately describe and predict the properties and behaviors of systems with both itinerant and localized electrons present. Our theories and methods will accurately and efficiently treat the interactions among both itinerant and localized electrons in an equal footing so as to greatly enhance the predictive power of *ab initio* calculations for correlated materials. Such theory and method development will eventually lead to effective *ab initio* calculations and predictions of the energies and properties of any strongly correlated materials, just like DFT does for most of weakly correlated materials today.

We will perform ab initio calculations to reveal complex material physics governed by delicate interplays among electron correlation, spin fluctuation, and magnetism. Such complex materials physics include spin correlation and dynamics, spin state crossover, magnetic anisotropy, structural and magnetic phase transitions caused by pressure, as well as multiplet states in crystalline environments. These properties are critical in determining the functionalities of the materials containing 3d and/or 4f electrons. Fundamental understanding the microscopic interactions in these systems are vital for guiding the design and discovery of novel materials or optimization of existing materials for energy relevant applications. However, a correct theoretical description of electronic structures and properties of such systems, especially those with 4f electrons remains an outstanding challenge. Our studies will provide key ingredients for achieving the DOE mission and Ames Laboratory strategic goals, especially in (a) Enable prediction and control for rare earth systems and magnetic behavior and (b) Discover, predict, and control novel quantum-driven phenomena.

We will Integrate the accurate ab initio calculations and our expertise in crystal structure predictions with machine learning (ML), data science and experiment to establish a robust ML-guided framework for efficient discovery of novel materials, especially those contains RE elements. A major challenge in materials design and discovery for energy relevant applications is to effectively predict synthesizable materials with a targeted functionality. This requires effective approaches to select promising chemical elements and compositions, and then link them with stable crystal structures and desired functionalities. Our ML-guided framework with feedback from experimental validation will greatly accelerate materials design, discovery, and synthesis to meet the mission of DOE and the strategic goals of Ames Laboratory.

References

- [1] J. Liu, X. Zhao, Y. X. Yao, C. Z. Wang, and K. M. Ho, *J. Phys. Condensed Matter* **33**, 095902 (2021). DOI: 10.1088/1361-648x/abbe78
- [2] J. Liu, Y. X. Yao, J. H. Zhang, K. M. Ho, and C. Z. Wang, *Phys. Rev. B (Letter)*, **104**, L081113 (2021). DOI: 10.1103/PhysRevB.104.L081113
- [3] Z. Ye, F. Zhang, Y. X. Yao, C. Z. Wang, and K. M. Ho, *Molecular Physics*. Published online (2020), DOI: 10.1080/00268976.2020.1797917.
- [4] Z. Ye, F. Zhang, Y. X. Yao, C. Z. Wang, and K. M. Ho, *Phys. Rev. B* **101**, 205122 (2020). DOI: 10.1103/PhysRevB.101.205122
- [5] R. H. Wang, Y. Sun, V. P. Antropov, Z. J. Lin, C. Z. Wang, K. M. Ho, *Applied Physics Letters* **115**(6), 182601 (2019). DOI: 10.1063/1.512448
- [6] L. Tang, Z. J. Yang, T. Q. Wen, K. M. Ho, M. J. Kramer, and C. Z. Wang, *Phys. Chem. Chem. Phys.* **22**, 18467-18479 (2020). DOI: 10.1039/D0CP01689F
- [7] L. Tang, Z. J. Yang, T. Q. Wen, K. M. Ho, M. J. Kramer, and C. Z. Wang, *ACTA Materialia*, **204** 116513 (2021). DOI: 10.1016/j.actamat.2020.116513

Publications (Selected from FY20 and FY21 publications)

- [1] J. Liu, Y. X. Yao, J. H. Zhang, K. M. Ho, C. Z. Wang, “Role of Coulomb interaction in the phase formation of fcc Ce: Correlation matrix renormalization theory”, *Phys. Rev. B (Letter)*, **104**, L081113 (2021). DOI: 10.1103/PhysRevB.104.L081113
- [2] J. Liu, X. Zhao, Y. X. Yao, C. Z. Wang, K. M. Ho, “Correlation matrix renormalization theory in -band lattice systems” *Journal of Physics: Condensed Matter*, **33**, 095902 (2021). DOI: 10.1088/1361-648x/abbe78.
- [3] C. Liu, Y. X. Yao, C. Z. Wang, K. M. Ho, V. P. Antropov, “Calculations of anisotropic magnetic properties using spin-orbit energy variations”, *Phys. Rev. B* **102**, 205119 (2020). DOI: 10.1103/PhysRevB.102.205119
- [4] Y. Sun, Y. X. Yao, M. C. Nguyen, C. Z. Wang, K. M. Ho and V. P. Antropov, “Spatial decomposition of magnetic anisotropy in magnets: application for doped Fe_{16}N_2 ”, *Phys. Rev. B*, **102**, 134429 (2020). DOI: 10.1103/PhysRevB.102.134429
- [6] L. Tang, Z. J. Yang, T. Q. Wen, K. M. Ho, M. J. Kramer, and C. Z. Wang, “Short- and medium-orders in $\text{Al}_{90}\text{Tb}_{10}$ glass and their relation to the metastable crystalline phases”, *ACTA Materialia*, **204**, 116513 (2021). DOI: 10.1016/j.actamat.2020.116513
- [7] G. Bhaskar, V. Gvozdetzkyi, M. Batuk, K. M. Wiaderek, Y. Sun, R. H. Wang, C. Zhang, S. L. Carnahan, X. Wu, R. A. Ribeiro, S. L. Bud'ko, P. C. Canfield, W. Y. Huang, A. J. Rossini, C. Z. Wang, K. M. Ho, J. Hadermann, J. V. Zaikina, “Topochemical Deintercalation of Li from Layered LiNiB : toward 2D MBene”, *J. Amer. Chem. Soc.* **143** (11), 4213-4223 (2021). DOI: 10.1021/jacs.0c11397
- [8] K. Lee, D. X. Mou, N. H. Jo, Y. Wu, B. Schrunck, J. M. Wilde, A. Kreyssig, A. Estry, S. L. Bud'ko, N. C. Nguyen, L. L. Wang, C. Z. Wang, K. M. Ho, P. C. Canfield, A. Kaminski, “Evidence for a large Rashba splitting in PtPb_4 from angle-resolved photoemission spectroscopy”, *Phys. Rev. B* **103**, 085125 (2021). DOI: 10.1103/PhysRevB.103.085125.
- [9] I. S. Han, J. T. McKeown, L. Tang, C. Z. Wang, H. Parsamehr, Z. C. Xi, Y. R. Lu, M. J. Kramer, and A. J. Shahani, “Dynamic observation of dendritic quasicrystal growth upon laser induced solid-state transformation”, *Phys. Rev. Lett.*, **125**, 195503 (2020). DOI: 10.1103/PhysRevLett.125.195503
- [10] B. Q. Song, Mingyu Xu, Vladislav Borisov, Olena Palasyuk, C. Z. Wang, Roser Valentí, Paul C. Canfield, and K. M. Ho, “Construction of A–B heterolayer intermetallic crystals: Case studies of the 1144-phase TM-phosphides $\text{AB}(\text{TM})_4\text{P}_4$ (TM=Fe, Ru, Co, Ni)”, *Phys. Rev. Materials* **5**, 094802 (2021). DOI: 10.1103/PhysRevMaterials.5.094802
- [11] Z. Ye, F. Zhang, Y. X. Yao, C. Z. Wang, K. M. Ho, “Ground state properties of one-dimensional and two-dimensional Hubbard model from Gutzwiller conjugate gradient minimization theory”, *Phys. Rev. B* **101**, 205122 (2020). DOI: 10.1103/PhysRevB.101.205122
- [12] R. H. Wang, Y. Sun, V. P. Antropov, Z. J. Lin, C. Z. Wang, K. M. Ho, “Theoretical prediction of a highly responsive material: Spin fluctuations and superconductivity in FeNiB_2 system”, *Appl. Phys. Lett.* **115**, 182601 (2019). DOI: 10.1063/1.512448
- [13] S. Ren, Y. Sun, F. Zhang, A. Travesset, C. Z. Wang, K. M. Ho, “Phase Diagram and Structure Map of Binary Nanoparticle Superlattices from a Lennard-Jones Model”, *ACS Nano*, **14**, 6795-6802 (2020). DOI: 10.1021/acsnano.0c00250
- [14] L. Tang, Z. J. Yang, T. Q. Wen, K. M. Ho, M. J. Kramer, and C. Z. Wang, “Development of Interatomic Potential for Al-Tb Alloy by Deep Neural Network Learning Method”, *Phys. Chem. Chem. Phys.* **22**, 18467-18479 (2020). DOI: 10.1039/D0CP01689F
- [15] D. Vaknin, S. Pakhira, D. Schlageel, F. Islam, J. H. Zhang, D. Pajerowski, C. Z. Wang, D. C. Johnston, R. J. McQueeney, “Localized singlets and ferromagnetic fluctuations in the dilute magnetic topological insulator $\text{Sn}_{0.95}\text{Mn}_{0.05}\text{Te}$ ”. *Phys. Rev. B* **101**, 140406 (2020). DOI: 10.1103/PhysRevB.101.140406

Disorder and Interaction in Correlated Electron Materials

Principal investigator: Ziqiang Wang

Department of Physics, Boston College, Chestnut Hill, MA 02467

wangzi@bc.edu

Project Scope

The program investigates correlated and topological quantum electronic states and their low energy properties in transition metal oxides, pnictides, chalcogenides, shandites, and antimonides. These include Cu and Fe-based high- T_c superconductors (SC), kagome lattice magnets, and the newly emerged vanadium-based kagome lattice SC. This part of the program maintains close collaborations with experimental groups. These collaborative efforts have led to impactful discoveries and advanced the theoretical understanding of the low-temperature collective quantum mechanical properties of the charge, spin, orbital, and lattice degrees of freedom as well as their interplay with lattice geometry and electronic topology. They inspired in turn new experimental discoveries.

Some of the research findings since 2020 include: (1) In 2019, we put forth the theory of quantum anomalous vortex (QAV) that nucleates spontaneously at the magnetic ions in SC with strong spin-orbital coupling, in the absence of an applied magnetic field. A continuous transition from the Yu-Shiba-Rosinov vortex free impurity state to the QAV state was predicted, as well as the Majorana zero mode (MZM) in the vortex core at the interstitial excess Fe atoms in Fe(Te,Se) SC form the superconducting topological surface states. This led to the new experimental discovery of the QAVs with MZMs by STM at the Fe adatoms introduced by atomic surface deposition in both LiFeAs and FeTeSe SCs [8, 28], and the observation of reversible transitions between Yu-Shiba-Rosinov states and Majorana vortices as a function of the exchange coupling [28, 35]. These advances demonstrated a field-free Majorana platform in SCs with Z_2 nontrivial topological band structure. (2) The discovery of chiral edge states inside the superconducting gap in heavy-fermion metal UTe_2 [1], which ignited the field searching for intrinsic chiral topological SC. (3) The discovery of zero-energy bound states localized at *both* ends of atomic line defects in monolayer FeTeSe/STO with the highest T_c in Fe-based SC [3], followed by the theoretical proposal of emergent quasi-1D topological SC with Majorana end states in naturally embedded quantum structures in unconventional spin-singlet high- T_c SC [23]. (4) Discovering competition between electronic nematicity and superconductivity on the nanometer scale in Fe-based SC $FeTe_{1-x}Se_x$ [22]. (5) Several original contributions to kagome lattice magnets and SC [2, 10-16, 18-21, 31-34, 36] highlighted below.

Recent Progress

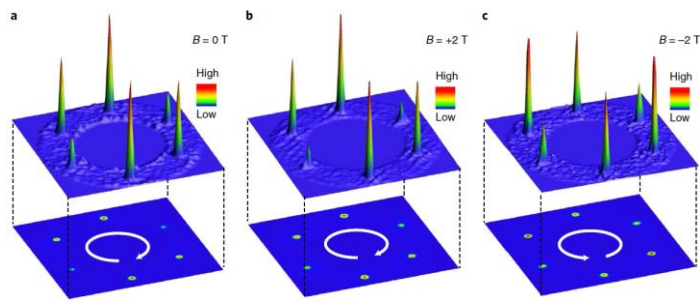
The search and discovery of correlated topological quantum states in transition metal kagome materials can be summarized as a trilogy. The first part began around 2007 and focused on strongly correlated insulator Herbertsmithite for the novel quantum spin liquid state and fractionalized excitations. The role of the kagome lattice geometry is essentially to

provide strong magnetic frustration. However, it is known that the special kagome geometry also frustrates the kinetic motion of electrons traversing the lattice. The quantum interference effects produce a noteworthy kagome lattice electronic structure signified by flat band, Dirac points, and van Hove singularities that naturally promote topological and correlation effects. It is thus equally desirable to study kagome metals.

The second part of the trilogy began around 2018, when a family of Fe, Co, and Mn-based kagome lattice transition metal shandites emerged. They are typically magnetic metals with the Fermi level lying close to either the flat band or the Dirac points of the kagome band structure. A fascinating set of correlated topological quantum states have been discovered, including massive Dirac fermions with giant magnetic field tunability enabled by the Berry curvature induced orbital magnetic moments, the magnetic Weyl semimetal with Fermi arc surface states and large anomalous Hall effect (AHE), the localized spin-orbital polarons [10, 11], and lightly doped topological Chern magnets with chiral fermion edge states close to the quantum limit [2].

The third part of the trilogy began in 2019 following the discovery of a new family of vanadium-based kagome lattice nonmagnetic metals AV_3Sb_5 ($A=K, Rb, Cs$), AVS for short, where V atoms form perfect kagome net. These compounds are nonmagnetic, exhibit Z_2 -nontrivial band structures with the Fermi level very close to the van Hove singularities. They develop unconventional charge density wave (CDW) orders accompanied by giant AHE despite the absence of magnetism. The field has leapt forward following the discovery of superconductivity in 2020, with more than 100 papers posted on the arXiv, reporting novel symmetry breaking quantum states, including chiral CDW, time-reversal symmetry breaking, rotation symmetry breaking, pseudogap and pair density waves, and chiral topological superconductivity. We made several original contributions since December.

Chiral and time-reversal symmetry breaking charge order in KV_3Sb_5 (Nature Materials 2021) – To investigate the nature of the CDW state, in collaboration with Zahid Hasan’s group at Princeton, we studied the topography and density of states using STM/S. We found



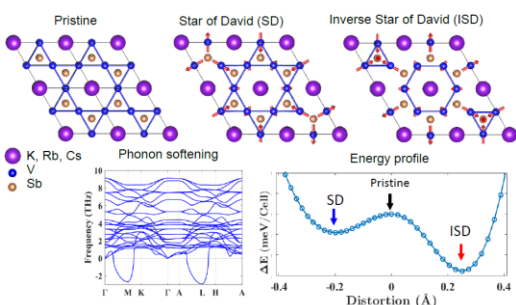
that the V electrons on the exhibits a triple-Q (3Q) CDW with 2×2 period. Surprisingly, the Fourier peaks of the dI/dV conductance maps at the CDW wave vector $\mathbf{Q}_{2 \times 2}$ have different intensity that breaks all reflection symmetry and exhibits a well-defined handedness, giving rise to a remarkable chiral charge order. Even

more intriguingly, we discovered that the chirality of the CDW couples to an applied magnetic field along the c-axis, and can be switched when the direction of the magnetic field is flipped. We thus concluded that the kagome metal hosts a chiral CDW that also breaks time-reversal symmetry (TRS), and conjectured that the long-sought-after TRS-breaking orbital current state proposed for the high- T_c cuprates may be present [20]. The robustness of the chiral CDW has been widely debated by STM groups, with some confirming our results and others finding the 2×2 CDW to have C_2 and reflection symmetry [31]. Our work has

stimulated the community to probe TRS breaking. Two μ SR groups have found evidence for TRS breaking onset inside the CDW phase, while the most recent optical polar Kerr rotation experiments detected TRS-breaking at the onset of the CDW.

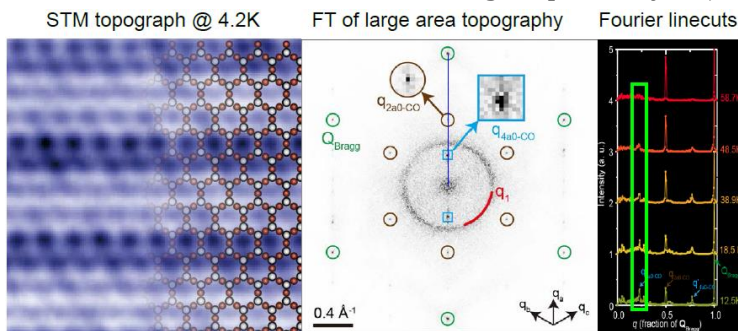
Orbital current and flux phase in kagome AV_3Sb_5 (*Science Bulletin* 2021) – Motivated by our conjecture of the orbital current in the chiral CDW phase from STM and AHE experiments, we studied the symmetry properties of a single-orbital model on the kagome lattice. We proposed a 2×2 CDW with TRS breaking orbital current and chiral flux that is competitive in energy and contributes to intrinsic anomalous Hall effect.

Electronic structure, phonon softening and CDW in kagome AV_3Sb_5 (*Physical Review Letters* 2021) – We carried out theoretical studies of the electronic structure and electron-



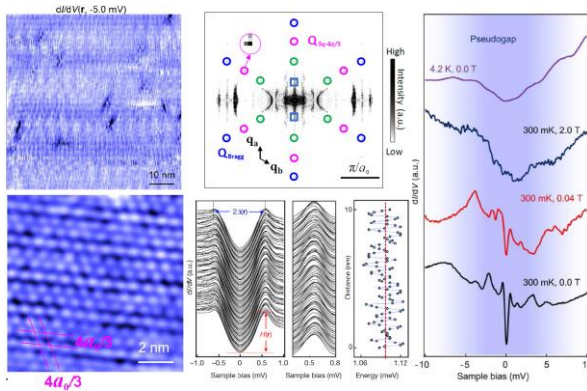
phonon coupling in collaboration with Binghai Yan from the Weizmann Institute. We found that the undistorted AVS is unstable due to phonon softening and leads to the 3Q CDW with 2×2 lattice distortions. Both Star of David (SD) and inverse SD (ISD) are locally stable. The ISD charge order pattern is lower in total energy. Although electron-phonon coupling is strong, we find that it alone cannot describe the superconductivity in AVS.

Cascade of correlated states and $4a_0$ unidirectional CDW in CsV_3Sb_5 (*Nature* 2021) – We studied the nature of the CDW state in CVS with our in-house STM group led by Ilija Zeljkovic. In addition to the 2×2 3Q-CDW order at wave vector $Q_{2 \times 2}$, we discovered a unidirectional charge order with $4a_0$ periodicity at $Q_{1 \times 4}$ that onsets at around 50-60K [16] and breaks both translation and rotational symmetry. We further observed strongly anisotropic quasiparticle interference pattern, suggesting orbital-selective correlation effects in the multiorbital vanadium kagome band structure. The 2×2 CDW and the $4a_0$ unidirectional charge order are found to persist into the superconducting state below the transition temperature 2.5K.



Roton pair density wave (PDW) and pseudogap behavior in CsV_3Sb_5 (*Nature* 2021) – Collaborating with Hongjun Gao's group at IOP, we studied [15] the nature of the superconducting state using the 30mK capability of the STM/S with high resolution. We found that the superconducting state has a V-shaped density of states with a pairing energy gap ~ 0.5 meV. Thus the SC is in the strong coupling regime with a two-gap to T_c ratio about 5. The dI/dV maps and their Fourier transforms reveal that, in addition to the coexisting 3Q-CDW peaks at $Q_{2 \times 2}$ and 1Q-CDW peaks at $Q_{1 \times 4}$, a new set of triple-Q peaks at $Q_{4/3 \times 4/3}$ emerges at low energies, suggesting that an underlying PDW at these wave vectors becomes coherent due to the superconducting condensate. Remarkably, the gap size, coherence peak height,

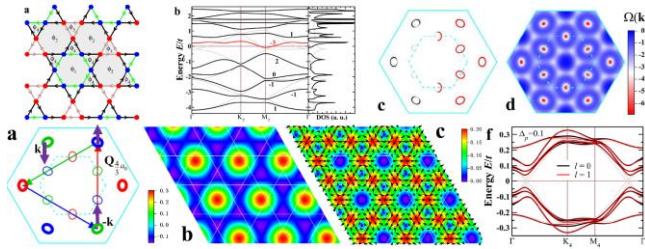
gap depth, and zero-bias density of states show $4a_0/3 \times 4a_0/3$ spatial modulations. We



discovered that the primary PDW is responsible for the observed pseudogap behavior, with striking analogies and distinctions to the high- T_c cuprates. In the pseudogap phase above T_c and the zero-temperature pseudogap phase under high magnetic field, the fluctuating PDW induces intertwined electronic order at the same wave vectors. We conjectured a roton PDW with an emergent vortex-antivortex lattice.

Chern Fermi pockets and chiral topological PDW in kagome superconductors – We

have been investigating theoretically the physical mechanism behind these remarkable properties in kagome superconductors. In our recent paper posted on the arXiv [36], we argued that the essential part of the phenomenology can be described by doped orbital Chern insulators. The Fermi level crosses the Chern bands of the TRS breaking 2×2 CDW state with orbital current, giving rise to the Chern Fermi pockets (CFPs) with sizes comparable to those detected by quantum oscillations. The CFPs carry concentrated Berry curvature of the Chern band and semi-quantitatively describe the large intrinsic anomalous Hall effect observed in the CDW phase. Remarkably, these CFPs



are connected by $3/4$ of the reciprocal lattice vectors and produce the novel $4/3 \times 4/3$ PDW observed in the superconducting and pseudogap phases in our Nature paper, including the conjectured “roton” PDW. Most intriguingly, due to the unique hexagonal symmetry, the PDW is intertwined with a uniform superconducting condensate, and is a never-before-encountered chiral topological PDW superconductor with chiral Majorana edge modes. Our findings point to a new orbital-based mechanism in a kagome materials platform for *intrinsic* chiral topological density waves and superconductors.

Future Plans

In the coming year, the research activities will focus on developing microscopic theories for the TRS breaking chiral CDW and the topological PDW in the kagome superconductors. Beyond providing theoretical descriptions of the remarkable experimental observations, we aim to fully establish by concrete correlated model calculations that the doped orbital Chern insulators with CFPs embody a rich set of correlated and topological states. They offer a new orbital-based mechanism and a prominent kagome materials platform for *intrinsic* chiral topological density waves and superconductors. We will explore the PDW mechanism for *intrinsic* chiral topological superconductivity and other novel paired states with unconventional and fractionalized vortices, and study its potential relevance for twisted bilayer graphene and other hexagonal quantum materials.

Recent Publications (Since 2020)

1. L. Jiao, et al., **Nature** 579, 523 (2020).
2. J. -X. Yin, et al., **Nature** 583, 533 (2020).
3. Cheng Chen, et al., **Nature Physics** 16, 536 (2020).
4. Sen Zhou, et al., **Physical Review B** 101, 035106 (2020).
5. Chaofei Liu, et al., **Science Advances** 6, eaax7547 (2020).
6. J. Q. Liu, et al., **Physical Review Research** 2, 033260 (2020).
7. Yi Zhang, et al., **Physical Review B** 102, 035136 (2020).
8. Songtian S. Zhang, et al., **Physical Review B** 101, 100507 (2020).
9. J. -X. Yin, et al., **Physical Review B** 102, 054515 (2020).
10. Yuqing Xing, et al., **Nature Communications** 11, 5613 (2020).
11. Jia-Xin Yin, et al., **Nature Communications** 11, 4415 (2020).
12. Songtian S. Zhang, et al., **Physical Review Letters** 125, 046401 (2020).
13. J. -X. Yin, et al., **Nature Communications** 11, 4003 (2020).
14. Zhonghao Liu, et. al., **Nature Communications** 11, 4002 (2020).
15. Hui Chen, et al., **Nature** (2021). <https://doi.org/10.1038/s41586-021-03983-5>
16. He Zhao, et al., **Nature** (2021). <https://doi.org/10.1038/s41586-021-03946-w>
17. Yun-Peng Huang, et al., **Physical Review B** 104, 165145 (2021).
18. Hengxin Tan, et al., **Physical Review Letters** 127, 046401 (2021).
19. Xilin Feng, et al., **Science Bulletin** 66, 1384 (2021).
20. Yu-Xiao Jiang, et al., **Nature Materials** 20, 1353 (2021).
21. C. Mielke, III, et al., **Physical Review Materials** 5, 034803 (2021).
22. He Zhao, et al., **Nature Physics** 17, 903 (2021).
23. Yi Zhang, et al., **Physical Review X** 11, 011041 (2021).
24. Zheng Ren, et al., **Nature Communications** 12, 10 (2021).
25. He Zhao, et al., **Science Advances** 7, eabi6468 (2021).
26. Chang-Jiang Zhu, et. al., **Chinese Physics B** 30, 106802 (2021).
27. Kun Jiang, et al., **Physical Review B** 103, 045108 (2021).
28. Peng Fan, et al., **Nature Communications** 12, 1348 (2021).
29. Geng Li, et al., [arXiv:2110.07813](https://arxiv.org/abs/2110.07813) (2021).
30. Chun-Jiong Huang, et al., [arXiv:2011.05919](https://arxiv.org/abs/2011.05919) (2020).
31. Hong Li, et al., [arXiv:2104.08209](https://arxiv.org/abs/2104.08209) (2021).
32. Haitao Yang, et al., [arXiv:2110.11228](https://arxiv.org/abs/2110.11228) (2021).
33. Haoxiang Li, et al., [arXiv:2109.03418](https://arxiv.org/abs/2109.03418) (2021).
34. H. Miao, et al., [arXiv:2106.10150](https://arxiv.org/abs/2106.10150) **Physical Review B**, in press (2021).
35. Ching-Kai Chiu and Ziqiang Wang, [arXiv:2109.15227](https://arxiv.org/abs/2109.15227) (2021).
36. Sen Zhou and Ziqiang Wang, [arXiv:2110.06266](https://arxiv.org/abs/2110.06266) (2021).

Exploiting locality in electronic structure: tensor networks, gausslets, blue electrons, and machine-learning

Principal Investigator: Professor Steven R. White

Department of Physics & Astronomy, University of California, Irvine, CA 92697

srwhite@uci.edu

Co-Principal Investigator: Professor Kieron Burke

Department of Chemistry and of Physics, University of California, Irvine, CA 92697

kieron@uci.edu

Program Scope

The overarching theme of this project is to bring an unprecedented combination of high accuracy and efficiency to correlated electronic structure calculations of solids using the density matrix renormalization group and tensor networks, and to make this accuracy widely available for complicated systems by density functional methods. In a nutshell, by using several novel techniques, including entirely new ways of choosing optimal basis sets for strongly correlated systems, we can make correlated wavefunction calculations with Density Matrix Renormalization group (DMRG) far more efficient than before. We then use recently developed machine learning (ML) techniques to create density functionals which correct the errors in standard semi-local approximations, to yield “chemical accuracy” (errors less than 1.6 milliHartree) for strongly correlated systems. In addition to ML techniques, we also develop an alternative to standard Kohn-Sham (KS) density functional theory (DFT) called conditional probability (CP) DFT which attempts to avoid several blatant errors made in KS-DFT approximations, such as bond breaking and self-interaction errors, by bypassing the need to approximate the exchange-correlation (XC) energy functional.

Initial progress was driven by the meticulous creation of a one-dimensional (1D) mimic of real electronic structure calculations, in which approximate density functionals make errors that are quantitatively similar to those in realistic simulations. We developed algorithms and tuned the interaction so that DMRG calculations are extremely efficient in this 1D world, and even include a mimic of the electron-electron cusp. This has allowed us to run a near endless sequence of calculations to create/refine/test our new basis set approaches, and to generate sufficient data to train ML density functionals on strongly correlated systems, and in the thermodynamic limit.

We demonstrated how efficient local basis functions could be in quasi-one-dimensional realistic calculations. For 3D systems, we developed multi-sliced gausslets, which when used with DMRG solves hydrogen chain systems in the complete-basis-limit with exact correlation. In the last year we have completed development of hybrid Gaussian/gausslet bases, where the Gaussians are utilized to efficiently capture core electrons. Simultaneously, we are creating the machinery to train ML density functionals on the output from these multi-sliced calculations, thus reproducing this high accuracy in routine low-cost DFT calculations. The DMRG approach is crucial for rapidly generating data for training functionals, and for treating the most correlated systems. For a broad range of other systems, the ML density functional will provide high accuracy ground-state energies and densities with much lower computational cost.

Keywords: Density Matrix Renormalization group, Density functional theory development, Machine-learned physics

Recent Progress

Hybrid gausslet/Gaussian basis sets

Recently we completed a paper describing the next steps in developing 3D gausslet basis functions, where we form a hybrid basis with gausslets and an ordinary Gaussian basis [1]. Gausslets are not efficient in representing cores of large Z atoms, whereas Gaussians are. The key issue in combining the bases is in preserving the diagonal nature of the two-electron Hamiltonian when the Gaussians are added to the basis. As part of this work, we also studied how one can accelerate the approach to the complete basis set limit. We developed a cusp correction based on the double occupancy of each local basis function. As shown in Figure 1, these corrections allows us to achieve accuracies at the micro-Hartree level. The demonstration here is for a two electron system, where the complete basis set energy is known nearly exactly, but the correction is easily applied in the many electron case.

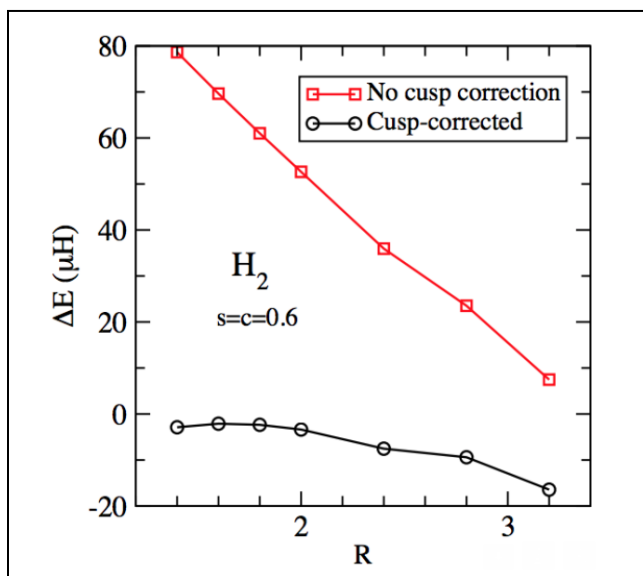


Figure 1. Energy for H_2 in a hybrid gausslet/Gaussian basis compared with nearly exact variational calculations, showing the effect of a cusp correction based on the double occupancy of each gausslet. The energy errors are due to the incompleteness of the basis; the cusp correction eliminates the errors down to the microHartree scale.

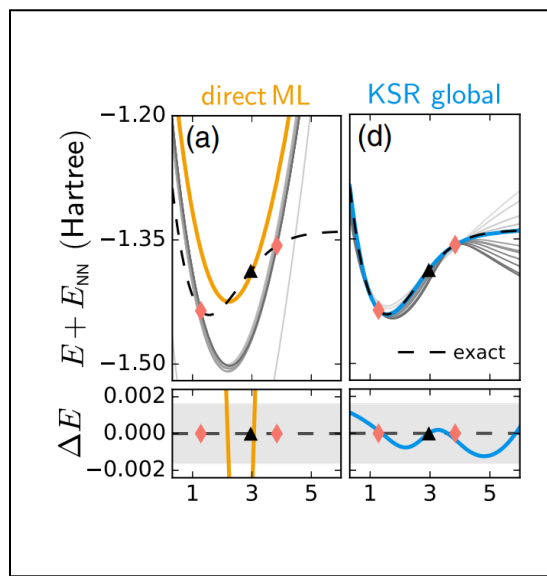


Figure 2. One-dimensional H_2 dissociation curve for ML models trained from two molecules (red diamonds) with optimal models (highlighted in color) selected by the validation molecule at $R = 3$ (black triangle). The exact curve is represented as a black dashed line. The bottom panel shows the difference from the exact curve. (a) an ML model that directly predicts E from geometries. (d) a fully non-local (global) neural XC functional model trained using the KSR method. Figure repurposed from [2].

Kohn-Sham regularizer

Recently, there has been substantial interest in using ML methods to improve DFT approximations. When creating effective ML models in physics, including prior knowledge is important and is often incorporated explicitly using loss terms or constraints on model architectures. In recent work, we additionally embed prior knowledge in the computation itself by solving the KS equations when training neural network models for the XC functional [2]. We find that this method provides an implicit regularization during training and greatly improves the generalization of the resulting XC models. For example, using this KS regularizer (KSR) method and 1D analog model systems, we show that only two training points are needed to learn the entire 1D H_2 dissociation curve within chemical accuracy, including the strongly correlated region, see Figure 2. We have also extended this method for spin-polarized systems by proposing an analogous spin-adapted version [4]. We assess generalizability by training on a handful of 1D atomic systems and testing on a set of unseen 1D equilibrium-bonded molecules. In particular, we find that our non-local neural XC model obtains near chemical accuracy for ground-state properties of 1D molecules in the test set [4].

Conditional probability DFT

In recent work [3] we proposed a theoretical framework called conditional probability DFT (CP-DFT). CP-DFT is an alternative to KS-DFT, in which we directly calculate conditional probability (CP) densities, from which the energy can be calculated. Instead of relying on an XC functional approximation, which have many well-known deficiencies, CP-DFT extracts the XC energy from a sequence of density functional calculations of conditional probabilities. Such CP calculations are naturally carried out using Gausslet basis functions and are embarrassingly parallelizable. In [3] we analyze results

from a simple CP approximation, dubbed the blue electron approximation, that satisfies several important exact conditions, such as the electron-electron cusp condition. It was shown that this simple CP approximation yields usefully accurate results for the uniform gas, two-electron ions, including H^- , and the hydrogen dimer, even as the bond is stretched. CP-DFT has no self-interaction error for one electron, and correctly dissociates H_2 , both major challenges in standard KS-DFT. A highlight of results is presented in Figure 3.

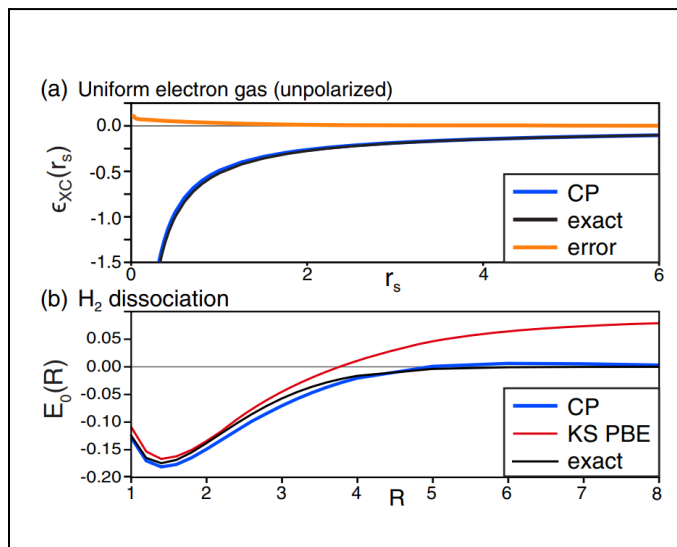


Figure 3. Results from CP approximation (blue curve) and exact (black curve). (a) XC energy per electron in uniform gas at increasing Wigner-Seitz radii, r_s . (b) binding energy curve for H_2 . The red curve is standard KS-DFT using the PBE XC functional. Figure repurposed from [3].

Future Plans

For the gausslet work, we will be focusing on a decimation procedure that starts with a gausslet or hybrid gausslet basis and "decimates it" to reduce the number of functions while maintaining the diagonal property. We require as input for the decimation an approximate single particle reduced density matrix (1-RDM). If we did not care about the diagonal property, the best basis would be the largest occupancy eigenstates of the 1-RDM, the natural orbitals. The problem is much more difficult when one wants to maintain diagonality. We require that the basis includes not only the natural orbitals, but also a good representation of their products (as in the "density-fitting" method). Additional functions must be added to make the basis localizable, and an approximate joint diagonalization method is used to obtain the localized functions. Localized functions are necessary but not sufficient, however, to produce the diagonal property, and we use automatic differentiation based optimization to modify the functions slightly to produce the diagonal properties. Preliminary tests show that this decimation procedure can reduce the size of the bases by roughly an order of magnitude while maintaining chemical accuracy.

The KSR and spin-adapted KSR methods have shown promising potential so far. However, the generalization of trained neural XC models has not been thoroughly explored. In particular, it would be useful to demonstrate transferability of trained models to a more diverse set of unseen, and strongly-correlated systems. Another major step is to extend the KSR method and associated neural XC models to 3D systems in a computationally efficient manner. The hybrid gausslet basis set could be especially useful here to generate high accuracy training data.

In our most recent CP-DFT approach, the initial results were based off a fairly rudimentary approximation and are surprisingly accurate. We plan to further explore the formal theory of CP-DFT, such as deriving more exact conditions and extending the theory to spin-polarized systems. To gain further insight, we also plan to implement and test CP-DFT approximations and concepts on a more diverse set of systems. The hybrid gausslet basis set will be useful here to both carry out and benchmark CP calculations.

Publications

[1] Qiu, Yiheng, and White, S.R. "Hybrid gausslet/Gaussian basis sets", accepted in the Journal of Chemical Physics, arXiv:2103.02734 (2021)

[2] Li, Li, et al. "Kohn-Sham equations as regularizer: Building prior knowledge into machine-learned physics." Physical review letters 126.3 (2021): 036401.

[3] McCarty, Ryan J., et al. "Bypassing the Energy Functional in Density Functional Theory: Direct Calculation of Electronic Energies from Conditional Probability Densities." Physical Review Letters 125.26 (2020): 266401.

[4] Kalita, Bhupalee, et al. "Generalizability of density functionals learned from differentiable programming on weakly correlated spin-polarized systems." arXiv preprint arXiv:2110.14846 (2021).

First principles thermodynamics of intrinsically disordered matter

Michael Widom, Carnegie Mellon University, Department of Physics

Program Scope

Even in nominally ordered materials such as crystals, a certain degree of disorder inevitably occurs. Counterintuitively, such intrinsic disorder actually enhances the thermodynamic stability of matter by raising its entropy and thereby reducing its free energy. In contrast to the internal energy, where well established methods such as electronic density functional theory allow accurate and reasonably efficient calculation, the entropy has resisted a simple and universally applicable approach. Hence, methods to calculate the entropy play a central role in this project. Alongside that effort, we are modeling the disorder present in a variety of interesting material systems including high entropy alloys, quasicrystals, and liquid metal alloys. Through this modeling we seek to quantify the short-range chemical order and phase transformations that lead to long-range chemical order. Our approaches include Monte Carlo simulations, analytical tools such as the Cluster Variation Method, and generalizations of the Coherent Potential Approximation.

Keywords: Long- and short-range chemical order; information-based entropy calculation methods; thermodynamics of intrinsically disordered materials.

Recent Progress

Entropy is a function of the thermodynamic state, and as such it should be calculable from a representative member of the equilibrium ensemble. Specifically, it equals (in suitable units) the *information* required to specify the instantaneous state. The greater the disorder, the amount of information that must be provided to specify the position and chemical species of every atom. This information can be captured in the form of correlation functions, which in turn can be simulated from first principles Monte Carlo or molecular dynamics. We have applied this idea to propose methods for calculation of entropy in three different types of material: liquid metals and alloys, in which we calculate the deviation from the absolute entropy of an ideal gas as a functional of the pair correlation functions; chemical substitutions of high entropy alloys, in which we employ multi-point chemical species correlations as in the Cluster Variation Method; vibrational entropy of solids, based on the covariances of atomic displacements during molecular dynamics simulations.

Recently [1] we calculated absolute free energies of liquid alkali metal alloys by combining first principles simulated total energies with absolute entropies obtained from simulated pair correlation functions. We were able to predict that Li-Na would phase separate owing to strongly unfavorable interatomic interactions that exceed the entropy of mixing at all but extremely high

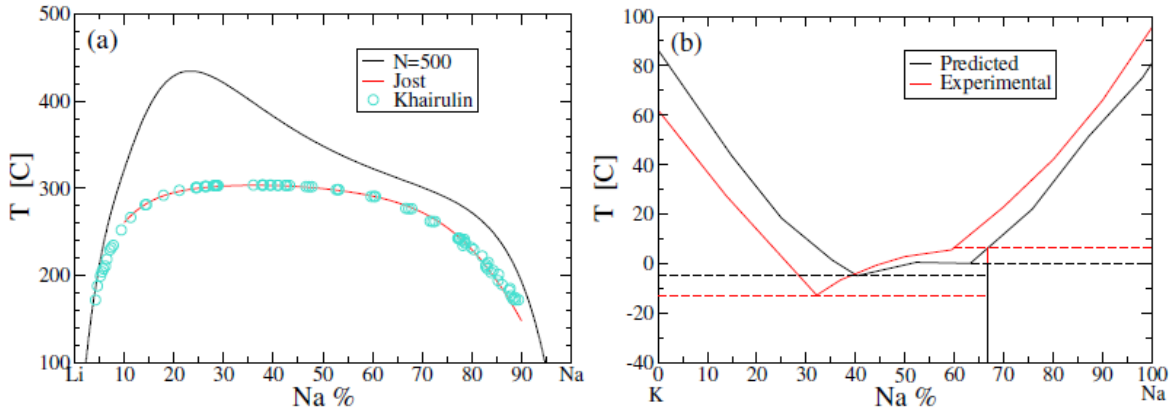


Figure 1. Phase diagrams of (a) Li-Na and (b) K-Na as predicted by first-principles absolute free energy calculations.

temperatures, while Na-K would mix at all but extremely low temperatures, despite mildly unfavorable interactions. Indeed, Na-K exhibits a deep eutectic and remains liquid down to $T = -13\text{C}$. Fig. 1 displays our predicted phase diagrams. For Na-K we closely reproduce experiment, while for Li-Na our results are a good way from the critical point. Near the critical point we see deviations that we attribute to critical fluctuations and the diverging correlation length.

Whereas the absolute entropy of liquids is obtained by reducing the ideal gas entropy by the mutual information content of the pair correlation functions, we obtain the chemical substitutional entropy of high entropy alloys by reducing the ideal entropy of mixing by the information content of correlation functions. Previously [2] we included only pair correlations (the equivalent of the Warren-Cowley order parameters), while now we extend up to four-point correlations defined at the vertices of a tetrahedron. The entropy at this level is obtained via the formalism of Kikuchi's Clustr Variation Method. The pair correlation function overestimates the entropy reduction because of the mutual reinforcement of correlations around closed loops. Together with Wissam Al-Saidi we have employed machine learning potentials for MoNbTaW to obtain accurate higher order correlations that illustrate this. We also verified the effect through the use of high temperature series expansions.

As shown in Fig. 2 for a MoNbTaW high entropy alloy, nearest neighbor pair correlations (CVM-NN) lower the entropy relative to ideal mixing ($\log(4)$), while the tetrahedron approximation (CVM-Tetra) raises the predicted entropy at low

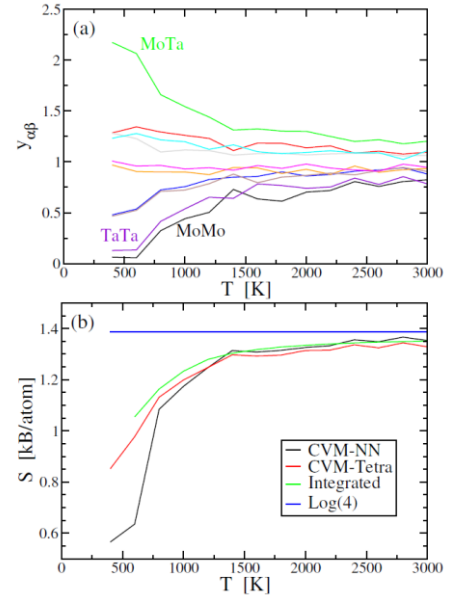


Figure 2. (a) Nearest neighbor pair frequencies normalized by concentrations. (b) Predicted entropy at different levels of approximation compared with thermodynamic integration.

temperatures relative to the pair approximation. To validate the accuracy at this level of approximation, we compare with the prediction of thermodynamic integration. However, thermodynamic integration does not yield absolute entropy, so we shifted that curve vertically to match up with the others at high temperature.

All solids have vibrational entropy related to small thermally excited displacements from ideal lattice sites. While these are fairly well described by harmonic theory, with anharmonicity included via thermal expansion. At elevated temperatures, molecular dynamics is required to include the full effects of anharmonicity. We have derived an expression for the entropy as a functional of the covariance matrix for interatomic displacements. At low temperatures we apply quantum corrections to correct the negative divergence of classical entropy. This approach works with high accuracy for Al and fairly well for Na. We are investigating the role of higher order cumulants of displacement for the case of Na, and also the applicability to the vibrational entropy of high entropy alloys. Fig. 3 illustrates the predicted entropy of Al and the covariance matrix on which it is based.

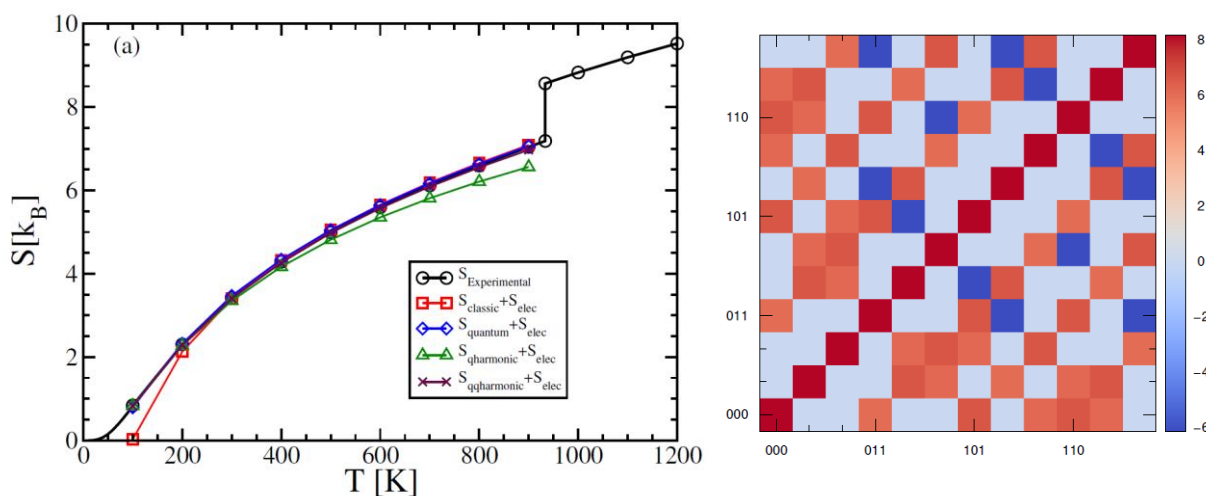


Fig. 3. Entropy of solid Al (a) as predicted by the covariance matrix obtained from first principles molecular dynamics. Classic is the classical prediction, while quantum quantizes the vibrational levels. Qharmonic is the quasiharmonic theory, while qqharmonic utilizes experimental thermal expansion. Covariance matrix (b) reveals correlations among neighboring atomic displacements.

In addition to our work on entropy, we are investigating the impact of substitutional disorder and short-range chemical order on the electronic structure of alloys. The coherent potential approximation is an efficient approximation for the limit of complete disorder. The top panel of Fig. 4 illustrates the principle: the disordered CPA medium (purple) is represented as a concentration-weighted average C_i of the individual atomic species i (red and blue) embedded in the CPA medium. In our approach [3] shown in the bottom panel of Fig. 4, we bias the concentrations in the neighborhoods of the red and blue atoms according to short-range order

parameters W_{ij} . We apply density functional theory to calculate the electronic structure and total energy using the KKR multiple scattering Green function method. Applying this method to the model binary alloy CuZn and to the high entropy alloy AlCrTiV, we were able to resolve the preferred patterns of short-range chemical order and sublattice ordering. We made the code publicly available on GitHub.

As a follow-on to this effort, we are developing methods to calculate the electrical conductivity of alloys in the presence of short-range chemical order. Currently [4] we have implemented only the CPA theory, and we have applied it to predict conductivity trends in high entropy alloy families. Future code development will be carried out under a recently obtained NSF-CSSI project, while applications of the method to high entropy alloys and other model systems such as K-state alloys, thermoelectrics, and spin-Hall systems will be carried out under the current project.

Future Plans

Our plan for the near future focuses on modeling the structure and thermodynamics of Al-Co-Cu decagonal quasicrystals. We have obtained excellent interatomic potentials for simulation that allow us to obtain enthalpies close to the convex hull. Chemical substitutional entropy will likely explain the stability at elevated temperatures.

References

- [1] Y. Huang, “M. Widom and M. C. Gao, “Ab-initio free energies of liquid metal alloys: application to the phase diagrams of Li-Na and K-Na”, *Phys. Rev. Mat.* (under review 2021)
- [2] M.C. Gao, C. Zhang, P. Gao, F. Zhang, L.Z. Ouyang, M. Widom, and J.A. Hawk, “Thermodynamics of Concentrated Solid Solution Alloys”, *Curr. Opin. Solid State Mat. Sci.* **21** (2017) 238-251
- [3] V. Raghuraman, Y. Wang and M. Widom, “An averaged cluster approach to including chemical short range order in KKR-CPA”, *Phys. Rev. B* **102** (2020) 054207
- [4] V. Raghuraman, Y. Wang and M. Widom, "An investigation of high entropy alloy conductivity using first-principles calculations", *Appl. Phys. Lett.* **119** (2021) 121903

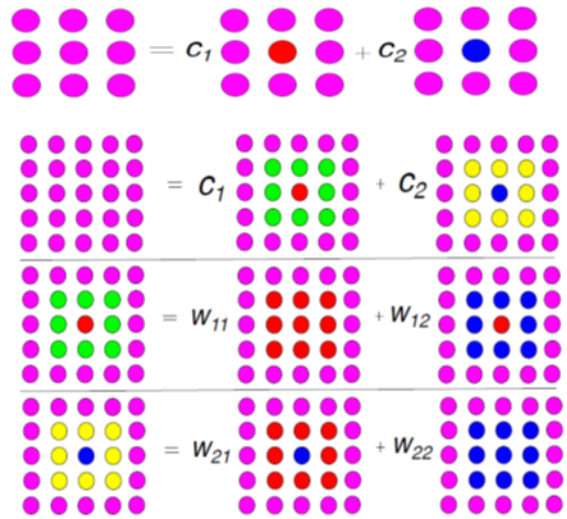


Fig. 4. The CPA approximation (top) models the limit of complete disorder, while our method (bottom) incorporates short-range chemical order.

Publications

R. Feng, B. Feng, M. C. Gao, C. Zhang, J. C. Neuefeind, J. D. Poplawsky, Y. Ren, K. An, M. Widom, and P. K. Liaw, "Superior high-temperature strength in a supersaturated refractory high-entropy alloy", (*Adv. Mat.*, to appear, 2021)

V. Raghuraman, Y. Wang and M. Widom, "An investigation of high entropy alloy conductivity using first-principles calculations", *Appl. Phys. Lett.* **119** (2021) 121903

C. Lee, F. Maresca, R. Feng, Y. Chou, T. Ungar, M. Widom, K. An, J. D. Poplawsky, Y.-C. Chou, P. K. Liaw and W. A. Curtin, "Strength Can be Controlled by Edge Dislocations in Refractory High-Entropy Alloys", (*Nat. Comm.* to appear 2021, <https://arxiv.org/pdf/2008.11671>)

R. Feng, C. Zhang, M.C. Gao, Z. Pei, F. Zhang, Y. Chen, D. Ma, K. An, J.D. Poplawsky, L. Ouyang, Y. Ren, J.A. Hawk, M. Widom and P.K. Liaw, "High-throughput design of high-performance lightweight high-entropy alloys", *Nat. Comm.* **12** (2021) 4329

Y. Huang, M. Widom and M.C. Gao, "Ab-initio free energies of liquid metal alloys: application to the phase diagrams of Li-Na and K-Na", (*Phys. Rev. Mat.*, under review) <http://arxiv.org/abs/2105.08491>

S. Dutta, Y. Yun, M. Widom and A.J. Gellman, "2D Ising Model for Adsorption-induced Enantiopurification of Racemates", *ChemPhysChem* **22** (2020) 197-203

N. Hoffman and M. Widom, "Cluster variation method analysis of correlations and entropy in BCC solid solutions", *Mat. Met. Trans. A* **52** (2020) 1551-8

V. Raghuraman, Y. Wang and M. Widom, "An averaged cluster approach to including chemical short range order in KKR-CPA", *Phys. Rev. B* **102** (2020) 054207

F. Lupke, D. Waters, S.C. de la Barrera, M. Widom, D.G. Mandrus, J. Yan, R.M. Feenstra, B.M. Hunt, "Coexistence of quantum spin hall edge state and proximity-induced superconducting gap in monolayer 1T'-WTe₂", *Nat. Phys.* **16** (2020) 526-30

M. Mihalkovic and M. Widom, "Spontaneous formation of thermodynamically stable Al--Cu--Fe icosahedral quasicrystal from realistic atomistic simulations", *Phys. Rev. Resch.* **2** (2020) 013196

E. Eklof, A. Fischer, A. Ektarawong, A. Jaworsky, A. Pell, J. Grins, S. Simak, B. Alling, Y. Wu, M. Widom, W. Scherer and U. Haussermann, "Mysterious SiB₃: Identifying the relation between α - and β -SiB₃", *ACS Omega* **4** (2019) 20

DECODE: Data-driven Exascale Control of Optically Driven Excitations in Chemical and Material Systems

PI: Bryan M. Wong (University of California, Riverside), Co-PIs: Christian Shelton (University of California, Riverside), Zizhong Chen (University of California, Riverside), Ibrahim Khaled (Lawrence Berkeley National Laboratory), Mauro Del Ben (Lawrence Berkeley National Laboratory)

Program Scope

This collaborative project will harness exascale computing and non-conventional machine-learning approaches to design tailored optical excitations for controlling electron-driven dynamics in chemical/material systems. **Figure 1** summarizes the overall scope and inter-connected approaches used in this project for designing tailored, optically-driven excitations to control and manipulate the long-term dynamics of chemical/material systems. Within this coordinated approach, (1) RT-TDDFT calculations are first utilized to create a simulation set (i.e., pulse width, excitation frequency, and amplitude) for (2) calculating target “control” descriptors for enhanced electron/energy transfer efficiency. These computationally-intensive calculations will be (3)

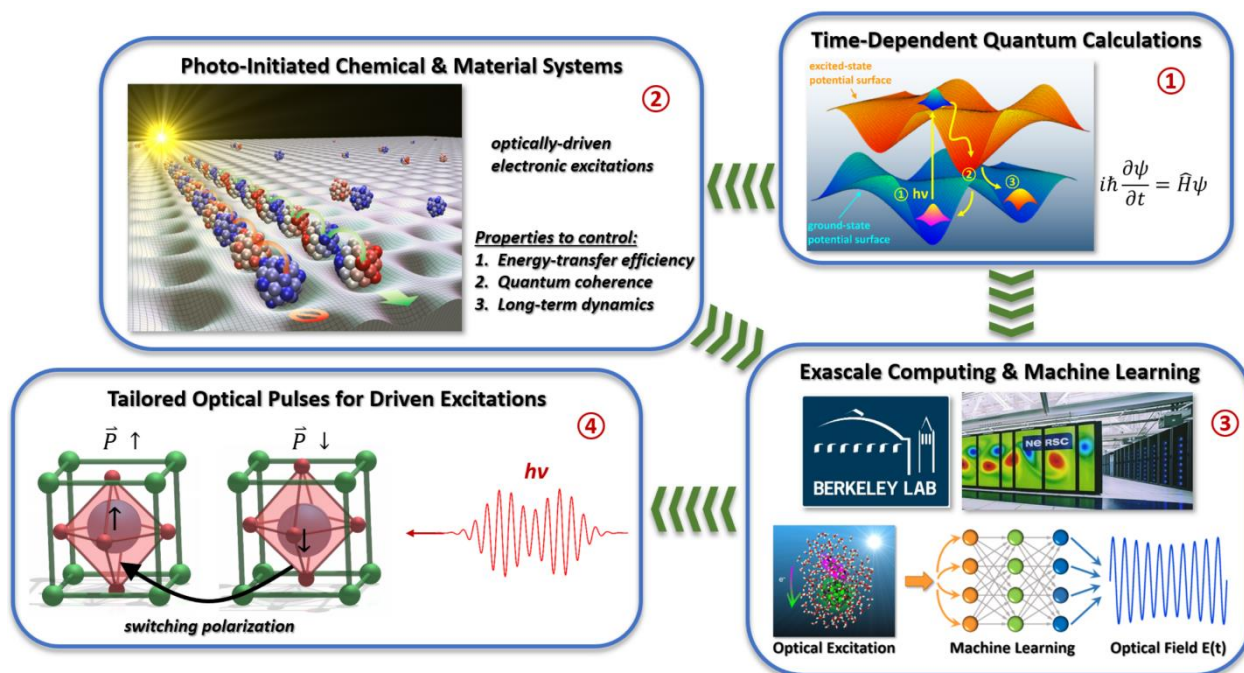


Figure 1: Overall scope and interconnected approaches for optimizing optically driven excitations to control the dynamics of chemical/material systems. (1) RT-TDDFT calculations with periodic boundary conditions are first utilized to generate data for (2) calculating target control parameters for enhanced electron/energy transfer efficiency in material systems. The ability to generate this high-quality data is enabled by (3) exascale computing and machine-learning approaches with the end goal of constructing tailored optimal pulse shapes for (4) controlling specific, driven excitations in chemical/material systems.

optimized to efficiently run on leadership-class pre-exascale and exascale HPC systems to finally enable (4) Bayesian-based hyperparameter optimization algorithms to construct tailored optimal pulse shapes for controlling specific, driven excitations in chemical/material systems (such as polarization switching in ferroelectric materials¹ or directed electron-transfer excitations on surfaces). Collectively, these four synergistic approaches address far-from-equilibrium phenomena with advanced scientific computing, behavior of properties in electric/magnetic fields, and ultimately controlling chemical/material processes under the influence of driven excitations to predict their long-term dynamics. Due to the sheer volume of data and number of CPUs/GPUs used in these calculations, this project also addresses fault-tolerance computational issues, which has not received appropriate attention in most large-scale parallelization efforts. Finally, the LBNL team members in this project are also directly involved in the architecture exploration path for NERSC10 and beyond, which ensures that this project has direct relevance to upcoming DOE ASCR and exascale initiatives.

Keywords: time-dependent density functional theory, quantum control, machine learning

Recent Progress

The official start date of this project was 08/15/2021, and during the past month, we have started to profile our RT-TDDFT code in preparation for the parallelization efforts on DOE HPC systems by the LBNL team (see **Figure 2**). To this end, the initial versions of our code have been implemented in the open-source PySCF code.² Most importantly, the PySCF code utilizes

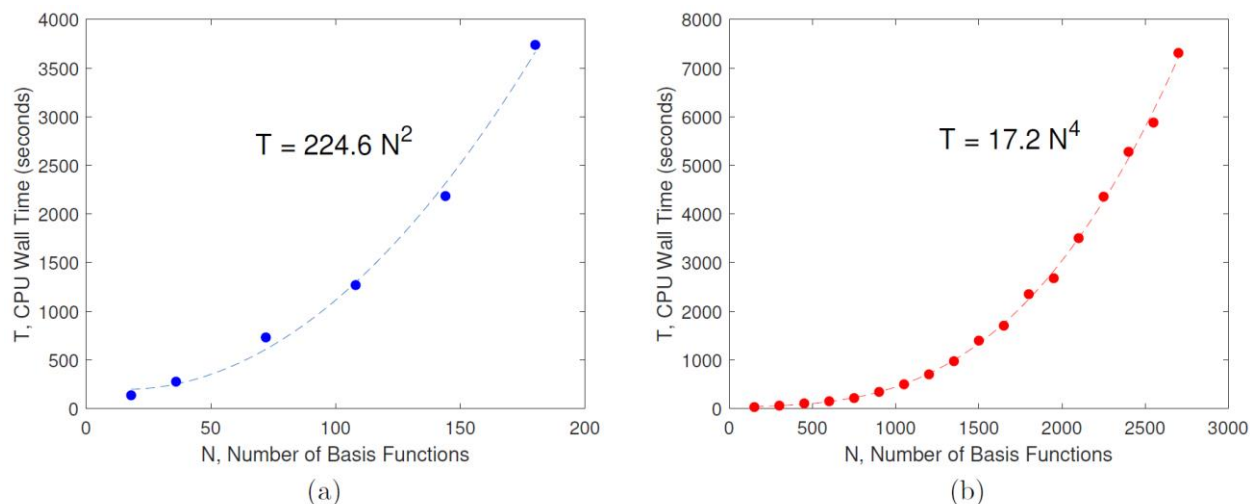


Figure 2: Computational scaling of (a) Hartree Fock exchange and (b) RT-TDDFT propagation for periodic supercells of diamond. The data points were obtained with a customized PySCF code for RT-TDDFT calculations in the PI's group, and the dotted lines in each graph denote a polynomial fit to the data. The evaluation of nonlocal exchange scales as N^4 with basis set size, whereas the real-time propagation scales as N^2 . One goal of this project is to scale these calculations to large periodic systems with hybrid functionals and hundreds of thousands of basis sets.

Gaussian basis sets that are more computationally efficient for hybrid functionals and solid surfaces than plane-wave expansions. For the RT-TDDFT calculations described previously, the most computationally intensive routines are the generation and propagation of the time-dependent Hamiltonian matrix. This is particularly crucial in the case of hybrid exchange-correlation functionals where the computational bottleneck is building the Hartree-Fock exchange (HFX) part of the Hamiltonian. When using a localized basis in the PySCF code, the evaluation of periodic HFX involves a tensor-like contraction of a rank 4 tensor (i.e., the four-center, two-electron repulsion integrals (ERIs)) with the density matrix at each step of the SCF procedure.

We have recently carried out preliminary scaling tests on our customized PySCF code for RT-TDDFT calculations of periodic systems in **Figure 2**. The most salient point of this graphical analysis is that while the evaluation of HFX scales as N^4 , the pre-factor for the real-time propagation of the RT-TDDFT equations is large and not negligible. It is worth mentioning that the RT-TDDFT calculations are nearly embarrassingly parallel over the number k (momentum) points. As such, accelerating both the generation and propagation of the hybrid-tuned periodic RT-TDDFT equations in this project will also improve parallelization over k points to ensure a comprehensive, rigorously sound, and validated computational capability upon completion.

Future Plans

For our future plans (based on the computational challenges mentioned above), we are pursuing the following parallelization activities: (1) Screening of ERIs combined with the sparsity of the density matrix can lead to linear scaling techniques that mitigate the $O(N^4)$ scaling for the formation of the Fock matrix (cf. **Figure 2b**). We anticipate that parallelization will be strongly system dependent, which dictates the effective sparseness of the density matrix and ERI tensors. (2) Our existing implementation of hybrid-XC periodic RT-TDDFT will be further profiled, computational bottlenecks will be identified, and computational kernels simulating the full application running at scale will be isolated. (3) A performance-portable design for accelerator technologies on the isolated kernels will be implemented. The isolated kernels will themselves be optimized to define best portability strategies, and kernel refactorization will be utilized to exploit available accelerated libraries and data structures (for accelerated ERI tensor contractions). (4) The kernel's performance will be improved to leverage near-peak performance usage on an accelerator. Accelerated libraries will be explored for the computation of ERIs to reduce load imbalance and increase arithmetic intensity. (5) Low-rank approximations and density fitting techniques will be exploited (such as the resolution of the identity approximation³) to speed-up the prefactor of the integral evaluation. (6) GPU-accelerated alternatives will be explored for distributed matrix-multiplications⁴⁻⁵ and iterative eigensolvers.⁶

References

1. Chao Lian, Zulfikhar A. Ali, Hyuna Kwon, and Bryan M. Wong. Indirect but efficient: Laser-excited electrons can drive ultrafast polarization switching in ferroelectric materials. *Journal of Physical Chemistry Letters*, 10:3402-3407, 2019.
2. Qiming Sun, Timothy C. Berkelbach, Nick S. Blunt, George H. Booth, Sheng Guo, Zhendong Li, Junzi Liu, James D. McClain, Elvira R. Sayfutyarova, Sandeep Sharma, Sebastian Wouters, and Garnet Kin-Lic Chan. Pyscf: the python-based simulations of chemistry framework. *WIREs Computational Molecular Science*, 8:e1340, 2018.
3. Xinguo Ren, Patrick Rinke, Volker Blum, Jurgen Wieferink, Alexandre Tkatchenko, Andrea Sanfilippo, Karsten Reuter, and Matthias Scheffler. Resolution-of-identity approach to Hartree-Fock, hybrid density functionals, RPA, MP2 and GW with numeric atom-centered orbital basis functions. *New Journal of Physics*, 14:053020, 2012.
4. Grzegorz Kwasniewski, Marko Kabic, Maciej Besta, Joost VandeVondele, Raffaele Solca, and Torsten Hoefler. Red-blue pebbling revisited: Near optimal parallel matrix-matrix multiplication. *Proceedings of the International Conference for High Performance Computing, Networking, Storage and Analysis, SC '19, New York, NY, USA, 2019. Association for Computing Machinery.*
5. Mark Gates, Jakub Kurzak, Ali Charara, Asim YarKhan, and Jack Dongarra. SLATE: Design of a modern distributed and accelerated linear algebra library. In *Proceedings of the International Conference for High Performance Computing, Networking, Storage and Analysis, SC '19, New York, NY, USA, 2019. Association for Computing Machinery.*
6. Andreas Stathopoulos and James R. McCombs. PRIMME: PREconditioned Iterative MultiMethod Eigensolver - methods and software description. *ACM Transactions on Mathematical Software*, 37:21, 2010.

Publications

This project started less than one month ago with funding allocated to the team recently on September 29, 2021; as such, no publications acknowledging this award have been published to date.

Dispersive Interactions in Quantum Materials: Interplay between Anisotropy, Doping, and Non-linearity

Lilia M. Woods,

Department of Physics, University of South Florida, Tampa, FL 33620

Program Scope

Ubiquitous interactions originating from electromagnetic fluctuations have become increasingly important in light of rapid discoveries of novel materials. Such forces are major players for the stability of many layered composites and the operation of devices at the nanoscale. The expanding materials library with systems having Dirac fermions and nontrivial topology has opened up new opportunities to probe fluctuation induced interactions and uncover unusual scaling laws, dependences on physical constants, and sign variations. Specifically, materials, such as silicene, germanene, and stanene (newly added members of the graphene family) can experience force phase transitions with topologically non-trivial signatures accessible via external fields. Bilayers formed of such constituents are highly unexplored and they offer new perspectives of how novel properties of the individual honeycomb staggered layers further evolve. Additionally, surface states and the associated Fermi arcs have different from bulk properties of Weyl semimetals, also considered as 3D graphene analogs. The goal of the project is by investigating Casimir/van der Waals interactions in such materials to bring forward basic understanding of their fundamental properties and serve as an excellent platform for probing light-matter interactions. Additionally, the project involves a balanced approach of analytical and computational methods to explore the relation between electronic and optical response and topological textures in staggered bilayers and Weyl semimetals. In-depth calculations of van der Waals/Casimir-like interactions focusing on highlighting the role of novel materials features are also part of this project for better understanding and control of such ubiquitous forces. Novel physical phenomena involving materials where van der Waals interactions play a stability role are also studied.

Keywords: Casimir/van der Waals interactions, topological materials, optical response

Recent Progress

Investigating dispersive interactions brings forward the necessity to understand the optical response properties of the involved materials. Given that it is closely related to the electronic structure of the materials, we turned to first principles computational techniques. It is realized that the optical conductivity tensor can be obtained within the Kubo formalism, for which the eigenstates and eigen-energies of the system's Bloch Hamiltonian are needed. For this purpose, we developed an in-house simulations tool that takes results from density functional theory (DFT) codes, such as Quantum ESPRESSO and VASP, and interfaces them with WANNIER90 code. This in-house scheme interpolates the DFT electronic structure into a maximally localized Wannier functions basis. In this way, we obtain the eigenstates, eigen-energies, and Hamiltonian

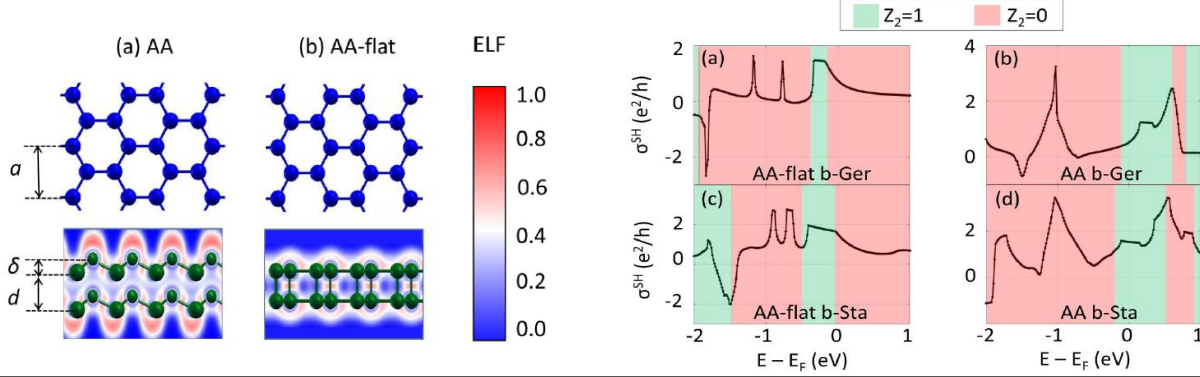


Figure 1 Top and side view of the (a) AA and (b) AA-flat bilayers. The lattice constant a , lattice staggering δ , and interlayer separation d are denoted. Results for the Electron Localization function (ELF) are also shown. Corresponding spin Hall conductivity is shown for some bilayers with AA and AA-flat stacking, where regions for $Z_2 = 1$ and $Z_2 = 0$ are shaded in green and red, respectively.

for the studied system, which are the necessary ingredients for calculating observables. In this way, we are able to calculate diagonal and Hall conductivity components and separate their interband and intraband contributions as a function of frequency, include relaxation scattering times and wave vector dispersion.

We have applied this computational tool to bilayered materials composed of silicene (b-Sil), germanene (b-Ger), and stanene (b-Sta). While Sil, Ger, and Sta have similar to graphene honeycomb structure, there is also significant spin orbit (SOC) due to the heavier Si, Ge, and Sb atoms [1]. The AA and AB are the most recognized stacking patterns for bilayered graphene, however, we find that due to the finite lattice staggering of the monolayers there are six such stacking patterns for the considered systems and they have quite different energy band structures. To probe Dirac physics, we calculate the spin Hall conductivity σ^{SH} , which is a measure of the nontrivial spin Berry curvature. As representative examples here, we show 2 cases of AA stacking and the corresponding σ^{SH} as a function of Fermi level (Fig. 1). While metals with strong SOC are expected to have nonzero σ^{SH} , quantized values of σ^{SH} (as is the case around the Fermi level for the shown cases here) are a signature of nontrivial topology. In Fig. 1

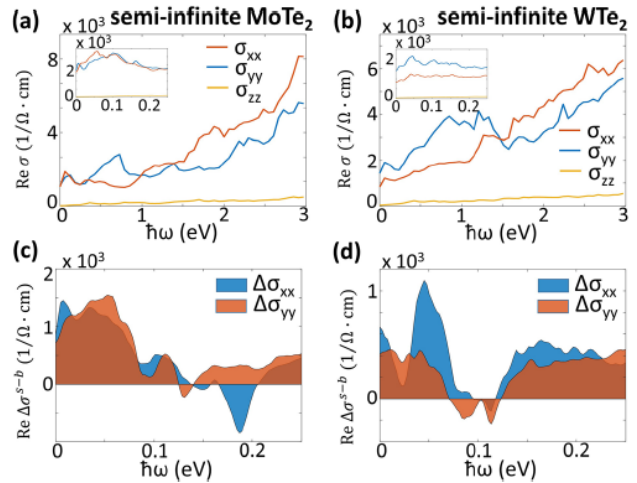


Figure 2 Real parts of σ_{xx}, σ_{yy} components of the optical conductivity tensor as a function of frequency. The real part of $\Delta\sigma_{ii} = \sigma_{ii}^{semi} - \sigma_{ii}^{bulk}$ is also shown.

we also show the calculated Z_2 index associated with the time-reversal-invariant-momenta points (TRIM). The regions corresponding to $Z_2 = 1$ indicate that these materials are quantum Hall insulators. A complete analysis of the electronic structure, its orbital composition, Berry curvature, spin Hall conductivity, and vibrational properties for these bilayers is obtained.

Weyl semimetals are a special class of 3D systems with linearly dispersive bands whose crossing points are monopoles of Berry curvature in momentum space giving rise to Fermi arc surface states [2]. The optical response of MoTe₂ and WTe₂, representatives of type II Weyl semimetals, was recently measured, but several features remained unexplained [3]. We investigated the optical conductivity components using our DFT/Wannier/Kubo computational approach. To resolve the contribution from the surface states, the standard Kubo approach is modified and we implement *Kubo-Greenwood formalism* [4], which relies on a Green's function method by representing the material as a stack of principal layers.

There is a plethora of new features in the response, which is found to be anisotropic with peaks associated with particular features from the bulk and surface states. Signatures of Weyl physics are also identified. The optical response of MoTe₂ and WTe₂ monolayers is compared to their bulk counterparts giving a comprehensive picture of the optical response of these materials. In Fig. 2 some results for the semi-infinite materials are shown, where the second row of panels gives a visual representation of the surface states contributions.

It turns out that analytical studies of the optical conductivity of Weyl systems within the minimum two-band crossing model are also quite complicated with difficulties arising from the dimensionality of the system. To study Casimir interactions and resolve characteristic behaviors, analytical expressions for the different components are obtained by considering an effective two band model taking into account the tilting of the Weyl cones. The bulk and surface energy band structure of type I and type II Weyl semimetals are determined, which are then used to obtain all components of the bulk and surface response. The analytical expressions we obtained for the plasma frequencies, Hall conductivity response, and surface conductivity due to the Fermi arc states are complex, but they are necessary to identify key features in the Casimir interactions.

Significant efforts in deriving the Fresnel reflection matrices for the electromagnetic boundary conditions (which enter into the formalism for the Casimir energy calculations) are also reported. Furthermore, it turns out that the Lifshitz formalism had to be revised in order to properly account for propagating and evanescent waves in such materials. We uncovered many ways to modulate the interaction between Weyl semimetals and some results are shown in Fig. 3. We find that the interaction is essentially dominated by the diagonal bulk conductivity components, while the Hall response and Fermi arc states play much smaller role. This is unlike 2D graphene for

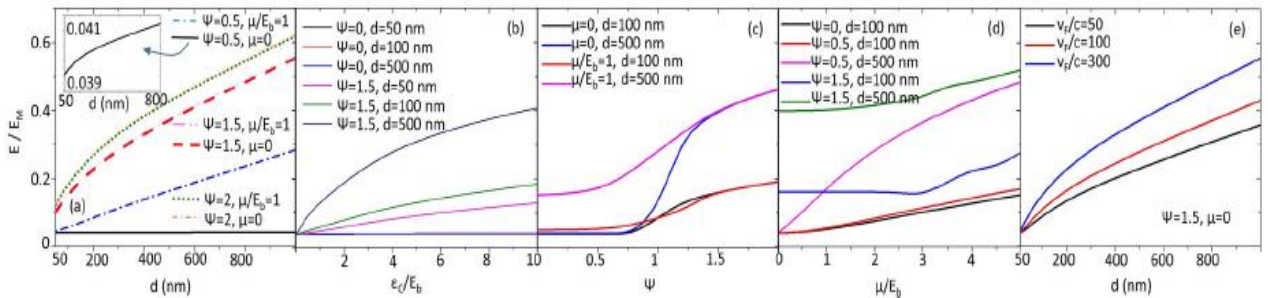


Figure 3 Quantum Casimir energy for Weyl semimetals normalized to the energy for perfect metals. The parameter Ψ quantifies the cone tilting, and $\Psi < 1$ corresponds to type I and $\Psi > 1$ for type II Weyl semimetal. The parameter E_b is a measure of the separation between the Weyl cones, and ϵ_c is the cutoff energy.

which the nontrivial topology is much more important and it can lead to quantization and repulsion in their Casimir interactions, as we have found earlier in [5].

Future Plans

The materials landscape is rapidly expanding with many topologically nontrivial systems characterized by enhanced nonlinear optical properties. Additionally, layered materials such as transition metal dichalcogenides, can exhibit different types of phases tunable by layer stacking or external fields. In specific, plasmonic excitations with negative dispersion have been found in some metallic dichalcogenides. Doping is another important factor that can change the structural phases of many layered Weyl semimetals, which in turn affects their optical response. These recent discoveries motivate investigating the ubiquitous van der Waals/Casimir forces with apparent prominence in distance separations ranging from Angstroms to micrometers.

The future research builds on the PI's extensive work on novel materials properties and their role in van der Waals/Casimir forces. Computed optical response of transition metal dichalcogenides emphasizing their plasmon excitations will be utilized to probe negative dispersion modes and their effects in such interactions. Examining the role of propagating and evanescent modes will broaden our understanding of dispersion in various separation regimes. Analytical and computational studies considering such forces beyond the linear response regime are also part of our plans. Development of computational schemes to delineate linear vs. nonlinear response in different materials is planned. Models beyond the Lifshitz approach to take into account nonlinearity in materials is also included in this project. Our theoretical efforts on evanescent mode contributions and nonlinear optical response effects in vdW/Casimir phenomena will address previously unexplored problems, which we believe are highly beneficial for the scientific community at large. The development and implementation of contemporary computational schemes can be utilized for problems beyond this work.

References

1. S. Balendhran, S. Walia, H. Nili, S. Sriram, and M. Bhaskaran, Elemental analogues of graphene: Silicene, germanene, stanene, and phosphorene, *Small* **11**, 640 (2015)
2. N. P. Armitage, E. J. Mele, and A. Vishwanath, Weyl and Dirac semimetals in three-dimensional solids, *Rev. Mod. Phys.* **90**, 015001 (2018)
3. A. J. Frenzel, C. C. Homes, Q. D. Gibson, Y. M. Shao, K. W. Post, A. Charnukha, R. J. Cava, D. N. Basov, *Phys. Rev. B* **95**, 245140 (2017)
4. P. B. Allen, in *Conceptual Foundations of Materials*, Vol. 2 (Eds: S. G. Louie, M. L. Cohen), Elsevier Science, New York **2006**.
5. P. Rodriguez-Lopez, W.J.M. Kort-Kamp, D. A. R. Dalvit, and L. M. Woods, Casimir force phase transitions in the graphene family, *Nature Commun.* **8**, 14699 (2017)

Publications

1. L. M. Woods, M. Kruger, and V. V. Dodonov, *Perspective on recent and future developments in Casimir interactions*, Appl. Sciences, accepted (Special Issue on “Radiative Processes in Quantum Electrodynamics: Theory, Experiments and Applications”), 2020
2. D. T. Nga, A. D. Phan, V. D. Lam, L. M. Woods, and K. Wakabayashi, *Enhanced solar photothermal effect of PANI fabrics with plasmonic nanostructures*, RSC Advances **10**, 28447 (2020)
3. P. Rodriguez-Lopez, A. Popescu, I. Fialkovsky, N. Khusnutdinov, and L. M. Woods, *Signatures of Complex Optical Response in Casimir Interactions of Type I and II Weyl Semimetals*, Comm. Materials (Nature), **1**, 14 (2020)
4. V. Kalappattil, R. Das, R. Geng, H. Luong, M. Pham, T. Nguyen, A. Popescu, L. M. Woods, H. Srikanth, and M. H. Phan, *Giant spin Seebeck effect through an interface organic semiconductor*, Mater. Horiz. **7**, 1413 (2020)
5. G. L. Klimchitskaya, V. M. Mostepanenko, K. Yu, and L. M. Woods, *The Casimir force, causality, and the Gurzhi model*, Phys. Rev. B **101**, 075418 (2020)
6. A. Popescu, A. Pertsova, A. V. Balatsky, and L. M. Woods, *Optical Response of $MoTe_2$ and WTe_2 Weyl Semimetals: Distinguishing Between Bulk and Surface Contributions*, Adv. Theory Simul. **3**, 1900247 (2020)
7. A. Popescu, P. Rodriguez-Lopez, and L. M. Woods, *Composition and stacking dependent topology in bilayers from the graphene family*, Phys. Rev. Mater. **3**, 064002 (2019)
8. N. Khusnutdinov and L. M. Woods, *Casimir effects in 2D Dirac materials*, JETP Lett. **110**, 183 (2019)
9. A. D. Phan, N. B. Le, N. T. H. Lien, L. M. Woods, S. Ishi, and K. Wakabayashi, *Confinement effect on the solar thermal heating process of TiN nanoparticle solutions*, Phys. Chem. Chem. Phys. **21**, 19915 (2019)
10. T. Stedman, C. Timm, and L. M. Woods, *Multiband effects in equations of motion of observables beyond the semiclassical approach*, New J. Phys. **21**, 103007 (2019)

First Principles Investigations for Magnetic Properties of Innovative Materials

Principle investigator: Ruqian Wu
Department of Physics and Astronomy
University of California Irvine
Irvine, CA 92697-4575
wur@uci.edu

Project scope

The goal of this project is to conduct creative research on low-dimensional heterostructures by developing and using theoretical approaches based on the density functional theory, with an eye towards finding new materials and phenomena for technological breakthroughs. The interactions among electron, spin, phonon and magnon excitations are investigated to establish new rules for the control and use of dynamical properties of two dimensional (2D) materials. Our results have been found useful by collaborators for the explanation of their important experimental data and, furthermore, we have also provided significant new insights and predictions for different material systems.

Recent major progress

Control magnetic and topological properties with a van der Waals ferroelectrics

Ferroelectric materials can generate a strong local electric field from their spontaneous electric polarization, e.g., $\sim 80 \mu\text{Ccm}^{-2}$ in $\text{PbZr}_{0.2}\text{Ti}_{0.8}\text{O}_3$, whose direction can be actively controlled. The electric tunability of ferroelectric materials can hence be incorporated into a variety of spintronic devices for achieving nonvolatile control of the spin degree of freedom for future spin memory and logic devices. As an important magnetic property, for example, the Dzyaloshinskii-Moriya interaction has attracted considerable theoretical and experimental research attention as it plays an essential role in multiferroicity, magnon Hall effect, magnetic skyrmions and chiral domain walls.

As an example, magnetic properties of a MnBi_2Te_4 (MBT) monolayer can be effectively controlled in contact with $\text{III}_2\text{-VI}_3$ two-dimensional ferroelectric substrates. As the electric polarization in the ferroelectric films is switched, a semiconductor to half-metal transition occurs in MBT, and its magnetic easy axis in several cases reorients. As an example, the Curie temperature of MBT/ In_2Se_3 can be enhanced to 21.5 or 32 K under the influence of electric polarization and biaxial strain, much higher than that of the pristine MBT monolayer, which is 14.5 K in our calculations. Our results suggest effective ways to tune magnetic properties of MBT and provide useful insights for the further development of these important van der Waals functional materials. As shown in Fig. 1, there is a potential drop of 1.078 eV across the two sides of In_2Se_3 because of the inherent electric field, leading to distinctly different band shifts in MBT when contacting with opposite sides. When the polarization is upward, the CBM of In_2Se_3 locates above the VBM of MBT. Therefore, the electrons cannot transfer between MBT and In_2Se_3 , but are slightly redistributed in the interfacial region. In contrast, for the downward polarization, the CBM of In_2Se_3 becomes lower than the VBM of MBT, leading to

electron transfers from MBT to In_2Se_3 . This can also be seen from the projected density of states (PDOS).

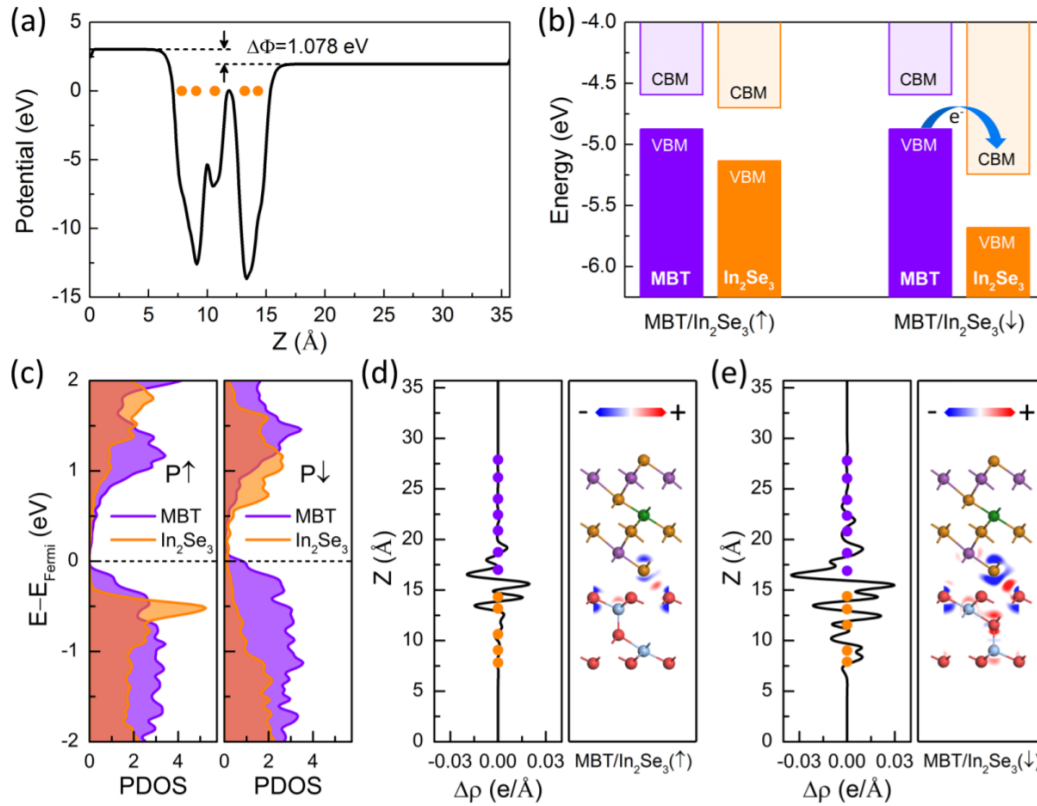


Fig. 1 (a) The planar-averaged electrostatic potential of the In_2Se_3 monolayer. The orange dots represent positions of atoms. (b) Band alignments of $\text{MBT}/\text{In}_2\text{Se}_3(\uparrow)$ and $\text{MBT}/\text{In}_2\text{Se}_3(\downarrow)$ with respect to the vacuum level of MBT. (c) PDOS of $\text{MBT}/\text{In}_2\text{Se}_3(\uparrow)$ and $\text{MBT}/\text{In}_2\text{Se}_3(\downarrow)$. (d) and (e) Planar averaged and 2D charge density difference of $\text{MBT}/\text{In}_2\text{Se}_3$ heterostructure. The violet and orange dots represent positions of MBT and In_2Se_3 atoms, respectively. The blue and red areas indicate loss and gain electrons, respectively.

New magnetic and topological materials from endohedral fullerene molecules

Well-protected magnetization, tunable quantum states and long coherence time are desired for the use of magnetic molecules in spintronics and quantum information technologies. We recently studied a variety of endohedral fullerene molecules $\text{M}@C_{28}$ ($\text{M}=3\text{d}, 4\text{d}$ and 5d transition metals) through systematic first-principles calculations and spin dynamics analyses. Individually, many of these molecules have stable magnetization, giant magnetic anisotropy energy ($>30\text{meV}$ per molecule) and bias-tunable structure. Some of them may have coherence time up to several milliseconds for their quantum spin states at a reasonably high temperature ($\sim 10\text{K}$) after full consideration of spin-vibration couplings. We further designed a series of 2D materials based on these endohedral fullerenes and revealed that many of them may integrate different functions in a single system, such as ferroelectricity with large electric dipole moments, multiple magnetic phases with both strong magnetic anisotropy and high

Curie temperature, quantum spin Hall effect or quantum anomalous Hall effect with robust topologically protected edge states. These findings provide a strategy of using fullerenes 1) for the development of single-molecule magnets, magnetic molecular junctions, and molecular qubits; and 2) as building blocks for the synthesis of novel 2D materials which can be easily controlled with a local electric field.

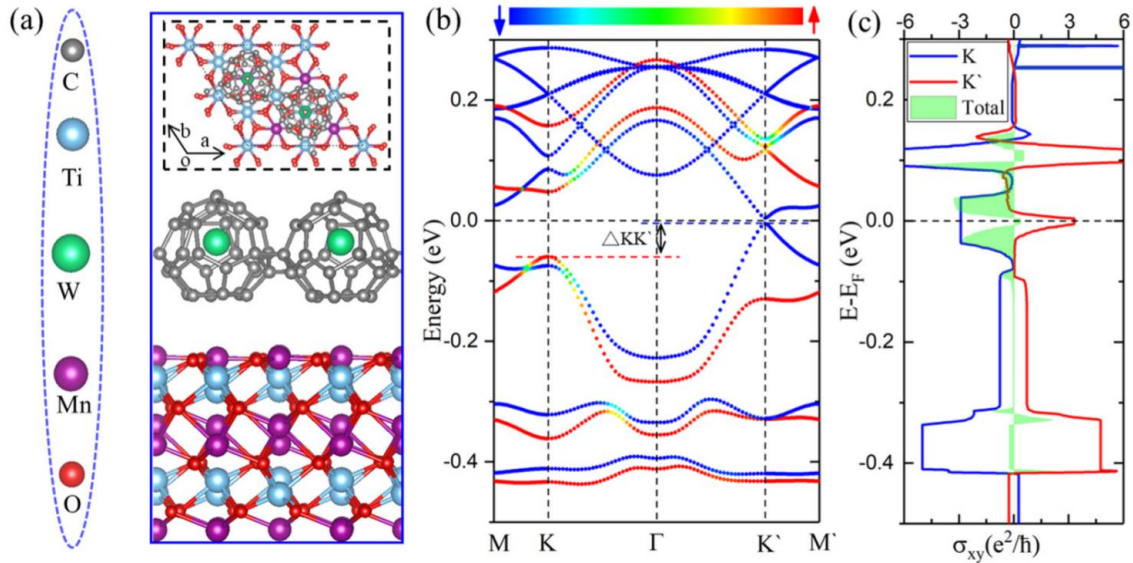


Fig. 2. (a) The side view of the structure of 2D W@C₂₈ on the MnTiO₃ (001) surface. (Inset is the top view.) (b) The calculated band structure of 2D W@C₂₈ on the MnTiO₃ (001) surface. [The valley splitting $\Delta_{KK'} = E(K) - E(K')$, where $E(K)$ ($E(K')$) represents VBM at the K (K') point.] (c) The corresponding anomalous Hall conductivity σ_{xy} as a function of Fermi level.

Fig. 2 demonstrates the results of using W@C₂₈ lattice on a magnetic MnTiO₃ (001) surface for the production of valleytronic properties. As the valley and spin degrees of freedom are interlocked, the proximity effect of the magnetic MnTiO₃ substrate on the two valleys is nonequivalent, as seen in the band structure of two-dimensional W@C₂₈/MnTiO₃. A large valley splitting ($\Delta_{KK'}$) of ~ 55 meV can be found as a result of low symmetry of the 2D W@C₂₈ lattice and the inequivalent proximity effect on two spin channels. The K and K' valleys have band gaps of ~ 100 and ~ 8.8 meV, respectively. Obviously, the valley-polarized anomalous Hall effect is analogous to the quantum anomalous Hall effect and falls into the same category as the Berry-phase related topological transport phenomena. The anomalous Hall conductivity as a function of the position of the Fermi level.

Planned activities: 2021-2022

1. Study topological properties of MBT and related materials with defects and substrates
2. Explore high order topological properties of different structures and molecular networks.
3. Develop code for studies of nonlinear optical properties of topological materials.
4. Investigate spin-phonon coupling in 2D and 3D materials.
5. Explore the effect of ferroelectric materials on magnetic and topological properties of 2D materials.

Publications through Summer 2020

14. Jie Li and R. Q. Wu, "Bias-tunable two-dimensional magnetic and topological materials", *Nanoscale* **13**, 12513 (2021). [pdf](#)
13. B. H. Zhang, Z. Wang, R. Q. Wu, "First-principles studies of the unconventional spin-phonon coupling mediated by spin-orbit coupling in pyrochlore $Cd_2Os_2O_7$ ", *Phys. Rev. B* **104**, 024411 (2021). [pdf](#)
12. Y. S. Hou, S. Ardo, and R. Q. Wu, "Hybrid density functional study of band gap engineering of $SrTiO_3$ photocatalyst via doping for water splitting", *Phys. Rev. Mater.* **5**, 065801 (2021). [pdf](#)
11. Yipeng An, Kun Wang, Shijing Gong, Yusheng Hou, Chunlan Ma, Mingfu Zhu, Chuanxi Zhao, Tianxing Wang, Shuhong Ma, Heyan Wang, Ruqian Wu, and Wuming Liu, "Nanodevices engineering and spin transport properties of $MnBi_2Te_4$ monolayer", *npj Computational Materials*, **7**, 45 (2021). [pdf](#)
10. J. Li and R.Q. Wu, "Two-dimensional multifunctional materials from endohedral fullerenes", *Phys. Rev. B*, **103**, 115417 (2021). [pdf](#)
9. Y.S. Hou and R.Q. Wu, "Alloying vanadium in $MnBi_2Te_4$ for robust ferromagnetic coupling and quantum anomalous Hall effect", *Phys. Rev. B*, **103**, 064412 (2021). [pdf](#)
8. B.H. Zhang, Y.S. Hou, Z. Wang, R.Q. Wu, "Tuning Dzyaloshinskii-Moriya Interactions in Magnetic Bilayers with Ferroelectric Substrate", *Phys. Rev. B*, **103**, 054417 (2021). [pdf](#)
7. Xingxu Yan, Chengyan Liu, Chaitanya A. Gadre, Lei Gu, Toshihiro Aoki, Tracy C. Lovejoy, Niklas Dellby, Ondrej L. Krivanek, Darrell G. Schlom, Ruqian Wu and Xiaoqing Pan, "Local Phonon Spectral Density of Single Defects Imaged by Electron Microscopy", *Nature*, **589**, 65 (2021). [pdf](#)
6. Jie Li and Ruqian Wu, "Metal-organic Frameworks: Possible New Two-Dimensional Magnetic and Topological van der Waals materials", *Nanoscale* **12**, 23620 (2020). [pdf](#)
5. J. Karel, D.S. Bouma, C. Fuchs, S. Bennett, P. Corbae, S.B. Song, B.H. Zhang, R.Q. Wu, F. Hellman, "Anomalous Hall Angle in Amorphous Transition Metal Thin Films", *Phys. Rev. Mater.* **4**, 114105 (2020). [pdf](#)
4. Yipeng An, Yusheng Hou, Kun Wang, Shi-Jing Gong, Chuanxi Zhao, Tian-Xing Wang, Zhao-Yong Jiao, Heyan Wang, and Ruqian Wu, "Multifunctional Lateral Transition-Metal Disulfides Heterojunctions", *Advanced Functional Mater.*, **30**, 2002939 (2020). [pdf](#)
3. Gui-Fang Du, Hua-Hua Fu, and Ruqian Wu, "Vibration-enhanced spin-selective transport of electrons in the DNA double helix", *Phys. Rev. B*, **102**, 035431 (2020). [pdf](#)
2. Mei Fang, Yanmei Wang, Hui Wang, Yusheng Hou, Eric Vetter, Yunfang Kou, Wenting Yang, Lifeng Yin, Zhu Xiao, Zhou Li, Lu Jiang, Ho Nyung Lee, Shufeng Zhang, Ruqian Wu, Xiaoshan Xu, Dali Sun, Jian Shen, "Tuning the interfacial spin-orbit coupling with ferroelectricity", *Nature Communications*, **11**, 2627 (2020). [pdf](#)
1. Feng Xue, Zhe Wang, Yusheng Hou, Lei Gu, Ruqian Wu, "Control magnetic properties of $MnBi_2Te_4$ with a van der Waals ferroelectric III_2-VI_3 film and biaxial strain", *Phys. Rev. B*, **101**, 184426 (2020). [pdf](#)

Synthesis of motif and symmetry for accelerated learning, discovery, and design of electronic structures for energy conversion applications

Qimin Yan, Temple University

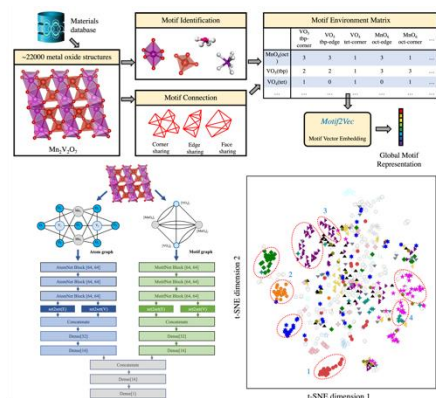
Program Scope

The scope of the proposed research is to develop symmetry-incorporated and motif-centric machine learning frameworks with a focus on the prediction of materials properties related to electronic structures at a dramatically reduced cost compared to *ab-initio* atomistic simulations. The developed machine learning (ML) models will be combined with symmetry tools and high-throughput computations to discovery and design functional oxides and 2D materials for energy conversion applications.

Keywords: structure motif, graph neural network, solid-state material

Recent Progress

Machine learning especially graph-based learning frameworks have been successfully applied to solid-state material systems for material property predictions.^{1,2} Moving beyond atom-level models and motivated by the existing motif-property-functionality correlations,³ we demonstrated how structure motifs in crystal structures can be combined with both unsupervised and supervised ML techniques to enhance the effective representation of solid-state material systems. We propose a novel machine learning framework, so-called atom-motif dual network (AMDNet), in which structure motifs can be incorporated in a graph-based learning architecture to make reliable property predictions for solid-state materials. AMDNet is a fundamental step toward the incorporation of physical principles in machine learning framework design for solid-state materials.



The proposed motif-centric learning framework for solid-state materials, including the architecture of the atom-motif dual network (AMDNet) and the motif representations obtained from unsupervised learning.

Future Plans

We will develop novel symmetry-incorporated and attention-based graph neural networks for the effective prediction of electronic band structures. Site symmetries and irreducible representations will be incorporated to enhance the prediction performance for complex electronic structures. Another effort will be to initiate symmetry-driven and ML-aided functional materials discovery for energy conversion, including transparent conducting materials and 2D light emitters.

References

1. T. Xie, J. C. Grossman, *Phys. Rev. Lett.* 120, 145301 (2018)
2. C. Chen, W. Ye, Y. Zuo, C. Zheng, S. P. Ong, *Chem. Mater.* 31, 3564 (2019)
3. Q. Yan, *et al.*, *PNAS* 114, 3040-3043 (2017)

Publications

1. H. Banjade, S. Hauri, S. Zhang, F. Ricci, W. Gong, G. Hautier, S. Vucetic, Q. Yan, “Structure motif centric learning framework for inorganic crystalline systems” *Sci. Adv.* 7, eabf1754 (2021)
2. W. Gong, Q. Yan, *Comput.* “Graph-based deep learning frameworks for molecules and solid-state materials” *Mater. Sci.* 195, 110332 (2021)
3. H. R. Banjade, J. Pan, Q. Yan, “Monolayer 2D semiconducting tellurides for high-mobility electronics” *Phys. Rev. Mater.* 5, 014005 (2021)
4. H. Bai, P. Chu, J.-Y. Tsai, N. Wilson, X. Qian, Q. Yan, and H. Ling, “Graph Neural Network for Hamiltonian-Based Material Property Prediction” *Neural. Comput. Appl.* *accepted* (2021)

Quantum Computing Enhanced Gutzwiller Variational Embedding Method for Correlated Multi-Orbital Materials

Yongxin Yao, Cai-Zhuang Wang, Kai-Ming Ho and Peter P. Orth
Ames Laboratory, Ames, IA 50011

Program Scope

This project aims to leverage existing noisy intermediate-scale quantum computers technology to achieve highly accurate total energy and quantum dynamics calculations in correlated multi-orbital materials. Specifically, we develop and integrate algorithmic components for a hybrid quantum-classical computational framework that combines a Gutzwiller embedding approach with variational quantum circuit simulation techniques that is optimized for current quantum hardware. This approach allows use of larger correlation projectors that systematically improve simulation accuracy. The key idea is that quantum embedding Hamiltonians of higher Hilbert space dimension can be solved more efficiently on quantum computers. We have demonstrated proof-of-principle calculations of competing phases of a model correlated electron lattice, which represents the first bulk correlated material simulation achieved on a real quantum device. The capability of this new approach will be further established by benchmarking it on multi-orbital systems to advanced classical algorithms. This methodology will then be used to investigate a series of rare-earth based strongly correlated materials to discover their complex phase diagrams and coherent quantum dynamics. On a broader level, this work will facilitate the discovery and design of correlated functional materials by building an efficient hybrid quantum-classical computational framework for simulating equilibrium and out-of-equilibrium behavior of correlated materials. The codes that are being developed during this project are all open source and made freely available to other researchers.

Keywords: Quantum Computing, Quantum Embedding, Correlated Materials.

Recent Progress

The main achievements of the project include the development and implementation of a hybrid quantum-classical computational framework based on the Gutzwiller embedding method and variational quantum eigensolver (VQE), and self-adaptive variational quantum algorithms to enable quantum imaginary time evolution (QITE) for ground state preparation and real-time evolution for nonequilibrium dynamics simulation. This Gutzwiller quantum-classical embedding (GQCE) is benchmarked on real quantum processing units (QPUs) by comparing solution of the periodic Anderson lattice model to exact solutions obtained by Dynamical Mean-Field Theory (DMFT). The adaptive variational QITE (AVQITE) and quantum dynamics simulations (AVQDS) algorithms provide scalable quantum impurity solvers for ground state and dynamics simulations of multi-orbital materials within the GQCE framework. More details are described below.

1. **Gutzwiller quantum-classical embedding (GQCE) framework.** We developed a hybrid quantum-classical simulation framework for correlated electron systems based on the Gutzwiller variational embedding approach, as illustrated in Fig.1. This GQCE framework is implemented on Rigetti QPUs and applied to the periodic Anderson model, which describes a correlated heavy electron band hybridizing with non-interacting conduction electrons. Our simulation results quantitatively reproduce the known ground state quantum phase diagram including metallic, Kondo and Mott insulating phases (see Fig.2). This is the first fully self-consistent hybrid quantum-classical simulation of an infinite correlated lattice model executed on QPUs, demonstrating that the Gutzwiller hybrid quantum-classical embedding framework is a powerful approach to simulate correlated materials on NISQ hardware. This benchmark study also puts forth a concrete pathway towards practical quantum advantage on NISQ devices.

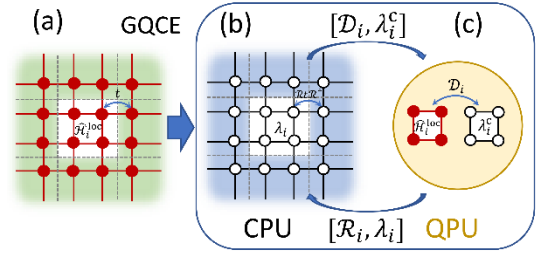


Fig. 1: Schematic illustration of GQCE framework.

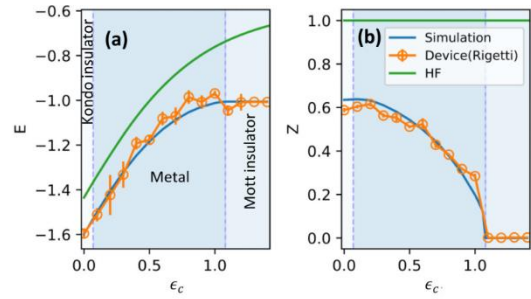


Fig. 2: Accurate ground state simulations of periodic Anderson model on Rigetti hardware

The work is published in Phys. Rev. Research [1]. The GQCE software package that is used in the benchmark calculations is publicly available at the repository <https://doi.org/10.6084/m9.figshare.11987616>. The detailed calculation data are also available online at <https://doi.org/10.6084/m9.figshare.11992011>.

2. **Adaptive variational quantum dynamics simulations (AVQDS).** We introduce a general-purpose, self-adaptive approach to construct variational wavefunction ansätze for

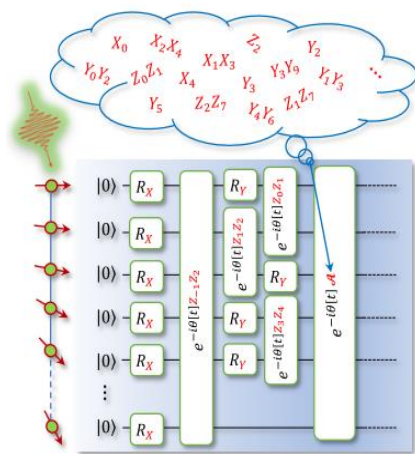


Fig. 3: Schematic illustration of AVQDS.

highly accurate quantum dynamics simulations based on McLachlan's variational principle, as illustrated in Fig. 3. The key idea is to dynamically expand the variational ansatz along the time-evolution path such that the McLachlan distance, which is a measure of the simulation accuracy, remains below a set threshold. This adaptive variational quantum dynamics simulation (AVQDS) approach is applied to the integrable Lieb-Schultz-Mattis spin chain and the nonintegrable mixed-field Ising model, where it captures both finite-rate and sudden post-quench dynamics with high fidelity. The AVQDS quantum circuits that prepare the time-evolved state are much

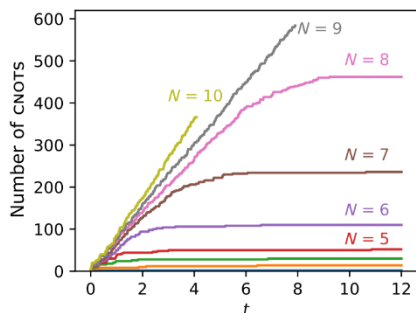


Fig. 4: Circuit saturation and scalability of N -site model calculations for fixed times.

shallower than those obtained from first-order Trotterization and contain up to two orders of magnitude fewer CNOT gate operations. A linear system-size scaling for simulations with fixed times is also demonstrated. This scalable algorithm creates opportunities to study quantum dynamics of significantly larger systems on current and near-term quantum devices. AVQDS will be used as a quantum dynamics solver for GQCE material simulations of dynamical properties.

This work is published at PRX Quantum [2]. The associated open-source code and data have been released at <https://doi.org/10.6084/m9.figshare.14920074>.

3. **Adaptive variational quantum imaginary time evolution (AVQITE)**. An adaptive variational quantum imaginary time evolution (AVQITE) approach is introduced that yields efficient representations of ground states for interacting Hamiltonians on near-term quantum computers. It is based on McLachlan's variational principle applied to imaginary time evolution of variational wave functions, and avoids difficult nonconvex high-dimensional optimization that plagues other variational approaches such as the variational quantum eigensolver. The variational parameters evolve according to equations of motions that minimize the difference to the exact imaginary time evolution, which is quantified by the McLachlan distance. Rather than working with a fixed variational ansatz, where the minimal McLachlan distance is constrained by the quality of the ansatz, the adaptive method iteratively expands the ansatz along the dynamical path to ensure the McLachlan distance remains below a chosen threshold. AVQITE is used to prepare ground states of H_4 , H_2O and BeH_2 molecules and yields compact variational ansätze and ground state energies beyond chemical accuracy. Polynomial scaling of circuit depth with system size is demonstrated through a set of AVQITE calculations of quantum spin models. Finally, quantum Lanczos calculations can also be naturally performed alongside AVQITE without additional quantum resource costs. AVQITE will be used as a ground state solver on real device for GQCE simulations of ground state properties of multi-orbital materials.

The preprint of this work is available at arXiv [3]. The associated code and data will be released after the publication.

Future Plans

The future work plan focuses on two main directions: (i) implementing and benchmarking the Gutzwiller embedding Hamiltonian solvers of ground state, and (ii) quantum dynamics simulations on noisy quantum simulators and real quantum hardware for multi-orbital correlated electron systems.

We will use quantum circuit implementations of AVQITE approach for ground state preparation, and AVQDS for quantum dynamics simulations. The effects of quantum noise and device noise

on the calculations will be systematically studied. Measurement frugal techniques and error mitigation approaches will be adopted. Multiband e_g and t_{2g} Hubbard models will be two primary benchmark examples in the coming year. The results will be compared with other static and dynamics quantum solver. Algorithms for the calculation of nonlinear response functions (such as shift currents and second-harmonic generation) or interacting quantum models on current (and future) quantum hardware will also be developed and tested.

The formulation similarity for calculations of ground state and quantum dynamics in term of imaginary and real time evolution will be leveraged to develop a modularized code, where most functionalities can be shared between the static and dynamics calculation codes. This will greatly improve the efficiency for code development and benefit from the cross-benchmark in two different application domains.

References

- [1] Y. Yao, F. Zhang, C.-Z. Wang, K.-M. Ho, and P. P. Orth, *Gutzwiller Hybrid Quantum-Classical Computing Approach for Correlated Materials*, Phys. Rev. Res. **3**, 013184 (2021).
- [2] Y.-X. Yao, N. Gomes, F. Zhang, C.-Z. Wang, K.-M. Ho, T. Iadecola, and P. P. Orth, *Adaptive Variational Quantum Dynamics Simulations*, PRX Quantum **2**, 030307 (2021).
- [3] N. Gomes, A. Mukherjee, F. Zhang, T. Iadecola, C.-Z. Wang, K.-M. Ho, P. P. Orth, and Y.-X. Yao, *Adaptive Variational Quantum Imaginary Time Evolution Approach for Ground State Preparation*, ArXiv210201544 (2021).

Publications

- [1] N. Gomes, F. Zhang, N. F. Berthusen, C.-Z. Wang, K.-M. Ho, P. P. Orth, and Y. Yao, *Efficient Step-Merged Quantum Imaginary Time Evolution Algorithm for Quantum Chemistry*, J. Chem. Theory Comput. **16**, 6256 (2020).
<https://doi.org/10.1021/acs.jctc.0c00666>.
- [2] Y. Yao, F. Zhang, C.-Z. Wang, K.-M. Ho, and P. P. Orth, *Gutzwiller Hybrid Quantum-Classical Computing Approach for Correlated Materials*, Phys. Rev. Research **3**, 013184 (2021).
<https://doi.org/10.1103/PhysRevResearch.3.013184>.
- [3] F. Zhang, N. Gomes, N. F. Berthusen, P. P. Orth, C.-Z. Wang, K.-M. Ho, and Y. Yao, *Shallow-Circuit Variational Quantum Eigensolver Based on Symmetry-Inspired Hilbert Space Partitioning for Quantum Chemical Calculations*, Phys. Rev. Research **3**, 013039 (2021).
<https://doi.org/10.1103/PhysRevResearch.3.013039>.
- [4] Y. Yao, N. Gomes, F. Zhang, C.-Z. Wang, K.-M. Ho, T. Iadecola, and P. P. Orth, *Adaptive Variational Quantum Dynamics Simulations*, PRX Quantum **2**, 030307 (2021).
<https://doi.org/10.1103/PRXQuantum.2.030307>.
- [5] F. Zhang, N. Gomes, Y. Yao, P. P. Orth, and T. Iadecola, *Adaptive Variational Quantum Eigensolvers for Highly Excited States*, Phys. Rev. B **104**, 075159 (2021).
<https://link.aps.org/doi/10.1103/PhysRevB.104.075159>
- [6] N. Gomes, A. Mukherjee, F. Zhang, T. Iadecola, C.-Z. Wang, K.-M. Ho, P. P. Orth, and Y. Yao, *Adaptive Variational Quantum Imaginary Time Evolution Approach for Ground State Preparation*, ArXiv:2102.01544 (2021).
<http://arxiv.org/abs/2102.01544>

Topological spin textures in chiral magnets: from 2D to 3D

Jiadong Zang, Department of Physics and Astronomy, University of New Hampshire

Program Scope

This grant award focuses on the study of both fundamental physical property and material realization of magnetic spin textures with nontrivial topology. It consists of three major parts:

1. Realizing and manipulating skyrmion and related skyrmionic textures. A zoo of skyrmion-like topological spin textures can be enabled in chiral magnets, and their controlled current driven dynamics will be designed through simulations.
2. Investigating transport signatures of spin textures. Topological Hall effect (THE) has been widely used for identifying skyrmions. We have identified THE in various systems. Alternative mechanisms to THE-like feature have been proposed.
3. Unlocking 3D topological hopfion textures. Energy landscape, transport signature, and novel dynamics of hopfions will be discussed.

Theoretical developments in this project are also supported by intensive experimental collaborations.

Keywords: Magnetic skyrmion, hopfion, topological Hall effect

Recent Progress

Magnetic skyrmion is a nanostructured spin texture in which magnetic moments point in all directions wrapping a unit sphere. The one-to-one correspondence between a skyrmion and a unit sphere grants the skyrmion a nontrivial topology, which is quantitatively captured by the invariant topological charge $Q = \frac{1}{4\pi} \int d^2x \mathbf{m} \cdot (\partial_x \mathbf{m} \times \partial_y \mathbf{m})$, where \mathbf{m} is the direction of local magnetic moment. $Q = -1$ for each magnetic skyrmion. The integrand serves as an emergent magnetic field acting on itinerant electrons traverse skyrmions, resulting in the so-called topological Hall effect (THE). Similar as magnetic domains, the skyrmion moves under an electric current, while accompanied by the skyrmion Hall effect. Understanding transport and dynamical properties of skyrmions is vital for advancing topological spintronics. Extending zoology of topological spin textures in real materials can greatly deepen our understanding of topological magnetism on the nanometer scale. We have achieved significant progress in the three categories listed in the Program Scope:

1. Novel skyrmion textures and their dynamics.

From center to periphery of a skyrmion, spins have rotated by an angle of π . Such rotation angle can be generalized to other integer multiples of π , giving rise the target skyrmion we predicted and realized in confined geometries[1]. In particular, the structure with 2π rotation

is dubbed the skyrmionium (Fig. 1). In a recent work [2], we demonstrated free-moving skyrmionium in chiral magnets. Due to its zero topological charge, a skyrmionium under electric current can move straight without any transverse velocity. A skyrmionium can be visualized as a conventional skyrmion wrapped by a circular helical stripe, which can enclose more skyrmions and give rise to the skyrmion bundle states. The topological charge of a skyrmion bundle can be arbitrary integer values depending on the number of skyrmions enclosed. Using nonequilibrium states during the field reversal, skyrmion bundle states were predicted by our micromagnetic simulation and confirmed experimentally.

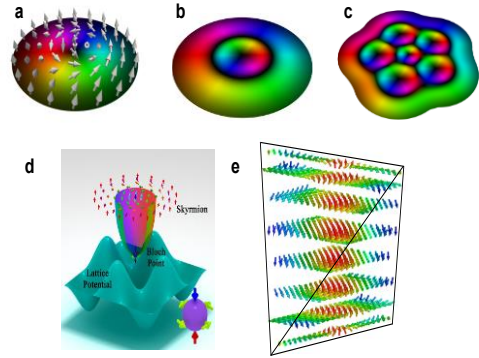


Figure 1: Spin configurations of (a) skyrmion, (b) skyrmionium, (c) skyrmion bundle, (d) chiral bobber, and (e) chiral tetrahedron.

Actually the skyrmion bundle has complex three-dimensional (3D) structure. Cross sections of top and bottom surfaces exhibit chiral vortex structures. By integrating electron holography and micromagnetic simulations, we recently uncovered a similar skyrmionic vortex structure confined in a FeGe tetrahedral nanoparticle[3]. Formation of the skyrmionic vortex is enabled by the geometrical chiral frustration at edges of the tetrahedron. This work also indicates the possibility of 3D magnetic structure reconstruction by simulation-guided tomography.

Another important skyrmion-related 3D spin texture is the chiral bobber (ChB). It is composed of a skyrmion tube and a Bloch point. The Bloch point is length-less due to its singular nature, while the skyrmion has its own length scale. The ChB as a composite must acquire novel dynamics while driven by current. Using high performance micromagnetic simulation, we showed that the Bloch point experiences strong atomic scale pinning[4]. As a result, ChB acquires Hall motion, especially at low current. During ChB's motion, the Bloch point undergoes frequent pinning and depinning. Spin-wave excitation is thus generated. The excitation frequency can be two orders of magnitude higher than that of skyrmions. It can be even finely tuned by the velocity of ChB.

2. Topological Hall effect (THE) in quantum materials

Ever since its first identification in MnSi[5], THE has been observed in many other materials, those include not only standard skyrmion materials like FeGe, Ir/FeCoPt multilayers, but also topological insulators (TIs) and strongly correlated materials (see Fig. 2). In the past year, we have performed extensive experimental collaborations worldwide, and discovered THE in a broad spectrum of materials. In magnetic doped topological insulators (MTI), typical hump feature of THE was observed. Using integrated Kubo formula and Monte Carlo simulation, we revealed linear correlation between the THE resistivity and chiral domain density[6]. This correlation was confirmed by magnetic force microscopy measurement. In another MTI/TI multilayer sample, crossover between THE and quantum anomalous Hall effect was observed.

Using linear response theory, we evaluated the variation of spin-orbit interaction induced Dzyaloshinskii-Moriya interaction as a function of the gate voltage. The result is in qualitative consistence with experimental observations[7].

We are among the earliest players on THE in 2D materials. We identified THE in $\text{Fe}_3\text{GeTe}_3/\text{WTe}_2$ [8]. In order to explain the observation of skyrmions using transmission electron microscopy, our simulation revealed the possible presence of chiral bobber at the interface between 2D materials. We are currently working extensively on skyrmions in CrTe_2 -based 2D materials[9]. As an example, we identified THE in Cr_3Te_5 , where excessive Cr atoms are randomly distributed in the van de Waals gap between CrT_2 layers. It is quite possible that it is an RKKY-driven skyrmion system.

A hump at $\rho_{xy} - B$ curve is widely believed as unequivocal feature of THE. However, we provided a clear counter example. In EuCd_2As_2 , a typical THE hump was observed. But our symmetry analysis and Monte Carlo simulation rule out the possibility of skyrmions therein[10]. Using DFT calculation, we revealed momentum space Berry phase origin of THE. Under field-driven magnetization evolution, a gap is opened at the Fermi surface, and elevation of the Berry phase takes place. This work advocates alternative explanations of THE.

3. Magnetic hopfions and their dynamics

Fig. 3 shows a typical hopfion structure. Spins with the same z-component form torus planes, far away from which, spins point to the z-direction. Furthermore, any two equal-spin lines, dubbed as the preimages, in the hopfion are linked by integer times.

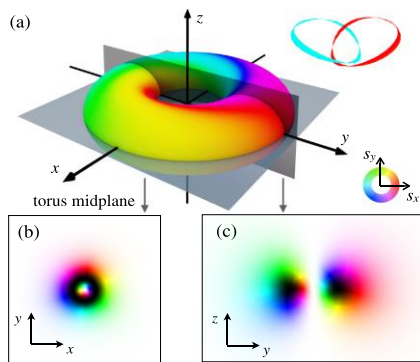


Figure 3: (a) Spin configuration of a hopfion. (b, c) cross sections of the hopfion onto two orthogonal planes.

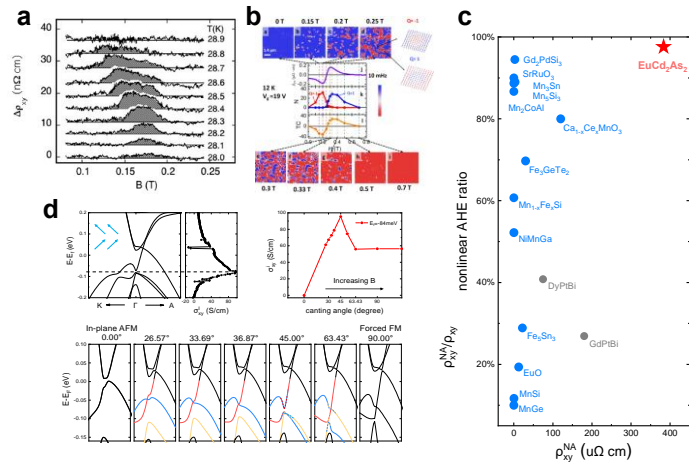


Figure 2: Topological Hall effect in (a) MnSi and (b) MTI. (c) A summary of THE in quantum materials. (d) DFT calculation of intrinsic Hall conductivity in EuCd_2As_2 .

We made the first predict of hopfion in real magnetic materials[11]. Hopfion can be stabilized in chiral magnet nanodisk sandwiched in between two spin polarized layers. This prediction was recently confirmed by Fischer's group from Lawrence-Berkeley Lab. Inspired by realization of hopfion, we further studied hopfion dynamics. Under spin transfer torque, hopfion exhibits rich dynamics including longitudinal motion along the current direction, transverse motion perpendicular to the current

direction, rotational motion, and even dilation[12]. Such complex dynamics can be fully understood in terms of spin Berry phase, which can be expressed using hopfion displacement and rotation angle as collective coordinates. Our calculations exhibit highly entangled collective coordinates in hopfion's phase space.

Electron transport in hopfion and other exotic topological spin textures is a field largely uninvestigated. Using higher order Born approximation, we showed topological Hall effect of the hopfion, even though its overall topological charge is zero. Scattering amplitude is also related to the toroidal moment of the hopfion[13].

Future Plans

We plan to explore other exotic topological spin textures, especially those related to skyrmions. Composites of skyrmions, Bloch points and helical stripes will be extensively studied. These composites have the potential to own novel dynamics and exhibit rich topological transport phenomena. On the other hand, study of hopfion is still in its infancy. Exploration of more material realizations is extremely important. How transport signature can be related to the topological index is another interesting question to explore.

Inspired by many works on 3D topological magnetism, we plan to spend significant effort on developing new methods for 3D magnetic reconstruction. This is a typically challenging inverse problem that can be potentially addressed by advanced algorithm and/or machine learning skills.

References

1. F. Zheng, et. al, Phys. Rev. Lett. 119, 197205 (2017)
2. J. Tang, Y. Wu, W. Wang, L. Kong, B. Lv, W. Wei, J. Zang, M. Tian, H. Du, Nature Nanotechnology, in press
3. K. Niitsu, Y. Liu, A. Booth, X. Yu, N. Mathur, M. Stolt, D. Shindo, S. Jin, J. Zang, N. Nagaosa, Y. Tokura, Research Square preprint DOI:10.21203/rs.3.rs-311043/v1,
4. Z. Gong, et. al, Phys. Rev. B 104, L100412 (2021)
5. A. Neubauer, et. al, Phys. Rev. Lett. 102, 186602 (2013)
6. W. Wang, Y. F. Zhao, F. Wang, M. W. Daniels, C. Z. Chang, J. Zang, D. Xiao, W. Wu, Nano Lett. 21, 1108 (2021).
7. J. Jiang, et. al, Nature Materials, 19, 732 (2020)
8. Y. Wu, et. al, Nature Communications 11, 1 (2020).
9. M. Huang, et. al, Nano Letters, in press.
10. X. Cao, J. X. Yu, P. Leng, C. Yi, Y. Yang, S. Liu, L. Kong, Z. Li, X. Dong, Y. Shi, J. Zang, F. Xiu, arXiv:2103.09395.
11. Y. Liu, R. K. Lake, J. Zang, Phys. Rev. B 98, 174437 (2018)
12. Y. Liu, W. Hou, X. Han, J. Zang, Phys. Rev. Lett. 124, 127204 (2020)
13. S. S. Pershoguba, D. Andreoli, J. Zang, Phys. Rev. B 104, 075102 (2021).

Publications

1. Y. Liu, W. Hou, X. Han, J. Zang, Three-Dimensional Dynamics of a Magnetic Hopfion Driven by Spin Transfer Torque, *Physical Review Letters* 124, 127204 (2020)
2. Z. Li, S. Shen, Z. Tian, K. Hwangbo, M. Wang, Y. Wang, F. M. Bartram, L. He, Y. Lyu, Y. Dong, G. Wan, H. Li, N. Lu, J. Zang, H. Zhou, E. Arenholz, Q. He, L. Yang, W. Luo, P. Yu, *Nature Communications* 11, 1 (2020).
3. Z. Dai, J. X. Yu, B. Zhou, S. A. Tenney, P. Lampen-Kelley, J. Yan, D. Mandrus, E. A. Henriksen, J. Zang, K. Pohl, J. T. Sadowski, *2D Materials*, 7, 035004 (2020).
4. C. H. Back, V. Cros, H. Ebert, K. Everschor-Sitte, A. Fert, M. Garst, T. Ma, S. Mankovsky, T. Monchesky, M. V. Mostovoy, N. Nagaosa, S. Parkin, C. Pfleiderer, N. Reyren, A. Rosch, Y. Taguchi, Y. Tokura, K. von Bergmann, and J. Zang, *Journal of Physics D*, 53, 363001 (2020)
5. J. Jiang, D. Xiao, F. Wang, J. H. Shin, D. Andreoli, J. Zhang, R. Xiao, Y. F. Zhao, M. Kayyalha, L. Zhang, K. Wang, J. Zang, C. Liu, N. Samarth, M. HW Chan, C. Z. Chang, *Nature Materials*, 19, 732 (2020)
6. Y. Wu, S. Zhang, J. Zhang, W. Wang, Y. L. Zhu, J. Hu, G. Yin, K. Wong, C. Fang, C. Wan, X. Han, Q. Shao, T. Taniguchi, K. Watanabe, J. Zang, Z. Mao, X. Zhang, K. L. Wang, *Nature Communications* 11, 1 (2020).
7. D. Khadka, T. Thapaliya, S. H. Parra, X. Han, J. Wen, R. F. Need, P. Khanal, W. Wang, J. Zang, J. M. Kikkawa, L. Wu, S. X. Huang, *Science Advances* 6, eabc1977 (2020).
8. W. Wang, Y. F. Zhao, F. Wang, M. W. Daniels, C. Z. Chang, J. Zang, D. Xiao, W. Wu, *Nano Letters* 21, 1108 (2021).
9. M. Huang, L. Gao, Y. Zhang, X. Lei, G. Hu, J. Xiang, H. Zeng, X. Fu, Z. Zhang, G. Chai, Y. Peng, Y. Lu, H. Du, G. Chen, J. Zang, B. Xiang, *Nano Letters*, in press.
10. J. Tang, Y. Wu, W. Wang, L. Kong, B. Lv, W. Wei, J. Zang, M. Tian, H. Du, *Nature Nanotechnology*, in press
11. S. S. Pershoguba, D. Andreoli, J. Zang, *Physical Review B* 104, 075102 (2021)
12. W. Sun, W. Wang, J. Zang, H. Li, G. Zhang, J. Wang, Z. Cheng, *Advanced Functional Materials*, 2104452 (2021)
13. Z. Dai, Z. Gao, S. S. Pershoguba, N. Tiwale, A. Subramanian, Q. Zhang, C. Eads, S. A. Tenney, R. M. Osgood, C. Y. Nam, J. Zang, A. T. C. Johnson, J. T. Sadowski, *Physical Review Letters* 127, 086805 (2021)
14. Z. Gong, J. Tang, S. S. Pershoguba, Z. Xie, R. Sun, Y. Li, X. Yang, J. Liu, W. Zhang, X. Zhang, W. He, H. Du, J. Zang, Z. H. Cheng, *Physical Review B* 104, L100412 (2021)
15. X. Cao, J. X. Yu, P. Leng, C. Yi, Y. Yang, S. Liu, L. Kong, Z. Li, X. Dong, Y. Shi, J. Zang, F. Xiu, arXiv:2103.09395, submitted to *Nature Physics*.
16. K. Niitsu, Y. Liu, A. Booth, X. Yu, N. Mathur, M. Stolt, D. Shindo, S. Jin, J. Zang, N. Nagaosa, Y. Tokura, *Research Square preprint*: <https://doi.org/10.21203/rs.3.rs-311043/v1>, under review in *Nature Materials*.

Fundamental and Defect Properties of Electronic Materials

Shengbai Zhang and Damien West

Department of Physics, Applied Physics & Astronomy, Rensselaer Polytechnic Institute,
Troy, NY 12180

Program Scope

We solved a longstanding puzzle in condensed matter physics with potential implications in device design and redox chemistry. The puzzle is on the nature of band alignment between materials. Naively, one may think the alignment is straightforward, since one can always use the vacuum level as a common reference as is widely adopted in quantum chemistry. However, computational solid-state physics is made possible in large because of the Bloch theorem, which is a theorem for infinite solid. On the positive side, such an approach isolates bulk properties from those of surfaces and interfaces; on the flip side, however, we lose track of the vacuum level. In fact, before our work, people had argued [1] and widely believed that the vacuum level in an infinite solid is illly defined. In 2018, we showed [2] for the first time that the vacuum level is not illly defined. In 2020, we further showed [3] that the widely used reference energy, i.e., the average potential of a solid is offset from the vacuum level by a previously unknown dipole term D_Q , which arises at surfaces due to the quadrupole moment of bulk solid.

These findings have led to more questions: (1) what is the physical significance of D_Q ? (2) What are the implications of the specific crystal truncation which is deemed necessary by elementary electromagnetism to have a uniquely defined bulk quadrupole? Interestingly, using (2), we can calculate polarizations of solids – both spontaneous polarization (without the widely used Berry phase approach) and free carrier polarization at a finite size. This opens the door for studying ferroelectric nanostructures and potentially spontaneously polarized metallic systems. Regarding (1), D_Q can be used to define an innate workfunction (φ_I), which is the position of bulk Fermi level relative to bulk vacuum level. Band alignment is now an alignment between φ_I 's plus a contribution from interfacial charge relaxation.

The latter merely reflects the charge density difference across the interface. Taking lattice matched semiconductor heterostructures such as GaAs/AlAs as an example, since the charge density difference is negligible, the band alignment should simply be that of φ_I 's [3].

To put the theory on more solid footing, we examine the extreme case, i.e., surfaces, that maximizes the effect of charge relaxation. This is done over a wide range of matter – metal, semiconductor, and insulator. As one may recall, half a century ago, Lang and Kohn showed [4] that for simple metals, the workfunction can be nicely described by a surface charge relaxation using a simple jellium model. Their success reveals the insignificance of atomic positions on the charge relaxation. However, they also assumed that the vacuum level is that of the average potential, i.e., $D_Q = 0$. Not surprisingly,

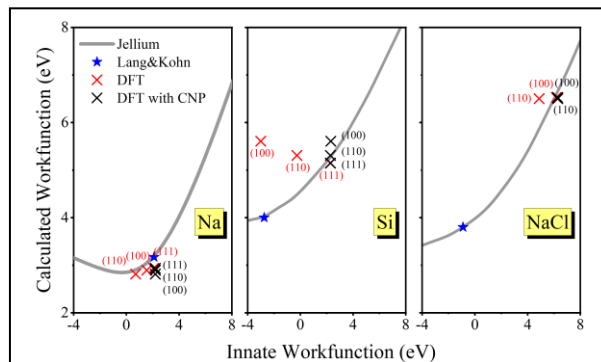


Fig. 1. Calculated workfunction versus φ_I for (a) Na, (b) Si, and (c) NaCl. Solid lines are jellium results as a function of φ_I , which are expected to approach φ_I at large φ_I . Blue stars are the Lang and Kohn results with $D_Q = 0$, red crosses are the DFT results for slabs with electronic relaxation, and black crosses are those when the effect of CNP on φ_I is also included.

the theory failed miserably for semiconductors and insulators, as can be seen in Fig. 1. On the other hand, once we add D_Q to the jellium model, significant improvement is obtained across the board, for example, for Na (metal), Si (semiconductor), and NaCl (widegap insulator).

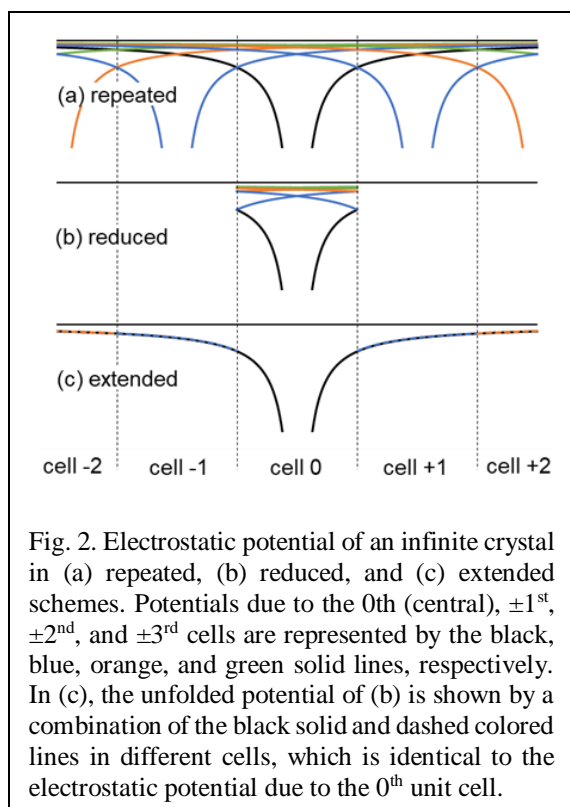
These results can be further improved by avoiding planar truncations which may improperly cut into the atomic charge (note the better agreement for Si (111), in which the cutting plane bisects the covalent bonds perpendicularly). As suggested by Tung and Kronik [5] recently, a charge neutral polyhedron (CNP) is the proper description of surfaces when truncating a bulk solid into slabs, as it minimizes the surface energy. When taking this effect into account, the results for Si are also significantly improved in par with those of metals and insulators.

In short, the mystery around the position of the vacuum level has been resolved. The physics of surface workfunction and that of band alignment between matter become transparent and surprisingly simple. For the future, we see straightforward definitions of other quantities of physical significance, such as intrinsic deformation potentials and intrinsic redox potentials of solids. We also start to understand what happens to atoms when they form a solid, i.e., one should replace spherical charge balls in vacuum by CNPs of crystal symmetry with characteristic atomic sizes.

Keywords: vacuum level in bulk, band alignment, and workfunction

Recent Progress

(1) *Revealing the vacuum level in infinite solid by real-space potential unfolding (publications 4 and 6).* One of the most puzzling problems in electrostatics of infinitely large systems is the average electrostatic potential, \bar{V} , with respect to the vacuum. Its ambiguity was first introduced perhaps by Ihm, Zunger, and Cohen in 1979. After years of debate, a general consensus developed that \bar{V} is an ill-defined quantity because the vacuum level in bulk cannot be unambiguously determined. The ambiguity can be alternatively explained in two ways: (1) a direct integration of charge density is a conditionally convergent quantity whose value depends explicitly on how the integral is taken. (2) Equivalently, in the Fourier representation of the electrostatic potential, the limit $\bar{V} = \lim_{\mathbf{G} \rightarrow 0} V(\mathbf{G})$ is not generally well defined,



but instead depends on the direction from which the limit is taken. Recently, we devised an analytic approach, which is pictorially represented in Fig. 2, to determine the vacuum level position in infinite solids. This method unfolds the local electrostatic potential within one unitcell, with contributions from all its translationally equivalent duplicates, into an extended potential associated with a localized charge, reintroducing the vacuum level reference into the infinite periodic bulk. Figure 2 shows that the average of the total electrostatic potential over one unitcell is equal to the average of one-unitcell-induced electrostatic potential over the entire space. We further found that the average electrostatic potential with respect to the vacuum level is exactly equal to the quadrupole per volume

of the unit cell under consideration. We also extended the above concept for scalar potential to vector potential, predicting a ferromagnetic anomaly at the surfaces of antiferromagnetic bulk materials (publication 6).

(2) *Polarization at the nanoscale (publication 1)*. Size-dependent permanent dipole moment and those induced by surface strain or surface charges have been observed in wurtzite nanostructures. Unlike its zincblende counterpart, the wurtzite structure has intrinsic spontaneous polarization due to its low crystal symmetry. Size-dependent polarization field of

PbTiO₃ nanomaterials has also been demonstrated and been used to improve photocatalytic activity. At the interface between KNbO₃ and BaTiO₃ and between LaMoO₃ and SrMnO₃, there is supposed to exist the so-called polar catastrophe due to spontaneous polarization, which is, however, quenched. Such quenching might be explained as a band-bending effect: namely, bulk CBM lines up with VBM, when the film thickness L exceeds a critical thickness L_c , or alternately, because surface dangling bonds (DBs) come into play. Most recently, permanent dipoles were also observed in zincblende CdSe nano-platelets by transient electric birefringence measurements. Importantly, zincblende is a high-symmetry structure which should not have any spontaneous polarization due to bound charge. Clearly, none of the above can be explained in terms of a spontaneous polarization of bulk. In this work, we develop a theory of polarization charge, which can be applied to polarization at the nanoscale. We show that not only can the polarization charge be uniquely defined following Ref. [2], but also its spatial distribution along the normal direction to the surfaces can be obtained. The approach is applied to seven wurtzite (I-VII, II-VI, III-V, and IV-IV) semiconductor slabs, as well as the perovskite BaTiO₃. We see that for passivated surfaces the total polarization charge is consistent with what is expected from Berry-phase calculations (see Fig. 3). For unpassivated surfaces at the nanoscale, however, charge transfer between DBs can dominate the total polarization. Furthermore, even when surface DBs are fully passivated, the entire system is semiconducting only when the polarization is relatively weak, and the length scale is small so that charge transfer between valence and conduction bands at opposing ends of the materials does not take place. In this semiconducting regime, piezoelectric effects are quenched in qualitative agreement with experiment.

(3) *Realization of double-layer honeycomb structure (publication 5)*. The ability to grow 2D vdW phases of ordinarily covalent 3D bulk materials would greatly increase the available candidates of 2D materials for exploring new physics and functionalities for device applications. Recently, we theoretically proposed that a large family of traditional binary semiconductors are stable in the 2D double layer honeycomb (DLHC) structure [6]. Namely, traditional III-V, II-VI, and I-VII semiconductors, with wurtzite or ZB structure in their 3D bulk form, can be kinetically stable as 2D materials at the ultra-thin limit. These newly proposed 2D materials are intrinsically stable, in distinct contrast to those ‘extrinsically stable’ ones such as stanene and bismuthene, which are in essence an extension of the surface as their interaction with the substrate is required to prevent buckling. Furthermore, this new class of 2D material is not only large but expected to exhibit rich phenomena, including a novel type of topological insulator based on vdW interlayer interactions and excitonic insulators driven by reduced screening [7]. In this joint experimental and theoretical work, few layer AlSb have been grown by MBE. The substrate is graphene covered

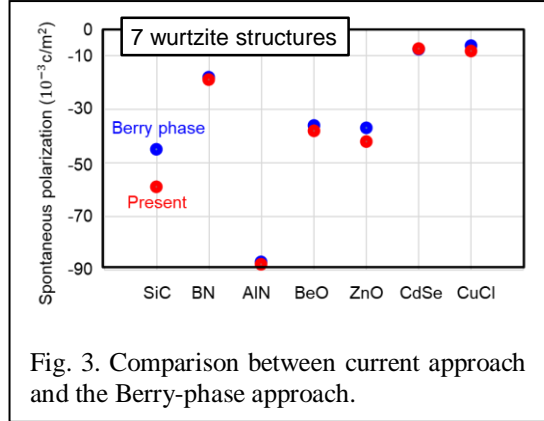


Fig. 3. Comparison between current approach and the Berry-phase approach.

single crystal SiC(0001), in which the weak vdW interaction of graphene with the grown materials makes it possible to examine the intrinsic nature of the resulting 2D grown films. The characterized structure and electronic properties of the resulting AlSb films via spectroscopic imaging STM and cross-sectional imaging STEM are completely consistent with our proposed DLHC structure.

(4) *Prediction of two-dimensional dark excitonic insulators (publications 7 and 8)*. Excitonic insulator (EI) is an exotic phase of solid with a long-range ordered ground state. In an EI, the exciton binding energy exceeds the band gap, leading to the renormalization of the single-particle spectrum associated with the spontaneous formation of excitons. In Ref. [7], we showed that a dark EI may form in materials with parity-forbidden transitions at the fundamental band gap. In these works, we further showed that *any* symmetry-forbidden transitions, not necessarily parity-forbidden, can prompt the stabilization of a dark EI. For example, in the strongly correlated transition metal dihalides, the strong localization of electrons leads to orbital-forbidden selection rules, which are different for the spin-up and spin-down channels. As such, half-exitonic insulators (HEIs) can result wherein only one spin channel has a bosonic condensation of excitons, while the other still has the usual fermions. Being a simultaneous EI and band insulator, quasiparticles in a HEI should respond very differently to applied stimulus. Our argument also applies to spin-forbidden selection rules, leading to spin triplet EIs. As a matter of fact, owing to exchange interactions, triplet excitons are omnipresent in solids. However, a majority of them will not exhibit the desired spin gap to be experimentally measurable. We showed that the semi-hydrogenated graphene may be a good platform to study spin-forbidden EIs, as they are predicted to spontaneously form. From an experimental point of view, possibly the most straightforward way to detect an EI phase is to directly measure condensation, i.e., the long-range coherent superfluid of excitons. However, as charge-neutral particles, the flow of excitons cannot provide easily detected electrical signals. As the spin-triplet excitons carry a finite spin moment, they could provide a new opportunity for the detection of EI, as spin superfluidity will occur when they condense into a single quantum state.

Future Plans

We will conclude our pursue of physics behind the band alignment, while examining the extent to which our new findings apply to the prediction of deformation potentials, electrode potentials, and redox potentials. We will expand the study of polarization-without-the-Berry-phase to poor- and semi-metals to which, to the best of our knowledge, no good theory/model applies. We will pursue the physics of emergent strong interaction in 2D materials and its impacts on defect formation and transport. Particularly, we are interested in the formation of polarons, as an interplay between localization due to Hubbard U and the more traditional one due to electron-phonon coupling, such as the Jahn-Teller distortion. We will determine if conduction can be reached by ionizing defects to the polaronic state, i.e., exciton/polaron crossover, instead of ionization to the band edge. We will also examine the implications of carrier localization to excitonic instability at point defects and how it renormalizes the defect spectrum, ionization, and conductivity. We will revisit our unfortunately “never-ending” goal of finding an accurate formalism to correct errors in bulk charged defect calculations, as new clues have emerged. We are interested in the fundamental limit in crystal stability upon intrinsic defect formations, targeting the non-traditional, non-zincblende and hence lesser-known semiconductors and widegap materials, especially the oxides, as well as the fundamental limits of doping. For the latter, we will examine the effects of resonant doping in hard to dope materials, as resonant doping seems to be a good candidate to achieve higher mobility. Finally, we will calculate light matter interactions in heterovalent interfacial structures to examine how the linear and non-linear responses are affected at the atomic level and by the formation of exotic interfacial bonds.

References

1. L. Kleinman, Phys. Rev. B 24, 7412 (1981).
2. D-H. Choe, D. West, S. B. Zhang, Phys. Rev. Lett. 121, 196802 (2018).
3. D-H. Choe, D. West, S. B. Zhang, Phys. Rev. B 103, 235202 (2020).
4. N. D. Lang and W. Kohn, Phys. Rev. B 3, 1215 (1971).
5. R. T. Tung and L. Kronik, Phys. Rev. B 94, 075310 (2016).
6. M. C. Lucking, W. Xie, D.-H. Choe, D. West, T.-M. Lu, S. B. Zhang, Phys. Rev. Lett. 120, 086101 (2018).
7. Z. Jiang, Y. Li, S. Zhang, W. Duan, Phys. Rev. B 98, 081408 (2018).

Publications

1. K. Yang, Z. Jiang, D-H. Choe, D. West, S. B. Zhang, “Polarization at the Nanoscale”, arXiv preprint arXiv:2108.13950.
2. R. Besse, J. F R V Silveira, Z.Jiang, D. West, S. B. Zhang, and J. L F Da Silva, “Beyond the Anderson rule: importance of interfacial dipole and hybridization in van der Waals heterostructures”, 2D Mater. **8**, 041002 (2021).
3. D. Ghoshal, H. Shang, X. Sun, X. Wen, D. Chen, T. Wang, Z. Lu, T. Gupta, H. Efstathiadis, D. West, N. Koratkar, T-M. Lu, S. B. Zhang, and S-F Shi, “Orientation-Controlled Large-Area Epitaxial PbI₂ Thin Films with Tunable Optical Properties”, ACS Appl. Mater. Interfaces **13(27)**, 32450–32460 (2021).
4. D-H. Choe, D. West, and S. B. Zhang, “Revealing the vacuum level in an infinite solid by real-space potential unfolding”, Phys. Rev. B **103**, 235202 (2021).
5. L. Qin, Z-H. Zhang, Z. Jiang, K. Fan, W-H. Zhang, Q-Y. Tang, H-N. Xia, F. Meng, Q. Zhang, L. Gu, D. West, S. B. Zhang, and Y-S. Fu, “Realization of ALSb in the Double-Layer Honeycomb Structure: A Robust Class of Two-Dimensional Material”, ACS Nano **15**, 8184–8191 (2021).
6. Z. Y. Jiang, D. West, S. B. Zhang, “Vector potential and surface magnetic field in magnetoelectric antiferromagnetic materials”, Phys. Rev. B **102**, 174411 (2020).
7. Z. Jiang, W. Lou, Y. Liu, Y. Li, H. Song, K. Chang, W. Duan, S. B. Zhang, “Spin-Triplet Excitonic Insulator: The Case of Semihydrogenated Graphene”, Phys. Rev. Lett. **124**, 166401 (2020).
8. Z. Jiang, Y. Li, W. Duan, S. B. Zhang, “Half-Excitonic Insulator: A Single-Spin Bose-Einstein Condensate”, Phys. Rev. Lett. **122**, 236402 (2019).
9. C. Si, D. Choe, W. Xie, H. Wang, Z. Sun, J. Bang, S. B. Zhang, “Photoinduced Vacancy Ordering and Phase Transition in MoTe₂”, Nano Lett. **19**, 3612-3617 (2019).
10. D. Wang, D. Han, D. West, N.-K. Chen, S.-Y. Xie, W. Q. Tian, V. Meunier, S. B. Zhang & X.-B. Li, “Excitation to defect-bound band edge states in two-dimensional semiconductors and its effect on carrier transport”, npj Comp. Mater. **5**, 8 (2019).

Data-driven Discovery of Inorganic Electrides for Energy Applications

Qiang Zhu,

Department of Physics and Astronomy,

University of Nevada Las Vegas

Program Scope

Electrides are ionic solids with cavity-trapped electrons, which serve as anions. Both the localization of electrons in the interstitial and their mutual interactions provide early examples of quantum confinement. Due to the presence of interstitial electrons around the Fermi level (Fig. 1), electrides exhibit unique properties, such as low work function and high electron mobility. A variety of applications in catalysis, batteries and superconducting electronics have been proposed [1].

Despite over thirty years of research, only tens of electride materials are known today. Our fundamental understanding, as well as utilization, of these exotic materials remain limited by the small library of candidate electride materials. In the last decade, it has become possible to discover new materials through computation, and the path to this breakthrough has been paved by the development of structure prediction methods. Two largely complementary approaches exist: data mining [3] and first-principles [4] crystal structure prediction (CSP). The former is capable of quickly scanning the materials over a vast chemical space but will fail if the target material does not have any analogue in the database. On the other hand, the latter is based on powerful exploratory computer algorithms capable of making predictions with little pre-existing knowledge. Yet, each CSP study requires very significant computational resources. Therefore, such studies were limited to only a few systems.

This research aims to accelerate the discovery of electrides through developing an advanced materials screening method that combines structure prediction, machine learning and high-throughput screening. Specific objectives of this research include: (1) to incorporate symmetry relations into materials structure screening, (2) to develop machine learning models that can perform quick evaluations of materials' structural and electronic properties; 3) to construct an electride database by screening promising within a large chemical space. The simulation results will provide the materials community with a large number of potential electrides, allowing the experimental researchers to test predictions and probe potential technological applications.

Keywords: Electron Localization, Materials Data Mining, Physics-informed Machine learning

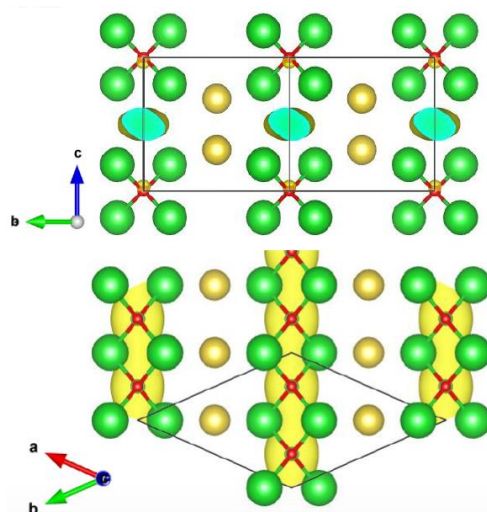


Fig. 1. An example of 1D electride NaBa₂O [2].

Recent Progress

Since 2018, my group has been actively developing two open source codes PyXtal [5] and PyXtal_FF [6], which provide the foundation to carry out the methodology developments for materials structure prediction and atomistic simulation. Both codes have started to become popular for the general purpose of materials modeling. In electrider research, we have performed the following researches in the past three years.

1. We were one of the first groups to introduce a truly high-throughput computational scheme to allow screening of potential electrideres from the entire inorganic materials database [7].
2. We performed the first principles structure prediction to identify a brand new electrider material Rb_3O with the presence of both topological and electrideres from the existing materials database electrider properties [8].
3. We recently screened over 600 2D monolayer materials to search for the existence of

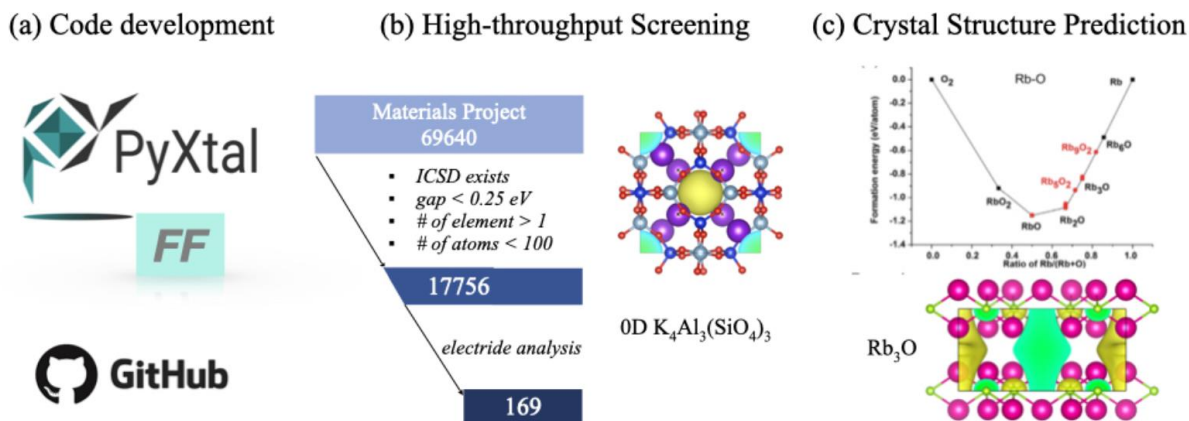


Fig. 2. Preliminary works on (a) code developments; (b) high-throughput screening and (c) crystal structure prediction on electrider design.

potential electrideres that can be switched on by strain engineering [9].

Future Plans

For the next five years, we aim to accelerate the discovery of electrider materials by improving the existing CSP methods with both group theory and data-intensive approaches as follows.

A. Reducing the search space in global structure optimization from symmetry constraints.

To explore the entire structural space for a given chemical system, many structure prediction

methods, such as simulated annealing and evolutionary algorithms, involve repetitive generation and perturbation of structures based on the random processes. However, most of the computation time will be wasted on sampling high-energy and disordered regions in the structural space. To avoid the unnecessary sampling, we propose to develop a new structural initialization and variation scheme in a reduced space constrained by symmetry. Based on the current PyXtal code, we will further implement the new functions to enable the structural variation by following the group-subgroup relations with mathematical rigor. We expect the the new method will serve as a fundamental library to improve the existing structure predictions methods.

- B. Developing the machine learning models to predict materials' structural and electronic properties.** Even under the reduced search space that considers symmetry constraints, a typical structure prediction requires hundreds/thousands of trial structures to be evaluated by expansive first-principles calculations. Recently, there has been rapid progress in the development of machine learning force fields which can deliver the same accuracy as first-principles methods, but with a speed up of 2-4 orders of magnitude greater. However, the previous models are limited to the properties associated with atomic energy only (e.g., total energy, forces, stress), while the electronic information is missing. In the proposal, we will develop a physics-informed machine learning model based on the tight-binding formalism. With this new model, we expect to improve the extrapolability of energy prediction. More importantly, the electronic properties can be derived as well.
- C. Discovering new electrified materials with the advanced CSP methods and machine learning.** To search for better electrified materials, we plan to apply the improved CSP method from Task A to predict materials in a broad chemical space, as opposed to the traditional CSP which deals with only one chemical system. To avoid massive quantum mechanical calculations, we will train the machine learning (ML) models from Task B to relax the geometry and predict the physical properties for the trial structures. We anticipate that such low-cost ML models may be also beneficial to high-throughput materials screening beyond the CSP activities.
- D. Establishing the database for electrified materials.** From task C, we expect to identify a large number of electrified materials. Their fundamental physical properties, including thermal stability, work function, carrier mobility and topological properties will be carefully examined by the means of ML and first-principle calculations. We expect that the resulting electrified material database will make a profound impact on the materials design community.

References

- [1] Dye, J.L. *Acc. Chem. Res.* (2009) doi: 10.1021/ar9000857.
- [2] Wang, J-J et al. *Phys. Rev. B* (2019) doi: 10.1103/PhysRevB.99.064104
- [3] Curtarolo, S. et al. *Nat. Mater.*, 12, 191 (2013) doi:10.1038/nmat3568
- [4] Oganov, A.R. et al. *Nat. Rev. Mater.* (2019) doi:10.1038/s41578-019-0101-8
- [5] Fredericks, S., et al. *Comp. Phys. Comm.* doi:10.1016/j.cpc.2020.107810
- [6] Yanxon, H. et al. *Machine Learning: Sci. Tech.* (2020) doi:10.1088/2632-2153/abc940
- [7] Zhu, Q. et al. *Matter* (2019) doi:10.1016/j.matt.2019.06.017
- [8] Zhu, S-C et al. *Phys. Rev. Mater.* (2019) doi:10.1103/PhysRevMaterials.3.024205

[9] Yang, X. et al. Phys. Rev. B (2021) doi: 10.1103/PhysRevB.103.125103

Publications

N/A

RECONSIDERING ELECTRONIC PHASES: THE ROLE OF OTHER MICROSCOPIC DEGREES OF FREEDOM

PI: Alex Zunger,
University of Colorado, Boulder, Colorado, USA

The traditional approach to the understanding of “electronic phases” in model Hamiltonian approaches to correlated electron problems in CMP centers on the electron degrees of freedom [1-3]. Other microscopic degrees of freedom (m-DOF), such as lattice distortions, or the configurations of local magnetic and dipole moments, were often considered as *consequences* of the primary electron localization, afterthoughts that can be dealt with later as separate problems and not a possible *cause* of the opening of the insulating gap itself. Unlike the mean-field like Density Functional Theory (DFT), an entirely different mathematical machinery based largely on the Hubbard Hamiltonian and its extensions has been created, emphasizing electron correlation and localization in the presence of non-interacting “spectator” DOF’s [1-3].

The repeated demonstrations of failures of DFT by the correlated electron community (as recently as this year [4]) were generally based on the use of the highest possible symmetry described by the smallest possible unit cell. It turned out that such imposed symmetry constraint constituted a ‘self-fulfilling prophecy’ being a key reason [5-9] for the false metal predictions in Mott insulators [4] by mean field approaches. But this fault was not part of the DFT method itself. Members of the DFT community pointed out that there are avenues for removing the constraints on naive DFT [5-10] other than disposing of DFT altogether. This entailed allowing m-DOF, all sanctioned by the DFT single-determinant, mean-field framework, without necessarily appeal to strong correlation.

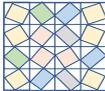
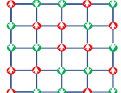
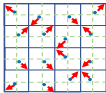
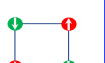
m-DOF’s can include (schematic figure below) structural motifs (column a); magnetic motifs (column b), or dipole motifs (column c). At low temperatures these motifs tend to give rise to long range ordered (LRO) configurations (row 1), whereas configurations that are not the stablest ones (‘para phases’) give rise to partially ordered configurations (rows 2 and 3). Such para phases were traditionally imagined to be made of single motifs (‘monomorphous’ in row 3), a tradition sanctioned by the structural characterization techniques (e.g. X Ray diffraction) that delivered the *global, averaged structure*. Consequently, properties are still most commonly explained and linked to simple monomorphous descriptions of a material’s structure.

However, experimental evidence for the existence of local features (indicated schematically in Row 2a,2b,2c) started to accumulate early on (see review in [11]). This happened as X ray and Neutron local characterization probes became available (primarily in National Laboratories), able to ‘see’ the local positional, magnetic and dipolar configurations, unmasked by the averaging procedure attendant in the traditional, volume-averaging probes such as X Ray Diffraction [11]. Recent observations from the experimental community, reported symmetry breaking in nominally cubic paraelectric oxide phases such as BaTiO₃ and KNbO₃ *being piezoelectric* [12]. This is surprising (but technologically exciting), given that along with chiral dichroism, second harmonic generation and the Rashba spin splitting, the classic piezoelectricity requires an absence of inversion center. Remarkably, piezoelectricity was observed in what used to be considered nominally cubic perovskites.

We point out [5-9] that a realistic picture of para phases could entail significantly larger unit cells, having a range of *local motifs* (‘polymorphous networks in row 2). The significance of this realization lies in the fact that polymorphous networks can have profoundly different materials properties than the hitherto conceived monomorphous simplifications (row 3). For example, whereas use of monomorphous description of Mott paramagnets (3b) such as NiO or LaMnO₃ as input to band theory produces a false metallic band structure, use of the correct polymorphous description (2b) predicts the observed insulating phase. Also, use of the polymorphous structure of paraelectric (2c) such as BaTiO₃ predicts loss of inversion symmetry, consistent with the recently observed piezoelectric effect, the use of the monomorphous structure (3c) fails. Other examples include larger band gaps and stable phonons in para-elastics, (2a vs 3a) s-p bonded perovskites. It

was pointed out that this broken symmetry mean-field approach correctly described the local structural motif measured via pair distribution function (PDF), while at the same time producing gapping, mass enhancement [8], orbital order in paramagnetic Mott insulators, and loss of inversion symmetry in paraelectric piezoelectric phases, all without invoking strong correlation. Furthermore, P. Ghosez et al [10], have used in 2017 symmetry-broken DFT, pointing out how this leads to metal-insulator transitions in Nickelates, triggered specifically by lattice degrees of freedom.

Global vs local

Type of m-DOF Phase of m-DOF	(a) μ =Position displacement	(b) μ =spin moments	(c) μ =dipole moments
(3) Para-phase Sym. unbroken $\mu_{\text{global}} = 0$ $\mu_{\text{local}} = 0$	(3a) Simple paraelastic 	(3b) Simple paramagnetic 	(3c) Simple paraelectric 
(2) Para-phase Sym. broken $\mu_{\text{global}} = 0$ $\mu_{\text{local}} \neq 0$	(2a) Paraelastic (polymorphous) 	(2b) Paramagnetic (polymorphous) 	(2c) Paraelectric (polymorphous) 
(1) Ordered Ground state Sym. broken $\mu_{\text{global}} \neq 0$ $\mu_{\text{local}} \neq 0$	(1a) Long-range ordered displacements (orth-, tetra-) 	(1b) Long-range ordered magnetic moments (AFM, FM)  ● spin up ● spin down	(1c) Long-range ordered dipole moments (FE, AFE)  ▲ local dipole

3

The apparent explanations of similar physical effects by symmetry broken mean field like DFT and sometimes by explicitly highly correlated symmetry preserving methods begs the obvious question: what happened to the strong correlation when symmetry was broken in a larger cell? This is reminiscent of the classic case of failure of symmetry preserving mean field for stretched bonds in hydrogen molecule or chain, but the successful answer for the symmetry-broken dissociation to two separate hydrogen atoms [9]. Thus, 'what is strongly-correlated for one reference state can be weakly-correlated or even uncorrelated for another reference state'[12]. In other words, *strong correlation may be representation-dependent, rather than being an absolute statement on the intrinsic physical nature of a compound or a phase.*

The experimental and theoretical communities working on complex phenomena discussed here must join forces with open minds to solve the essential remaining difficult problems in this field. We all want to know what are the *minimal (not maximal), enabling physics concepts* needed to understand the trend across the Periodic Table in these field. One is not denying the elegance, physical depth and mathematical beauty of some of the highly correlated methods [1-3]. We are questioning if (or when) they are actually *needed*.

We are not denying the existence of correlation. This is likely to be the case for multiplets in Kondo systems or in open shell free atoms and ions such as carbon, (where the many body effects disappear when carbon forms graphite or diamond). It is important, however, to figure out specifically when this highly correlated description is unescapable. For example, determine which systems would maintain correlated behavior even if it cannot be symmetry broken. No longer can one cry out that "strong correlation is everywhere". Indeed, identifying compounds and properties where DFT fails fair-and-square will provide legitimate opportunities for explicitly correlated, symmetry preserving theories to (deservingly) shine. These questions are highly consequential, deciding which theoretical/computational methods to use for predicting the properties of technologically relevant materials, including fixing the metal vs. insulator description of many oxides in the computational data bases (as demonstrated in Ref. [5])

- [1] J. Hubbard, Proc. R. Soc. London, Ser. A 276, 238 (1963).
- [2] D. P Arovas, Erez Berg, Steven Kivelson, Srinivas Raghu [The Hubbard Model](#) arXiv:2103.12097
- [3] A. Georges, W. Krauth, and M. J. Rozenberg, Rev. Mod. Phys. 68, 13 (1996)
- [4] Eva Pavarini "Solving the strong-correlation problem in materials" La Rivista del Nuovo Cimento; 11 2021
- [5] O. I. Malyi and Alex Zunger "False metals, real insulators, and degenerate gapped metals" Applied Physics Reviews, 7, 041310 (2020)
- [6] J. Varignon, M. Bibes and Alex Zunger, "Origin of band gaps in 3d perovskite oxides" Nature Commu., 10, 1658 (2019).
- [7] Zhi Wang, Xin-Gang Zhao, Robert Koch, Simon J. L. Billinge, and Alex Zunger, "Understanding electronic peculiarities in tetragonal FeSe as local structural symmetry breaking" Phys. Rev. B 102, 235121 (2020)
- [8] Zhi Wang, Oleksandr I. Malyi, Xingang Zhao, and Alex Zunger, "Mass enhancement in 3d and s-p perovskites from symmetry breaking" Phys. Rev. B 103, 165110 (2021)
- [9] Yubo Zhang, James Furness, Ruiqi Zhang, Zhi Wang, Alex Zunger, and Jianwei Sun, "Symmetry-breaking polymorphous descriptions for correlated materials without interelectronic U" Phys. Rev. B 102, 045112 (2020)
- [10] M B Jordan, J Iniguez, P Ghosez "Structurally triggered metal-insulator transition in rare earth nickelates" Nature Communications 8, 177 (2017).
- [11] T Egami, SJL Billinge Underneath the Bragg peaks: structural analysis of complex materials(2003)
- [12] J.P. Perdew et al., PNAS 118, e2017850118 (2021).

Work was supported by the U.S. Department of Energy, Office of Science, Basic Energy Sciences, Materials Sciences and Engineering Division under Grant No.DE-SC0010467. The ab initio calculations of this work used resources of the National Energy Research Scientific Computing Center, which is supported by the Office of Science of the U.S. Department of Energy. See related poster entitled "The peculiarities of para phases of oxide perovskites explained as consequences of symmetry breaking".

Spin-Orbit Coupled Systems: From Triplet Superconductivity to Topological Kink States

PI: Igor Zutic, University at Buffalo, State University of New York, zigor@buffalo.edu

Program Scope

Advances in semiconductors and their nanostructures provide fascinating opportunities to reveal novel quantum phenomena and transfer them to other classes of materials. Our proposed research reflects the renewed interest in emergent and many-body phenomena in semiconductor nanostructures, which can support magnetism, spin-orbit coupling, and superconductivity, as well as novel ways to implement such nanostructures. Rather than with the MBE growth, atomically sharp interfaces can be also realized by mechanical exfoliation of van der Waals materials. The resulting monolayers are a striking example of ultrathin nanostructures which can be transformed through proximity effects. However, the presence of strong Coulomb interaction and nontrivial topological properties offers an important opportunity to revisit the role of spin-orbit coupling and description of proximity effects beyond the single-particle picture.

Keywords: proximity effects, spin-orbit coupling, topological materials

Recent Progress

Interfacial Spin-Orbit Coupling: Spin-Triplet Superconductivity and Magnetoanisotropy

Spin-orbit coupling (SOC) is a key interaction in spintronics, allowing electrical control of spin or magnetization and, vice versa, magnetic control of electrical current [1]. However, recent advances have revealed much broader implications of SOC that is also central to the design of topological states with potential applications from low-energy dissipation and faster magnetization switching to high tolerance of disorder. SOC and the resulting emergent interfacial spin-orbit fields are simply realized in junctions through structural inversion asymmetry, while the anisotropy in magnetoresistance (MR) allows their experimental detection. Surprisingly, we demonstrate that an all-epitaxial ferromagnet/MgO/metal junction with a single ferromagnetic region and only negligible MR anisotropy undergoes a remarkable transformation below the superconducting transition temperature of the metal. The superconducting junction has a MR anisotropy 3 orders of magnitude higher and could enable novel applications in superconducting spintronics. In contrast to common realizations of MR effects that require a finite applied magnetic field, our system is designed to have two stable zero-field states with mutually orthogonal magnetizations: in plane and out of plane [2]. This behavior is illustrated in Figs. 1(a)-(c).

A common path to superconducting spintronics, Majorana bound states, and topologically protected quantum computing relies on spin-triplet superconductivity. While naturally occurring spin-triplet pairing is elusive, and even common spin-triplet candidates, such as Sr_2RuO_4 [3], support alternative explanations [4,5], proximity effects in heterostructures can overcome these limitations. It is expected that robust spin-triplet superconductivity in magnetic junctions should rely on highly spin-polarized magnets or complex magnetic multilayers [6]. Instead, we predict that the interplay of interfacial SOC and the barrier strength in simple magnetic junctions, with only a small spin polarization and *s*-wave superconductors, can lead to nearly complete spin-triplet superconducting proximity effects, as depicted in Fig. 1(d) [7]. This peculiar behavior arises from an effective perfect transparency: interfacial SOC counteracts the native potential barrier for states

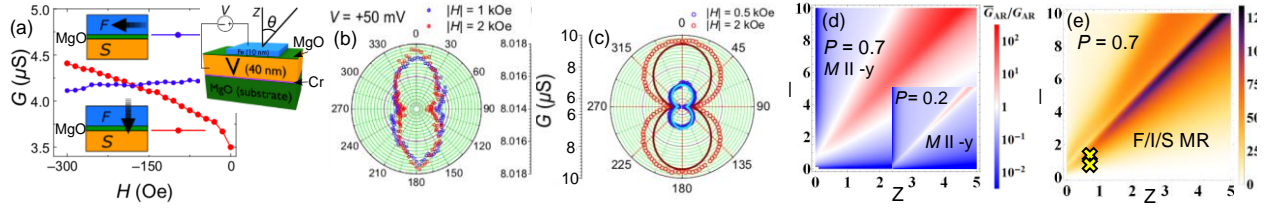


Fig. 1 (a) Fe/MgO/V junction, θ is the angle between the magnetization \mathbf{M} and the interface normal. Zero-bias ($V = 0$) conductance, G , with in-plane, out-of-plane H . Our design allows for two $H = 0$ stable states (in-, out-of-plane \mathbf{M}). (b), (c) $G(\theta)$ at $T = 0.3$ K in the normal ($V = 50$ meV) and superconducting state, solid lines: our theoretical fits [2]. (d) Zero-bias G ratio between the spin-flip (equal spin) and conventional Andreev reflection as a function of the normalized barrier, Z , and Rashba SOC strength, λ [7], shows the relative contribution of the singlet and triplet superconductivity. (e) The corresponding magnetoresistance (MR), crosses denote the modeled Fe/MgO/V samples in [2].

of a given spin and wave vector. We show that the enhanced spin-triplet regime is characterized by a huge increase MR anisotropy, orders of magnitude larger than in the normal state. This suggests measuring such MR anisotropy, as studied in Ref. [2], probes the presence of equal-spin triplet superconductivity, we recently confirmed in junctions with van der Waals magnets [8].

Robust Topology and Spin-Valley-Momentum Locking: From Concept to Materials Design

Two-dimensional (2D) hexagonal lattices offer a versatile platform to manipulate charge, spin, and valley degrees of freedom and implement different topological states. While pioneering predictions for the quantum anomalous and quantum spin Hall (QSH) effects were guided by graphene-like systems, graphene poses inherent difficulties with its weak SOC and a gap of only $\Delta \sim 40 \mu\text{eV}$ [9]. The quest for different 2D hexagonal monolayers (MLs) with a stronger SOC on one hand reveals, as in transition metal dichalcogenides (TMDs), an improved control of valley-dependent phenomena, while on the other hand, as in a ML Bi on SiC substrate, topological states remain even above room temperature with a huge topological gap ~ 0.8 eV [10]. However, with its inversion symmetry Bi/SiC has no valley-dependent effects and examples where valley degrees of freedom support robust topological states remain scarce.

We reveal how to overcome these challenges by recognizing the opportunities from the quantum valley Hall kink (QVHK) states [11,12], realized in bilayer graphene (BLG) systems supporting the reversal of the Berry curvature $\Omega(\mathbf{k})$ [see also Fig. 2] along an internal boundary. The resulting topological defect supports counter-propagating 1D chiral electrons, topologically protected by the valley-inversion symmetry. However, with a small BLG gap ~ 20 meV, such QVHK excludes high-temperature applications, and QVHK states were limited to 5 K [14]. Crucially, disorder easily induces inter-valley scattering, preventing the expected ballistic transport in QVHK states. Specifically, we propose a robust platform

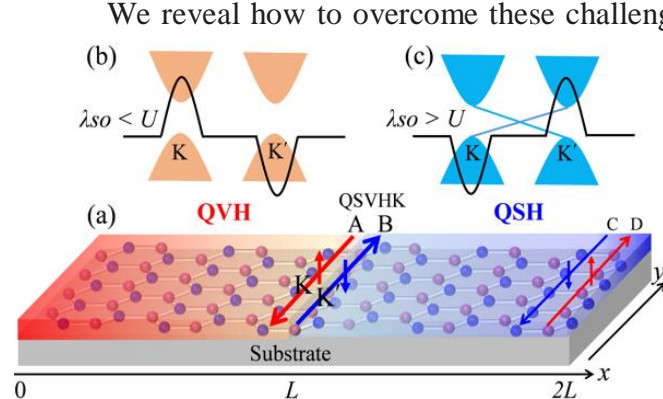


Fig. 2 (a) Quantum spin-valley Hall kink (QSVHK) states (A,B), at the K, K' valleys and QSH edge states (C, D) in a junction of quantum valley Hall (QVH) and QSH insulators. The arrows: spin channels. (b) and (c) schematic of the bands and Berry curvatures (black) for QVH and QSH insulators, distinguished by the relative SOC strength, λ_{SO} , and staggered potential, U . (c) QSH edge states in blue [13].

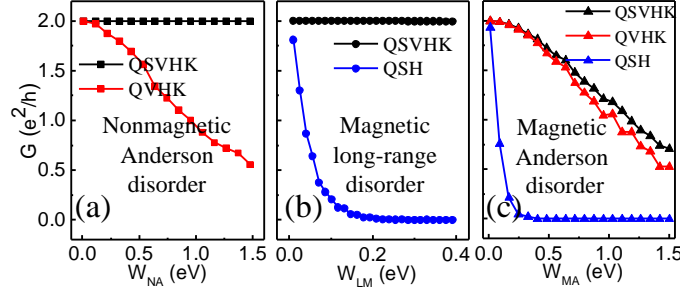


Fig. 3 (a) Junction conductance G vs nonmagnetic Anderson disorder strength W_{NA} at the Fermi level for the QSVHK and QVHK states. (b) Same as (a) but for the QSVHK and QSH states vs magnetic long-range disorder strength W_{LM} . (c) Same as (b) but vs magnetic Anderson disorder strength W_{MA} . The parameters U , λ_{SO} for the QVH and QSH regions are taken from the BiAs/SiC and Bi/SiC. The hopping parameter is $t_{1,2} = 1$ eV.

QVHK state in BLG, the QSVHK state is fully spin-polarized. As illustrated in Fig. 2, The kink state A (B) at K (K') valley has a spin-up (down) channel, see Fig. 2, demonstrating an example of *spin-valley-momentum locking*, derived from a simultaneous protection by time-reversal and valley-inversion symmetries. Based on first-principles results and our fabricated samples, we show that QSVHK states, protected with a gap up to 287 meV, can be realized in bismuthene by alloy engineering, surface functionalization, or electric field, supporting nonvolatile applications of spin-valley filters, valves, and waveguides even at room temperature [13].

Future Plans

Motivated by our prediction for an enhanced proximity-induced spin-triplet superconductivity [7], we have guided its realization in junctions of van der Waals ferromagnets and s -wave superconductors. While our expectation that the maximum MR, which signals the presence of spin-triplet contribution, appears to be experimentally confirmed for intermediate values of junction resistance [8], we recognize that our theoretical approach needs to be generalized. Instead of the assumption for a step function pair potential, we will develop its self-consistent description. This picture will allow us to study superconducting correlations and compare their signature with the inferred equal spin-triplet contribution which we found to be non-monotonic both in the strength of the SOC and the interfacial barrier, as shown in Fig 1(d). These studies will allow us to further examine the use of MR anisotropy as the probe for spin-triplet superconductivity and provide a more complete understanding of the ongoing experiments [8].

While we have focused on the transport signature of the spin-valley-momentum locking, we will also explore what are the implications of the underlying topological properties on the optical response. This will be guided by our DOE-supported work showing a gate-controlled helicity reversal of the emitted light, reflecting the changes in band topology of the participating excitons, which we have studied from Bethe-Salpeter equation in similar Bi-based systems [15].

In the quest to realize robust topological states in 2D materials, such as the nodal-line topological semimetals, we will explore how they could be implemented by creating periodic vacancies. This approach provides an alternative method to support desirable nonsymmorphic symmetries, even in common symmorphic materials [16,17], while ensuring that the nodal lines remain robust under external perturbations due to spin-orbit coupling or magnetic exchange.

to realize arrays of spin-polarized QVHK states at room temperature based on a 2D hexagonal topological insulator, where the QVHK states are simultaneously the QSH edge states, forming along the QSH-quantum valley Hall (QVH) interface, shown in Fig. 2 [13].

Remarkably, the conductance of QSVHK states remains quantized against both nonmagnetic short- and long-range and magnetic long-range disorder, verified by the Green-function calculations shown in Fig. 3 and contrasted by more fragile quantization of QSH and QVHK states. Unlike the

References

1. I. Zutic, J. Fabian, and S. Das Sarma, Spintronics: Fundamentals and Applications, *Rev. Mod. Phys.* **76**, 323 (2004).
2. I. Martinez, P. Högl, C. Gonzalez-Ruano, J. Pedro Cascales, C. Tiusan, Y. Lu, M. Hehn, A. Matos-Abiague, J. Fabian, I. Zutic, and F. G. Aliev, Interfacial Spin-Orbit Coupling: New Platform for Superconducting Spintronics, *Phys. Rev. Appl.* **13**, 014030 (2020).
3. A. P. Mackenzie and Y. Maeno, The superconductivity of Sr_2RuO_4 and the physics of spin-triplet pairing, *Rev. Mod. Phys.* **75**, 657 (2003).
4. I. Zutic and I. Mazin, Phase-Sensitive Tests of the Pairing State Symmetry in Sr_2RuO_4 , *Phys. Rev. Lett.* **95**, 217004 (2005).
5. A. N. Petsch, M. Zhu, M. Enderle, Z. Q. Mao, Y. Maeno, I. I. Mazin, and S. M. Hayden, Reduction of the Spin Susceptibility in the Superconducting State of Sr_2RuO_4 Observed by Polarized Neutron Scattering, *Rev. Lett.* **125**, 217004 (2020).
6. M. Eschrig, Spin-polarized supercurrents for spintronics: A review of current progress, *Rep. Prog. Phys.* **78**, 104501 (2015).
7. T. Vezin, C. Shen, J. E. Han, and I. Zutic, Enhanced Spin-Triplet Pairing in Magnetic Junctions with s-Wave Superconductors, *Phys. Rev. B* **101**, 014515 (2020).
8. R. Cai, Y. Yao, P. Lv, Y. Ma, W. Xing, B. Li, Y. Ji, H. Zhou, C. Shen, S. Jia, X. C. Xie, I. Zutic, Q.-F. Sun and W. Han, Evidence for anisotropic spin-triplet Andreev reflection at the 2D van der Waals ferromagnet/superconductor interface, preprint, under review in *Nat. Commun.*
9. J. Sichau, M. Prada, T. Anlauf, T. J. Lyon, B. Bosnjak, L. Tiemann, and R. H. Blick, Resonance Microwave Measurements of an Intrinsic Spin-Orbit Coupling Gap in Graphene: A Possible Indication of a Topological State, *Phys. Rev. Lett.* **122**, 046403 (2019).
10. F. Reis, G. Li, L. Dudy, M. Bauernfeind, S. Glass, W. Hanke, R. Thomale, J. Schäfer, and R. Claessen, Bismuthene on a SiC substrate: A candidate for a high-temperature quantum spin Hall material, *Science* **357**, 287 (2017).
11. I. Martin, Y. M. Blanter, and A. F. Morpurgo, Topological Confinement in Bilayer Graphene, *Phys. Rev. Lett.* **100**, 036804 (2008).
12. J. Jung, F. Zhang, Z. Qiao, and A. H. MacDonald, Valley-Hall kink and edge states in multilayer graphene, *Phys. Rev. B* **84**, 075418 (2011).
13. T. Zhou, S. Cheng, M. Schleenvoigt, P. Schuffelgen, H. Jiang, Z. Yang, and I. Zutic, Spin-Valley Hall Kink States: From Concept to Materials Design, *Phys. Rev. Lett.* **129**, 116402 (2021).
14. J. Li, R.-X. Zhang, Z. Yin, J. Zhang, K. Watanabe, T. Taniguchi, C. Liu, and J. Zhu, A valley valve and electron beam splitter, *Science* **362**, 1149 (2018).
15. G. Xu, T. Zhou, B. Scharf, I. Zutic, Optically Probing Tunable Band Topology in Atomic Monolayers, *Phys. Rev. Lett.* **125**, 157402 (2020).
16. F. Liu, F. Qu, I. Zutic, S. Xie, D. Liu, A. L. A. Fonseca, and M. Malard, Robust Topological Nodal-Line Semimetals from Periodic Vacancies in Two-Dimensional Materials, *J. Phys. Chem. Lett.* **127**, 5710 (2021).
17. F. Liu, F. Qu, I. Zutic, and M. Malard, Less is more: Vacancy-engineered nodal-line semimetals, [arXiv:2108.05502](https://arxiv.org/abs/2108.05502)

Publications

1. T. Vezin, C. Shen, J. E. Han, and I. Zutic, Enhanced Spin-Triplet Pairing in Magnetic Junctions with s-Wave Superconductors, *Phys. Rev. B* **101**, 014515 (2020).
2. I. Martinez, P. Högl, C. Gonzalez-Ruano, J. Pedro Cascales, C. Tiusan, Y. Lu, M. Hehn, A. Matos-Abiague, J. Fabian, I. Zutic, and F. G. Aliev, Interfacial Spin-Orbit Coupling: New Platform for Superconducting Spintronics, *Phys. Rev. Appl.* **13**, 014030 (2020).
3. T. Zhou, S. Cheng, M. Schleenvoigt, P. Schuffelgen, H. Jiang, Z. Yang, and I. Zutic, Spin-Valley Hall Kink States: From Concept to Materials Design, *Phys. Rev. Lett.* **129**, 116402 (2021).
4. G. Xu, T. Zhou, B. Scharf, I. Zutic, Optically Probing Tunable Band Topology in Atomic Monolayers, *Phys. Rev. Lett.* **125**, 157402 (2020).
5. T. C. Zhu, A. J. Bishop, T. Zhou, M. Zhu, D. J. O'Hara, A. A. Baker, S. Cheng, R. C. Walko, J. J. Repicky, J. A. Gupta, C. M. Jozwiak, E. Rotenberg, J. Hwang, I. Zutic, R. K. Kawakami, Magnetic Properties and Electronic Structure of Magnetic Topological Insulator MnBi_2Se_4 , *Nano Lett.* **21**, 5083 (2021).
6. J. Joshi, T. Zhou, S. Krylyuk, A.V. Davydov, I. Zutic, and P. M. Vora, Localized Excitons in NbSe_2 - MoSe_2 Heterostructures, *ACS Nano* **14**, 8528 (2020).
7. F. Liu, F. Qu, I. Zutic, S. Xie, D. Liu, A. L. A. Fonseca, and M. Malard, Robust Topological Nodal-Line Semimetals from Periodic Vacancies in Two-Dimensional Materials, *J. Phys. Chem. Lett.* **127**, 5710 (2021).
8. F. Liu, F. Qu, I. Zutic, and M. Malard, Less is more: Vacancy-engineered nodal-line semimetals, [arXiv:2108.05502](https://arxiv.org/abs/2108.05502)
9. K. Chen, K. Qi, T. Zhou, T. Yang, Y. Zhang, Z. Guo, C.-K. Lim, J. Zhang, I. Zutic, H. Zhang, P. N. Prasad, Water-Dispersible CsPbBr_3 Perovskite Nanocrystals with Ultra-Stability and its Application in Electrochemical CO_2 Reduction, *Nano-Micro Lett.* **13**, 172 (2021).
10. R. Cai, Y. Yao, P. Lv, Y. Ma, W. Xing, B. Li, Y. Ji, H. Zhou, C. Shen, S. Jia, X. C. Xie, I. Zutic, Q.-F. Sun and W. Han, Evidence for anisotropic spin-triplet Andreev reflection at the 2D van der Waals ferromagnet/superconductor interface, preprint, under review in *Nat. Commun.*
11. Y. Luo, T. Zhou, M. R. Neupane, A. Matos-Abiague, R. Bailey-Crandell, M. Newburger, I. Iyalin, I. Zutic, and R. K. Kawakami, van der Waals Photothermoelectric Effect in Atomic Layer Heterojunctions, preprint.

Author Index

Agterberg, Daniel	1	Del Maestro, Adrian	158
Amoo, M.	58	Deslippe, Jack R.	221
Andrade, Xavier	286	Devereaux, T. P.	82
Antropov, Vladimir	418	Di Ventra, Massimiliano	88
Balents, Leon	6	Du, M.-H.	322
Bansil, A.	58	Dubois, J.	186
Barraza-Lopez, Salvador	11	Dufty, J. W.	383
Barros, Kipton	158, 191	Dykman, M. I.	231
Batista, Cristian	158	Eisenbach, M.	322
Benali, A.	172	Engel-Herbert, Roman	44, 146
Berlijn, T.	72	Eom, Chang-Beom	146
Bernardi, Marco	39	Eriksson M.	186
Bernevig, B. Andrei	16	Ertekin, Elif	30
Bhattacharya, A.	172	Faoro, L.	186
Bondarev, Igor	20	Feiguin, Adrian E.	58, 91
Brar, V.	186	Ferguson, Andrew	108
Broido, David	25	Fernandes, Rafael M.	93
Burke, Kieron	427	Fishman, R. S.	72
Carlson, Erica	146	Fong, Dillon	276
Ceperley, David	30	Freericks, James	98, 103
Chamon, Claudio	33	Friesen, M.	186
Chan, Garnet Kin-Lic	37, 39	Galitski, Victor	111
Chan, Maria	108	Galli, G.	108
Chandra, Premala	41	Ganesh, P.	172
Chelikowsky, James R.	221	Ginsberg, Naomi S.	221
Chen, L. Q.	44	Glazman, Leonid	119
Chen, Zizhong	437	Gopalan, V.	44
Chern, Gai-Wei	49, 191	Govoni, Marco	108, 124
Chernyshev, Alexander	54	Greenblatt, Martha	191
Choi, Sangkook	191	Griffin, Sinéad	126
Chowdhury, S.	58	Guistino, Feliciano	114
Choy, J.	186	Gull, Emanuel	39
Chubukov, Andrey V.	60	Gygi, François	108
Chudnovsky, Eugene M.	65	Hamlin, J. A.	137
Classen, Laura	398	Haule, Kristjan	191
Clay, R.	172	Hautier, Geoffroy	126
Cohen, Marvin L.	216	Heinonen, Olle	172, 281
Coleman, Piers	69	Hennig, R. G.	137
Cooper, V. R.	72	Henry, M. D.	231
Correa, Alfredo	286	Heremans, Joseph	108
da Jornada, Felipe H.	221	Hermele, Michael	128
Dabo, I.	44	Hirschfeld, P. J.	133, 137
Dagotto, Elbio	77	Ho, Kai-Ming	418, 452
de Pablo, Juan	108	Hosur, Pavan	142
Dean, Mark	158, 191	Hunt, Benjamin M.	146
Del Ben, Mauro	437	Ibrahim, Khaled	415

Irvin, Patrick	146	Mazin, Igor I.....	243
Jain, Jainendra	149	McDermott, R.....	186
Jia, C.....	58, 82	Mele, E. J.	247
Jiang, H.....	82	Melnick, Corey.....	191
Johnson, Duane D.....	154	Millis, Andrew.....	39
Johnson, Harley.....	30	Mitas, Lubos.....	172, 251
Johnston, Steven.....	158	Mitra, Aditi.....	255
Jordan, Andrew N.....	163	Moore, J. E.	82
Kas, J. J.	82, 327	Moreno, Juana	257
Ke, Liqin	167	Moreo, Adriana	77
Kemper, Alexander	103	Moritz, B.	82
Kent, P. R. C.	172	Morr, Dirk K.	262
Khaled, Ibrahim.....	437	Mulligan, Michael	267
Khatami, Ehsan	158	Nandkishore, Rahul	272
Khemani, Vedika.....	177	Narang, Prineha	146
Kim, Eun-Ah.....	182	Narayanan, Badri.....	276
Kioupakis, Emmanouil	114	Nashed, Y.....	58
Kolkowitz, S.....	186	Neaton, Jeffrey B.....	216, 221
Konik, Robert.....	191, 398	Neuhauser, Daniel	221, 415
Kotliar, Gabriel	191, 415	Nevidomskyy, Andriy.....	30
Kovalev, Alexey.....	196	Norman, Michael.....	281
Krogel, J.....	172, 322	Ogitsu, Tadashi.....	286
Kutepov, Andrey	191	Okamoto, Satoshi	77
Lambrecht, Walter R. L.	201	Orth, Peter P.	452
Lany, Stephan.....	407	Parashar, Manish	191
Lee, Dung-Hai.....	216	Park, Hyowon.....	281
Lee, H. N.....	172	Parker, D. S.	72
Lee, Patrick A.	206	Pashov, Dimitar	407
Levchenko, A.	186	Pemmaraju, C. D.	82, 286
Levy, Jeremy.....	146	Perkins, Natalia	291
Li, Ying Wai	158	Persson, Kristin	295
Lin, Lin	415	Petrovic, Cedomir.....	191
Lindenberg, Aaron M.	58, 286	Pleimling, Michel	375
Lindsay, Lucas	72, 211	Ponomareva, Inna	300
Littlewood, Peter.....	281	Potter, Andrew.....	346
Liu, Jian	158	Prendergast, David.....	286
Lordi, V.....	186	Qiu, Diana Y.	221, 304
Louie, Steven G.....	216, 221	Rabani, Eran.....	39, 221
Luo, Y.....	172	Raghu, Srinivas	307
Lyanda-Geller, Yuli.....	226	Rahman, Talat S.	312
Lyon, S. A.....	231	Raja, Archana	126
MacDonald, Allan H.	235	Rappe, Andrew M.....	317
Maier, Thomas	77, 158	Ray, K.	186
Marianetti, Chris A.....	238	Reboredo, F. A.	322
Martin, Ivar	281	Rehr, J. J.....	82, 327
Matveev, Kostya	281	Reichman, David	39

Romero, Aldo H.	331	van Schilfgaarde, Mark	407
Rosen, Y.	186	Vasseur, Romain.....	410
Rubenstein, B.	172	Vila, F.	82
Ruzsinszky, Adrienn.....	334	Vlcek, Vojtech.....	415
Sachdev, Subir	338	Wagner, Lucas.....	30
Sankaranarayanan, Subramanian	276	Wang, Cai-Zhuang.....	418, 452
Scalettar, Richard	158, 341	Wang, Feng	221
Shaner, E. A.	231	Wang, Lin-Wang	216
Shankar, Shyam.....	346	Wang, Ziqiang	422
Sharifzadeh, Sahar.....	350	Weber-Bargioni, Alexander	126
Shastry, B. Sriram	355	Weichselbaum, Andreas	398
Shelton, Christian	437	West, Damien	462
Shelton, William A.....	154	Whaley, K. Birgitta.....	415
Sheng, Dong-Ning.....	360	White, Steven R.....	427
Shin, H.	172	Whitmer, Jonathan.....	108
Shulenburger, L.....	172	Widom, Michael	432
Si, Qimiao	365	Wong, Bryan M.	437
Singh, David J.	370	Woods, Lilia M.....	441
Singh, Prashant.....	154	Woodward, Carol	39
Sipahigil, Alp	126	Wu, Ruqian	446
Smirnov, Andrey V.	154	Xiao, Di.....	146
Stewart, G. R.....	137	Xu, J.	44
Talapin, Dmitri.....	108	Yan, Qimin	450
Tan, Liang Z.....	286	Yang, Chao.....	39, 221, 415
Täuber, Uwe C.	375	Yao, Yongxin	191, 418, 452
Tennant, Alan.....	158	Yin, Weiguo	398
Thayer, J.	58	Yoon, C.....	58
Todadri, Senthil.....	380	Yoon, M.	322
Townsend, J.	172	Zang, Jiadong	457
Trickey, Samuel B.	383	Zgid, Dominika	415
Tse, Wang-Kong	388	Zhang, Feng.....	418
Tserkovnyak, Yaroslav	393	Zhang, Shengbai	462
Tselik, Alexei	398	Zhu, Qiang	467
Turk, Matthew.....	30	Zunger, Alex	471
Turner, J.	58	Zutic, Igor.....	474
Ullrich, Carsten A.....	403		

Participant List

Name	Email	Organization
Agterberg, Daniel	agterber@uwm.edu	University of Wisconsin, Milwaukee
Barraza-Lopez, Salvador	sbarraza@uark.edu	University of Arkansas
Bernevig, Andrei	bernevig@gmail.com	Princeton University
Bondarev, Igor	ibondarev@ncsu.edu	North Carolina Central University
Broido, David	broido@bc.edu	Boston College
Cantoni, Claudia	claudia.cantoni@science.doe.gov	US Department of Energy - BES
Ceperley, David	ceperley@illinois.edu	University of Illinois, Urbana-Champaign
Chamon, Claudio	chamon@bu.edu	Boston University
Chan, Garnet	gkc1000@gmail.com	Caltech
Chandra, Premi	pchandra@physics.rutgers.edu	Rutgers University
Chen, Long-Qing	lqc3@psu.edu	Pennsylvania State University
Chern, Gia-Wei	gchern@virginia.edu	University of Virginia
Chernyshev, Sasha	sasha@uci.edu	University of California, Irvine
Chowdhury, Sugata	sugata.chowdhury@howard.edu	Howard University
Chubukov, Andrey	achubuko@umn.edu	University of Minnesota
Chudnovsky, Eugene	eugene.chudnovsky@lehman.cuny.edu	The City University of New York
Coleman, Piers	pcoleman@physics.rutgers.edu	Rutgers University
Cooper, Valentino	coopervr@ornl.gov	Oak Ridge National Laboratory
Correa, Alfredo	correa@llnl.gov	Lawrence Livermore National Laboratory
Dagotto, Elbio	edagotto@utk.edu	ORNL/University of Tennessee
Devereaux, Thomas	tpd@stanford.edu	SLAC National Accelerator Laboratory
Di Ventra, Massimiliano	diventra@physics.ucsd.edu	University of California, San Diego
Feiguin, Adrian	a.feiguin@northeastern.edu	Northeastern University
Fernandes, Rafael	rfernand@umn.edu	University of Minnesota
Fiechtner, Gregory	gregory.fiechtner@science.doe.gov	Department of Energy
Freericks, James	james.freericks@georgetown.edu	Georgetown University
Galitski, Victor	galitski@umd.edu	University of Maryland
Galli, Giulia	gagalli@uchicago.edu	University of Chicago
Giustino, Feliciano	fgiustino@oden.utexas.edu	University of Texas, Austin
Glazman, Leonid	leonid.glazman@yale.edu	Yale University
Gopalan, Venkatraman	vgopalan@psu.edu	Pennsylvania State University
Govoni, Marco	mgovoni@anl.gov	Argonne National Laboratory
Graf, Matthias	matthias.graf@science.doe.gov	Department of Energy
Gull, Emanuel	egull@umich.edu	University of Michigan, Ann Arbor
Hautier, Geoffroy	geoffroy.hautier@dartmouth.edu	Dartmouth College
Hennig, Richard	rhennig@ufl.edu	University of Florida
Hermele, Michael	michael.hermele@colorado.edu	University of Colorado, Boulder
Hirschfeld, Peter	pjh@phys.ufl.edu	University of Florida
Holder, Aaron	aaron.holder@science.doe.gov	Department of Energy
Horton, Matthew	mhorton@lbl.gov	Lawrence Berkeley National Laboratory
Hosur, Pavan	phosur@uh.edu	University of Houston
Hunt, Benjamin	bmhunt@andrew.cmu.edu	Carnegie Mellon University

Jain, Jainendra	jkj2@psu.edu	Penn State University
Jiang, Hong-Chen	hcjiang@stanford.edu	SLAC National Accelerator Laboratory
Johnson, Duane	ddj@ameslab.gov	Ames Laboratory
Johnston, Steven	sjohn145@utk.edu	University of Tennessee
Jordan, Andrew	jordan@chapman.edu	Chapman University
Ke, Liqin	liqinke@ameslab.gov	Ames Laboratory
Kemper, Alexander	akemper@ncsu.edu	North Carolina State University
Kent, Paul	kentpr@ornl.gov	Oak Ridge National Laboratory
Kerch, Helen	helenkmd@gmail.com	Department of Energy
Khemani, Vedika	vkhemani@stanford.edu	Stanford University
Kim, Eun-ah	ek436@cornell.edu	Cornell University
Kolkowitz, Shimon	kolkowitz@wisc.edu	University of Wisconsin, Madison
Konik, Robert	rmk@bnl.gov	Brookhaven National Laboratory
Kotliar, Gabriel	kotliar@physics.rutgers.edu	Rutgers/Brookhaven National Laboratory
Kovalev, Alexey	alexey.kovalev@unl.edu	University of Nebraska, Lincoln
Lambrecht, Walter	walter.lambrecht@case.edu	Case Western Reserve University
Lee, Patrick	palee@mit.edu	Massachusetts Institute of Technology
Levy, Jeremy	jlevy@pitt.edu	University of Pittsburgh
Lindsay, Lucas	lindsaylr@ornl.gov	Oak Ridge National Laboratory
Louie, Steven G.	sglouie@berkeley.edu	Lawrence Berkeley National Laboratory
Lu, Jiwei	jiwei.lu@us.af.mil	Air Force Office of Scientific Research
Lyanda-Geller, Yuli	yuli@purdue.edu	Purdue University
Lyon, Stephen	lyon@princeton.edu	Princeton University
MacDonald, Allan	macd@physics.utexas.edu	University of Texas, Austin
Marianetti, Chris	chris.marianetti@columbia.edu	Columbia University
Martin, Ivar	ivar@anl.gov	Argonne National Laboratory
Mazin, Igor	imazin2@gmu.edu	George Mason University
Mele, Eugene	mele@physics.upenn.edu	University of Pennsylvania
Mewes, Claudia	ckmewes@ua.edu	University of Alabama
Mitas, Lubos	lmitas@ncsu.edu	North Carolina State University
Mitra, Aditi	aditi.mitra@nyu.edu	New York University
Moreno, Juana	moreno@phys.lsu.edu	Louisiana State University
Moritz, Brian	Brian.Moritz@science.doe.gov	Department of Energy
Morr, Dirk	Dkmorr@uic.edu	University of Illinois, Chicago
Mulligan, Michael	michael.c.mulligan@gmail.com	University of California, Riverside
Nandkishore, Rahul	rahul.nandkishore@colorado.edu	University of Colorado, Boulder
Narayanan, Badri	badri.narayanan@louisville.edu	University of Louisville
Neaton, Jeff	jbneaton@lbl.gov	Lawrence Berkeley National Laboratory
Norman, Michael	norman@anl.gov	Argonne National Laboratory
Ogitsu, Tadashi	ogitsu1@llnl.gov	Lawrence Livermore National Laboratory
Parazzoli, Paul	paul.parazzoli@science.doe.gov	Department of Energy
Pechan, Michael	michael.pechan@science.doe.gov	Department of Energy
Perkins, Natalia	nperkins@umn.edu	University of Minnesota

Ponomareva, Inna	Iponomar@usf.edu	University of South Florida
Qiu, Diana	diana.qiu@yale.edu	Yale University
Raghu, Srinivas	sraghu@stanford.edu	Stanford University
Rahman, Talat	talat.rahman@ucf.edu	University of Central Florida
Rappe, Andrew	rappe@sas.upenn.edu	University of Pennsylvania
Ray, Keith	ray30@llnl.gov	Lawrence Livermore National Laboratory
Reboredo, Fernando	reboredofa@ornl.gov	Oak Ridge National Laboratory
Rehr, John	jjr@uw.edu	University of Washington
Romero, Aldo	alromero@mail.wvu.edu	West Virginia University
Ruzsinszky, Adrienn	aruzsinszky@temple.edu	Temple University
Sachdev, Subir	sachdev@g.harvard.edu	Harvard University
Scalettar, Richard	scalettar@physics.ucdavis.edu	University of California, Davis
Schlueter, John	JSchluet@nsf.gov	National Science Foundation
Schwartz, Andrew	andrew.schwartz@science.doe.gov	Department of Energy
Shankar, Shyam	shyam.shankar@utexas.edu	University of Texas, Austin
Sharifzadeh, Sahar	ssharifz@bu.edu	Boston University
Shastry, Sriram	sriram@physics.ucsc.edu	University of California, Santa Cruz
Sheng, Dong-Ning	donna.sheng@csun.edu	California State University, Northridge
Si, Qimiao	qmsi@rice.edu	Rice University
Singh, David	singhdj@missouri.edu	University of Missouri
Tauber, Uwe C	tauber@vt.edu	Virginia Tech
Thiyagarajan, Pappannan	p.thiyagarajan@science.doe.gov	Department of Energy
Todadri, Senthil	senthil@mit.edu	Massachusetts Institute of Technology
Trickey, Sam	trickey@qtp.ufl.edu	University of Florida
Tse, Wang-Kong	wktse@ua.edu	University of Alabama
Tserkovnyak, Yaroslav	yaroslav@physics.ucla.edu	University of California, Los Angeles
Tselik, Alexei	tselik@gmail.com	Brookhaven National Laboratory
Tumas, Bill	bill.tumas@nrel.gov	National Renewable Energy Laboratory
Turkowski, Volodymyr	Volodymyr.Turkowski@ucf.edu	University of Central Florida
Turner, Joshua	joshuat@slac.stanford.edu	SLAC/Stanford University
Ullrich, Carsten	ullrichc@missouri.edu	University of Missouri
van Schilfgaarde, Mark	Mark.vanSchilfgaarde@nrel.gov	National Renewable Energy Laboratory
Vasseur, Romain	rvasseur@umass.edu	University of Massachusetts, Amherst
Vlcek, Vojtech	vlcek@ucsb.edu	University of California, Santa Barbara
Wagner, Lucas	lkwagner@illinois.edu	University of Illinois, Urbana-Champaign
Wang, Ziqiang	wangzi@bc.edu	Boston College
Wang, Cai-Zhuang	wangcz@ameslab.gov	Ames Laboratory
White, Steven	srwhite@uci.edu	University of California, Irvine
Widom, Michael	widom@cmu.edu	Carnegie Mellon University
Wong, Bryan	bryan.wong@ucr.edu	University of California, Riverside
Woods, Lilia	lmwoods@usf.edu	University of South Florida
Wu, Ruqian	wur@uci.edu	University of California, Irvine
Yan, Qimin	qiminyan@temple.edu	Temple University

Yao, Yongxin
Zang, Jiadong
Zhang, Shengbai
Zhu, Qiang
Zunger, Alex
Zutic, Igor

ykent@ameslab.gov
jiadong.zang@unh.edu
zhangs9@rpi.edu
qiang.zhu@unlv.edu
alex.zunger@colorado.edu
zigor@buffalo.edu

Ames Laboratory
University of New Hampshire
Rensselaer Polytechnic Institute
University of Nevada, Las Vegas
University of Colorado, Boulder
University at Buffalo